The Role of GPR84 in Chronic Pain Mechanisms

Nicol, Louise

Awarding institution:
King's College London

The Role of GPR84 in Chronic Pain Mechanisms

Louise Samantha Concetta Nicol

Thesis presented for the degree of Doctor of Philosophy
at King's College London

Wolfson Centre for Age Related Diseases
King's College London
2009 - 2013

Abstract

Increasing pre-clinical evidence supports a role of neuronal-immune interactions in chronic pain. Here, we investigated the involvement of G-protein receptor 84 (GPR84), an immune cell receptor that is markedly induced in monocytes/macrophages and microglia under inflammatory conditions, in chronic pain signalling.

GPR84 knock-out (KO) mice exhibited normal acute pain thresholds but showed deficits in neuropathic and inflammatory pain responses. Thus, in contrast to wild-type (WT) mice, KOs did not develop mechanical allodynia or thermal hyperalgesia subsequent to partial sciatic nerve ligation (PNL) and exhibited attenuated mechanical, thermal and cold hyperalgesia after intraplantar injection of complete Freund's adjuvant (CFA). Nerve injury or inflammation also resulted in increased Iba1 and phosphorylated p38 mitogen-activated protein kinase (MAPK) immunoreactivity in spinal microglia, as well as increased Iba1 expression in macrophages of the sciatic nerve post PNL, with no difference between genotypes.

In WT mice, GPR84 mRNA expression was up-regulated in the spinal cord and sciatic nerve at 7 and 21 days post PNL, as well as in microglia or macrophage cultures at 3 hours post lipopolysaccharide (LPS) stimulation. Concurrent with these changes, we identified 86 dysregulated genes in the sciatic nerve and spinal cord following injury and 30 dysregulated mediators in macrophages following treatment. Interestingly, expression of arginase-1 (ARG1), a marker for anti-inflammatory macrophages, was considerably up-regulated by 20.8-fold in KO sciatic nerve at 7 days post PNL. In addition, forskolin-induced levels of 3'-5'-cyclic adenosine monophosphate (cAMP) were greater in KO than WT macrophages. Together these data are indicative of an anti-inflammatory macrophage phenotype in KO mice under pathological conditions.

We suggest that GPR84 is a pro-inflammatory receptor involved in nociceptive signalling in animal models of persistent pain, possibly mediating its effects via the modulation of peripheral macrophages. Based on these results GPR84 may be a promising new target with therapeutic potential in chronic pain.

Abstracts Arising from this Work

Louise Nicol, Clive Gentry, Daisy Mcinnerney, John B. Davis, Marzia Malcangio and Stephen B. McMahon **(2013)**. *Inflammatory Pain Behaviour is Attenuated in GPR84 Knock-out Mice*. Society for Neuroscience Annual Meeting, San Diego.

Louise Nicol, John M. Dawes, Clive Gentry, John B. Davis, Stephen B. McMahon and Marzia Malcangio **(2012)**. *Neuropathic Pain Behaviour is Attenuated in GPR84 Knock-out Mice*. 14th World Congress on Pain (IASP), Milan.

Louise Nicol, John M. Dawes, John B. Davis, Stephen B. McMahon and Marzia Malcangio **(2011)**. *Chronic Pain Mechanisms: The Role of GPR84/EX33 Expressed on Spinal Microglial Cells*. New Frontiers in Persistent Pain (ABCAM), Paris.

Acknowledgements

I would firstly like to thank my supervisors Dr Marzia Malcangio and Prof Stephen McMahon for all their support throughout my PhD. Marzia, thank you for all your encouragement, guidance and engaging conversations. Mac, your enthusiasm and passion for science is truly inspiring and I will never forget our surgical experiences and moments of scrutinising down the microscope. I am extremely grateful for the fantastic opportunity you have both given me and for all the skills I have acquired that shall equip me throughout the rest of my life.

I would also like to thank our collaborators from GlaxoSmithKline, particularly Dr John Davis for providing the transgenic animals and his continued contribution throughout the project. I am indebted to Dr Anna Clark and Dr Amelia Staniland for their time spent teaching me many of the techniques that form the groundings of the research presented in this thesis. I would also like to thank Anna for the fun and memorable trip around Vienna and for all her support throughout the years as a teacher and a friend. A special mention to the super-fast John Grist for all his assistance with surgeries and saving me on occasions where my surgery plans had been overly optimistic. Clive Gentry, the master of animal behaviour, thank you for your time and assistance with the intrathecal/intraplantar injections and the paw-pressure data presented in this thesis. My gratitude goes to everyone that helped: Dr Andy Grant for teaching me calcium fluorometry and helping out with the microscope setup. Dr John tomato-cola Dawes, the molecular king and office buddy, for his patience and teaching on a number of molecular techniques in addition to his assistance with all the PCR array data. Dr Margarita Calvo for technical support on a number of issues, including how to block tissue on my very first day. Dr Trinidad Montero-Melendez for teaching me how to culture bio-gel elicited macrophages, Elizabeth Old for the cortical microglia cultures, Hannes Kiesewetter for showing me resident macrophage cultures and my student, Daisy Mcinnerney, for her assistance. I would also like to thank Vivien Cheah and Caroline Abel (along with John Grist) for all their administrative solutions for any problems and the smooth running of my PhD.

I am thankful to the past and current members of the Mac lab who have made my time a pleasant experience. We shared many fun moments together, including girly nights at Mary Janes feasting on huge burgers and happy hour piña coladas, eventful Christmas parties, the Mac lab Sports Day, our trip to the beach, the pub crawls, random nights in Belushi's or The Blue Eyed Maid and the awesome conference trip to Paris. A special mention should also be made to my two sets of office buddies: the originals, Nicky, Tommy H, cake-loving Sara and Karen Bosch woman with her mini sausages. My disagreements with the boys over how cold the office was and continuous banter made a tough day of work an enjoyable experience.

Nicky, you were one of my first friends in the lab and have remained close to me throughout the years. I thank you for all your support in times of good and bad, which have been full of fizzy fangs and sweetie gifts. My second set of office buddies upstairs, lovely Umut, Ariana the small malteaser, Andrea-boomting/dancing buddy, Rie the chatterbox, the flexible Olivia and Francisco. We shared many laughs and fun office moments together. A special note to Rose, Margarita, Federica and Dee for being supportive friends and Juan for his invaluable chats and care. Thank you to Alex, Amanda, Ana, Andrew, Claudia, Franziska, Jorge, Katalin, Kathryn, Lisa, Lan, Maggie, Matthew, Natalie, Ning, Ping, Richard, Sanam/Salmon, Sebastian, Steven, Thanos and Tom P - you all made this a good experience.

Alexander Bell and Lucy Bee, it was with you that I discovered my interest in neuroscience research and your encouragement gave me the confidence to pursue a PhD, which was one of the best decisions I have ever made. My friends, Jale Dolucan, Salvatore Lobue, Sarah Headley, Mariella and Annabella Nigrelli, thank you for your supportive and caring friendships, your interest in my work and your words of encouragement to keep me motivated throughout this journey.

The first lab technique I learned was *in situ* hybridisation, which was a memorable experience with Christopher Tsantoulas. I quickly adapted to his bat-like hours and strictness. Although some of our experiments didn't work out, we did. Now as my partner I'm grateful for your understanding, patience and support. You opened my eyes to many things and I'm tremendously appreciative of all your time spent reading this thesis word by word. Thank you for all your love and care.

Words cannot express the gratitude I have for my parents Kwame and Jose, my brother Antony and sister Nicola. Dad and mum, you have always aspired to build a strong and supportive family home, which set the foundations to a successful future. You instilled the importance and power of education in me from the very beginning when reading my first words in Janet and John books and continued your endless encouragement in every path I chose. I thank you all for your unconditional support and love that drove me to reach for the stars and achieve my dreams no matter how hard they were to follow. I hope that I have made you proud.

Table of Contents

List of Figures

List of Tables

Abbreviations

AC - Adenylate cyclase
AIF1 - Allograft inflammatory factors-1
AM - Acetoxymethyl
AMP - Adenosine monophosphate
AMPAR - α-amino-3-hydroxy-5-methyl-4 isoxazolepropionic acid
ANOVA - Analysis of variance
AREG - Amphiregulin
ARG1 - Arginase-1
ARRIVE - Animal Research: Reporting of *In Vivo* Experiments
ARTN - Artemin
ASIC - Acid sensing ion channel
ATF2 - Activating transcription factor 2
ATP - Adenosine-5'-triphosphate
AUC - Area under curve

B_1 - Bradykinin receptor 1
B_2 - Bradykinin receptor 2
BDNF - Brain derived neurotrophic factor
B-GEPM - Bio-Gel elicited peritoneal macrophage
BMM - Bone-marrow derived macrophage
BTC - Betacellulin

C5a - Complement 5a
CA - Capric acid
Ca^{2+} - Calcium
CaM - Calmodulin
CAMK - Calcium/calmodulin-dependent kinase
CAMKK - Calcium/calmodulin-dependent kinase kinase
cAMP - 3'-5'-cyclic adenosine monophosphate
CatS - Cathepsin S
CBP - CREB binding protein
CCI - Chronic constriction injury
CCL - Chemokine (C-C motif) ligand
CCR - C-C chemokine receptor type
CD3D - T-cell surface glycoprotein cluster of differentiation 3 delta chain
cDNA - Complementary deoxyribonucleic acid
CFA - Complete Freund's adjuvant
CGRP - Calcitonin-gene related peptide
CHO - Chinese hamster ovary
Cl^- - Chloride
cNOS - Constitutive NOS
CNS - Central nervous system
COX - Cyclooxygenase
CR - Complement receptor
CRAC - Calcium release-activate Calcium channel
CREB - Cyclic adenosine monophosphate response element-binding protein
CRPS - Complex regional pain syndrome
CSF - Cerebral spinal fluid
CSF1R - Colony stimulating factor 1 (macrophage) receptor
CSF3R - Colony stimulating factor 3 (granulocyte) receptor
CST - Complete sciatic nerve transection
CT - Cycling time
CX_3CR1 - CX3C chemokine receptor 1
CXCL - Chemokine (C-X-C motif) ligand
CXCR - C-X-C chemokine receptor type
CXCR1 - CXC chemokine receptor 1

DAG - Diacyl-glycerol
DAPI - 4',6-diamidino-2-phenylindole
DMEM - Dulbecco's Modified Eagle's medium
DNase - Deoxyribonuclease
DRG - Dorsal root ganglion

EAE - Experimental autoimmune encephalomyelitis
EAN - Experimental autoimmune neuritis
ECM - Extracellular matrix
EDTA - Ethylenediaminetetraacetic acid

EGF - Epidermal growth factor
EGFR/ERBBI - Tyrosine-kinase epidermal growth factor receptor
eNOS/NOS3 - Endothelial NOS
EP - Prostaglandin
EPSC - Excitatory postsynaptic current
ER - Endoplasmic reticulum
EREG - Epiregulin
ERK - Extracellular signal-regulated kinase

FBS - Fetal bovine serum
FC - Fold change
FCεRI - Immunoglobulin E receptor
FDR - False discovery rate
FFA - Free fatty acid

GABA - γ-aminobutyric acid
GAP - GTPase-accelerating protein
GAPDH - Glyceraldehyde-3-phosphate dehydrogenase
GBS - Guillain-Barré Syndrome
GDNF - Glial-derived neurotrophin factor
GDP - Guanosine diphosphate
GEF - Guanine nucleotide exchange factor
GFAP - Glial fibrillary acidic protein
GFP - Green fluorescent protein
GPCR - G-protein-coupled receptor
GPR84 - G-protein 84
GRK - G-protein-coupled receptor kinase
GTP - Guanosine triphosphate
GTPase - Guanosine triphosphatase

H^+ - hydrogen
H1 - Histamine receptor 1
H2.EB1 - Histocompatibility 2, class II antigen Eβ
HBEGF - Heparin-binding EGF-line growth factor
HET - Heterozygous
HIV - Human immunodeficiency virus
HK - Housekeeping
HPRT – Hypoxanthine phosphoribosyltransferase
HSP - Heat shock protein

I.p. - Intraperitoneal
IASP - International Association for the Study of Pain
IB4 - Isolectin B4
Iba1 - Ionised calcium binding adaptor molecule 1
IBS - Irritable bowel syndrome
IFN - Interferon
IKK - Kinase complex
IL - Interleukin
IL-1ra - Interleukin-1 receptor antagonist
iNOS - Inducible nitric oxide synthase
$[Ca^{2+}]_i$ - Intracellular calcium concentration
IP_3 - Inositol 1, 4, 5-triphosphate
IP_3R - Inositol 1, 4, 5-triphosphate receptor
IPSC - Inhibitory post-synaptic current
IRAK4 - IL-1 receptor-associated kinase 4
ITGAM - Integrin alpha M/CD11b
IκB - Inhibitory κB

JNK - c-Jun N-terminal

K^+ - Potassium
KCC2 - Potassium chloride co-transporter 2
KO - Knock-out

LCFFA - Long chain free fatty acid
LPS - Lipopolysaccharide
LTA - Lipoteichoic acid
LTB_4 - leukotriene-B4
LTP - Long-term potentiation

MAPK - Mitogen-activated protein kinase
MCFFA - Medium chain free fatty acid
Mg^{2+} - Magnesium
mGLUR - Metabotropic glutamate receptor
MKK - MAPK kinase
MMP - Matrix metalloproteinase
MRC1 - Mannose receptor c-type 1
MS - Multiple sclerosis
MUFA - monounsaturated

MyD88 - Myeloid differentiation primary response gene 88

Na^+ - sodium
NADPH - Nicotinamide adenine dinucleotide phosphate
NCX - Sodium/calcium exchanger
ND - Non-detectable
NeuN - Neuronal nuclei
NF200 - Neurofilament 200
NF-κB - Nuclear factor kappa-light-chain-enhancer of activated B cell
NGF - Neurotrophin growth factor
NK1 - Neurokinin 1
NMDAR - N-methyl-D-aspartate receptor
nNOS - NOS
NNT - Numbers needed to treat
NNH - Numbers needed to harm
NO - Nitric oxide
NOS2 - Nitric oxide synthase 2
NRG1 - Neuregulin 1
NSAID - Non steroidal anti-inflammatory drug

OA - Osteoarthritis
6-OAU - 6-n-octylamino uracil
OCT - Optimum cutting temperature
OX-42 - Cluster of differentiation molecule 11B (CD11B)

P2X - Purigenic ionotropic receptor
P2Y - Purigenic metabotropic receptor
PAG - Periaqueductal grey matter
PAMP - Pathogen associated molecular pattern
PB - Parabrachial
PB - Phosphate buffer
PBS - Phosphate buffered saline
PCR - Polymerase chain reaction
PDE - Phosphodiesterase
PET- Positron emission tomography
PFA - Paraformaldehyde
PG - Prostaglandin
PGE_2 - prostaglandin E2
PGI_2 - Prostacyclin
PI3K - Phosphoinositide 3-kinase
PIP_2 - Phosphatidylinositol 4,5-bisphosphate
PKA - Protein kinase A
PKC - Protein kinase C
PLA_2 - Phospholipase A2
PLC - Phospholipase C
PLT - Paucity of lymph node T-cells
PMCA - Plasma membrane calcium-ATPase
PMN - Polymorphonuclear leukocyte
PNL - Partial nerve ligation
PNS - Peripheral nervous system
P-p38 - Phosphorylated p38
PROX - Proximal
PRR - Pattern recognition receptor
PTGS2 - cyclooxygenase-2
PUFA - polyunsaturated
PWL - Paw withdrawal latency
PWT - Paw withdrawal threshold

qRT-PCR - Quantitative real-time PCR

3Rs - Replacement Refinement and Reduction
RA - rheumatoid arthritis
Rag-1 - Recombinant activating gene-1 null mice
RET - Receptor tyrosine kinase
RGS - Regulator of G-protein signalling protein
RM - Repeated measure
ROC - Receptor-operated channel
RVM - Rostral ventromedial medulla
RyRs - Ryanodine receptors

SCFFA - Small chain free fatty acid
SD - Standard deviation
SEM - Standard error of the mean
5HT - Serotonin/5-hydroxytryptamine
SNARE - Soluble N-ethylmaleimide-sensitive factor attachment protein receptor
SNI - Spared nerve injury
SNK - Student-Newman-Keul
SNL - Spinal nerve ligation

SOC - Store-operated channel
SP - Substance P
SSNRIs - Serotonin and norepinephrine reuptake inhibitors
STZ - Streptozotocin

TAB - TAK-1 binding protein
TAK1 - Transforming growth factor-β-activated kinase
Tc - cytotoxic T cell
TCA - Tricyclic antidepressant
TGF - Transforming growth factor
Th - T-helper cells
TIR - Toll-interleukin-1 receptor
TLR - Toll-like receptor
TNF - Tumor necrosis factor
TRAF6 - Tumor necrosis factor receptor-associated factor 6
Tregs - regulatory T cells
Trk – Tropomyosin receptor kinase
TRPA - Transient receptor potential cation channel, subfamily A, member
TRPC - Transient receptor potential cation channel subfamily C, member
TRPM - Transient receptor potential cation channel subfamily M, member
TRPV - Transient receptor potential cation channel subfamily V, member
TTX - Tetrodotoxin
TXA_2 - Thromboxane

VGCC - Voltage-gated calcium channel
VZV - Varicella zoster virus

WD - Wallerian degeneration
WDR - Wide dynamic range neuron
WT - Wild-type

XCL - Chemokine (C motif) ligand

ΔΔCT - Delta delta cycling time

Chapter 1

General Introduction

1.1 The clinical problem of chronic pain

The nervous system is a specialised network of cells that integrates sensory information from an organism's internal and external environment and coordinates an appropriate response. The sensation of pain is mediated by a complex system of neuronal activity, providing a protective mechanism against potential tissue injury and facilitating the process of healing in the event of damage. According to the International Association for the Study of Pain (IASP), pain is defined as 'an unpleasant sensory and emotional experience associated with actual or potential tissue damage, or described in terms of such damage'. The importance of pain as a survival mechanism is particularly evident when considering individuals born with genetic abnormalities that affect the normal function of this system. For example, congenital insensitivity to pain is a rare disorder characterised by the inability to detect and thus respond to a painful stimulus. It can be caused by mutations in the tropomyosin receptor kinase A (TrkA) gene, which render the encoded neurotrophin growth factor (NGF) receptor unresponsive to NGF (Pezet and McMahon, 2006), or by mutations in the SCN9A gene encoding the α-subunit of the voltage-gated sodium (Na^+) channel, $Na_v1.7$ (Cox et al., 2006). As a result these individuals tend to have extensive burns, bruises and lacerations, particularly during childhood, and often die prematurely from repetitive illness (Verpoorten et al., 2006).

On the other hand, when pain becomes maladaptive and outlasts healing of the underlying tissue damage it surpasses its usefulness as a protective mechanism. Such pain chronicity may be broadly classified into three categories: pain caused by tissue disease or damage (inflammatory pain), pain owing to disease or damage of the somatosensory system (neuropathic pain) and the coexistence of the former two (mixed pain) (Baron et al., 2010). Currently chronic pain is a major public health concern, impacting on millions of people with epidemiological studies reporting a prevalence of 7-8% in the European population (Bouhassira et al., 2008). Symptoms of chronic pain are severely debilitating and inflict considerable personal suffering in relation to ensuing co-morbidities such as insomnia, depression and social isolation. In one study it was reported that around 60% of patients were less able or unable to work and that 20% had lost their jobs as a result of their medical condition (Breivik et al., 2006). In Europe it is estimated that chronic pain results in enormous socioeconomic costs in lost productivity that amounts to 1.5% of the total gross domestic product (Phillips, 2006).

1.2 Treatments

Many patients report a lack of satisfaction with currently available pain treatments, with less than 50% experiencing effective pain relief and 64% reporting that their treatment inadequately controls their pain (Breivik et al., 2006). Furthermore, many prescription drugs require long-term use due to a lack of disease-modifying capabilities and as a result are accompanied by adverse and intolerable side effects. Despite the increase in the number of clinical trials, many drugs have failed to show efficacy, most likely due to the underlying heterogeneity of chronic pain and the complex contribution of psychological and emotional factors. This poor prognosis indicates the continuing challenge of chronic pain and the need for better understanding of its pathology. In addition, the implementation of 'tailor-made' therapeutic approaches where specific drugs are targeted at particular groups of patients may provide a promising approach towards the development of safer and more effective treatments (Baron et al., 2010).

For a long time non-steroidal anti-inflammatory drugs (NSAIDs), weak opioids, anticonvulsants and anti-depressants have been the mainstay of conventional chronic pain treatment. NSAIDs such as aspirin, ibruprofen and the related compound, paracetamol, are amongst the most widely used, with more than 50 types currently available on the market. NSAIDs generally provide pain relief and alleviation of swelling in chronic inflammatory joint diseases such as osteoarthritis (OA) and rheumatoid arthritis (RA) as well as in acute inflammatory conditions such as fractures and soft tissue damage. The primary mode of action of this class of drugs is inhibition of cyclooxygenase (COX) enzymes and resultant reductions in the synthesis of prostaglandins (PGs), which are nociceptor sensitisors (Ferreira, 1980). Most NSAIDs share similar anti-inflammatory, analgesic and antipyretic effects and thus also tend to induce similar adverse reactions typically involving irritation of the gastric system.

Opioids are currently commonly used analgesics by chronic pain patients due to their proven efficacy in several types of peripheral and central neuropathic pain disorders (Dworkin et al., 2010). Opioids such as morphine, oxycodone, methadone, levorphanol and tramadol exert their effects at pre- and post-synaptic μ-opioid receptors. Oxycodone also antagonises the κ-receptor and tramadol inhibits the uptake of monoamines (Baron et al., 2010). The downstream effect of opioids is the closure of voltage-gated calcium (Ca^{2+}) channels (VGCCs) and the opening of potassium (K^{+}) channels, resulting in reduced neuronal excitability and neurotransmission. Although opioids are amongst the most effective

analgesics available, they are associated with many adverse side effects including constipation, nausea and sedation. Furthermore, there are still major concerns related to long-term use, such as misuse and addiction as well as complications such as immunologic changes, hypogonadism and opioid-associated hyperalgesia. Therefore, routine use of this class of drugs is strongly discouraged except in exceptional circumstances where immediate pain relief is necessary (O'Connor and Dworkin, 2009). For example, patients who are waiting upon first-line medications or have acute neuropathic pain symptoms or patients with chronic neuropathic pain suffering from bouts of exacerbated pain symptoms will be treated with opioids.

The anticonvulsants gabapentin and pregabalin, are routinely used for treating neuropathic pain, both of which act by binding to the α_2-δ1 subunit of T-type Ca^{2+} channels on primary afferent nociceptors and in CNS neurons. This consequently reduces the release of excitatory neurotransmitters including glutamate and substance P (SP). These drugs are well characterised in animal models of chronic pain and have exhibited efficacy in several clinical trials across various peripheral and central neuropathic pain conditions. However pregabalin has failed to relieve HIV neuropathy and there is no conclusive evidence for superior efficacy of either of these α_2-δ1 binding agents (Finnerup et al., 2010). Gabapentin was originally developed for the treatment of epilepsy and designed as a blood brain barrier–penetrating γ-aminobutyric acid (GABA) analogue, but was later found to also be an effective analgesic. Both gabapentin and pregabalin have moderate drug interactions but patients do exhibit some side-effects such as sedation, dizziness and peripheral oedma (Baron et al., 2010; Dworkin et al., 2010).

Anti-depressant drugs such as the tricyclic antidepressants (TCAs; amitriptyline, desipramine, nortriptyline) and selective serotonin and norepinephrine reuptake inhibitors (SSNRIs; duloxetine, venlafaxine) constitute first-line treatments for neuropathic pain patients. TCAs have demonstrated efficacy in central pain but amitriptyline was ineffective in patients with HIV or chemotherapy-induced neuropathies. Duloxetine and venlafaxine are particularly efficacious in painful poly-neuropathy, however, in a single study venlafaxine failed to relieve neuropathic pain of various aetiologies (Finnerup et al., 2010). Generally, their mode of action involves the inhibition of serotonin and norepinephrine uptake by monoaminergic nerve terminals, leading to increased extracellular concentrations of these transmitters. Besides providing pain relief, the anti-depressant effect is an additional benefit for patients who frequently suffer from chronic pain-associated depression. Like opioids, antidepressants have demonstrated efficacy in various types of neuropathic pain disorders

but also elicit a number of unwanted side effects, such as mouth dryness, blurred vision, constipation and urinary retention (Dworkin et al., 2010).

Patients with postherpetic neuralgia or focal neuropathy who require localised peripheral pain relief can be treated with topical application of 5% lidocaine (non-specific Na^+ channel blocker) in a patch or gel form. The lidocaine patch is recommended as a first-line drug treatment for such patients based on three published positive trials. Besides providing satisfactory pain relief in these cases, another advantage of this treatment is the minimal adverse side effects (erythema or rash) due to limited systemic absorption. Furthermore, since the risk of neuropathic pain is greater in the increasingly aging population, the use of topical drugs with fewer side effects is well suited for this group of patients. However, two trials have failed to demonstrate efficacy of the lidocaine patch/cream in patients with peripheral nerve injury or mixed neuropathic pain. Therefore results for this treatment option in placebo-controlled trials remain conflicting (Finnerup et al., 2010).

Meta-analysis studies and systematic reviews are particularly informative for comparing the efficacy and safety of compounds used for different neuropathic pain conditions. Here, measurements such as numbers needed to treat (NNT) or numbers needed to harm (NNH) can be used in conjunction with the National Institute for Health and Care Excellence guidelines to provide appropriate treatment recommendations for individual patients. Whilst NNT is the number of patients treated with a drug until one experiences 50% pain relief, NNH is the number of patients needed to treat until one drops out as a result of adversive effects. Table 1 summarises combined NNT and NNH values across different neuropathic conditions. However, one must consider that such head-to-head comparisons can be misleading due to the heterogeneity of the studies involved (e.g. different drug doses, study design and placebo responses). Likewise, adverse side effects differ in severity and relevance, depending on a patient's condition and dropout rates may also be influenced by trial duration. Therefore NNH values do not necessarily provide a definitive measure of long-term side effects (Finnerup et al., 2010).

	Painful poly-neuropathy	Postherpetic neuralgia	Peripheral nerve injury	HIV neuropathy	Central pain	Mixed neuropathic pain	NHH
Antidepressants							
TCAs	2.1	2.8			2.7		15.9
SNRIs	5.0						13.1
SSRIs	6.8						ns
Anticonvulsants							
Gabapentin	6.4	4.3					32.5
Pregabalin	4.5	4.2			5.6	3.8	10.6
Lacosamide							7.8
Valproate		2.1					ns
Lamotrigine							11.7
Topiramate							6.3
Levetiracetam							ns
Carbamazepine/ Oxcarbazepine	3.7						6.6
Opioids							
Opioids	2.6	2.6	5.1			2.1	17.1
Tramadol	4.9	4.8					13.3
Various							
Cannabinoids					3.4	8.3	ns
Topical lidocaine							ns
NMDA antagonists	3.5						12.5
Topical/NGX capsaicin	11.0	3.2		6.5			11.5

Table 1.1: Combined NNT and NNH for different classes of drugs commonly used for the treatment of several types of neuropathic pain conditions

The data presented here is from a systematic review of 174 randomized, double-blind, placebo controlled trials showing combined NNT and NNH values for drugs used for neuropathic pain treatment (95% confidence interval). Ns, relative risk not significant (Finnerup et al., 2010).

Besides the aforemented drug classes that are commonly used for various neuropathic pain conditions, in many acute and chronic inflammatory diseases such as RA, irritable bowel syndrome (IBS), multiple sclerosis (MS) and psoriasis, natural and synthetic glucocorticoids are at the forefront of available therapies. The anti-inflammatory and immunosuppressive actions of these drugs are mainly attributed to the suppression of nuclear factor kappa-light-chain-enhancer of activated B cells (NF-κB) mediated transcription of pro-inflammatory chemokines/cytokines in leukocytes (Coutinho and Chapman, 2011). However, their excellent clinical efficacy is compromised by serious metabolic side effects associated with long term use.

Although a diverse range of pharmacological treatments are available for a number of chronic pain conditions many are associated with adverse side effects and there is a lack of

patient satisfaction. This suggests that pain management requires further improvement via the development of new drugs with better efficacy, tolerability and safety. Despite this pessimistic outlook, treatment strategies have profoundly changed over the years and are continuing to evolve. This is particularly illustrated by the great wealth of research over the past two decades on the contribution of the immune system and its multiple pro-inflammatory mediators in nociceptive transmission, which has subsequently led to more recent biological therapies. These include receptor antagonists of the cytokines, interleukin (IL)-1β (Anakinra), tumor necrosis factor (TNF)-α (Etanercept) and IL-6 (Tocilizumab), which have proven to be particularly efficacious in patients with RA. However, as with all forms of treatment, biological inhibitors are associated with some side effects related to their immunosuppressive actions such as increased susceptibility to infections. Regardless of this, they are generally well tolerated and form a promising new approach as disease-modifying agents from the conventional symptomatic relieving medications (Upchurch and Kay, 2012).

1.3 Pain transmission

1.3.1 Sensory neurons

Over a century ago, Charles Sherrington proposed the existence of primary sensory neurons (nociceptors), which are activated by stimuli deemed as potentially tissue damaging (Sherrington, 1906). This view was later reinforced by Ed Perl, who postulated that pain is mediated by specialised high threshold nociceptive sensory neurons (Bessou and Perl, 1969), in strong opposition to Patrick Wall's and Ron Melzack's argument for a central origin of pain (Melzack and Wall, 1965). Today, we recognise that nociceptors do indeed form a peripheral pathway for pain detection and that altered processing in the central nervous system (CNS) may contribute to hypersensitivity.

Sensory neurons are located within the dorsal root ganglion (DRG) and originate from multipotent neural crest stem cells that delaminate from the neural tube during the third wave of neurogenesis. DRG neurons consists of four main functional components; the peripheral terminal which transduces external inputs via action potential generation; the axon whereby these action potentials are propagated; the soma which maintains neuronal function and integrity and the central terminals, which engage in synaptic communication with central post-synaptic neurons via the release of neurotransmitters across the synaptic cleft (Marmigere and Ernfors, 2007).

1.3.2 Anatomical and electrophysiological properties of sensory neurons

There are three main classes of sensory neurons. The first class are the thinly myelinated, medium diameter Aδ-fibre afferents, some of which convey acute well-localised 'fast/sharp' pain, and coduct at a velocity of approximately 2.2-8 m/s in rats. The second class are the unmyelinated small diameter C-fibre afferents, which conduct poorly localised 'slow/dull' pain at a velocity of < 1.4 m/s (Harper and Lawson, 1985b, a). Due to their cutaneous innervation and role in mediating painful sensations, together these two classes have been historically termed as nociceptors and constitute 70% of all neuronal cell bodies in the DRG (Ralston et al., 1984). Aδ nociceptors may be further categorised into type I high threshold mechanical nociceptors, which respond to mechanical, chemical and high threshold thermal stimuli (> 50°C) and type II low thermal threshold / high mechanical threshold nociceptors (Basbaum et al., 2009). Similarly, C-fibres consist of a heterogenous population of polymodal afferents that include mechano-heat-responsive, heat-responsive, and mechanically insensitive 'silent' nociceptors that develop mechanical sensitivity subsequent to injury (Schmidt et al., 1995). Notably, some C-fibres respond to cooling or innocuous stroking and thus not all C-fibres are involved in mediating noxious stimuli (Olausson et al., 2008). Lastly, the thickly myelinated large diameter Aβ-fibre afferents rapidly conduct stimuli at 14-30 m/s and belong to large DRG neurons (constituting approximately 12% of DRG neurons) (Harper and Lawson, 1985a). Under normal conditions these fibres are predominantly low-threshold mechanoreceptors that are responsive to innocuous stimulation of the skin, muscle and joint. However, approximately 20% of A-fibre nociceptors appear to conduct within the Aβ- conduction velocity range, and may be referred to as the 'Aβ-nociceptors' (Djouhri and Lawson, 2004).

1.3.3 Biochemical and molecular properties of sensory neurons

Nociceptors have also been classified according to their neurochemical properties, which encompasses an extensive list of cell markers utilised for the study of these neurons. Immunohistochemical studies have revealed two large groups of C-fibre neurons. The peptidergic population makes up 40% of DRG neurons and characteristically contain the neuropeptides SP and calcitonin-gene related peptide (CGRP) and express TrkA receptors (McCarthy and Lawson, 1989; Averill et al., 1995; Lawson, 2002). The non-peptidergic population makes up 30% of DRG neurons and express the glial-derived neurotrophin factor (GDNF) sensitive receptors, receptor tyrosine kinase (RET) in complex with GDNF family receptor α1/α2. Many RET-positive neurons also bind *Bandeiraea simplicifolia* isolectin B4 (IB4) and express the ionotropic purinergic receptor, $P2X_3$ as well as Mrg class

G-protein-coupled receptors (GPCRs) (Molliver et al., 1997; Bradbury et al., 1998; Snider and McMahon, 1998; Vulchanova et al., 1998; Bennett et al., 2000). Lastly, the Aβ-fibres can be immunohistochemically labelled for phosphorylated neurofilament 200 (NF200) and express both tyrosine kinase receptor B (TrkB) and tyrosine kinase receptor C (TrkC) receptors, which are responsive to the neurotrophins, brain derived neurotrophic factor (BDNF), neurotrophin (NT) -3, 4, 5, respectively (McMahon et al., 1994).

In addition, molecular studies have identified selective expression of receptors and ion channels that are involved in the modulation of pain transmission in nociceptors (Basbaum et al., 2009). For example, most C-fibres express transient receptor potential (TRP) channels sensitive to thermal stimuli (TRPV1) (Caterina et al., 1997; Michael and Priestley, 1999) and Aδ-fibres express both TRPV1 and TRPV2 (Bridges et al., 2003). Differential expression of other ion channels such as those responding to cold stimuli (TRPM8) (Bautista et al., 2007) or chemical irritants (TRPA1) (Bautista et al., 2006) as well as the acid sensing ion channels (ASICs) can potentially be used to distinguish between sensory neuron sub-populations (Garcia-Anoveros et al., 2001; Julius and Basbaum, 2001).

1.4 The dorsal horn of the spinal cord

DRG neurons relay sensory information to the spinal cord where their primary afferent terminals synapse with second order dorsal horn neurons. Work pioneered by Bror Rexed in the cat led to the establishment of an organised system of 10 laminae, which constitute the grey matter of the spinal cord according to the size and packing density of neurons (Rexed, 1952). A majority of dorsal horn neurons (laminae I – VI) are interneurons that are confined to the spinal cord and innervate localised regions. Interneurons may be electrophysiologically or immunohistochemically classified as excitatory (glutamatergic) or inhibitory (GABA-ergic). Many inhibitory neurons may also express glycine suggesting that in some cases both GABA and glycine are co-released (Todd, 2010). The dorsal horn also contains ascending and descending projection neurons to and from supraspinal sites. Lamina I, also referred to as the marginal layer, is a thin cell layer that covers the top of the dorsal horn. This lamina has the greatest number of projection neurons in the dorsal horn but mainly consists of interneurons, 45% of which are positive for the SP receptor, neurokinin 1 (NK1) (Todd et al., 1998). The interneurons are smaller than the projection neurons and hence there is some variation in size and shape within this layer. Lamina II (substantia gelatinosa) is much wider than lamina I and is divided into two parts; lamina II inner (IIi) or outer (IIo). Lamina II consists of densely packed interneurons in the outer

region and together laminae I and II are collectively referred to as the superficial dorsal horn and are mainly targeted by nociceptive afferents (Light and Perl, 1979a, b). The neurons in this region respond to noxious input and many are electrophysiologically classified as nociceptor specific. Lamina III is densely packed with interneurons that are larger than the ones that constitute lamina II and the border between these laminae can be clearly identified by the characteristic presence of myelinated axons in lamina III. Deeper laminae (III - VI) receive both innocuous and noxious input (Light and Perl, 1979a, b) and are thus electrophysiologically classified as wide dynamic range neurons (WDR), responding to a broad range of stimulus intensities. Lastly, laminae VII - IX comprise the motor neuron-containing ventral horn, while lamina X surrounds the central canal.

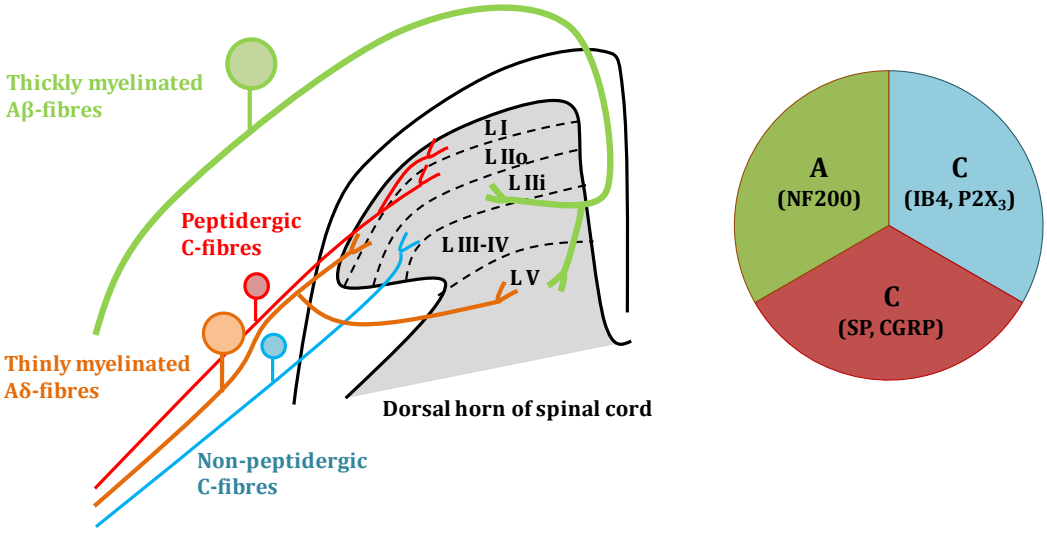

Figure 1.1: Anatomical characterisation of primary afferent fibres, their DRG neurons and connections with the spinal cord

Simplified schematic illustrating anatomical features of the three main classes of primary afferent sensory neurons. Thickly myelinated Aβ-fibres, with large neuronal cell bodies terminate in laminae III - V and also have some extensions into lamina II. Thinly myelinated Aδ-fibres with medium sized neuronal cell bodies aborize laminae I, IIo and V. A-fibres may be identified with the neurochemical marker NF200. Unmyelinated C-fibres with small sized neuronal cell bodies are further categorised as peptidergic (SP, CGRP) or non-peptidergic (IB4, $P2X_3$) and terminate superficially in lamina I/IIo and IIi, respectively.

The functional class of primary afferents determines their specific termination patterns. Cutaneous nociceptors (Aδ- and C-fibres) generally innervate laminae I and II. However, there are some subclass differences; for instance Aδ- nociceptors primarily terminate in lamina I, whilst Aδ- hair follicle afferents innervate the border region between lamina II and III (Light and Perl, 1979a). Likewise, non-peptidergic C-fibres terminate centrally in lamina IIi, whereas peptidergic heavily arborize laminae I and IIo. C-fibres may also polysynaptically innervate lamina III - V (Light and Perl, 1979a, b; Todd, 2010). Finally the Aβ-fibres, arborize laminae III - V but also have some extensions into lamina II (Light and Perl, 1979a). Termination patterns and neurochemical markers for the different sensory neuron classes is presented in Fig. 1.1.

1.5 Supraspinal centres and pain

Information regarding noxious stimuli is transmitted from the dorsal horn of the spinal cord along ascending neuronal pathways to higher centres located in the brain. These projection neurons are particularly concentrated in lamina I and dispersed throughout laminae III – VI (Todd, 2010). Retrograde and anterograde tracing approaches have been valuable in enhancing our understanding of neuronal networks between the spinal cord and the brain. Lamina I ascending pathways, also referred to as the spinoparabrachial tract, target supraspinal areas such as the periaqueductal grey matter (PAG), the parabrachial (PB) and nuclei of the thalamus. Eighty percent of these projection neurons are NK1 positive (Hunt and Mantyh, 2001) and may project onwards to areas such as the amygdala and hypothalamus, which are involved in the affective/emotional aspects of the pain experience (Hunt and Mantyh, 2001). The NK1 receptor has attracted considerable attention due to its nociceptor-specific anatomical location. Studies in rodents using antagonists or the SP-conjugated neurotoxin saporin, which selectively ablates NK1 positive cells, have demonstrated analgesic effects in experimental models of neuropathic and inflammatory pain (Mantyh, 1997; Ma and Hill, 1999). However, despite their success in animals, NK1 antagonists failed to show efficacy in clinical trials, perhaps due to physiological species differences (Hill, 2000). This failure shed some doubt on the relevance of SP/NK1 signalling in pain pathways and brought forward the hypothesis that ablating NK1 positive cells produces analgesic effects due to loss of projection neurons rather than diminished nociceptor transduction.

Arising from the deeper laminae (III - VI) of the dorsal horn is the spinothalamic pathway, which predominantly projects to the thalamus and carries information regarding the

sensory/discriminative aspects of the pain experience (Doyle and Hunt, 1999). In addition, a third pathway originating from lamina II interneurons that are in contact with IB4 positive C-fibres, primarily targets the amygdala, hypothalamus and globus pallidus through contact with lamina V projection neurons. This ascending pathway is connected to non-peptidergic nociceptors and parallels lamina I projection neurons that are connected to peptidergic nociceptors, indicating that the two nociceptive classes may possess their own pain pathways (Braz et al., 2005).

Amongst the various pathways descending from the brain to the spinal cord are the two main monoamine-containing pathways: the serotonergic system, originating in the nucleus raphe magnus and the noradrenergic system, derived from the locus coeruleus and adjacent pontine regions. These descending axons terminate diffusely throughout the dorsal horn but mainly in superficial laminae I and II. Monoaminergic descending pathways projecting from the rostral ventromedial medulla (RVM) critically modulate nociceptive spinal cord activity and exert both facilitatory (Serotonin/5-hydroxytryptamine $(5HT)_3$ receptors) and inhibitory (α_2 adrenoceptors) control (Suzuki and Dickenson, 2005; D'Mello and Dickenson, 2008; Todd, 2010).

1.6 Peripheral sensitisation

Abnormal pain sensations such as hyperalgesia, allodynia and spontaneous pain may be caused by tissue inflammation and nerve injury. According to IASP, hyperalgesia is defined as an increased pain response to normally noxious stimuli. The change in threshold within the proximity of the injury site is referred to as primary hyperalgesia, whereas secondary hyperalgesia defines threshold changes in the surrounding undamaged tissue. Allodynia is defined by IASP as a noxious response to a normally innocuous stimulus. However, this terminology was recently clarified so that unless a pain response is known to be evoked by low-threshold fibres it is referred to as hyperalgesia (Sandkuhler, 2009). Thus with regards to the peripheral nervous system (PNS), hypersensitivity refers to a decrease in thresholds so that a previously innocuous stimulus can now recruit nociceptors, as well as an increase in neuronal excitability so that a noxious stimulus elicits a greater response; this augmented activity is a phenomenon referred to as peripheral sensitisation.

Peripheral sensitisation is typically a result of changes in the chemical milieu caused by cell damage and mediator release from keratinocytes, fibroblasts, endothelial cells, peripheral nerve terminals glial and immune cells (see *Chapter 3*). These locally released mediators

facilitate the inflammatory process, and are commonly referred to as an 'inflammatory soup' consisting of prostanoids, kinins, histamine, neuropeptides (SP, CGRP), 5HT, adenosine triphosphate (ATP), adenosine, growth factors, protons, cytokines and chemokines (Marchand et al., 2005; Woolf and Ma, 2007; Basbaum et al., 2009). Subsequent to release these agents may act directly on nociceptor terminals or indirectly on other target cells via their cognate membrane ion channels/receptors, resulting in the induction of multiple intracellular signalling pathways including protein kinase A (PKA), protein kinase C (PKC), phosphoinositide 3-kinase (PI3K), and the MAPKs: extracellular signal-regulated kinase (ERK), p38, c-Jun N-terminal (JNK). This leads to the phosphorylation of various proteins and a substantial increase in the transcription of neuropeptides, growth factors and receptors/ion channels in the somata of nociceptors (Costigan et al., 2002; Xiao et al., 2002). Consequentially, primary sensory neurons undergo a phenotypic switch that alters their neurochemical characters and properties. This results in raised basal sensitivity to noxious and innocuous stimuli and a subsequent increase in excitability and action potential firing. Voltage-gated Na^+ channels are responsible for the initiation of action potentials and together with K^+ channels regulate the excitability of sensory neurons and communicate amplified sensory information from the periphery to the spinal cord. Thus the combination of phosphorylation- and transcriptional-dependent events drives peripheral sensitisation and contributes to enhanced central transmission (Woolf and Ma, 2007). These mechanisms are summarised in Fig. 1.3.

The receptors of inflammatory mediators fall into three broad classes: ionotropic receptors/ion channels (ATP receptors, $P2X_2$ and $P2X_3$; TRP channels); receptor tyrosine kinases (NGF and BDNF receptors, TrkA and TrkB, respectively) and GPCRs (bradykinin receptors 1 and 2 (B_1 and B_2); chemokine receptors e.g. chemokine (C-C motif) receptor 2 (CCR2), chemokine (CX3C-motif) receptor 1 (CX_3CR1)). These receptor classes shall be addressed below.

1.6.1 Ionotropic receptors/ion channels

Thermal hyperalgesia is a key sensory maladaptation associated with inflammation and is mediated by TRPV1, which is one of the most studied vanilloid receptors in pain research. TRPV1 is a six transmembrane domain non-selective cation channel and its activation produces an influx of Na^+ and Ca^{2+}, which depolarises the neuron and activates downstream signalling molecules (Caterina et al., 1997). TRPV1 is expressed by small- to medium- sized DRG neurons and is activated by noxious temperatures (> 42 °C), capsaicin (extract from hot chilli peppers) and protons. The most compelling evidence for a role of this ion channel

in nociception is the reported alleviation of CFA or mustard oil-induced thermal hyperalgesia in the TRPV1 null mouse. In contrast, nerve injury induced thermal and mechanical hypersensitivity was normal in TRPV1 KOs as well as responses to acute thermal stimuli in intact animals, except at high temperatures (Caterina, 2000). The participation of TRPV1 in inflammatory pain is well documented but in neuropathic pain the role of this receptor is less understood. TRPV1 expression up-regulates in models of inflammatory pain but contrastingly down-regulates in a number of models of neuropathic pain, except for some up-regulation in surviving DRG somata (Hudson et al., 2001; Rasband et al., 2001; Schafers et al., 2003a). These polymodal signal integrators can be substantially modulated by components of the inflammatory soup, which may involve the lowering of temperature- or agonist-dependent thresholds required for activation. This results in the firing of neurons to a stimulus that was previously innocuous, which correlates with acute hyperalgesia. Concurrently, long-term changes encompass increased protein expression and insertion of TRPV1 channels into the plasma membrane of nociceptor terminals (Ji et al., 2002; Linley et al., 2010).

Extracellular protons and lipids behave as direct allosteric modulators of the channel, whereas bradykinin, ATP and NGF can indirectly modulate TRPV1 through the mobilisation of down-stream intracellular signalling cascades (Basbaum et al., 2009). NGF/TrkA and bradykinin/B_2 mediated sensitisation was previously proposed to be via phospholipase C (PLC) mediated hydrolysis of phosphatidylinositol 4,5-bisphosphate (PIP_2), which is a tonic inhibitor of TRPV1 (Chuang et al., 2001; Prescott and Julius, 2003). However, later findings opposed this accepted model and demonstrated that in fact PIP_2 promotes the activation of TRPV1. Instead it was proposed that NGF mediated activation of PI3K subsequently activates Src kinase, which phosphorylates tyrosine residues on the N-terminus of TRPV1 and promotes trafficking of the receptor to the plasma membrane (Zhang et al., 2005d; Stein et al., 2006). This enhanced expression at the plasma membrane is thought to be the main contributor to thermal hyperalgesia. NGF/TrkA is also retrogradely transported in endosomes to the cell bodies of sensory neurons, where it activates p38 MAPK, leading to increased translation and transport of TRPV1 to peripheral nociceptor terminals (Ji et al., 2002). However, NGF may also mediate transcriptional-dependent effects, and in a model of CFA, up-regulation in the expression of TRPV1 was dependent on both NGF and GDNF in Trk-A and IB4/RET positive neurons, respectively (Amaya et al., 2004). In addition, PKA and/or PKC have been documented to facilitate TRPV1 signalling possibly via increasing the open probability of the channel, which consequently augments TRPV1 currents (Lopshire and Nicol, 1998; Bhave et al., 2003). For example, prostaglandin E2 (PGE_2) sensitises TRPV1 channels through both PKA (EP4) and PKC (EP1) dependent signalling pathways (Lopshire

and Nicol, 1998; Moriyama et al., 2005). In addition to the mediators mentioned above, a number of other pro-algesic substances may exert sensitising effects on TRPV1 channels during peripheral inflammation including glutamate, 5HT, adenosine, histamine, chemokines and cytokines (Ma and Quirion, 2007).

Tissue injury results in local acidosis and the production of hydrogen ions, which is a hallmark of a physiological inflammatory response that can be detected by TRP and ASIC channels. TRPA1 mediates sensory responses to many chemical irritants such as mustard oil, garlic and membrane permeable electrophiles (allyl isothiocyanate from wasabi or allicin from garlic) as well as endogenous proalgesic agents that are produced in response to damage or stress. Like TRPV1, these channels are expressed by peptidergic C-fibres and consist of six transmembrane domains with a non-cation selective central pore (Nilius et al., 2012). Pharmacological blockade of TRPA1 was shown to inhibit formalin responses and attenuate mechanically evoked C-fibre firing in rodents, indicating a role in the transduction of both noxious chemical and mechanical stimuli (Kerstein et al., 2009). Interestingly, in a study utilising TRPA1 null mice, the channel was demonstrated to be a target of pro-inflammatory factors such as bradykinin, which elicit hypersensitivity in pain pathways via PLC signalling (Bautista et al., 2006). Bradykinin is a peptide cleaved by enzymes (kallikreins) from circulating plasma proteins upon tissue injury and directly activates nociceptive DRG neurons causing pain in animals and humans (Levine et al., 1993). Subsequent to activation of the bradykinin B_2 receptor, mobilisation of PLC and cAMP-induced PKA contributes to TRPA1 sensitisation, probably via a phosphorylation dependent mechanism (Wang et al., 2008). Conversely, in a number of nerve injury models of neuropathic pain the expression of TRPA1 is down-regulated (Andrade et al., 2012). Although one study showed that whilst TRPA1 mRNA was down-regulated in the injured-L5 DRG, it was up-regulated in the un-injured L4 DRG and was found to contribute to the development of cold hyperalgesia (Katsura et al., 2006).

ASICs are sodium selective cation channels that are activated by low extracellular pH and are thought to play a role in sensing tissue acidosis during inflammation, where pH values may drop as low as 5.4 (Jacobus et al., 1977; Wang et al., 2013). ASIC channels consist of two transmembrane domains and are located in sensory neurons innervating the skin and in DRG somas of variable sizes (Wemmie et al., 2006). Similar to the TRPA1s, ASIC channels exhibit changes in activity subsequent to exposure to inflammatory mediators. For example, application of NGF, bradykinin, 5HT and IL-1β enhanced ASIC3 mRNA expression in cultured DRG neurons, which showed some correlation with augmented channel activity and increased sensory neuron excitability (Mamet et al., 2002). It was also previously

reported that ASIC expression in small DRG neurons increases in CFA treated rats (Voilley et al., 2001). A recent study demonstrated that 5HT-induced nociceptive behaviours are attenuated in ASIC3 KO mice and inhibited by the non-selective antagonist, amiloride, in WT mice. It was proposed that 5HT enhances proton-evoked currents of ASIC3 channels by binding to the non-proton ligand sensing domain and sensitising the channel to respond to extracellular mild pH (Wang et al., 2013).

Enhanced activity of voltage-gated Na^+ and Ca^{2+} channels and suppression of voltage-gated K^+ channels is also implicated in the establishment of hyperalgesia. For example, the K_v7 family of K^+ channels are inhibited via the activation of PLC coupled receptors as a result of PIP_2 depletion (Li et al., 2005) or inositol triphosphate (IP_3) -mediated increases in intracellular Ca^{2+} levels (Gamper and Shapiro, 2003). K_v7 channels are involved in the regulation of neuronal excitability and so inhibition results in augmented neuronal activity. Similarly, in the setting of nerve injury and inflammation several voltage gated K^+ channels have been reported to be down-regulated ($K_v4.3$, $K_v3.4$, $K_v9.1$ and the K_v2 subunit), which has been linked to a heightened neuronal excitability (Takeda et al., 2006; Chien et al., 2007; Takeda et al., 2008; Tsantoulas et al., 2012; Tsantoulas and McMahon, 2014; Tsantoulas et al., 2014). Small DRG neurons express a combination of tetrodotoxin (TTX) -sensitive fast kinetics ($Na_v1.7$) and TTX-resistant slow kinetics ($Na_v1.8$, $Na_v1.9$) Na^+ channels. Evidence from multiple KO studies support the considerable contribution of these Na^+ channels to inflammation-induced hypersensitivity (Kerr et al., 2001; Nassar et al., 2004; Amaya et al., 2006), as well as studies utilising animal models of inflammation. For example, intraplantar CFA was shown to evoke an increase in the expression of $Na_v1.7$ and $Na_v1.8$ in the DRG (Gould et al., 2004) and sensitising agents released during inflammation such as PGE_2, adenosine and 5HT enhanced Na^+ conductance, induced a hyperpolarising shift and accelerated current activation (Gold et al., 1996). Likewise, $Na_v1.9$ currents were potentiated by a combination of pro-inflammatory mediators in rat DRG neurons (Maingret et al., 2008) possibly via PKC mediated phosphorylation (Liu and Wood, 2011). In contrast, TTX-resistant Na^+ channels seem unlikely to participate in neuropathic pain. Both $Na_v1.8$ and $Na_v1.9$ are down-regulated in injured neurons and KO studies show little impact on pain thresholds (Dib-Hajj et al., 1999; Priest et al., 2005; Amaya et al., 2006). For example, $Na_v1.7$ and $Na_v1.8$ double KO mice continue to develop neuropathic pain behaviours after nerve injury (Nassar et al., 2005). In addition to changes in the properties of voltage-gated Na^+ and K^+ channels, Ca^{2+} channels are also altered by inflammatory mediators. Low voltage activated T-type Ca^{2+} channels expressed in nociceptors are activated by weak depolarisation and facilitate the initiation of action potentials (Coste et al., 2007). Increases in their density as a result of exposure to inflammatory mediators such as hydrogen

sulphide, enhances their currents (Kawabata et al., 2007). C-fibre expressed N- and T-type Ca^{2+} channels are also up-regulated in models of nerve injury, and $Ca_v2.2$ or 3.2 deficient mice exhibit attenuated pain behaviours after inflammation or nerve injury, respectively (Cao, 2006).

ATP released from damaged cells, skin keratinocytes exposed to mechanical or chemical stimuli, or sensory neurons, activates ionotropic purinergic receptors such as $P2X_2$ and $P2X_3$ (Linley et al., 2010). These non-cation selective receptors are expressed in small DRG neuronal cell bodies and their axons, and the opening of these receptors results in an influx of Na^+ and Ca^{2+} and an efflux of K^+ (Lewis et al., 1995). This initiates depolarisation and a secondary influx of Ca^{2+} via VGCCs. The substantial rise in intracellular Ca^{2+} and subsequent activation of kinases such as ERK leads to the release of secondary mediators (Dai et al., 2004). Intraplantar injection of ATP has exhibited dose-dependent pro-nociceptive effects, and was reported to enhance pain behaviours in three independent paradigms of peripheral sensitisation (Hamilton et al., 1999). Notably, $P2X_3$ expression falls by ~ 50% in the DRG following nerve transection (Bradbury et al., 1998) but increases following intraplantar CFA (Xu and Huang, 2002) possibly due to an NGF/GDNF mediated effect (Ramer et al., 2001). Furthermore, $P2X_2$ and $P2X_2/P2X_3$ KO mice exhibit attenuated pain-related behaviours in response to intraplantar formalin, and DRG neurons from these mice show minimal ATP responses, indicating that these subunits account for virtually all ATP responses in sensory neurons (Cockayne et al., 2005).

1.6.2 Receptor tyrosine kinases

The neurotrophins NGF and BDNF and their cognate receptors TrkA and TrkB, respectively, form a well-documented pro-nociceptive signalling system (Pezet and McMahon, 2006). The Trk receptors are tyrosine kinase receptors that dimerise and autophosphorylate upon ligand binding to initiate two major biochemical pathways involving PI3K and MAPK. These signalling pathways contribute to transcriptional and post-translational regulation of neuropeptides/neuromodulators (CGRP, SP, BDNF), receptors (TRPV1, ASIC, $P2X_3$, μ-opioid) and voltage-gated ion channels (TTX -sensitive and -resistant Na^+ channels) in nociceptive neurons (Pezet and McMahon, 2006). As aforementioned, NGF/TrkA-induced hyperalgesia through TRPV1 sensitisation has been demonstrated to occur through a number of downstream second messengers including, PKA, PKC, PLC, PI3K and MAPK (Chuang et al., 2001; Ji et al., 2002; Zhang et al., 2005d; Stein et al., 2006; Zhu and Oxford, 2007).

1.6.3 GPCRs

The purpose of this thesis was to examine the role of GPR84 in chronic pain mechanisms. Therefore, a more in depth discussion about the GPCR class of receptors is appropriate with regards to the aim of this thesis.

GPCRs are the largest family of membrane proteins with more than 800 genes and remarkably orchestrate a diverse range of biological processes from hormonal and neurotransmitter signalling, to mediating sensory responses such as sight and smell. Thus it isn't surprising that the majority of currently used drugs in the clinic target these receptors. Pioneering work by Rall and Sutherland in the 1950's lead to the establishment that a series of hormones bind to specific heptahelical receptors linked to highly specialised intracellular transducer systems. These receptors generically consist of 7 transmembrane domains connected by 3 intracellular and extracellular loops, in addition to a cytoplasmic domain which interacts with G-proteins. GPCRs are grouped into three families according to sequence similarity within the transmembrane core or the presence of certain conserved residues or motifs (Pierce et al., 2002). Family A constitutes the largest group of these receptors and includes the rhodopsin, adrenergic and olfactory receptors. Family B is considerably smaller and includes gastrointestinal peptide hormone receptors, such as vasoactive intestinal peptide. Lastly, family C is the smallest class and consists mainly of the metabotropic glutamate and GABA receptor families. This group characteristically possesses very large extracellular amino terminals that are important for the binding of ligands and subsequent activation (Pierce et al., 2002). Once activated, the GPCR initiates signal transduction by interacting with a heterotrimeric G protein (α, β, γ) and so in effect acts as a guanine nucleotide exchange factor (GEF) for Gα subunits and facilitates the exchange of guanosine diphosphate (GDP) for guanosine triphosphate (GTP) (Siderovski and Willard, 2005). This leads to the dissociation of the Gα-GTP complex from the inhibitory βγ subunit (Hamm, 1998), enabling Gα-GTP and the βγ dimer to interact with downstream effectors which drive further intracellular signalling cascades (see Fig. 1.2). The duration of these signalling events is determined by the rate of guanosine triphosphatase (GTPase) mediated hydrolysis of the Gα-subunit and consequential re-association of Gα-GDP with Gβγ (Hamm, 1998). This process is accelerated in heterotrimeric G-proteins by regulator of G-protein signalling (RGS) proteins, which stimulate signal termination by acting as GTPase-accelerating proteins (GAPs) for Gα (Siderovski and Willard, 2005).

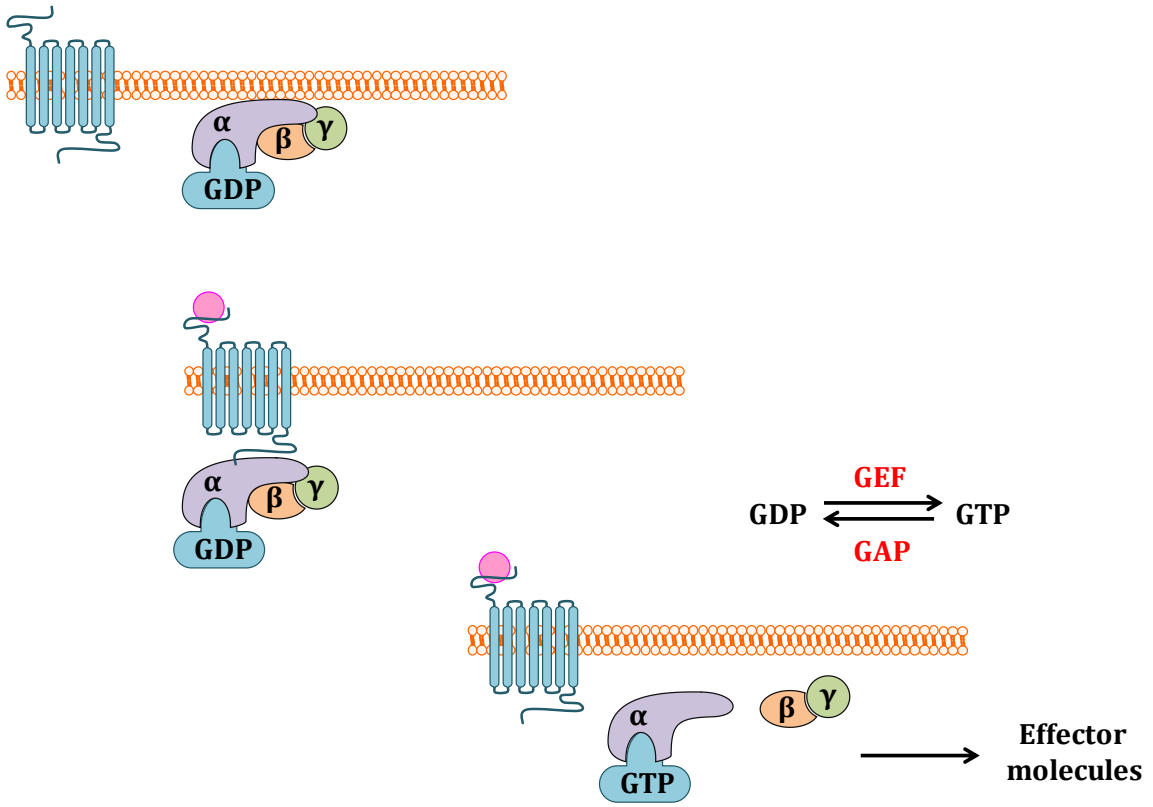

Figure 1.2: Generic heterotrimeric GPCR activation model

Ligand binding to a hepathelical GPCR leads to a conformational change and the interaction of the receptor with the αβγ complex bound to GDP. GDP is subsequently exchanged for GTP, initiating the dissociation of Gα-GTP and Gβγ, which go on to activate down-stream second messengers such as cAMP and Ca^{2+}. RGS proteins stimulate signal termination by acting as GAPs. Here GTP is rapidly hydrolysed into GDP and inorganic phosphate.

Based on the homology of the α-subunit sequences, G-proteins are classically divided into four main families: $G\alpha_s$ (activates adenylate cyclase (AC)), $G\alpha_{i/o}$ (inhibits AC), $G\alpha_{q/11}$ (activates PLC) and $G\alpha_{12/13}$ (activates Rho-GEFs) (Hamm, 1998; Cabrera-Vera et al., 2003). The Gα-subunits are comprised of two specific domains, a GTPase domain that mediates binding and hydrolysis of GTP and a helical domain that buries GTP within the protein core. The Gγ-subunit extensively interacts with the Gβ-subunit through N-terminal coiled coils (Lambright et al., 1996) and is bound to Gα-GDP via a hydrophobic pocket. Upon GTP binding to Gα the hydrophobic pocket is removed, causing loss of affinity for Gβγ (Cabrera-Vera et al., 2003).

Gαs family

An important aspect of the regulation of receptors/ion channels in the context of peripheral hypersensitivity is the mechanisms by which the channels become sensitised or desensitised as a result of alterations in the surrounding chemical milieu of nociceptive terminals. GPCRs are of particular interest as their various secondary pathways have been implicated in nociceptor sensitisation. Furthermore, many of the mediators released during an inflammatory response act via GPCRs and initiate many intracellular signalling cascades that contribute to the modulation of ion channels and the generation of hyperalgesia. For instance, the prostaglandin (EP2, EP4, IP and DPI) (Smyth et al., 2009) and 5HT receptors ($5HT_{4,6,7}$) (Cardenas et al., 2001) are coupled to the $G\alpha_s$ family, which stimulate the enzyme AC to catalyse the formation of cAMP from ATP. Newly synthesised cAMP subsequently binds to PKA, initiating the dissociation of the PKA regulatory and catalytic subunits and passive diffusion into the nucleus (Taylor et al., 1992). In turn, activated PKA phosphorylates numerous targets such as cAMP response element-binding protein (CREB), which binds to the conserved cAMP response element expressed within the promoter region of many cAMP-responsive genes. CREB may then form a complex with its transcription co-activator, CREB binding protein (CBP), subsequent to phosphorylation and translocate to the nucleus to initiate RNA synthesis (Mayr and Montminy, 2001; Racioppi and Means, 2008).

PGE_2/EP4 signalling induces the sensitisation of TRP channels (Lopshire and Nicol, 1998) and TTX-resistant Na^+ channels (Gold et al., 1996) and suppresses K^+ channels (Nicol et al., 1997) probably via PKA mediated phosphorylation. As previously mentioned, Lopshire and Nicol (1988) demonstrated that PGE_2 or cAMP analogs transiently increase capsaicin-gated channel activity in embryonic rat sensory neurons by enhancing the amplitude of whole cell currents. They also demonstrated that this sensitising effect could be blocked by a PKA inhibitor, leading to the suggestion that capsaicin-gated ion channels may be modulated by PKA-mediated phosphorylation of the serine residue S116 (Lopshire and Nicol, 1998; Bhave et al., 2002). Cyclic AMP was in fact one of the first second messengers implicated in pain and nociceptor sensitisation, and elevated levels of this signalling molecule is associated with increased neuronal excitability. This is illustrated by a study showing that intradermal injection of cAMP-inducing agents such as forskolin in rats produces dose-dependent hyperalgesia that can be blocked via the cAMP analog, RP-cAMP (Taiwo and Levine, 1991). Furthermore, transgenic mice that do not express particular isoforms of AC exhibit attenuated pain behaviours and correspondingly pre-treatment with AC inhibitors

decreases PGE_2-induced behavioural hyperalgesia (Aley and Levine, 1999; Wei et al., 2002; Kim et al., 2007b).

$G\alpha_{q/11}$ family

The histamine (H1), bradykinin (B_2), prostaglandin (EP1) and SP (NK1) receptors are coupled to the $G\alpha_{q/11}$ family of G-proteins, which activate PLC. The PLC family consists of a diverse group of enzymes that are divided into 3 subtypes. There are 4 members of the PLCβ family, 2 members of the PLCγ family and 4 members of the PLCδ family. The Gα subunits (α_q, α_{11}, α_{14}, α_{16}) belonging to the G_q subfamily selectively activate PLC-β isozymes via interaction with its COOH-terminal. Activation of PLC results in the biosynthesis of diacyl-glycerol (DAG) and IP_3 from the membrane-bound lipid precursor, PIP_2. DAG may then activate PKC, whilst IP_3 binds to its IP_3 receptors (IP_3Rs), expressed by intracellular stores. This leads to the mobilisation of a Ca^{2+} response and consequently activates an array of Ca^{2+} dependent kinases. PKC has a well documented role in nociceptor activation and sensitisation, which is thought to be mainly via the direct phosphorylation of receptors and ion channels (Hucho and Levine, 2007). For example, PKCε is able to augment TRPV1 channel activity and restore currents subsequent to desensitisation by directly phosphorylating S800 residues (Mandadi et al., 2006). PKC also promotes soluble N-ethylmaleimide-sensitive factor attachment protein receptor (SNARE) -dependent trafficking of TRPV1 to the membrane, which enhances channel currents and thus contributes to thermal hyperalgesia (Morenilla-Palao et al., 2004). As previously discussed it was thought that bradykinin-B_2 signalling sensitised TRPV1 via PLC activation and subsequent PIP_2 depletion (Chuang et al., 2001), however this mechanism has been questioned in light of new findings (Stein et al., 2006).

$G\alpha_{i/o}$ family

Stimulation of the $G\alpha_{i/o}$ pathway in nociceptors usually involves the inhibition of AC and the activation of phosphodiesterases, which reduces cAMP levels and the activity of PKA. $G\alpha_{i/o}$ activation also leads to an inhibition of presynaptic VGCCs and a consequential suppression of synaptic transmission. Therefore this pathway is associated with a state of reduced excitability and analgesia that is best illustrated by the activation of opioid receptors, which are expressed in 29-38% of C-fibre axons (Ingram and Williams, 1994; Coggeshall et al., 1997). However, the most compelling evidence for the involvement of $G\alpha_{i/o}$ signalling in peripheral sensitisation is the direct and indirect effects of chemokines. Chemokine receptors are widely distributed in neurons, leukocytes and glial cells and signal via the

$G\alpha_{i/o}$ family of G-proteins (Kiguchi et al., 2012). Activation of these receptors leads to the mobilisation of Ca^{2+} via a PLC-β-dependent pathway and the subsequent initiation of various intracellular kinases such as the calmodulin-kinases (CAMKs) and MAPKs (Elzi et al., 2001; Sassone-Corsi, 2012). Ultimately, via a combination of phosphorylation and/or transcription-dependent events there is an increase in receptor/ion channel membrane density and currents in nociceptors as well as enhanced release of mediators; immune and glial cells may also show enhanced secretion and expression of cell surface receptors. The contribution of some chemokine receptors to peripheral sensitisation is well documented (Abbadie et al., 2009) and will be discussed more thoroughly later in this chapter.

Termination of receptor activation is crucial for the tight regulation of intracellular signalling. One of the most widespread mechanisms for regulating GPCR activity is via G-protein-coupled receptor kinase (GRK) driven receptor desensitisation. GRKs only phosphorylate the receptor in its agonist bound state and promote the binding of arrestin proteins, which act as sterical inhibitors of receptor/G-protein interaction. Second messenger kinases such as PKA and PKC may also serve as negative feedback regulators and promote G-protein uncoupling by phosphorylating receptors. Besides acute phosphorylation-dependent effects, dampening of receptor signalling may also entail slower regulatory mechanisms such as receptor degradation and gene transcription/translation, in addition to the intrinsic regulation of GTPase activity via RGS proteins. On the other hand, receptor internalisation serves as a mechanism by which receptors are resensitised and made ready to respond to a subsequent stimulus. This usually involves β-arrestin-dependent mechanisms via clathrin coated or uncoated vesicles (Pierce et al., 2002).

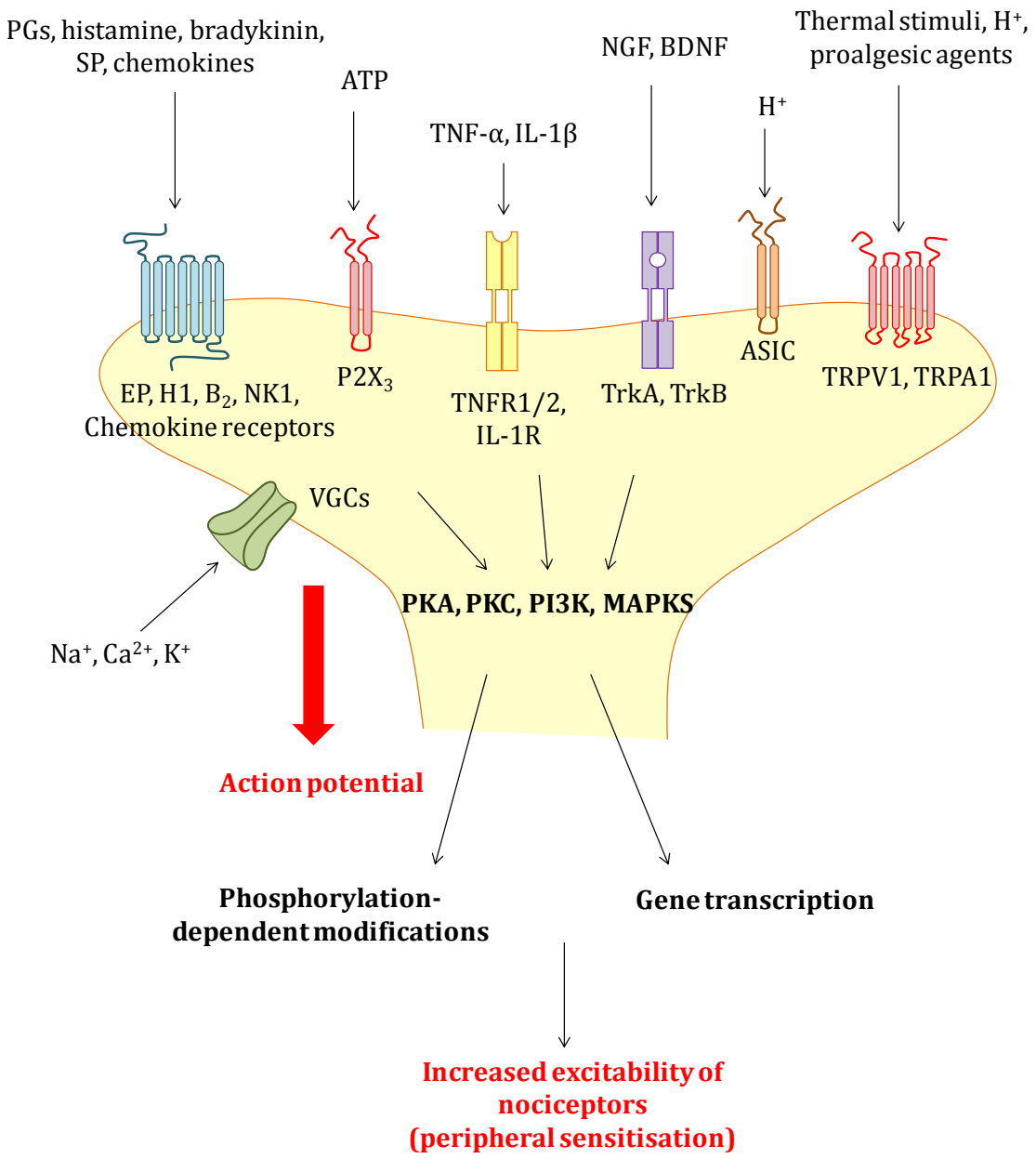

Figure 1.3: Signalling pathways involved in peripheral sensitisation

Keratinocytes, fibroblasts, endothelial cells, peripheral nerve terminals, glial and immune cells release mediators such as PGs, histamine, bradykinin, SP, chemokines (CCL2, CCL3), ATP, cytokines (TNF-α, IL-1β), growth factors (NGF, BDNF), protons (H^+). These mediators act via their cognate receptors (GPCR, ionotropic receptors, tyrosine kinase receptors) expressed by peripheral nerve terminals and activate multiple intracellular signalling pathways (PKA, PKC, PI3K, MAPK's). This leads to the phosphorylation of various proteins and post-translational modifications such as increased trafficking/changes in properties of receptors/ion channels. There is also a substantial increase in the transcription of neuropeptides, growth factors and receptors/ion channels in the somatas of nociceptor neurons. The combination of phosphorylation-dependent and transcriptional-dependent events sensitises nociceptors and drives peripheral sensitisation.

1.7 Central sensitisation

Nociceptor afferents terminate in the superficial dorsal horn of the spinal cord and synapse with second-order neurons, transferring incoming peripheral information about the intensity and duration of a noxious stimulus to the CNS. Central sensitisation is manifested as a state of hyperexcitability of dorsal horn neurons, which can be electrophysiologically characterised as an elevation in spontaneous activity, a reduction in thresholds, heightened responses to incoming stimuli and an increase in receptive fields (Latremoliere and Woolf, 2009). In contrast to peripheral sensitisation, central sensitisation contributes to hypersensitivity in unaffected areas (secondary hyperalgesia). Peripheral sensitisation is most certainly involved in changes in the nociceptive system and constitutes the trigger for central changes; this form of hypersensitivity is localised to the site of injury/damage (primary hyperalgesia) and plays a major role in thermal hyperalgesia. On the other hand, central sensitisation is thought to be the main driver of mechanical hyperalgesia as a result of CNS plasticity that alters responsiveness to stimulus inputs (Woolf and Salter, 2000; Latremoliere and Woolf, 2009). Evidence of this striking phenomenon in the context of pain was first shown by Woolf in 1983, who measured the flexor reflex withdrawal response of α-motorneurons as an output indicator to noxious stimuli. He reported that under normal conditions spontaneous activity was absent and that activation of motor neurons required a noxious input. However, after repeated application of a noxious heat stimulus to the paw, he observed an increase in motor neuron excitability, a reduction in thresholds and an increase in cutaneous receptive fields. This meant that a peripheral stimulus such as light touch was consequentially able to evoke a response. He verified that these findings were exclusively due to a central mechanism by showing that electric stimulation of Aβ-fibres elicited responses only after induction of inflammation, and that local administration of an anaesthetic at the site of injury bore no effect on the enlarged receptive fields. Importantly, he also confirmed that this central hypersensitive state could be recapitulated by repeated electrical stimulation at C-fibre strength (Woolf, 1983).

Glutamate is the primary fast excitatory neurotransmitter of the CNS and mediates its effects via its ionotropic receptors: N-methyl-D-aspartate receptor (NMDAR), α-amino-3-hydroxy-5-methyl-4-isoxazolepropionic acid receptor (AMPAR) and kainate receptors and metabotropic glutamate receptors (mGluR). AMPAR and NMDAR receptors are found at virtually every synapse in the superficial laminae, whereas mGluRs are more localised to extrasynaptic sites (Alvarez et al., 2000; Antal et al., 2008). Excitatory postsynaptic currents (EPSCs) are mainly generated via the activation of AMPA and kainate receptors expressed

by second order dorsal horn neurons whilst NMDARs are normally blocked by magnesium ions (Mg^{2+}) (Mayer et al., 1984). In the setting of tissue damage or injury, the sustained release of neurotransmitters and neuromodulators such as glutamate, BDNF, SP and CGRP from nociceptor terminals into the superficial dorsal horn contribute to the summation of EPSCs in second order neurons. This eventually generates a sufficient level of depolarisation that removes the NMDAR Mg^{2+} block and opens the pore (Mayer et al., 1984; Mannion et al., 1999; Woolf and Salter, 2000; Kawasaki et al., 2004; D'Mello and Dickenson, 2008). The activation of NMDARs produces a large inward Ca^{2+} current and the mobilisation of multiple downstream signalling cascades (MAPK, PKA, PKC, PI3K, Src) that facilitate C-fibre mediated central sensitisation of dorsal horn neurons (Latremoliere and Woolf, 2009). Essentially, these Ca^{2+}-dependent protein kinases contribute to phosphorylation-dependent modifications of NMDAR and AMPAR, as well as numerous other receptors and ion channels. Such modifications may include changes in channel kinetics, as well as increased synaptic density caused by enhanced synthesis and trafficking of ion channels and scaffold proteins. These changes subsequently strengthen nociceptive transmission by increasing membrane excitability and synaptic efficacy (Costigan et al., 2009a; Latremoliere and Woolf, 2009).

In addition to phosphorylation-dependent modifications, longer-lasting transcription-dependent (phosphorylation-independent) processes contribute to the establishment of central hyperexcitability. A body of literature supports a key role of the MAPK, ERK, in neuronal plasticity. One of the earliest studies demonstrated that MAPK phosphorylation in the dorsal horn was very much dependent on nociceptive activity (Ji et al., 1999; Ji et al., 2009). This was shown to depend on the intensity and duration of the noxious stimulus i.e. only noxious stimuli of a duration greater than ten seconds was capable of activating ERK; however, this may well change in the setting of injury (Ji et al., 1999; Wang et al., 2004; Wei et al., 2006). As the ERK pathway integrates multiple protein kinases that are triggered by various receptors (NMDARs, mGluRs, TrkB, NK1 or CGRP), many signalling pathways converge to activate ERK. In addition, raised intracellular Ca^{2+} levels via the glutamatergic receptors critically mobilises several Ca^{2+} dependent kinases (PKC, PI3K) that phosphorylate ERK in dorsal horn neurons (Pezet et al., 2008). Correspondingly, the distribution of phosphorylated ERK reveals neurons that have been stimulated with nociceptive input. The activation of ERK is necessary for the phosphorylation of CREB and other transcription factors that drive the expression of genes such as c-Fos, NK1, COX-2 and TrkB (Latremoliere and Woolf, 2009). Such transcriptional regulation is critical for long-term changes that drive the maintenance of central sensitisation, whereas posttranslational regulation is only sufficient for inducing central sensitisation.

Another mechanism which contributes to central sensitisation is the loss of inhibitory control. GABAergic or glycinergic inhibitory interneurons are densely found in the superficial dorsal horn. Experimentally induced inhibition of $GABA_A$ or glycine receptors via spinal administration of bicuculline or strychnine, respectively, generates behavioural hypersensitivity in rats similar to that seen after peripheral nerve injury (Sivilotti and Woolf, 1994). In accordance with these findings, nerve injury results in diminished GABAergic currents and suppressed glycinergic currents, suggested to be a result of inhibitory neuron cell death (Moore et al., 2002). Other studies have shown that BDNF release from microglial cells may contribute towards a state of disinhibition in the spinal cord. Under physiological conditions the potassium chloride co-transporter 2 (KCC2) drives chloride (Cl^-) out of the cell. Therefore the opening of Cl^- channels causes hyperpolarisation of neurons due to the influx of Cl^- along the electrochemical gradient. However, after peripheral nerve injury microglial derived BDNF induces a down-regulation of KCC2 in lamina I projection neurons (Coull et al., 2003). The decrease in expression of KCC2 produces a rise in the intracellular Cl^- concentration and a depolarising shift in the anion reversal potential, hence impeding the inhibitory tone of GABA and glycine channels (Coull et al., 2005). In addition, disinhibition may occur via PGE_2/EP2 -induced activation of the cAMP/PKA pathway, where the phosphorylation of glycine receptors consequently inhibits the responsiveness of neurons to glycine (Harvey et al., 2004).

Finally, glial cells may also contribute to the development and maintenance of central sensitisation, which will be discussed below.

1.8 Immune cells and pain

Tissue or peripheral nerve damage is accompanied by an immune cell response, which encompasses the activation of resident immune cells, infiltration of inflammatory cells and the release of immune mediators. This response is evident in damaged tissues or nerves, the DRG and spinal cord as well as supraspinal sites. Accumulating evidence has supported the critical involvement of immune cells and immune mediators in the development of hyperalgesia. Microglia and macrophages are the key phagocytic cells of the innate immune system in CNS and PNS, respectively, and are the most studied immune cells in the field of pain with a wealth of literature supporting their contribution to nociceptive transmission.

1.8.1 Mast cells

Bone marrow derived mast cells are a heterogenous population originating from haematopoietic progenitors and are easily recognised by their distinctive heavily granulated appearance. These cells are typically found in body tissues exposed to the external environment such as the skin and mucosal layers of the airways and intestines, but are also found in nerves. Like other immune cells, mast cells engage in numerous immunological activities ranging from phagocytosis and antigen processing to the synthesis and secretion of cytokines (Metcalfe et al., 1997; Galli et al., 2005; Urb and Sheppard, 2012). Mast cells are major players in inflammatory responses and are considered as effector cells in allergic disorders. As one of the resident classes of immune cells in peripheral nerves they are thought to play a role in the development of inflammation and the establishment of a hypersensitive state. The most characterised mechanism of activation of these cells is via their high-affinity immunoglobulin E receptors (FCεRI). However, mast cells may also be activated via the engagement of their pattern recognition receptors (PRRs) in a similar fashion to other leukocytes. Upon activation mast cells rapidly degranulate releasing histamine, heparin, 5HT and proteases (e.g. tryptase) in addition to secreting prostaglandins and a number of chemokines and cytokines (Urb and Sheppard, 2012). Several of the mediators released have demonstrated pro-nociceptive properties that contribute to hyperalgesia. For example, histamines, TNF-α, 5HT and tryptase are able to both activate and sensitise nociceptors, and TNF-α has been shown to directly increase firing rates of sensory axons (Rueff and Dray, 1993; Sorkin et al., 1997; Herbert et al., 2001; Kawabata et al., 2001). Correspondingly, treatment of neuropathic rats with histamine inhibitors has been shown to alleviate the development and maintenance of mechanical and thermal hyperalgesia (Zuo et al., 2003). However, as expected, this method of treatment only provided partial relief as multiple mediators contribute to neuropathic pain. Many mast cell derived mediators also possess chemoattractant properties and thus are able to recruit other immune cell types, particularly neutrophils that release further algogenic and pro-inflammatory mediators at the site of injury (Moalem and Tracey, 2006).

One of the most striking studies supporting the involvement of mast cells in neuropathic pain demonstrated that the development of behavioural hyperalgesia was alleviated in rats treated pre and post PNL surgery with sodium cromoglycate, an agent that stabilises mast cells and prevents them from degranulating. This effect was also associated with a reduction in the recruitment of neutrophils and macrophages to the site of nerve injury (Zuo et al., 2003). Cromoglycate treatment also exhibited analgesic effects in the second-phase of formalin evoked pain (Parada et al., 2001). Furthermore, depletion of mast cell granules via

chronic treatment with compound 48/80 results in attenuated CFA or zymosan and acetic acid-induced hyperalgesia (Woolf et al., 1996; Ribeiro et al., 2000). Conversely, subcutaneous injection of a single dose of 48/80 evoked acute nociceptive behaviours in rats (Parada et al., 2001).

Interestingly, mast cell depletion results in a loss of NGF-induced thermal sensitisation in skin preparations of the saphenous nerve attached to dorsal skin of the hind paw (Rueff and Mendell, 1996). NGF indirectly augments an inflammatory response by exerting cytokine-like action on TrkA-positive inflammatory cells such as mast cells, basophils, lymphocytes and neutrophils. This results in proliferation and the synthesis of cytokines that contribute to the sensitisation of peripheral nerve terminals. In addition, NGF promotes mast cell survival and degranulation. Depletion of mast cells results in a reduction in the NGF sensitising effect and prevents an increase in NGF from baseline levels in CFA treated rats. This is not only because mast cell depletion eliminates the indirect effect of NGF in evoking mediator release (which in turn induces NGF production in other cell types), but also because mast cells are themselves sources of NGF (Woolf et al., 1996).

1.8.2 Neutrophils

Neutrophils, also referred to as polymorphonuclear leukocytes (PMNs), are the most abundant type of white blood cell in mammals, comprising 60-70% of the total white blood cell pool. These short-lived (24 hours) cells form a crucial component of the inflammatory response by orchestrating the recruitment, activation and programming of antigen presenting cells (Witko-Sarsat et al., 2000; Nathan, 2006; Caielli et al., 2012). Under normal conditions neutrophils are in a circulating non-adherent state and are undetectable in peripheral nerves. However, subsequent to nerve injury/tissue damage, the local appearance of inflammation-induced adhesion molecules enables the extravasation and migration of these cells to the site of inflammation where their numbers become considerably greater (Clatworthy et al., 1995; Perkins and Tracey, 2000; Zuo et al., 2003; Nathan, 2006; Cunha et al., 2008a). For example, a 3-fold increase in neutrophils was reported in the rat ipsilateral DRG at 7 days post chronic constriction injury (CCI) surgery (Morin et al., 2007).

As neutrophils migrate towards a stimulus along the concentration gradient of chemoattractants such as NGF-β, chemokine (C-X-C motif) ligand (CXCL)1 and leukotriene-B4 (LTB_4) (Scholz and Woolf, 2007) they discharge two distinctive sets of granules, the peroxidase-negative and the peroxidise-positive granules (Nathan, 2006). Peroxidase-

negative granules are secreted first and contain large amounts of lactoferrin, lipocalin, lysozymes and the chemotactic antimicrobial peptide LL37. They also contain matrix metalloproteinase (MMP) 8, 9 and 25, which facilitate neutrophil recruitment and tissue break-down. The second group of granules released are peroxidase-positive and contain small α-defensins, myeloperoxidase and a selection of potent antibiotics (Nathan, 2006). The release of these factors, particularly superoxides and other reactive oxygen species as well as many pro-inflammatory cytokines (IL-1β, TNF-α, IL-6), contribute to inflammation by directly or indirectly exciting sensory neurons (Cunha et al., 1992; Schafers et al., 2003b; Zelenka et al., 2005; Nathan, 2006). In addition, the release of CCL3, CCL4 and defensins co-ordinates the recruitment of macrophages, which perpetuate the inflammatory response once neutrophil numbers begin to dwindle subsequent to their initial peak at 24 hours post injury (Scapini et al., 2000; Witko-Sarsat et al., 2000; Zuo et al., 2003).

The most convincing evidence for the involvement of neutrophil invasion in neuropathic pain is derived from studies examining the effects of neutrophil recruitment/depletion on pain behaviours. For example, it was shown that the hypernociceptive effects of the potent neutrophil chemoattractants, LTB_4 and complement 5a (C5a), were dependent on neutrophil migration (Levine et al., 1984; Levine et al., 1985). Administration of PMX53, which is a C5a receptor antagonist, exerted analgesic effects in the zymosan, carrageenan and LPS models of peripheral inflammation (Ting et al., 2008). Similarly, a single study showed that inhibition of neutrophil migration via orally administered DF 2162, a selective inhibitor of the CXC chemokine receptors 1 and 2 (CXCR1 and CXCR2), prevented pro-nociceptive behaviours induced by LPS, CFA or zymosan in rats (Cunha et al., 2008b). Cunha et al. (2008) also showed that this compound could reduce neutrophil infiltration, oedema and behavioural hypersensitivity in a model of collagen-induced arthritis. Accordingly, early depletion of neutrophils in rats with a PNL injury was reported to considerably attenuate the development of hyperalgesia (Perkins and Tracey, 2000; Zuo et al., 2003).

Integrin α4β1, is expressed by human and rat neutrophils as well as other immune cell types and mediates the process of extravasation, including neutrophil tethering, rolling and firm adhesion, by binding to vascular cell adhesion molecule-1. Early treatment with a neutralising antibody against α4β1 produced a reduction in neutrophil infiltration at the site of injury and alleviated mechanical allodynia in spinal cord injured rats (Fleming et al., 2009). In a related study, pre-treatment with a leukocyte adhesion inhibitor (fucoidin), which prevents neutrophil infiltration, alleviated carrageenan-induced hyperalgesia in a dose-dependent manner but bore no effect on the induction of inflammatory cytokines (IL-1β, TNF-α, CXCL1) (Cunha et al., 2008a). It was also found that *in vitro* stimulation of

neutrophils with IL-1β resulted in the production of PGE_2, whilst intraplantar IL-1β elicited PGE_2 production in the hind paw that was abolished via pre-treatment with fucoidin. Furthermore, depletion of the neutrophil population at a later stage of nerve injury-induced pathology (8 days post PNL) had no effect on behavioural hypersensitivity (Zuo et al., 2003). Thus together these data indicate that neutrophils are important in the induction of inflammatory hyperalgesia via the release of numerous pro-nociceptive mediators such as PGE_2 and chemoattractant cytokines. However, neutrophils are unlikely to contribute significantly at later stages of neuropathic pain, which corresponds with their succeeding decrease in numbers subsequent to the initial peak.

Early on in the inflammatory response, neutrophils may also release opioid peptides, which exert anti-nociceptive effects via their neuronally expressed opioid receptors (Brack et al., 2004). This adds to the complexity of an inflammatory response and may be a mechanism which is lost or outweighed in the pathology of neuropathic pain. Netherless, what we can gather from these experimental studies is that although the neutrophil response is limited and relatively short-lived, these cells release important mediators that attract other immune cell types, particularly macrophages, which surpass the initial contribution of neutrophil cells and maintain the inflammatory response by releasing further mediators.

1.8.3 Macrophages

Macrophages are large phagocytic cells of the innate immune system that are distributed throughout the body and can be broadly categorised into tissue or circulating macrophages. Under normal conditions macrophages closely survey their microenvironment for pathogens or tissue injury and maintain homeostasis by phagocytosing necrotic cells and rapidly responding to local disturbances. In the bone marrow, myeloid progenitor cells give rise to monoblasts, pro-monocytes and eventually monocytes, which are subsequently released into the bloodstream where they are thought to continue developing and maturing (Mosser and Edwards, 2008). In mice and humans there are two main subsets of monocytes that exhibit specific migration and functional differences, the 'inflammatory' and 'resident' monocytes. These subsets are thought to be derived from macrophage dendritic cell precursors and whilst inflammatory monocytes may further differentiate into dendritic cells, resident monocytes give rise to macrophages upon migration from the blood into the tissue (Zhang and Mosser, 2008; David and Kroner, 2011). Resident monocytes are $CD115^+$ (cluster of differentiation 115; macrophage colony stimulating factor receptor) and possess high levels of CX_3CR1 but lack expression of C-C chemokine receptor type (CCR)2, GR1 (Ly6C) and CD62L (L-selectin). On the other hand, inflammatory monocytes are

characterised as $CD115^+$ and $GR1^+$ (Ly6C), express high levels of CCR2 and CD62L and low levels of CX_3CR1 (Zhang and Mosser, 2008; David and Kroner, 2011).

Macrophages are also classified according to their functional characteristics as either M1 (classically activated pro-inflammatory macrophages) or M2 (alternatively activated anti-inflammatory macrophages). M1 macrophages, which are associated with the inducible nitric oxide synthase (iNOS) marker, are produced during a cell-mediated immune response. These macrophages are induced by interferon (IFN)-γ released from other immune cell types (natural killer cells and Th-1 lymphocytes), exhibit greater microbiocidal capacity and secrete higher levels of the pro-inflammatory mediators IL-1β, IL-6 and IL-23 compared to the M2 class (Mosser and Edwards, 2008; David and Kroner, 2011). In contrast, M2 macrophages express higher levels of some anti-inflammatory cytokines such as IL-10 and transforming growth factor (TGF)-β and up-regulate ARG1 whilst down-regulating pro-inflammatory mediators during a response. This subtype may be further subdivided into M2a (immunity against parasites), M2b (pro- and anti-inflammatory function) and M2c (pro-healing/regulatory) (David and Kroner, 2011).

Subsequent to injury or infection, macrophages form one of the first lines of defence of the immune system and become rapidly activated in response to various exogenous and endogenous 'danger signals' such as pathogen associated molecular patterns (PAMPs), alarmins and heat shock proteins (HSP) (Zhang and Mosser, 2008). Macrophages also respond to the release of mediators from other innate immune cells. One of the most well established modes of activation is via a family of highly conserved PRRs such as the toll-like receptors (TLRs) which are able to recognise PAMPs, including the typical LPS and lipoteichoic acid (LTA) outer membrane components of Gram-negative and -positive bacteria, respectively. Once activated macrophage cells undergo profound physiological changes and up-regulate a number of cell surface receptors, secrete a range of mediators and exhibit enhanced phagocytic activity (Zhang and Mosser, 2008).

Macrophages also play a key role in the process of Wallerian degeneration (WD) by phagocytosing damaged axons, myelin sheaths, debris and necrotic cells distal to the site of injury (Perrin et al., 2005). As previously discussed, peripheral macrophages consist of a heterogenous population of resident and infiltrating cells. The faster responding resident macrophages are important in initiating the clearance response and are assisted by a large influx of the hematogenous derived infiltrating population (Ton et al., 2013). The clearance process is orchestrated by a number of chemokines including CCL2, CCL3 and IL-1β and is necessary for axonal regeneration. In the PNS, this process occurs rapidly within a matter of

days, in the CNS, WD is much slower and can take as long as months (Perry et al., 1987; Perrin et al., 2005). Interestingly, WD may be interrupted by the application of CCL2, CCL3 or IL-1β neutralising antibodies (Perrin et al., 2005), which prevents the infiltration of macrophages, or enhanced by the application of TLR2 or TLR4 ligands (zymosan and LPS, respectively) (Boivin et al., 2007). Furthermore, mice pre-treated with the glucocorticoid dexamethasone, or deficient in TLR signalling exhibit reduced recruitment/activation of macrophage cells and a delayed clearance of myelin debris and regeneration of the injured nerve (Boivin et al., 2007). TLR signalling is coupled to the activation of NF-κB, which orchestrates the transcription of many pro-inflammatory mediators in response to PAMPs such as HSP60 and 70, necrotic cells and components of the extracellular matrix (ECM) that are abundantly found at sites of injury (Nguyen et al., 2002; Willis et al., 2005). Based on these studies it is evident that TLRs do indeed contribute to the process of WD and in this setting are activated by a number of endogenous ligands.

The findings of Perrin et al. (2005) and Boivin et al. (2007) are particularly interesting as they implicate impairment of WD and the macrophage response in the alleviation of pain-related behaviours. Their work is supported by a previous study that used C57BL/WLD mice, which exhibit reduced rates of WD as a result of over-expression of the nicotinamide mononucleotide adenylyltransferase gene (Myers et al., 1996; Mack et al., 2001). These mice displayed delayed macrophage recruitment and WD that correlated with attenuated nerve injury-induced thermal hyperalgesia compared to WT controls (Myers et al., 1996). In addition, macrophage depletion via systemic administration of clodronate-containing liposomes not only reduced axonal degeneration but also alleviated mechanical and thermal hyperalgesia (Liu et al., 2000; Barclay et al., 2007). Correspondingly, mechanical thresholds increased by the time the macrophage population recovered at 8 days post injury, as revealed by ED1 and ED2 immunoreactivity in the spleen (Barclay et al., 2007). Notably, macrophages have been shown to play a limited role in mechanical allodynia and neither systemic/perineural administration of a macrophage inihibitor nor depletion or transfer of activated macrophages to the perineurium can alter mechanical thresholds (Rutkowski et al., 2000; Barclay et al., 2007).

Interestingly, evidence from pain models of disease associated pathologies suggests that macrophages play a modality specific role in neuropathic pain mechanisms that is very much dependent on aetiology. For example, in a model of streptozotocin (STZ) -induced diabetes (where macrophages infiltrate L4/L5 DRGs by 1 week and diabetic nerves by weeks 2 and 3) depletion via clodronate treatment alleviated beta cell damage and mechanical allodynia, but not thermal hyperalgesia (Conti et al., 2002; Mert et al., 2009; Ton

et al., 2013). Similarly, in rat models of HIV-1 or chemotherapy-induced neuropathy, the infiltration of peripheral macrophages into the sciatic nerve and DRG correlated with mechanical allodynia (Peters et al., 2007b; Peters et al., 2007a; Wallace et al., 2007b; Liu et al., 2010; Kamerman et al., 2012). Accordingly, pre-treatment with minocycline diminished paclitaxel-evoked allodynia and attenuated macrophage infiltration (Liu et al., 2010). In a model of vincristine-induced pain it was reported that expression of IL-6 was co-localised with infiltrating macrophages in the sciatic nerve and lumbar DRG. Correspondingly, administration of an IL-6 neutralising antibody to the sciatic nerve attenuated mechanical allodynia and IL-6 KO mice showed reduced behavioural hypersensitivity (Kiguchi et al., 2008b).

Attenuation in neuropathic pain-associated behaviours in TLR2, 3 and 4 null mice has mainly been attributed to an impaired microglial response (Tanga et al., 2005; Kim et al., 2007a; Obata et al., 2008). However, a recent study using TLR2 null mice supported a prominent role of peripheral macrophages in behavioural hypersensitivity and found no evidence of microglial involvement (Shi et al., 2011). Here, it was reported that thermal hyperalgesia was abolished in nerve-injured TLR2 KO mice whilst mechanical allodynia was partially attenuated. This correlated with a reduction in macrophage infiltration as well as a decrease in the expression of IκB-α and TNF-α in the injured sciatic nerve of KO mice at 14 days post injury. In contrast, WT mice exhibited normal thresholds and an increase in these markers, which co-localised with $ED1^+$ cells (Shi et al., 2011). In contradiction with previous findings (Kim et al., 2007a), Shi et al. (2011) found no evidence of a microglial phenotype and reported that expression of TLR2 and IκB-α mRNA was undetectable in the spinal cords of WT mice, but strikingly induced along with TNF-α in injured sciatic nerves.

Peripheral inflammatory models such as carrageenan and CFA are thought to mediate their effects in a TLR-dependent manner (Bhattacharyya et al., 2008) and evoke the release of ATP from monocytes, which in turn activates $P2X_4$ receptors via autocrine signalling. This leads to the mobilisation of Ca^{2+} and subsequent phosphorylation of p38 and the release of pro-inflammatory PGE_2. Mice deficient in the expression of $P2X_4$ show attenuated formalin, CFA or carrageenan-induced pain behaviours due to a reduction in PGE_2-driven neuronal hyperexcitability (Ulmann et al., 2010). This effect is attributed to resident macrophages in the paw, as the expression of $P2X_4$ is restricted to this cell type. In support of this, transfer of ATP-primed WT but not KO macrophages to the hind paws of naïve mice recapitulated pain behaviours (Ulmann et al., 2010). Interestingly, CCR2 null mice also exhibit marked reductions in inflammatory and neuropathic pain behaviours, linked to a diminished

microglial response and evidence of reduced monocyte recruitment (Izikson et al., 2000; Abbadie et al., 2003).

Macrophages contribute significantly to inflammatory pain by releasing many inflammatory mediators (Marchand et al., 2005). Intraperitoneal administration of zymosan and acetic acid elicited dose-dependent writhing responses which could be enhanced by peritoneal pre-treatment with thioglycollate, or reduced by macrophage removal via saline lavage (Ribeiro et al., 2000). The aforementioned experiments illustrate that the pain response is dependent on the number of macrophages present in the peritoneal cavity. Furthermore, it was also shown that this response was dependent on the release of TNF-α, IL-1β and IL-8/CXCL8, as pre-treatment with corresponding neutralising antibodies attenuated nociceptive behaviours, whereas administration of all three recombinant cytokines induced hypernociception in mice (Ribeiro et al., 2000). These findings are further supported by a study that demonstrated that intraperitoneal administration of LPS-stimulated macrophage supernatants produced nociceptive writhing responses in rats that could be inhibited via pre-treatment with dexamethasone, paracetamol or indomethacin (Thomazzi et al., 1997). It was also shown that pre-incubation of LPS stimulated macrophage supernatants with neutralsing antibodies for TNF-α, IL-1β and IL-8/CXCL8 produced some alleviation of pain behaviours (Thomazzi et al., 1997). Accordingly, intraplantar administration of LPS or carrageenan evoked mechanical hyperalgesia and an increase in TNF-α and IL-1β immunoreactivity in the skin of treated paws (Cunha et al., 2000).

Macrophage-derived mediators such as TNF-α, IL-1β, IL-6, CCL3, PGs and nitric oxide (NO) may directly or indirectly contribute to the development of hyperalgesia (Woolf and Ma, 2007; Austin and Moalem-Taylor, 2010). For example, PGs are up-regulated in macrophages located in the peripheral nerve and contribute to the development of pain behaviours by directly sensitising nociceptors and increasing neuronal excitability (Samad et al., 2002; Ma and Eisenach, 2003b). TNF-α and IL-1β have been documented to increase in the sciatic nerve and spinal cord of STZ-treated rats, and IL-1β was co-localised with ED-1 positive macrophages in the nerve (Conti et al., 2002; Drel et al., 2010; Bishnoi et al., 2011). TNF-α has also been reported to co-localise with ED-1 positive macrophages in the sural nerves of patients with established diabetic neuropathy, though this was not a model of pain (Kawamura et al., 2008). In the injured sciatic nerves of mice, the dramatic up-regulation of CCL3 is thought to contribute to macrophage recruitment and hence the development of neuropathic pain (Kiguchi et al., 2010a). Perineural administration of anti-CCL3 delays the onset of hypernociception, whereas intraneural or perineural application of recombinant CCL3 evokes allodynia and thermal hyperalgesia. Furthermore, perineural application of

nicotine, which acts at nicotinic acetylcholinergic receptors to suppress cell migration and cytokine expression, reduces both pain behaviours and the expression of CCL2 and IL-1β (Cloez-Tayarani and Changeux, 2007; Kiguchi et al., 2010a).

1.8.4 T cells

T lymphocytes are effector cells of the adaptive immune system and are derived from haematopoietic stem cells in the bone marrow. Later these cells transit into the blood stream and populate the thymus where they mature into thymocytes (Schwarz and Bhandoola, 2006). T cells are a heterologous population of immune cells comprising of $CD4^+$ T-helper (Th) cells, $CD8^+$ cytotoxic T (Tc) cells or $CD4^+$ regulatory T cells (Tregs) and upon maturation and selection they exit the thymus and enter the blood circulation. Th cells may be further subdivided into pro-inflammatory Th1 cells or anti-inflammatory Th2 cells, which depends greatly on the transcription factors they induce and a number of external cues (cytokines). A Th1 phenotype is directed by IL-12 and these cells produce INF-γ through a STAT 4 dependent pathway, whereas a Th2 phenotype is directed by IL-4 and these cells also produce IL-4 along with IL-5 through a STAT 6 dependent pathway (O'Garra and Arai, 2000). Th1 cells promote cellular immunity and play an important role in the removal of various types of pathogens such as bacteria, parasites, yeasts and viruses. Characteristically, this T cell phenotype produces INF-γ and TNF-α and tends to be associated with the recruitment of NK cells and cytotoxic $CD8^+$ T cells. On the other hand Th2 cells mainly mediate humoral immunity and typically produce IL-4, IL-5 and IL-13. This class of T cells engage mast cells and eosinophils in the removal of parasites and suppress macrophage activation and the production of pro-inflammatory cytokines (O'Garra and Arai, 2000).

The first implication of T cells in nociception came from a study examining the inflammatory response in three models of neuropathic pain in rats. Here it was found that after CCI, PNL or ischaemic lesion/transection injury, there was a considerable increase in T cells in the injured sciatic nerve compared to sham controls (Cui et al., 2000). Moalem and Yu (2004) later reported that T cell infiltration into the sciatic nerve occurs as soon as 3 days post CCI, which peaks at day 21 and remains present for 5-6 weeks. They also demonstrated that nerve-injured congenitally athymic nude rats, which lack mature T cells, exhibit attenuated mechanical allodynia and thermal hyperalgesia. To further elucidate the role of T cells in neuropathic pain, Moalem and Yu (2004) subsequently showed that the application of Th cells polarised to either a pro-inflammatory Th1 phenotype or anti-inflammatory Th2 phenotype elicited behavioural hypersensitivity in nude rats or modestly attenuated pain

behaviour in littermate controls, respectively. These findings were later confirmed in nude and recombinant activating gene-1 null mice (Rag-1; encodes an enzyme essential for T-cell maturation) that again exhibited attenuated mechanical hypersensitivity after nerve injury, which was reversed by adoptive transfer of $CD4^+$ leukocytes (Cao and DeLeo, 2008; Costigan et al., 2009b). It has also been reported that T cells infiltrate the dorsal horn, peaking at 7 days post injury. Interestingly, nude rats exhibited reduced GFAP immunoreactivity in the spinal cord, which is suggestive of a possible T cell-glial interaction in nociceptive transmission (Cao and DeLeo, 2008).

In contrast to adult rats, nerve-injured neonatal rats do not develop neuropathic pain, which is a striking phenomenon also observed in humans. One of the most important studies illustrating the T cell contribution to neuropathic pain delineated the transcriptional profile differences in the dorsal horn between adult and neonatal rats. It was identified that in the setting of nerve injury a greater microglial and T cell response occurred in adult rats compared to younger animals. Central chemokine profiles were also different between these two age groups and INF-γ was particularly up-regulated in the dorsal horns of adults but not neonates (Costigan et al., 2009b). Furthermore, it has also been shown that although neonates have a limited Th population, they possess a relatively larger Th2 population, which may account for the differences in pain responses compared to adults (Morein et al., 2007).

Despite the selection process which only allows functional, non self-reactive T cells into the periphery, some autoreactive T cells escape thymic censorship and are released into the circulation. T cells are associated with many autoimmune diseases that are accompanied by debilitating pain symptoms, such as Guillain-Barré Syndrome (GBS). In a model of experimental autoimmune neuritis (EAN) that mimics acute inflammatory demyelinating polyradiculoneuropathy in GBS, rats exhibited neuropathic pain-associated behaviours that coincided with significant T cell infiltration into the sciatic nerve (Moalem-Taylor et al., 2007). Similarly, in experimental autoimmune encephalomyelitis (EAE; model of MS) mice developed mechanical allodynia during the early disease stages, where significant T cell infiltration into the superficial dorsal horn was accompanied by increased glial reactivity (Olechowski et al., 2009).

1.9 Glia and pain

In the CNS, glial cells (astrocytes, oligodendrocytes and microglia) account for approximately 70% of the total cell population and are involved in the formation of the blood brain barrier, the development of the myelin sheath and defence against invading pathogens or damage. Glial cells also regulate neuronal function via neurotransmitter release and express an array of receptors/ion channels that allow them to directly respond to neuronal signals. In the PNS, glial cells (satellite cells and Schwann cells) also undertake numerous roles in metabolic and ionic homeostasis, myelin sheath development and trophic support.

Over the past two decades glial cells, particularly microglia and astrocytes, have received considerable attention for their involvement in chronic pain, stemming from some of the early work of Garrison et al. (1991).

1.9.1 Microglia

Del Río-Hortega was the first to introduce the concept of microglia with a series of published studies between 1919 and 1927, which adopted the classic silver carbon labelling technique. The origin of these cells has long been the subject of great controversy within the glial field. Initially it was believed that microglia were of mesodermal origin and Rio-Hortega postulated that these cells invaded the brain early during development where they matured into amoeboid cells. Although this view was widely accepted, others disagreed and proposed that glioblasts of the neuroectoderm were the precursors of microglial cells and thus argued that all glial cells shared a common stem cell population (Paterson et al., 1973; Kitamura et al., 1984). The third view, which was originally proposed by Leblond and colleagues in the 1930s was that microglia are of the monocytic lineage. This theory was later verified using autoradiography, which showed that amoeboid microglia exhibiting monocytic characteristics later transformed into ramified microglia (Imamoto and Leblond, 1978; Ling et al., 1980). These findings were further validated by subsequent studies and the use of newly developed immunohistochemical markers (Perry et al., 1985; Graeber et al., 1988).

It is now generally accepted that microglial cells are of the monocytic lineage and share many functional similarities of peripheral monocytes/macrophages. Recent findings suggest that these cells originate from the foetal yolk sac and migrate into the CNS during early

embryonic development; however microglia are also thought to differentiate from circulating monocytes entering the CNS during the early stages of postnatal development (Perry et al., 1985; Saijo and Glass, 2011). Under normal conditions microglia are in a 'quiescent' state and are involved in immune surveillance and CNS homeostasis. In this state microglia morphology is typically ramified with a small cell body and fine long projections that continuously survey the local microenvironment. However, subsequent to infection or injury microglia undergo considerable morphological changes; their processes shorten and thicken and their distal branches become de-ramified. Their cell bodies also increase in size and adopt a more rounded 'amoeboid' shape. Microglia also up-regulate multiple cell surface glycoproteins (MHC-II, CD45), considerably increase in numbers by means of proliferation and enhanced migratory capacity, become more phagocytic and release a range of pro-inflammatory substances. This response is collectively referred to as microgliosis (Ransohoff, 2007; Ransohoff and Perry, 2009). As microglia express a repertoire of ionotropic and metabotropic receptors, it is apparent that a single mechanism of activation is unlikely, and that these cells are engaged by various signals that lead to different morphological and secretory responses. Such signals include invading pathogens or nerve/tissue damage, which is accompanied by the release of a number of mediators such as ATP, glutamate, cytokines, chemokines, PGs, neuropeptides and NO. In turn microglia release a repertoire of neuroexcitatory substances, which directly/indirectly excite and sensitise dorsal horn neurons and thus enhance nociceptive transmission, leading to hyperalgesia and allodynia (DeLeo and Yezierski, 2001; Watkins et al., 2001; Watkins and Maier, 2003).

The role of microglia in chronic pain mechanisms has been well characterised in a number of neuropathic and inflammatory pain paradigms. Many of the initial findings were based on studies using general glial inhibitors, which proved to be effective in reducing/preventing hyperalgesia and allodynia in animal pain models (Meller et al., 1994; Watkins et al., 1997; Sweitzer et al., 2001; Raghavendra et al., 2003a; Raghavendra et al., 2003b; Hua et al., 2005; Ledeboer et al., 2005; Clark et al., 2007a). Fluorocitrate attenuates metabolic activity specifically in glial cells by inhibiting the enzyme aconitase and consequently blocking the citric acid cycle (Goncharov et al., 2006). Propentofylline is a derivative of methyl xanthine and mediates its glia suppressing effects via the inhibition of adenosine transporters and phosphodiesterases, which leads to a reduction in cAMP (Tawfik et al., 2008). Minocycline belongs to the tetracycline class of antibiotics and exerts a number of inhibitory effects on microglial cells, including the suppression of iNOS and IL-1 as well as the phosphorylation of p38 MAPK (Lai and Todd, 2006). Although much of the work using propentofylline and fluorocitrate illustrated the involvement of glial cells in the regulation of pain sensitivity,

these inhibitors failed to distinguish which glial cell type is involved. Furthermore, their biological actions lacked the necessary selectivity to be entirely convincing, with even suspected effects on neuronal function. On the other hand, the literature supports a selective mode of action of minocycline in microglial cells. In one study minocycline reduced the development of nerve injury induced neuropathic pain but failed to attenuate existing mechanical allodynia and hyperalgesia (Raghavendra et al., 2003a), indicating that microglia may play a more important role in the initiation rather than maintenance of chronic pain. Conversely, it has also been demonstrated that administration of agents capable of directly activating microglia, including LPS and the HIV glycoprotein 120, evoke nociceptive behaviours in naïve rats (Milligan et al., 2000; Cahill et al., 2003; Clark et al., 2006).

Out of the three glial inhibitors discussed, propentofylline is the only one that has been taken to a high-profile clinical trial and failed to show efficacy in alleviating pain associated with post-herpetic neuralgia. In cases like this, the lack of translation from pre-clinical rodent models of pain to humans is thought to be due to a number of reasons such as the lack of predictability of animal models, functional differences between rodent and human microglia and different methods of pain measurement (evoked pain vs spontaneous pain). Such failures highlight the limitations of preclinical research and emphasise the importance of using human tissues and primary cells to improve translation to the human condition (Landry et al., 2012).

Progression on to more targeted interventions has led to a wealth of literature exploring specific microglial receptors using pharmacological tools and transgenic technology. Like peripheral macrophages, microglia express a number of TLRs, which initiate a cellular response upon detection of numerous endogenous and exogenous danger signals, as previously described (section 1.8.3). The expression of TLR4 is exclusive to microglia in the CNS, which has been shown to up-regulate in the spinal cord of nerve-transected rats as soon as 4 hours post surgery up until day 14 (Tanga et al., 2004). In a later study, Tanga et al. (2005) showed that nerve-injured TLR4 KO mice exhibited attenuated mechanical allodynia and thermal hyperalgesia compared to WT controls, which correlated with reduced microglia reactivity in the spinal cord as revealed by OX-42 (cluster of differentiating molecules 11b; CD11b) staining. These studies suggest that TLR4 signalling contributes to the activation of microglia during the induction of neuropathic pain. Moreover, as reduced microglia activity is associated with attenuated pain behaviours it is evident that these cells are important in chronic pain pathways. This is further supported by studies examining the function of other microglial receptors in models of neuropathic pain,

such as CX_3CR1, $P2X_4$, $P2X_7$ and CCR2 (Abbadie et al., 2003; Tsuda et al., 2003; Chessell et al., 2005; Tanga et al., 2005; Clark et al., 2010b; Staniland et al., 2010).

In contrast to neuropathic models of traumatic nerve injury, evidence for microglial involvement in models of peripheral inflammatory pain is circumstantial (McMahon et al., 2005; McMahon and Malcangio, 2009). Intraplantar administration of various inflammogens such as zymosan, formalin, carrageenan and CFA elicit hypersensitivity of the ipsilateral hind paw. However, the extent of the glial response is notably moderate and discrepancies between groups are evident throughout the literature. For instance, many studies have reported contradictory observations on the regulation of glial cell markers in numerous inflammatory models; whilst some failed to observe any change in the microglial response (Molander et al., 1997; Honore et al., 2000; Zhang et al., 2003; Clark et al., 2007a) others have reported clear changes (Fu et al., 1999; Sweitzer et al., 1999; Sweitzer et al., 2001; Yeo et al., 2001; Aumeerally et al., 2004; Raghavendra et al., 2004), which is supported by studies using glial inhibitors, particularly minocycline (Meller et al., 1994; Watkins et al., 1997; Hua et al., 2005). It should be noted, however, that differences between inflammatory models and time points examined may account for some of the discrepancies. Furthermore, many of these studies have used markers such as OX-42 and ionised calcium binding adaptor molecule 1 (Iba1) to illustrate microglia activation but it remains unclear whether these markers are associated with pain hypersensitivity. Nevertheless, certain microglial markers such as $P2X_4$, CX_3CR1 and TLR4 are up-regulated in the context of injury/inflammation and inhibition of these receptors attenuates neuropathic/ inflammation-induced pain (Tsuda et al., 2003; Tanga et al., 2004; Zhuang et al., 2007; Clark et al., 2012). In addition to these exclusive markers, strong evidence for microglial involvement in inflammation-induced pain has been demonstrated using p-p38 MAPK as a marker of microglia activation, which is a nociceptive specific kinase (Kim et al., 2002; Kumar et al., 2003; Svensson et al., 2003a; Svensson et al., 2003b; Ji and Suter, 2007; Ji et al., 2009; Clark et al., 2012).

MAPKs are an evolutionally conserved family of molecules that possess various roles in gene expression and cell signalling. MAPKs are comprised of three main members: ERK (1 and 2), p38 (α,β,γ,δ) and JNK (1-3), which are activated via MAPK kinase mediated phosphorylation and exert a range of transcriptional-dependent and independent effects (Ji et al., 1999). Phosphorylated p38 is induced by pro-inflammatory cytokines and a number of cell stressors, and has a crucial role in inflammatory responses. Accordingly, the administration of p38 inhibitors in models of inflammatory and neuropathic pain confers analgesia (Ji and Woolf, 2001; Ji et al., 2002; Kumar et al., 2003; Svensson et al., 2003a; Svensson et al.,

2003b; Tsuda et al., 2004; Clark et al., 2006; Ji and Suter, 2007). Activated microglia produce numerous inflammatory mediators such as IL-1β, IL-6, TNF-α, PGE_2, NO and BDNF (Ji and Suter, 2007), some of which can induce the activation of p38 (Ji and Woolf, 2001; Abbadie et al., 2003; Svensson et al., 2005). In turn, p38 regulates the transcription of many mediators in an NF-κB dependent manner, particularly IL-1β, IL-6 and TNF-α (Ji and Woolf, 2001; Svensson et al., 2003a; Sung et al., 2005; Clark et al., 2006). These cytokines contribute to central sensitisation via a combination of modulatory effects on excitatory and inhibitory synaptic transmission, which involve the phosphorylation of CREB and transcription of pro-nociceptive genes (Kawasaki et al., 2008).

The modulation of microglial activation has also proven to be efficacious in some pain models of disease-associated pathologies. For example, inhibition of p-p38, pERK1/2, p-Src and p-JNK via the administration of gabapentin, minocycline, lidocaine or MAPK inhibitors prevented/reversed microglial activation and hence alleviated the development of diabetic and paclitaxel-induced neuropathic pain in rats (Sweitzer et al., 2004; Daulhac et al., 2006; Tsuda et al., 2008; Wodarski et al., 2009; Pabreja et al., 2011; Suzuki et al., 2011; Burgos et al., 2012). Correspondingly, the inhibition or modulation of mediators released by activated microglia also attenuates behavioural hypersensitivity. Intrathecal administration of a TNF-α neutralising antibody or an IL-1 receptor antagonist reduced vincristine or paclitaxel-induced mechanical allodynia, respectively, whilst IL-10 gene therapy prevented and reversed the allodynic state in paclitaxel-treated rats (Ledeboer et al., 2007; Kiguchi et al., 2008a). Similarly, gp120-treated rats exhibited spinal microgliosis that correlated with the development of behavioural hypersensitivity, whereas treatment with minocycline or a TNF-α neutralising antibody attenuated these behaviours (Herzberg and Sagen, 2001; Wallace et al., 2007b; Wallace et al., 2007a; Zheng et al., 2011b; Blackbeard et al., 2012). Microglial activation is also documented to contribute to bone cancer-induced neuropathic pain (Zhang et al., 2005b; Mao-Ying et al., 2012). Early minocycline treatment prevented bone cancer-induced behavioural hypersensitivity by inhibiting the release of BDNF from microglial cells. Concurrent treatment with fluorocitrate or an ERK kinase inhibitor reduced spinal p-ERK expression and attenuated mechanical allodynia (Wang et al., 2011; Wang et al., 2012a; Wang et al., 2012b). Furthermore, intrathecal administration of a CCL2 neutralising antibody attenuated bone cancer-induced pain possibly by inhibiting microglial-neuronal communication (Hu et al., 2012).

1.9.2 Astrocytes, Schwann cells and satellite cells

Astrocytes are the most abundant cell population of the CNS and arise from neuroepithelial stem cells, sharing the same origin as oligodendrocytes and neurons. These cells form close connections with neurons and capillaries and are active cells that are normally involved in regulating most aspects of neuronal function (Butt, 2011). Garrison et al. (1991) were amongst the first to propose a role for astrocytes in neuropathic pain by describing astrocytic hypertrophy in the spinal cord of nerve-injured rats, which was evident by an increase in glial fibrillary acidic protein (GFAP) immunoreactivity. This result triggered many more studies that confirmed the reactive astrocytic phenotype in a number of models of inflammatory and neuropathic pain (Sweitzer et al., 1999; Ma and Quirion, 2002; Gao et al., 2009).

Astrocytes are believed to play a prominent role in the maintenance of neuropathic pain, as illustrated by studies that show astrocytic activation succeeding microglial activation at 4 days and lasting up to 12 weeks post peripheral nerve injury in rats (Tanga et al., 2004). This temporal dissociation between microglia and astrocytes is supported by the fact that neuropathic GFAP null mice exhibit initial development of behavioural hypersensitivity but the duration of these pain behaviours is considerably shorter (Kim et al., 2009). In the context of injury/tissue damage, astrocytes, like microglia, are engaged by a wide range of neurotransmitters that initiate the transition into a reactive astrocytic state. Once activated, these cells may in turn release many mediators including PGs, NO, glutamate, ATP, cytokines and chemokines (Hansen and Malcangio, 2013; Mika et al., 2013) that directly or indirectly contribute to pain hypersensitivity.

In the PNS there are two main types of glial cells, the Schwann and satellite cells. Schwann cells are derived from the neural crest and comprise of two main phenotypes: the myelinating Schwann cell and the ensheathing/non-myelinating Schwann cell (Campana, 2007). Myelinating Schwann cells wrap around medium and large diameter axons and provide a lipid rich membrane that facilitates axonal conduction, whereas non-myelinating Schwann cells ensheath unmyelinated small diameter axons in small bundles known as Remak bundles (Murinson and Griffin, 2004). Satellite cells surround neuronal somas within the DRG and are thought to exert similar metabolic homeostasis functions as astrocytes (Lu and Richardson, 1991). In the context of nerve injury, Schwann cells mediate the process of WD by orchestrating demyelination and nerve regeneration (Campana, 2007). Shortly after nerve injury Schwann cells undergo a phenotypic switch and stop producing myelin proteins, proliferate, migrate and release multiple mediators such as cytokines (IL-1β, TNF-

α, IL-6, CCL2), growth factors (NGF, BDNF, GDNF), PGE_2 and ATP. These mediators sensitise nociceptors through direct or indirect mechanisms and promote the recruitment of other immune cells, namely via CCL2-mediated recruitment of macrophages (Shamash et al., 2002; Tofaris et al., 2002; Muja and DeVries, 2004; Austin and Moalem-Taylor, 2010; Gaudet et al., 2011). In the DRG, satellite cells also become activated and proliferate extensively (Lu and Richardson, 1991), leading to an increase in GFAP immunoreactivity and the release of pro-inflammatory cytokines (IL-1β, TNF-α), which contribute to enhanced neuronal firing (Takeda et al., 2007).

From the literature it is clear that the release of mediators from immune cells significantly contributes to the development and maintenance of hypersensitivity. Therefore it is plausible that blocking the release of these signalling molecules or their receptors may alleviate pain. For example, anti-NGF treatment effectively reverses established hyperalgesia in rodent models of inflammatory and neuropathic pain (Wild et al., 2007), whilst anti-TNF-α therapy is a clinical success in the treatment of RA (Haraoui, 2005).

1.10 Cytokines and chemokines

The contribution of pro-inflammatory cytokines and chemokines to the exacerbation of inflammatory and neuropathic pain is supported by a wealth of studies. These signalling molecules are released by resident dendritic cells, macrophages, lymphocytes and mast cells as well as other cell types of the nervous system in response to various stimuli. Cytokines/chemokines signal in an autocrine, paracrine or hormonal fashion and have multiple roles in the modulation of the immune system and the inflammatory response (Sommer and Kress, 2004; Wells et al., 2006; Kiguchi et al., 2012).

Cytokines are small polypeptides (5-140kDa) with diverse molecular structures and relatively short half-lives and can be categorised into four main groups: growth factors, interleukins, interferons and TNF. The members of these groups can also be further classified as pro- or anti-inflammatory, depending on their primary function. Pro-inflammatory cytokines (IL-1β, TNF-α, IL-6, IL-12, IL-15, IL-17, IL-18, IFN-γ) promote an inflammatory response and are implicated in nociception by facilitating neurogenic inflammation (Opree and Kress, 2000). In contrast, anti-inflammatory cytokines (IL-4, IL-10, TGF-β) suppress the immune response. On the other hand, chemokines form a distinct group of chemotactic cytokines that possess exclusive chemical properties. They are typically much smaller than cytokines with a molecular weight ranging from 8-10kDa and

act on cell membrane expressed GPCRs coupled to the inhibitory $G\alpha_{i/o}$ family of G-proteins. Functionally, this group of approximately 50 signalling molecules exhibits great redundancy and overlap, as there are several ligands for each of the 20 receptors. Likewise, single chemokines are recognised by multiple receptors expressed by a range of cell types including leukocytes, neurons and glial cells (Ubogu et al., 2006). Generally, chemokines consist of four or more cysteine residues that form disulphide bonds, and are thus classified into 4 main groups according to the position of the first two conserved cysteine residues near the N-terminus (see Fig. 1.4). The CC group constitutes the largest family of chemokines and possesses 2 adjacent cysteines (CCL2, CCL3, CCL4, CCL5). This chemokine group predominantly attracts macrophages and eosinophils. The CXC group has a single amino acid between the two cysteine residues and may be further divided based on the presence or absence of an ELR motif (glutamic acid-leucine-arginine) on the N-terminus just before the CXC (CXCL5, CXCL8). These chemokines primarily recruit neutrophils, while the non-expressing ELR motif chemokines are involved in lymphocyte recruitment (CXCL9, CXCL10, CXCL12, CXCL13) (Clark-Lewis et al., 1991; Ubogu et al., 2006; Verri et al., 2006). The CX_3C group features 3 amino acids between the two cysteine residues and has currently a single member (CX_3CL1 (fractalkine)) that acts on multiple cell types including monocytes, T lymphocytes and natural killer cells. Unlike the other groups, chemokines of the C family only have a total of 2 cysteines (Chemokine (C motif) ligand (XCL) 1 and 2) and preferentially recruit lymphocytes (Zlotnik and Yoshie, 2000; Verri et al., 2006).

A number of groups have demonstrated the onset of mechanical and thermal hyperalgesia subsequent to local, intraneural, systemic or intrathecal injection of cytokines and chemokines, which can be reversed via neutralising antibodies or inhibitors (Ferreira et al., 1988; Follenfant et al., 1989; Cunha et al., 1992; Safieh-Garabedian et al., 1995; Woolf et al., 1997; Sung et al., 2004; Zelenka et al., 2005). Furthermore, in experimental models of neuropathic and inflammatory pain these cytokines and their receptors are up-regulated in the sciatic nerves and DRG neurons of rodents. Accordingly, pre-treatment with neutralising antibodies or inhibitors exhibits analgesic effects (Ferreira, 1980; Cunha et al., 1991; Cunha et al., 1992; Murphy et al., 1995; Safieh-Garabedian et al., 1995; DeLeo et al., 1996; Woolf et al., 1997; Cunha et al., 2000; Ribeiro et al., 2000; Shubayev and Myers, 2000; Okamoto et al., 2001; Homma et al., 2002; Sommer and Kress, 2004; Svensson et al., 2005; Marchand et al., 2009). Some of these experiments are discussed in more detail in *Chapters 2* and *3*.

Cytokines generate a state of hypersensitivity by exerting a combination of direct and indirect effects. This is supported by evidence of the expression of cytokine receptors on peripheral axons, suggesting that their ligands are able to directly mediate sensitising

effects on nociceptors (Sommer and Kress, 2004). For example, subsequent to nerve injury there is a marked increase in the expression of the TNF-α receptors, TNF 1 and 2, in peripheral nerve axons, DRG somata, peripheral immune cells and spinal microglia (Ohtori et al., 2004; George et al., 2005). Therefore, it is likely that TNF-α signalling can directly induce the excitation of sensory neurons and contribute to the development of hypersensitivity. The IL-1β receptor, IL-1R, is also expressed by DRG neurons indicating that IL-1β may mediate direct sensitising effects via an IL-1R/tyrosine kinase/PKC-dependent pathway (Sommer and Kress, 2004). However, in most cases the algesic effects of cytokines are mediated indirectly via the induction of other mediators such as PGE_2, which directly bind to their cognate receptors on nociceptor afferents and sensitise them. Evidence of this was shown in earlier studies, where pre-treatment with intraplantar indomethacin (COX inhibitor) attenuated IL-1β or IL-6 evoked behavioural hyperalgesia, whilst pre-treatment with atenolol (B_1 blocker) attenuated IL-8/CXCL8 evoked hyperalgesia (Cunha et al., 1991; Cunha et al., 1992), indicating that these cytokines can elicit their effects indirectly via the COX pathway or the sympathetic nervous system, respectively. In accordance with these findings, later studies showed that IL-1β and TNF-α signalling induces NF-κB mediated transcription of a number of genes including COX-2, NO, IL-1β, TNF-α and IL-6 (Pahl, 1999; Moalem and Tracey, 2006). IL-1β has also been shown to mediate thermal hyperalgesia via activating the iNOS-NO cascade in the spinal cord (Sung et al., 2004). Furthermore, IL-6 promotes the induction of BDNF in rat DRG neurons, which is attenuated in IL-6 KO mice (Murphy et al., 2000). These mice also exhibited attenuated pain hypersensitivity after injury, suggesting that IL-6 contributes to sensitisation via BDNF synthesis (Murphy et al., 2000). IL-6 also promotes OX-42 expression in spinal microglia as well as the up-regulation of the chemokine CX_3CR1 (Latremoliere et al., 2008; Lee et al., 2010).

In the spinal cord, pro-inflammatory cytokines secreted by microglia and astrocytes enhance neuronal excitability and synaptic transmission, which are characteristic features of central sensitisation (Woolf and Salter, 2000; DeLeo and Yezierski, 2001; Watkins et al., 2001). IL-1β, TNF-α and IL-6 perfusion can augment excitatory AMPAR and NMDAR-induced currents, while IL-1β can inhibit GABAergic and glycinergic currents in lamina II neurons (Kawasaki et al., 2008). These modulatory effects are possibly via the induction of protein kinases, which phosphorylate excitatory and inhibitory receptor subunits and mediate transcriptional-dependent changes that contribute towards long-term neural plasticity (Ji et al., 2003; Kawasaki et al., 2008).

During inflammation the most important role of chemokines is the promotion of leukocyte migration and recruitment to the site of damage. Experimental evidence suggests that these

signalling molecules contribute to nociception mainly by activating immune cells in the periphery or spinal microglia. However, chemokines may also be able to exert direct effects via chemokine receptors expressed by primary afferent neurons or second order dorsal horn neurons. Similar to previous studies on cytokines; peripheral or central administration of chemokines elicits pain behaviours in rodents, which can be reversed via the administration of neutralising antibodies (Clark et al., 2007b; Thacker et al., 2009; Kiguchi et al., 2010b; Kiguchi et al., 2010a; Dawes et al., 2011). In addition, the development of pain behaviours is abolished in CCR2 and CX_3CR1 (CX_3CL1/fractalkine receptor) KO mice in various pain models (Abbadie et al., 2003; Staniland et al., 2010).

In response to nerve injury macrophages infiltrate the peripheral nerve and DRG and up-regulate the expression of the fractalkine receptor CX_3CR1 and the production of the protease cathepsin S (CatS) and the chemokine IL-8/CXCL8 (Barclay et al., 2007; Holmes et al., 2008). CXCL8 was one of the first chemokines implicated in nociceptive transmission as intradermal injection produces hypersensitivity in rats, as previously discussed (Cunha et al., 1991). Similarly fractalkine is also pro-nociceptive when administered intrathecally and CX_3CR1 null mice exhibit attenuated pain behaviours after nerve injury (Milligan et al., 2005; Clark et al., 2007b; Staniland et al., 2010). In the spinal cord the membrane-bound form of fractalkine is cleaved from neurons by the microglial-derived CatS and may subsequently bind to CX_3CR1, which is exclusively expressed by spinal microglia (Clark and Malcangio, 2012). This feedback mechanism initiates the activation of the p38 MAPK pathway and subsequent release of pro-inflammatory mediators that contribute to pain hypersensitivity (Clark et al., 2007b; Clark et al., 2011). In addition, intraplantar injection of CatS elicited transient mechanical hyperalgesia in naïve rats, whereas systemic administration of an irreversible CatS inhibitor reversed mechanical hyperalgesia in nerve-injured rats (Barclay et al., 2007).

Other chemokines suggested to contribute to neuron-glia nociceptive transmission are CCL2 and CCL3. Spinally released CCL2 and CCL3 from sensory neurons may recruit and activate $CCR2^+$ and $CCR1/CCR5^+$ microglia cells, respectively. This is supported by studies demonstrating that the exogenous application of CCL2 or CCL3 to the spinal cord induces microglia activation and hyperalgesia in rodents, which is abolished in CCR2 null mice or via the administration of CCL2 or CCL3 neutralising antibodies (Zhang et al., 2007; Kiguchi et al., 2010b). In the periphery CCL2 is released in large amounts from Schwann cells and constitutes a crucial chemoattractant for infiltrating $CCR2^+$ macrophages. The migration of macrophages occurs 2-3 days post injury, in accordance with the onset of WD (Gaudet et al., 2011). Thus it is not surprising that CCR2 null mice show attenuated macrophage

recruitment and WD as well as reduced behavioural hypersensitivity (Siebert et al., 2000; Abbadie et al., 2003). CCL3-CCR1 signalling has also been proposed to elicit some interesting peripheral actions that contribute to pain hypersensitivity, such as the sensitisation of TRPV1 receptors in DRG neurons. CCR1 and TRPV1 are co-expressed in small to medium sized DRG neurons. Activation of CCR1 initiates PLC mediated hydrolysis of PIP_3 and Ca^{2+} mobilisation. This leads to the activation of PKC, which is proposed to phosphorylate TRPV1 and remove inhibitory PIP_2, leading to thermal hyperalgesia (Zhang et al., 2005a).

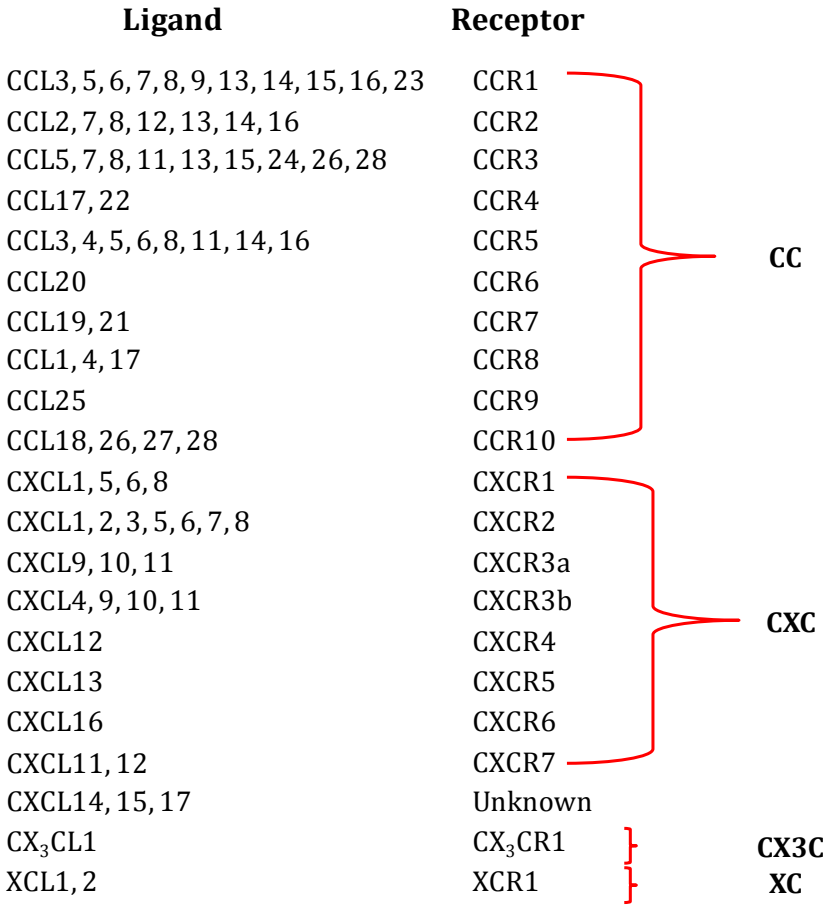

Figure 1.4: Chemokine ligands and their receptors

Chemokines are classified into 4 main groups (CC, CXC, CX3C, XC) according to the position of the first two conserved cysteine residues near the N-terminus. Functionally, this group of approximately 50 signalling molecules exhibits great redundancy and overlap, as there are several ligands for each of the receptors. Likewise, single chemokines are recognised by multiple receptors expressed by a range of cell types including leukocytes, neurons and glial cells (Wells et al., 2006).

Although only some of the literature concerning cytokines and chemokines in pain has been discussed, it is evident that these signalling molecules play a crucial and complex role in the development and maintenance of chronic pain in the nervous system. The immune system and its array of signalling molecules have been implicated in various diseases associated with chronic pain such as diabetes, MS, RA, fibromyalgia, Crohn's disease and IBS (Sommer and Kress, 2004; Abbadie, 2005; McMahon et al., 2005; Austin and Moalem-Taylor, 2010; Calvo et al., 2012). In the clinic, evidence of elevated levels of chemokines and cytokines as well as increased leukocyte counts in diseased tissues have been reported in patients with various pain associated pathologies. For example, in patients with inflammation of the connective tissue, the severity of reported pain correlates with levels of TNF-α in the synovial fluid (Nordahl et al., 2000). Similarly, raised levels of CXCL8 or CCL2 were found in the cerebral spinal fluid (CSF) of patients with back pain and demyelinating polyneuropathy (Brisby et al., 2002; Ochi et al., 2003). In cohorts of patients with complex regional pain syndrome (CRPS), painful neuropathy or spinal cord injury, levels of pro-inflammatory TNF-α, IL-2 and IL-6 were raised, whilst levels of anti-inflammatory IL-4 and IL-10 were reduced. Conversely, patients with painless neuropathy exhibited increased levels of anti-inflammatory cytokines (Davies et al., 2007; Uceyler et al., 2007b; Uceyler et al., 2007a). In addition to raised expression of cytokines, evidence of increased inflammatory cell recruitment has been reported in patients. For example, patients with CRPS showed an enhanced pro-inflammatory monocyte phenotype, in contrast to healthy control patients (Ritz et al., 2011) and in nerve biopsies from neuropathic pain patients the severity of immune cell infiltration correlated with the extent of experienced pain (Lindenlaub and Sommer, 2003). Microgliosis in the thalamus of patients suffering from chronic phantom-limb pain has also been documented in a PET scan study (Banati et al., 2001) and evidence of gliosis in the spinal cord has been reported in a post-mortem examination of a CRPS patient (Del Valle et al., 2009). Furthermore, patients with inflammatory diseases such as interstitial cystitis and chronic pancreatitis, where pain is a cardinal sign, have increased levels of mast cells compared to patients without pain (Oberpenning et al., 2002; Hoogerwerf et al., 2005). Approximately 90% of MS patients exhibit elevated levels of immunoglobulin G in the brain or cerebrospinal fluid, which is indicative of CNS inflammation (Gilden, 2005). Unsurprisingly CNS diseases such as Parkinson's disease, Alzheimer's disease and stroke may also be associated with a pro-inflammatory component and an altered immune cell presence (DeLeo and Yezierski, 2001), however further research is required to fully understand the mechanisms and implications of this.

In conclusion, it is apparent that basic research as well as some clinical evidence strongly supports the role of immune cells and pro-inflammatory cytokines/chemokines in chronic

pain mechanisms. Therefore, the development of novel immunomodulatory analgesics that are selective for particular receptors could provide a successful approach in the treatment of chronic pain. Moreover, as chemokines signal via GPCRs, they are plausible targets for pharmacological manipulation with regards to the immense success of current drugs on the market that largely act on this class of receptors.

1.11 GPR84 (EX33)

In a series of screening studies GlaxoSmithKline identified the orphan GPR84 as a promising immune cell target in chronic pain pathways. Therefore, this thesis examines GPR84 as a novel candidate for the treatment of chronic pain. Despite being discovered well over a decade ago, very little is known about GPR84 and its functional role. However, some groups have utilised transgenic mice and heterologous *in vitro* systems to elucidate the contribution of GPR84 in neuroimmune and neuroinflammatory processes.

GPR84 consists of a generic heptahelical structure of a typical GPCR and is thought to belong to the rhodopsin superfamily, with little similarity to other known receptors. Expression analysis has revealed that this receptor is predominantly expressed in hematopoietic tissues in both humans and mice, and that particularly high levels of GPR84 mRNA are found in bone marrow. In the mouse there is also some expression in the spleen, lung and lymph nodes (Wittenberger et al., 2001; Yousefi et al., 2001; Wang et al., 2006a). Strikingly, GPR84 expression is restricted to immune cells and exclusive to microglia in the CNS, while upon appropriate immune stimulation such as LPS exposure, GPR84 expression is considerably up-regulated. TNF-α and IL-1β can also induce GPR84 expression and accordingly, LPS-induced GPR84 expression was attenuated in TNF-α and IL-1β null mice (Wang et al., 2006a; Bouchard et al., 2007; Lattin et al., 2008). This finding is consistent with the up-regulation of GPR84 mRNA in cortical and spinal microglia in a model of endotoxemia (systemic administration of LPS) and EAE and perhaps indicates a role in neuroinflammation (Bouchard et al., 2007). Furthermore, its restricted expression and up-regulation only upon immunostimulation makes it an appealing target for selective pharmacological manipulation. A selective ligand for GPR84 is yet to be identified. However, free fatty acids (FFAs) of a medium chain length of C9-C14, including undecanoic acid (C11:0), capric acid (C10:0) and lauric acid (C12:0), have exhibited efficacy in GPR84 transfected Chinese hamster ovary (CHO) cells (Wang et al., 2006a). Little is known about the signalling pathway of this receptor, although in one study Wang et al. (2006) showed that capric acid inhibited forskolin-induced cAMP in CHO cells with greater efficacy than other screened ligands. It

was also shown that this effect was *Bordetella pertussis* toxin-sensitive, indicating that GPR84 may be coupled to the $G\alpha_{i/o}$ family (Wang et al., 2006a; Suzuki et al., 2013). However, these findings were opposed by a later study that demonstrated that medium chain free fatty acids (MCFFAs) do not signal via a $G\alpha_{i/o}$ coupled pathway in neutrophils (Versleijen et al., 2009). FFAs have diverse actions on a number of different tissues and are associated with diseases such as diabetes, obesity and dyslipidemia (Hwang, 2000; Evans et al., 2004). Therefore, it is possible that FFAs have an immunomodulatory role via GPR84 mediated signalling, providing a feasible link between obesity-related metabolic syndromes and inflammation. Intriguingly, GPR84 has been reported to be up-regulated in adipocytes of high fat chow induced obese mice in response to TNF-α release from infiltrating macrophages, suggesting a potential link between GPR84 signalling and inflammation-induced adiposity and diabesity (Nagasaki et al., 2012).

There is some evidence suggesting that GPR84 may be involved in the regulation of a subset of chemokines and cytokines. Wang et al. (2006) showed that undecanoic acid, capric acid and lauric acid were able to dose-dependently increase the secretion of IL-12p40 from macrophages under LPS stimulated conditions. Pro-inflammatory IL-12 plays a key role in promoting Th1-driven immunity and inhibiting Th2 anti-inflammatory responses. This indicates that activation of GPR84 promotes Th1 differentiation and the production of Th1-associated cytokines such as INF-γ and IL-2. In accordance with this finding, Venkataraman and Kuo (2005) found that when stimulated under Th1 or Th2 differentiation conditions, GPR84 null T-cells exhibited enhanced production of Th2 cytokines IL-4, IL-5 and IL-13. Interestingly, Th1-driven immunity is associated with many autoimmune and inflammatory diseases such as MS, IBS and RA (Verri, 2005). However, despite a hyper Th2 cytokine phenotype and augmented anti-CD3 induced production of IL-4, GPR84 null mice exhibit normal T and B cell proliferation (Venkataraman and Kuo, 2005).

More recent studies using modified medium chain FFAs with additional hydroxyl groups or the surrogate agonist, 6-n-octylamino uracil (6-OAU), revealed that GPR84 promotes leukocyte and macrophage chemotaxis. It was also found that under LPS-stimulated conditions GPR84 activation via these ligands resulted in the production of pro-inflammatory IL-8/CXCL8 from leukocytes and TNF-α from macrophages (Suzuki et al., 2013). In addition, systemic administration of 6-OAU in rats increased plasma levels of the potent neutrophil and macrophage chemoattractant, CXCL1 (Suzuki et al., 2013).

Owning to the compelling body of evidence on the interaction between neurons, immune and glial cells, it is now recognised that the pathogenesis of chronic pain is not limited to the

aberrant activity of neurons but also depends on a self-perpetuating neuro-immune component (Marchand et al., 2005; Scholz and Woolf, 2007; Thacker et al., 2007; Austin and Moalem-Taylor, 2010; Calvo et al., 2012). Therefore, researchers are challenged with the diversity of neuronal-immune-glial interactions in their quest to identify novel exploitable targets for the treatment of neuropathic pain. Pro-inflammatory GPR84 is an exciting new candidate in the field of chronic pain, not only because it is restricted to immune cells but also due to the fact that it is only up-regulated upon appropriate immunostimulation. Thus pharmacological manipulation of this receptor is likely to have limited side effects, which is always a detrimental set back in patient health care treatment. Although there is currently no evidence for a role of this receptor in nociceptive transmission, up-regulation of GPR84 has been observed in clinically relevant animal models of diabesity and EAE, which feature pain-associated pathologies (Bouchard et al., 2007; Nagasaki et al., 2012). Furthermore, the current literature indicates that GPR84 promotes a pro-inflammatory T cell phenotype and the release of a subset of cytokines known to contribute to inflammation and nociceptive signalling. Therefore, GPR84 is a promising and relevant target to examine in the context of chronic pain.

1.12 Aims of thesis

The aim of this thesis is to investigate the role of GPR84 in chronic pain mechanisms. In *Chapters 1* and *2* we characterise mechanical and thermal thresholds of GPR84 transgenic mice using a range of behavioural tests in a model of nerve injury (PNL) and in two models of inflammation (CFA, LPS). We immunohistochemically examine the spinal microglial and peripheral macrophage responses in these models, as GPR84 is an immune cell expressed receptor and these cells are well documented to play a prominent role in persistent pain mechanisms. To gain an understanding of the functional role of GPR84 in pain pathways, we investigate the transcriptional regulation of 92 different chemokines, cytokines, growth factors and cell markers known to be immune-regulated in the sciatic nerve and spinal cord tissues of nerve injured GPR84 WT and KO mice. Similarly, we profile LPS-induced gene transcription in GPR84 WT and KO macrophages to investigate whether GPR84 regulates the pro-inflammatory response of these immune cells. Lastly, *Chapter 3* entails a screening study of three potential GPR84 ligands, examining their selectivity and efficacy using Ca^{2+} and cAMP signalling assays. Here the aim is to identify a selective agonist that could be utilised in further studies to facilitate our understanding of the role of GPR84 in chronic pain mechanisms.

To summarise, in this thesis we have used a combination of behavioural testing, molecular and biochemical techniques to test the hypothesis that pro-inflammatory GPR84 contributes to persistent pain pathways via the modulation of immune cells.

Chapter 2

The Role of GPR84 in Neuropathic Pain

2.1 Introduction

2.1.1 Neuropathic pain

Neuropathic pain is defined as ‘‘pain arising as a direct consequence of a lesion or disease affecting the somatosensory system” (Treede et al., 2008). Aside from traumatic nerve injuries such as mechanical damage during surgery or compression injury in carpal tunnel syndrome, neuropathic pain is associated with a wide spectrum of neuropathologies. Such diverse aetiologies include metabolic diseases (diabetic polyneuropathy); viral infections (Human Immunodeficiency Virus (HIV), *Varicella zoster* virus (VZV)); neurotoxicity (chemotherapeutic drugs or anti-viral therapy); autoimmune diseases (MS) and sympathetic nervous system dysfunction (CRPS) (Zimmermann, 2001). Symptoms of neuropathic pain are typically associated with sensory abnormalities that clinically manifest as a combination of paraesthesias (tickling, tingling, burning, pricking, numbing); dysaesthesias (electrical, ‘pins and needles’, itching); evoked pain (mechanical allodynia, thermal hyperalgesia) and spontaneous pain. While these are considered as positive symptoms that are caused by hyperexcitability of the nervous system, patients also experience negative symptoms (hypoesthesia and hypoalgesia) as a result of axonal degeneration and neuronal necrosis. Due to treatment side effects and accompanying co-morbidities such as poor sleep, depression and anxiety, neuropathic pain severely debilitates the lives of patients. Despite the overwhelming number of analgesics available, therapeutic treatment is still considered to be insufficient and many patients report lack of adequacy in the management of their pain. Therefore, optimal pain care continues to remain elusive (Breivik et al., 2006).

2.1.2 Animal models of neuropathic pain

Due to difficulties in studying the underlying pathophysiological mechanisms of neuropathic pain in humans, several animal pain models have been developed as tools to assist research for more effective treatments. Many of these involve surgical injury to the sciatic nerve to induce sustained pain-related behaviours of the hind paw (see Fig. 2.1). Complete sciatic nerve transection (CST) was one of the first models employed to study neuropathic pain mechanisms and closely simulates symptoms of phantom limb pain seen after complete axotomy in humans (Wall et al., 1979). As a result of motor dysfunction caused by complete deinnervation of the limb, the assessment of pain behaviours to an applied stimulus is not

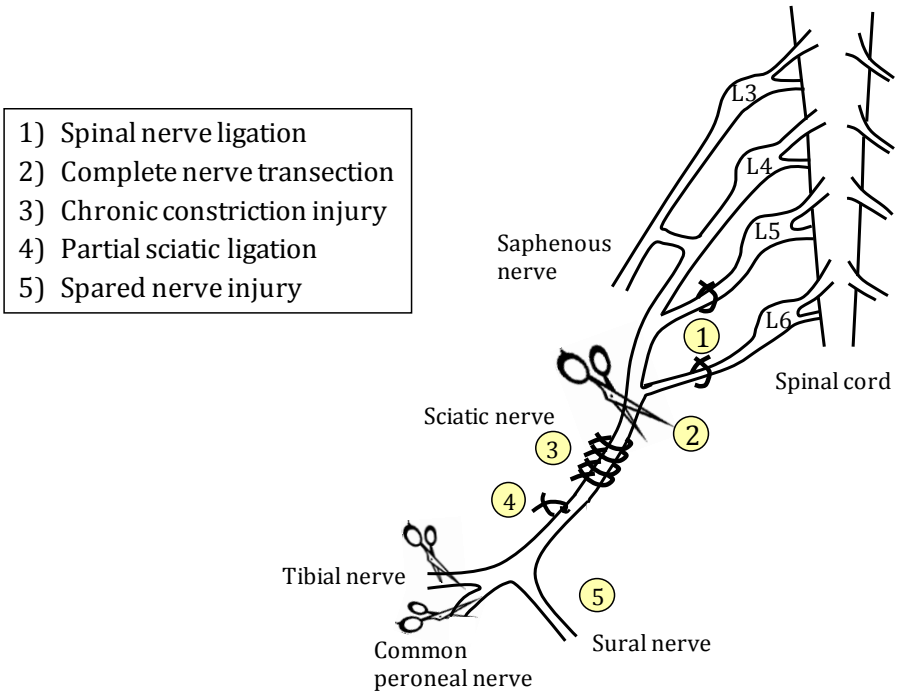

Figure 2.1: Commonly used traumatic nerve injury models of neuropathic pain

possible in this model. However, animals do show autotomy (self-mutilation), which is thought by many to reflect a level of spontaneous activity in the damaged sensory neurons and has thus been used to quantify the degree of neuropathic pain. Although in similar models of nerve lesions this autotomic behaviour is absent due to the presence of some sensory innervation. Therefore the self-mutilating response in the CST model may be attributed to excessive grooming in the absence of sensory feedback from the affected hind paw rather than representing an abnormal pain state (Rodin and Kruger, 1984).

The CCI model, entails loosely tying the sciatic nerve with four chromic catgut ligatures to simulate a chronic nerve compression injury and is accompanied by an inflammatory response and a subsequent degree of peripheral nerve axotomy (Bennett and Xie, 1988). Simulation of partial injuries encountered in the clinic is achieved by the PNL model (Seltzer et al., 1990). This model involves the tight ligation of 1/3 to 1/2 of the sciatic nerve, which keeps some fibres intact so that painful sensory information can still be detected from the periphery. In this model a greater number of axons are injured, and these consist of a random subset of damaged and intact L4 and L5 fibres. Due to inconsistencies in constriction, both the PNL and CCI models exhibit some variability.

The spinal nerve ligation (SNL) (Kim and Chung, 1992) and spared nerve injury (SNI) (Decosterd and Woolf, 2000) models are popular for their accuracy and minimal variability.

SNL is performed via the tight ligation of both or either of the L5 or L6 spinal nerves so that whilst the primary sensory neurons of the L5/L6 DRG are axotomised, L4 is left uninjured. This allows the investigator to determine the relative contribution of injured and intact neurons in the development of pain associated behaviours. SNI entails the sectioning of the tibial and peroneal nerves while the sural nerve is left intact, thus enabling the study of injured and non-injured neuronal populations. These models of traumatic peripheral nerve injury (schematically presented in Fig. 2.1) have been shown to produce neuropathic symptoms such as allodynia and hyperalgesia (except CST). However, the duration and magnitude of these pain components vary considerably (Kim et al., 1997; Dowdall et al., 2005).

In addition to traumatic nerve injury models there are also disease-based models that are considered to be more clinically relevant and representative of the diverse human neuropathic pain condition. These include models of painful diabetic neuropathy such as the streptozocin-induced diabetic neuropathy model (Wuarin-Bierman et al., 1987); models of viral infections such as HIV associated neuropathy (Wallace et al., 2007b) and post-herpetic neuralgia (Fleetwood-Walker et al., 1999); neuropathy induced by chemotherapy and antiretroviral therapy (Aley et al., 1996; Polomano et al., 2001; Wallace et al., 2007a), and bone cancer pain models (Medhurst et al., 2002), although in the latter model there is debate about the degree of nerve injury.

A majority of work published on pain testing in rodents involves the application of mechanical or thermal stimuli to the affected hind paw. This initiates a spinally mediated reflex flexion withdrawal response as a result of the activation of peripheral nociceptors. The application of graded filaments to the plantar surface of the hind paw as a measure of sensitivity to punctuate mechanical stimuli was first described by von Frey (1986). This method was later adapted to enable the calculation of the 50% paw withdrawal threshold (PWT) (Chaplan et al., 1994). Likewise, the application of a heat source in the form of radiant light to the plantar hind paw surface can be used to examine sensitivity to thermal stimuli. This method was developed by Hargreaves and colleagues (1988) and the latency of the withdrawal reflex is measured as an indicator of sensitivity. In addition to these two key methods, the paw-pressure test as a measure of mechanical hypersensitivity, hot-plate and tail-flick tests as measures of thermal sensitivity and cold-plate and acetone tests as measures of cold sensitivity are also regularly used. Whilst these forms of behavioural pain assessment in rodent models are well established in the literature, they do not account for the presence of spontaneous pain or the global impact of pain and poorly address

ethological validity (Andrews et al., 2012). As previously mentioned, the behaviours typically measured are spinal reflexes (paw withdrawal), spino-bulbospinal reflexes (jumping) or innate behaviours (biting, licking, scratching, vocalization and guarding). Importantly, one must note that evoked withdrawal responses are a measure of hypersensitivity (allodynia and hyperalgesia) rather than the pain itself (Mogil, 2009). Furthermore, in the clinical setting spontaneous pain is a much better indicator of a patient's pain rating than measures of hypersensitivity. Moreover, while von Frey fibres are generally used for testing static/punctate allodynia, the most problematic symptom in patients is dynamic allodynia. Consequentially, the clinical reality is poorly reflected by the behavioural measures adopted in animal experiments (Mogil, 2009), an issue that needs careful consideration when interpreting animal pain studies and their translation to the human condition. Hence some research groups are now attempting to establish alternative animal pain paradigms focused on operant measures (Rice et al., 2008; Mogil, 2009; Andrews et al., 2011; Andrews et al., 2012), which can also be used in conjunction with conventional behavioural tests.

2.1.3 Mechanisms of Neuropathic pain: Immune and glial cells

Traumatic nerve injury animal models have been used by many research groups to study peripheral and central neuronal mechanisms in neuropathic pain. However, as a result of tissue damage caused by nerve injury, an inflammatory response generated by the immune system undoubtedly marks the contribution of these non-neuronal cells to neuropathic pain mechanisms (Bennett, 1999). Therefore, it is now recognised that the pathogenesis of neuropathic pain is not limited to the aberrant activity of neurons but also depends on a self-perpetuating neuro-immune component (Marchand et al., 2005; Scholz and Woolf, 2007; Thacker et al., 2007; Austin and Moalem-Taylor, 2010; Calvo et al., 2012).

Nerve injury results in immediate and irreversible interruption of electrical nerve conduction and the intrinsic degeneration of damaged axons in a process referred to as WD, which triggers a vigorous cascade of non-neuronal responses (Gaudet et al., 2011). Schwann cells, the principle glial cells of the PNS that support neuronal function, rapidly undergo a phenotypic switch which involves the secretion of numerous pro-inflammatory cytokines, including IL-1β, TNF-α, IL-6 and PGE_2 as well as MMPs, which coordinate WD and immune cell recruitment (Campana, 2007). In juxtaposition, growth factors such as BDNF and GDNF are also released and transported retrogradely to promote axonal growth and re-myelination (Ramer et al., 2003; Scholz and Woolf, 2007; Austin and Moalem-Taylor, 2010).

One of the first responders to a peripheral insult are the resident mast cells, which degranulate at the site of injury releasing histamine, serotonin, proteases, PGs and chemokines that mediate sensitisation of primary afferent axons and attract neutrophils and macrophages (Austin and Moalem-Taylor, 2010). Experimental evidence has shown that inhibition of mast cell degranulation reduces the infiltration of neutrophils and macrophages, attenuating nerve injury induced hyperalgesia (Zuo et al., 2003).

Subsequent to nerve injury, resident macrophages (the primary phagocytic cells of the PNS) proliferate extensively and circulating monocytes are attracted to the lesion site via chemokines, resembling a 'rapid-response team'. These later acting cells play a crucial role in WD and the phagocytosis of necrotic tissue, cellular debris and axotomised processes (Perry et al., 1987; Austin and Moalem-Taylor, 2010). Inhibition of macrophage infiltration or activation has been experimentally demonstrated to interrupt WD. Here, Perrin et al. (2005) showed that application of neutralising antibodies for the chemokines CCL2 and IL-1β interrupts macrophage recruitment and suppresses myelin clearance, whereas administration of recombinant forms of these chemokines elicits a rapid macrophage response (Perrin et al., 2005). Boivin et al. (2007) demonstrated that mice deficient in TLR signalling exhibited a significant attenuation in the recruitment/activation of macrophage cells and the persistence of myelin debris, delaying regeneration of the injured nerve. In contrast, WD was accelerated via the administration of TLR ligands, and this effect was thought to be partially mediated by macrophages as glucocorticoid treatment resulted in delayed clearance and functional recovery (Boivin et al., 2007). In addition to their role in phagocytosis and regeneration of injured nerves, macrophages have also been implicated in pain-associated behaviour. The most compelling evidence for the role of these cells in neuropathic pain mechanisms comes from a study on C57BL/WLD mice, which have an intrinsic genetic defect in peripheral axons that causes an abnormal rate of WD and delayed macrophage recruitment (Myers et al., 1996). Here it was observed these mice exhibited delayed macrophage recruitment and WD that correlated with reduced CCI-induced thermal hyperalgesia (Myers et al., 1996). Furthermore, it has been demonstrated that systemic depletion of macrophages in a range of animal models of nerve injury not only reduced axonal degeneration but alleviated mechanical and thermal hyperalgesia (Liu et al., 2000; Barclay et al., 2007). Notably, other groups have reported the inability to relieve mechanical allodynia using this approach, hence highlighting the distinct mechanisms underlying different pain modalities (Rutkowski et al., 2000; Barclay et al., 2007).

'Activated' macrophages release many algesic mediators such as TNF-α, IL-1β, IL-6, PGs and NO that directly or indirectly sensitise nociceptors by binding to their cognate receptors and activating various intracellular signalling pathways (Woolf and Ma, 2007). Aptly, this pro-inflammatory macrophage phenotype has also been observed in patients with CRPS, who exhibit raised blood monocyte levels (Ritz et al., 2011). Furthermore, a number of gene profiling studies in rodents have illustrated a dramatic regulation of cytokines in the context of neuropathic pain, highlighting the importance of temporal and spatial expression patterns of pro-inflammatory (particularly IL-1β, IL-6 and TNF-α) and anti-inflammatory (IL-10) cytokines, in correlation with behavioural hypersensitivity and a delayed resolution component (Gillen et al., 1998; Okamoto et al., 2001; Costigan et al., 2002; Tanga et al., 2005). Many of the cytokines and chemokines released following nerve injury modulate the transduction properties of nociceptive sensory axons and evoke ongoing activity in myelinated and unmyelinated axons. Ectopic firing is a crucial component underlying spontaneous activity in neuropathic pain and has been shown to arise in multiple locations, such as at the site of injury and in the DRG (Amir et al., 2005). Increased density of cytokine receptors in nociceptive afferents as a result of enhanced membrane trafficking means that these fibres also become more sensitised and hyper-responsive to inflammatory factors, which may contribute to ectopic firing. For example, raised TNF-α expression has been documented in the injured nerves of patients and rodents (Empl et al., 2001; George et al., 2004). This cytokine is able to directly stimulate neurons, evoke action potential firing and elicit pain behaviours when injected intraneurally in rodents (Wagner and Myers, 1996; Schafers et al., 2003b). Conversely, pre-emptive pharmacological blockade studies using the competitive TNF-α inhibitor, Etanercept, have demonstrated attenuation of pain-associated behaviour in rodents (Sommer et al., 2001; Svensson et al., 2005) and thus this conceptual approach has progressed on to trials of anti-TNF-α therapy in humans.

In addition to the mobilisation of the immune system and accumulation of a large 'inflammatory soup' of mediators within the endoneurium, an immune response also occurs within the proximity of the cell bodies of injured and spared sensory neurons. In response to the release of ATP and perhaps other factors, satellite glial cells become activated, proliferate and release soluble molecules such as TNF-α and IL-1β (Ohara et al., 2009), accompanied by the rapid recruitment of neutrophils, macrophages and T lymphocytes. T lymphocytes have been shown to infiltrate the nerve at a much later stage than their innate immune system counterparts and enter the DRG via deep ganglionic blood vessels and cell surface meninges. This recruitment is perhaps driven by signals originating from neurons and satellite cells that project into the axons of damaged nerves (Hu and McLachlan, 2002;

Moalem et al., 2004). T cells have also been implicated in nerve injury-induced neuropathic pain behaviour and a key study showed that congenetically athymic nude rats, which lack functional T cells, had attenuated mechanical allodynia and thermal hyperalgesia post CCI in contrast to their WT littermate controls (Moalem et al., 2004). Alongside the immune response, the DRG also undergoes cascades of transcriptional changes that encompass the up- and down-regulation of pro-inflammatory mediators, ionotropic and metabotropic receptors, neuropeptides, ion channels, signalling molecules and vesicular proteins (Costigan et al., 2002; Xiao et al., 2002). This extensive phenotypic change contributes to an increase in DRG neuronal excitability, which is synaptically communicated to first order dorsal horn neurons of the spinal cord.

In the CNS, microglia are one of the first responders to disturbances in the homeostasis of the microenvironment by pathogens or damage and undergo a repertoire of morphological, immunophenotypic and gene expression changes (as described in *Chapter 1*). Their numbers increase drastically by means of proliferation and migration in a process defined as microgliosis, a phenomenon also observed in the thalamus of amputee patients with chronic phantom-limb pain and in a post-mortem study of a patient with CRPS where 'reactive' microglia were observed in the spinal cord (Banati et al., 2001; Del Valle et al., 2009). The transition from a normally 'quiescent' to a 'pain-related' enhanced response state (McMahon and Malcangio, 2009) is thought to be initiated by multiple endogenous signals from primary afferent nociceptive inputs, as well as mediators released from localised astrocytes, microglia and neurons. Such mediators are thought to include adenosine, ATP, glutamate, cytokines/chemokines, arachadonic acid, neuropeptides (SP, CGRP) and NO, some of which act on their respective ionotropic or metabotropic microglial expressed receptors (DeLeo and Yezierski, 2001; Watkins et al., 2001). This in turn drives signalling pathways involving the phosphorylation of the MAPKs, p38 and ERK and the subsequent initiation of several transcription factor cascades including NF-κB, which controls the expression of a plethora of pro-inflammatory mediators such as IL-1β, IL-6, TNF-α, PGE2, NOS, COX-2, ATP, BDNF and CatS (DeLeo and Yezierski, 2001; Watkins et al., 2001; Coull et al., 2005; Ji and Suter, 2007; Kawasaki et al., 2008; Clark et al., 2009). The secretion of pro-inflammatory mediators contributes to central sensitisation via enhancing excitatory synaptic transmission and suppressing synaptic inhibition. IL-1β, IL-6 and TNF-α have been shown to augment EPSCs and suppress inhibitory post-synaptic currents (IPSCs) in the superficial dorsal horn of the spinal cord, inducing central sensitisation, hyperalgesia and long-term synaptic plasticity via the induction of CREB induced gene transcription (Kawasaki et al., 2008). Spinal blockade of pro-inflammatory cytokines is analgesic, whilst

spinal injection of recombinant factors is pro-nociceptive (DeLeo et al., 1996; DeLeo and Yezierski, 2001; Watkins et al., 2001).

TLR4 is also an important player in the activation of microglial cells, triggering a cascade of downstream signalling pathways that culminate to engage NF-κB (Baeuerle and Henkel, 1994). In pathological states the TLRs respond to cell body damage, components of the ECM, HSPs 60 and 70, cations and proteoglycan fragments (Tanga et al., 2005). Importantly, data suggests that the TLRs co-ordinate WD in the injured nerve and neuroinflammation via the modulation of Schwann cells/macrophages or microglial cells, respectively (Aravalli et al., 2007). Conversely, pharmacological or genetic manipulation of this single transmembrane receptor results in impairment of these processes and attenuation of behavioural hypersensitivity (Tanga et al., 2005; Boivin et al., 2007). Similar studies involving the manipulation of specific microglial receptors in the CNS: CX_3CR1, $P2X_4$, $P2X_7$, CCR2 and TLR4 (see *Chapter 1*) (Abbadie et al., 2003; Tsuda et al., 2003; Chessell et al., 2005; Tanga et al., 2005; Clark et al., 2010b; Staniland et al., 2010) or the use of general glial inhibitors (Sweitzer et al., 2001; Ledeboer et al., 2005; Clark et al., 2007a) demonstrate inhibition or reversal of neuropathic pain behaviours and together form a wealth of evidence supporting the contribution of microglial cells to experimental pain states. Furthermore, the role of microglial cells in pain has also been explored in humans with post-mortem evidence of 'reactive' microglia and astrocytes in the spinal cords of patients with CRPS (Del Valle et al., 2009). In addition to reports of raised pro-inflammatory and reduced anti-inflammatory cytokine profiles in the CSF of two CRPS patients compared to control patients, which correlated with pain intensity (Alexander et al., 2005).

Microglia are also involved in the recruitment of T cells, which have been shown to infiltrate the spinal cord, peaking in cell numbers at 7 days post nerve injury (Cao and DeLeo, 2008). Cao and DeLeo (2008) reported a significant reduction in behavioural hypersensitivity in $CD4^+$ KO mice that was reversed via the adoptive transfer of $CD4^+$ leukocytes and hypothesised that T cells interact with both microglia and astrocytes to exacerbate inflammation and neuronal sensitisation (Cao and DeLeo, 2008). Subsequent to nerve injury, astrocytes proliferate and undergo considerable morphological and immunophenotypic changes, which was first documented by Garrison et al. (1991). These changes are characterised by hypertrophy and a dramatic increase in GFAP staining that parallels with the extent of behavioural hyperalgesia in rats (Garrison et al., 1991). Recruitment of reactive astrocytes is thought to be due an array of signals from neighbouring microglia, astrocytes and neurons. Once 'activated', astrocytes release many

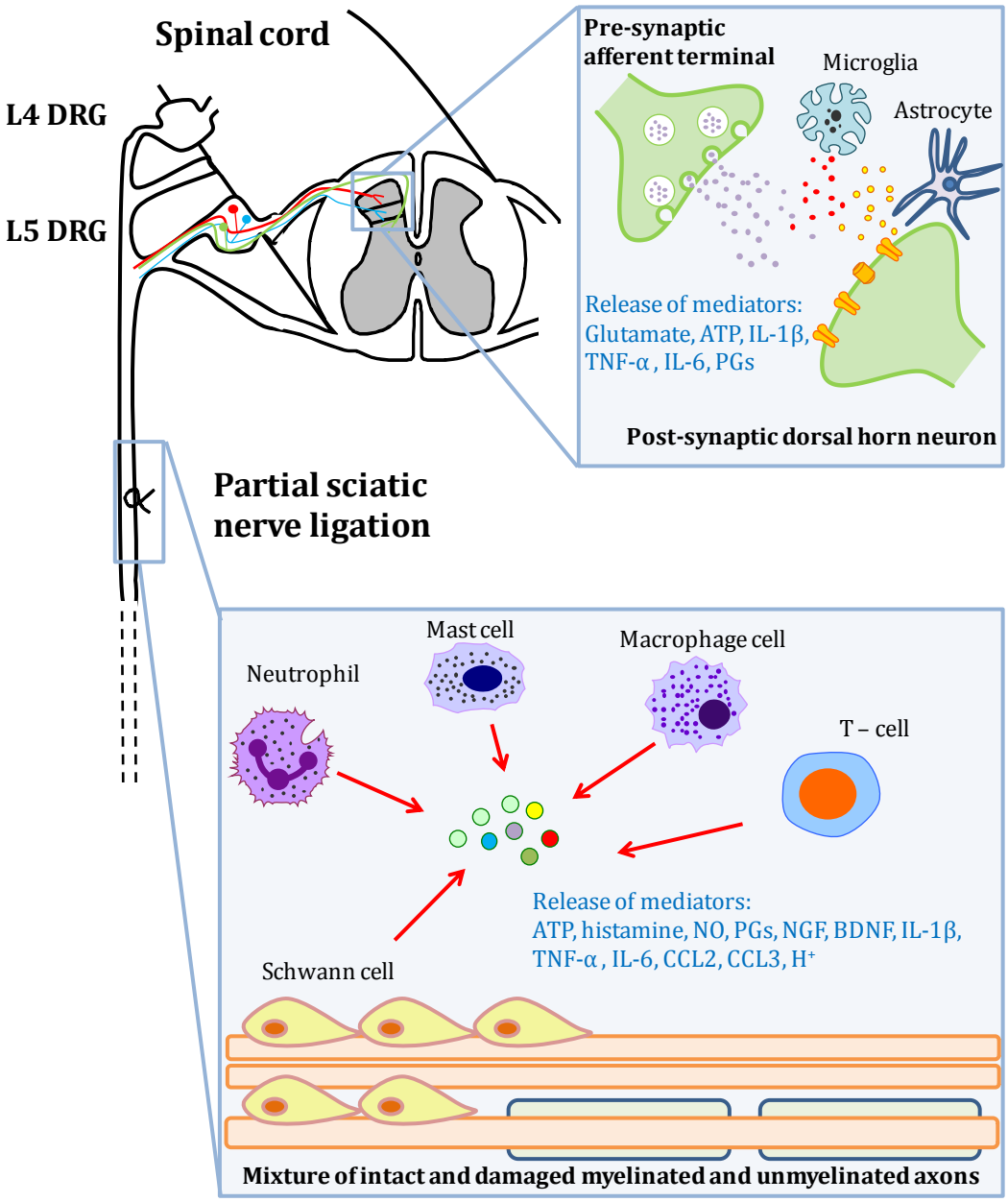

Figure 2.2: Neuroimmune interactions occuring subsequent to peripheral nerve injury

At the site of peripheral nerve injury, Schwann cells and resident mast cells proliferate and release a combination of ATP, growth factors, histamines, cytokines, and TLR ligands, which sensitise axons or may be transported retrogradely to the DRG where they alter gene transcription. The release of mediators also activates resident macrophages and neutrophils and contributes to the recruitment of other immune cells, such as infiltrating monocytes and T-cells. These non-neuronal cells in turn release further algogenic substances that contribute to ectopic activity of the injured nerve. In the CNS, incoming signals from the periphery lead to the activation of dorsal horn neurons, microglia and astrocytes. Activated microglia proliferate and release cytokines such as IL-1β, TNF-α and IL-6, which activate intracellular signalling pathways and initiate further sustained release of mediators that enhance excitability of dorsal horn neurons.

factors through JNK mediated cellular pathways and are essentially thought to play a role in the persistence of pain (Ji et al., 2006; Gao et al., 2009; Ji et al., 2009; Ransohoff and Perry, 2009). Fig. 2.2 summarises the neuroimmune interactions that can occur subsequent to peripheral nerve injury.

In conclusion, experimental evidence has pointed towards a critical role of immune and glial cells as well as pro-inflammatory mediators in the generation of neuropathic pain. It is apparent that specific roles of individual cells and molecules are regarded as particularly important. In terms of translational human research, the immune cell component in chronic pain is very much dependent on genetic and environmental factors as well as the nature of the associated pathology. Despite the growing amount of clinical evidence supporting immune cell involvement in chronic pain, neuro-immune interactions are complex and their role in the induction and maintenance of pain are not yet fully understood. In light of this credible evidence, scientists are challenged with the diversity of neuronal-immune-glial interactions to identify novel exploitable targets in the treatment of neuropathic pain.

GPR84 was identified by GSK as a potential new target for the development of analgesics for chronic pain patients. GPR84 is an immune cell expressed receptor that is up-regulated upon appropriate immunostimulation and has some implications in neuroinflammation (see *Chapter 1*). Although there is currently no evidence for the role of this receptor in nociceptive transmission, an increase in GPR84 expression has been documented in animal models that feature pain-associated pathologies (Bouchard et al., 2007; Nagasaki et al., 2012). Therefore GPR84 qualifies as a valid and interesting new target to examine within the context of chronic pain mechanisms.

2.1.4 Aims

In this chapter we utilised the PNL model (Seltzer et al., 1990) in transgenic mice to examine GPR84 in neuropathic pain mechanisms. The PNL model is documented to produce consistent and reproducible pain-associated behaviours in rodents, which correlates with robust peripheral and central immune and glial reactivity. We assessed neuropathic pain behaviours of GPR84 WT and KO mice in conjunction with a prominent focus on the macrophage and microglia response. We also investigated mRNA transcript expression of 92 different chemokines, cytokines, growth factors and cell markers known to be immune-regulated in the sciatic nerve and spinal cord tissue of nerve injured WT and KO mice. This

approach enabled us to identify putative mediators that are modulated by GPR84 and may thus contribute to neuropathic-pain behaviour via down-stream signalling of this receptor.

2.2 Materials and methods

2.2.1 Generation, Breeding and Genotyping of GPR84 knock-out Mice

GPR84 (NM_030720, ENSMUSG00000063234) KO mice were provided by Deltagen Inc. under a GlaxoSmithKline license agreement (CA). Genomic DNA from recombinant embryonic stem cells 129/OlaHsd was used for gene targeting and assayed for homologous recombination using long range polymerase chain reaction (PCR) analysis (Fig. 2.2A). PCR was used to confirm correctly targeted ES clones using one primer within the LacZ/Neo Cassette and another primer outside the targeting construct for both 5′ and 3′ ends of the targeted locus, as follows:

5′ end: 5' external primer #28016; TGGTCAATCATTGTCCTCTCTGAACC and LacZ/Neo primer #2416; GGGATCTTGGCCATGGTAAGCTGAT; expected amplicon size 4.6kb. 3′ end: 3' external primer #28005 AAACCACAGTTTATCACTTACTAGCCC and LacZ/Neo primer 1431 ACGTACTCGGATGGAAGCCGGTCTT; expected amplicon size 4.0kb.

PCR cycling conditions were 96 °C for 20 s; 30 cycles of 96 °C for 8 s, 63 °C for 10 s, 68 °C for 2 min 15 s; followed by 5 cycles of 96 °C for 8 s, 63 °C for 10 s and 68 °C for 8 min. Those ES cells that were correctly targeted were injected into C57BL/6 host blastocyts to generate chimeric mice. Male chimaeras were crossed with C57BL/6 females to produce heterozygous (HET) N1F0 offspring. HET's were repeatedly bred, or backcrossed, onto the C57BL/6 genetic background, which was later verified using 98 single nucleotide polymorphism markers (Markel et al., 1997; Wakeland et al., 1997). Fully backcrossed mice exhibited > 98% coverage with the C57BL/6 marker. HET backcrossed mice were inter-mated to produce F1 animals homozygous for the GPR84 mutation or WT littermate controls. Mice were genotyped by PCR using the following primers:

GS(E) #35788 5':-ACAGCTCAGATGCCAACTTCTCCTG ;-3',

GS (TE)#35789 5':-TCCTAGAGCAATGAGACAGAGGGTG;-3'

and Neo(T) #40610 5':- GACGAGTTCTTCTGAGGGGATCGATC;-3'

Ear punched samples were lysed and the DNA was run with a Taq polymerase (Qiagen) mix. PCR cycling conditions were 95°C for 3 min, followed by 30 cycles—95°C for 30 s, 58°C for 30 s, 72°C for 30 s, with a final extension at 72°C for 3 min and maintained at 4°C. The PCR products were run and visualised on a 2% agarose gel; the WT allele generated a 344-bp band using primers GS(E) 35788 and GS (TE) 35789, whereas the mutant allele generated a 583-bp band from primers GS (TE) 35789 and Neo(T) 40610 (Fig. 2.2B). All experiments were conducted according to the requirements of the United Kingdom Animals (Scientific Procedures) Act (1986) and conformed to GlaxoSmithKline ethical standards.

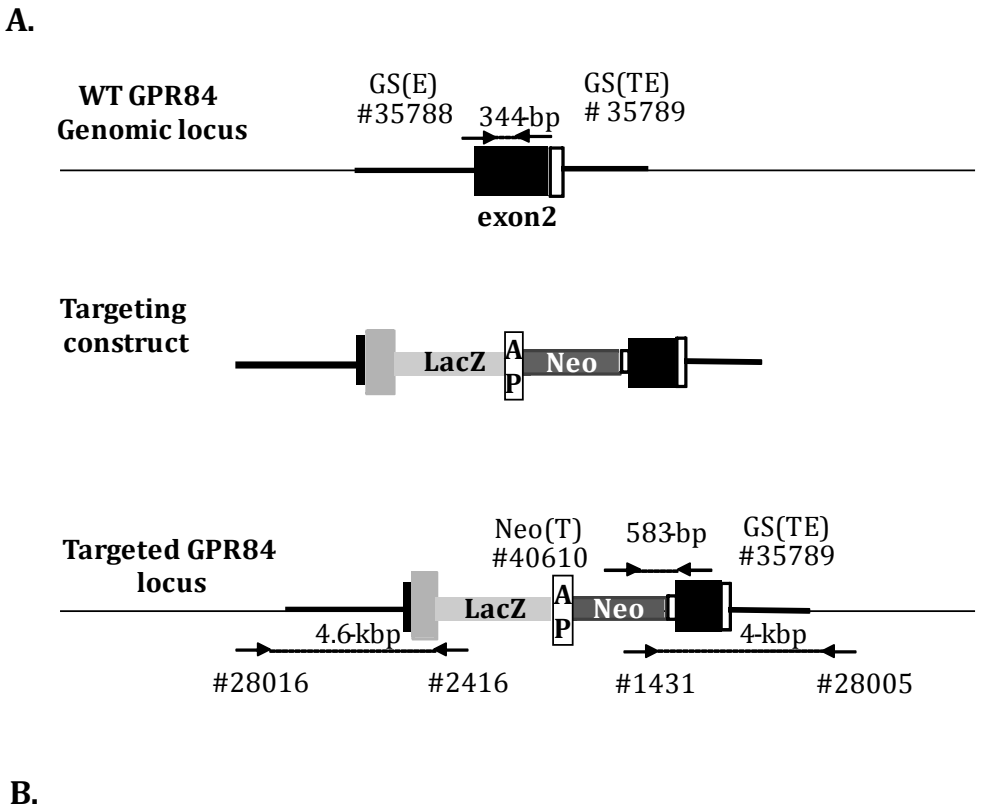

Figure 2.3: Generation of GPR84 KO mice

(A) Schematic of single coding exon 2 is shown. Thicker lines indicate the relative positioning of the gene target. Targeting replaced 257 bp of coding sequence with an Internal Ribosome Entry Site - LacZ-polyA expression cassette and a positive selection cassette that contains the neomycin phosphotransferase gene driven by the PGK promoter (Neo). Correctly targeted ES clones were identified via the PCR primers indicated, which were also used to genotype F1 mice. The insertion of the LacZ IRESLacZ introduces a premature translational stop signal that deletes the first three predicted trans-membrane domain sequences of the seven transmembrane domain receptor molecule. (B) An example of GPR84 genotyping results from F1 intercross. The genotyping primers (GS(T) #35788, GS(TE) #35789, Neo(T) #40610) generate a 344 bp and 558 bp product for WT and KO mice, respectively. In HETs both products are observed.

2.2.2 Animals

Breeding and husbandry

Mice forming the initial breeding pairs were supplied by GlaxoSmithKline, which consisted of HET F1 offspring from WT and KO breeding. HET pairs were bred from 8 weeks old to produce litters of mixed genotypes according to Mendelian genetics: 50% HETS, 25% homozygous WT and 25% homozygous KO. Breeding pairs and their litters were delegated identity codes. From 10 days of age each mouse received an identity ear notch mark and a unique corresponding animal number and was genotyped as previously described. Breeding pairs had a maximum of 6 litters before the pair were retired. On average, litter sizes were around 4-12 pups and weaning occurred 21 days after birth. WT and KO mice were used for experimental purposes from 7-14 weeks of age and HETS were only used for breeding.

Experimental animals

Experiments were conducted on randomly selected mixed sex and age-matched mice weighing 20-25 g (7-14 weeks old). Mice were housed individually or in groups (no more than 4 per cage) in standard environmental conditions (12 hour light/dark cycle) with *ad libitum* access to food and water. Animal husbandry and experiments were carried out in a non-sterile housing environment in accordance with the United Kingdom Animals (Scientific Procedures) Act 1986.

To calculate the number of animals required for behavioural studies *a priori* power analysis was carried out using G*Power (v-3.1.7) software. Based on an estimated 60% reduction effect (deduced from previous experimental studies in our lab), the software estimated that a total sample size of 32 (n = 8 per group) would be required to detect statistical differences ($\alpha = 0.05$, $1-\beta = 0.95$, $d = 7$). Four groups of animals were tested including a control sham-operated group and a nerve-injured group for each genotype. For all studies the experimenter was blinded to genotype and treatment. Allocation concealment was carried out by assigning individual animals with identification numbers (as previously mentioned) and by employing an independent investigator to re-blind animals after surgery. Blinding codes were broken after completion of behavioural experiments to determine if further anatomical assessment was necessary. According to pre-determined exclusion criteria, animals were excluded from experimental analysis if they died during surgery, if the surgery

was flawed or if animals reached end points as specified by the project license e.g. excessive self-mutilation.

2.2.3 Neuropathic pain model: PNL

Animals were anesthetised with 2-3% isoflurane (Abbott Animal Health, UK) inhalation anaesthesia. The left hind paw was secured, shaved and sterilised. The sciatic nerve was carefully exposed and isolated from neighbouring connective tissue via a small incision midway of the left thigh. At a site within close proximity of the trochanter, distal to the posterior biceps semitendinosus nerve branch, a 5-0 vicryl suture (Ethicon, UK) was inserted into the nerve and ligated so that 1/3 to 1/2 of the nerve was held tightly within the ligature, as previously described (Seltzer et al., 1990). In sham operated mice the same procedure was carried out except that the nerve was not ligated. Mechanical (von Frey) and thermal (Hargreaves) withdrawal thresholds were examined pre-surgery (at least three baseline measurements) and post-surgery on days 4, 7, 11, 14, 18 and 21.

2.2.4 Mechanical withdrawal threshold

Von Frey

Tactile mechanical thresholds of alert and unrestrained mice were examined via von Frey hair application (0.008-1 g, Touch Test, Stoelting, USA) to the plantar surface of the hindpaw via the 'up-down' method (Chaplan et al., 1994). Before testing mice were acclimatised for a period of 1 hr in individual acrylic testing cubicles (8 x 5 x 10 cm) on an elevated wire mesh floor. Placement in testing cubicles was selected at random for each testing day. This enabled access to the lateral paw surface. Calibrated von Frey hairs were applied starting with the 0.6 g filament, in an alternate fashion to the left and right hind paw. The flexible nylon hair was applied so that the fibre bent for a duration of 3 s or until a paw withdrawal reflex occurred that was not coupled with movement or grooming. A positive withdrawal response is followed by a lower force hair and vice versa for a negative response until a change in behaviour occurs. Using this 'up-down' sequence four subsequent hairs were assessed and the 50% PWT was calculated according to the method described by Dixon (1980).

Paw pressure

Noxious mechanical thresholds were examined in the hindpaws of restrained alert mice via an Analgesymeter (7200; Ugo Basile, Italy) (Randall and Selitto, 1957). Each hindpaw was tested separately; briefly, the plantar surface was placed on a pedestal with a probe resting on the dorsal surface. Increasing pressure was applied via the probe, up to a maximum of 120 g to prevent tissue damage. The nociceptive threshold was taken as the force at which the mouse responded.

2.2.5 Thermal withdrawal threshold

Hargreaves

Thermal thresholds in unrestrained and alert mice were determined with the Hargreaves method using the Plantar Test (7370; Ugo Basile, Italy) (Hargreaves et al., 1988). Prior to testing, mice were acclimatised for 1 hr in individual acrylic testing cubicles (8 x 5 x 10 cm) on a glass plate. Placement in testing cubicles was selected at random for each testing day. An infrared light source of an arbitrary intensity of 30 (calibrated to elicit a paw withdrawal latency (PWL) of 10-15 s in naïve mice) was directed onto the plantar surface of the hind paw through the glass plate. The PWL was automatically recorded in secs upon a withdrawal reflex. The left and right paws were tested alternately and responses were recorded for each paw on three separate occasions with at least 2 mins between assays. Each test had a maximum latency of 23 s to prevent tissue damage.

Tail immersion-withdrawal

Thermal thresholds of the tails of lightly restrained mice were examined via the tail immersion-withdrawal test (Mogil et al., 1999). The distal third of the tail was directly immersed in water at a set temperature of either 49°C or 52°C ± 0.2°C (Grant SUB14; Grant Instruments Ltd, UK). The thermal withdrawal latency was recorded to the nearest 0.01 s as a characteristic abrupt tail reflex. A maximum latency of 20 s and 10 s was permitted at temperatures of 49°C and 52°C, respectively, to prevent tissue damage.

Hot plate

Noxious thermal thresholds of the hind paws were examined via the hot plate test (Eddy and Leimbach, 1953) using a hot/cold plate (IITC Life Sciences, USA) set at a temperature of 49°C ± 0.1°C. Unrestrained mice were placed on the hot plate in a 10 cm-diameter acrylic testing box. A jumping, licking and stamping reflex was taken as the latency to respond and recorded to the nearest 0.01 s. A maximum latency of 20 s was permitted to prevent tissue damage.

Cold plate

Noxious cold thresholds of the hind paws of lightly restrained mice were examined using the cold plate (IITC Life Sciences, USA) set at a temperature of 10°C ± 0.1°C. Each paw was tested separately by being placed with the plantar surface touching the plate. The latency to withdraw was taken as the threshold and recorded to the nearest 0.01 s. A 20 s cut-off was implemented to prevent tissue damage.

Locomotor function (RotaRod)

Balance and co-ordination was examined via the locomotor test, using a RotaRod that accelerates from 2 to 40 rpm over a period of 300 s (7650; Ugo Basile, Italy). Mice were initially trained before testing. Unsuccessful test runs were trialled again and no mice remained on the apparatus after 100 s.

2.2.6 Tissue preparation and immunohistochemistry

On days 7 or 21 following PNL or sham surgery, GPR84 WT and KO mice were anaesthetised with sodium pentobarbital (0.2 g/mL intraperitoneal (i.p.); Euthatal, Merial Animal Health Ltd) and perfused transcardially with a 0.9% saline and 0.1% heparin solution (Leo Laboratories Ltd, UK) followed by fixation with 4% paraformaldehyde (PFA) (VWR, UK) in 0.1 M phosphate buffer (PB). Lumbar spinal cord and sciatic nerve were dissected and post-fixed for 2 hrs in PFA and cryoprotected in a 20% sucrose/0.1 M PB solution (VWR, UK) for a minimum of 3 days at 4°C. Subsequently, tissue was embedded in Optimum Cutting Temperature (OCT) medium (VWR, UK), snap frozen with liquid nitrogen and stored at -80°C. Prior to embedding sutures were removed from injured sciatic nerves. Transverse spinal cord sections of the L4 and L5 lumbar region and longitudinal nerve sections were

cut on the cryostat in sets of 8 series at 20 μm and 15 μm thickness, respectively, and subsequently thaw-mounted onto Superfrost plus microscope slides (VWR, UK). After drying, 7 day post-PNL or sham surgery spinal cord sections were incubated overnight with primary antibody solution for p-p38 (rabbit anti-p-p38; 1:100; Sigma, UK), and visualised with extra avidin-FITC following two stages of signal amplification with Avidin Biotin Complex (ABC; Vector Laboratories, USA) and biotinyl tyramide (PerkinElmer Life Sciences, UK) as previously shown (Clark et al., 2006). The sections were then incubated overnight with the second primary antibody, raised against rabbit anti-Iba1 (1:1000; Wako Chemicals, Germany). Spinal cord (21 day) and sciatic nerve sections were only incubated with Iba1. After anti-Iba1 incubation sections were incubated with the secondary antibody solution for 2 hrs (1:1000; IgG conjugated Alexa Fluor 488 or 546; Invitrogen, USA). All antibodies were prepared in PBS supplemented with 0.1% Triton X-100 (VWR, UK) and 0.2% sodium azide (Sigma, UK). Slides were carefully cover slipped with Vectashield Mounting Medium containing 4',6-diamidino-2-phenylindole (DAPI) (Vector Laboratories, UK), nail-varnished and dried.

Quantification of immunoreactivity

Images were visualised and captured using a Zeiss Axioplan microscope (Zeiss, UK) and for blinding purposes were labelled according to the identification code of the animal. Blinding codes were broken after study completion. Analysis of p-p38 and Iba1 immunoreactivity was performed by counting the number of positive profiles within three fixed $4x10^4$ μm^2 boxes in the lateral, central and medial areas of the dorsal horn, using the nuclear marker DAPI to assist in determining positive cells, as previously described (Clark et al., 2007a). A mean value was obtained for both the ipsilateral and contralateral dorsal horns of a minimum of three sections per animal. For analysis of Iba1 staining in the sciatic nerves, four boxes of $4x10^4$ μm^2 area, two distal and two proximal to the nerve lesion, were placed randomly along the nerve. The number of Iba1 positive cell profiles were counted within the boxes and a mean value was obtained for both the distal and proximal regions of the nerve. A minimum of three sections per animal were assessed. The experimenter was blinded to both the genotype and treatment throughout the analysis.

2.2.7 RNA extraction and cDNA synthesis

On days 7 or 21 following PNL or sham surgery, mice were anaesthetised with sodium pentobarbital (0.2 mg/mL i.p.); Euthatal, Merial Animal Health Ltd, UK). The lumbar regions

of the spinal cord were quickly dissected, separated into the ipsilateral and contralateral sides and placed into separate 1.5 mL Eppendorf tubes. The ipsilateral and contralateral sciatic nerves of approximately 1 cm in length were also collected and stored in separate Eppendorf tubes. The collected tissue was immediately snap frozen in liquid nitrogen and stored at -80°C for further processing. RNA was extracted via homogenising the tissue samples using a hybrid method of phenol extraction (Trizol, Invitrogen, UK) and column purification (RNeasy, Qiagen, UK). For injured sciatic nerves, the sutures were removed prior to RNA extraction and mini elute columns (Qiagen, UK) were used, which are optimized for samples with small RNA amounts. Sham nerves were pooled to increase the yield of RNA isolation. After purification the RNA was eluted using RNAse-free water and its concentration and purity were estimated using a NanoDrop ND-100 Spectrophotometer (Thermo Fischer Scientific, UK). All 260:280 absorbance ratios were in the range of 1.96-2.15. Samples were also deoxyribonuclease (DNase; Qiagen, UK) treated during RNA isolation to prevent genomic contamination. RNA integrity was confirmed by running samples on a RNA 6000 Nano Chips Bioanalyzer (Agilent). Complementary deoxyribonucleic acid (cDNA) was subsequently synthesised from the ribonucleic acid (RNA) using the SuperScript II reverse transcriptase kit (Invitrogen, UK) according to the manufacturers protocol.

2.2.8 Taqman array set-up and quantitative real-time PCR

Taqman® PCR mouse mediator arrays cards were custom designed using the Applied Biosystem website (http://www.appliedbiosystems.com). The cards use micro-fluidic technology, comprising of 384 wells and 4 sets of 96 different primer/probe pairs against specific genes within the mouse genome, including four housekeeping (HK) genes: glyceraldehyde-3-phosphate dehydrogenase (GAPDH), 18S ribosomal RNA, β-actin, and hypoxanthine phosphoribosyltransferase (HPRT). Spinal cord and sciatic nerve cDNA samples from 7 and 21 days post PNL or sham surgery were diluted and added in a 1:1 ratio to Taqman universal PCR master mix (Applied Biosystems, UK; contains DNA Taq polymerase and dNTPs). Dnase-free water was added to the sample mix producing a final [cDNA] of 2 ng/µl in a total volume of 20 µl. The sample mix was loaded into the appropriate port and the cards were centrifuged so that 1 µl was channelled into each well. Cards were then sealed and placed into a 7900 HT Fast Real-Time PCR system (Applied Biosystems, UK), where cDNA samples underwent 40 amplification cycles, and amplification products were analysed in real time with DSD 2.1 software. Real-Time PCR records fluorescence emitted from a reporter molecule upon the amplification of target DNA. Thus upon

amplification the complementary Taqman probe is degraded releasing a reporter molecule from local proximity of the quencher, which produces fluorescent emissions during each amplification cycle. The number of cycles required to pass an arbitrary threshold of fluorescence (calculated for each individual card) is measured to quantify the amount of the target sequence present in the sample. Hence the lower the cycling time (CT) the greater the expression of a particular transcript. Relative expression values of gene transcripts using the delta delta cycling time (ΔΔCT) method as previously described (Schmittgen and Livak, 2008) were calculated for each sample and normalised against the mean of the CT values of the four HK genes via the R packages ReadPCR and NormqPCR (Perkins et al., 2012). For each transcript the ΔΔCT values are presented as fold change (FC = PNL/sham for each genotype). Transcripts with undetermined values in more than 50% of the samples were assigned an average default CT value of 38. If this occurred in both PNL and sham sample groups, no FC value was calculated. Transcripts that were undetermined in less than 50% of samples obtained an average CT value based on the remaining data values.

2.2.9 Data and statistical analysis

All behavioural and immunohistochemical data were analysed using SigmaPlot 12.3 and SigmaStat software. For single comparisons between two groups, a paired student t-test was applied (behavioural data). For multiple comparisons, one-way (immunohistochemical data) or two-way (behavioural data) analysis of variance (ANOVA) was used, followed by Student-Newman-Keuls (SNK) post hoc test to determine individual group differences. For the Taqman mouse PCR array card data, two-sided Welch's t-test were run in the R programme on the ΔCT values. The p values were adjusted using the false discovery rate (FDR) to correct for multiple hypothesis testing, as previously described (Benjamini et al., 2001). Non-parametric tests were applied where the data was not normally distributed. In all cases the data is presented as the mean ± standard error of the mean (SEM) and $p < 0.05$ was set as the statistical significance level.

2.3 Results

2.3.1 Acute pain thresholds and locomotor ability are normal in GPR84 KO mice

In order to investigate whether deletion of the GPR84 gene impacts on acute pain thresholds of naïve mice, GPR84 WT and KO mice were behaviourally assessed following acute peripheral application of a range of mechanical and thermal stimuli (Fig. 2.4). GPR84 KO mice exhibited normal thermal pain thresholds to varying levels of intensity applied to the hind paw or tail compared to WT mice (A, WT: 10.5 ± 0.4 s, KO: 11.6 ± 0.4 s; B, WT: 5.2 ± 0.3 s, KO 5.0 ± 0.3 s; C, WT: 2.2 ± 0.1 s, KO: 2.0 ± 0.2 s; D, WT: 14.0 ± 1.2 s, KO: 12.6 ± 2.0 s; Fig. 2.4A-D). In addition, acute cold pain thresholds were unaffected (WT: 20.1 ± 2.1 s, KO: 20.3 ± 1.6 s; Fig. 2.4E). GPR84 KO mice also exhibited normal mechanical thresholds of low and high intensity (Fig. 2.4F & G) compared to WT mice and showed no deficits in locomotor function (F, WT: 0.72 ± 0.05 g, KO: 0.71 ± 0.1 g; G, WT: 104.8 ± 2.0 g, KO: 118.2 ± 4.4 g; H, WT: 87.6 ± 1.9 s, KO: 82.1 ± 2.6 s; Fig. 2.4H). There were no significant differences between the genotypes in any of the acute tests. These data indicate that naïve GPR84 KO mice exhibit normal thermal and mechanical acute thresholds and are equally capable as their WT littermate controls to elicit paw withdrawal responses to an applied stimulus.

2.3.2 GPR84 KO mice do not develop pain-associated behaviours after nerve injury

It is well established that peripheral nerve injury results in the development of evoked pain-associated behaviours such as mechanical allodynia and thermal hyperalgesia in the ipsilateral, but not the contralateral hindpaw, which serves as a control. In our studies we utilised the PNL model, which is a well documented model of peripheral nerve injury. To demonstrate the reproducibility of this model and confirm that we were also able to induce a neuropathic pain state in mice, mechanical and thermal thresholds were examined before and after PNL or sham surgery. As expected, nerve injured mice showed a significant reduction in mechanical and thermal paw withdrawal thresholds (data not shown).

Having demonstrated the ability to reiterate pain-associated behaviours using the PNL model as reported in the literature we then compared mechanical and thermal thresholds of nerve injured GPR84 KO mice to WT littermate controls. As before, injured WT mice showed an average reduction of 68.8% in mechanical thresholds from baseline (D0, 0.8 ± 0.1 g) and thresholds remained reduced from day 4 (0.3 ± 0.1 g) up to day 21 (0.1 ± 0.1 g). On days 18 (0.2 ± 0.1 g) and 21 there was a significant difference compared to WT sham controls (D18,

0.6 ± 0.1 g; D21, 0.5 ± 0.1 g; Fig. 2.5A). Similarly, WT PNL mice exhibited an average reduction of 25.4% in thermal thresholds from baseline (D0, 10.1 ± 1.0 s) over the 21 testing days, which was significant from baseline on days 4 and 21 and WT sham controls on days 4, 7 and 21 (D4, 6.1 ± 0.8 s; D7, 7.6 ± 1.4 s; D21, 6.5 ± 0.6 s vs WTS: D4, 11.7 ± 1.1 s; D7, 11.1 ± 1.7 s; D21, 11.5 ± 1.3 s; Fig. 2.5B). Strikingly, nerve injured GPR84 KO mice did not develop mechanical (Fig. 2.5C) or thermal (Fig. 2.5D) hypersensitivity over the 21 testing days and thresholds did not drop from baseline or differ from KO sham controls; (KOPNL mechanical: D0, 0.7 ± 0.1 g to D21, 0.6 ± 0.1 g vs KOS: D0, 0.8 ± 0.1 g to D21, 0.5 ± 0.1 g; KOPNL thermal: D0, 11.3 ± 1.1 s to D21, 11.1 ± 1.4 s vs KOS: D0, 12.1 ± 0.8 s to D21, 11.9 ± 1.1 s).

Data are presented separately for each genotype and only the ipsilateral paw withdrawal responses of each experimental group are shown for clarity. However, statistical analysis was performed across all four experimental groups. These data suggest that deletion of the GPR84 gene impairs the development of neuropathic pain behaviours in nerve injured mice. This result was obtained across three independent experiments; in every one of them, experimental procedures were carried out exactly the same and the experimenter was blind to treatment and genotype. One animal was excluded as a result of death during surgery.

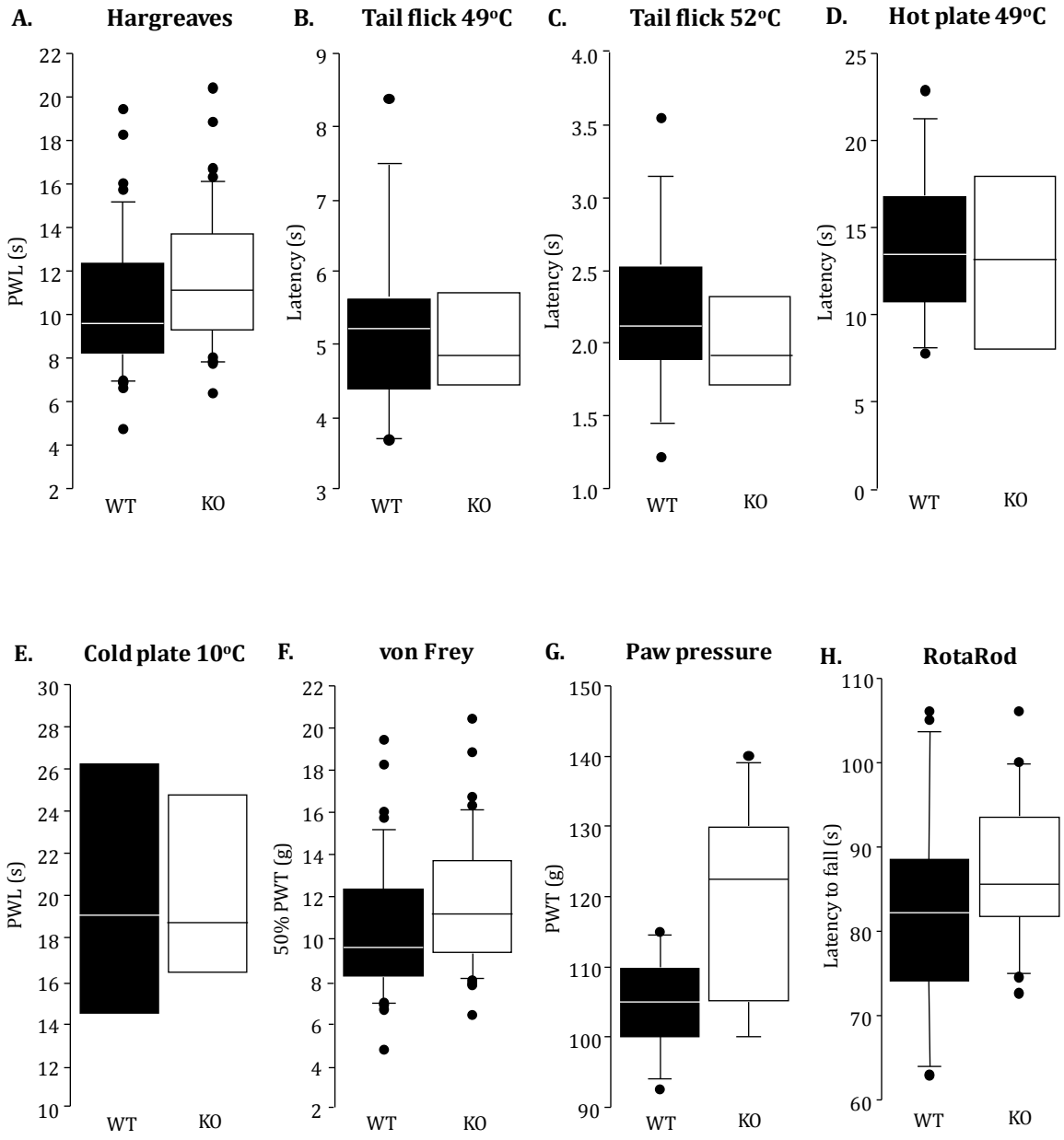

Figure 2.4: GPR84 KO mice display normal responses to acute painful stimuli and normal locomotor ability

To assess acute nociception in naïve GPR84 WT and KO mice, responses to a range of thermal and mechanical acute pain tests were compared. There were no significant differences in the responses of WT and KO mice in the temperature threshold tests (Hargreaves, (A); tail immersion withdrawal at 49°C, (B), or 52°C, (C); hot plate at 49°C, (D); cold plate at 10°C, (E)) or mechanical threshold tests (von Frey, (F); paw pressure, (G)). GPR84 KO mice also displayed normal locomotor function using the RotaRod apparatus, (H). Data are presented as the mean ± SEM. $p > 0.05$, independent Student's t-test, n = 8-14.

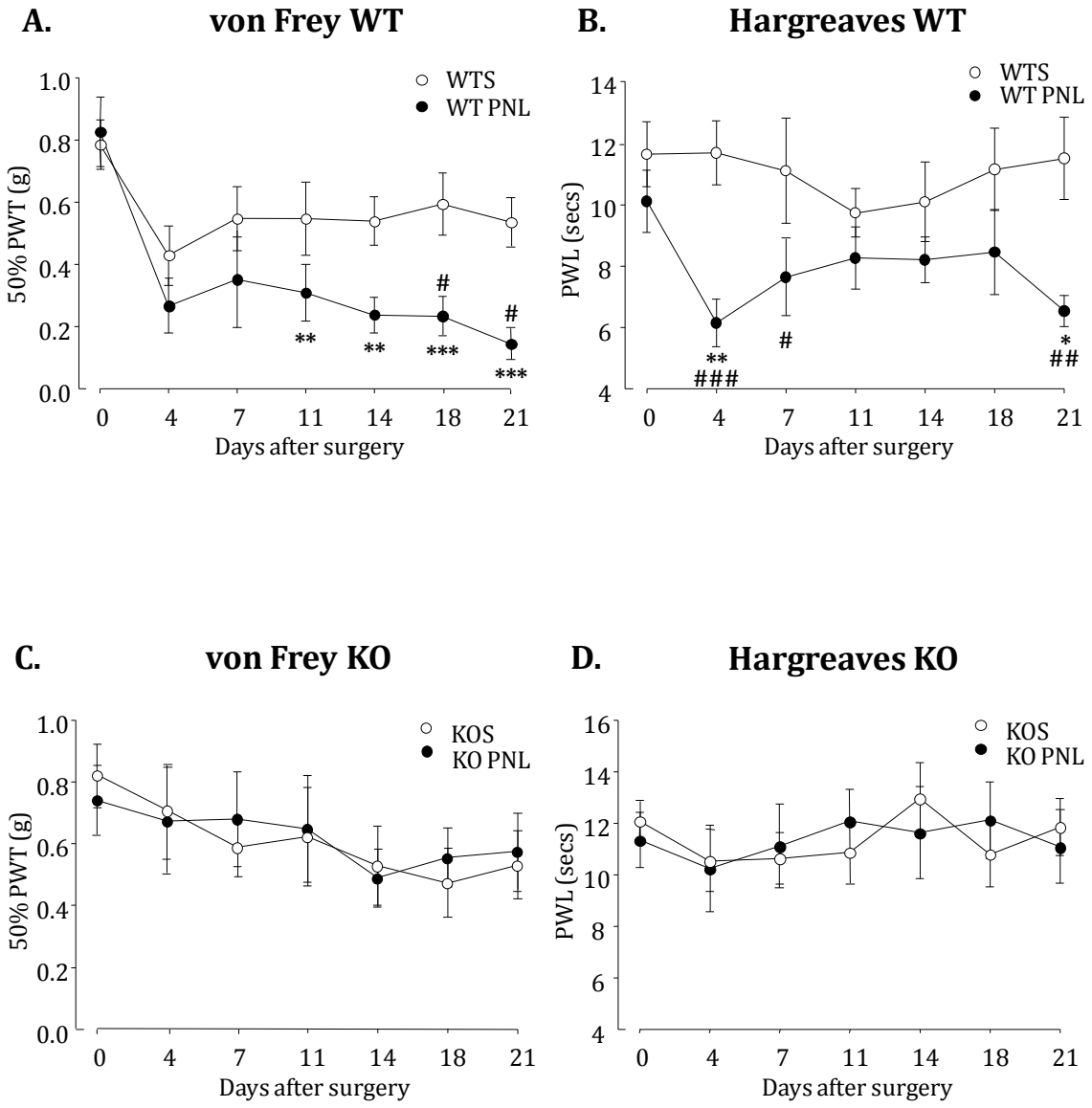

Figure 2.5: Reduced neuropathic pain in GPR84 knockout mice

Mechanical (A, C) and thermal (B, D) withdrawal responses of GPR84 WT (A, B) and KO (C, D) mice were measured before (day 0) and up to 21 days post PNL or sham surgery. WT mice developed significant mechanical hypersensitivity and showed reduced thermal thresholds compared to sham (WTS) controls. Mechanical allodynia and thermal hyperalgesia were absent in KO mice and did not differ from sham values at any time (KOS). Data are presented as the mean ± SEM. *$p < 0.05$, **$p < 0.01$, ***$p < 0.001$ vs baseline (day 0). $^{\#}p < 0.05$, $^{\#\#}p < 0.01$, $^{\#\#\#}p < 0.001$ vs sham control, two-way repeated measure (RM) ANOVA with SNK post hoc, n = 9-12.

2.3.3 GPR84 KO mice exhibit a normal microglial response 7 days post PNL

Having established a behavioural phenotype, we then sought to correlate these findings with histological analysis. Microglia are known to play a key role in the initiation of pain-associated behaviours and GPR84 is exclusively expressed on these cells in the CNS (Bouchard et al., 2007); we therefore investigated the microglial phenotype after nerve injury in WT and KO mice to elucidate if GPR84 deletion alters the microglial response. To achieve this we examined immunohistochemical changes of microglia in lumbar spinal cord sections at 7 days post PNL; a time point where anatomical changes in response to nerve injury such as microgliosis are robust.

To investigate whether deletion of GPR84 specifically alters microglial numbers, we stained for Iba1, which is a marker of microglial cells. Quantification of immunoreactivity revealed that there was no significant difference between GPR84 WT and KO microglial cell numbers in the ipsilateral or contralateral dorsal horns of sham controls (Fig. 2.6). Therefore, under normal conditions GPR84 deletion has no effect on microglial numbers. Furthermore, we also observed that under these conditions, microglia morphology in the KO was no different to that of the WT and microglial cells exhibited characteristic long, thin processes and a ramified appearance. Subsequent to peripheral nerve injury both GPR84 WT and KO mice showed a significant 3.2 fold increase in Iba1 positive cells in the ipsilateral dorsal horn (WTPNL, 21.1 ± 1.7/4x10^4 μm^2; KOPNL, 21.6 ± 2.4/4x10^4 μm^2) compared to sham controls (WTS, 6.6 ± 2.0/4x10^4 μm^2; KOS, 6.7 ± 0.7/4x10^4 μm^2; Fig. 2.6). There was no significant difference between the genotypes. Microglia morphology in response to nerve injury was typically de-ramified and amoeboid in shape, which was again exhibited by both genotypes. This indicates that GPR84 KO mice are capable of launching a normal microgliosis response subsequent to peripheral nerve injury and thus this receptor does not play a role in regulating microglial numbers under neuropathic conditions.

Although there were no differences in microglial numbers, we also investigated whether GPR84 deletion may effect phosphorylation of p38 MAPK, which is a key kinase in nociceptive pathways and a marker of microglial activation (Ji and Suter, 2007; Ji et al., 2009). In sham animals, we found no significant difference in the number of p-p38 positive cell numbers in ipsilateral or contralateral dorsal horn between GPR84 WT and KO (Fig. 2.6). Therefore, under normal circumstances GPR84 deletion has no effect on microglial activation. Subsequent to peripheral nerve injury both GPR84 WT and KO mice showed a significant 3.4 and 4.1 fold increase in p-p38 positive cells, respectively, in the ipsilateral

dorsal horn (WTPNL, 20.4 ± 2.1/4x10^4 μm^2; KOPNL, 18.6 ± 3.7/4x10^4 μm^2) compared to sham controls (WTS, 6.0 ± 2.3/4x10^4 μm^2; KOS, 4.5 ± 1.3/4x10^4 μm^2; Fig. 2.6) and there was no significant difference between genotypes. These results suggest that GPR84 is not important for the regulation of p-p38 expression in microglial cells under neuropathic pain states.

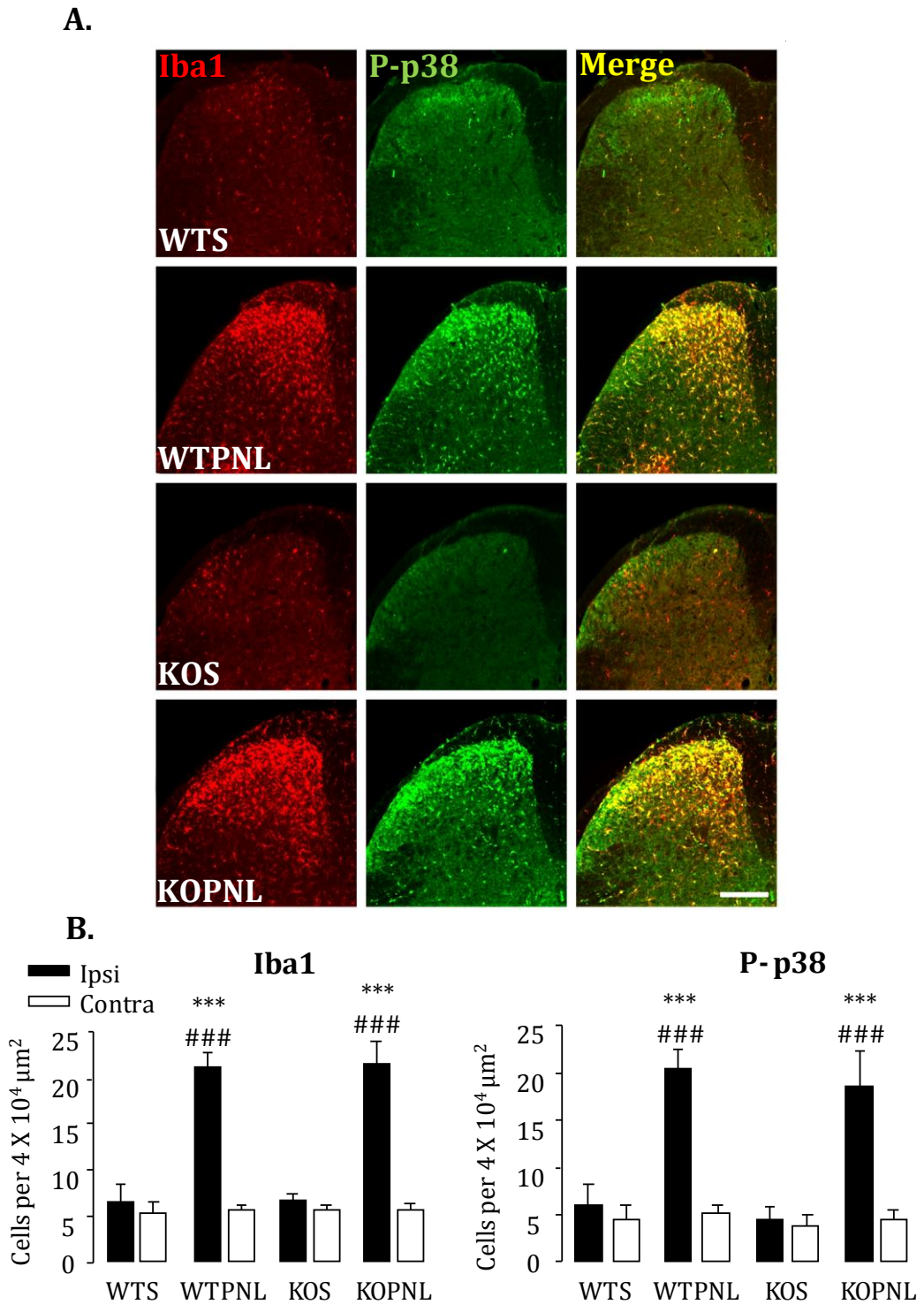

Figure 2.6: Nerve injured GPR84 KO mice exhibit a normal microglial response in the spinal cord 7 days post PNL

Subsequent to peripheral nerve injury there was a significant increase in Iba1 and p-p38 positive cells in the ipsilateral dorsal horn of the spinal cord of GPR84 WT (WTPNL) and KO (KOPNL) mice, compared to control sham groups (WTS and KOS, respectively) (A), quantified in (B). There was no significant difference between genotypes. Data are presented as the mean ± SEM. ***$p < 0.001$ vs contralateral; ###$p < 0.001$ vs sham, one-way RM ANOVA with SNK post hoc, n = 4-6. Scale bar = 200 µm.

2.3.4 GPR84 KO mice exhibit a normal microglial response 21 days post PNL

So far we have seen no evidence of a role of GPR84 in the microgliosis response at 7 days post PNL, therefore we investigated whether deletion of this receptor affects the microglial phenotype at a later time point of 21 days. Although there may be an element of resolution at this later time point, there is still a significant difference in the mechanical and thermal paw withdrawal thresholds of the WT PNL group compared to the WT sham group. Importantly, this difference is absent in the KO at this later time point. Furthermore, behavioural hypersensitivity correlating with increased microglial cell numbers in the ipsilateral dorsal horn has been reported up to 50 days post PNL in rats (Clark et al., 2006).

To investigate if deletion of GPR84 specifically alters microglial numbers, we stained for Iba1 in L4 and L5 spinal sections. Similar to our findings at day 7 post PNL, there was no significant difference between GPR84 WT and KO microglial cell numbers in the ipsilateral or contralateral dorsal horns of sham controls at 21 days post surgery (Fig. 2.7). Microglial morphology was also observed to be no different between genotypes. Subsequent to peripheral nerve injury both GPR84 WT and KO mice showed a significant 1.8 fold increase in Iba1 positive cells in the ipsilateral dorsal horn compared to sham controls (WTPNL, 9.3 ± 0.7/4x10^4 μm^2; KOPNL, 11.1 ± 0.8/4x10^4 μm^2 vs WTS, 5.3 ± 0.6/4x10^4 μm^2; KOS, 6.1 ± 0.9/4x10^4 μm^2; Fig. 2.7). The increased number of microglial cells in response to injury 21 days post PNL was similar to that seen at the earlier time point, and there was no significant difference between the genotypes. Again, morphological changes of microglial cells in response to nerve injury were similar and no different between the genotypes. However, it is worth noting that the increase in microglial numbers at 21 days post PNL was approximately 50% of that at 7 days post injury, confirming a degree of resolution at this later time point. These data illustrate that GPR84 KO mice are capable of an extensive microgliosis response over the course of traumatic neuropathy and that GPR84 deletion does not alter microglial numbers.

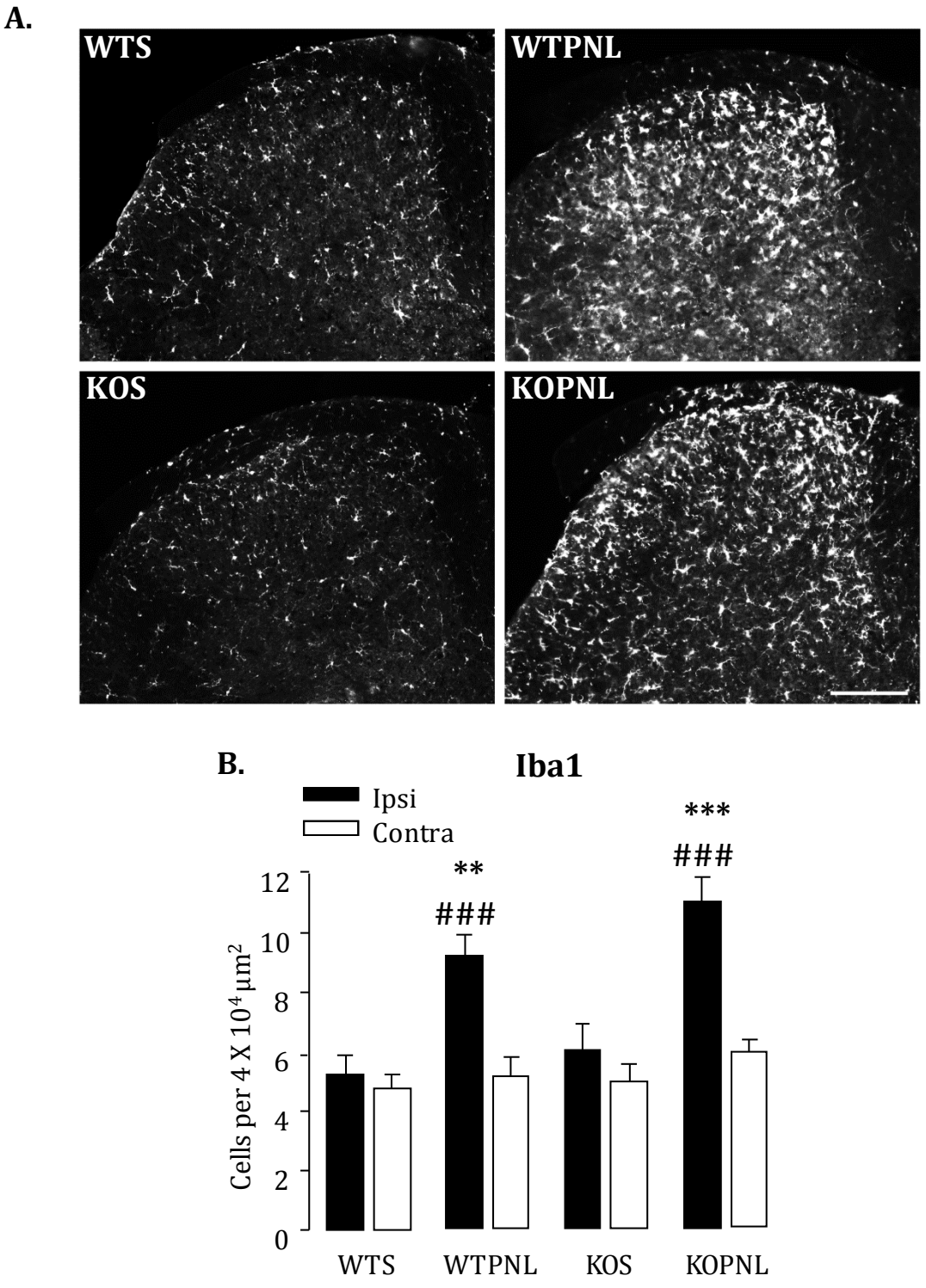

Figure 2.7: Nerve injured GPR84 KO mice exhibit a normal microglial response in the spinal cord 21 days post PNL

Subsequent to peripheral nerve injury there was a significant increase in Iba1 positive cells in the ipsilateral dorsal horn of the spinal cord in WTPNL and KOPNL mice compared to control sham groups (WTS and KOS, respectively) (A), quantified in (B). There was no significant difference between the genotypes. Data are presented as the mean ± SEM. $^{**}p < 0.01$, $^{***}p < 0.001$ vs contralateral; $^{###}p < 0.001$ vs sham, one-way RM ANOVA with SNK post hoc, n = 4. Scale bar = 200 µm.

2.3.5 GPR84 KO mice exhibit a normal macrophage response 7 days post PNL

So far we have seen no evidence of a CNS change in the microglial profile of GPR84 KO mice that correlates with the behavioural phenotype after injury. As GPR84 expression is restricted to immune cells, we decided to examine the response of macrophages in the sciatic nerves. These are the key phagocytic immune cells of the PNS and have been well documented to play a role in nerve injury-induced behavioural hypersensitivity (Myers et al., 1996; Liu et al., 2000; Barclay et al., 2007).

To elucidate whether deletion of GPR84 may alter the peripheral inflammatory response to nerve damage mediated by infiltrating macrophage cells, we carried out immunostaining of Iba1 in longitudinal sciatic nerve sections, distal and proximal to the site of injury. We examined this marker of macrophage cells at 7 days post PNL, as the immune response at this time point is robust and correlates with the behavioural hypersensitivity seen in WT mice. We found that there was no significant difference between GPR84 WT and KO macrophage cell numbers in the ipsilateral sciatic nerves of sham controls (Fig. 2.8.). Therefore GPR84 deletion has no effect on macrophage cell numbers per se. Following peripheral nerve injury both WT and KO mice showed a 95.1% and 91.3% increase in Iba1 positive cells, respectively, in the ipsilateral sciatic nerve, distal to the lesion site compared to sham controls (WTPNL, 10.0 ± 1.2/4x10^4 μm^2; KOPNL, 9.4 ± 0.3/4x10^4 μm^2 vs WTS, 0.5 ± 0.2/4x10^4 μm^2; KOS 0.8 ± 0.1/4x10^4 μm^2; Fig. 2.8). Due to a degree of macrophage infiltration into intact axons of the nerve injury site, proximal counts of the injured nerve were also greater than sham controls, which were significant in WT mice (WTPNL, 3.0 ± 1.0/4x10^4 μm^2; KOPNL, 2.0 ± 0.5/4x10^4 μm^2). There was no significant difference between the genotypes. These data demonstrate that GPR84 has no effect on macrophage infiltration in response to nerve injury and therefore these cells are not essential for the behavioural phenotype observed in GPR84 KO mice. However, we must acknowledge that following nerve injury macrophage cells can also infiltrate the CNS and contribute to the Iba1 cell population in the dorsal horn, and thus a CNS macrophage involvement cannot be excluded (Zhang et al., 2007). The contribution of macrophage infiltration into the DRG in GPR84 WT and KO mice is yet to be established.

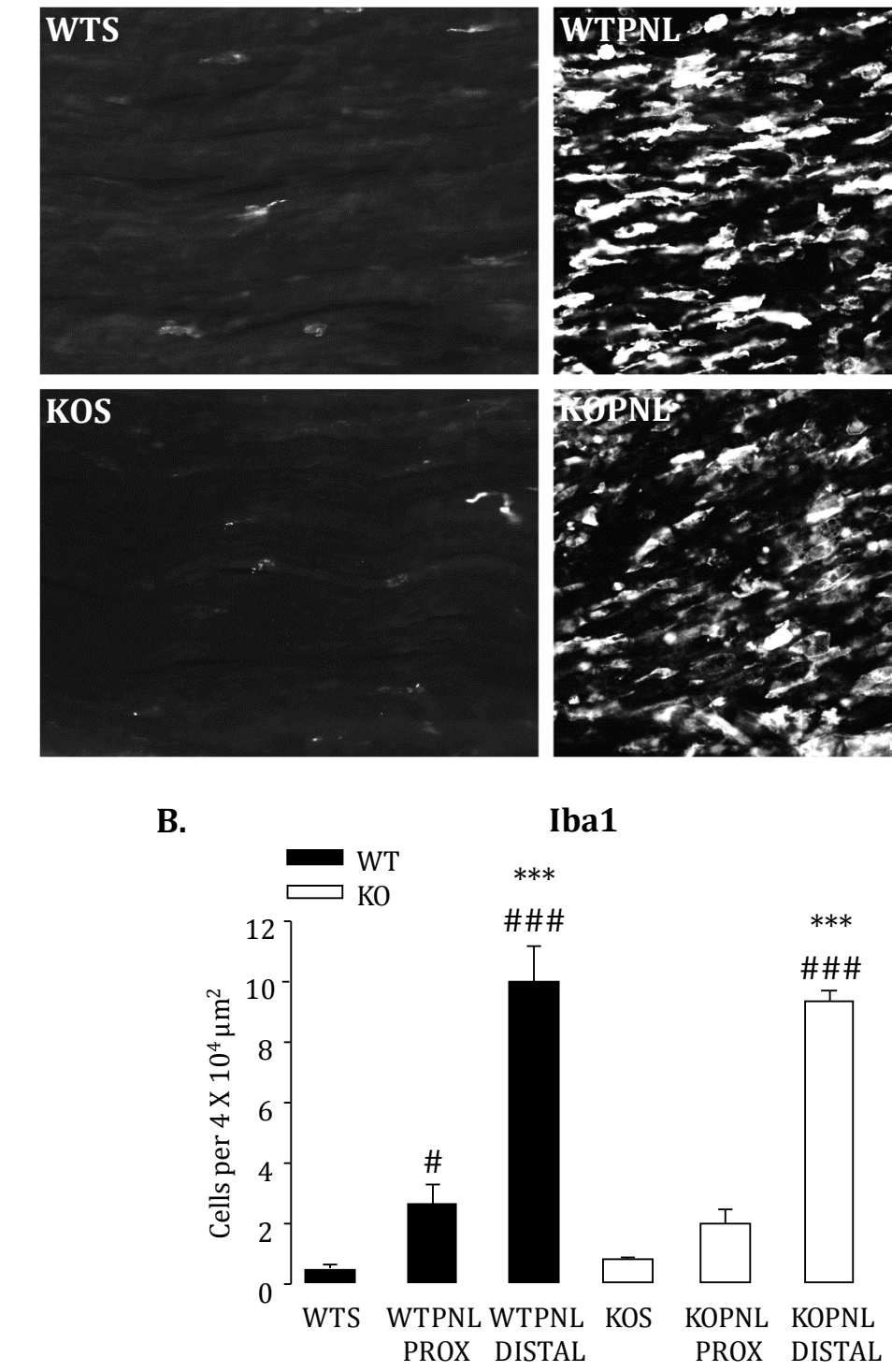

Figure 2.8: GPR84 KO mice exhibit a normal macrophage response in the sciatic nerve 7 days post PNL

There was a significant increase in Iba1 positive cells in the injured ipsilateral sciatic nerve in GPR84 WTPNL and KOPNL mice compared to their corresponding control sham groups (WTS and KOS, respectively) (A), quantified in (B). There was no significant difference between genotypes. Data are presented as the mean ± SEM. $^{***}p < 0.001$ vs corresponding proximal (PROX); $^{\#}p < 0.05$, $^{\#\#\#}p < 0.001$ vs corresponding sham group, one-way RM ANOVA with SNK post hoc, n = 4. Scale bar = 200 µm.

2.3.6 Raw PCR array data: Comparing nerve injury induced mediator transcript changes in GPR84 WT and KO mice

We have shown that deletion of GPR84 results in the prevention of behavioural hypersensitivity after nerve injury (Fig. 2.5). To investigate whether this correlates to changes in mediator expression induced by peripheral nerve injury we utilised high through-put custom-made Taqman array cards, to compare the expression of a range of putative mediators of interest (a majority of which were chemokines and cytokines) in sciatic nerve and spinal cord tissue of GPR84 WT and KO at two time points. An explanation of analysis is provided in the methods section (2.2.8) and in more detail in (Perkins et al., 2012).

Appendix Tables 1-8 display the raw CT values of 92 different chemokine/cytokines, growth factors and cell markers as well as raw CT values of control HK genes in the sciatic nerve at 7 and 21 days post sham or PNL surgery (1, 2), (5, 6) respectively; and in the spinal cord at 7 and 21 days post PNL or sham surgery (3, 4), (7, 8) respectively, in GPR84 WT and KO mice. Transcripts which had amplification curves that failed to pass a set threshold within the exponential phase were denoted as non-detectable (ND). Note that ARG1, Mannose receptor c-type 1 (MRC1), Colony stimulating factor 3 (granulocyte) receptor (CSF3R), neuregulin 1 (NRG1) were only examined at 7 days post PNL; CCL26, CCL28, Colony stimulating factor 1 (macrophage) receptor (CSF1R), Histocompatibility 2, class II antigen E beta (H2.EB1) were only examined at 21 days post PNL.

Gene expression was measured via the amplification of a target cDNA sequence that corresponds to a particular gene of interest. The samples were subjected to 40 cycles of temperature controlled PCR amplification, which entails three key phases of denaturation, primer annealing and elongation. During amplification the level of fluorescence was measured and once it reached above background to a set threshold within the exponential phase, the number of cycles required to reach this threshold were used to estimate the amount of cDNA sequence present and hence the amount of transcript in the original sample (Perkins et al., 2012). A CT value of 1 corresponds to doubling of a transcript and so the lower the CT value the greater the expression of the gene.

Incomplete reverse transcription of RNA or error in sample loading can result in faulty reactions and incorrectly calculated CT values. However, the raw CT values of individual genes were generally consistent within experimental groups (*Appendix* Tables 1-8),

implicating biological differences rather than experimentally-driven variability. At the end of each table within an experimental group are the raw CT values for the four HK genes, which are used to normalise the data. We observed that the CT values of the HK genes within experimental groups varied no more than 1 cycle, particularly in the spinal cord tissue, which is indicative of consistency. In the sciatic nerve tissue the CTs were slightly more variable at both time points, perhaps reflecting differences in tissue compositions. Overall consistency was also exhibited between experimental groups of both genotypes, where the average CT values for HK genes varied no more that 1 cycle in the spinal cord tissue at both time points and in the sciatic nerve tissue at D7. Likewise, in the D21 sciatic nerve tissue, all HK genes except 18s exhibited an average increase of 1 CT in the WT PNL group and 2 CTs in the KO PNL group, compared to corresponding sham groups. Despite this, an up-regulation in the HK genes in fact reduces the FC values of up-regulated transcripts rather than enhances them and hence limits significance. Therefore, we can assume that the data is consistent enough to limit the incidence of false positives.

It was observed that a majority of fluorescent readings for each gene transcript crossed the arbitrary threshold within the exponential phase generally between 15 and 35 cycles. Transcripts that were below detection level, and did not cross the threshold or had CT values close to 38 were denoted as ND (*Appendix* Tables 1-8). As stated in the methods section, transcripts that attained a ND CT value in more than 50% of the samples within an experimental group were given a default value of 38, and if this occurred in both experimental groups (i.e. PNL and sham) then the transcript did not obtain a FC value. In all cases the amplification plots of individual transcripts for each card were checked for faulty reactions caused by bubbles or evaporation of the reaction mixture due to unsealed wells. Hence we can be confident that lack of gene detection was due to a biological factor rather than a technical error.

2.3.7 Top dysregulated mediators in nerve injured GPR84 WT and KO mice

Tables 2.1-2.4 display the top differentially regulated genes in GPR84 KO mice. Data are displayed as the mean FC relative to control levels (see *Appendix* Tables 11 and 12 for FC values of all genes profiled). The standard deviation (SD) values are only those of the case samples where variability is considered to be the greatest, rather than the control samples. A FC threshold of ≥ 2 in one or both genotypes for a particular gene was set to reduce noise by eliminating those genes that showed marginal expression changes. A FC ratio (KO FC/WT FC) threshold of ≥ 1.5 was also set and genes were ranked according to this ratio. The FC

ratio was employed in the screening criteria so that unless a particular transcript changed by ≥ 1.5 fold between genotypes, it would not be considered to be transcriptionally regulated by GPR84. This enabled us to efficiently filter irrelevant genes that are un-related to the behavioural pain phenotype despite a correlated expression and thus focus on transcripts that were considerably dysregulated between genotypes. With such a large data set it is important to implement careful criteria to dissociate genes of interest from those not showing substantial transcriptional changes (Antunes-Martins et al., 2013). However, setting up a very stringent threshold also creates the possibility that some genes of relevance may be disregarded.

The concept that the development of behavioural hypersensitivity is driven by an increased expression of mediators has led many genomic studies to focus on those genes that are up-regulated after nerve injury. However, nociception is also driven by a down-regulation in the expression of some genes, hence why we have examined both up- and down-regulated transcripts. Table 2.1A displays the top ranking down-regulated genes in the sciatic nerve of GPR84 KO mice 7 days post PNL. These genes are of particular interest because they were either up-regulated or more greatly expressed in WT than KO mice after nerve injury by a FC ratio of ≥ 1.7, correlating with an absence of behavioural hypersensitivity in the KO. As expected GPR84 was not detectable in the KO, but was strikingly up-regulated in WT sciatic nerve tissue after nerve injury (FC: 51.3). Intriguingly, of the top 10 down-regulated transcripts half, were epidermal growth factors (EGFs): amphiregulin (AREG) (WT FC: 12.2, KO FC: ND); betacellulin (BTC) (WT FC: 4.1, KO FC: 2.0); artemin (ARTN) (WT FC: 4.5, KO FC: 2.4); epiregulin (EREG) (WT FC: 55.3, KO FC: 30.5); heparin-binding EGF-line growth factor (HBEGF) (WT FC: -3.3, KO FC: -5.7). Unlike the other EGFs, which exhibited similar patterns of up- or down-regulation between the genotypes, amphiregulin was particularly interesting despite a lack of significance as it was not detectable in the KO and was considerably up-regulated in the WT. The other top five down-regulated transcripts were cytokines, including the pro-inflammatory IL-23a and IL-5. However, since these were down-regulated in both genotypes (although considerably more in the KO) they are unlikely to be related to the KO behavioural phenotype.

Table 2.1B ranks the top up-regulated genes in KO sciatic nerve 7 days post PNL compared to WT. Intriguingly, the pro-inflammatory mediators IL-1β, IL-6, TNF-α, CCL2 and CCL3, which are well documented to play a role in nociception (Thacker et al., 2007; Austin and Moalem-Taylor, 2010) were up-regulated in both genotypes but to a greater extent in the KO. This finding was unexpected as KO mice did not display neuropathic pain-related

behaviour at this time point. IL-1β, TNF-α and CCL3 were significantly expressed in both genotypes, where IL-6 and CCL2 were detected only in the KO: (IL-1β: WT FC: 24.9, KO FC: 71.9; IL-6: WT FC: 1.8, KO FC: 14.3; TNF-α: WT FC: 6.8, KO FC: 18.3; CCL2: WT FC: 1.9, KO FC: 4.9; CCL3 WT FC: 10.2, KO FC: 25.7. A majority of up-regulated transcripts in the KO were chemokines, reflecting their important role in neuropathology. Pro-inflammatory IL-12b, CCL4, CCL7, CCL8, CCL9, CXCL9, CXCL10 and chemotactic XCL1 were significantly induced in the KO and showed a greater FC increase than the WT (Table 2.1B) along with a few immune cell markers including ARG1, allograft inflammatory factors-1 (AIF1), and T-cell surface glycoprotein CD3 delta chain (CD3D). AIF1 (Iba1 gene) was up-regulated in both genotypes but was 2.1 times more greatly expressed in the KO (AIF1: WT FC: 4.3, KO FC: 9.2). This complies with our previous observation that macrophage infiltration into the sciatic nerve after injury is normal in the KO (Fig. 2.8). Interestingly ARG1, a marker of a sub-population of anti-inflammatory macrophages was significantly up-regulated in the KO in contrast to the WT (WT FC: 5.7, KO FC: 20.7).

In the spinal cord 7 days post PNL, very few transcripts met the threshold criteria. FC values of individual genes were also smaller than that seen in the sciatic nerve and did not reach significance (Table 2.2). CXCL3 and IL-24 were up-regulated in the WT and were undetectable or less expressed in the KO, respectively; however, these proteins are not documented to have a role in nociception (Table 2.2A). Top up-regulated transcripts in the KO included a mixture of chemokines and cytokines (Table 2.2B), three of which are implicated in pro-nociceptive transmission: CCL5, TNF-α and IL6 (DeLeo et al., 1996; Homma et al., 2002; Benamar et al., 2008). Notably, CXCR3 (the receptor for pro-inflammatory CXCL10) was the top up-regulated transcript in the KO and was down-regulated in the WT (WT FC: -1.5, KO FC: 7.0). CXCL10 mRNA was found to be significantly induced in both the sciatic nerve and spinal cords of KO mice 7 days post PNL (Table 2.1B). Therefore, elevated expression of CXCR3 could be a result of infiltrating T-cells via the chemotactic properties of CXCL10 (Taub et al., 1993), a hypothesis also supported by an increased expression of the T cell receptor, CD3D, in the spinal cord tissue of KO mice.

We also examined transcriptional changes induced by the PNL model in the sciatic nerves and spinal cords of GPR84 WT and KO mice at a later time point as behavioural hypersensitivity was absent throughout the 21 testing days in the KOs (Fig. 2.5). Table 2.3 illustrates a range of chemokines, cytokines and growth factors differentially regulated between the genotypes in the nerve. However, none of these changes were significant except for BTC which was up-regulated in the KO (unlike the earlier time point where it was up-

regulated in the WT) (Table 2.3B). The only other top regulated EGF at this later time point was EREG, which showed considerably less induction in the WT compared to day 7 and was not detectable in the KO (Table 2.3A). Despite a lack of significance, the pro-nociceptive mediators IL-1β, IL-6, COX-2 (PTGS2), inducible nitric oxide synthase 2 (NOS2) and CCL3 were amongst the top 17 ranking genes that showed a greater expression in the WT sciatic nerve than the KO, correlating with the observed behavioural hypersensitivity in neuropathic WT mice (Table 2.3A). At the earlier time point these mediators were in fact considerably up in the KO as opposed to the WT, which represents a striking transcriptional switch between the genotypes at the later time point. Consistent with the earlier time point, CXCL17, CCL8 and CXCL9 were up-regulated in the KO but down-regulated or undetectable in the WT and the pro-nociceptive mediators IL-12b, BDNF and CCL21a,b also had a higher expression in the KO. The immune cell marker, integrin alpha M (ITGAM; CD11b), was amongst the top hits and showed a greater induction in the KO, which again supports our observation that the macrophage response to nerve injury is indistinguishable from the WT (Fig. 2.8).

In spinal cord tissue at 21 days post PNL fewer genes met the threshold criteria and transcript changes were smaller and lacked significance, similar to the D7 time point (Table 2.4). None of the top up-regulated (A) or top down-regulated (B) transcripts in the KO were consistent with the earlier time point except for CCL8, which was consistently up-regulated in the KO spinal cord. Top regulated mediators included pro-inflammatory IL-12b, IL-23a, CCL7, and CXCL9; with only IL-12b and CXCL9 being previously implicated in nociceptive transmission. Contrary to the early time point, CXCR3 exhibited reduced expression in the KO, although there was an increase in the selective ligand CXCL9 (Table 2.4). CXCR3 is preferentially expressed by pro-inflammatory T helper type 1 (Th1) lymphocytes and so this could indicate resolution of T cell infiltration into the spinal cord at this later time point, consistent with the behavioural phenotype in the KO mice. On the other hand, the greater expression of CXCR3 in the WT is suggestive of increased T-cell infiltration into the spinal cord, which could mark the slower onset of the T-cell contribution to neuropathic pain (WT FC: 3.5, KO FC: 1.2).

In summary, we have identified a number of genes which were dysregulated in the nerves and spinal cords of GPR84 KO mice at two time points after nerve injury. It is evident that the greatest transcriptional changes occurred in the sciatic nerve at both time points, an observation further highlighted in the profile distribution graphs (Fig. 2.9). This representation shows the distribution of average FC values relative to sham controls and the

FC ratios of genes in the sciatic nerve and spinal cord of GPR84 WT and KO mice at 7 and 21 days post PNL. The gene profiles are ranked in order of FC ratio from the greatest down-regulated to the most up-regulated in the WT as opposed to the KO. The blue shaded region corresponds to the cut off threshold of a FC of 2.

The profile distribution graphs illustrate the important temporal relationships in gene expression as well as the differences in gene regulation between distinct tissue types. Considering that a majority of the transcripts screened are driven by intrinsic immunological activity, gene expression changes may be somewhat diluted in the spinal cord compared to the sciatic nerve due to different cellular compositions. As previously discussed, both tissues exhibited greater transcriptional changes at the early time point. The spatial temporal relationship with transcriptional regulation is an interesting aspect of these data sets and would require additional studies examining different time points to gain further understanding. Interestingly, at the earlier time point in both tissue types a subset of genes were more strongly induced in the KO than the WT (Fig. 2.9A & B). However, the vast majority of FC ratio values resided below threshold and only a minority of genes were differentially regulated between the genotypes. These results indicate that transcriptional changes in response to peripheral nerve injury are generally similar between the two genotypes, as illustrated by the tight correlation profiles of the FC values. In contrast to the earlier time point, more genes are differentially regulated between the genotypes in the sciatic nerve at D21 as indicated by the FC ratio profile (despite lower FC values). In the spinal cord, the FC profiles are tighter at the later time point but there is a similar number of dysregulated genes as in the D7 data set.

In each genotype FC data points that clearly resided outside the threshold are differentially regulated from control tissue and those genes that also have FC ratios ≥ 1.5 are differentially regulated between the genotypes. These genes are of particular interest as they could potentially play a role in behavioural hypersensitivity modulated by GPR84 and are presented and evaluated in the tables below.

Table 2.1: Top down- (A) and up- (B) regulated genes in GPR84 KO sciatic nerve 7 days post PNL

2.1 (A)	Top down-regulated genes in GPR84 KO sciatic nerve tissue 7 days post PNL			
Rank	**ID**	**WT**	**KO**	**KOFC / WTFC RATIO**
1	GPR84	51.3 (22.43-117.2)**	ND	-51.3
2	AREG	12.2 (2.5-59.1)	ND	-12.2
3	IL5	-1.5 (0.1-3.6)	-16.2 (0.05-0.08)***	-10.8
4	IL23A	-3.0 (0.3-0.4)*	-7.3 (0.02-1.2)	-2.4
5	BTC	4.1 (2.2-7.4)*	2.0 (0.5-7.6)	-2.0
6	IL34	-4.5 (0.1-0.4)*	-8.7 (0.03-0.4)	-1.9
7	ARTN	4.5 (2.4-8.3)*	2.4 (1.3-4.6)	-1.9
8	EREG	55.3 (18.6-163.9)*	30.5 (11.8-78.6)*	-1.8
9	HBEGF	-3.3 (0.2-0.4)**	-5.7 (0.09-0.4)*	-1.7
10	CXCL13	-11.7 (0.05-0.1)***	-20.1 (0.02-0.2)*	-1.7

2.1 (B)	Top up-regulated genes in GPR84 KO sciatic nerve tissue 7 days post PNL			
Rank	**ID**	**WT**	**KO**	**KOFC / WTFC RATIO**
1	IL6	1.8 (0.3-9.5)	14.3 (4.8-42.6)*	8.0
2	CCL1	-1.3 (0.2-3.1)	8.0 (2.5-25.8)	6.4
3	CCL7	1.6 (0.7-4.0)	7.6 (3.5-16.6)*	4.7
4	XCL1	4.7 (0.9-24.3)	19.8 (9.5-41.0)*	4.2
5	CCL4	8.3 (6-11.4)**	32.0 (17.7-57.7)**	3.9
6	IL12B	7.1 (1.4-36.2)	26.2 (16-43.1)*	3.7
7	ARG1	5.7 (4.7-7.0)	20.7 (9.8-43.8)**	3.6
8	CXCL17	-6.2 (0.02-1.3)	-1.9 (0.2-1.2)	3.2
9	CXCL10	1.8 (1.0-3.1)	5.5 (2.4-12.3)*	3.1
10	IL1B	24.9 (13.7-45.2)*	71.9 (42.1-123.0)***	2.9
11	CXCL9	3.5 (2.4-5.0)*	9.8 (4.4-21.8)*	2.8
12	CXCL2	20.0 (13.3-30.0)**	55.9 (41.9-74.7)**	2.8
13	CCL8	7.6 (7.0-8.2)	21.0 (9.0-49.3)*	2.8
14	TNF	6.8 (5.3-8.6)**	18.3 (13.3-25.2)**	2.7
15	CCL2	1.9 (1.1-3.3)	4.9 (2.8-8.5)*	2.5
16	CCL3	10.2 (8.3-12.5)**	25.7 (17.0-38.9)***	2.5
17	CSF2	-1.4 (0.1-3.8)	3.5 (0.9-13.9)	2.4
18	CD3D	2.5 (0.4-14.2)	5.9 (3.1-11.0)*	2.4
19	CCL9	1.8 (1.6-2.1)	4.2 (2.6-6.6)*	2.3
20	AIF1	4.3 (3.2-5.8)**	9.2 (5.8-14.6)**	2.1

Table 2.2: Top down- (A) and up- (B) regulated genes in GPR84 KO spinal cord 7 days post PNL

2.2 (A)	Top down-regulated genes in GPR84 KO spinal cord tissue 7 days post PNL			
Rank	**ID**	**WT**	**KO**	**KOFC / WTFC RATIO**
1	GPR84	2.6 (1.5-4.4)	ND	-2.6
2	IL19	-1.4 (0.6-0.9)	-3.1 (0.1-1.5)	-2.3
3	CXCL3	2.0 (0.8-5.2)	ND	-2.0
4	IL24	9.0 (2.3-35.1)	5.7 (2.1-15.8)	-1.6

2.2 (B)	Top up-regulated genes in GPR84 KO spinal cord tissue 7 days post PNL			
Rank	**ID**	**WT**	**KO**	**KOFC / WTFC RATIO**
1	CXCR3	-1.5 (0.4-1.1)	7.0 (3.5-13.9)	4.7
2	CCL8	1.2 (0.7-2.3)	3.8 (2.4-6.0)	3.0
3	CCL5	1.0 (0.6-1.6)	2.3 (1.0-5.8)	2.3
4	TNF	2.2 (1.5-3.1)	4.1 (3.1-5.3)	1.9
5	CD3D	-2.3 (0.1-1.9)	3.9 (2.1-7.1)	1.7
6	IL6	1.5 (0.6-3.3)	2.4 (1.5-3.8)	1.6

Table 2.3: Top down- (A) and up- (B) regulated genes in GPR84 KO sciatic nerve 21 days post PNL

2.3 (A)	Top down-regulated genes in GPR84 KO sciatic nerve tissue 21 days post PNL			
Rank	**Gene**	**WT FC**	**KO FC**	**KOFC/WTFC RATIO**
1	IL1B	42.8 (17.7-103.6)	3.2 (0.6-17.8)	-13.3
2	IL27	16.4 (9.8-27.6)	2.2 (0.8-6.2)	-7.4
3	XCL1	17.2 (0.3-1140.4)	2.5 (1.1-5.6)	-7.0
4	CCL3	17.8 (6.9-46.2)	4.0 (1.7-9.7)	-4.4
5	GPR84	3.6 (1.1-11.5)	ND	-3.6
6	IL6	-1.4 (0.2-2.8)	-4.4 (0.1-0.5)	-3.1
7	CXCL11	-3.7 (0.3-0.6)	-11.1 (0.02-0.4)	-3.0
8	EREG	2.9 (0.8-11.1)	ND	-2.9
9	PPBP	-2.6 (0.2-0.8)	-7.1 (0.1-0.3)	-2.8
10	PTGS2	-1.5 (0.2-2.1)	-3.7 (0.1-1.0)	-2.5
11	CCL4	8.0 (4.6-14.0)	3.3 (0.8-13.9)	-2.4
12	IL23A	-6.0 (0.04-0.6)	-14.3 (0.01-0.4)	-2.4
13	CXCL1	2.2 (0.9-5.7)	1.0 (0.1-7.5)	-2.1
14	CCL28	-3.2 (0.2-0.5)	-6.4 (0.1-0.4)	-2.0
15	NOS2	4.3 (3.5-5.4)	2.2 (1.7-2.9)	-2.0
16	CCL22	3.1 (0.8-12.3)	1.8 (0.4-8.7)	-1.7
17	CXCL3	18.1 (3.0-107.5)	12.4 (1.5-100.8)	-1.5

2.3 (B)	Top up-regulated genes in GPR84 KO sciatic nerve tissue 21 days post PNL			
Rank	**Gene**	**WT FC**	**KO FC**	**KOFC/WTFC RATIO**
1	CXCL17	-2.1 (0.1-0.9)	12.1 (4.1-35.7)	5.7
2	IL12B	ND	4.7 (1.3-16.7)	4.7
3	CCL8	3.3 (2.3-4.6)	13.4 (7.1-25.3)	4.1
4	IL34	-3.6 (0.2-0.5)	-1.1 (0.1-11.5)	3.2
5	STAT4	-9.4 (0.03-0.4)	-3.4 (0.1-0.6)	2.8
6	BDNF	8.3 1.1-62.2)	23.0 (3.1-310.0)	2.8
7	CXCL14	1.2 (0.6-2.2)	3.2 (1.3-7.7)	2.7
8	CCL24	-4.2 (0.1-0.4)	-1.7 (0.3-1.2)	2.4
9	CCL21A,B	-4.5 (0.2-0.4)	-1.9 (0.2-1.9)	2.4
10	CXCL9	1.3 (0.7-2.2)	2.9 (1.9-4.6)	2.3
11	CCL25	-3.5 (0.2-0.5)	-1.6 (0.4-0.9)	2.2
12	FGF7	-4.5 (0.1-0.4)	-2.4 (0.1-1.7)	1.9
13	CXCL13	-9.9 (0.03-0.4)	-5.5 (0.1-0.2)	1.8
14	BTC	2.8 (1.3-6.3)	5.0 (3.3-7.4)*	1.8
15	ITGAM	2.0 (0.9-4.3)	3.2 (1.2-8.0)	1.6
16	CCL19	-2.3 (0.2-1.1)	-1.5 (0.2-2.3)	1.6
17	IL18	-3.2 (0.2-0.6)	-2.1 (0.3-0.9)	1.5
18	IL1A	11.5 (1.7-79.0)	17.3 (6.3-47.1)	1.5

Table 2.4: Top down- (A) and up- (B) regulated genes in GPR84 KO spinal cord 21 days post PNL

2.4 (A)	Top down-regulated genes in GPR84 KO spinal cord tissue 21 days post PNL			
Rank	**ID**	**WT FC**	**KO FC**	**KOFC/ WTFC RATIO**
1	CXCR3	3.5 (2.7-4.6)	1.2 (0.6-2.5)	-2.9
2	CXCL17	4.2 (3.2-5.5)	2.2 (1.3-3.8)	-1.9
3	IL23A	1.3 (1.0-1.6)	-2.3 (0.04-4.5)	-1.8
4	IL12B	2.0 (0.5-8.5)	-3.1 (0.1-1.3)	-1.6

2.4 (B)	Top up-regulated genes in GPR84 KO spinal cord tissue 21 days post PNL			
Rank	**ID**	**WT FC**	**KO FC**	**KOFC/ WTFC RATIO**
1	CCL7	1.6 (0.6-4.6)	7.5 (3.7-15.2)	4.6
2	AREG	-1.1 (0.3-3.5)	2.6 (0.7-9.7)	2.4
3	IL11	-1.2 (0.6-1.2)	-2.1 (0.2-1.0)	1.7
4	CXCL9	1.5 (0.4-6.4)	2.5 (0.9-6.9)	1.7
5	CXCL13	2.9 (0.6-13.4)	4.7 (0.7-31.3)	1.7
6	IL19	1.4 (0.8-2.5)	2.2 (0.5-10.0)	1.5
7	CCL8	2.4 (0.9-6.3)	3.7 (2.5-5.6)	1.5

Tables 2.1-2.4: Top down- (A) and up- (B) regulated gene transcripts in the sciatic nerve and spinal cord of nerve injured GPR84 KO mice

Tables displaying the top down-regulated (A) and the top up-regulated (B) genes in the ipsilateral sciatic nerve at 7 and 21 days post PNL (2.1 and 2.3, respectively) and ipsilateral spinal cord at 7 and 21 days post PNL (2.2 and 2.4, respectively). The genes are ranked in descending order of FC ratio. FC ratio = KO FC/WT FC, where FC = PNL/sham within each genotype. Only genes with a FC of ≥ 2 within one or both of the genotypes and a FC ratio of ≥ 1.5 have been ranked. This enables the identification of transcripts that exhibit the greatest FC from control and are considerably dysregulated between genotypes. Genes with a FC ratio of less than 1.5 are considered to be similarly expressed between genotypes. Data are presented as the mean FC (± 1 SD range of the case samples (PNL tissue)). $P < 0.05$*, $p < 0.01$**, $p < 0.001$*** vs sham; T-test with FDR correction for multiple testing, n = 4. ND, not detected.

A. Sciatic nerve tissue day 7 post PNL

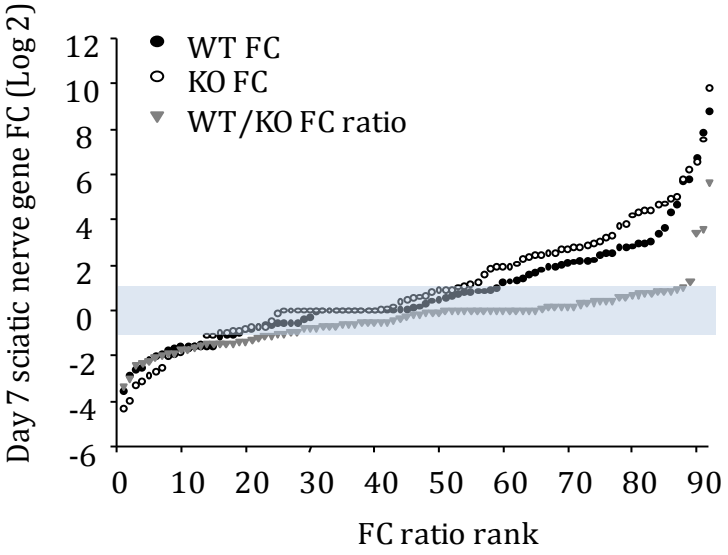

B. Spinal cord tissue day 7 post PNL

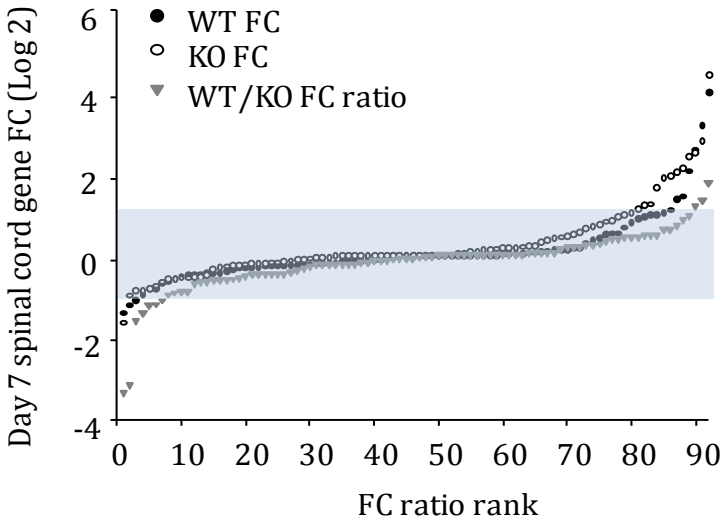

C. Sciatic nerve tissue day 21 post PNL

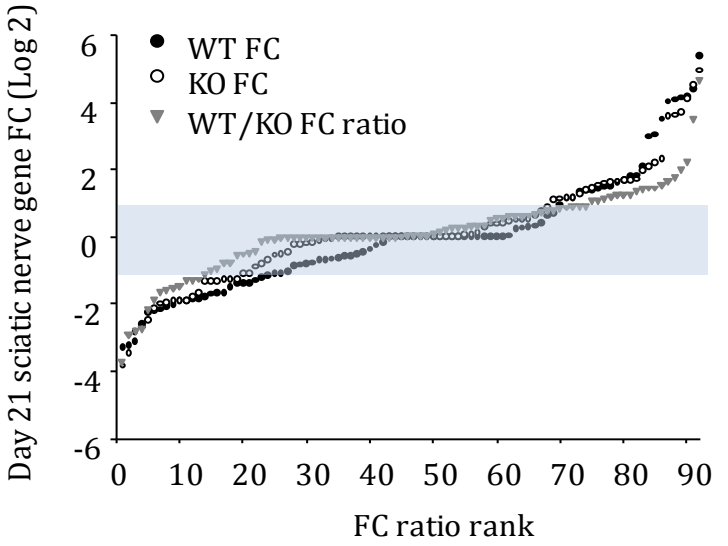

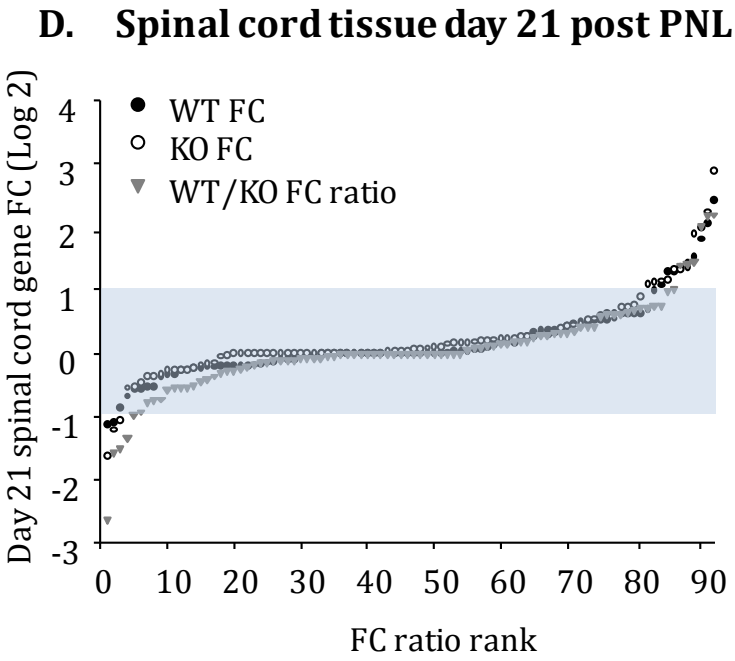

Figure 2.9: Distribution of PNL induced gene transcript changes in the sciatic nerve and spinal cord of GPR84 WT and KO mice

Transcript expression profiles of a range of cytokines, growth factors and cell markers 7 and 21 days post PNL in ipsilateral sciatic nerve (A & C, respectively) and ipsilateral spinal cord (B & D, respectively) of GPR84 WT and KO mice relative to appropriate sham control tissue. Transcripts are ranked in order of increasing FC ratio. Where FC ratio = WT FC/KO FC; FC = PNL/sham. The distribution profiles for most genes are similar between the genotypes, however a subset are considerably dysregulated. The greatest transcript FCs occur in the sciatic nerve 7 days post PNL (A), where a greater subset of transcripts appear to be up- or down-regulated in KO mice as opposed to day 21 (C), where transcript FCs are smaller but exhibit greater dysregulation between the genotypes. In the spinal cord, transcript changes post PNL are much smaller compared to the nerve, particularly at day 21 and show tighter FC profiles and hence greater similarity between the genotypes. The data points show the average FC or FC ratio for each gene transcript ranked from the most down-regulated to the most up-regulated. The blue shaded box represents an area of > 2 and each data point shows the mean FC for each individual transcript. Adjacent FC data points represent the same gene transcript, n = 92. The x-axis is on a log 2 scale.

2.3.8 Correlation of PNL induced gene expression between GPR84 WT and KO mice

To directly compare nerve injury induced transcriptional changes between genotypes, average FC values for each gene in GPR84 WT and KO mice are plotted against each other (Fig. 2.10). As indicated by the Pearson's correlation coefficient, there is a positive correlation between the WT and KO data sets in each tissue and at each time point, which is significant ($p < 0.001$). This relationship is stronger in the sciatic nerve (0.868 (A), 0.734 (C)) than the spinal cord (0.643 (B), 0.360 (D)) and at 7 days (0.868 (A), 0.643 (B)) than 21 days post PNL (0.734 (C), 0.360 (D)). These data indicate that mediator changes induced by PNL required for the development of behavioural hypersensitivity is generally similar between genotypes. Although, the R values for the D21 data sets are notably lower than the D7 data sets, particularly in the spinal cord, the correlations are significant. However, this leaves us some room to speculate that transcriptional regulation in the nerve and spinal cord at D21 is different between the genotypes. Therefore, our focus is on the few outlying transcripts, which are identified as data points that deviate markedly from the correlation of the data sets. These data points skew the Pearson's correlation coefficient as they are differentially regulated between genotypes and have been highlighted in red on the graphs. GPR84 is denoted as a red triangle.

Presenting the transcript changes in this format enables the assessment of data scatter and the identification of genes that do not conform to the rest of the data. In the sciatic nerve 7 days post PNL amphiregulin showed a strong induction in the WT but was not detectable in the KO (A). At 21 days post PNL, IL-1b showed a marked up-regulation in the WT sciatic nerve tissue compared to the KO, whereas contrariwise CXCL17 showed a considerable induction in the KO and down-regulation in the WT tissue (C). In the spinal cord at 7 days post PNL, CXCR3 and CD3D were more abundant in the KO tissue than the WT and at 21 days IL-12b went up in the WT and down in the KO tissue, whereas CCL7 was induced more substantially in the KO (D). All these outliers are top hits in the gene ranking tables above.

2.3.9 A direct comparison between nerve injured GPR84 WT and KO tissues

Figure 2.11 compares transcriptional changes between GPR84 WT and KO nerve injured tissues directly where the FC is expressed as KOPNL/WTPNL. In this case, FC values of gene transcripts in nerve injured KO mice are expressed relative to those in nerve injured WT mice, where the WT serves as a control. Figure 2.11A presents the FC profiles of transcripts across the tissue types and time points examined, which are ranked from the lowest to the

highest FC. Adjacent data points do not necessarily correspond to the same gene across the experimental groups. We found that processing the data in this format yields similar key findings to the alternative method of analysis presented previously. The greatest transcriptional changes in response to nerve injury occurred in the sciatic nerve, with more genes up-regulated at 7 days post PNL and down-regulated at 21 days post PNL in the KO relative to the WT. Not surprisingly, the three most down-regulated data points correspond to GPR84 as it is non-detectable in the KO (7 day sciatic nerve, 7 and 21 day spinal cord). The overall trend indicates that most genes are not differentially regulated between genotypes and lie below the threshold, implicating a similar transcriptional response to nerve injury in WT and KO mice.

To compare gene changes between the two time points (7 and 21 days post PNL) the average FC values for each transcript are plotted against each other. As indicated by the Pearson's correlation coefficient there is no relationship between the sciatic nerve time point data sets (-0.0622), which implies no consistency in transcriptional regulation between 7 and 21 days post PNL and that overall changes in gene expression vary considerably over time in the sciatic nerve (Fig. 2.11B). The few genes that were consistently up- or down-regulated in the sciatic nerve at both time points are highlighted in red: CXCL17 (D7 FC: 2.9 (1.3-6.6), D21 FC: 2.1 (0.7-6.2)) or IL23a (D7 FC: -2.3 (0.1-3.7), D21 FC -2.5 (0.1-2.2)), respectively. GPR84 is denoted as a red triangle. Intriguingly, the anti-inflammatory chemokine, CXCL17, has continuously been a top ranking gene in the data analysis and thus may be a plausible target for further validation.

Despite a significant positive correlation (0.740), which is clearly driven by a single data point rather than a relationship in the scatter between the two data sets, most of the gene changes in the spinal cord have a FC < 2 (Fig. 2.11C). The only consistent transcript changes between the two time points above the threshold criteria was IL-19 (D7 FC: -2.4 (0.1-1.9), D21 FC -3.5 (0.1-1.3)) and GPR84, which are highlighted in red. None of the average FC values for individual genes were significant via this method of analysis (except for GPR84 in the sciatic nerve at D7).

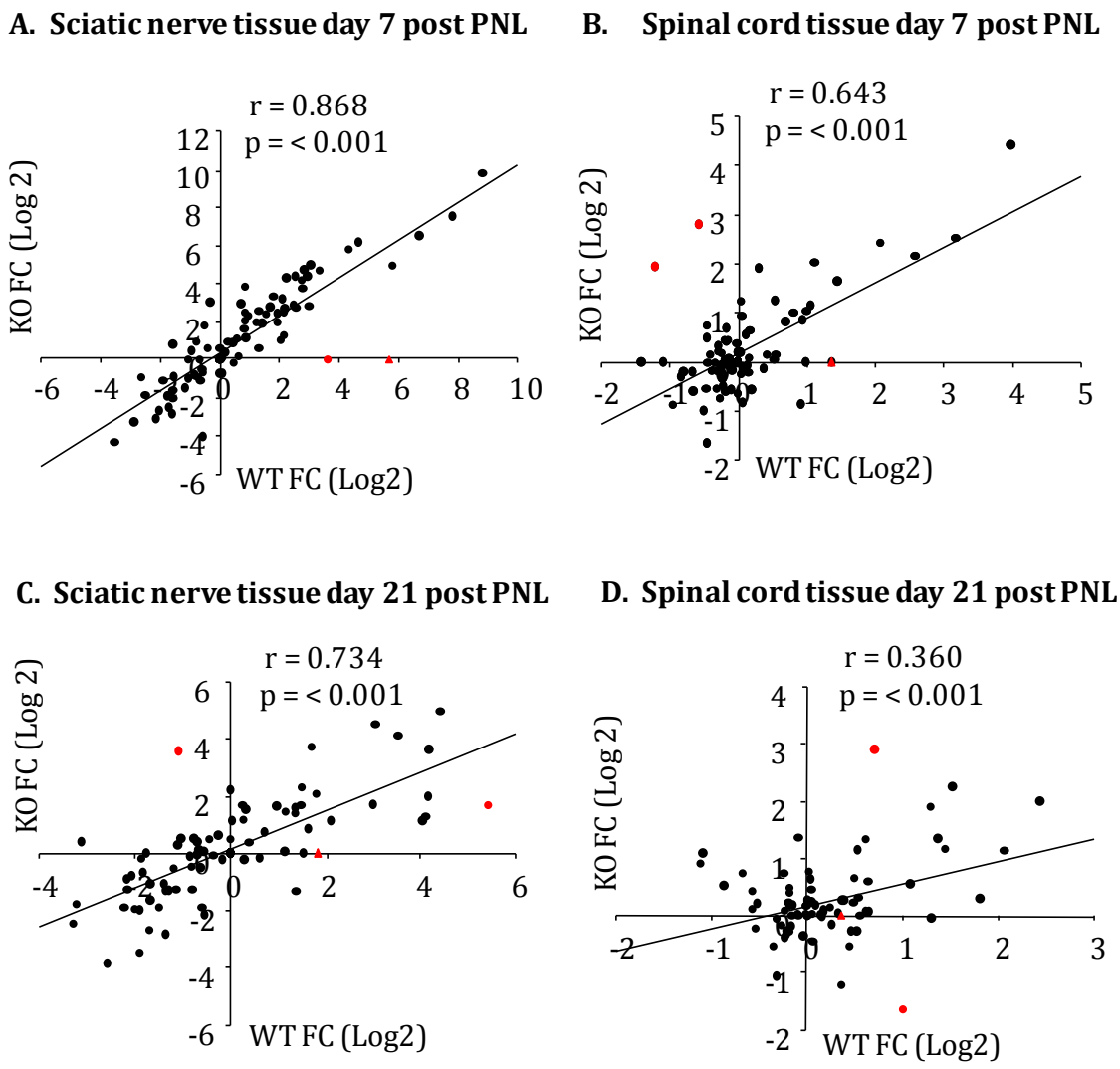

Figure 2.10: Correlation of injury-induced transcriptional changes in the sciatic nerve and spinal cord of GPR84 WT and KO mice

Transcript expression changes of a range of cytokines, chemokines, growth factors and cell markers in the ipsilateral sciatic nerve and spinal cord of nerve injured GPR84 WT and KO mice relative to sham tissues are plotted against each other on a log 2 scale. The Pearson's correlation coefficient for the sciatic nerve (0.868 (A), 0.734 (C)) and spinal cord (0.643 (B), 0.360 (D)) at 7 and 21 days post PNL, respectively, indicate a significant relationship between genotypes ($p < 0.001$). Expression of the data in this format enables the identification of gene transcripts that have a FC induction or reduction ≥ 2, where FC = PNL/sham. Visual analysis of the FC scatter identifies gene transcripts that show differential regulation between genotypes (highlighted in red, see text). Red triangle denotes GPR84 FC. Data is presented as the mean FC. Pearson's correlation coefficient, n = 92.

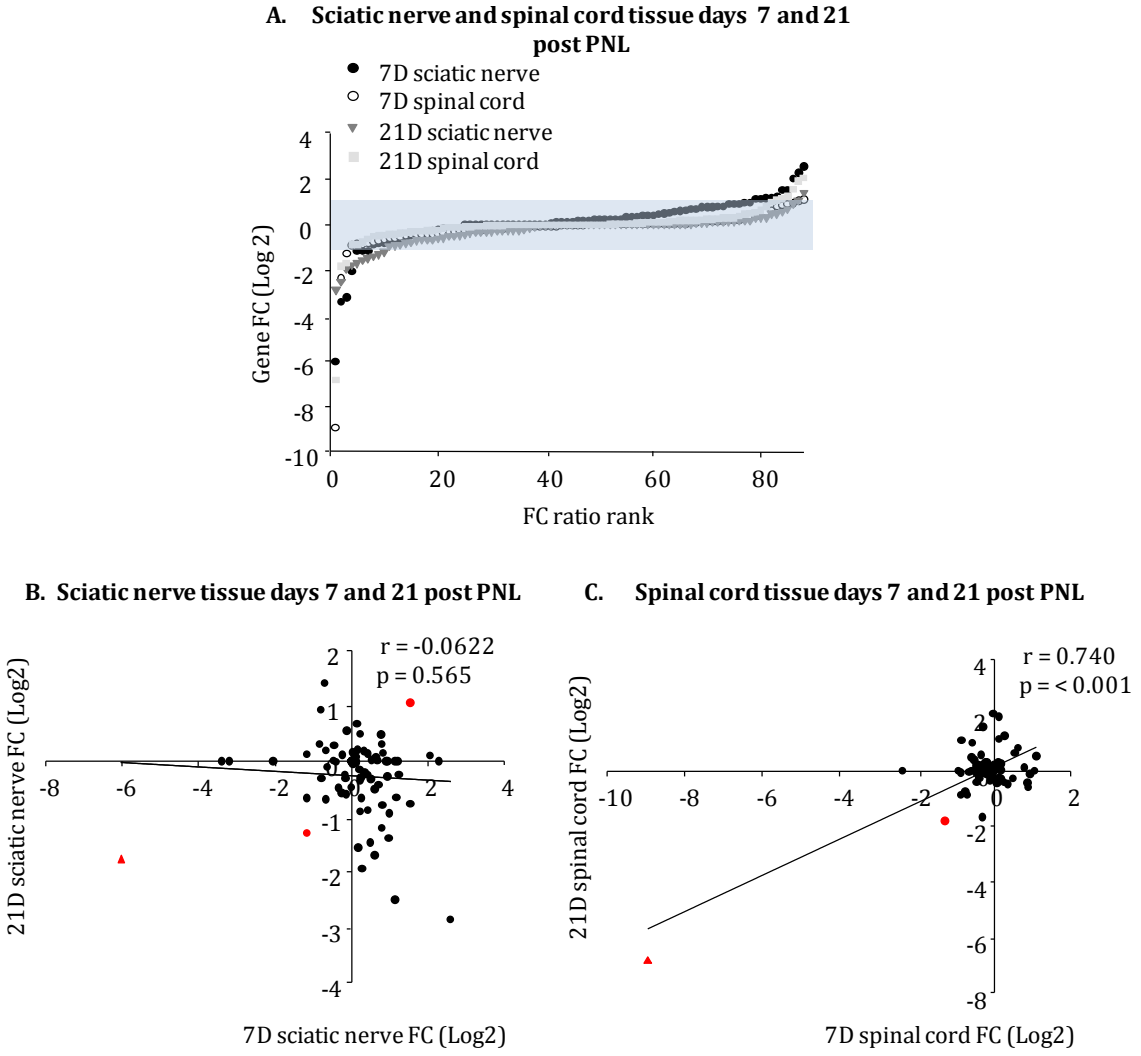

Figure 2.11: Analysis of the distribution and correlation of gene transcripts induced by PNL in the sciatic nerve and spinal cord of nerve injured GPR84 KO mice relative to nerve injured WT mice

Direct comparison of nerve injury-induced gene expression changes in GPR84 WT and KO mice showing expression profiles of a range of cytokines, chemokines, growth factors and cell markers at 7 and 21 days post PNL in ipsilateral sciatic nerve and spinal cord (A). Transcripts are ranked in order of increasing FC; FC = (KOPNL/WTPNL). Generally, the gene distribution profiles between the two genotypes are similar. The greatest transcript FCs occur in the sciatic nerve tissue where at 7 days post PNL where a subset of transcripts appear to be more strongly up- or down-regulated in the KO. In both tissues at 21 days post PNL, a greater proportion of transcripts appear to be down-regulated in the KO relative to the WT in contrast to transcriptional changes at the earlier time point. In the spinal cord transcriptional changes are much smaller compared to the nerve, at both time points. The data points show the average FC for each gene transcript ranked from most down- to most up-regulated. The blue shaded box represents an area of < 2 and each data point shows the mean FC for

each individual transcript. Adjacent data points do not necessarily represent the same gene transcript, n = 88. The x-axis is on a log 2 scale. Transcript expression changes in the sciatic nerve and spinal cord at the two examined time points are plotted against each other to investigate the factor of time, on a log 2 scale. The Pearson's correlation coefficients for the sciatic nerve (-0.0622) (B) and spinal cord (0.740) (C) at 7 and 21 days post PNL indicate that there is no correlation between both time points in sciatic nerve and a significant positive relationship between both time points in spinal cord tissue ($p < 0.001$). Expression of the data in this format enables the identification of gene transcripts that have a consistent FC induction or reduction of ≥ 2 between the two time point data sets. Red triangle denotes GPR84 FC. Data is presented as the mean FC. Pearson's correlation coefficient, n = 88.

These analyses exclude the following genes as they were not examined at both time points: ARG1, MRC1, CSF3R, NRG1, CCL26, CCL28, CSF1R and H2EB1.

Table 2.5: The top five down- and up-regulated super ranked genes in the sciatic nerve and spinal cord of nerve injured GPR84 KO mice compared to WT mice

2.5 (A)	Top down-regulated genes in GPR84 KO mice				
Super rank	Nerve 7 + 21 days	Spinal cord 7 + 21 days	7 days nerve + spinal cord	21 days nerve + spinal cord	All tissues
1	GPR84	IL23A	GPR84	IL23A	GPR84
2	EREG	CXCL2	AREG	CCL22	IL23A
3	IL23A	CCL11	IL23A	CXCL1	CCL11
4	CXCL11	CCL22	CCL11	CCL3	CCL22
5	AREG	IL25	CXCL3	GPR84	TXLNA

2.5 (B)	Top up-regulated genes in GPR84 KO mice				
Super rank	Nerve 7 + 21 days	Spinal cord 7 + 21 days	7 days nerve + spinal cord	21 days nerve + spinal cord	All tissues
1	CXCL9	CCL8	CD3D	CXCL9	TNF
2	CCL8	CCL21A,B	CCL8	CCL21A	ARG1
3	ARG1	CCL5	CXCL17	CCL8	CCL21A,B
4	CXCL17	STAT4	IL6	STAT4	STAT4
5	IL12B	CD3D	CCL17	IL5	CCL8

Tables displaying the top five down-regulated (A) and top 5 up-regulated (B) genes super ranked by FC ratio in GPR84 KO mice from left to right, where FC ratio = (KOPNL/KO sham)/(WTPNL/WT sham). Genes are super ranked via the FC ratio's of genes from either two data sets: sciatic nerve 7/21 days; spinal cord 7/21 days; time point 7, sciatic nerve/cord; time point 21, sciatic nerve/cord; or all four data sets: sciatic nerve/spinal at 7/21 days excluding those genes that were only examined at one time point: ARG1, MRC1, CSF3R, NRG1 (only examined at 7 days post PNL); CCL26, CCL28, CSF1R, H2EB1 (only examined at 21 days post PNL).

The extensive analysis of transcriptional profiles in WT and KO tissues before and after injury highlighted some interesting outliers that are differentially regulated between genotypes. Super ranking the data permits the identification of transcripts that are consistently down- or up-regulated in the KO across time points or tissues (Table 2.5) and hence strengthens the hypothesis that these genes warrant further investigation. Genes are super-ranked by cross-comparing top up- and down-regulated transcripts ranked by FC ratio in each of the four data sets. For each data set, those genes with the largest FC obtained the lowest value, whilst undetected genes were given a rank of 84. The average rank values across different data sets, as specified in the table 2.5A and B, was used to give a super-rank value for each gene so that those transcripts with lower values were the most consistently up- or down-regulated.

Many of the top super ranking hits are common denominators within the top hit tables (2.1-2.4). In the sciatic nerve these include; top down-regulated: IL23a, EREG, GPR84 (Table 2.5A); top up-regulated: IL-12b, CCL8, CXCL9, CXCL17 (Table 2.5B). In the spinal cord none of the super-ranked down-regulated genes were previous hits (Table 2.5A) and only CCL8 was a top up-regulated hit (Table 2.5B). At D7, GPR84 was a top down-regulated gene and IL-6, CCL8 and CD3D were top up-regulated genes (Table 2.5A,B). At D21, IL-23a was a top down-regulated gene and CCL8 was a top up-regulated gene in this data set and across all four data sets (Table 2.5A,B). IL-23a and CCL8, are in fact consistently regulated across 3-4 data sets, but these pro-inflammatory mediators are unlikely to play a role in the behavioural phenotype as IL-23a is down-regulated in both genotypes but more substantially in the KO and CCL8 is consistently up-regulated in the KO. By super-ranking the data many top regulated genes in particular tissues and time points are substituted by lower ranking genes that are more commonly regulated across data sets. These genes tend to show little relevance to the behavioural phenotype such as IL-23a and CCL8. Therefore, it may be more appropriate to analyse individual data sets to identify genes of interest rather than conducting cross analysis over multiple data sets.

In agreement with our hypothesis that GPR84 is a target in chronic pain mechanisms, its expression in the WT was up-regulated in both sciatic nerve and spinal cord after PNL in comparison to sham at both time points; however this trend was only significant in the nerve 7 at days post PNL (Fig.2.12A & B). Hence, in conjunction with the stiking behavioural phenotype observed in nerve injured GPR84 KO mice this receptor is clearly a potential pain-mediating target. ARG1 was also amongst the top up-regulated genes in the sciatic nerves of KO mice 7 days post PNL. This anti-inflammatory macrophage marker increased

significantly after nerve injury compared to the WT, along with a marginal increase in Mrc1. Mrc1 is an alternative anti-inflammatory macrophage marker that also showed a greater induction in the sciatic nerves of KO mice compared to WT mice, although not significant (Fig. 2.13). ARG1 is a potentially interesting target as there is a substantial degree of dysregulation between the genotypes after nerve injury and its anti-inflammatory role corresponds with the absence of behavioural hypersensitivity in nerve injured KO mice. It would therefore be interesting to further validate this transcript and examine the M1 and M2 macrophage populations in the sciatic nerves of neuropathic WT and KO mice.

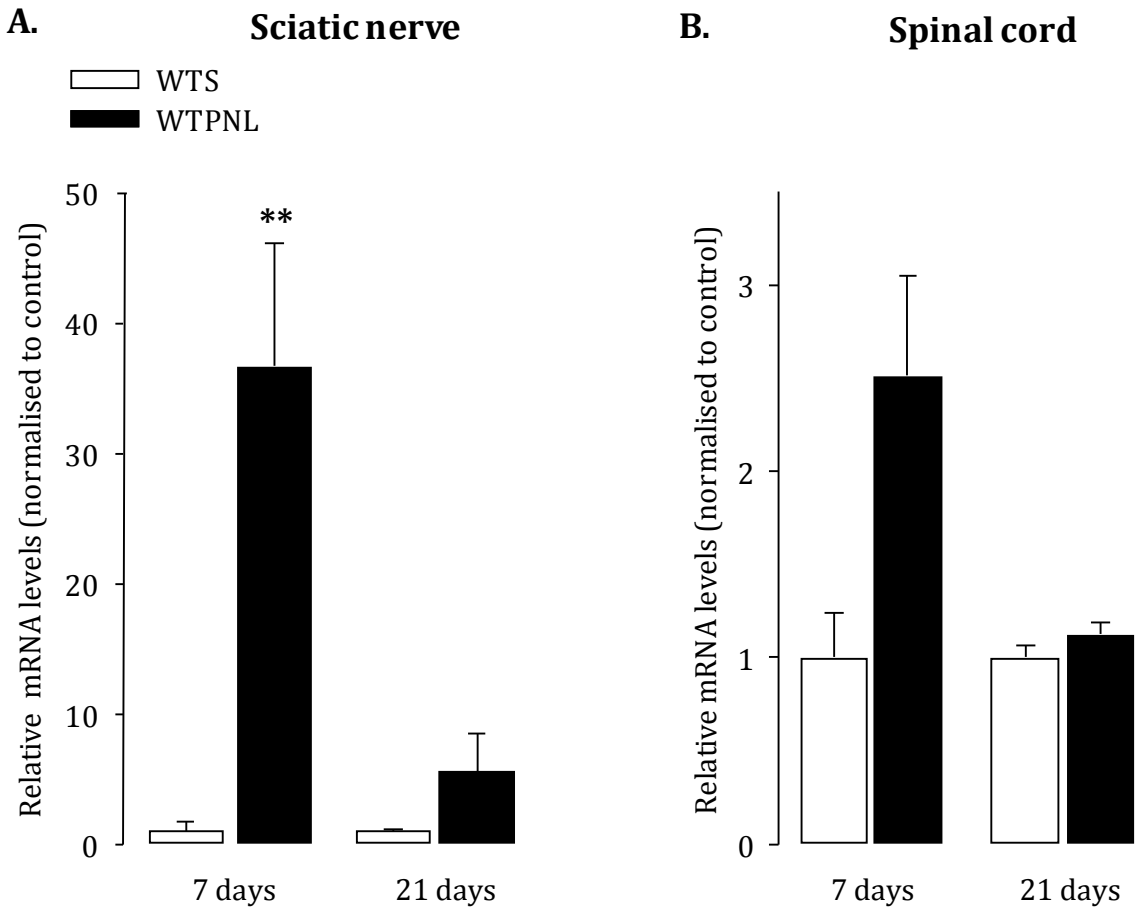

Figure 2.12: Nerve injury induces an increase in GPR84 expression in the sciatic nerve and spinal cord of WT mice

Subsequent to nerve injury there is an induction of GPR84 expression in the sciatic nerve (A) and spinal cord (B) at 7 and 21 days post PNL compared to sham tissue. This was only significant in the sciatic nerve at 7 days post PNL. Changes in mRNA expression are normalised to the mean ΔCT of sham groups, where ΔCT = (mean GPR84 CT) – (mean CT of the HK genes). Data are presented as the mean ± SEM. $P < 0.01$** vs sham, T-test with FDR for multiple testing correction, n = 4.

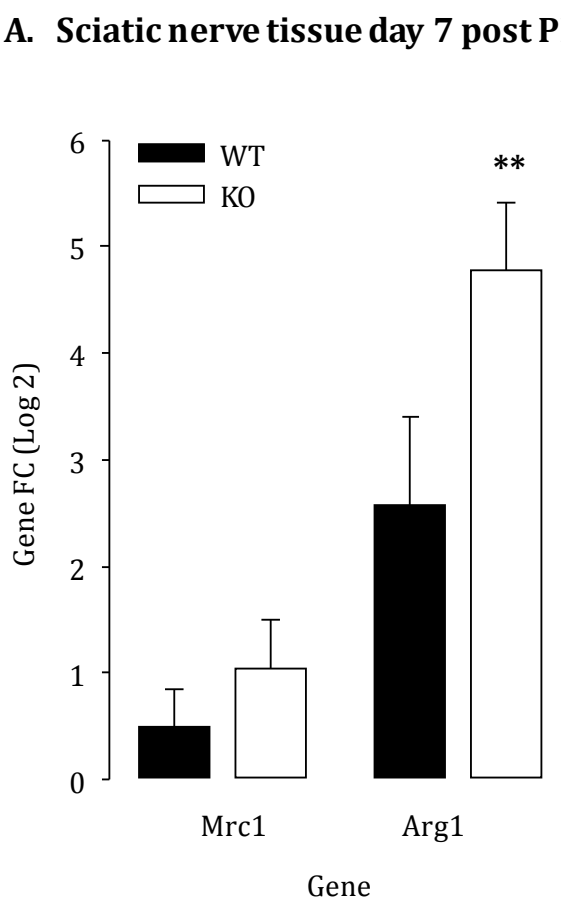

Figure 2.13: Nerve injured GPR84 KO mice show a greater induction of the anti-inflammatory macrophage markers, Arginase 1 (Arg1) and Mannose receptor c-type 1 (Mrc1)

(A) Nerve injury induces a significant increase in the expression of Arginase 1 and a greater induction in the expression of Mannose receptor c-type 1 in sciatic nerve of GPR84 KO mice 7 days post PNL, in comparison to their WT littermate controls. Changes in mRNA expression are relative to the four HK genes and expressed as a FC (PNL/sham). Data are presented on a log 2 scale as the mean ± SEM. $p < 0.01$** vs WT, T-test with FDR for multiple testing correction, n = 4.

2.4 Discussion

Neuropathic pain is a debilitating disease affiliated with a spectrum of pathologies. Neuronal-immune and glial interactions as well as the vast signalling networks of immune mediators play a principal role in neuropathic pain. In this chapter we utilised transgenic mice, exploiting the PNL model (Seltzer et al., 1990) to examine the role and function of GPR84 in neuropathic pain states. Peripheral nerve injury elicits profound adaptive and maladaptive transcriptional changes in metabolism, cell survival, excitability and transmitter synthesis, ultimately leading to the generation of neuropathic pain (Costigan et al., 2002). Amongst the many receptor classes that show substantial up- or down-regulation in response to nerve injury, GPCRs are one of the foremost classes. We have demonstrated that following PNL, the relative expression of GPR84 increased in the sciatic nerves and spinal cords of WT mice and that deletion of this GPCR abolished mechanical and thermal hypersensitivity; consistent with a critical role in neuropathic pain modulation. GPR84 appears to be exclusively expressed on immune cells and is therefore a new alternative non-neuronal target in therapeutic treatment of chronic pain.

2.4.1 GPR84 plays a role in neuropathic pain mechanisms independent of microglia and macrophage recruitment

The PNL paradigm (Seltzer et al., 1990) is a well established model of peripheral nerve injury that results in considerable damage to both myelinated and unmyelinated axons. As a partial nerve injury model, the preservation of some input enables behavioural responsiveness to mechanical and thermal stimuli to be tested. This model shows highly consistent pain-related changes in rodents (Malmberg and Basbaum, 1998). Although many groups initially employed rats to determine the molecular basis of pain pathology, there is an increasing shift towards the use of transgenic mice. The use of transgenic mice enables researchers to study specific proteins in complex pain mechanisms, which is an approach we have also adopted in our own studies to investigate the role of GPR84.

We showed that after nerve injury there was a significant reduction in mechanical and thermal thresholds of neuropathic mice in contrast to sham controls, recapitulating the literature. An accumulating body of literature has reported that these pain-related behaviours correlate with a rapid spinal cord glial response (Garrison et al., 1991). Alongside neuronal changes in the dorsal horn, microglial cells undergo extensive proliferative and morphological changes (Kreutzberg, 1996) by increasing the expression of

an array of cell surface receptors (e.g. CD11b, MHCII, $CD4^+$) and by releasing algesic mediators (Watkins et al., 2001; Coull et al., 2005; Clark et al., 2007a). This rapid phenotypic switch, which can be visualised by Iba1 and OX-42 antibody markers, normally correlates with the presence of hyperalgesic and allodynic behaviours. Pharmacological blockade of glial metabolism via inhibitors such as minocycline, fluorocitrate and propentofylline has demonstrated anti-allodynic properties and the attenuation of microglial activation, as revealed by reduced OX-42 immunofluorescence (Sweitzer et al., 2001; Ledeboer et al., 2005; Clark et al., 2007a). Targeting of specific microglial pathways or receptors in the CNS also alleviates pain associated behaviours; TLR4 and CX_3CR1 null mice exhibit decreased microglial proliferation and activation, as shown by reduced OX-42/Iba1 immunoreactivity and p-p38 expression (Tanga et al., 2005; Staniland et al., 2010). Moreover, neuropathic pain was inhibited with intrathecal administration of CCL2 neutralising antibody and abolished in the CCR2 null mouse (Abbadie et al., 2003; Thacker et al., 2009). In both cases this correlated with decreased microglial activation. However, there is some controversy with regards to the cell types that express CCR2, which has been reported to be exclusively neuronal in contrast to evidence of predominant microglial expression (Abbadie et al., 2003; Gosselin et al., 2005; Gao et al., 2009). Furthermore, the role of the purigenic microglial expressed receptors, $P2X_4$ and $P2X_7$ has been underscored by studies using null mice or selective antagonists, which also report diminished neuropathic pain (Tsuda et al., 2003; Chessell et al., 2005; Clark et al., 2010b). Thus, an overwhelming amount of data deriving from the manipulation of microglial signalling in the CNS, supports a role of these immune cells in the pathology of neuropathic pain (Watkins and Maier, 2003; McMahon and Malcangio, 2009).

On the other hand, in the periphery macrophages are the key immune cell players. Here, they infiltrate damaged axons, mediate WD via the phagocytosis of cell debris (Perry et al., 1987) and release a repertoire of pro-inflammatory mediators that sensitise primary afferent axons. This temporal relationship has been shown to strongly correlate with behavioural hypersensitivity (Myers et al., 1996). Importantly, pharmacological manipulation of macrophage expressed receptors, systemic depletion or attenuation of macrophage cell recruitment and infiltration is linked to reduced neuropathic pain behaviours (Myers et al., 1996; Perrin et al., 2005; Barclay et al., 2007; Boivin et al., 2007). Furthermore, a recent study showed that administration of the anti-inflammatory transforming growth factor-β1 (TGF-β1) directly into partially ligated sciatic nerves of mice reduced pro-inflammatory MAC^+ (CD11b/CD18) macrophages at the site of injury with a corresponding decrease in IL-6 and CCL3 and reduced neuropathic pain behaviours

(Echeverry et al., 2013). Treatment with this cytokine had no effect on the ED1^{+} (CD68) population of phagocytic macrophages and the WD process was normal. Based on these findings the authors proposed the notion of targeting specific macrophage populations to alleviate neuropathic pain without compromising nerve regeneration (Echeverry et al., 2013).

In light of this evidence and the fact that GPR84 is selectively expressed by immune cells, we focused on characterising the microglia and macrophage response to nerve injury in GPR84 WT and KO mice. To quantify these populations, reliable and sensitive methods are required. We used Iba1 and p-p38, which are well established immunohistochemical markers used to quantify the abundance and activation status, respectively, of microglia in the dorsal horn. We also stained for Iba1 in the sciatic nerve to quantify the presence of macrophages. It is well documented that nerve injury results in increases in both the activation and population size of microglia in the dorsal horn and macrophages in the injured sciatic nerve (Thacker et al., 2007; Austin and Moalem-Taylor, 2010; Gaudet et al., 2011; Calvo and Bennett, 2012; Calvo et al., 2012). Moreover, attenuation of behavioural hypersensitivity by pharmacological manipulation of membrane receptors or metabolic activity of these cells results in a reduction in these markers (Liu et al., 2000; Sweitzer et al., 2001; Ma and Eisenach, 2003b; Ledeboer et al., 2005; Tanga et al., 2005; Clark et al., 2007a).

We report that neuropathic pain is abolished in nerve injured GPR84 KO mice in contrast to WT littermates. As expected, WT mice demonstrated a significant reduction in mechanical and thermal withdrawal thresholds. This induction in behavioural hypersensitivity correlated well with a significant increase in microglial numbers and activation in the ispilateral dorsal horn, as revealed by enhanced Iba1 and p-p38 immunoreactivity, respectively. A significant degree of macrophage infiltration into the injured sciatic nerve was also shown by an increase in Iba1 positive cells. Interestingly, although behavioural hypersensitivity was absent, nerve injured GPR84 KO mice exhibited microgliosis and macrophage infiltration similar to that of the WT mice. Put together, these data suggest that GPR84 is a novel and promising target as gene deletion diminished neuropathic pain but did not alter acute pain thresholds. Although the recruitment of microglia and macrophage cells appears to play a limited role in neuropathic pain mechanisms mediated by GPR84, perhaps other features of these cells may be important or other immune cell types. We set out to test the former possibility with PCR array cards as discussed below.

2.4.2 GPR84 regulates the expression of a subset of pro-inflammatory mediators

In order to correlate the observed KO behavioural phenotype to altered genomic regulation, we next investigated whether GPR84 deletion affects transcriptional changes of mediators induced by nerve injury. Using custom designed mouse PCR array cards we examined changes in the sciatic nerve and spinal cord tissue of GPR84 WT and KO mice in the PNL model at two different time points. This produced four sets of gene expression data. Despite the immense potential of large data sets, the amount of information gathered can be difficult to interpret and manage. In addition, there are concerns about the representation, sensitivity and reproducibility of such data (Costigan et al., 2002). Therefore the implementation of a standard criteria, as well as the validation of gene changes at both mRNA and protein level are crucial steps for the conclusive determination of novel pain mediators.

We analysed the data sets via implementing a strict threshold criteria of a FC ≥ 2 and a FC ratio ≥ 1.5 and conducted multiple comparisons. Based on this approach, we examined the top ranking genes for consistency within and across data sets in addition to analysing transcriptional profiles and correlations between genotypes. Despite extensive analysis of the data it is unclear as to which mediators are contributing to the KO behavioural phenotype. It is evident that the largest transcriptional changes occurred in the sciatic nerve, some of which were only significant at 7 days post PNL. Greater changes in gene expression were observed at 7 days than at 21 days in both tissues and more genes were dysregulated in the sciatic nerve than in the spinal cord (at both 7 and 21 days). Therefore, as the more robust regulatory response was observed in the sciatic nerve at 7 days, we chose to subject this data set to further analysis. Here, nerve injury induced an up-regulation of 33 genes in the WT and 44 genes in the KO, and a down-regulation of 18 genes in the WT and 16 genes in the KO. It is well recognised that rodent models of peripheral nerve injury possess an inflammatory component (some to a greater extent than others) (Bennett, 1999; Bridges et al., 2001), which is accounted for in our data by an induction of pro-inflammatory genes. However, unexpectedly the induction of gene expression was similar between genotypes and KO mice exhibited as great, if not greater, increases in some pro-inflammatory mediators, particularly algogenic factors such as IL-1β, IL-6, TNF-α, PTGS2, NOS2 and CXCL5 (Follenfant et al., 1989; DeLeo et al., 1996; Aley et al., 1998; Homma et al., 2002; Ma and Eisenach, 2002; Dawes et al., 2011). There was also an increase in the cell surface markers AIF and ITGAM, which corresponded with our previous

immunohistochemical findings of a normal macrophage response in the KO as discussed in *2.3.5*.

2.4.3 GPR84 is involved in the regulation of a subset of growth factors in the sciatic nerve 7 days post PNL

Strikingly, many of the top down-regulated transcripts in the injured sciatic nerves of GPR84 KO mice (compared to WT) were EGFs. AREG, was not detected in the KO but was induced by nerve injury in the WT. BTC and EREG were induced in both genotypes but to a greater extent in the WT. HBEGF was down-regulated in both genotypes but more so in the KO. EGFs mediate multiple and versatile cellular functions including cell proliferation, survival, development and homeostasis via binding to their tyrosine-kinase epidermal growth factor receptors (EGFR/ERBBI) to initiate receptor dimerisation, autophosphorylation and the activation of vast signalling cascades (Schneider and Wolf, 2009). In the last decade, experimental evidence has revealed that GPCRs are able to augment potent mitogenic signals via a signalling partnership with EGFRs in a metalloprotease-dependent process. This pathway has been linked to many crucial physiological events such as cell proliferation, apoptosis, migration and disease (Schneider and Wolf, 2009). Little is known about EGFs in association with pain transmission, although one study reported that intradermal administration of EGF did not generate mechanical hyperalgesia and blocked PGE_2-mediated sensitisation, indicating a role in the attenuation of nociception (Andres et al., 2010). Then again, ERBB mediated signalling has been implicated in pain pathways (Calvo et al., 2010; Calvo et al., 2011).

ARTN, a member of the GDNF family, was induced in both genotypes after nerve injury but more substantially in the sciatic nerves of WT mice. Neurotrophins derived from immune cells such as mast cells and T lymphocytes exert multiple actions on sensory neurons and after nerve injury some neurotrophins and their receptors including NGF, BDNF and GDNF are markedly increased, particularly in Schwann cells (Woolf and Salter, 2000). We observed that NGF and BDNF were similarly induced by nerve injury in both genotypes, indicating that GPR84 is not involved in the regulation of these growth factors. Unlike NGF and BDNF, which are well documented in literature to play a role in pain transmission via sensitising nociceptors and increasing the excitability of dorsal horn neurons (Woolf, 1996; Latremoliere and Woolf, 2009), the story around GDNF is contradictory. GDNF has been postulated to have a neuroprotective role (Bennett et al., 2000; Ramer et al., 2003), and intrathecal administration was shown to reverse nerve injury induced behavioural

hypersensitivity; an effect attributable to normalised expression of sodium channels in the DRG (Boucher, 2000; Wang et al., 2003). Systemic administration of ARTN was also shown to reverse neuropathic pain behaviours in a dose and time-dependent manner and morphological/neurochemical manifestations generated by nerve injury were normalised by treatment (Gardell et al., 2003; Bennett et al., 2006). On the other hand, GDNF has also been shown to contribute to inflammatory induced pain in a model of CFA (Fang et al., 2003) and acute administration of GDNF induced mechanical hyperalgesia in the rat by sensitising nociceptors (Bogen et al., 2008).

2.4.4 GPR84 is involved in the regulation of cytokine/chemokine expression in the sciatic nerve 7 days post PNL

We report that nerve injury induces an increase in expression of many chemokines and cytokines that have been well documented for their pro-nociceptive properties. Interestingly, many of the pro-nociceptive cytokines, such as TNF-α, IL-1β, and IL-6, were amongst the top up-regulated hits in the sciatic nerve of KO mice. Subsequent to peripheral nerve injury Schwann cells, resident macrophages and mast cells release TNF-α, whose expression peaks concurrently with the maximal decrease in pain thresholds (Shubayev and Myers, 2000). Subcutaneous administration of TNF-α elicits mechanical allodynia and thermal hyperalgesia, which is rapidly reversed via the application of neutralising antibodies (Homma et al., 2002). IL-1β is up-regulated within hours of peripheral nerve injury and intraplantar or intraneural administration of the rat sciatic nerve produces a rapid onset of hypersensitivity (Follenfant et al., 1989; Zelenka et al., 2005). The role of IL-6 in pain is less clear due to its multifunctional role that has caused conflicting experimental reports. After nerve injury the expression of IL-6 and its receptor, IL-6R, increase proximal to the site of damage, in the DRG and in the spinal cord (Murphy et al., 1995; DeLeo et al., 1996). Whilst some have demonstrated that spinal administration of IL-6 produces dose-dependent anti-allodynic effects in SNL rats (Flatters et al., 2003, 2004), others have shown that intrathecal administration of IL-6 generates pain behaviours, which can be markedly attenuated in several models of neuropathy via anti-IL-6 neutralising antibodies (DeLeo et al., 1996; Lee et al., 2010). Amongst the top down-regulated transcripts in the sciatic nerves of KO mice were IL-5, IL-11, IL-23a, IL-34 and CXCL13. Little is known about these mediators in the context of pain but given that they were down-regulated in both genotypes (albeit to a greater extent in the KO) they are unlikely to play a role in the attenuated behavioural pain phenotype of KO mice.

A majority of the top ranking up-regulated genes in the KO vs WT were chemokines including CCL1, 2, 3, 4, 7, 8, 9; CXCL9, 10, 17 and XCL1. Chemokines have also been reported in pain transmission, acting on their neuronal, immune and glial cell expressed receptors, which are coupled to $G\alpha_{i/o}$ signalling pathways (see *Chapter 1*). These pathways play a pivotal role in inflammation and orchestrate numerous cellular functions such as leukocyte trafficking, angiogenesis and haematopoiesis (White et al., 2013). As previously discussed, neuropathic pain is abolished in CCR2 null mice and hypersensitive behaviours are attenuated with the administration of CCL2 neutralising antibodies. These observations correlate not only with an attenuated microglial response, but also with a reduction in macrophage recruitment (Abbadie et al., 2003). CCL3 is similarly postulated to contribute to neuropathic pain; peripheral or central administration of this ligand elicits pain behaviours that are reversed via antibody neutralisation (Kiguchi et al., 2010b). After nerve injury increased expression of CCL3 facilitates WD and nociceptor sensitisation via direct action on its $CCR1^+$ and $CCR5^+$ Schwann and macrophage cells (Kiguchi et al., 2012). The receptor for the chemokine IL-8 (CXCL8), CXCR2, was interestingly up-regulated 2.8 times more in the KO than in the WT. IL-8 is thought to facilitate inflammation and studies using CXCR2 null mice report defective neutrophil recruitment (Chapman et al., 2009). Chemotactic chemokines CCL4, CCL7 and CCL8 are involved in the recruitment of macrophages, acting through the same receptors that confer the pro-nociceptive properties of CCL2, CCL3 and CCL5 and thus could potentially play a role in nociceptive pathways (Wells et al., 2006). In addition, these chemokines also act through CCR1, 2 and 5, which have been well documented to increase in expression in a range of PNS inflammatory disorders in humans. For instance, sural nerve biopsies from patients with Guillain-Barré syndrome exhibited an increase in CCR1 and CCR5 due to infiltrating endoneurial macrophages (Kieseier et al., 2002).

Pro-inflammatory CXCL9 and CXCL10 interact independently and synergistically at their receptor, CXCR3, which is primarily expressed by T lymphocytes. In chronic inflammatory conditions such as RA and experimental models of MS, CXCL9 and CXCL10 are considerably up-regulated in synchrony with their receptors, where they critically orchestrate leucocyte entry into the nervous system (Iwamoto et al., 2008; Kohler et al., 2008). Increased expression of these chemokines may be indicative of enhanced nerve injury-induced T-cell recruitment in the KO. Despite a lack of significance, intriguingly, CCL1 was up-regulated in the KO but down-regulated in the WT sciatic nerve. The relevance of CCL1 signalling via its receptor, CCR8, in pain or inflammation is yet to be determined. Nevertheless, CCL1 has

been shown to possess chemotactic properties and induce the expression of pro-inflammatory cytokines (Reimer et al., 2011).

The anti-inflammatory chemokines, CXCL17 and XCL1, were up-regulated in the sciatic nerves of KO mice 7 days post PNL. CXCL17 is thought to be involved in tissue repair in response to injury and XCL1, also known as lymphotactin, harbours its chemotactic effects via its receptor, XCR1. Both chemokines are involved in the regulation of T cell function and the suppression of the immune response, but little is known with regards to their contribution to nociceptive pathways (Nguyen et al., 2008; Lee et al., 2013). Based on these data, we can conclude that the deletion of GPR84 causes an up-regulation of a subset of chemokines and cytokines in the injured sciatic nerve; unexpectedly a majority of which are pro-inflammatory or implicated in nociception. However, it is possible that GPR84 mediated signalling may usually exert a suppressive role over these particular mediators. It is a common concept that heterotrimeric $G\alpha_{i/o}$ protein signalling in macrophage cells favours a pro-inflammatory cytokine response, although intriguingly inhibition of $G\alpha_{i}$ subunits in murine macrophages has been documented to augment LPS induced cytokines (Fan et al., 2007). This striking observation parallels our own studies as we to report increased expression of many pro-inflammatory mediators as a result of the deletion of a $G\alpha_{i/o}$ coupled receptor. In relation to the behavioural phenotype this finding is unexpected and does not coincide with our original hypothesis that GPR84 deletion would in fact attenuate the expression of some key pro-nociceptive mediators, hence emphasising the differential regulation of chemokines via $G\alpha_{i/o}$ proteins and the possibility of compensatory systems.

2.4.5 GPR84 signalling

Under basal conditions GPR84 has a low level of expression in macrophage and microglial cells but is markedly induced by factors that activate the NFκB pathway such as LPS, TNF-α, IL-1β and MCFFAs (Wang et al., 2006a; Bouchard et al., 2007). IL-1β and TNF-α null mice exhibit reduced expression of GPR84 mRNA in the cerebral cortex, while the addition of IL-1β and TNF-α blocking antibodies also reduces GPR84 transcripts in microglial cell cultures (Bouchard et al., 2007). Interestingly, we did not see differential regulation between the genotypes of these mediators in our studies, suggesting that these cytokines are not positively regulated by GPR84 activation after nerve injury. Wang et al. (2012) were the first to report that MCFFAs with carbon chain lengths of 9-12 residues may serve as endogenous ligands of GPR84. During a screen of more than 20 cytokines, MCFFA stimulation was shown to dose-dependently amplify LPS-stimulated production of pro-inflammatory IL-12p40 (IL-

12b) (Wang et al., 2006a). This indicated that activation of GPR84 promotes Th1 differentiation and the production of Th1-associated cytokines such as INF-γ and IL-2. Therefore, we may have expected to see IL-12p40 expression decrease or remain unchanged in the injured sciatic nerve tissue of GPR84 KO mice along with decreased/unchanged expression of Th1-associated cytokines and an increase in Th2-associated cytokines such as IL-4, 5, 6, 10 and 13. Interestingly, another study examining GPR84 KO T-cells showed an increased IL-4 production in response to *in vitro* stimulation with anti-CD3 (Venkataraman and Kuo, 2005). Thus, GPR84 is implicated in the regulation of T cells and the production of a subset of cytokines. However, in contrast to what we would anticipate from the Wang (2012) study, we found an increase in IL-12p40 expression in the injured sciatic nerves of KO mice compared to WT. Moreover, there was no change or detection of IL-2, 4 and 13 and a decrease in IL-5 expression, although we did observe an increase in IL-6 and IL-10. Although our data does not entirely coincide with previous findings, we must consider the fact that functional *in vitro* assays do not necessarily reflect the *in vivo* situation. Furthermore, IL-12p40 may either form a functional pro-nociceptive IL-12p70 subunit (via heterodimersation with the IL-12p35 (a)), or a biological blocker of IL-12p70 (via homodimerisation with other IL-12p40 subunits), which has been documented to produce analgesic effects when administered to nerve injured mice (Chen et al., 2013). Therefore, we can postulate that the observed decrease in IL-12p35 mRNA in the injured sciatic nerves of KO mice indicates a consequential increase in IL-12p40 homodimerisation; this would inhibit IL-12 and attenuate the pro-inflammatory Th1 phenotype, consistent with the behavioural phenotype of GPR84 null mice.

More recent studies using modified MCFFAs with added hydroxyl groups revealed that GPR84 mediates granulocyte and macrophage chemotaxis and the production of pro-inflammatory IL-8 and TNF-α, respectively, under LPS stimulated conditions (Suzuki et al., 2013). Systemic administration of the surrogate agonist, 6-OAU, was also shown to raise CXCL1 levels in rats (Suzuki et al., 2013). We did not see corresponding changes in the expression of these cytokines in GPR84 KO mice, but as previously discussed, these experimental conditions may diverge from cytokine/chemokine changes induced by the PNL model.

2.4.6 Future work

The expression of GPR84 was significantly up-regulated in the sciatic nerve at 7 days after peripheral nerve surgery. This finding, in conjunction with the striking behavioural

phenotype of null mice, suggests that GPR84 is critical for neuropathic pain. In light of this evidence we hypothesised that GPR84 deletion might affect transcriptional changes of pro-nociceptive mediators that are normally induced by nerve injury; these mediators may be involved in the activation of GPR84 and/or downstream signalling effects of this receptor in neuropathic states. We also characterised the microglia and macrophage response as key immune cell players in neuropathic pain mechanisms. However, we unexpectedly found that key allogenic mediators were up-regulated in the KO and that the microglia and macrophage phenotype did not differ between the genotypes. Thus the mechanisms behind GPR84 nociceptive signalling are unclear.

It is apparent that GPR84 is not necessary for global changes in inflammatory mediators but may be important in regulating specific factors produced by microglia and/or macrophage cells. Our screening study indicated that the gene for the anti-inflammatory macrophage cell marker, ARG1, may be of particular importance. We observed a striking up-regulation of ARG1 in the injured sciatic nerve of KO mice in contrast to WT mice. Macrophages can be broadly categorised into two basic subsets: the pro-inflammatory classically-activated M1 class and the anti-inflammatory alternatively-activated M2 class, as discussed in *Chapter 1*. In a study investigating the role of TNF-α in a model of EAN, clinical severity scores were attenuated in TNF-α null mice, correlating with a pro-M2 macrophage phenotype (Zhang et al., 2012b). In another study, IL-12p40 null mice exhibited enhanced polarity for the M2 phenotype as well as increased secretion of the anti-inflammatory TGF-β (Bastos et al., 2002). Therefore, it would be instrumental to further validate the pro-M2 phenotype we observed in the PNL model and examine the expression of M1 and M2 macrophages in the injured sciatic nerves of GPR84 WT and KO mice.

Importantly, we must note that our examination was limited to a set array of 92 genes of interest to our group, and thus further studies profiling alternative mediators may prove more informative. We utilised the PNL model not only because it is mechanistically simple but also due to the remaining innervation of un-ligated nerve fibres, which allowed us to measure reproducible behavioural outcomes between the genotypes. However, we found that transcript changes were only significant in the sciatic nerve at 7 days and so a more robust nerve injury model may be more appropriate. For example, the SNI model (Decosterd and Woolf, 2000) would induce greater transcriptional changes as more neurons are damaged, hence providing a larger scope to observe differential regulation of transcripts between the genotypes. We did not observe positive evidence for the involvement of microglia or macrophage cell recruitment in GPR84 mediated nociceptive signalling.

Therefore, it would be interesting to further investigate other immune cell types known to play a role in neuropathic pain behaviours, such as neutrophils and T-cells.

In light of the behavioural phenotype in null mice and up-regulation of GPR84 mRNA in response to nerve injury, GPR84 appears to be a promising new target in pain research. Unfortunately, we were unable to visualise staining of this receptor in the PNL model as protein expression was not high enough for detection via this method (data not shown). It would be interesting to determine whether intrathecal or subcutaneous administration of a GPR84 blocking antibody to nerve injured mice would alleviate behavioural hypersensitivity. Conversely, the putative role of this receptor could be thoroughly tested by administration of a selective agonist to determine whether direct GPR84 activation can generate behavioural hypersensitivity in naïve mice.

Chapter 3

The Role of GPR84 in Chronic Inflammatory Pain

3.1 Introduction

3.1.1 Inflammatory pain

Inflammation is a protective response that is usually a result of tissue damage, infection or irritation and is classically associated with symptoms of redness (rubor), heat (calor), pain (dolor), swelling (tumor) and loss of function (function laesa). Vasodilation of blood vessels during inflammation decreases vascular resistance and thus enables increased blood flow to the area of damage, resulting in redness and heat. Increased vascular permeability facilitates the exudation of plasma proteins and fluid into the tissue, producing swelling (oedema). Concurrently, the process of inflammation activates free nerve endings, ultimately leading to the sensation of pain (Chiu et al., 2012). In doing so, the inflammatory response facilitates tissue healing by removing damaged tissue and limiting the use of the affected area. The final stage of a successful acute inflammatory response is resolution, which is a passive but highly co-ordinated sequence of events that restores homeostasis (Lee and Surh, 2012). However, in some cases where the pro-inflammatory signals persist and the immune response is uncontrolled, inflammatory pain outlasts the healing process of the underlying tissue damage and so no longer serves as a protective mechanism, leading to the development of chronic pain (Lee and Surh, 2012). Chronic inflammatory pain is a major clinical problem in many human diseases such as RA, OA, cancer, diabetes, fibromyalgia, inflammatory back pain and IBS and not only compromises the quality of lives of patients but also amounts to huge socioeconomic costs in patient care. Furthermore, increasing evidence has highlighted the role of neuroinflammatory processes in the etiology of many neurological diseases such as Alzheimer's, Parkinson's disease and multiple sclerosis (DeLeo and Yezierski, 2001). Therefore, the convergent involvement of the immune system and its multiple signalling molecules in the genesis of many inflammatory diseases is an important avenue for the development of successful therapeutic treatments.

3.1.2 Models of inflammatory pain

Hyperalgesia is a symptom that follows various forms of tissue injury and is typically characterised by a reduction in nociceptive thresholds. Such abnormal sensations may also be accompanied by allodynia and spontaneous pain, which are measurable behavioural outcomes in animal models of pain, although interpretation of the latter is subjective. To study chronic inflammatory pain, a number of experimental models in rodents have been developed that entail the cutaneous or subcutaneous application of an inflammogen or

chemical irritant to the hind paw, joint or muscle tissue followed by behavioural tests to examine changes in thermal and mechanical pain thresholds (Zhang and Ren, 2010). Some of the classical models routinely used include CFA (inactivated *mycobacteria tuberculosis* emulsified in mineral oil), zymosan (extract of yeast cell wall), carrageenan (seaweed extract) and formalin (Pillemer and Eaker, 1941; Freund, 1947; Dubuisson and Dennis, 1977; Svensson et al., 2003b). CFA, zymosan and carrageenan produce a rapid local inflammatory response, paw oedema and persistent pain. The hyperalgesia and allodynia last for approximately 1-2 weeks in the CFA model and 24 hours in the carrageenan and zymosan models. On the other hand, formalin consists of two phases; an initial 5 minute period of guarding, licking and biting behaviour, which is attributed to direct activation of nociceptor afferent terminals followed by a second phase of shaking and licking that lasts approximately 40 minutes and is thought to be mediated by central sensitisation of dorsal horn neurons within the spinal cord (Dubuisson and Dennis, 1977; Dickenson and Sullivan, 1987). Formalin treated rodents may also exhibit behavioural hypersensitivity lasting up to 4 weeks as a result of central sensitisation caused by ongoing peripheral signals from inflamed tissues and nerve damage (Fu et al., 1999). Several clinically relevant models of inflammatory pain have also been developed including the application of CFA into the knee joint or base of the tail to induce models of monoarthritis or polyarthritis, respectively (De Castro Costa et al., 1981). Type II collagen emulsified in Freund's incomplete adjuvant may also be injected into the base of the tail to induce polyarthritis (Baek et al., 2005).

CNS inflammation is a common feature of many neurological pathologies associated with pain (Felts et al., 2005). A number of inflammogens have been injected into the CNS to experimentally induce central inflammation. These include the cytokines IL-1β, TNF-α and INF-γ as well as LPS (Andersson et al., 1992a, b; Minghetti et al., 1999). LPS is a cell wall component of Gram-negative bacteria and is an amphiphillic compound consisting of a lipid A, a core oligosaccharide and an O side-chain. LPS is one of the most potent inflammatory inducing agents of the immune system and may be administered in several ways; for instance, systemic administration is used as a model of endotoxemia, while intrathecal treatment generates an inflammatory response that is isolated from immune-mediated disease processes (Andersson et al., 1992b; Felts et al., 2005).

3.1.3 LPS/TLR4 signalling pathway

LPS stimulation of mammalian cells occurs via the interaction with several binding proteins including CD14, MD2 and TLR4 followed by a cascade of signalling pathways. TLR4 is

believed to be unable to directly bind to LPS and so LPS/TLR4 signalling is permitted by the physical association of the MD2 protein on the cell surface, which may also be facilitated by the TLR4 co-receptor, CD14 (Lu et al., 2008). The Toll protein was first discovered in *Drosophila* and research carried out on the C3H/HeJ mouse, which possesses a defective LPS response, warranted the notion that TLR4 signalling is an essential component of the LPS response (Poltorak, 1998). Briefly, upon LPS recognition, TLR4 undergoes oligomerization and interacts with one of the five Toll-interleukin-1 receptor (TIR) domain-containing adaptor proteins, most commonly, the myeloid differentiation primary response gene 88 (MyD88) (Poltorak, 1998). Once associated with the TIR domain of the TLR, MyD88 recruits the serine/threonine kinase, IL-1 receptor-associated kinase 4 (IRAK4), to the TLR complex via an interaction between the death domains of both molecules and undergoes rapid phosphorylation and re-association with tumor necrosis factor receptor-associated factor 6 (TRAF6) (Cao et al., 1996a; Cao et al., 1996b). TRAF6 and phosphorylated TRAK1 subsequently dissociate from the receptor complex and go on to interact with TGF-β activated kinase (TAK1) and TAK-1 binding proteins (TAB) where a cascade of ubiquitination reactions occur on TRAF6 (Doyle and O'Neill, 2006). Eventual phosphorylation of TAK1 and TAB2 triggers the dissociation of the membrane bound TRAF6/TAK1/TAB1,2 complex to the cytosol where IRAK-1 is subsequently degraded. As a result, TAK1 is activated and phosphorylates the inhibitory κB (IκB) kinase complex (IKK) (Cao et al., 1996a; Cao et al., 1996b). The activated IKK complex in turn mediates phosphorylation and degradation of the IκB protein and subsequent liberation of NF-κB. NF-κB may then translocate to the nucleus to initiate the transcriptional regulation of many pro-inflammatory cytokines and immune-related genes (Lu et al., 2008). In parallel TAK1 also activates the MAPK kinases (MKKs), resulting in the eventual phosphorylation and activation of MAPKs such as p38 and JNK. Initiation of MAPK pathways leads to the activation of transcription factors, which drive the synthesis of many pro-inflammatory cytokines that facilitate pain-signalling (Lu et al., 2008). Fig. 3.1 summarises the LPS/TLR4 signalling pathway.

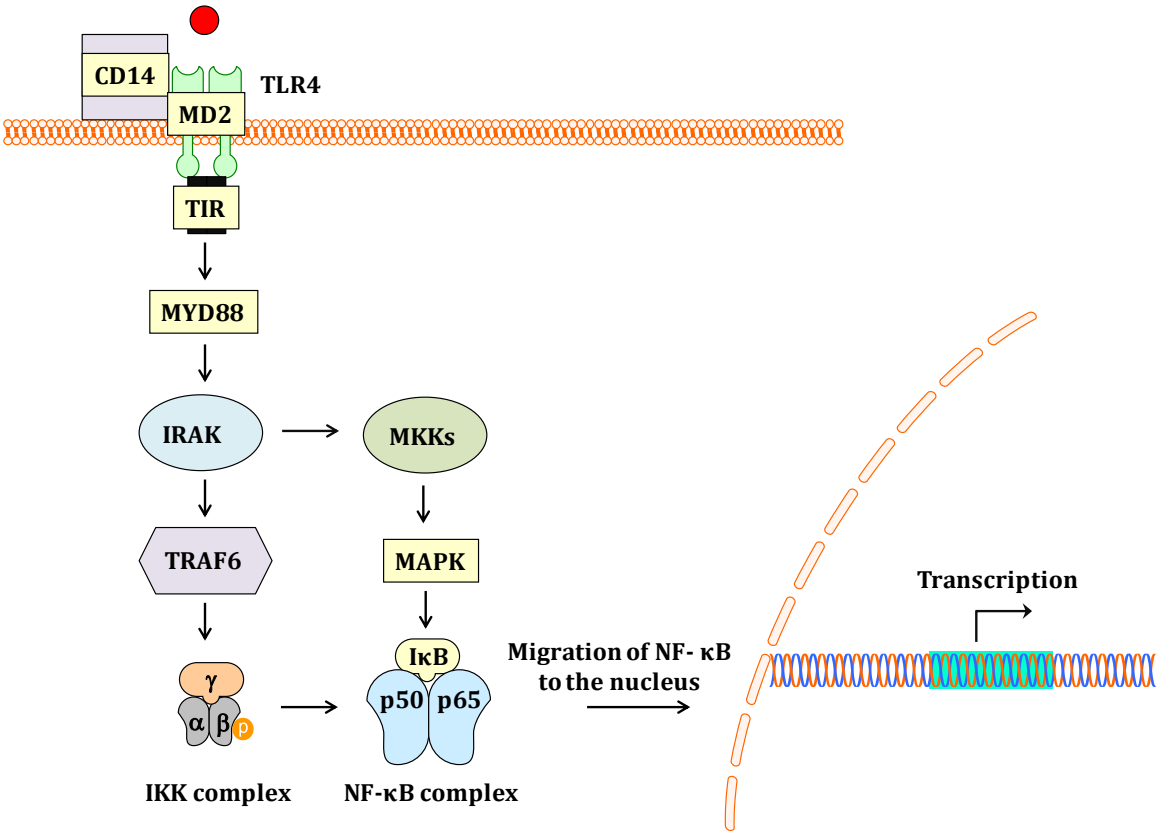

Figure 3.1: Diagram of LPS/TLR4 signalling pathway

Molecular components involved in TLR4 signalling pathway. Activated TLR4 interacts with MyD88, leading to the recruitment of IRAK, which undergoes rapid phosphorylation and re-association with TRAF6. After a series of phosphorylation-dependent events, the IKK complex is activated and mediates the phosphorylation and degradation of the IκB protein. Liberated NF-κB may then translocate to the nucleus to initiate the transcriptional regulation of many target genes. TRAF6 mediated activation of MKK leads to the mobilisation of MAPKs such as p38, which may also activate NF-κB.

In this chapter, we utilised a peripheral (CFA) and a central (LPS) model of inflammation. Injection of CFA to the hind paw produces a dose-dependent inflammation and behavioural hyperalgesia in rodents via the activation of the innate immune system and subsequent activation of the adaptive immune system in a TLR dependent manner (Freund, 1947; Marta et al., 2009). As GPR84 is normally only expressed by immune cells, the CFA model is appropriate for investigating the role of this receptor in persistent inflammatory induced pain. Intrathecal administration of LPS into the lumbar spinal cord is also associated with hyperalgesia in the hind paw (Cahill et al., 2003) and triggers the production of cytokines

such as IL-1β, TNF-α and IL-6 that contribute to the initiation and maintenance of behavioural hypersensitivity (DeLeo and Yezierski, 2001; Wieseler-Frank et al., 2005). Since TLR4 serves as a specific sensor of LPS and is exclusively expressed by microglial cells in the CNS (Lehnardt et al., 2002) we employed the LPS-induced CNS inflammatory model to selectively evaluate the response of microglial cells to a robust inflammatory stimulus in the absence of GPR84. Notably, GPR84 expression is up-regulated in microglia and macrophage cells by LPS or cytokines which are capable of stimulating the NF-κB pathway, such as TNF-α and to a lesser extent IL-1β (Wang et al., 2006a; Bouchard et al., 2007). Therefore, we also measured GPR84 expression in cultured microglia and macrophage cells subsequent to LPS stimulation and examined LPS-induced mediator profiles in WT and KO macrophages.

3.1.4 Mechanisms of chronic inflammatory pain

Subsequent to an inflammatory insult, multiple factors are released from damaged cells, producing an 'inflammatory soup' rich in protons (K^+, H^+), histamine, 5HT, PGs, growth factors, bradykinin, ATP and cytokines (Scholz and Woolf, 2002; Marchand et al., 2005; Linley et al., 2010). These nociceptor sensitizers act via their cognate receptors expressed on C-fibre terminals and generate an axonal reflex response by inducing the release of the neuropeptides, SP and CGRP (Chiu et al., 2012). SP and CGRP are considered to be the main initiators of neurogenic inflammation and upon C-fibre stimulation are released into the periphery where they act directly on vascular endothelial smooth muscle cells to elicit vasodilation and plasma extravasation, respectively. This results in the aforementioned characteristic redness and swelling (Chiu et al., 2012). Other mediators released in response to tissue damage such as PGE_2 and bradykinin, contribute to peripheral sensitisation of nociceptors by driving the activation of multiple intracellular transduction signalling pathways such as PKA, PKC and PI3K, as well as the MAPKs, p38, ERK and JNK (Fig. 3.2) (Woolf and Ma, 2007). There are two main downstream effects of these cascades, one being rapid phosphorylation-dependent modifications in ionotropic and metabotropic receptors, receptor subunits and subsets of ion channels, which alter activation thresholds and kinetic properties of nociceptor terminals. The other encompasses changes in transcriptional programmes that generate long-term effects (Linley et al., 2010). For example, sensitising agents such as PGE_2, adenosine and 5HT may enhance Na^+ conductance of TTX resistant channels by shifting the voltage-dependence and accelerating channel activation (Gold et al., 1996). Products of the COX pathway may also induce a transcriptional increase in the expression of $Na_v1.7$ and $Na_v1.8$ in large and small DRG neurons (Gould et al., 2004). In addition to increased excitability of primary afferent neurons, thermal hypersensitivity is a cardinal sign of an inflammatory response, and appears to be largely driven by enhanced

TRPV1 currents. NGF mediated activation of PI3K via TrkA activation leads to the down-stream phosphorylation of TRPV1 by src kinase and hence an increase in membrane current (Zhang et al., 2005d). Increased membrane currents of ion channels is mainly attributed to sensitisation or greater trafficking out of the DRG cell bodies to the surface membrane of peripheral processes (Coggeshall et al., 2004; Zhang et al., 2005d). In addition to post-translational effects, NGF may also mediate transcriptional regulation over multiple ionotropic (TRPV1, $P2X_3$, ASIC3) and metabotropic (B_2 receptor, μ-opiod receptor) receptors and voltage-gated ion channels (Na^+, Ca^{2+}, K^+) (Pezet and McMahon, 2006). NGF is a major contributor to inflammatory hyperalgesia and has been shown to be up-regulated in various experimental models of inflammation as well as in a number of human diseases with some correlation to the extent of reported pain. Correspondingly, anti-NGF treatment has successfully demonstrated alleviation of behavioural hyperalgesia in experimental models of inflammation using rodents (Pezet and McMahon, 2006).

Mobilisation of the resident immune cell response occurs in conjunction with the activation of sensory neurons. Here, activated mast cells and dendritic cells release a range of chemokines and cytokines that contribute to the localised pool of accumulating signalling molecules, many of which possess chemotactic properties for neutrophils, eosinophils, macrophages and T-cells (Chiu et al., 2012). The synthesis and release of chemotactic and cellular adhesion molecules establishes a concentration gradient, which is essential for the re-orientation, homing and migration of target leucocytes to active sites of inflammation (DeLeo and Yezierski, 2001). Immune cell infiltration and migration to the injury site is a hallmark of the stereotypical inflammatory response, where the initial activation of the innate immune system results in further production of cytokines and the expression of cell surface antigens, leading to the recruitment of the adaptive immune system (DeLeo and Yezierski, 2001).

In effect, activation of the immune system generates a second series of signals, which unanimously contribute to changes in the chemical milieu and transduction properties of nociceptive neurons. Cytokines are well documented to play an important role in the pathogenesis of many inflammatory diseases via their direct or, more commonly, indirect actions (Arai et al., 1990; Woolf et al., 1997). Characteristically, cytokines exhibit functional redundancy and overlap as they tend to share multiple receptors to carry out various autocrine, paracrine and hormonal effects. The complex signalling pathways of these molecules encompass a combination of pro- and anti-inflammatory actions on a broad range of cell types. This may involve transcription-dependent or independent effects that contribute to peripheral sensitisation and hence inflammatory pain hypersensitivity (Woolf

et al., 1997; Verri et al., 2006). The first cytokines described to play a role in inflammatory and/or neuropathic pain mechanisms were IL-1β, TNF-α, IL-6 and IL-8/CXCL8 followed by the more recently discovered contribution of IL-12 and IL-18. IL-1β and TNF-α are expressed by a range of cells and are prototypically involved in the establishment of peripheral sensitisation via recruiting and activating immune cells (Verri et al., 2006). These cytokines may also induce the expression of NGF and PGE_2 and exert direct effects on nociceptive neurons, which exacerbates neuronal excitability and evokes spontaneous firing (Woolf et al., 1997; Binshtok et al., 2008). Intraplantar administration of IL-1β was shown to elicit mechanical hypersensitivity in rodents that was dependent on the release of prostanoids, whereas local injection of the anti-inflammatory IL-1 receptor antagonist (IL-1ra) inhibited carrageenan and LPS induced hyperalgesia by means of competitive action at the IL-1R (Ferreira et al., 1988; Cunha et al., 2000). Consistent with this, mechanical and thermal hypersensitivity in the CFA model, were reported to be alleviated with pre-treatment of IL-1ra or an NGF neutralising antibody (Safieh-Garabedian et al., 1995).

TNF-α is a potent pro-inflammatory cytokine predominantly produced by macrophage cells in response to aberrant stimuli and mediates its effects through its high affinity receptors, TNFR1 and TNFR2. Similar to IL-1β, TNF-α has been experimentally demonstrated to evoke mechanical hypersensitivity subsequent to intraplantar administration and pre-treatment with anti-TNF-α antiserum attenuated CFA induced mechanical and thermal hyperalgesia (Woolf et al., 1997). In models of overt pain, subcutaneous injection of formalin or intraperitoneal zymosan/acetic acid evoked the release of IL-1β, TNF-α and IL-8/CXCL8, which are concomitantly involved in the writhing response, whereas administration of their corresponding anti-serums inhibited nociceptive behaviours (Ribeiro et al., 2000). Patients with chronic inflammation of the connective tissue exhibit raised levels of TNF-α in the temporomandibular joint synovium, which correlates with reported symptoms of local allodynia at the joint (Nordahl et al., 2000). Encouragingly, anti-TNF-α therapy is beneficial in some inflammatory diseases such as OA and psoriatic arthritis and has exemplified clinical success in RA treatment (Rankin et al., 1995; Haraoui, 2005).

IL-6 elicits a range of bio-activities that encompass both anti- and pro-inflammatory effects. Like the previously discussed cytokines, IL-6 administration to the hind paw induces a bilateral dose- and time-dependent mechanical hypersensitivity, which is indicative of systemic distribution (Cunha et al., 1992; Verri et al., 2006). This concept is supported by the fact that smaller doses of IL-6 produce correspondingly smaller effects in the contralateral paw and that intraplantar administration of IL-6 antagonists and neutralising antibodies inhibit hypersensitivity of the ipsilateral paw, with no effect on the contralateral

paw (Cunha et al., 1992). Furthermore, pre-treatment with indomethacin (COX inhibitor) specifically attenuated IL-1β or IL-6 evoked behavioural hyperalgesia whilst bearing no effect on IL-8 evoked hyperalgesia. Likewise, pre-treatment with atenolol (B_1 blocker) attenuated IL-8 but not IL-1β or IL-6 evoked hyperalgesia (Cunha et al., 1991; Cunha et al., 1992). This suggests that these cytokines elicit their effects via different mechanisms, involving either the COX pathway (IL-1β/IL-6) or the sympathetic nervous system (IL-8) (Cunha et al., 1991; Cunha et al., 1992). In a model of carrageenan evoked hyperalgesia, it was further demonstrated that co-administration of atenolol and anti-IL-8 serum were not additive in contrast to co-administration of indomethacin and anti-IL-8 serum, which exhibited additive effects and abolished behavioural hypersensitivity in the rat (Cunha et al., 1991). In addition, TNF-α induced mechanical hypersensitivity is partially attenuated with pre-treatment of indomethacin or atenolol and is abolished by co-treatment of these drugs (Verri et al., 2006). Correspondingly, anti-IL-1β, anti-IL-8 or anti-IL-6 treatment partially attenuated TNF-α induced hypersensitivity, whereas the combination of anti-IL-1β and anti-IL-8 or anti-IL-6 and anti-IL-8 neutralising antibodies abolished pain behaviours (Cunha et al., 1992; Verri et al., 2006). This evidence therefore suggests that TNF-α possess a pivotal role in inflammatory mechanisms and its effects are mediated by two distinguishable pathways: TNF-α/IL-1β/IL-6/prostaglandin and TNF-α/IL-8/sympathetic (Cunha et al., 1992; Verri et al., 2006).

Subsequent to inflammatory stimuli, IL-12 and IL-18 are also released from a range of immune cells including monocytes, macrophages, B cells and dendritic cells (Nakanishi et al., 2001; Verri et al., 2006) and synergistically promote Th1 differentiation and the production of IFN-γ (Nakanishi et al., 2001). Like IL-6, IL-12 exhibits dual roles; while it exacerbates collagen-induced arthritis when administered during the early stages of the disease, it exerts anti-inflammatory effects when administered at later stages (Joosten et al., 1997). IL-12 has also been shown to consistently produce pain in humans. For example, a cohort of renal cancer patients receiving intravenous recombinant IL-12 therapy presented cases of arthralgias in the finger joints and shoulder region (Gollob et al., 2000). Intraplantar administration of IL-12 also elicits hypernociceptive behaviours in rodents (Verri, 2005). IL-18 is a member of the IL-1 family and shares caspase 1 with IL-1β, which is the enzyme that catalyses the cleavage of its pro-IL-18 precursor molecule to yield the active glycoprotein (Bazan et al., 1996). Normally IL-18 is constitutively expressed in many cell types, unlike many other cytokines that are induced upon appropriate stimulation. In various inflammatory diseases including Crohn's disease, type 1 diabetes and RA, IL-18 expression increases in specific tissues associated with the particular disease (Nakanishi et al., 2001). In a collagen-induced arthritis model, IL-18 null mice were reported to show attenuated

disease severity, which correlated with reduced levels of TNF-α. The authors postulated that this was a neutrophil mediated mechanism as IL-18 promotes neutrophil migration via inducing TNF-α, which in turn up-regulates the neutrophil chemoattractant molecule LTB_4 (Canetti et al., 2001; Wei et al., 2001).

Incoming signals from the periphery and subsequent release of neurotransmitters into the dorsal horn generates changes in the chemical milieu of the CNS. Microglia and astrocytes respond via gliosis and a concomitant release of mediators (see *Chapter 1*) that contribute to the development of central sensitisation and behavioural hypersensitivity (Watkins et al., 2001; Watkins and Maier, 2003). Centrally released glutamate and SP directly activate NMDA and NK1 receptors expressed by microglial cells, which induces the activation of NF-κB and the sequential synthesis of pro-inflammatory mediators (Rasley et al., 2002). Upon neuronal activation the chemokine, fractalkine, is diffusely released from neuronal cell membranes and binds to its exclusively expressed microglial receptor, CX_3CR1. This forms a direct neuronal to glial cell signalling pathway, which essentially drives p38 activation and down-stream events that maintain hyperalgesia (Chapman et al., 2000). Once activated p38 is translocated to the nucleus where it phosphorylates transcriptional factors including activating transcription factor 2 (ATF-2), which mediates the biosynthesis of many mediators such as IL-1β, TNF-α, COX-2 and iNOS (Kumar et al., 2003; Svensson et al., 2003b; Ji and Suter, 2007; Ji et al., 2009). In addition to orchestrating transcriptional events, p38 is also thought to exert its effects via direct interaction with enzymes, receptors and ion channels (Svensson et al., 2003a). For example, during inflammation spinal p38 activates phospholipase A2 (PLA_2) leading to the generation of arachidonic acid and the production of PG. Conversely, it was shown that pre-treatment with intrathecally administered p38 inhibitors (SB20358 or SD-282) prevented COX-2 up-regulation with a concomitant attenuation of intraplantar formalin/carrageenan- and intrathecal SP-induced hyperalgesia (Svensson et al., 2003a; Svensson et al., 2003b). Similarly, Clark et al. (2006) showed that the release of IL-1β from LPS stimulated spinal cord slices was mediated by p-38 activation in spinal microglia, which could be prevented by the administration of a p-38 inhibitor. This was later shown to be dependent on the activation of the $P2X_7$ receptor as a result of LPS evoked ATP release (Clark et al., 2010b). Neuronally released ATP activates microglial cells via a selection of purigenic metabotropic (P2Y) and ionotropic ($P2X_4$ and $P2X_7$) receptors, which in turn initiate the release of several cytokines (Franke et al., 2007). As previously discussed (*Chapter 2*) the central release of proinflammatory cytokines (IL-1β, TNF-α, IL-6) enhances EPSCs and potentiates AMPA and NMDA currents in lamina II dorsal horn neurons via a combination of direct and indirect effects on neuronal properties (Kawasaki et al., 2008). Here chemokines are critical players in neuroinflammatory responses to a peripheral

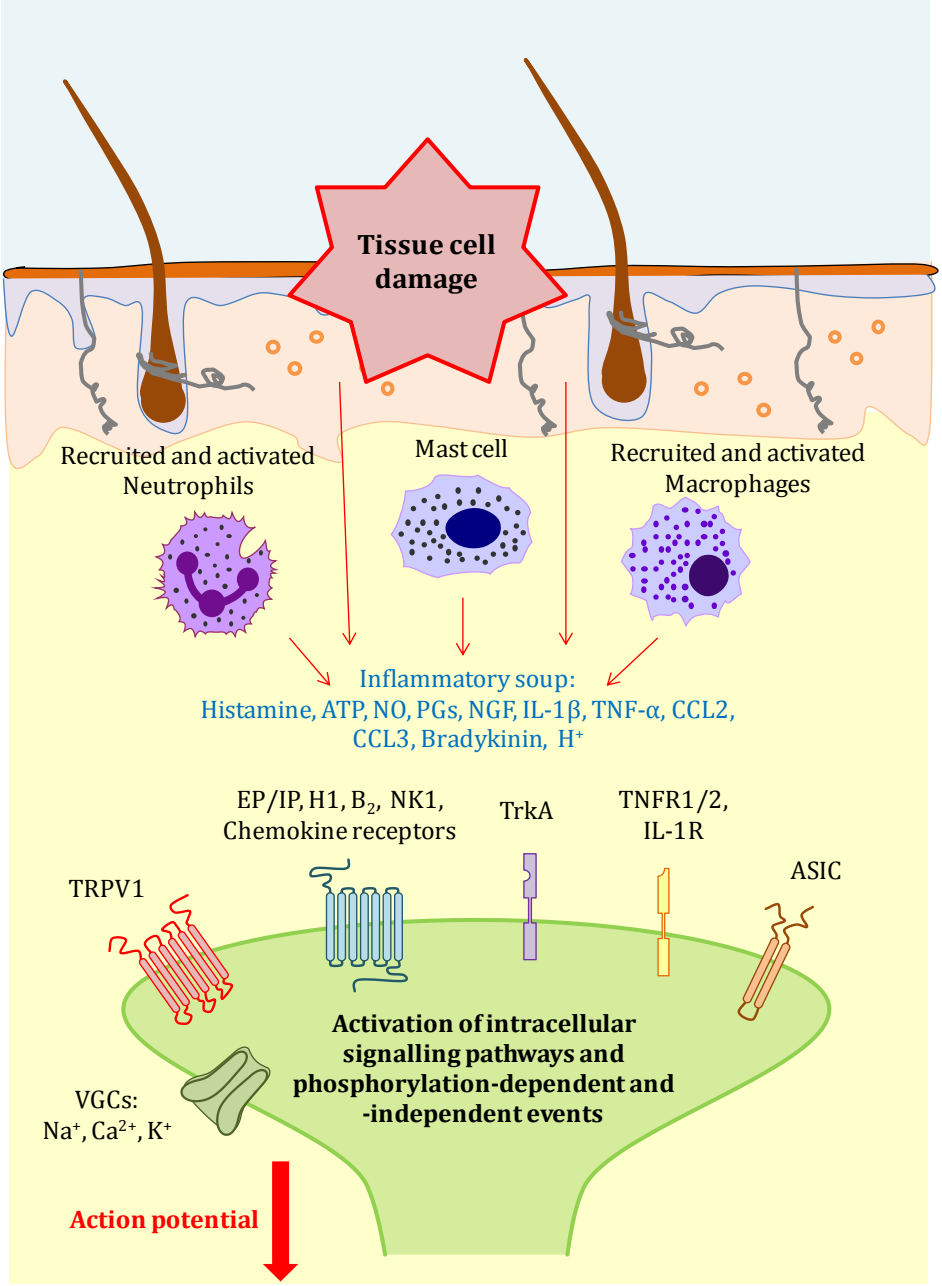

Figure 3.2: Inflammation-induced pain mechanisms

Subsequent to tissue damage, resident mast cells and macrophages are activated and blood-borne immune cells (neutrophils and monocytes) infiltrate the site of inflammation. Various mediators are released from damaged tissue cells and immune cells, which act via their cognate receptors expressed on primary afferent neurons. For example, TNF-α/TNFR, histamine/H1, bradykinin/B_2, NGF/TrkA, PGE_2/EP2, CCL2/CCR2, CCL3/CCR1,5 signalling leads to the activation of intracellular kinases (PKA, PKC, PI3K, MAPK), which initiate post-translational modifications such as phosphorylation and increased trafficking of ion channels and receptors. Chemokines and cytokines may exert their pro-nociceptive effects directly by binding to their receptors expressed on nociceptors. They may also act indirectly via recruiting immune cells and initiating the release of other mediators such as PGs, which can activate and sensitise nociceptors. Modified from Marchand et al. (2005).

insult and in addition to neuronal modulation they may also induce further release of COX2, NOS and SP. Ultimately, microglial activation and the subsequent release of cytokines, glutamate, ATP, prostanoids, NO and proteases drives multiple signalling pathways that contribute to increased excitability, the up-regulation of neuronal receptors and enhanced neurotransmission leading to centrally maintained hypersensitivity (DeLeo and Yezierski, 2001; Watkins et al., 2001; Watkins and Maier, 2003).

3.1.5 Aims

In this chapter we utilised a peripheral (CFA) and a central (LPS) model of inflammation in transgenic mice to evaluate the role of GPR84 in persistent inflammatory pain mechanisms. In both models we characterised pain behaviours of GPR84 WT and KO mice and examined the spinal microglial phenotype. Lastly, we investigated changes in mRNA transcript expression of 92 different chemokines, cytokines, growth factors and cell markers in LPS stimulated WT and KO macrophage cells. This approach enabled us to identify putative mediators that are modulated by GPR84 and hence may contribute to inflammatory-pain behaviour via down-stream signalling of this receptor.

3.2 Materials and methods

3.2.1 Animals

Breeding and genotyping of GPR84 WT and KO animals was carried out as described in the methods section in *Chapter 2*. Experiments were conducted on randomly selected mixed sex and age-matched mice weighing 20-25 g (7-14 weeks old). Mice were housed individually or in groups (no more than 4 per cage) in standard environmental conditions (12 hour light/dark cycle) with *ad libitum* access to food and water. Animal husbandry and experiments were carried out in a non-sterile housing environment in accordance with the United Kingdom Animals (Scientific Procedures) Act 1986.

To calculate the number of animals required for behavioural studies *a priori* power analysis was carried out using G*Power (v-3.1.7) software. Based on an estimated 60% reduction effect (deduced from previous experimental studies in our lab), the software estimated that a total sample size of 36 (n = 9 per group) would be required to detect statistical differences ($\alpha = 0.05$, $1-\beta = 0.95$, d = 3 or 6). For the CFA study two groups of animals were tested and the contralateral paw was used as a control for both genotypes. For the CNS inflammatory model four groups of animals were tested including a saline-treated control group and an LPS-treated group for each genotype. For all studies the experimenter was blinded to genotype and treatment. Allocation concealment was carried out by assigning each animal with an individual identification number (see *Chapter 2*) and by employing an independent investigator to prepare treatments. Blinding codes were broken after completion of behavioural experiments to determine if further anatomical assessment was necessary. According to pre-determined exclusion criteria, animals were excluded from experimental analysis as specified by the project license e.g. excessive self-mutilation.

3.2.2 Inflammatory pain models

Complete Freund's Adjuvant (CFA)

A single 15 µl dose of CFA (1 mg/mL, Mycobacterium tuberculosis in mineral oil; Sigma, UK) was injected into the plantar surface of the left hind paw. The contralateral paw served as a control. Mechanical (von Frey, paw pressure) and thermal/cold (Hargreaves, cold plate) withdrawal thresholds were examined pre- and post-CFA on days 1, 3, 7, 10 and 14. To

quantify the degree of paw oedema the dorsal-ventral thickness was measured using a pocket thickness gauge (Mitutoyo, UK) pre and post CFA treatment.

Lipopolysaccharide (LPS) – induced mechanical hyperalgesia

Animals were anesthetised with 2-3% isoflurane (Abbott Animal Health, UK) inhalation anaesthesia. Two intrathecal injections of LPS were administered into the lumbar region of the spinal cord, an initial 'priming' dose and a second dose 24 hrs later. Intrathecal injections were carried out using a 25 G needle on a Hamilton syringe, which was inserted at a 20° angle between the L5/L6 vertebrae as previously described (Hylden and Wilcox, 1980). LPS-treated mice received two 5 µl doses of 2 µg of LPS (Sigma, UK; dissolved in 0.9% saline) while control mice received two 5 µl doses of 0.9% saline. Mechanical (von Frey, paw pressure) and cold (cold plate) withdrawal thresholds were examined pre- and at 1 and 3 hrs post-LPS (Clark et al., 2006; Clark et al., 2010b).

3.2.3 Mechanical withdrawal threshold

Von Frey

Tactile mechanical thresholds of alert and unrestrained mice were examined via von Frey hair application (0.008-1 g, Touch Test, Stoelting, USA) to the plantar surface of the hindpaw via the 'up-down' method (Chaplan et al., 1994). Before testing, mice were acclimatised for a period of 1 hr in individual acrylic testing cubicles (8 x 5 x 10 cm) on an elevated wire mesh floor. Placement in testing cubicles was selected at random for each testing day. This enabled access to the lateral paw surface. Calibrated von Frey hairs were applied starting with the 0.6 g filament, in an alternate fashion to the left and right hind paw. The flexible nylon hair was applied so that the fibre bent for a duration of 3 s or until a paw withdrawal reflex occurred that was not coupled with movement or grooming. A positive withdrawal response is followed by a lower force hair and vice versa for a negative response until a change in behaviour occurs. Via this 'up-down' sequence four subsequent hairs were assessed and the 50% PWT was calculated according to the method described by (Dixon, 1980).

Paw pressure

Noxious mechanical thresholds were examined in the hindpaws of restrained alert mice via an Analgesymeter (7200; Ugo Basile, Italy) (Randall and Selitto, 1957). Each hindpaw was tested separately; briefly, the plantar surface was placed on a pedestal with a probe resting on the dorsal surface. Increasing pressure was applied via the probe, up to a maximum of 120 g to prevent tissue damage. The nociceptive threshold was taken as the force at which the mouse responded.

3.2.4 Thermal withdrawal threshold

Hargreaves

Thermal thresholds in unrestrained and alert mice were determined with the Hargreaves method using the Plantar Test (7370; Ugo Basile, Italy) (Hargreaves et al., 1988). Prior to testing, mice were acclimatised for 1 hr in individual acrylic testing cubicles (8 x 5 x 10 cm) on a glass plate. Placement in testing cubicles was selected at random for each testing day. An infrared light source of an arbitrary intensity of 30 (calibrated to elicit a PWL of 10-15 s in naïve mice) was directed onto the plantar surface of the hind paw through the glass plate. The PWL was automatically recorded in secs upon a withdrawal reflex. The left and right paws were tested alternately and responses were recorded for each paw on three separate occasions with at least 2 mins between assays. Each test had a maximum latency of 23 s to prevent tissue damage.

Cold plate

Noxious cold thresholds of the hind paws of lightly restrained mice were examined using the cold plate (IITC Life Sciences, USA) set at a temperature of 10°C ± 0.1°C. Each paw was tested separately by being placed with the plantar surface touching the plate. The latency to withdraw was taken as the threshold and recorded to the nearest 0.01 s. A 20 s cut-off was implemented to prevent tissue damage.

3.2.5 Tissue preparation and immunohistochemistry

On completion of behavioural testing, mice were anaesthetised with sodium pentobarbital (0.2 g/mL i.p.; Euthatal, Merial Animal Health Ltd) and perfused transcardially with a 0.9% saline and 0.1% heparin solution (Leo Laboratories Ltd, UK) followed by fixation with 4%

paraformaldehyde (PFA; VWR, UK) in 0.1 M PB. Lumbar spinal cords were dissected and post-fixed for 2 hrs in PFA and cryoprotected in a 20% sucrose/0.1 M PB solution (VWR, UK) for a minimum of 3 days at 4°C. Subsequently, tissue was embedded in OCT medium (VWR, UK), snap frozen with liquid nitrogen and stored at -80°C. Transverse spinal cord sections of the L4 and L5 lumbar region were cut on the cryostat in sets of 8 series at 20 μm thickness and subsequently thaw-mounted onto Superfrost plus microscope slides (VWR, UK). After drying, spinal cord sections were incubated overnight with primary antibody solution for p-p38 (rabbit anti-p-p38, 1:100; Sigma, UK) or GPR84 (goat anti-GPR84, 1:100; Santa Cruz, UK), and visualised with extra avidin-FITC following two stages of signal amplification with Avidin Biotin Complex (ABC; Vector Laboratories, USA) and biotinyl tyramide (PerkinElmer Life Sciences, UK) as previously shown (Clark et al., 2006). The sections were then incubated overnight with the second primary antibody, raised against Iba1 (rabbit anti-Iba1, 1:1000; Wako Chemicals, Germany), neuronal nuclei (mouse anti-NeuN clone A60, 1:500; UK) or GFAP (rabbit anti-GFAP, 1:1000; DakoCytomation, Denmark), and subsequently incubated with the appropriate secondary antibody solution for 2 hrs (1:1000; IgG conjugated Alexa Fluor 350, 488 or 546; Invitrogen, USA). All antibodies were prepared in PBS supplemented with 0.1% Triton X-100 (VWR, UK) and 0.2% sodium azide (Sigma, UK). Slides were carefully cover slipped with Vectashield Mounting Medium with or without DAPI (Vector Laboratories, UK), nail-varnished and dried.

Quantification of immunoreactivity

Images were visualised and captured using a Zeiss Axioplan microscope (Zeiss, UK) and for blinding purposes were labelled according to the identification code of the animal. Blinding codes were broken after study completion. Analysis of p-p38 and Iba1 immunoreactivity was performed by counting the number of positive profiles in the whole dorsal horn (7.3 x 10^5 μm^2) or within three fixed 4 x 10^4 μm^2 boxes in the lateral, central and medial areas of the dorsal horn, using the nuclear marker DAPI to assist in determining positive cells, as previously described (Clark et al., 2007a). A mean value was obtained for both the ipsilateral and contralateral dorsal horns of a minimum of three sections per animal. The experimenter was blinded to both the genotype and treatment throughout the analysis.

3.2.6 *In vitro* assays

Bio-gel elicited peritoneal macrophage (B-GEPM) cell culture and stimulation

Adult GPR84 WT and KO mice were given an i.p. injection (1 mL) of Bio-Gel P-100 2% polyacrylamide beads (Bio-Rad, UK). Four days later mice were culled via neck dislocation, and the layer of skin covering the peritoneum was wiped with 70% ethanol. A total volume of 20 mL of sterile cold phosphate-buffered saline (phosphate buffered saline (PBS); Invitrogen, UK) containing ethylenediaminetetraacetic acid (EDTA; 3 mM; Invitrogen, UK) was injected into the peritoneal cavity using a 25 G needle. After gentle massaging the buffer was retrieved in 14 mL Falcon tubes, filtered to remove the polyacrylamide beads and spun to obtain a pellet. Cells were then re-suspended and plated at a density of 2 x 10^6 cells/well in Dulbecco's Modified Eagle's medium (DMEM) with 10% fetal bovine serum (FBS) (Invitrogen, UK) and incubated at 37°C. The cells were washed 2 hrs after plating and the medium was replaced. Twenty four hrs later the media was replaced with FBS-free medium for 2 hrs, followed by 3 hrs of LPS stimulation (1 μg/mL; Sigma, UK). The culture medium of control wells was replaced with fresh FBS-free medium without subsequent stimulation.

Microglial cell culture and stimulation

Mixed primary cell cultures of glial cells were isolated from the cortical tissue of P7 rat pups (Staniland et al., 2010). Cultures were maintained for two weeks at 37°C (5% CO_2/95% O_2) in medium containing 1% penicillin-streptomycin (Sigma, UK) and 15% FBS (Invitrogen, UK), which was changed every 2-3 days. Two weeks later the microglial cells were harvested via forceful shaking of the flask and plated in 6 well plates at a density of 5 x 10^5 cells/well. Forty eight hrs later the medium was replaced with FBS-free medium, for a duration of 2 hrs followed by 3 hrs of LPS stimulation (1 μg/mL; Sigma). For control experiments, culture medium was replaced with FBS-free media and the stimulation step was omitted.

3.2.7 RNA extraction and cDNA synthesis

Following LPS stimulation of cultured microglia and B-GEPMs, cells were homogenised by removing the media and adding Trizol (Invitrogen, UK) directly to the well and pipetting up and down. RNA was extracted and cDNA was synthesised as described in *Chapter 2*.

3.2.8 Taqman array set-up and quantitative real-time PCR

Taqman® PCR mouse mediator arrays cards were custom designed using the Applied Biosystem website (http://www.appliedbiosystems.com). Each card contained 92 different transcripts and 4 HK genes and was run and subsequently analysed as described in *Chapter 2*. For each transcript the ΔΔCT values are presented as FC (FC = LPS/control). Transcripts with undetermined values in more than 50% of the samples were assigned an average default CT value of 38. If this occurred in both LPS and control sample groups, no FC value was calculated. Transcripts that were undetermined in less than 50% of samples obtained an average CT value based on the remaining data values.

To validate GPR84 and CCL19 expression in microglia and macrophage cells, respectively, individual quantitative real-time PCR (qRT-PCR) was performed using the Corbett Rotor-Gene 6000. Samples were added to Roche LightCycler master mix containing SYBR Green (Roche, UK) to produce a final [cDNA] of 5 ng/µl in a total volume of 20 µl. Four samples per experimental group were run in duplicate and subjected to 40 cycles of amplification. Primer sequences were designed using the Primer Blast software (http://www.ncbi.nlm.nih.gov/tools/primer-blst/) and tested to ensure an amplification efficiency within the range of 0.8-1.2 (see table below). Transcript levels were calculated using the ΔΔCT method, normalised against GAPDH (for GPR84 quantification) or HPRT (for CCL19 quantification). For each transcript the ΔΔCT values are presented as FC (FC = LPS/control). Control reactions with RNAse-free water produced no amplification signal.

Gene	Primer sequence	Product size (bp)
GAPDH	Forward 5' - TGTGTCCGTCGTGGATCTGA - 3' Reverse 5' - TTGCTGTTGAAGTCGCAGGAG - 3'	150
HPRT	Forward 5' - GTCCTGTGGCCATCTGCCTAG - 3' Reverse 5' - TGGGGACGCAGCAACTGACA - 3'	93
GPR84 (rat)	Forward 5' - TCAGGTGAGTCTCCATCATGTGGAA - 3' Reverse 5' - AGAAAGGCTGCAGGAGCGTGC - 3'	246
CCL19 (mouse)	Forward 5' - CTTCTGCCAAGAACAAAGGCAA - 3' Reverse 5' - ACAGACTTGGCTGGGTTAGG - 3'	150

3.2.9 Data and statistical analysis

All behavioural and immunohistochemical data were analysed using SigmaPlot 12.3 and SigmaStat software. For single comparisons between two groups, a paired Student's t-test was applied (behavioural data). For multiple comparisons, one-way (immunohistochemical data) or two-way (behavioural data) ANOVA was used, followed by SNK post hoc test to determine individual group differences. For the Taqman mouse PCR array card data, two-sided Welch's t-tests were run in the R programme on the ΔCT values. The p values were adjusted using the FDR method to correct for multiple hypothesis testing, as previously described (Benjamini et al., 2001). Non-parametric tests were applied where the data was not normally distributed. In all cases the data is presented as the mean ± SEM and $p < 0.05$ was set as the statistical significance level.

3.3 Results

3.3.1 GPR84 KO mice show attenuation of pain-associated behaviours after CFA

Having established that GPR84 plays a role in neuropathic pain mechanisms (see *Chapter 2*) we investigated whether this receptor may also contribute to chronic inflammatory pain pathways, especially in light of its documented role in clinically-relevant pathologies associated with inflammatory pain such as endotoxemia, EAE (model of MS), obesity and diabetes (Bouchard et al., 2007; Nagasaki et al., 2012). It is well established that experimental administration of inflammogens to the hind paw of rodents produces nociceptive hypersensitivity (Raghavendra et al., 2004; Clark et al., 2007a). Therefore, we utilised the CFA model as a relatively 'pure' model of persistent peripheral inflammation.

To investigate whether GPR84 deletion alters inflammatory pain-associated behaviours, CFA was administered to the hind paw of GPR84 WT and KO mice and mechanical and thermal thresholds were examined. As expected, WT mice showed a significant reduction in ipsilateral paw pressure thresholds by day 3 (D3, 64.3 ± 2.7 g) which remained down up until day 14 (D14 76.3 ± 6.0 g) compared to baseline (D0, 118.1 ± 4.2 g) or the contralateral paw (D3, 104.4 ± 3.1 g; D14, 110.6 ± 5.6 g) which served as an additional control (Fig. 3.3A). In contrast, KO mice showed an initial reduction at day 1 (88.1 ± 3.5 g) in ipsilateral thresholds compared to baseline (117.5 ± 4.1 g) and the contralateral paw (D1, 110.0 ± 3.1 g), which recovered by day 3 (93.1 ± 3.1g) and reached contralateral values by day 7 (106.2 ± 3.5 g) and remained unchanged (Fig. 3.3A). There was an average reduction of 35.2% in WT mice and 14.8% in KO mice from baseline over the 14 testing days. In both genotypes contralateral values did not significantly differ from baseline at any point. Area under the curve (AUC) quantification revealed that, in contrast to WT, KO mice did not develop mechanical hyperalgesia in the CFA treated paw and that there was a significant difference in ipsilateral thresholds between genotypes (Fig. 3.3B). Mechanical thresholds were also assessed using von Frey filaments. Interestingly, both genotypes showed a non-significant reduction in mechanical paw withdrawal thresholds expressed as calculated AUC of the ipsilateral hind paw compared to the contralateral side (Fig. 3.3D). These data suggest that GPR84 is involved in the maintenance of nociceptor driven mechanical hyperalgesia induced by inflammation but not mechanical allodynia.

Following peripheral inflammation, WT mice also showed a significant reduction in thermal thresholds of the ipsilateral hind paw from day 1 to 7 (D1, 3.9 ± 0.4 s; D3, 3.0 ± 0.4 s; D7, 4.8 ± 1.3 s; Fig. 3.3C) compared to baseline (D0, 8.9 ± 0.5 s) or the contralateral paw (D1, 11.2 ±

0.9 s; D3, 10.7 ± 0.6 s; D7, 13.9 ± 1.1 s). On day 7 thresholds started to recover to baseline and by this time point there was an average reduction of 55.8%. By day 10 thresholds were no longer significantly different from baseline (D10, 8.9 ± 1.6 s). Contralateral values did not significantly differ from baseline at any point. Similarly, KO mice showed an average reduction of 35.1% in thermal thresholds of the ipsilateral paw by day 7, which recovered to baseline thereafter. However, this was attenuated on days 1 and 3 (D1, 8.9 ± 3.7 s; D3, 4.7 ± 0.5 s) compared to WT mice. At no point was the change in thermal thresholds significantly different to baseline (10.1 ± 0.7 s) and only on days 3, 7 and 10 (D10, 7.1 ± 1.3 s) was there a significant difference from the control contralateral paw (D3, 11.0 ± 1.4 s; D7, 13.2 ± 1.3 s; D10, 15.7 ± 1.2 s).

Changes in sensitivity to cold stimuli was assessed, and as expected, WT mice developed significant cold hyperalgesia of the ipsilateral hind paw post CFA by day 3, which lasted up to day 14 (D3, 7.5 ± 0.6 s; D7, 9.9 ± 0.9 s; D10, 10.4 ± 0.8 s; D14, 8.7 ± 0.9 s) compared to baseline (D0, 17.5 ± 0.7 s) and the contralateral paw (D3, 10.7 ± 0.7 s; D7, 16.1 ± 1.0 s; D10, 16.5 ± 0.9 s; D14, 15.3 ± 1.6 s; Fig. 3.3F). Although, perhaps surprisingly, induction of cold hypersensitivity did not occur before day 3. There was an average reduction of 38.0% from baseline. Strikingly, KO mice showed an initial reduction of 32.1% in ipsilateral cold thresholds compared to baseline (16.4 ± 1.6 s) on day 1 (11.1 ± 1.0 s), which rapidly recovered to contralateral thresholds by day 3 (ipsi: 11.7 ± 0.6 s vs contra: 12.7 ± 0.5 s) and baseline thresholds by day 7 (15.5 ± 1.8 s) and remained unchanged throughout the rest of the testing days. In both genotypes contralateral values did not significantly differ from baseline at any point. AUC analysis showed that WT but not KO mice developed significant cold hyperalgesia in the CFA treated paw and that there was a significant difference between ipsi values of the two genotypes (Fig. 3.3G). Together these data show that GPR84 KO mice developed a transient thermal and cold hypersensitivity after peripheral inflammation that quickly recovered back to baseline. In contrast, the development of thermal and cold hypersensitivity in WT littermate controls was maintained. This finding suggests that GPR84 may be important for the maintenance rather than the initiation of inflammatory thermal and cold hyperalgesia.

GPR84 is expressed by immune cells involved in peripheral inflammation. To compare levels of peripheral inflammation between genotypes, the extent of oedema in the ipsilateral hind paw was assessed by measuring dorso-ventral paw thickness (Fig. 3.3E). We observed paw oedema in both genotypes from 24 hrs post CFA, which became significant on days 3 (both genotypes) and 7 (only KO mice) in comparison to baseline. However, there was no significant difference between genotypes. This result suggests that GPR84 deletion has no

effect on the degree of hind paw inflammation (WT: D0, 1.6 ± 0.1 mm; D1, 3.4 ± 0.5 mm; D3, 3.2 ± 0.2 mm; D7, 2.8 ± 0.1 mm vs KO: D0, 1.7 ± 0.03 mm; D1, 3.12 ± 0.4 mm; D3, 3.1 ± 0.2 mm; D7, 3.2 ± 0.1 mm).

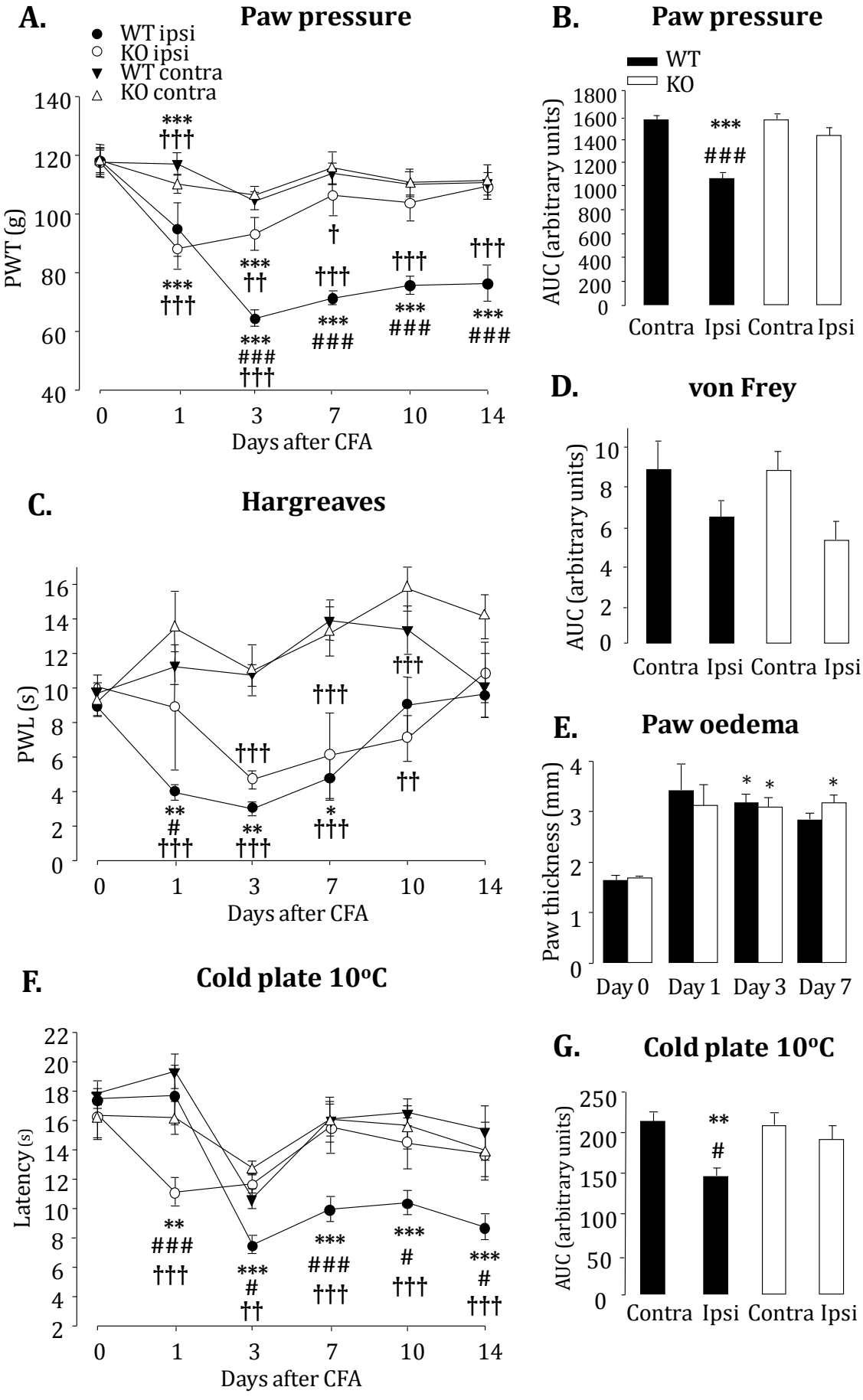
A.
Paw pressure
WT ipsi
KO ipsi
WT contra
KO contra
PWT (g)
Days after CFA
B.
Paw pressure
WT
KO
AUC (arbitrary units)
Contra Ipsi Contra Ipsi
C.
Hargreaves
PWL (s)
Days after CFA
D.
von Frey
AUC (arbitrary units)
Contra Ipsi Contra Ipsi
E.
Paw oedema
Paw thickness (mm)
Day 0 Day 1 Day 3 Day 7
F.
Cold plate 10°C
Latency (s)
Days after CFA
G.
Cold plate 10°C
AUC (arbitrary units)
Contra Ipsi Contra Ipsi

Figure 3.3: CFA treated GPR84 KO mice show attenuated inflammatory pain hypersensitivity

(A) Starting at 24 hrs post intra-plantar CFA administration (15 µl; 1 mg/mL), GPR84 WT mice showed a significant reduction in ipsilateral mechanical PWTs compared to baseline (day 0) and the control contralateral hind paw, which persisted throughout the 14 testing days. In contrast, GPR84 KO mice showed an initial reduction that recovered to baseline by day 7 and remained unchanged up until day 14. There was a significant difference between genotypes. ***$p < 0.001$ vs baseline; $^{\dagger\dagger\dagger}p < 0.001$ vs contralateral paw; $^{\#\#\#}p < 0.001$ vs KO, two-way RM ANOVA; post-hoc SNK. (B) AUC analysis for WT and KO ipsilateral and contralateral PWTs from baseline to 14 days post CFA were calculated (arbitrary units). In contrast to WT littermates, KO mice did not develop mechanical hyperalgesia in the ipsilateral hind paw. There was a significant difference between genotypes. ***$p < 0.001$ vs contralateral paw; $^{\#\#\#}p < 0.001$ vs KO, one-way ANOVA; post-hoc SNK. (C) WT mice showed a significant reduction in thermal PWLs of the ipsilateral paw from baseline on days 1 to 7, which recovered to baseline by day 14. In contrast, KO mice showed an attenuated level of reduction in thermal thresholds of the ipsilateral paw on days 1 and 3, which was significant on day 1. The thresholds of KO mice were not significantly different from baseline at any point. *$p < 0.05$, **$p < 0.01$ vs baseline; $^{\dagger\dagger}p < 0.01$, $^{\dagger\dagger\dagger}p < 0.001$ vs contralateral paw; $^{\#}p < 0.05$ vs KO; two-way RM ANOVA, post-hoc SNK. (D) WT and KO mice showed equivalent levels of mechanical allodynia in the ipsilateral hind paw, expressed as calculated AUC over the 14 day testing period. (E) Dorso-ventral paw thickness was measured as an indicator of paw oedema following CFA injection. WT and KO mice showed an equivalent increase in dorso-ventral paw thickness post CFA at all time points tested and there was no significant difference between genotypes at any point. *$p < 0.05$ vs baseline, Friedman RM ANOVA on Ranks, post-hoc Bonferroni–Dunn. (F) WT mice showed a long-lasting reduction in cold sensitivity thresholds post CFA injection in contrast to KO mice, which after an initial reduction recovered to baseline by day 3 and remained unchanged thereafter. There was a significant difference between genotypes on all testing days from 1 to 14. **$p < 0.01$, ***$p < 0.001$ vs baseline; $^{\#}p < 0.05$, $^{\#\#}p < 0.01$, $^{\#\#\#}p < 0.001$ vs KO; $^{\dagger\dagger}p < 0.01$, $^{\dagger\dagger\dagger}p < 0.001$ vs contralateral paw, two way RM ANOVA with SNK. (G) Calculation of AUC for cold PWLs of both genotypes from baseline to 14 days post CFA. WT, but not KO, mice developed significant cold hyperalgesia in the ipsilateral paw. There was a significant difference between genotypes. **$p < 0.01$ vs contralateral paw; $^{\#}p < 0.05$ vs KO, one-way ANOVA; post-hoc SNK. In all cases data are presented as the mean ± SEM, n = 8, except von Frey data where n = 16 up to day 7 and n = 8 thereafter.

3.3.2 CFA induced microgliosis is attenuated in GPR84 KO mice

Having established a behavioural phenotype, we then sought to correlate this with anatomical findings. In virtually all animal models of inflammation-induced pain, a microglial response has been immunohistochemically detected in the spinal cord (Sweitzer et al., 1999; Svensson et al., 2003b; Raghavendra et al., 2004; Hua et al., 2005; Guo et al., 2007; Sun et al., 2007). Therefore, to examine microglial cells in GPR84 mediated inflammatory pain we examined immunophenotypic changes of these cells in lumbar spinal cord sections of WT and KO mice at 14 days post CFA.

Quantification of Iba1 immunoreactivity revealed that at 14 days post CFA there was a significant 1.8-fold increase in microglia cell numbers in the ipsilateral dorsal horn of WT mice (8.7 ± 1.1/4x10^4 μm^2) compared to saline control (4.9 ± 0.5/4x10^4 μm^2; Fig 3.4A, B). This is in accordance with previous work where microglial activation was observed 4-14 days after CFA treatment (Raghavendra et al., 2004). In CFA treated KO mice there was a non-significant 1.8 fold increase (8.6 ± 1.6/4x10^4 μm^2) in microglial cells numbers in the ipsilateral dorsal horn compared to saline controls (4.9 ± 0.5/4x10^4 μm^2). Therefore both genotypes exhibited an equivalent increase in Iba1 positive cells and there was no significant difference between them. These data suggest that GPR84 does not play a role in regulating microglial numbers subsequent to a peripheral inflammatory insult. In CFA-treated mice both genotypes also exhibited similar microglial morphology, which varied from the typical ramified 'quiescent' state through to various stages of 'activation', in which cells appeared deramified and more amoeboid in shape with thicker and shorter processes.

We also investigated whether GPR84 deletion may alter the ability of microglial cells to respond to an inflammatory insult by examining staining for the microglia activation marker p-p38 MAPK (Ji and Suter, 2007; Ji et al., 2009). Quantification of immunoreactivity revealed a significant 1.8-fold increase in p-p38 positive cells in the ipsilateral dorsal horn of WT mice (8.6 ± 1.1/4x10^4 μm^2) compared to saline controls (4.9 ± 0.4/4x10^4 μm^2; Fig 3.4A, B). CFA treated KO mice showed a 1.7-fold increase (8.3 ± 1.8/4x10^4 μm^2) in p-p38 positive cells in the ipsilateral dorsal horn, which was not statistically significant compared to saline control (4.9 ± 0.3/4x10^4 μm^2). Again, there was no significant difference between the genotypes, suggesting that GPR84 signalling may not be important in the activation of microglial cells in inflammatory pain states.

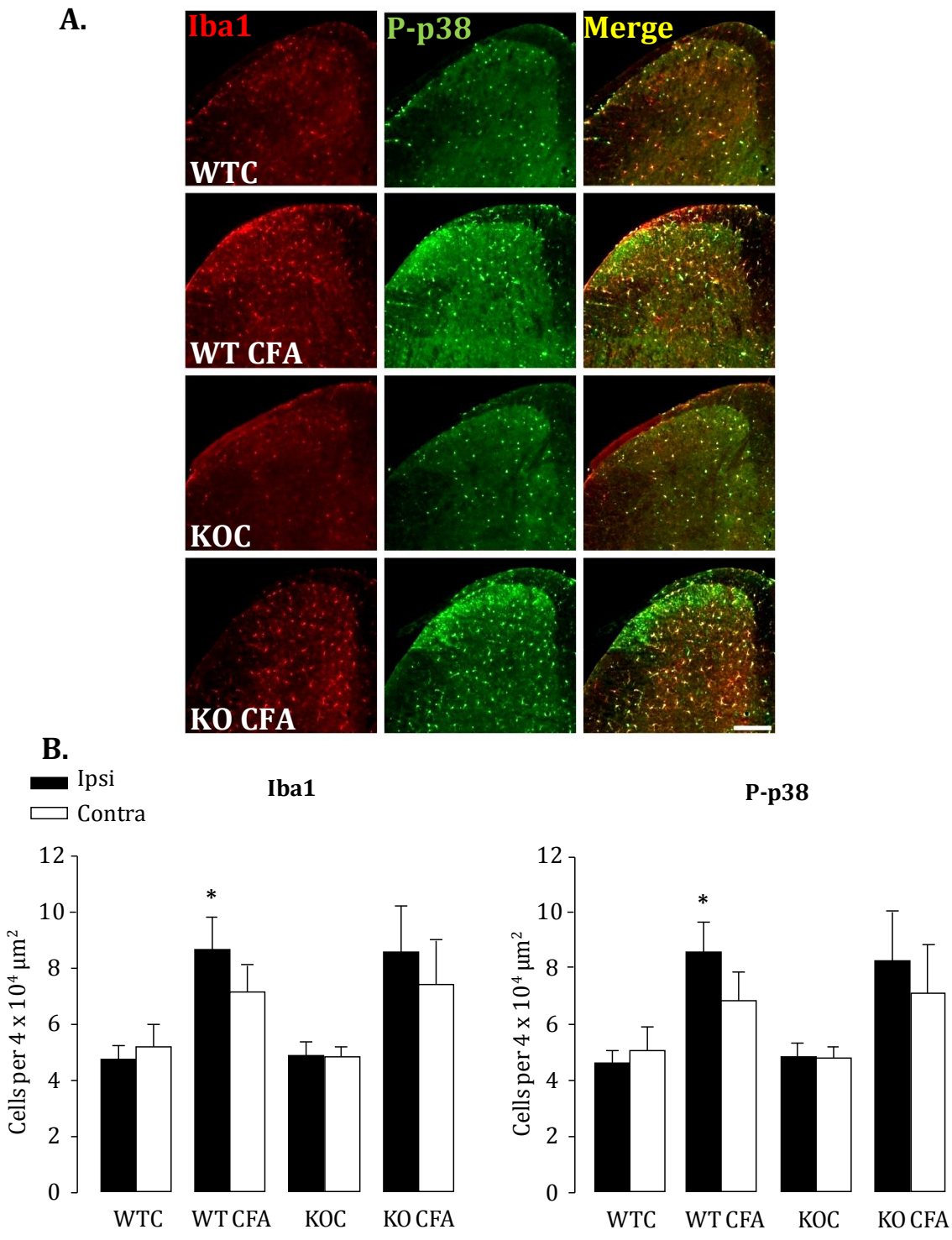

Figure 3.4: CFA induced microgliosis is attenuated in GPR84 KO mice

Subsequent to intraplantar CFA, there was a significant increase in Iba1 and p-p38 positive cells in the ipsilateral dorsal horn of the spinal cord in WT mice (WT CFA) compared to saline control (WTC). CFA-injected KO mice (KO CFA) also showed an increase in Iba1 and p-p38 positive cells compared to saline control (KOC), however, this was not significant (A); quantified in (B). There were no significant differences between genotypes. Data are presented as the mean ± SEM; $^{*}p < 0.05$, vs control; one-way ANOVA on ranks; post-hoc Tukey, n = 4-6. Scale bar = 200 µm.

3.3.3 LPS treated GPR84 KO mice show attenuated behavioural hyperalgesia

Although a number of experimental models of neuropathic and inflammatory pain demonstrate that microglia activation plays a role in the development of chronic pain (DeLeo and Yezierski, 2001; Watkins and Maier, 2003; McMahon et al., 2005; Clark et al., 2007a), we have been unable to correlate the behavioural phenotype of GPR84 KO mice after PNL or CFA to an altered microglial response. Therefore, to conclusively exclude the contribution of microglial cells in GPR84 mediated signalling we examined the role of these cells in the CNS by utilising the LPS-induced inflammatory model. Since intrathecal LPS specifically activates microglial cells via the TLR4 and is associated with heat and mechanical hyperalgesia (Lehnardt et al., 2002; Cahill et al., 2003), we investigated whether GPR84 deletion alters microglia mediated nociceptive behaviour.

Mice were primed with intrathecal LPS (2 μg/mouse) on day 1, which has been previously reported not to alter PWT to noxious or innocuous mechanical stimuli (Clark et al., 2006). As expected, the second dose of LPS 24 hrs later induced transient mechanical allodynia in GPR84 WT mice at 1 hr post treatment (0.4 ± 0.1 g), which rapidly recovered by 3 hrs (0.7 ± 0.1 g) and was no longer significantly different from baseline (0 hr, 0.9 ± 0.1 g) or control animals (0hr, 0.9 ± 0.1 g; 1hr, 0.9 ± 0.2 g; 3hr, 0.7 ± 0.1 g; Fig 3.5A). KO mice also showed a reduction in mechanical thresholds in response to intrathecal LPS however, this was not significant (LPS: 0hr, 0.8 ± 0.1 g; 1hr, 0.4 ± 0.1 g; 3hr, 0.6 ± 0.1 g vs control: 0hr, 0.8 ± 0.03 g; 1hr, 0.7 ± 0.2 g; 3hr, 0.7 ± 0.1 g; Fig 3.5B). One hr post LPS, WT and KO mice showed reductions of 57.5% and 52.2%, respectively, and there was no significant differences between genotypes.

Subsequent to priming and the second dose of intrathecal LPS, WT mice also developed significant mechanical hyperalgesia at 3 hrs post treatment (88.9 ± 1.6 g) in comparison to saline controls (100.8 ± 1.1 g; Fig. 3.5C). According to the literature, intrathecal LPS has been shown to induce significant mechanical hyperalgesia from as early as 1 hr post treatment that persists up to 6 hrs and returns to baseline thresholds by 24 hrs (Clark et al., 2006). Interestingly, we observed an increase in thresholds at 1 hr post treatment (112.5 ± 1.9 g) that dropped 15% below baseline (104.6 ± 1.7 g) by 3 hrs. Similarly KO mice also exhibited an increase in thresholds at 1 hr post treatment (112.5 ± 3.1 g) compared to baseline (101.9 ± 1.9 g) or saline controls (102.5 ± 0.6 g). However, at 3 hrs post LPS, KO mice showed a marginal 5.6% drop in mechanical thresholds (96.3 ± 4.0 g) from baseline and did not significantly differ from saline controls (101.3 ± 1.5 g) in contrast to WT mice (Fig. 3.5C).

In both genotypes cold sensitivity was unaltered 1 hr (WT: 13.1 ± 0.2 s; KO: 13.2 ± 0.5 s) after the second LPS dose but significantly dropped 3 hrs post treatment (WT: 10.7 ± 0.7 s; KO: 10.7 ± 0.4 s) in comparison to baseline (WT: 12.2 ± 0.4 s; KO: 12.4 ± 0.3 s; Fig 3.5D). There were no significant differences between genotypes. Together, the above data suggests that GPR84 may be involved in mediating mechanical hyperalgesia via the modulation of microglial cells but not mechanical allodynia or cold hyperalgesia. This modality-specific inhibition could be a result of phenotypic differences in populations of afferent fibres such as the expression of TRP channels and mechanosensors, which may be regulated down-stream of GPR84 activation under inflammatory conditions.

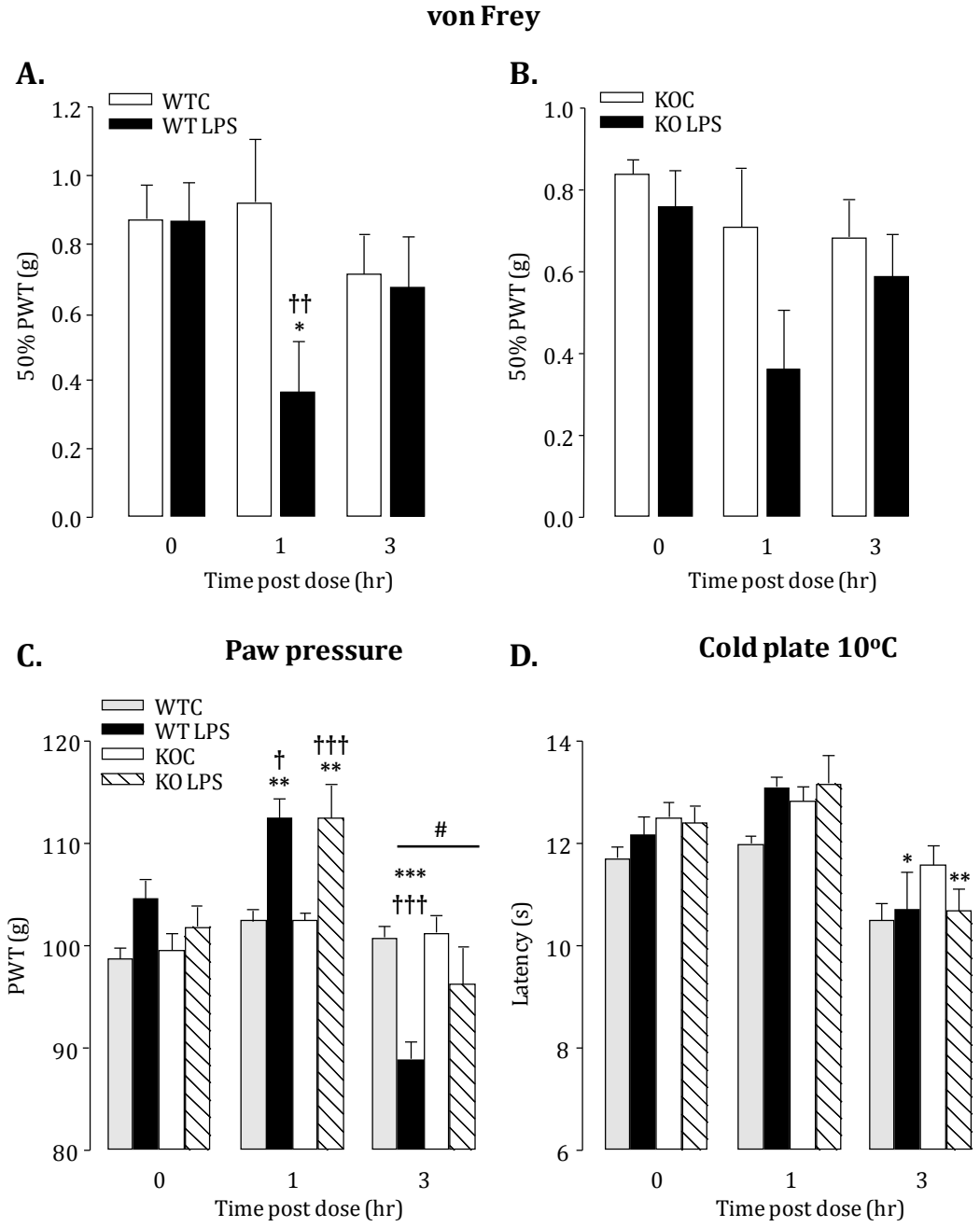

Figure 3.5: LPS treated GPR84 KO mice show attenuated behavioural hyperalgesia

GPR84 WT (A) and KO (B) mice showed a reduction in PWTs 1 hr after a second dose of intrathecal LPS, in comparison to vehicle treated mice (WTC, KOC, respectively). There was no significant difference between genotypes. (C) GPR84 WT, but not KO mice, mice showed a significant reduction in paw pressure thresholds 3 hrs post LPS in comparison to baseline and WTC. There was a significant difference between the LPS treated genotype groups. (D) Both GPR84 WT and KO mice showed significant increases in cold sensitivity at 3 hrs post LPS. There was no significant difference between genotypes. Data are presented as the mean ± SEM. *$p < 0.05$, ***$p<0.001$ vs baseline; †$p < 0.05$, ††$p < 0.01$, †††$p < 0.001$ vs saline control; #$p < 0.05$ vs KO, two-way RM ANOVA, post-hoc SNK, n = 6-9.

3.3.4 LPS treated GPR84 KO mice exhibit a normal microglia response

Despite a weak behavioural phenotype, we sought to immunohistochemically characterise the microglial response to LPS in order to determine whether direct activation of these cells is altered in the absence of GPR84. Therefore, we immunostained lumbar spinal cord sections for Iba1 and p-p38 to examine microglia numbers and activation, respectively, at 3 hrs after the second dose of LPS.

In accordance with literature (Clark et al., 2006), we observed a significant 1.5-fold bilateral increase in Iba1 and p-p38 positive cells (61.7 ± 3.9/7.3 x 10^5 μm^2 and 61.7 ± 3.9/7.3 x 10^5 μm^2, respectively) in the dorsal horns of LPS treated WT animals in comparison to saline controls (41.7 ± 3.4/7.3 x 10^5 μm^2; 41.6 ± 3.4/7.3 x 10^5 μm^2, respectively; Fig 3.6A, B). Interestingly, GPR84 KO mice exhibited a similar 1.5-fold bilateral increase in Iba1 and p-p38 positive cells (61.8 ± 3.7/7.3 x 10^5 μm^2 and 61.5 ± 3.7/7.3 x 10^5 μm^2, respectively) in LPS treated animals in comparison to saline controls (41.5 ± 5.1/7.3 x 10^5 μm^2; 41.4 ± 5.2/7.3 x 10^5 μm^2, respectively) (Fig 3.6A, B). These data indicate that deletion of GPR84 does not impair the ability of microglial cells to respond to a potent inflammatory stimulus and thus it is unlikely that the KO behavioural phenotype is mediated by microglial cells in a GPR84 dependent manner.

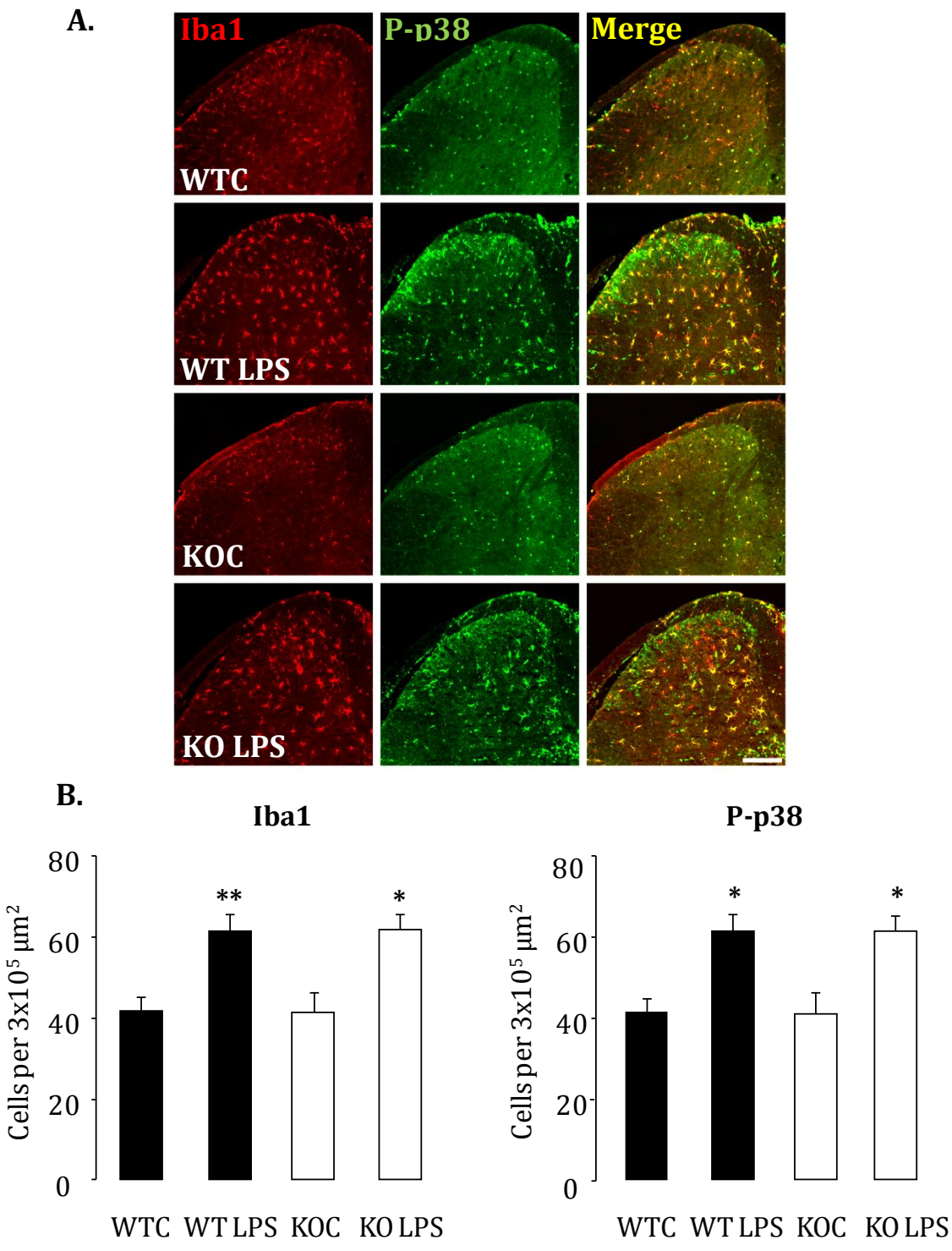

Figure 3.6: LPS treated GPR84 KO mice exhibit normal microgliosis

There was a significant bilateral increase in Iba1 and p-p38 positive cells in the dorsal horn of the spinal cord subsequent to intrathecal LPS in both GPR84 WT and KO mice (WT LPS, KO LPS, respectively) compared to vehicle control (saline) groups (WTC, KOC respectively) (A), quantified in (B). There was no difference between genotypes. Data are presented as the mean ± SEM. $^{*}p < 0.05$, $^{**}p < 0.01$ vs control, one-way ANOVA; post-hoc SNK, n = 4. Scale bar = 200 µm.

3.3.5 Immunohistochemical assessment of GPR84 protein expression

Under physiological conditions GPR84 expression is low and virtually undetectable even with a sensitive method like qPCR. However, subsequent to an appropriate immunological stimulus such as LPS, GPR84 expression increases in both monocytes/macrophages and microglial cells (Wang et al., 2006a; Bouchard et al., 2007). To characterise the protein expression of GPR84 we used a commercially available antibody against lumbar spinal cord sections from saline or LPS treated WT and KO mice.

In accordance with the literature (Bouchard et al., 2007), GPR84 immunostaining was absent in saline treated spinal cords of either WT or KO mice (Fig. 3.7A). However, characteristic bilateral GPR84 immunoreactivity was detected in LPS stimulated WT mice, which exhibited a punctate pattern that resembled microglial morphology (Fig. 3.7A). In contrast, GPR84 staining was completely absent in LPS treated KO mice, validating GPR84 silencing in this transgenic. To determine the identity of cells expressing GPR84 we carried out triple staining against GPR84, Iba1 (microglial marker), NeuN (neuronal marker) and GFAP (astrocytic marker; Fig. 3.7B). GPR84 immunoreactivity co-localised with a majority of Iba1 positive cells but did not co-label with NeuN or GFAP. This confirms that GPR84 is exclusively expressed by microglial cells and raises the possibility that only a subpopulation of microglia express this receptor.

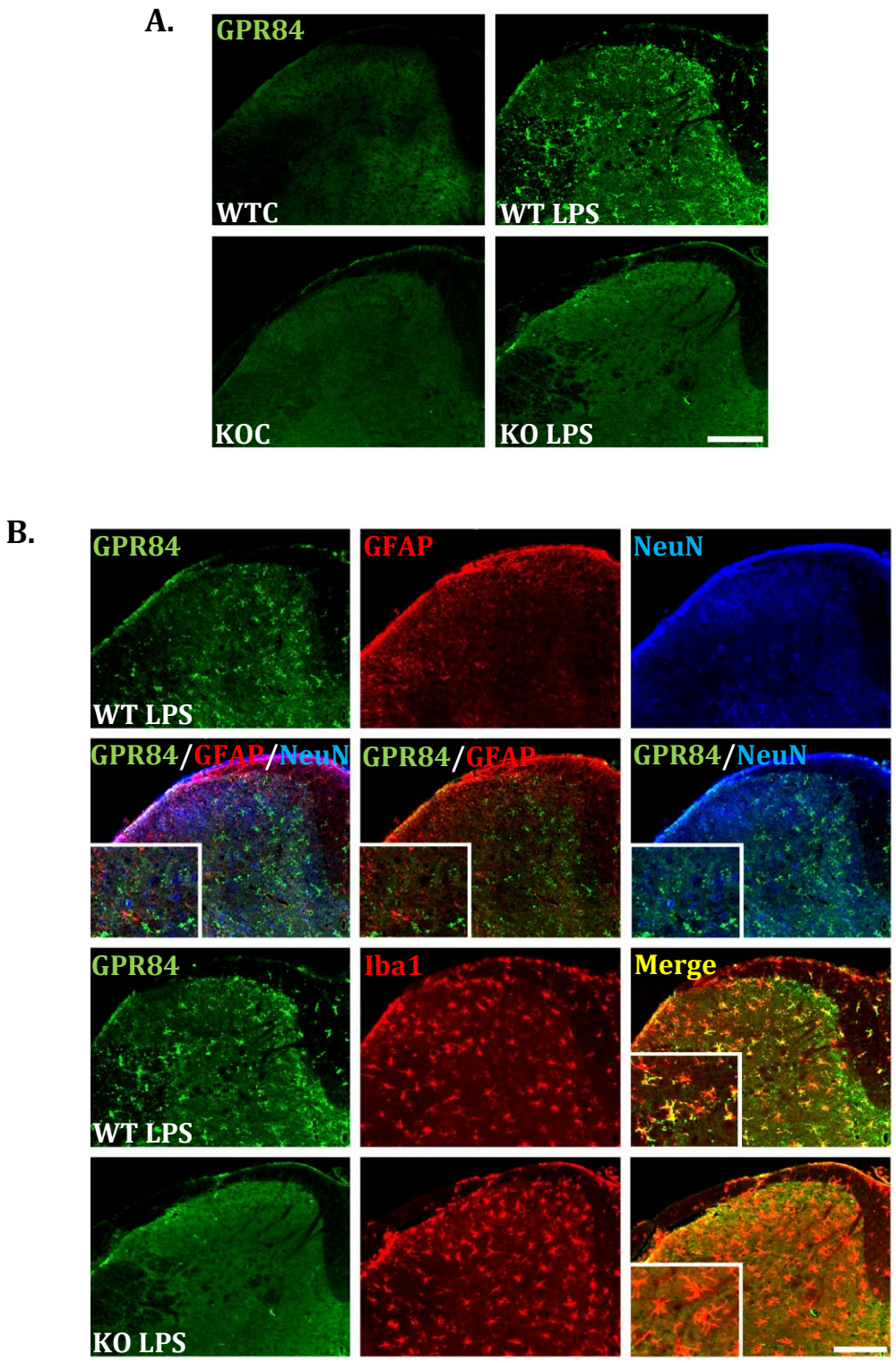

Figure 3.7: Protein verification of GPR84 deletion and co-localisation with microglia cells

GPR84 deletion was confirmed via the absence of staining in KO mice in both saline (KOC) and LPS stimulated conditions (KO LPS) (A). GPR84 immunoreactivity was not present in saline treated WT animals (WTC) but under LPS conditions (WT LPS) bilateral punctuate staining was evident (A). GPR84 immunoreactivity exclusively co-labelled with Iba1 positive cells under LPS stimulated conditions in WT mice (B). Scale bars = 200 µm.

3.3.6 GPR84 mRNA is induced in cultured microglia and macrophage cells subsequent to LPS stimulation

GPR84 gene transcription is strongly induced by diverse endogenous and exogenous inflammatory stimuli in a time dependent manner in subsets of central microglial cells and peripheral macrophages, as demonstrated by both *in vitro* and *in vivo* studies (Wang et al., 2006a; Bouchard et al., 2007). To verify our observation of GPR84 expression in central microglia in addition to peripheral macrophages, we cultured cortical microglial cells and peritoneal macrophage cells and measured GPR84 expression subsequent to 3 hrs of LPS (1 µg/ml) stimulation.

Since the moderate number of macrophage cells normally harvested from the peritoneum cavity are insufficient for extensive studies, eliciting agents such as Bio-Gel, thioglycollate and proteose-peptone are used to increase monocyte migration into the peritoneum and thus enhance yields (Zhang et al., 2008). Elicited macrophage populations consist of a mixture of resident and infiltrating cells of haematogenous origin similar to what we see in the *in vivo* situation. Both populations play an equal role in the response to a peripheral insult; the faster-acting resident cells initiate the response, followed by the later recruitment of infiltrating cells (Ton et al., 2013). We therefore utilised B-GEPMs not only for their practical advantages (ready availability, easy access and high yields), but also because this approach allowed us to study a heterogenous population of cells. In addition, these cells have been extensively studied in literature, where most of our understanding of tissue resident macrophages originates (Gordon, 2007; Zhang et al., 2008). B-GEPMs are also free of intracellular debris as they are unable to phagocytose the Bio-Gel beads. Nevertheless, B-GEPMs differ from resident cells in numbers and function and exhibit increased membrane turnover, respiratory and phagocytic capacity as well as alternative responses to various chemokines (Zhang et al., 2008). In comparison to other relevant sources of cells such as bone-marrow derived macrophages (BMM), elicited macrophages are similarly F4/80^{high}, CD11b^{high}, and CD68^{+}. However, GPR84 expression is restricted to BMMs and microglia in non-stimulated conditions and robustly increases in both BMMs and elicited peritoneal populations subsequent to LPS exposure (Lattin et al., 2008). Likewise, although we have focused on spinal microglia in this thesis, we have utilised cortical microglia in this study due to the requirement of greater cell yields.

Using qPCR, we observed a significant increase in GPR84 expression subsequent to LPS stimulation by 2.6-fold (1.7-3.6) in cortical microglial cells (A) and 30.8-fold (23.0-41.2) in B-GEPMs (B, Fig. 3.8). Therefore, GPR84 is highly inducible under inflammatory conditions

and is likely to act down-stream of pro-inflammatory mediators. Interestingly, there was a greater induction in macrophages than in microglia, which may indicate a more prominent role in regulating peripheral macrophages with regards to our previous findings (Fig 3.4 and 3.6). Furthermore, the exclusive expression of GPR84 in cells of the myelomonocytic lineage and the fact that its expression is only up-regulated in response to peripheral or central insult makes it an attractive therapeutic target.

3.3.7 Raw PCR array data: Comparing LPS induced mediator transcripts in GPR84 WT and KO Bio-Gel elicited macrophages

Using two models of inflammation (CFA and LPS) we have shown that GPR84 KO mice exhibit attenuated behavioural hypersensitivity that is restricted to particular modalities. We have verified that the microglial response does not correlate with GPR84 mediated nociceptive signalling in these models. The role of macrophages in chronic pain is well documented in models of inflammation and traumatic nerve injury. These cells promote the inflammatory response by releasing a range of mediators such as TNF-α, IL-1β, NGF, NO and PGE_2 (Marchand et al., 2005). TLR4 is an important player in the activation of macrophages and application of a potent exogenous TLR4 agonist (LPS) to cultured B-GEPMs provides a simple *in vitro* paradigm where the macrophage response can be evaluated. Therefore, to investigate whether there is any impairment in the ability of macrophage cells to launch an inflammatory response in the absence of GPR84, we have utilised high through-put custom-made Taqman array cards to analyse the relative expression of putative mediators in WT and KO B-GEPMs following LPS exposure. An explanation of analysis is provided in the methods section (2.2.8) and in more detail in (Perkins et al., 2012).

Appendix Tables 9 and 10 display the raw CT values of 92 different chemokines, cytokines, growth factors and cell markers as well as the HK genes of control and LPS stimulated GPR84 WT and KO macrophages. Generally, CT values exhibited consistency within experimental groups and the HKs varied no more than 1 cycle, except HPRT, which decreased by an average CT of 1.6 in LPS stimulated KO macrophages. Therefore, the data is consistent enough to assume a limited incidence of false positives and negatives. In the case of transcripts below detection level, the relevant amplification plots were checked for faulty reactions to confirm that the lack of gene detection was due to a biological factor rather than a technical error.

3.3.8 A subset of gene transcripts induced by LPS are differentially regulated by GPR84 WT and KO macrophages

Tables 3.1A and B display the top differentially regulated genes in GPR84 KO mice. Data are displayed as the mean FC relative to control (see *Appendix* Tables 11 and 12 for FC values of all genes profiled). The SD values are only those of the case samples where variability is considered to be the greatest, rather than the control samples. For each gene, a FC threshold of ≥ 2 in one or both genotypes was set to reduce noise by eliminating those genes that showed marginal expression changes. A FC ratio (KO FC/WT FC) threshold of ≥ 1.5 was also set and genes were ranked according to FC ratio. The FC ratio was employed in the screening criteria so that unless the FC value of a particular transcript differed by ≥ 1.5 – fold between genotypes, it would not be considered to be transcriptionally regulated by GPR84. This enabled us to efficiently filter irrelevant genes and focus on those transcripts that were considerably dysregulated between genotypes.

As expected, GPR84 was undetectable in KO macrophages but strongly up-regulated in LPS stimulated WT cells (FC: 30.8). Strikingly, both pro-inflammatory CCL19 and anti-inflammatory IL-13 were up-regulated in WT cells but remained un-detectable in the KO (FC: 71.0; FC: 7.7, respectively). Other pro-inflammatory mediators including IL-18, CCL2, CCL3, CCL7, CXCL5 and CXCL9 were significantly induced in both genotypes but to a greater extent in the WT (IL-18, WT FC: 4.0, KO FC: 2.6; CCL2, WT FC: 27.2, KO FC: 15.6; CCL3, WT FC: 249.5, KO FC: 165.1; CCL7, WT FC: 41.4, KO FC: 21.3; CXCL5, WT FC: 33.7, KO FC: 18.5; CXCL9, WT FC: 25.4, KO FC: 11.8), of which IL-18, CCL2, CCL3 and CXCL5 are documented to be pro-nociceptive (Wei et al., 2001; Abbadie et al., 2003; Kiguchi et al., 2010b; Dawes et al., 2011). These data suggest that in the absence of GPR84 mediated signalling macrophage cells exhibit an attenuated release of some pro-inflammatory cytokines/chemokines. However, key pro-inflammatory factors that are well documented to contribute directly or indirectly to pro-nociceptive behaviours were equivalently or more greatly induced in the KO subsequent to LPS stimulation compared to the WT, including IL-1β: (WT FC: 749.5 (548.0-1030.0), KO FC: 823.0 (555.0-1220.0)); IL-6: (WT FC: 1785.4 (1430.0-2220.0), KO FC: 1440.0 (878.0-2360.0)); TNF-α: (WT FC: 134.6 (119.0-152.0), KO FC: 267.0 (236.0-301.0)); PTGS2: (WT FC: 1120.5 (906.0-1390.0), KO FC: 1290.0 (902.0-1850.0)); PTGES: (WT FC: 30.1 (18.9-47.9), KO FC: 41.1 (24.5-69.0)) and NOS2: (WT FC: 130.0 (92.2-183.0), KO FC: 204.0 (81.8-510.0); ($p < 0.05$)). This suggests that under inflammatory conditions, GPR84 may suppress the expression of particular mediators whilst promoting the expression of others, thus reflecting the differential regulation of mediators by $G\alpha_{i/o}$ coupled

receptors. These data also indicate that on the whole, KO macrophages are equally capable of a robust inflammatory response as their WT controls.

Interestingly, IL-10, which is a potent anti-inflammatory interleukin, was one of the top five dysregulated factors and exhibited a greater induction in the WT. AIF1 (Iba1 gene) remained unchanged in the WT and was down-regulated in the KO, which is an unexpected finding with regards to our previous observations that LPS treated mice exhibited increased Iba1 immunoreactivity in the spinal cord (Fig 3.6). Notably, upon LPS stimulation all classical immune cell markers either remained unchanged or were down-regulated in both genotypes, including H2-EB1 (MHC class II), TLR4 and ITGAM (CD11b). Genes for IL-19, IL-20, CCL22, CCL24, CXCL3 and CXCL13 were also more greatly induced in the WT, some of which are implicated in inflammation but not documented to have a role in nociceptive pathways. Nevertheless, they may contribute via the exacerbation of inflammation or through binding to receptors that are known to mediate the effects of algogenic chemokines. For example, CXCL3 binds to CXCR2, which is the same receptor that pro-nociceptive CXCL5 binds to (Dawes et al., 2011).

Amongst the top up-regulated transcripts in the KO were the growth factors EREG and BDNF. EREG was significantly induced in both genotypes but by 1.8-fold more in the KO, whereas BDNF was down-regulated in the WT and remained unchanged in the KO. BDNF has a well established role in pain transmission (Latremoliere and Woolf, 2009), as opposed to EREG for which little is known. A selection of cytokines and chemokines were also more significantly induced in the KO, including IL-23A, IL-33, CCL20, CXCL11 and CSF2 (Table 3.1(B)). Of those, IL-33 and CXCL11 have been recently implicated in inflammatory pain pathways (Strong et al., 2012; Han et al., 2013; Zarpelon et al., 2013). In contrast, there is no established link between IL-23A, CCL20 and CSF2 and pain signalling and thus, although possible, a specific relevance to the KO behavioural phenotype is unlikely.

3.3.9 Distribution and correlation of LPS induced genes in GPR84 WT and KO macrophages

We have identified a number of genes which were dysregulated in GPR84 KO macrophages after a robust inflammatory stimulus. However, upon closer inspection it is evident that the majority of the 92 profiled transcripts exhibit similar changes in expression between genotypes. The distribution graph (Fig. 3.9A) illustrates the profiles of average FC values of individual genes relative to control (non-stimulated cells) for each genotype as well as the FC ratios of each gene. Gene profiles are ranked in order of FC ratio from the most down-

regulated to the most up-regulated in the WT vs the KO. The blue shaded region corresponds to the cut-off threshold of a FC ≥ 2. Within each genotype FC data points that clearly reside above or below this threshold are differentially regulated from control tissue and those genes that also have FC ratios ≥ 1.5 are differentially regulated between genotypes.

In both genotypes, it is evident that LPS exposure elicits a substantial induction of many of the 92 different transcripts examined, with very few genes down-regulated. In the WT 49 genes were up-regulated, 36 genes were unchanged and 7 genes were down-regulated. Similarly, in the KO 46 genes were up-regulated, 40 genes were unchanged and 6 genes were down-regulated. The FC profiles of the genotypes are tightly correlated, which indicates that the transcriptional response to LPS was similar (Fig 3.9A). This is further supported by the fact that a majority of FC ratio values are < 1.5 and only a small subset of genes are differentially regulated between the genotypes. These genes are of particular interest as they could potentially play a role in behavioural hypersensitivity mediated by GPR84 signalling and are presented and evaluated in the tables 3.1A and B.

To directly compare LPS induced transcriptional changes between genotypes, WT and KO average FC values are plotted against each other (Fig. 3.9B). Presenting the transcript changes in this format enables the assessment of data scatter and the identification of genes that do not conform to the rest of the data. As indicated by the Pearson's correlation coefficient, there is a positive correlation between the WT and KO data sets ($p < 0.001$). This indicates that the transcriptional changes in macrophage cells required to launch an inflammatory response are similar between genotypes and is not hindered in the absence of GPR84. Therefore, a majority of the 92 different pro-inflammatory genes profiled are not regulated by GPR84 except for those outliers highlighted in red (CCL19 and IL-13), which are also top hits in the ranking table 3.1A. These outliers are data points that skew the Pearson's correlation coefficient as they markedly deviate from the positive correlation of the two data sets, which is due to considerable differences in expression between the genotypes.

3.3.10 Validation of CCL19 expression

The extensive analysis of the Taqman PCR array data has led to the identification of two LPS induced mediators that are differentially regulated between WT and KO macrophages. Both CCL19 and IL-13 were undetectable in baseline conditions in both genotypes, however subsequent to LPS stimulation both mediators were up-regulated in WT cells in contrast to

KO cells. CCL19 is a pro-inflammatory chemokine with some implications in nociceptive transmission (Biber et al., 2011; Schmitz et al., 2013) and exhibited a significant up-regulation ($p < 0.001$), whereas IL-13 exhibited a non-significant up-regulation and possesses anti-inflammatory properties that are less fitting to the behavioural phenotype in question. Thus based on this evidence we decided to further validate the expression of CCL19 in WT and KO macrophage cells using conventional qRT-PCR. We found that the results were highly consistent with the original findings of the Taqman PCR array method; we observed a significant induction of CCL19 expression post LPS stimulation in WT but not in KO macrophages (WTC: 1.0 ± 0.3, WT LPS: 12.4 ± 7.3 vs KOC: 1.1 ± 0.1, KO LPS: 3.2 ± 1.1; Fig. 3.10A). However, when we repeated the experiment in an independent group of animals (Fig. 3.10B) CCL19 induction in the WT LPS group was considerably less and both genotypes showed an equivalent level of CCL19 up-regulation (WTC: 1.0 ± 0.6, WT LPS: 4.8 ± 0.4 vs KOC: 0.7 ± 0.2, KO LPS: 4.3 ± 1.0; $p < 0.05$ Fig. 3.10B). Due to time constraints, it was not possible to repeat the experiment; however, it would be worthwhile re-validating CCL19 expression alongside other differentially regulated mediators.

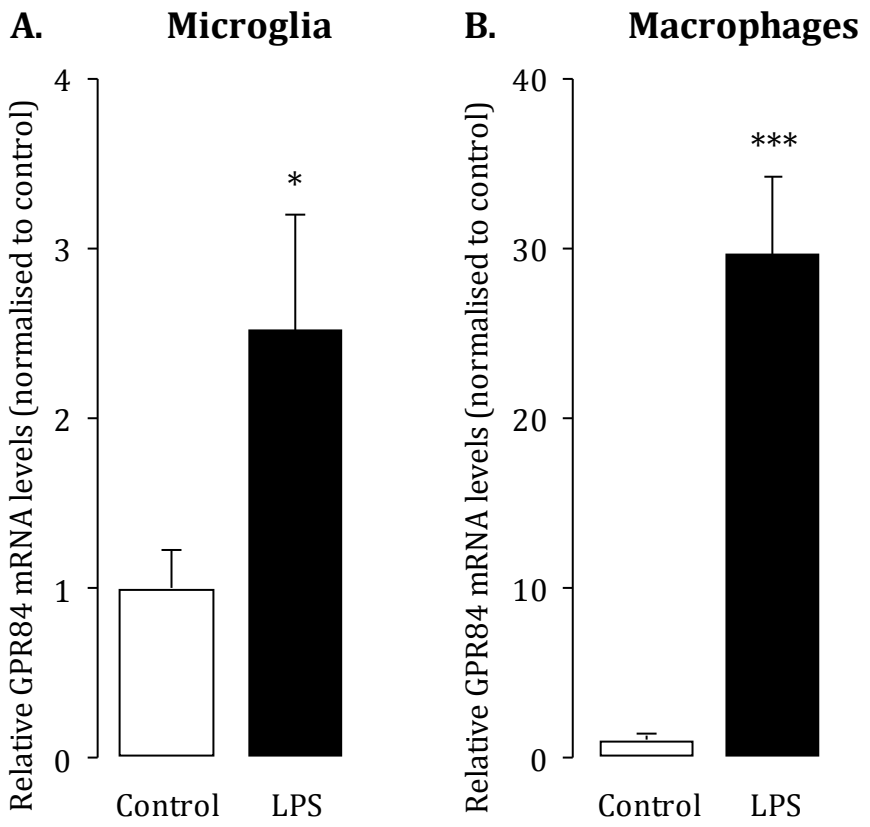

Figure 3.8: LPS stimulation induces an abundant increase in GPR84 expression in microglia and macrophage cells

The relative expression of GPR84 in WT cortical microglia (A) and Bio-gel elicited peritoneal macrophage cells (B), significantly increased subsequent to 3 hrs LPS (1 μg/ml) stimulation. Change in mRNA expression is normalised to the mean ΔCT of control cells where ΔCT = (mean GPR84 CT) – (mean HK CT). Data are presented as mean ± SEM. A, HK: GAPDH; t-test, *$p < 0.05$ vs control, n = 4. B, HKs: GAPDH, HPRT, X18S, ACTB, $p < 0.001$*** vs control, t-test with FDR for multiple testing correction, n = 4.

3.1 (A)	Top down-regulated genes in LPS stimulated GPR84 KO macrophages			
Rank	**Gene**	**WT FC**	**KO FC**	**KOFC/WTFC RATIO**
1	CCL19	71.0 (49.8-101.0)***	ND	-71.0
2	GPR84	30.8 (23.0-41.2)***	ND	-30.8
3	IL13	7.7 (1.9-31.8)	ND	-7.7
4	FGF7	-2.2 (0.3-0.8)	-12.1 (0.04-0.2)**	-5.0
5	IL10	153.2 (100.0-234.0)**	42.2 (34.0-524.0)**	-3.6
6	CXCL13	4.2 (2.4-7.3)	1.3 (0.6-2.8)	-3.2
7	CCL22	2360.1 (1080.0-5150.0)***	798.4 (142.0-450.0)**	-3.0
8	IL19	219.6 (17.4-27.7)*	100.0 (68.3-147.0)**	-2.2
9	CXCL9	25.4 (23.1-27.9)**	11.8 (7.1-19.6)**	-2.2
10	AIF1	1.0 (0.9-1.2)	-2.2 (0.2-2.2)*	-2.0
11	CCL7	41.4 (23.4-73.3)***	21.3 (10.4-43.6)**	-1.9
12	CXCL5	33.7 (23.7-47.8)***	18.5 (11.1-30.8)*	-1.8
13	CCL2	27.2 (17.0-43.6)***	15.6 (12.4-19.7)***	-1.7
14	IL20	13.1 (6.1-28.0)*	7.6 (2.9-20.1)*	-1.7
15	CXCL3	959.8 (796.0-1160.0)***	597.2 (394.0-905.0)***	-1.6
16	IL18	4.0 (3.2-4.9)**	2.6 (1.5-4.4)	-1.5
17	CCL3	249.5 (197.0-317.0)***	165.1 (129.0-211.0)***	-1.5
18	CCL24	3.0 (1.8-5.1)*	2.1 (1.5-2.9)	-1.5

3.1 (B)	Top up-regulated genes in LPS stimulated GPR84 KO macrophages			
Rank	**Gene**	**WT FC**	**KO FC**	**KOFC/WTFC RATIO**
1	CXCL11	35.1 (26.8-46.1)***	268.9 (112.0-647.0)***	7.7
2	CCL11	4.3 (1.1-17.4)	11.3 (2.1-61.6)	2.6
3	CCL20	28.7 (19.5-44.4)	66.6 (25.3-176)*	2.3
4	BDNF	-2.5 (0.1-1.9)	1.2 (0.3-5.9)	2.1
5	TNF	134.6 (119-152)***	266.6 (236-301)***	2.0
6	IL23A	1227.4 (812.0-1860)***	2374.0 (1300-4350)**	1.9
7	CCL28	-2.2 (0.2-1.0)	1.2 (0.5-2.5)	1.9
8	EREG	19.7 (14.9-26.2)**	35.6 (23.0-55.1)***	1.8
9	CSF2	6884.0 (3450.0-13800)***	11030.0 (2980.0-40800.0)**	1.6
10	NOS2	130.0 (92.2-183.0)***	204.2 (81.8-510.0)**	1.6
11	IL33	7.5 (4.3-13.1)**	11.5 (7.7-17.2)**	1.5

Table 3.1: Top down- and up-regulated gene transcripts in GPR84 KO macrophages subsequent to LPS stimulation

Tables displaying the top down- (A) and top up- (B) regulated gene transcripts 3 hrs post LPS stimulation (1 µg/ml) in GPR84 KO B-GEPMs ranked in order of FC ratio, where FC = LPS/control; FC ratio = KOFC/WTFC. Only genes with a FC ≥ 2 and a FC ratio of ≥ 1.5 have been ranked. Genes with a FC ratio < 1.5 are considered equally expressed between genotypes. Data are presented as the mean ± SD range of the case samples (LPS stimulated cells); $p < 0.05$*, $p < 0.01$**, $p < 0.001$*** vs control; t-test with FDR correction for multiple comparisons, n = 4.

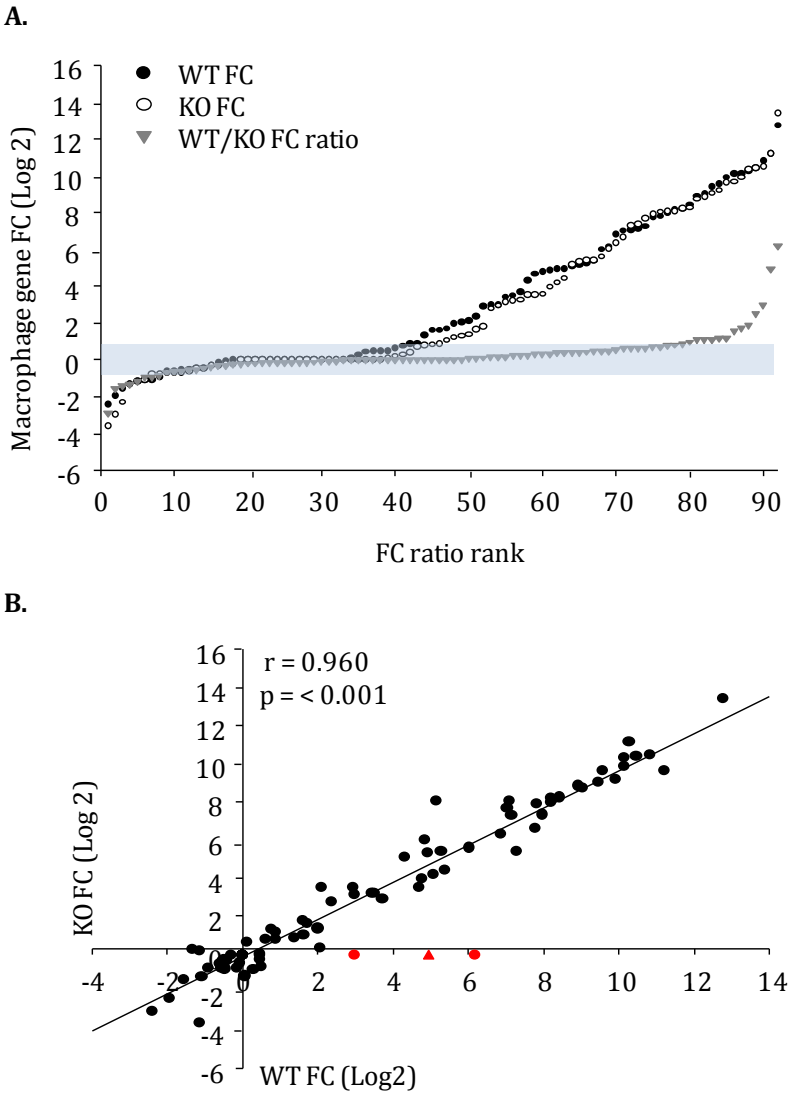

Figure 3.9: Distribution and correlation of LPS induced genes in GPR84 WT and KO macrophages

(A) Transcript expression profiles of a range of cytokines, growth factors and cell markers subsequent to 3 hrs LPS (1 μg/ml) stimulation of GPR84 WT and KO B-GEPMs. Transcripts are ranked in order of increasing FC ratio, where FC = LPS/control; FC ratio = WT FC/KO FC. Both genotypes demonstrate similar distribution profiles and only a few transcripts are differentially regulated as indicated by the FC ratio. The data points show the average FC or FC ratio for each gene transcript ranked from the most down-regulated to the most up-regulated in the WT. The blue shaded box represents an area of 2 ≤ FC and each data point shows the mean FC for each individual transcript. Adjacent FC data points represent the same gene transcript, n = 92. The x-axis is on a log 2 scale. (B) Transcript expression changes in WT and KO macrophages are plotted against each other on a log 2 scale. The Pearson's correlation coefficient (r = 0.960) indicates that there is a positive relationship between the two data sets ($p < 0.001$). Outliers are highlighted in red, see text. GPR84 is denoted as a red triangle. Data is presented as the mean FC. Pearson's correlation coefficient, n = 92.

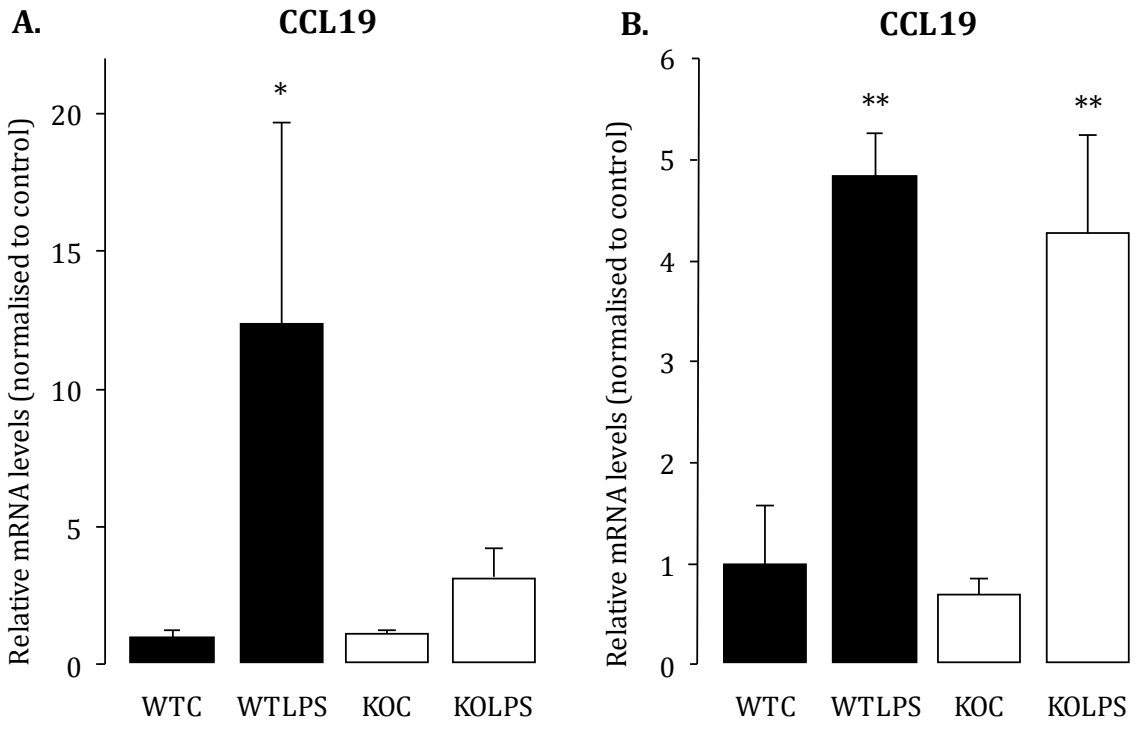

Figure 3.10: qRT-PCR validation of CCL19 expression in LPS stimulated GPR84 WT and KO macrophages

Following LPS stimulation (1 μg/ml), CCL19 mRNA expression increased in GPR84 WT but not KO macrophages (A). There was no significant difference between the LPS stimulated genotype groups. In an independent second experiment the expression of CCL19 significantly increased in both LPS stimulated GPR84 WT and KO macrophages compared to their appropriate control groups (B). There was no significant difference between the LPS stimulated genotype groups. Changes in mRNA expression is relative to the mean ΔCT of control cells where ΔCT = (mean CCL19 CT) – (mean HPRT CT). Data are presented as the mean ± SEM; *$p < 0.05$, **$p < 0.01$; (A): Kruskal one-way ANOVA on ranks, post hoc Dunn's method; (B): one-way ANOVA, post hoc Tukey; n = 4.

3.4 Discussion

Chronic inflammatory pain is associated with a range of pathologies from autoimmune and neurological diseases to OA and cancer. Patients often have to contend with additional associated co-morbidities and thus quality of life is greatly compromised with current therapeutic treatment largely inadequate. The immune system with its array of signalling molecules plays a principle role in inflammation and thus the identification of key immune targets is a viable approach in the development of new therapeutic treatments. In this chapter we utilised two well documented experimental models of inflammatory pain to investigate the role of the immune cell expressed GPR84 in nociceptive transmission. We have demonstrated that following intraplantar CFA or intrathecal LPS, GPR84 KO mice exhibit attenuated behavioural hyperalgesia restricted to particular modalities; this however did not correlate with an altered microglia phenotype. We also verified deletion of GPR84 in the KO at the protein level and showed exclusive co-localisation with microglia in the CNS. Finally, we showed that subsequent to LPS stimulation, GPR84 mRNA expression is induced in cultured microglia and macrophages and that a subset of transcripts are differentially regulated in LPS stimulated KO macrophages. Therefore, GPR84 is a pro-inflammatory receptor mediating inflammation-induced pain and is specifically up-regulated upon exposure to appropriate inflammatory stimuli, which makes it an appealing target in chronic pain treatment.

3.4.1 GPR84 plays a role in inflammatory pain pathways that is independent of microglial activation

Intraplantar administration of CFA to the hind paw is one of the most common models of persistent inflammation that possesses both a peripheral and a central component, where the development of central sensitisation is manifested as thermal and mechanical hyperalgesia. Microglia are active participants in the initiation of chronic pain states by releasing a plethora of algesic factors, which is well documented in experimental models of nerve injury-induced neuropathic pain. However, the involvement of these cells in experimental models of inflammatory pain is somewhat more questionable (DeLeo and Yezierski, 2001; Watkins et al., 2001; Watkins and Maier, 2003; McMahon et al., 2005; McMahon and Malcangio, 2009). In a study utilising the CFA model, sustained spinal microglia activation was observed up to 14 days post CFA, indicated by an up-regulation of TLR4, CD14 and Mac-1 mRNAs as well as elevated OX-42 immunoreactivity, which correlated with behavioural allodynia and hyperalgesia (Raghavendra et al., 2004). In an

earlier study using two models of peripheral inflammation, animals treated with intraplantar formalin and zymosan exhibited spontaneous pain and persistent mechanical allodynia at later time points (Sweitzer et al., 1999). Immunohistochemical analysis revealed that glial activation correlated with the development and maintenance of mechanical allodynia, however, this was only evident as a moderate bilateral increase in OX-42 and GFAP staining (Sweitzer et al., 1999). Administration of formalin to the hind paw produces two phases of spontaneous nociceptive behaviour followed by a later onset of prolonged allodynia for up to three weeks. Using this model many groups have reported an ipsilateral increase in microglia numbers as revealed by OX-42 staining in the superficial dorsal horn that correlates with the onset of allodynia (Fu et al., 1999; Aumeerally et al., 2004). However, discrepancies in the literature with regards to microglial markers and their temporal regulation suggests caution should be applied to the interpretation of these results. For example, Fu et al. (1999) reported an ipsilateral increase in OX-42 in the medial portion of the dorsal horn and gracile nucleus of the brainstem post formalin administration but failed to observe any change in OX-6 (marker for MHC class II). Likewise, Sweitzer et al. (2001) reported an absence of MHC class II as well as CD4 in the spinal cord following intraplantar zymosan and observed a mild glial activation that paralleled with behavioural allodynia. In contrast, Yeo and colleagues (2001) demonstrated an increase in microglial cell markers in the caudal spinal trigeminal nucleus, including OX-18 (marker for MHC class I), OX-42 and OX-6, 21 days post subcutaneous formalin injection into the lateral facial surface of rats. Notably, the most striking observations using the formalin model ultimately indicate that the microglia response tends to peak 3 to 7 days post treatment despite the fact that nociceptive behaviours are most prominent within the first 2 hours of treatment. This microglia response also parallels with the development of allodynia, which has been documented to persist for up to three weeks post formalin. Together, these data argue against a contribution of microglial cells in the early formalin-induced nociceptive behaviour phase; in contrast there appears to be an association with long-lasting inflammation and tissue damage, implying a relationship between microglial activation and the extent of nerve damage rather than nociception (Fu et al., 1999; Wu et al., 2004).

Evidence against a central microglial role has also been documented in other inflammatory as well as neuropathic pain models, where authors reported unaltered OX-42 staining in response to CFA, topical application of mustard oil and CCI surgery (Colburn et al., 1997; Molander et al., 1997; Honore et al., 2000; Zhang et al., 2003; Clark et al., 2007a). On the contrary, many recent studies have demonstrated that microglia do in fact show an early response to peripherally injected inflammogens with increases in OX-42 staining within hours of treatment (Svensson et al., 2003a; Hua et al., 2005; Clark et al., 2007a; Guo et al.,

2007; Sun et al., 2007). Notably, whilst early studies have relied on observing morphological changes or increases in the density of microglia markers as a criterion, more recent work reflects the importance of using markers that reflect alterations in intracellular function, such as p-p38, rather than markers like OX-42 that require *de novo* protein synthesis (DeLeo and Yezierski, 2001; Hua et al., 2005). Phosphorylated p-38 is a prerequisite for NF-κB mediated cytokine synthesis and release from microglial cells and since phosphorylation is a very rapid process, p-p38 is regarded as a sensitive marker of spinal microglia activation (Ji and Suter, 2007; Ji et al., 2009). Indeed, this marker has been reported to correspond closely with the development of behavioural hyperalgesia in a variety of experimental models of inflammation (Kim et al., 2002; Svensson et al., 2003b). While intrathecal or systemic infusion of p38 inhibitors alleviate pain symptoms (Kumar et al., 2003; Svensson et al., 2003a; Svensson et al., 2003b). Interestingly, contradictory temporal and expression findings are also present in studies using this marker of microglia activation. For example, Ji et al. (2002) failed to see p38 phosphorylation in the dorsal horn but observed an increase in p-p38 expression in small DRG neurons 6 hours to 7 days post CFA treatment. Svensson et al. (2003) and Kim et al. (2002) observed an increase in spinal microglia p-p38 immunoreactivity following intraplantar formalin, with the former reporting a transient peak at 5 minutes whilst the later observed an increase in immunostaining 12 hours-2 days post treatment (Kim et al., 2002; Svensson et al., 2003b). Despite some discrepancies in the literature, on the whole these data support a clear role of spinal microglial cells in numerous models of inflammation that correlates with the development of pain behaviours.

In light of this evidence and the fact that GPR84 is a pro-inflammatory receptor exclusively expressed by microglial cells in the CNS (Bouchard et al., 2007; Suzuki et al., 2013) we utilised the CFA model to investigate whether GPR84 contributes to inflammatory pain via the modulation of microglial cells. We report that GPR84 KO mice exhibited attenuated mechanical, thermal and cold hyperalgesia in contrast to WT littermate controls and that both genotypes exhibited non-significant mechanical allodynia. As expected WT mice developed significant mechanical, thermal and cold hyperalgesia subsequent to intraplantar CFA that correlated with a significant increase in microglial numbers and activation in the ipsilateral dorsal horn, as revealed by enhanced Iba1 and p-p38 immunoreactivity, respectively. Similarly, CFA treated KO mice exhibited increased ipsilateral Iba1 and p-p38 immunoreactivity in the dorsal horn, but this did not reach significance. Furthermore, we did not find a statistical difference between the CFA treated genotype groups and so these findings indicate that GPR84 may not be involved in the modulation of microglial cells in persistent inflammatory pain mechanisms. Together our data suggest that GPR84 mediated

nociceptive signalling encompasses specific modalities and is unlikely to involve the modulation of microglial cells.

Studies examining the role of microglial expressed $G\alpha_{i/o}$ coupled GPCRs in transgenic mice have demonstrated a strong correlation between the observed behavioural phenotype and an altered microglial response. For example, zymosan treated CX_3CR1 null mice developed mechanical allodynia but showed an absence of thermal hyperalgesia which, unlike our findings, correlated with reduced microglial numbers in the dorsal horn as revealed by Iba1 immunoreactivity (Staniland et al., 2010). Likewise, CFA treated CCR2 null mice exhibited attenuated mechanical allodynia compared to WT controls from 6 hours to 2 days post treatment, in addition to markedly reduced pain compared to WT controls in the 2nd formalin phase (Abbadie et al., 2003). Administration of a CCL2 neutralising antibody reversed both mechanical allodynia and microglial activation. However, the reversal effect of an anti-CCL2 antibody has only been documented in a model of nerve injury (Thacker et al., 2009). These studies showed that paw oedema occurred in both genotypes, indicating an equivalent level of peripheral inflammation, which was a finding we also documented (Abbadie et al., 2003; Staniland et al., 2010). The central role of microglial cells in the initiation and maintenance of pain states is further supported by studies using microglial inhibitors. For example, administration of fluorocitrate attenuated the 2nd phase of formalin evoked flinching behaviours and zymosan-induced hyperalgesia (Meller et al., 1994; Watkins et al., 1997). Intrathecal minocycline also alleviated formalin and carrageenan evoked hyperalgesia, which corresponded with reduced spinal p-p38 immunoreactivity (Hua et al., 2005). However, in the CFA model the role of microglial cells is not that well established. Clark et al. (2007) reported an absence of microgliosis 24 hours post CFA despite the presence of behavioural hyperalgesia and intrathecal fluorocitrate failed to reduce pain behaviours. Furthermore, Raghavendra et al. (2004) reported low levels of microgliosis 1 day post CFA and in a study using CFA treated CCR2 null mice, animals showed a non-significant reduction of mechanical allodynia (Abbadie et al., 2003). The expression of $P2X_4$, which has been shown to up-regulate in reactive microglia, also remained unaltered 7 days post CFA (Tsuda et al., 2003). However, these studies have examined earlier time points than the one we report, and in accordance with a study examining the microglia response 14 days post CFA we observed significant microgliosis in the dorsal horn (Raghavendra et al., 2004). Put together, these data suggest that microglia may not be involved in the early stages of acute pain but may play a more important role in the later chronic phase of this model.

Previously we were unable to correlate the behavioural phenotype of GPR84 KO mice to an altered microglial phenotype in a peripheral nerve injury model of neuropathic pain (see *Chapter 2*) and have found no evidence of microglial involvement in a peripheral inflammation model. Therefore, to directly evaluate the contribution of microglial cells to GPR84 mediated nociceptive signalling we examined the role of these cells in an LPS-induced CNS inflammatory model. Intrathecal LPS specifically activates microglial cells via the TLR4 and induces thermal hyperalgesia and tactile allodynia, which is dependent on a prior priming dose (Lehnardt et al., 2002; Cahill et al., 2003). Such acute activation of spinal microglia has relevance to both inflammatory and neuropathic pain mechanisms as nerve injured TLR4 null mice display attenuated behavioural hypersensitivity and decreased expression of proinflammatory cytokines (Tanga et al., 2005). LPS stimulation initiates dimerization of the TLR4 cytoplasmic domains and subsequent activation of p38 MAPK and NF-κB mediated transcription, which induces the release of pro-inflammatory cytokines such as IL-1β and TNF-α, leading to an increase in excitability of dorsal horn neurons (Reeve et al., 2000; Clark et al., 2006; Clark et al., 2010b). Phosphorylation of p38 MAPK in microglia is a key intracellular signal that orchestrates their pain-related actions and correlates with the development of behavioural hypersensitivity. This has been demonstrated by spinal cord administration of LPS in *ex vivo* and *in vivo* models of CNS inflammation and a number of nociceptive models (Svensson et al., 2003b; Clark et al., 2006). The effects of LPS are very much dependent on the induction of pro-inflammatory cytokines and systemic administration of LPS has been shown to induce an increase in IL-1β, TNF-α, IL-6, CCL2 and CCL5 in the DRG and spinal cord. Correspondingly, systemic or perineural administration of these individual cytokines elicits mechanical hypersensitivity and thermal hyperalgesia (Cunha et al., 1992; Safieh-Garabedian et al., 1995; Woolf et al., 1997; Cunha et al., 2000; Strong et al., 2012; Yoon et al., 2012). Conversely, administration of minocycline suppresses systemic LPS induced hyperalgesia by reducing microglial/macrophage cell numbers and cytokine expression (Yoon et al., 2012) and pre-treatment of BV-2 cells with a p38 inhibitor reduces LPS stimulated cytokine production (Horvath et al., 2008).

In a model of neonatal priming, which reflects the long-term neuro-developmental changes in adults associated with neonatal surgery and intensive care, adult rats exhibited a similar predisposition to enhanced sensory sensitivity and stress to that seen in humans (Beggs et al., 2012). It was shown that rodents which received a hind paw incision at 3 days of age had increased hyperalgesic responses in comparison to animals that did not experience an early life pain experience, and this change was correlated to increased microglial reactivity in the adult dorsal horn. Selective targeting of microglial cells via intrathecal administration of

minocycline prevented hypersensitivity and the early microglia response seen in animals that had a prior neonatal injury (Beggs et al., 2012). Together these studies underscore the key role of microglia in nociception and importantly the notion of a required priming stimulus for the development of behavioural hypersensitivity, which is a crucial factor in the LPS model presented in this chapter.

We report that GPR84 KO mice exhibited attenuated mechanical hyperalgesia subsequent to intrathecal LPS administration but showed an equivalent development of mechanical allodynia and cold hyperalgesia to WT mice. In accordance with literature, the development of behavioural hyperalgesia in WT mice correlated with a significant increase in dorsal horn Iba1 and p-p38 immunoreactivity; however, a similar microglial response was also observed in the KO despite the behavioural differences. It has been previously reported that LPS induced mechanical hypersensitivity is absent in $P2X_7$ null mice, which corresponds with reduced p38 MAPK phosphorylation of spinal microglia (Clark et al., 2010b). Therefore our findings are somewhat puzzling as one would expect the KO behavioural phenotype to correlate with an altered microglial response, considering that these cells have been selectively activated and solely express GPR84, which is itself robustly induced by LPS exposure. In conclusion, these data suggest that GPR84 exerts its effects through complex signalling pathways that may involve a specific subset of afferent fibres or mechanoreceptors but does not regulate microgliosis in response to CNS inflammation. Interestingly, a previous study showed that administration of $P2X_4$ antisense oligodeoxynucleotides does not prevent activation of microglial cells despite suppressing both allodynia and an increase in $P2X_4$ expression in nerve injured rats (Tsuda et al., 2003). In light of this evidence, the up-regulation of GPR84 expression alone in response to nerve injury or inflammation could perhaps be the important factor contributing to nociceptive transmission. However, we have been unable to investigate this due to a lack of pharmacological tools.

3.4.2 GPR84 expression is exclusive to spinal microglial cells and is up-regulated in response to inflammatory stimuli

GPR84 is a pro-inflammatory receptor that is highly inducible upon endogenous or exogenous inflammatory insult. In experimental models of endotoxemia, EAE and diabesity GPR84 is markedly up-regulated due to the release of soluble mediators (Bouchard et al., 2007; Nagasaki et al., 2012). Molecules able to stimulate the NF-κB pathway such as LPS, IL-1β and TNF-α enhance the expression of GPR84 in monocytes/macrophages and microglial cells, which can be blocked via the administration of NF-κB inhibitors (Wang et al., 2006a;

Bouchard et al., 2007; Lattin et al., 2008; Nagasaki et al., 2012). Furthermore heterologous expression systems have demonstrated that GPR84 is involved in the regulation of subsets of cytokines/chemokines (Venkataraman and Kuo, 2005; Wang et al., 2006a; Suzuki et al., 2013). Therefore, it is likely that the expression of this receptor is regulated by multiple pathways involving the activation of TLR4, TNFR or IL-1R, which eventually culminate in NF-κB mediated GPR84 transcription. In accordance with literature, we showed that under normal conditions GPR84 immunoreactivity was absent in the spinal cord of saline treated WT mice, in contrast to LPS treated mice which exhibited bilateral punctate staining that resembled microglial morphology. We also showed that GPR84 immunoreactivity exclusively co-localised with a majority of Iba1 positive cells and failed to co-label with NeuN and GFAP. This confirms that GPR84 expression is restricted to microglial cells and raises the possibility that only certain microglial subpopulations express this receptor. As expected, GPR84 staining was absent in the spinal cords of both saline and LPS treated KO mice. Lastly, in conjunction with these findings we demonstrated that GPR84 expression is robustly up-regulated in cortical microglia and B-GEPMs subsequent to LPS exposure.

3.4.3 A subset of LPS induced gene transcripts are differentially regulated in GPR84 WT and KO macrophages

As GPR84 is a highly inducible pro-inflammatory receptor we expected to observe a more robust behavioural phenotype in the two inflammatory models examined, similar to our previous findings in the neuropathic pain model. However, we saw a mild behavioural phenotype that was restricted to particular modalities, suggesting that the signalling pathway of GPR84 is complex and may encompass different mechanisms in animal models of persistent inflammatory and neuropathic pain. Due to the restricted expression of this GPCR to spinal microglial cells and marked up-regulation by an appropriate immunological stimulus, we expected to see an altered microglial phenotype in KO mice. However, the microglial response was equivalent between the genotypes in both the CFA and LPS-induced CNS inflammation models. We also demonstrated a dissociation of microglial and macrophage involvement in GPR84 mediated pain pathways in a nerve injury-induced model of neuropathic pain (*Chapter 2*). These findings are puzzling in light of the behavioural phenotype in KO mice as microglia and macrophage cells are well documented to contribute to pain behaviours. Based on this evidence and the fact that we observed a partial reduction in inflammation-induced hyperalgesia in the KO that was not associated with an altered microglia response, we sought to examine the possible contribution of peripheral macrophages by assessing the ability of B-GEPMs to launch an inflammatory response in the absence of GPR84. Here, we used a simple *in vitro* system to measure

transcriptional changes of a selection of putative mediators subsequent to LPS stimulation. Macrophage cells are central players in the innate immune response to a peripheral insult and promote inflammation by releasing a range of mediators such as TNF-α, IL-1β, NGF, NO and PGE_2 (Nathan, 1987; Tannenbaum and Hamilton, 1989; Marchand et al., 2005). LPS stimulation of cultured macrophage cells increases cytokine synthesis in a TLR4 dependent manner (Feng et al., 2002; Schmid et al., 2009) and application of LPS to the injured sciatic nerve enhances the recruitment of macrophage cells to the site of injury and the process of WD (Boivin et al., 2007). Therefore, our *in vitro* paradigm using a potent exogenous TLR4 agonist is a relevant representation of the *in vivo* situation.

Using custom designed mouse PCR array cards we examined LPS induced transcriptional changes in GPR84 WT and KO mice relative to appropriate control cells of each genotype. We analysed the data sets via implementing strict threshold criteria and examined top ranking up- or down-regulated genes in addition to transcriptional profiles and correlations between the two genotypes. We found that GPR84 KO macrophages were as equally capable as WT cells at launching a pro-inflammatory response upon LPS exposure and that there was an equivalent, if not greater induction of pro-nociceptive IL-1β, TNF-α, IL-6, PTGS2, PTGES and NOS2 in the KO than the WT. However, a subset of pro-nociceptive mediators (IL-18, CCL2, CCL3 and CXCL5) showed an attenuated induction in the KO in contrast to the WT. This reflects the differential regulation of mediators by $G\alpha_{i/o}$ proteins and suggests that GPR84 may concurrently down-regulate the expression of some mediators whilst up-regulating the expression of others. Together, these data indicate that GPR84 may be involved in the regulation of a small subset of cytokines that are known to contribute to nociceptive transmission.

IL-18 possesses a variety of functions particularly concerned with the regulation of T-cells, including the promotion of Th1 cell development and the activation/facilitation of IFN-γ and TNF-α secretion (Nakanishi et al., 2001). Intrathecal or intraplantar administration of this cytokine generates behavioural hypersensitivity (Verri, 2005; Verri et al., 2006; Miyoshi et al., 2008) and SNL-injured rodents exhibit increased expression of IL-18 and its receptor, IL-18R, in microglia and astrocytes, respectively (Miyoshi et al., 2008). It has also been reported that LPS stimulation potentiates IL-18 expression in microglial cells, indicating that IL-18 induction is downstream of TLR4-dependant activation of microglial cells (Miyoshi et al., 2008).

CCL2 is a chemotactic factor that contributes to the recruitment and activation of macrophages and microglial cells to the site of inflammation or injury (Charo and Ransohoff,

2006). Intraspinal administration of CCL2 in naïve rats results in microglial activation and pain behaviours, which are reversed via CCL2 neutralising antibodies (Thacker et al., 2009). Furthermore, CCR2 null mice show a reduction in pain behaviours in models of inflammatory and neuropathic pain (Abbadie et al., 2003). CCL3 is predominantly expressed in hematopoietic immune cells and exerts similar chemotactic properties to CCL2, regulating migration, proliferation and cytokine synthesis of immune cells via its cognate CCR1 and CCR5 receptors (Charo and Ransohoff, 2006). Intrathecal administration of CCL3 in naïve mice produced dose-dependent pain behaviours that were reversed via antibody neutralisation (Kiguchi et al., 2010b). CXCL5 is also involved in immune cell recruitment and activation and in an ultraviolet B model of inflammation high levels of expression of this chemokine correlated with peak behavioural hypersensitivity (Charo and Ransohoff, 2006; Dawes et al., 2011). In addition, intraplantar injection of CXCL5 evoked mechanical allodynia but not thermal hyperalgesia, attributed to the infiltration of macrophage and neutrophil cells (Dawes et al., 2011).

Among the top up-regulated genes in the KO were the growth factors BDNF and EREG. BDNF was down-regulated in the WT and remained unchanged in the KO after LPS, whereas EREG was up-regulated in both but to a greater extent in the KO. Little is known about EREG in nociceptive pathways and the expression pattern of pro-nociceptive BDNF (Latremoliere and Woolf, 2009) does not correspond to the behavioural phenotype in the KO. A subset of cytokines/chemokines were also induced in both genotypes but to a greater extent in the KO including IL-23a, IL-33, CCL20, CXCL11 and CSF2. Whilst a majority of these are currently unrelated to pain with only recent implications for IL-33 and CXCL11 (Strong et al., 2012; Han et al., 2013; Zarpelon et al., 2013), these expression patterns are unlikely to be relevant to the KO behavioural phenotype. This is because an increase in the expression of pro-nociceptive mediators does not coincide with our previous observations of an absence of mechanical hyperalgesia in CFA or LPS treated KO mice.

Pro-inflammatory CCL7, CCL19 and CXCL9 as well as IL-13, IL-19, IL-20, CCL22, CCL24, CXCL3 and CXCL13 showed attenuated induction in LPS stimulated KO cells. Whilst CCL7, CCL19 and CXCL9 have been linked to nociception (Biber et al., 2011; Dawes et al., 2011; Strong et al., 2012; Schmitz et al., 2013), the latter group have very little documentation in the context of pain. The transcriptional regulation of CCL19 was striking and under basal conditions this chemokine was undetectable, whereas subsequent to LPS stimulation CCL19 was markedly induced in WT but not KO cells. In response to inflammatory insult, CCL19 is co-released with CCL21a from a variety of stromal cells within the lymphoid organs where they act with similar affinities on $CCR7^{+}$ T-cells, B-cells and dendritic cells to promote

migration into lymphatic vessels and mediate the adaptive immune response (Comerford et al., 2013). Subsets of macrophage populations are also $CCR7^+$ and migrate in response to CCL19 and CCL21a to the marginal zone of the spleen where blood-borne pathogens are cleared (Ato et al., 2004). In a study utilising the *paucity of lymph node T-cells* (PLT) mice, which have a naturally occurring defect in the expression of both CCL19 and CCL21a, pain associated behaviours were absent subsequent to SNI and microglia failed to up-regulate $P2X_4$ mRNA expression (Biber et al., 2011). Intrathecal administration of CCL21a in these mice produced long lasting mechanical allodynia to a similar extent to that seen in the WT mice, which was dependent on $P2X_4$ receptor function. Although CCL19 was undetected in neuronal tissue and plays a minimal role in the behavioural phenotype of PLT mice, the contribution of this chemokine was not entirely excluded (Biber et al., 2011). A similar study also reported the anti-nociceptive effects of CCL19/21a deficient mice in the SNI model and again showed that this was not related to a reduced microglial response but rather due to an altered feature of microglial cells (Schmitz et al., 2013).

In light of this evidence and the intriguing transcriptional regulation of this chemokine we further validated the differential regulation of CCL19 between genotypes and were successfully able to re-produce the original Taqman PCR array data via individual qRT-PCR. However, we were unable to repeat these data in an independent group of animals. This could be due to the fact that the WT cells were not as stimulated as before and hence did not induce CCL19 to the same extent as seen previously or perhaps because the original findings were a false positive. It would therefore be interesting to re-validate our findings to clarify this discrepancy.

3.4.4 GPR84 signalling

The intriguing finding that GPR84 expression is restricted to immune cells sparked recent studies into the functional characterisation of this receptor under *in vitro* and *in vivo* conditions. In one study it was shown that T-cells from GPR84 null mice exhibited a hyper Th2 cytokine production of IL-4, IL-5 and IL-13 in contrast to WT controls, indicating that GPR84 may suppress anti-inflammatory cytokines. However, this hyper Th2 cytokine phenotype was not present in immunised KO mice *in vivo*, perhaps due to a degree of compensation driven by the effects of an active immune response or due to differences between *in vitro* and *in vivo* systems (Venkataraman and Kuo, 2005). As the expression of GPR84 is robustly induced by an inflammatory stimulus, many studies have examined the functional responses of immune cells subsequent to LPS stimulation, particularly since GPR84 has a very low level of expression under basal conditions. Exposure of RAW 264.7

cells to GPR84 ligands such as capric acid and lauric acid subsequent to LPS stimulation produced a dose-dependent increase in IL-12p40 transcription and secretion (Wang et al., 2006a). This was consistent with findings from Venkataraman and Kuo (2005) who reported increased Th2 cytokine production in KO T-cells. Suzuki et al. (2013) also showed that under LPS conditions, granulocyte and macrophage cells exhibited amplified production of IL-8 and TNF-α subsequent to stimulation with the GPR84 ligand 6-OAU. In addition, intravenous dosing with 6-OAU increased levels of CXCL1 in rodents (Suzuki et al., 2013). Based on this literature, we anticipated that LPS-stimulated GPR84 KO cells would exhibit enhanced production of Th2-associated cytokines: IL-4, IL-5, IL-6, IL-10 and IL-13 and decreased/unchanged production of Th1-associated cytokines: IFN-γ and IL-2 as well as decreased/unchanged levels of IL-12p40. We report non-detectable levels of IL-2 and IL-4 in LPS stimulated WT and KO macrophages; IL-13 increased in WT cells and was non-detectable in KO cells. There was also a robust up-regulation of IL-6, IL-10 and IL-12p40 in both genotypes. Although our findings do not entirely align with previous reports, we hypothesise that this is due to the use of different cell types where GPR84 may exert different functions.

As a $G\alpha_{i/o}$ coupled receptor, GPR84 is likely to be involved in the differential regulation of subsets of cytokines and chemokines exerting both positive or negative modulatory effects, which is also supported by our findings in this chapter. In a study examining the differential regulation of LPS-induced cytokines and chemokines in peritoneal macrophages from mice lacking particular isoforms of $G\alpha_i$ proteins, it was found that the KO mice generally exhibited attenuated induction of cytokines/chemokines except for some notable cases (Fan et al., 2007). TNF-α, IL-6 and IL-10 were all decreased in $G\alpha_{i2}$ and $G\alpha_{i1/3}$ KO mice in contrast to WT littermates, whereas CCL3 and CSF2 were more greatly expressed in $G\alpha_{i1/3}$ null mice and IL-1β remained unchanged in both $G\alpha_{i2}$ and $G\alpha_{i1/3}$ null mice (Fan et al., 2007). Therefore, it is apparent that $G\alpha_i$ proteins are capable of exerting both positive and negative regulatory effects on the expression of some pro-inflammatory cytokines and chemokines. Likewise, we observed equivalent or greater induction of pro-nociceptive mediators IL-1β, TNF-α, IL-6, PTGS2, PTGES and NOS2 in the KO than in the WT and attenuated expression of IL-18, CCL2, CCL3 and CXCL5, suggesting that GPR84 exerts both positive and negative effects.

3.4.5 Future work

In this chapter we examined the role of GPR84 in two experimental models of inflammatory pain and established a modality specific behavioural phenotype in KO mice, but found no evidence for the contribution of microglial cells. Resident or recruited macrophages have

been reported to contribute to inflammatory pain by the release of mediators such as TNF-α, IL-1β, NGF, NO and PGE_2 (Marchand et al., 2005). Experimental depletion or recruitment of these cells has been shown to significantly reduce or enhance zymosan and acetic acid induced pain (Ribeiro et al., 2000) while intraperitoneal administration of supernatants from LPS stimulated macrophages is hyperalgesic (Thomazzi et al., 1997). Furthermore, during an inflammatory response macrophage cells also contribute to the recruitment and activation of other immune cell types such as neutrophils (Souza et al., 1988). Therefore, it would be interesting to characterise the peripheral macrophage response in WT and KO mice via examining immunohistochemical markers of macrophage cells (Iba1 and F4/80) in the hind paws of CFA treated mice as well as profile transcriptional changes between genotypes in spinal cord and hind paw tissue. In addition, we characterised the peripheral response by measuring paw oedema and found no differences between the genotypes. However, the extent of peripheral inflammation could be further investigated by measuring myeloperoxidase activity and carrying out an assessment of leucocyte infiltration into the hind paw. Since we have only achieved successful GPR84 staining after LPS treatment it may also be interesting to behaviourally assess WT and KO mice subsequent to intraplantar administration of LPS, in conjunction with examining GPR84 immunoreactivity and immunophenotypic changes of peripheral macrophages that have infiltrated the hind paw.

As a pro-inflammatory receptor, it is likely that GPR84 may be involved in regulating the expression of subsets of mediators in response to an inflammatory insult. Therefore, the validation of CCL19 will need to be repeated alongside other top dysregulated genes (IL-18, CCL2, CCL3, CXCL5) in an independent group of animals, as this would prove instrumental in warranting further *in vivo* studies. Unfortunately, our examination was limited to a set selection of 92 genes and thus further studies profiling alternative mediators may prove to be more informative. The development of a selective agonist or antagonist would also permit the direct evaluation of the contribution of GPR84 activation or inhibition to pain pathways.

Chapter 4

GPR84 Cell Signalling

4.1 Introduction

Signal transduction is performed via membrane proteins and vitally determines cellular homeostasis and activity. Under normal conditions, GPCRs exist in an equilibrium of conformations, which are altered upon ligand binding. Activating ligands (agonists) stabilise receptor conformation and promote signalling via the coupled heterotrimeric G-protein subunit, whereas inhibitory ligands (antagonists) stabilise conformations that decrease signalling. Such pharmacological tools have been widely exploited in experimental studies investigating the physiological role and signalling pathways of receptors *in vitro* and *in vivo*. Throughout this thesis, we have utilised transgenic mice to examine GPR84 in chronic pain mechanisms, and have been able to show that this receptor indeed contributes to the development and maintenance of pain-associated behaviours. However, a lack of commercially available agonists or antagonists selective for GPR84 has hindered further progression in the characterisation of this receptor. Therefore, in this chapter we assessed three putative ligands using two different functional assays to identify a selective agonist that could be used in further characterisation studies.

GPR84 is an orphan receptor and its signalling pathway is currently unknown, with only a single study postulating that the free fatty acid, capric acid (CA), is the natural ligand that activates GPR84 in a $G\alpha_{i/o}$ -dependent pathway (Wang et al., 2006a). Based on this limited evidence we tested CA and two other ligands kindly provided by GSK/Convergence Pharmaceuticals (Embelin and CNV) for efficacy and selectivity in microglia and macrophage cells via Ca^{2+} and cAMP signalling assays.

4.1.1 Calcium signalling in microglia and macrophages

Calcium is a second messenger that regulates a range of cellular functions, including metabolism, secretion, proliferation, exocytosis and transcription (Kettenmann et al., 2011). Like any other eukaryotic cell, microglia and macrophages tightly control their intracellular Ca^{2+} concentration ($[Ca^{2+}]_i$), which is determined by a delicate balance between processes that introduce Ca^{2+} into the cell (channels, receptors, intracellular stores) and those that remove Ca^{2+} (buffers, pumps, exchangers) as summarised in Fig. 4.1. The influx and intracellular release of Ca^{2+} is a passive but gated function, whereas extrusion of Ca^{2+} from the cell or sequestration into intracellular stores is constitutive but energy-dependent (Moller, 2002).

In neurons, changes in $[Ca^{2+}]_i$ participates in electrical excitability (~ -70 mV to ~ +150 mV), neurotransmitter release and synaptic efficacy. In contrast, microglia and macrophages are non-excitable cells, meaning that they are unable to generate propagating electrical responses (action potentials). However, like neurons they express VGCCs and so are able to depolarise their membranes (~ -70 mV to ~ -10 mV) in response to external stimuli and thus can be considered as 'internally Ca^{2+} excitable'. Generally, extracellular Ca^{2+} levels are 20,000 fold higher than intracellular levels. In neurons Ca^{2+} signalling is at the fast end of the scale ranging from microseconds to milliseconds, with a resting $[Ca^{2+}]_i$ of ~100 nM that can rise to several μM (Clapham, 1995; Verkhratsky et al., 1998; Kettenmann et al., 2011). In non-excitable cells Ca^{2+} signalling is also a transient event, ranging from milliseconds to minutes, with a resting $[Ca^{2+}]_i$ of ~50 nM that can rise to several μM. This enables the cell to respond appropriately to extracellular signals, depending on the magnitude, duration and location of the Ca^{2+} signal. (Clapham, 1995; Moller, 2002).

The tight regulation of Ca^{2+} influx during numerous physiological mechanisms underlying cell activation is mediated via VGCCs (L-type), or receptor-operated channels (ROCs) (ionotropic glutamate and purinergic receptors), which are triggered by membrane depolarisation or ligand binding, respectively (Moller, 2002; Kettenmann et al., 2011). Essentially, ion channels control the flow of ions across the cell membrane and hence influence intracellular voltage-gated channels, membrane potential and cell volume. Correspondingly, the modulation of these features affects many processes such as respiration, proliferation, migration, secretion and cell morphology (Eder, 2005). Evidence for the existence of microglial expressed VGCCs is limited to a single study, in which the authors demonstrated the presence of a current with properties similar to that of L-type Ca^{2+} channels in rat microglial cells (Colton et al., 1994). It was shown that administration of the L-type Ca^{2+} channel opener, BAY K8644, enhanced the inward Ca^{2+} current, whereas the L-type antagonist, nifedipine, reduced the current and the production of superoxide anions (Colton et al., 1994). It was thus proposed that this small VGCC current contributed to nicotinamide adenine dinucleotide phosphate (NADPH) oxidase synthesis of superoxide anions, which are cytoactive molecules released in response to infection or injury (Colton et al., 1994). The presence of L-type VGCCs has also been documented in macrophages where increases in $[Ca^{2+}]_i$ during membrane depolarisation was dependent on external Ca^{2+} and blocked by nifedipine and verapamil whilst enhanced by BAY K8644 (Hijioka et al., 1992; Kong et al., 1992). Moreover, it has also been documented that non Ca^{2+} permeable voltage-gated channels may participate in Ca^{2+} signalling. For example, K^+ channels negatively regulate membrane potential, which enhances Ca^{2+} influx through non-selective cation

channels and intracellular stores, and in effect modulates functions such as proliferation and cell volume (Rouzaire-Dubois et al., 2000).

ROCs, such as the ionotropic ATP receptors ($P2X_4$ and $P2X_7$), were first identified in rodent and human microglial cultures (McLarnon et al., 1999; Kettenmann et al., 2011). Activation of P2X receptors results in Na^+ and Ca^{2+} influx and K^+ efflux through non-selective cationic channels and subsequent membrane depolarisation (McLarnon, 2005). Low levels of ATP (micromolar range) activate $P2X_4$ receptors while higher levels (millimolar range) also recruit $P2X_7$ receptors. $P2X_7$ receptors possess a large pore that is permeable to hydrophilic molecules of high molecular weights (> 600 Da) (Farber and Kettenmann, 2006b). Activation of these receptors produces a strong cellular depolarisation, a substantial increase in $[Ca^{2+}]_i$ and p38/ERK mediated release of signalling molecules such as TNF-α (Suzuki et al., 2004; McLarnon, 2005; Farber and Kettenmann, 2006a). ATP-induced Ca^{2+} signalling may also be facilitated via inward rectifying K+ channels, as blocking these using barium attenuates Ca^{2+} levels (Franchini et al., 2004).

In non-excitable cells, Ca^{2+} signals are predominantly produced via metabotropic receptors and subsequent mobilisation of the second messenger IP_3, which activates Ca^{2+} channels (IP_3Rs) expressed by the endoplasmic reticulum (ER) (Verkhratsky and Parpura, 2013). The ER is a major Ca^{2+} store and consists of a membranous network that extends from the cell membrane through the cytoplasm to the nuclear envelope. Here, Ca^{2+} release is executed by several different types of endomembrane-resident Ca^{2+} channels, including the well-characterised ryanodine receptors (RyRs) and IP_3Rs. Microglial cells possess both types of Ca^{2+} channels, but while RyRs are currently considered less important, IP_3R signalling pathways are the primary route for generating an increase in microglial $[Ca^{2+}]_i$ (Kettenmann et al., 2011). IP_3Rs are initiated via transduction pathways involving the activation of specific isoforms of PLC coupled to metabotropic GPCRs or receptor tyrosine kinases. For example, microglia express a number *Bordetella pertussis* toxin-sensitive heterotrimeric GPCRs for the chemokines CCL2 (CCR2), CCL3 and CCL4 (CCR1, 5, 9), CCL5 (CCR3) and fractalkine (CX_3CR1) (Murdoch and Finn, 2000; Flynn et al., 2003). Activation of PLC results in the biosynthesis of DAG and IP_3 from the membrane-bound lipid precursor, PIP_2. While DAG goes on to activate PKC, soluble IP_3 diffuses across the cytosol and binds to ER IP_3Rs. This results in increased IP_3Rs sensitivity to Ca^{2+} and the initiation of a biphasic Ca^{2+} signal; thus at low $[Ca^{2+}]_i$ the receptor is activated but subsequent to calcium release, high $[Ca^{2+}]_i$ inhibits the receptor (Murdoch and Finn, 2000; Kettenmann et al., 2011). In neurons, newly released Ca^{2+} binds to calmodulin (CaM), which possesses four high affinity Ca^{2+} binding sites. Upon formation of the Ca^{2+}/CaM complex, CaM increases its affinity for target enzymes

such as Ca^{2+}/calmodulin-dependent kinase kinase (CaMKK) and its substrates, Ca^{2+}/calmodulin-dependent kinase (CaMK) I and IV, which are phosphorylated and activated by CaMKK (Soderling, 1999; Racioppi and Means, 2008). The CaMK cascade orchestrates the activity of transcription factors such as CREB and may cross-talk with other intracellular pathways. For example, CaMKIV can inactivate AC and thus reduce levels of cAMP and may also interact with the MAPK signalling pathways (Soderling, 1999). There are reports of the CAMK pathway in microglia and macrophage cells but a majority of evidence coincides with neurons (Sola et al., 1999; Suh et al., 2005; Racioppi and Means, 2008, 2012; Racioppi et al., 2012). In immune cells the initiation of PKC and other Ca^{2+}-dependent kinases results in protein phosphorylation and a co-ordinated cascade of signalling events, which may also entail the activation of Ras and Rho proteins as well as $PLCA_2$, PI3k and MAPK pathways (Murdoch and Finn, 2000).

Following depletion of intracellular ER Ca^{2+} stores, which is sensed by stromal interaction molecules, Ca^{2+}-permeable store-operated channels (SOCs) such as the calcium release-activated Ca^{2+} channel (CRAC) and transient receptor potential channels (TRPM2,7; TRPC1-7) are opened to aid the replenishment of Ca^{2+} levels (Hoth and Penner, 1992; Zhang et al., 2005c; Feske et al., 2006; Worley et al., 2007). This mechanism is referred to as 'capacitative Ca^{2+} influx' and is employed by many non-excitable cells as the main route of Ca^{2+} entry (Putney, 1986, 1990; Semenova et al., 1999; Vig and Kinet, 2009; Gao et al., 2010; Verkhratsky and Parpura, 2013). Ca^{2+} entry in this manner tends to outlast the initial stimulus and thus provides a long-lasting influx that is crucial for regulating many aspects of microglial cell function such as morphology, proliferation, NO and cytokine production, antigen presentation, migration and phagocytosis (Farber and Kettenmann, 2006a; Kettenmann et al., 2011). This striking phenomenon was initially demonstrated in cultured microglia, where the activation of the $P2Y_{2/4}$ receptors via supramaximal doses of ATP or UTP resulted in complete depletion of the ER Ca^{2+} store and the prolonged opening of SOCs that lasted for tens of minutes (Toescu et al., 1998). Similarly, BDNF and LPS exposure acting via TrkB and TLR4, respectively, also induced long-lasting SOC activation in microglia (Hoffmann et al., 2003; Mizoguchi et al., 2009). This persistent SOC mediated increase in $[Ca^{2+}]_i$ is thought to perhaps account for the sustained elevation of basal $[Ca^{2+}]_i$ and associated attenuation of evoked Ca^{2+} signals upon further stimulation (Moller et al., 2000; Hoffmann et al., 2003). A corresponding elevated $[Ca^{2+}]_i$ profile has also been reported in cultured microglial cells incubated with toxic β-amyloid fragment (25-35) (Korotzer et al., 1995) as well as microglial cells isolated from post-mortem brains of Alzheimer patients, which exhibited reduced ATP or platelet aggregating factor induced Ca^{2+} signals (McLarnon et al., 2005). Furthermore, LPS stimulation induces the release of many cytokines including

TNF-α, IL-1β, IL-6, IFN-γ and IL-12. Accordingly, application of TNF-α, IL-1β or IFN-γ to human microglial cells has been demonstrated to evoke sustained Ca^{2+} signals via TNFR1/2, IL-1R and IL-6R, respectively (Goghari et al., 2000; McLarnon et al., 2001; Franciosi et al., 2002).

Abnormal Ca^{2+} signalling as a result of aberrant SOC activity has been implicated in several human inflammatory diseases such as IBS and allergy (Parekh, 2010). Interestingly, a recent study demonstrated that YM-58483, which inhibits SOCs in immune cells, alleviated CFA and SNI behavioural hypersensitivity as well as formalin-induced nociceptive behaviour, in addition to suppressing the release of pro-inflammatory mediators (Gao et al., 2013). Thus, the development of SOC channel inhibitors as a means to control aberrant Ca^{2+} activity could provide considerable clinical benefits for patients suffering from chronic inflammatory diseases and/or pain.

Ca^{2+} signalling in microglia/macrophages varies in magnitude as well as temporally and spatially (Moller, 2002; Kettenmann et al., 2011). Rapid Ca^{2+} signals are usually generated by Ca^{2+} released from internal stores and the fast opening of membrane channels is followed by a rapid decay. Other transient [Ca^{2+}] signals are characterized by an extended plateau phase and are attributed to an initial Ca^{2+} release and a subsequent Ca^{2+} influx through ROCs or SOCs, which play an important role in down-stream cellular events such as mediator release, transcriptional regulation and cell motility (Moller, 2002). More complex oscillatory Ca^{2+} signals are generated by Ca^{2+} release from internal stores and subsequent opening of SOCs, whereas slow rising Ca^{2+} signals are a result of modulatory effects on Ca^{2+} extrusion mechanisms (Moller, 2002). Subsequent to a cellular response and an elevation in $[Ca^{2+}]_i$, extrusion of Ca^{2+} is accomplished by plasma membrane Ca^{2+}-ATPase (PMCA) pumps, which are facilitated by Na^+/Ca^{2+} exchangers (NCX) (Carafoli, 1994; Nagano et al., 2004; Lytton, 2007; Staiano et al., 2013). These exchange proteins utilise the Na^+ gradient produced by Na^+ pumps to rapidly expel Ca^{2+} into the extracellular environment. In addition, Ca^{2+} may also be sequestered into the ER or mitochondria (Moller, 2002). Ca^{2+} -ATPase located on the ER membrane actively transports Ca^{2+} into the ER, whereas mitochondria act as potent Ca^{2+} buffers and uptake cytosolic Ca^{2+} via uniporters, which are highly selective integral membrane proteins (Carafoli, 1994; Gilabert and Parekh, 2000; Moller, 2002; Nagano et al., 2004; Staiano et al., 2013).

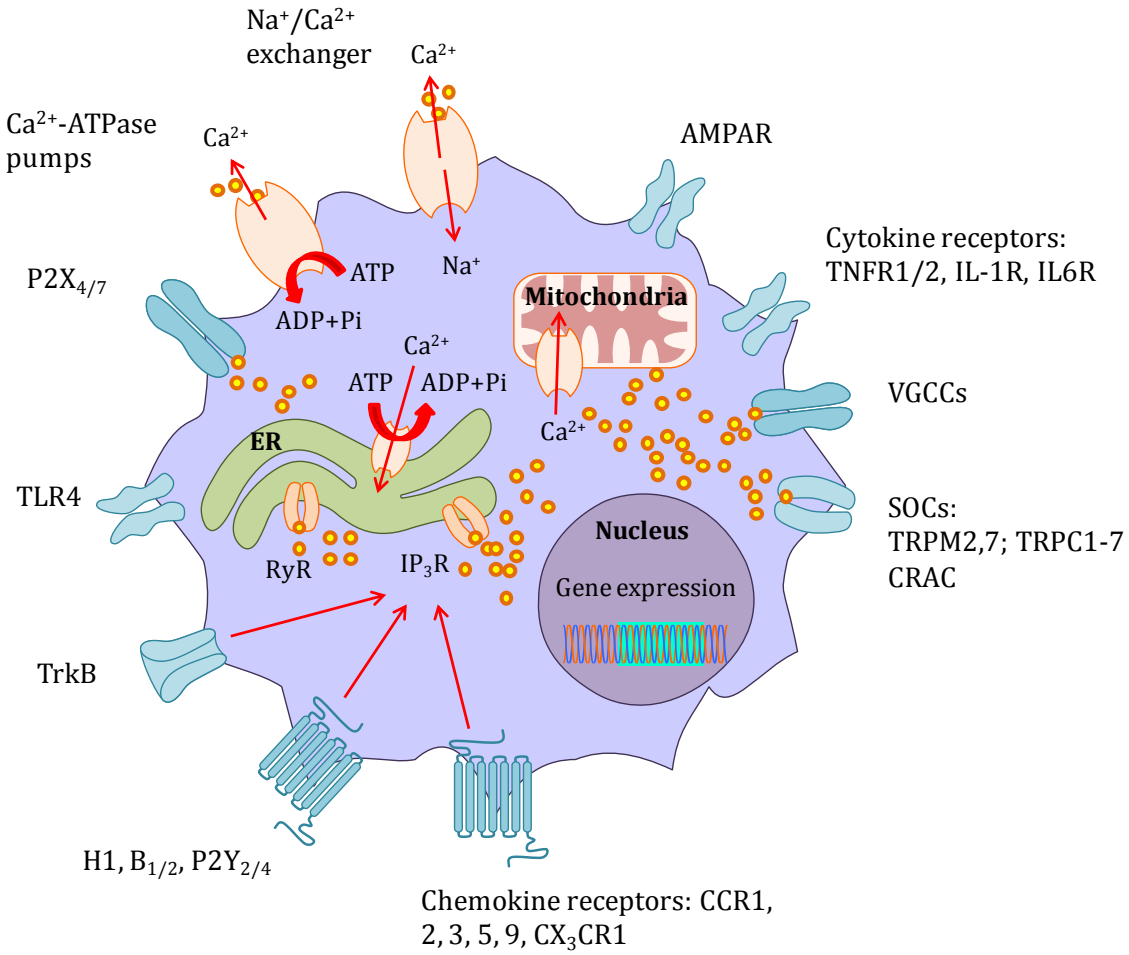

Figure 4.1: Intracellular calcium signalling

Simplified schematic of Ca^{2+} signalling in microglia and macrophage cells. Ca^{2+} may enter via ROCs ($P2X_{4/7}$, AMPAR), VGCCs (L-type) and SOCs (TRPM2,7, TRPC1-7, CRAC). Activation of GPCRs (H1, $B_{1/2}$, $P2y_{2/4}$, chemokine receptors) or tyrosine kinase receptors (TrkB) leads to the mobilisation of Ca^{2+} via IP_3Rs. Cytokine receptors and TLR4 also initiate Ca^{2+} release but the mechanisms are unclear. Ca^{2+} is extruded from the cell via Ca^{2+}-ATPase pumps and Na^+/Ca^{2+} exchangers (NCX) and may also be sequestered into the ER or mitochondria.

4.1.2 Cyclic AMP signalling in microglia and macrophages

Cyclic AMP was the first ubiquitous second messenger to be discovered and plays a crucial role in many cellular functions in response to hormones and neurotransmitters (Sutherland and Rall, 1958). Intracellular levels of cAMP are tightly regulated by two key enzymes, ACs and cyclic nucleotide phosphodiesterases (PDEs), which are involved in the biosynthesis or degradation of cAMP into adenosine monophosphate (AMP), respectively. Mobilisation of

AC is down-stream of the activation of GPCRs coupled to stimulatory $G\alpha_s$ by ligands such as epinephrine (β2), adenosine (A2a), histamine (H2) and PGE_2 (EP2) (Peters-Golden, 2009; Kettenmann et al., 2011). Subsequent to ligand binding, GPCRs undergo a conformational change and initiate the activation of a G-protein. This leads to the release of αs from the αβγ heterotrimeric complex, which binds to AC and catalyses the formation of cAMP from ATP. Newly synthesised cAMP then binds to PKA, which consists of a symmetrical complex of two regulatory and two catalytic subunits. Binding of cAMP to the two regulatory subunits initiates subunit dissociation and passive diffusion into the nucleus (Taylor et al., 1992). In turn, activated PKA phosphorylates numerous target proteins such as CREB, which binds to the conserved cAMP response element expressed within the promoter regions of many cAMP-responsive genes. CREB may then form a complex with its transcription co-activator, CBP (Mayr and Montminy, 2001). Alternatively, cAMP may also bind to guanine-nucleotide-exchange proteins, Epac-1 and 2, which are involved in the activation of the monomeric GTPase, Rap-1, which binds to B-Raf (Bos, 2006). The formation of the B-Raf-Rap-1 complex has been implicated in the activation of MAPKs such as ERK as well as the regulation of CREB-mediated gene transcription in various cell types including microglia and macrophages (Wang et al., 2006b). The cAMP/CREB pathway is summarised in Fig. 4.2.

Elevation in intracellular cAMP generally suppresses innate immune function such as phagocytosis, microbe killing and the production of pro-inflammatory mediators, whilst promoting the release of anti-inflammatory mediators (Bourne et al., 1974; Serezani et al., 2008; Peters-Golden, 2009). Upon activation, cells of the innate immune system (microglia/macrophages) produce an array of pro-inflammatory mediators. Many immune system molecules such as chemokines and cytokines act through inhibitory GPCRs and reduce the production of cAMP via preventing AC activity. However, the extent to which the immunostimulatory effects of these molecules depend on a reduction in intracellular cAMP is not clear (Serezani et al., 2008). Elevation of cAMP by mediators such as PGE_2 alters the release of many cytokines/chemokines and lipid mediators from 'activated' microglia or macrophage cells. For instance, the expression of pro-inflammatory TNF-α, IL-6, IL-12, CCL3, CCL4 and LTB_4 is reduced, while levels of anti-inflammatory IL-10 and IL-6 are enhanced (Martin and Dorf, 1991; Aloisi et al., 1997; Caggiano and Kraig, 1999; Prinz et al., 2001; Feng et al., 2002; Iwasaki et al., 2003; Uchiya et al., 2004; Aronoff et al., 2005; Aronoff et al., 2006). Notably, Aronoff and colleagues (2005) showed that this mechanism was PKA-dependent and Epac-1-independent and it was later found that PKA can directly regulate NF-κB (Wall et al., 2009). Aronoff et al. (2005) also demonstrated that pre-treatment with PGE_2 or an Epac-1 agonist prevented phagocytosis, whereas prior exposure of alveolar macrophages to a PKA inhibitor had no effect. Phagocytosis is a highly co-ordinated process

that entails the re-arrangement of the cytoskeleton and membrane upon complement receptor (CR) and FCγ receptor recognition of microbial particials (Gordon, 2007). An increase in cAMP levels suppresses CR and FCγ receptor mediated phagocytosis in an Epac-1-dependent manner and to a lesser extent PKA (Aronoff et al., 2005). However, this can very much depend on the cell type; both PKA and Epac-1 have been reported to inhibit phagocytic activity in microglia and peritoneal macrophages, but in monocytes this was found to be solely dependent on PKA (Bryn et al., 2006; Makranz et al., 2006). Elevated levels of intracellular cAMP also suppress microbicidal activity by down-regulating NADPH oxidase activity and hence the production of reactive oxygen intermediates such as hydrogen peroxide (Aronoff et al., 2005). Accordingly, pre-treatment with PGE_2, Epac-1 or PKA agonists inhibited the ability of alveolar macrophages to successfully kill ingested microbes (Aronoff et al., 2005). The role of cAMP in the regulation of inducible NO synthase and NO production is contradictory; while some groups have reported a facilitatory role of cAMP others have reported an inhibitory effect (Mustafa, 1998; Chen et al., 1999). Likewise, conflicting evidence also applies to phagolysosome maturation. For example, Muschel et al. (1977) showed that PKA was necessary for phagosomal acidification, whereas Kalamidas et al. (2006) demonstrated that elevated cAMP levels reduced phagolysosome formation and acidification via a PKA-dependent mechanism.

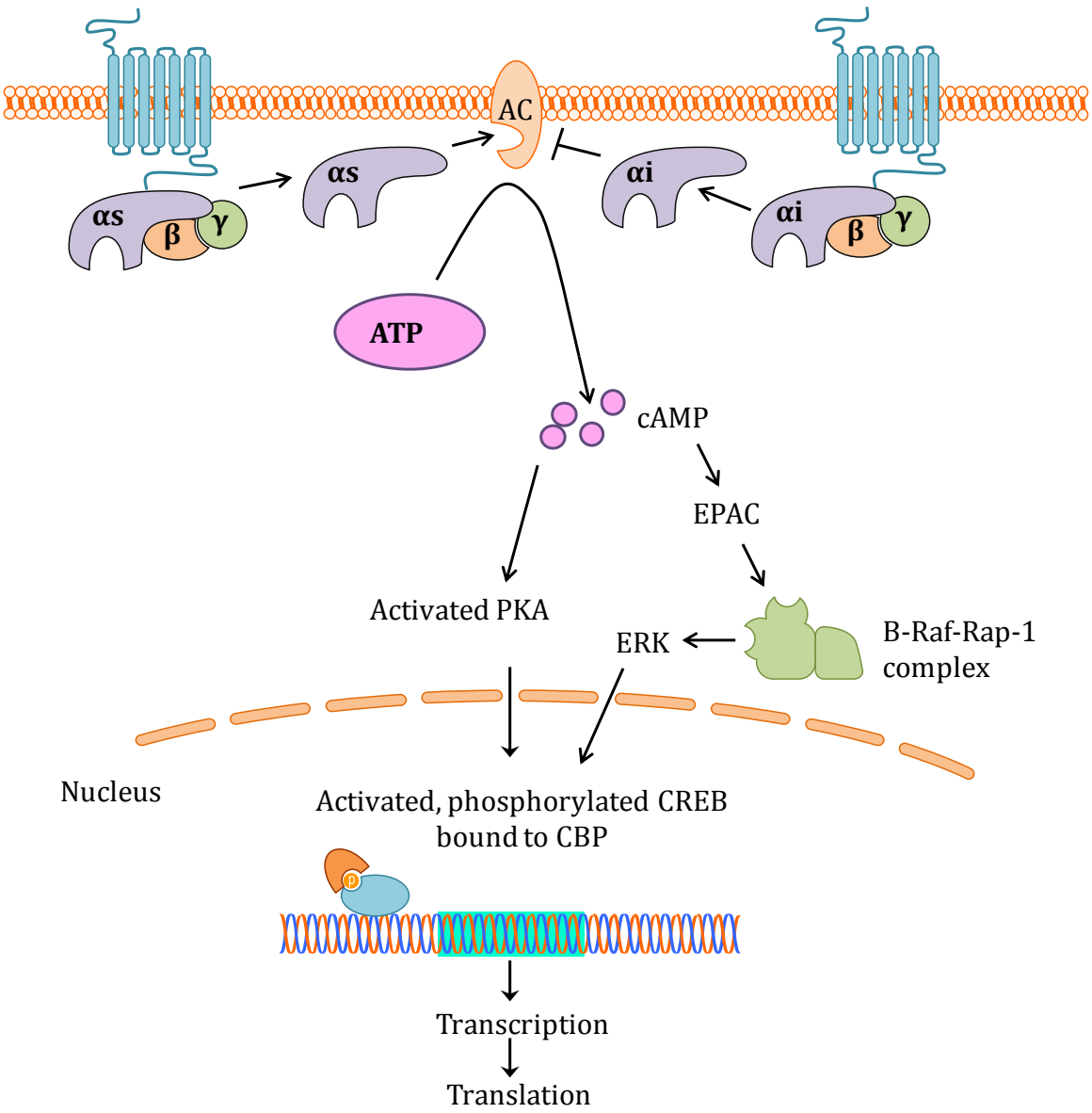

Figure 4.2: Cyclic AMP signalling in microglia and macrophages

Schematic illustrating the regulation of intracellular cAMP in microglia and macrophage cells. Activation of GPCRs leads to either the stimulation (Gαs) or inhibition (Gαi) of AC mediated synthesis of cAMP. Downstream effectors of cAMP (PKA and EPAC1/2) initiate the phosphorylation and activation of CREB, which associates with is coactivator, CBP, within the promoter region of target genes.

4.1.3 Putative GPR84 ligands

This chapter investigates the efficacy and selectivity of three GPR84 ligands in microglia and macrophage cells. The signalling pathway of GPR84 is unknown so we utilised Ca^{2+} and cAMP signalling assays to examine changes in the intracellular concentrations of two well-characterised second messengers that are down-stream of most classes of heterotrimeric GPCRs. There is very little data available on selective GPR84 agonists and antagonists. Embelin and CNV were identified as potentially interesting agonists in a series of screening assays performed by GSK/Convergence Pharmaceuticals (proprietary GSK/Convergence Pharmaceuticals data) and CA was identified by Wang et al. (2006a) as a natural ligand of GPR84.

Embelin

Embelin (2,5-dihydroxy-3-undecyl-1,4-benzoquinone) is a naturally occurring alkyl-substituted hydroxybenzoquinone derived from the *Embelia ribes* B_{URM} plant (Myrsinaceae family). Strikingly, embelin has demonstrated anti-inflammatory properties in several models of acute and chronic inflammation as well as analgesic, anti-tumor, anti-convulsant and neuroprotective effects in animals (Nikolovska-Coleska et al., 2004; Kalyan Kumar et al., 2011; Kumar et al., 2011; Mahendran et al., 2011b; Mahendran et al., 2011a; Thippeswamy et al., 2011b; Thippeswamy et al., 2011a). Despite its numerous well-documented pharmacological effects *in vivo*, little is understood about its molecular targets. However, it has been postulated that embelin mediates its effects via the inhibition of IκBα kinase and subsequent modulation of NF-κB, which is in agreement with its role in the regulation of genes associated with inflammation, tumorgenesis, proliferation and apoptosis (Ahn et al., 2007). In addition, embelin exerts inhibitory effects on X chromosome-linked inhibitor-of-apoptosis protein, which is thought to contribute to its anti-tumor properties (Nikolovska-Coleska et al., 2004). The biochemical structure of embelin is presented in Fig. 4.3.

Capric acid

CA is a MCFFA of a carbon chain length of 10 and is derived from animal fats and oils. Dietary fatty acids are the precursors for eicosanoids and other lipid mediators and were solely regarded as a source of calories. However, it is now well recognised that FFAs can behave as direct signalling molecules via cell surface GPCRs and exert many regulatory effects on metabolism and the immune system (Hwang, 2000). FFAs can be broadly classified into three groups depending on the length of their carbon backbone: short-chain

fatty acids (SCFFAs; 1-6 carbon atoms), MCFFAs (7-12 carbon atoms) and long-chain fatty acids (LCFFAs; 12 + carbon atoms) (Ulven, 2012). FFAs have obtained a lot of interest due to their association with diseases such as obesity and diabetes (Evans et al., 2004), which led to the identification of several GPCR receptors activated via lipids of various chain lengths (Ichimura et al., 2009). These include GPR40 (FFAR1), which is activated via LCFFAs (Briscoe et al., 2003), GPR41 (FFAR3) and GPR43 (FFAR2), which are activated by SCFFAs (Brown et al., 2003; Ulven, 2012) and GPR120, which is activated via LCFFAs (Hirasawa et al., 2005). GPR84 is thought to be activated by MCFFAs such as CA, which was shown to inhibit forskolin-induced cAMP production in transfected CHO cells (Wang et al., 2006a). MCFFAs have also been shown to activate leucocytes via the modulation of Ca^{2+} and PKC signalling as well as induce NF-κB transcription and the expression of pro-inflammatory markers such as COX-2 in RAW 264.7 cells, suggesting a contributory role in inflammation (Hwang, 2000; Lee et al., 2001; Wanten et al., 2004; Wanten and Naber, 2004; Wanten, 2006). The biochemical structure of CA is presented in Fig. 4.3.

CNV-0022600A

CNV (MW 268) is a novel GPR84 ligand identified by GlaxoSmithKline, which has exhibited characteristics of a full agonist in heterologous *in vitro* systems (proprietary GSK/ Convergence Pharmaceuticals data).

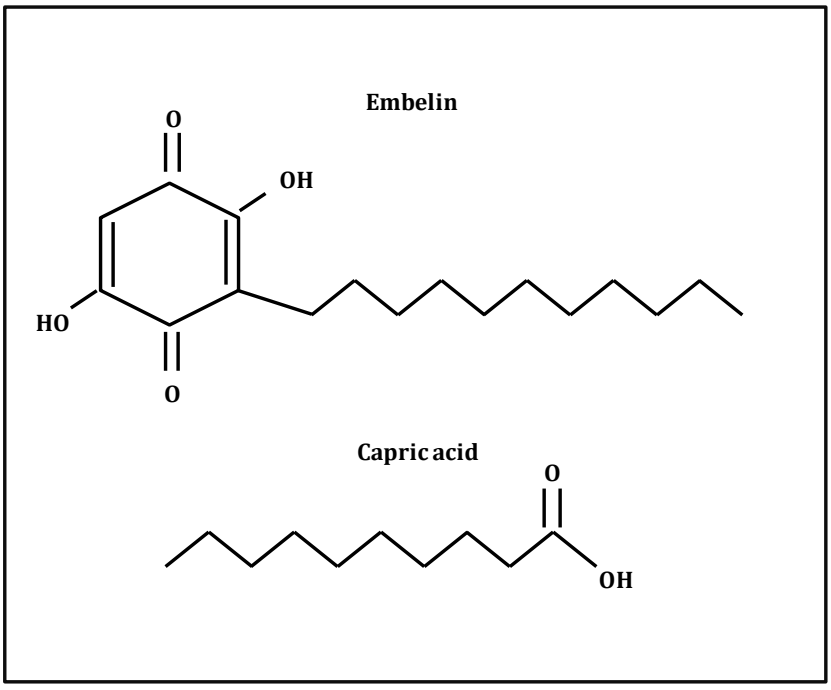

Figure 4.3: Molecular structures of Embelin and Capric acid

4.1.4 Fatty acid metabolism

Fatty acids are an important source of metabolic energy and can be stored as triglycerides until needed for oxidation. They are also substrates for membrane biogenesis and form the necessary building blocks for structurally complex glycolipid and phospholipid cell membrane components. Furthermore, their down-stream metabolites such as eicosanoids and resolvins serve as key intracellular signalling molecules that execute a number of physiological roles.

Fatty acids are hydrophobic molecules composed of long saturated, monounsaturated (MUFA) or polyunsaturated (PUFA) hydrocarbon chains and a terminal carboxylate group. Whilst saturated fatty acids have no double bonds between any of the carbon atoms, unsaturated fatty acids have double bonds between adjacent carbon atoms; MUFAs contain a single double bond and PUFAs have multiple. Both saturated and unsaturated fatty acids can be further sub-categorised according to their carbon chain lengths (Yaqoob, 2004; Kalish et al., 2012).

There are three main families of PUFAs: omega (ω) -3, derived from α-linolenic acid (18 : 3*n*-3); ω-6, derived from linoleic acid (18 : 2*n*-6); and ω-9, derived from oleic acid (18 : 1*n*-9) (Kalish et al., 2012). As linoleic acid and α-linolenic acid cannot be synthesised *de novo* (unlike oleic acid) and can be metabolised to form all downstream fatty acids, they are classified as essential dietary fatty acids. These two main families of PUFAs are uptaken by virtually every cell, possibly via diffusion or protein mediated translocation across the plasma membrane. Once inside a cell they bind to fatty acid binding proteins and undergo a series of desaturation and elongation steps. In humans, the three desaturase enzymes, Δ^5, Δ^6 and Δ^9, insert double bonds at the corresponding 5^{th}, 6^{th} and 9^{th} carbon atom in a fatty acid chain. The metabolism of α-linolenic acid, linoleic acid and oleic acid is a competitive process as all three fatty acids compete for the same Δ^5 and Δ^6 desaturases and elongases (Kalish et al., 2012). Linoleic acid is metabolised by Δ^6 to γ-linoleic acid, which is elongated to form dihomo-γ-linoleic acid and subsequently converted by the Δ^5 desaturase enzyme to arachidonic acid. Similarly, α-linolenic acid is converted to eicosapentaenoic acid via Δ^6 desaturation, elongation and Δ^5 desaturation. Eicosapentaenoic acid may undergo further elongation, desaturation and β-oxidation to form docosahexaenoic acid, however, very little α-linolenic acid proceeds along the entire metabolic pathway. As linoleic acid is abundantly found in vegetable oils, whilst α-linolenic acid is present in green leafy vegetables, vegetable and seed oils, the former pathway is more quantitatively important than the latter pathway. Finally, oleic acid may be metabolised into mead acid (Yaqoob, 2004; Kalish et al., 2012).

As previously mentioned, membrane-bound PUFAs serve as precursors to multiple second messengers, which may be pro- or anti-inflammatory. Eicosanoids are a dynamic class of signalling molecules that regulate a number of crucial biological functions such as host defence, vasoactivity and reproduction and are classically divided into PGs, prostacyclins (PGI_2s), thromboxanes (TXA_2s) and leukotrienes (Funk, 2001). These second messengers are not stored in cells but are synthesised upon demand by three key enzymes: COX, lipoxygenase and cytochrome P450. COX metabolises arachidonic acid, eicosapentaenoic acid and dihomo-γ-linoleic acid into pro-inflammatory PGs and TXA_2, whereas lipoxygenase mediates the synthesis of leukotrienes and anti-inflammatory lipoxins (see Fig. 4.4). Lastly, cytochrome P450 converts arachidonic acid into pro-inflammatory hydroxyeicosatetraenoic acid or anti-inflammatory epoxyeicosatrienoic acid. In addition, docosahexaenoic acid may be further metabolised to form the D-series of resolvins and protectins, which play immuno-protective roles during inflammation (Kalish et al., 2012).

Subsequent to nerve injury or inflammatory insult, COX is up-regulated in damaged nerve axons or tissues as well as in resident/infiltrating immune cells (Ma and Eisenach, 2002; Muja and DeVries, 2004; Durrenberger et al., 2006; Ma et al., 2012). This induces the production of pro-nociceptive PGs in nerve terminals and non-neuronal cells and the consequential development of behavioural hypersensitivity. PG acts via its four EP receptors expressed in DRG neurons to directly excite nociceptors and indirectly stimulate the release of SP and CGRP from nociceptors and their peripheral and central terminals (Vasko, 1995; Vanegas and Schaible, 2001). As previously described (*Chapter 3*), SP and CGRP are key mediators of neurogenic inflammation and nociception in the periphery, whilst centrally they may directly excite nociceptive specific dorsal horn neurons and thus contribute to central sensitisation and hyperalgesia. Accordingly, systemic or local administration of selective or non-selective COX inhibitors or EP1/EP4 antagonists alleviates neuropathic and inflammatory pain-associated behaviours in rodents and reduces the production of SP and CGRP in DRG neurons and the spinal cord (Kawahara et al., 2001; Ma and Eisenach, 2002, 2003a, b; Suyama et al., 2004; Staton et al., 2007; St-Jacques and Ma, 2011). Interestingly, in immune cells PG production exhibits immunosuppressive or anti-inflammatory effects as discussed in section 4.1.2. In addition, DHA-derived mediators such as D-series resolvins, docosatrienes and neuroprotectins, which are produced by COX-2, also exert anti-inflammatory actions and have been shown to be protective in various models of inflammation (Kalish et al., 2012). It is possible that the effects of these mediators are dampened in the presence of pathology and are thus potential therapeutic targets.

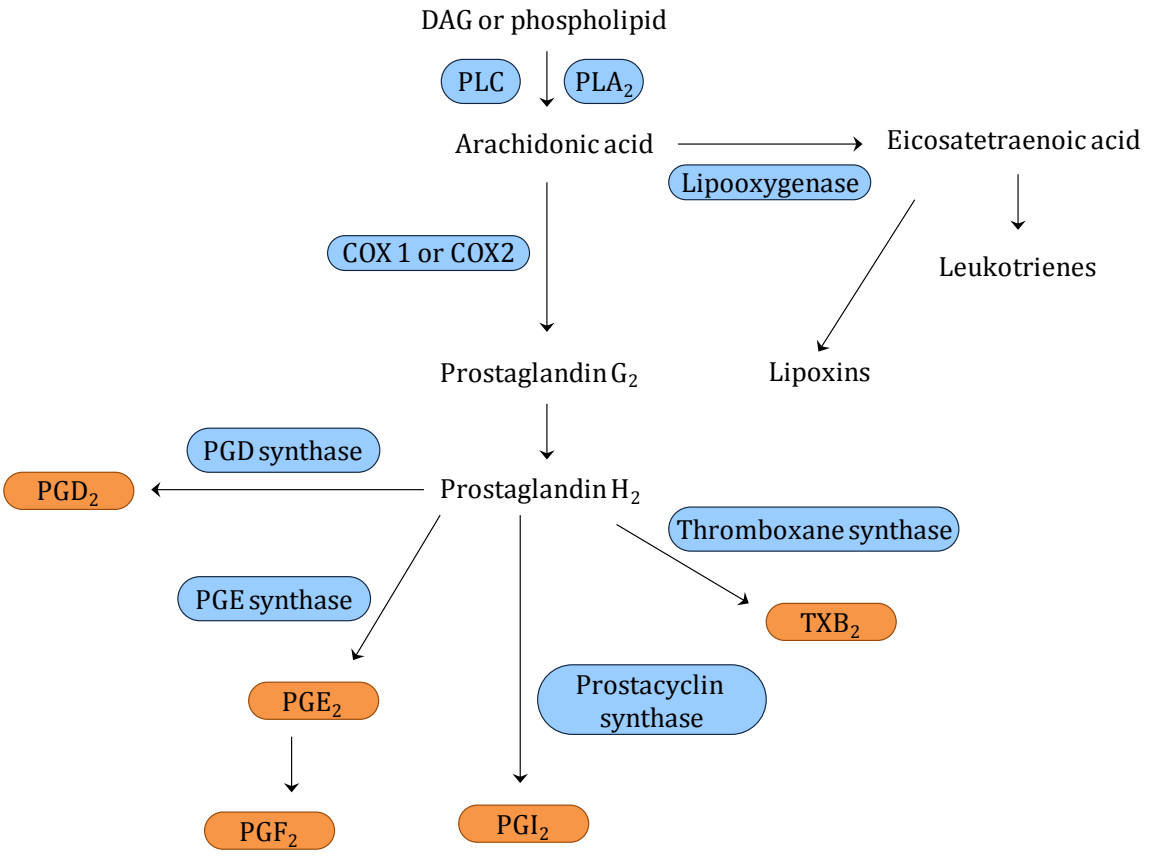

Figure 4.4: The biosynthesis of eicosanoids

Schematic presenting the pathways involved in the formation of eicosanoids from arachidonic acid. COX metabolises arachidonic acid, eicosapentaenoic acid and dihomo-γ-linoleic acid into PGs and TXA_2, whereas lipoxygenase mediates the synthesis of leukotrienes and lipoxins.

4.1.5 Aims

The use of pharmacological tools provides a valuable method in investigating the direct role of a particular receptor in a physiological system. Therefore, the aim of this chapter was to identify a GPR84 agonist that could be utilised in further studies to aid our understanding of the role of this receptor in chronic pain mechanisms. We explored the efficacy and selectivity of three potential GPR84 ligands, embelin, CA and CNV, in microglia and WT and KO macrophage cells via Ca^{2+} and cAMP signalling assays.

4.2 Materials and methods

4.2.1 Animals

Breeding and genotyping of GPR84 WT and KO animals was carried out as described in the methods section in *Chapter 2*. Randomly selected mixed sex and age-matched mice weighing 20-25g (7-14 weeks old) were used for cell culture. Mice were housed individually or in groups (no more than 4 per cage) in standard environmental conditions (12 hour light/dark cycle) with *ad libitum* access to food and water. Animal husbandry and experiments were carried out in a non-sterile housing environment in accordance with the United Kingdom Animals (Scientific Procedures) Act 1986.

4.2.2 Microglial cell culture and stimulation

Mixed primary cultures of glial cells were isolated from spinal cord tissue of P7 rat pups. Cultures were maintained for two weeks at 37°C (5% CO_2/95% O_2) in medium containing 1% penicillin-streptomycin (Sigma, UK) and 15% FBS (Invitrogen, UK), which was changed every 2-3 days. Two weeks later microglial cells were harvested via the forceful shaking of the flask and plated in 24 well plates at a density of 5 x 10^4 cells/well. Forty eight hrs later the microglial cells were stimulated for 3 hrs with LPS (1 μg/mL; Sigma, UK) (Clark et al., 2010a) to up-regulate the expression of GPR84. For control wells, culture medium was replaced with fresh medium and the stimulation step was omitted.

4.2.3 Resident and B-GEPM culture and stimulation

For the calcium-imaging assay resident peritoneal macrophages were cultured. For the cAMP assay B-GEPMs were cultured as previously described in *Chapter 3* as a higher yield of macrophages were required for this assay. Briefly, mice were culled via neck dislocation, and the layer of skin covering the peritoneum was wiped with 70% ethanol. A total volume of 20 mL of sterile cold PBS (Invitrogen, UK) containing 3 mM EDTA (Invitrogen, UK) was injected into the peritoneal cavity using a 25 G needle. After gentle massaging the buffer was retrieved in 14 mL Falcon tubes and spun to obtain a pellet. Cells were then re-suspended and plated in DMEM (Invitrogen, UK) with 10% FBS (Invitrogen, UK) and incubated at 37°C. The cells were washed 2 hrs after plating and the medium was replaced. Forty-eight hrs later, macrophage cells were stimulated for 3 hrs with LPS (1 μg/mL; Sigma, UK) to up-regulate the expression of GPR84. The culture medium of control wells was replaced with

fresh medium without subsequent stimulation. For B-GEPMs the LPS stimulation protocol was carried out 24 hrs after washing.

4.2.4 Cell preparation and immunocytochemistry

Microglia and macrophage cells were fixed with 4% PFA (VWR, UK) in 0.1 M PB for 30 mins followed by incubation with ice-cold methanol (VWR, UK) for 23 mins. Subsequently cells were washed three times with PBS and incubated for 2 hrs with primary antibody solution for Iba-1 (rabbit anti-Iba1, 1:1000; Wako Chemicals, Germany), followed by a 45 min incubation period with the secondary antibody solution donkey anti-rabbit Cy3 (1:1000; Stratech, UK). All antibodies were prepared in PBS supplemented with 0.1% Triton X-100 (VWR, UK) and 0.2% sodium azide (Sigma, UK). Slides were carefully cover slipped with Vectashield Mounting Medium with DAPI (Vector Laboratories, UK), nail-varnished and dried. Images were visualised and captured using a Zeiss Axioplan microscope (Zeiss, UK).

Cell cultures from the naïve peritoneal cavity contain ~ 40% macrophages, whilst elicited cultures contain 40-45% macrophages; purity increases to almost 80-90% by adherence in both types of culture. Eosinophils and neutrophils are the main cell types that contaminate peritoneal macrophage cultures and can affect the results of *in vitro* assays, leading to data misinterpretation (Fauve et al., 1983; Misharin et al., 2012). Mixed primary cultures of glial cells consist of heterogenous populations of astrocytes, oligodendrocytes and microglial cells and may become contaminated with fibroblasts. Upon adherence microglial cultures have a high purity in the range of ~ 95-99% (Ni and Aschner, 2010). In our studies, we visually verified the purity of microglia and macrophage cell cultures by examining Iba1 staining relative to DAPI expression as shown in Fig. 4.5. We found that almost all nuclear staining (DAPI) was co-localised with Iba1, indicating > 95% purity.

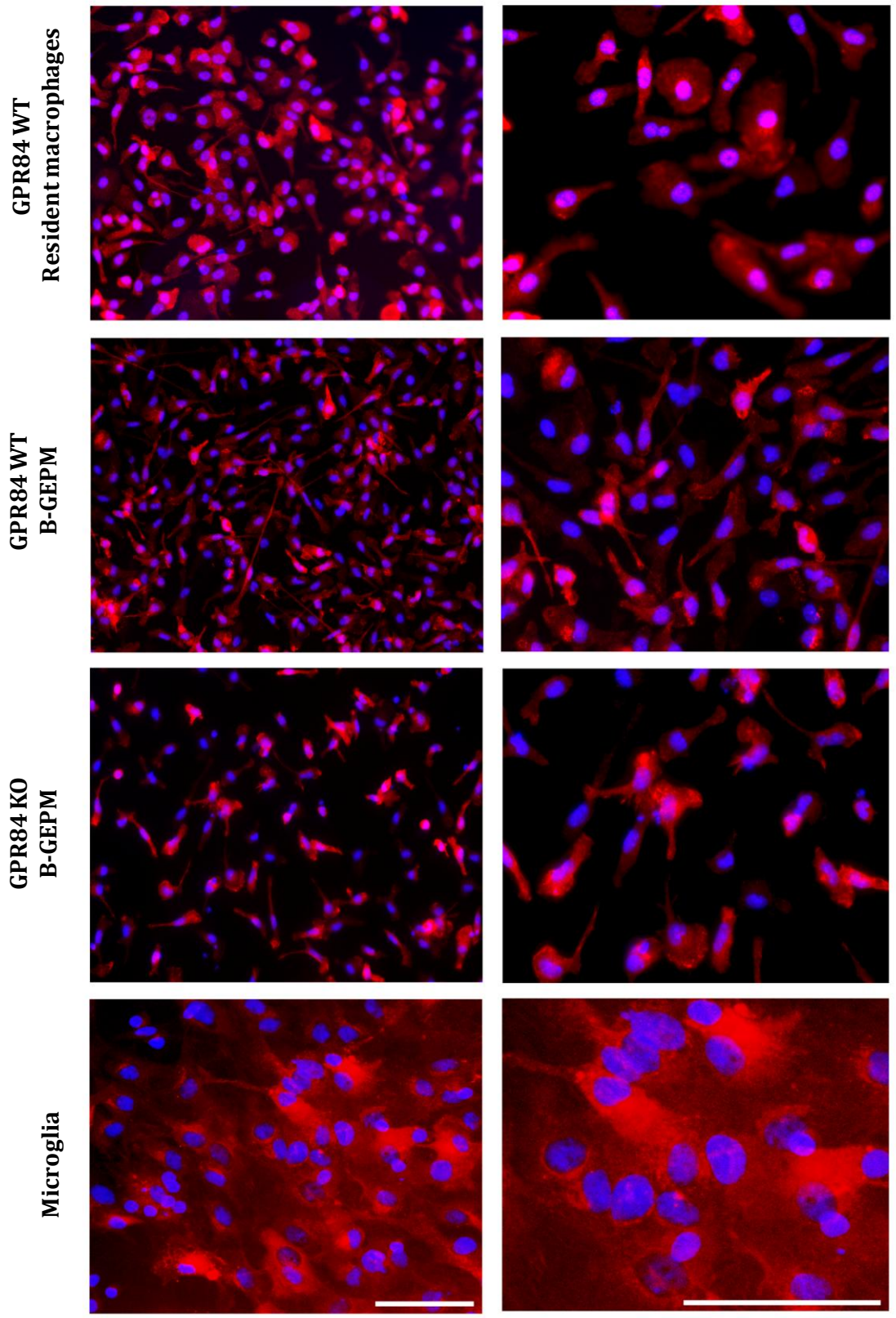

Figure 4.5: Verification of macrophage and microglia culture purity

The purity of microglia and macrophage cell cultures was verified via observing colocalisation of nuclear staining (indicated by DAPI in blue) with Iba1 (in red). Scale bars = 100 μm.

4.2.5 Calcium imaging

Control or LPS stimulated microglia and macrophage cells were incubated for 60-90 mins at 37°C with the Ca^{2+} indicator Fura-2AM (2 μM; Invitrogen, UK) in HBSS (Invitrogen, UK) containing probenecid (0.5 M; Sigma, UK). Cells were subsequently transferred to a perfusion chamber attached to an inverted microscope (Nikon, UK) equipped with a monochromator (Photon Technology, UK). Cells were washed and fluorescence was measured at 340 nm and 380 nm excitation and 510 nm emission. The baseline level was defined as the average $[Ca^{2+}]$ -based ratio taken over the first 2-5 mins of each run under continuous perfusion (4 mL/min) with HEPES buffer solution (hydroxyethyl piperazineethanesulfonic acid; 10 mM; 7 mM glucose; pH 7.4; Invitrogen, UK) prior to drug challenge. Calcium responses to embelin (Sigma, UK) or CA (Sigma, UK) were subsequently tested. Each dose was tested on a separate run and continuously perfused for a duration of 1 min followed by a 5 min wash out period using HEPES buffer. Ionomycin (Sigma, UK) or ATP (Sigma, UK) were used as positive controls to define viable microglia or macrophage cells, respectively. All experiments were conducted at room temperature. Results are expressed as a change (Δ) in the F340/380 emission ratio, which is proportional to the change in $[Ca^{2+}]_i$, where ΔF340/380 = max drug F340/380 – average baseline F340/380 (Fig. 4.6). In order to be defined as a responder, a cell's ratio change had to be 10% greater than the average baseline value of the cells examined per run, and respond positively to the application of ionomycin (microglia) or ATP (macrophages) (Dawes et al., 2011).

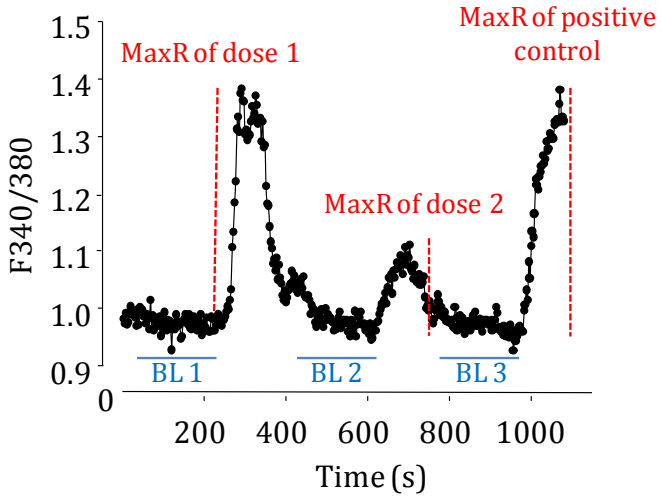

Figure 4.6: Diagram illustrating how ΔF340/380 is calculated

Drug or positive control response = maximum drug or positive control response – average baseline
Vehicle response (HEPES buffer) = maximum baseline value – average baseline
Baseline, BL; Maximum response, MaxR

4.2.6 cAMP-screen direct chemiluminescent ELISA

Bio-gel elicited GPR84 WT and KO macrophage cells were harvested as previously described in *Chapter 3* and plated in cAMP-Screen Direct® pre-coated 96-well assay plates (Invitrogen, UK) at a density of 150,000 cells/well. Two hrs later the cells were washed, replenished with fresh DMEM (Invitrogen, UK) and left overnight to settle. All cell stimulation protocols were carried out 24 hrs later and done in FBS-free DMEM (Sigma, UK) at 37°C. In order to increase GPR84 expression, WT cells were stimulated with LPS (1 µg/ml; Sigma, UK) for 3 hrs prior to incubation with a GPR84 ligand. WT and KO cells were then incubated for 20 min with embelin (Sigma, UK), CA (Sigma, UK) or CNV0022600A (CNV; GSK/Convergence Pharmaceuticals, UK), followed by 20 mins incubation with forskolin (R&D Systems, UK). Each GPR84 ligand was tested on a separate plate. Control wells were incubated with ligand solvents DMSO (0.005-0.1%), methanol (0.002%) and ethanol (0.002%).

To terminate the assay the media was aspirated and cells were incubated for 30 mins with 60 µl of lysis buffer at 37°C. During this time cAMP standards ranging from 0.006 to 6000 pM were prepared in lysis buffer. After lysis, 60 µl of each standard concentration was added to designated wells followed by the addition of 30 µl of cAMP-alkaline phosphatase solution and 60 µl of anti-cAMP antibody to every well. Following 1 hr incubation, the plate was washed 6 times with wash buffer and 100 µl of disodium 2-chloro-5-(4-methoxyspiro [1,2-dioxetane-3,2'-tricyclo [3.3.1.13,7] decan]-4-yl) phenyl phosphate (CSPD)®/Sapphire-II™ RTU substrate/enhancer solution was added for 30 min. Finally, the luminescence signal for each well was measured using a standard luminometer (1 sec/well) and the cAMP concentration was calculated via extrapolation from the standard curve (see Fig 4.7). All reagents were included in the cAMP-screen direct kit.

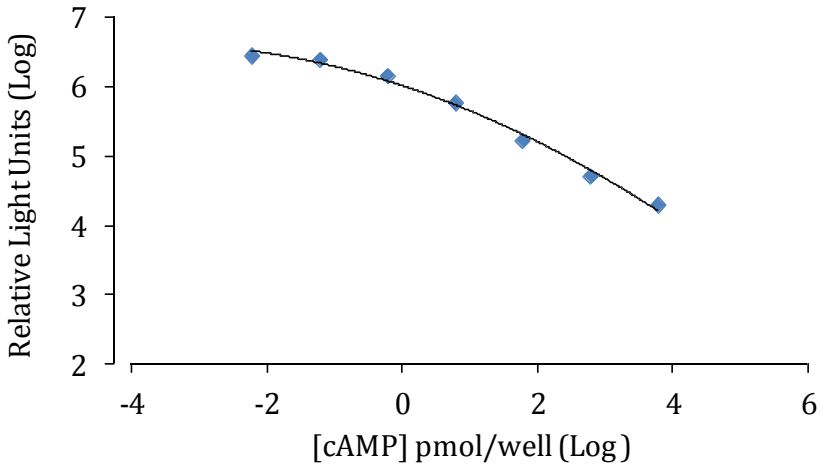

Figure 4.7: Example of a standard curve graph on a log scale

4.2.7 Data and statistical analysis

All data were analysed using SigmaPlot 12.3 and SigmaStat software. For single comparisons between two groups, a paired Student t-test was applied. For multiple comparisons, a one-way ANOVA was used with SNK post hoc test to determine individual group differences. For non-parametric data, Kruskal-Wallis one-way ANOVA on ranks was carried out, with Dunn's method. In all cases the data is presented as the mean ± SEM and $p < 0.05$ was set as the statistical significance level.

4.3 Results

4.3.1 Calcium fluorometry

Although the use of transgenic animals has been instrumental in our studies, there is the possibility of compensatory mechanisms operating to mask phenotypes. For this and other practical factors, the development of pharmacological tools could complement experiments and further advance our understanding of the role of GPR84 in chronic pain mechanisms. Currently, there are no commercially available compounds for GPR84 modulation and there is little evidence of a definitive signalling pathway for this receptor. Only a single study suggests that GPR84 is sensitive to MCFFAs with carbon chain lengths of 9-14, particularly CA. In this study Wang and colleagues showed that CA-mediated activation was dependent on a *Pertussis* toxin-sensitive $G\alpha_{i/o}$ coupled pathway, which produced a corresponding decrease in cAMP levels in transfected CHO cells (Wang et al., 2006a). MCCFAs have also been shown to modulate Ca^{2+} responses in leucocytes (Wanten et al., 2004; Wanten and Naber, 2004; Wanten, 2006) and so based on this evidence, we tested the efficacy and selectivity of CA in addition to two other agonists provided by GSK/Convergence Pharmaceuticals (embelin and CNV) via Ca^{2+} and cAMP signalling assays.

Intracellular Ca^{2+} is central to a multitude of cellular processes and may be studied using sensitive fluorescent Ca^{2+} indicators. These indicators can only bind to freely diffusible Ca^{2+} ions, however, a majority of intracellular Ca^{2+} is bound to various buffers, depending on cell type and compartment. In addition, because chemical Ca^{2+} indicators may themselves act as buffers and hence affect Ca^{2+} signalling kinetics, the type of Ca^{2+} indicator must be chosen with regards to spectral characteristics and binding properties (Paredes et al., 2008). In our studies, we utilised Fura-2 engineered with acetoxymethyl (AM) esters, which is one of the most popular ratiometric dyes. Addition of the ester permits sufficient hydrophobicity for membrane permeability so that the dye can passively diffuse into the cell when added extracellularly. Subsequent to loading esterases cleave the ester group, trapping the dye intracellularly and thus only alive cells are labelled (Paredes et al., 2008). Upon Ca^{2+} binding the Fura-2 peak absorbance shifts from 380 nm (unbound state) to 340 nm (Ca^{2+} bound state) while fluorescence is emitted at a peak wavelength of 510 nm. Ratiometric indicators enable accurate quantification of $[Ca^{2+}]_i$ and also control for uneven dye loading and changes in cell size (Paredes et al., 2008). As Fura-2 is resistant to photobleaching and has a high affinity for Ca^{2+}, less dye can be used thus reducing buffering and cytotoxicity (Di Virgilio et al., 1988). However, similar to other types of chemical indicators Fura-2 can become

compartmentalized, which is prevented via the addition of probenecid; an organic anion transport inhibitor (Di Virgilio et al., 1988).

4.3.2 ATP induces robust Ca^{2+} responses in microglial cells, whereas embelin exhibits poor efficacy

We initially tested the system setup and the ability to obtain calcium responses in microglial cells using ATP, which is a well-documented second messenger that generates Ca^{2+} responses via its ionotropic and metabotropic receptors (Farber and Kettenmann, 2006b). An intracellular Ca^{2+} response is represented as ΔF340/380 emission ratio. The ΔF340/380 ratio for individual cells was calculated by subtracting the average baseline F340/380 ratio of the cells examined per run, from the maximum F340/380 ratio upon stimulation. To accurately quantify Ca^{2+} responses we employed two criteria in the analysis of the data; a cell was regarded as a responder only if it a) had an average ΔF340/380 value greater than 10% of the average baseline F340/380 ratio of cells examined in a run and b) produced a Ca^{2+} response to the positive control, ionomycin. Quantification of responders was performed by calculating the number of cells that responded to a challenge as a percentage of the total number of cells that responded to ionomycin for each run. Ionomycin is an ionophore produced by the bacterium *Streptomyces conglobatus* and acts directly on intracellular Ca^{2+} stores to raise $[Ca^{2+}]_i$, and thus provides an excellent tool for our studies (Morgan and Jacob, 1994).

We found that perfusion (4 mL/min) of 100 μM ATP elicited a strong Ca^{2+} response (Fig. 4.8A, B). Quantification of the number of responders revealed that almost all viable cells examined responded to ATP (93.4 ± 3.5%) and showed a significant ΔF340/380 (0.4 ± 0.08) compared to vehicle (0.04 ± 0.01; Fig. 4.8C, D). Following validation of our assay by demonstrating ATP-induced Ca^{2+} transients in microglial cells in accordance with literature (Walz et al., 1993; McLarnon et al., 1999; Moller et al., 2000; Hoffmann et al., 2003; McLarnon, 2005), we investigated responses to embelin, a compound previously shown to possess a high affinity for GPR84 in transfected CHO cells (proprietary GSK data). We report that embelin produced small Ca^{2+} responses in microglial cells as illustrated by image (B) and the example trace (E) from a single cell response (Fig. 4.9). Quantification of the percentage of responders showed that there was a non-significant number of cells responding to embelin at 1 μM (10.7 ± 4.7%), 50 μM (12.5 ± 5.6%) and 100 μM (7.8 ± 3.8%; Fig. 4.9F) and only at the 1 μM dose (0.2 ± 0.05) was there a significant increase in the Fura-2AM based Ca^{2+} signal compared to vehicle (0.02 ± $5x10^{-6}$; Fig. 4.9G). The lack of consistency

and concentration dependence suggests that embelin does not effectively evoke receptor-mediated Ca^{2+} transients in microglial cells.

4.3.3 ATP induces robust Ca^{2+} responses in GPR84 WT and KO macrophages

Alongside our studies in microglial cells we also investigated embelin and capric acid selectivity for GPR84 by examining Ca^{2+} responses in WT and KO peritoneal macrophages. To confirm we could detect Ca^{2+} signals from this cell type we examined the responses of WT and KO macrophage cells to the positive control ATP, under non-stimulated or LPS simulated conditions (1 μg/mL; Fig. 4.10A, B). We observed that both WT and KO macrophages produced robust Ca^{2+} responses represented by the ΔF340/380 ratio (WT: ATP, 0.15 ± 0.01 vs vehicle, 0.02 ± 0.001; KO: ATP, 0.17 ± 0.02 vs vehicle, 0.02 ± 0.002), which was significantly enhanced by LPS (WT: ATP, 0.23 ± 0.02; KO: ATP, 0.24 ± 0.02; Fig. 4.10B). Virtually all cells examined in each run responded to ATP under non-stimulated (WT: 93.7 ± 5.2%; KO: 99.1 ± 0.4%) and LPS stimulated conditions (WT: 96.3 ± 1.4%; KO: 99.3 ± 0.4%; Fig. 4.10A). These observations are interesting, considering that previous groups have reported attenuated Ca^{2+} responses to ligands (including ATP) subsequent to LPS stimulation (Moller et al., 2000; Hoffmann et al., 2003). However, our protocol entailed a much shorter incubation period compared to these studies, which could pose as a reason for this discrepancy. Notably, there were no significant differences between genotypes or non- and LPS stimulated groups, suggesting that KO macrophages are just as capable as their WT controls in generating successful ATP induced Ca^{2+} responses. Therefore, ATP is an excellent positive control for exploring ligand selectivity in WT and KO macrophages.

4.3.4 Embelin-induced Ca^{2+} transients are attenuated in GPR84 KO macrophages

Having verified the ability to obtain Ca^{2+} responses from macrophages of both genotypes, we examined the selectivity of embelin by comparing the responses of WT and KO cells to different doses of this ligand (Fig 4.10). Although we previously observed modest responses in microglial cells to embelin, we hypothesised that embelin may be more effective at inducing Ca^{2+} signals in macrophage cells based on our previous findings that peripheral macrophages express greater levels of GPR84 mRNA than microglia upon stimulation (see *Chapter 3*). We found that GPR84 WT cells (D) exhibited greater embelin induced Ca^{2+} responses in contrast to KO (G) as illustrated in the example images and traces from single WT (I) and KO (J) cells responding to 10 μM embelin. Quantification of the number of responders shows that a greater percentage of WT cells responded to embelin than KO cells at doses 1, 10 and 50 μM, which was significant compared to vehicle at 10 μM (WT: 41.6 ±

10.8%; KO: 13.0 ± 7.6%) (Fig 4.10K). Quantification of the changes in the Fura-2AM signal showed that WT macrophages exhibited a greater increase in $[Ca^{2+}]_i$ than the KO, which was significant at 0.1, 1 and 10 μM (WT: 0.08 ± 0.01, 0.07 ± 0.01, 0.11 ± 0.02; KO: 0.05 ± 0.01, 0.07 ± 0.004, 0.05 ± 0.02, respectively) compared to vehicle (WT: 0.02 ± $9x10^{-4}$; KO: 0.02 ± $5x10^{-4}$). Notably, embelin recruited a greater number of responding WT macrophages than microglia (Fig 4.9F), however, interestingly the ΔF340/380 ratios were generally smaller but more consistent (Fig 4.10L). As the Ca^{2+} responses to embelin were generally greater in the WT than the KO, this suggests that embelin may exert selective actions at GPR84, particularly at a dose of 10 μM where both the percentage of responders and ΔF340/380 were significant compared to vehicle.

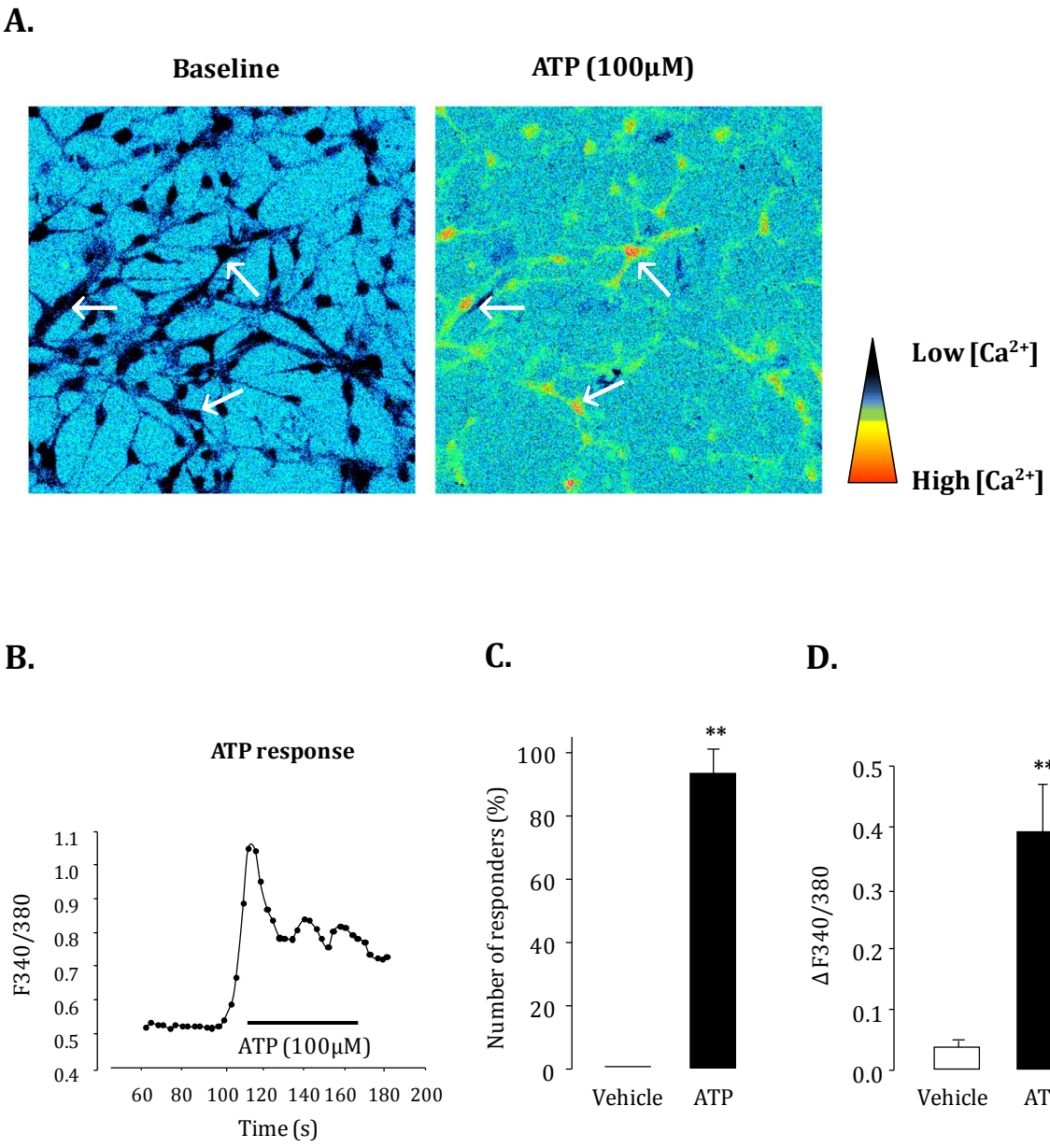

Figure 4.8: ATP induces an increase in $[Ca^{2+}]_i$ in microglial cells

Subsequent to application of ATP (100 µM) there is a change in $[Ca^{2+}]_i$ in comparison to baseline as indicated (arrows in A). Representative trace of a single microglial cell showing changes in the F340/380 emission ratio in response to ATP (B). Quantification of the number of responders shows that the percentage of microglial cells responding to ATP was significantly greater than vehicle treatment (HEPES; C). Quantification of the Ca^{2+} response is represented as a ΔF340/380 emission ratio (D). Microglial cells exhibit a robust increase in $[Ca^{2+}]_i$ in response to ATP. Data are presented as the mean ± SEM. **p < 0.01 vs vehicle, Mann-Whitney Rank Sum Test (C); Student's t-test (D), n = 5 experiments; average of ≥ 30 cells.

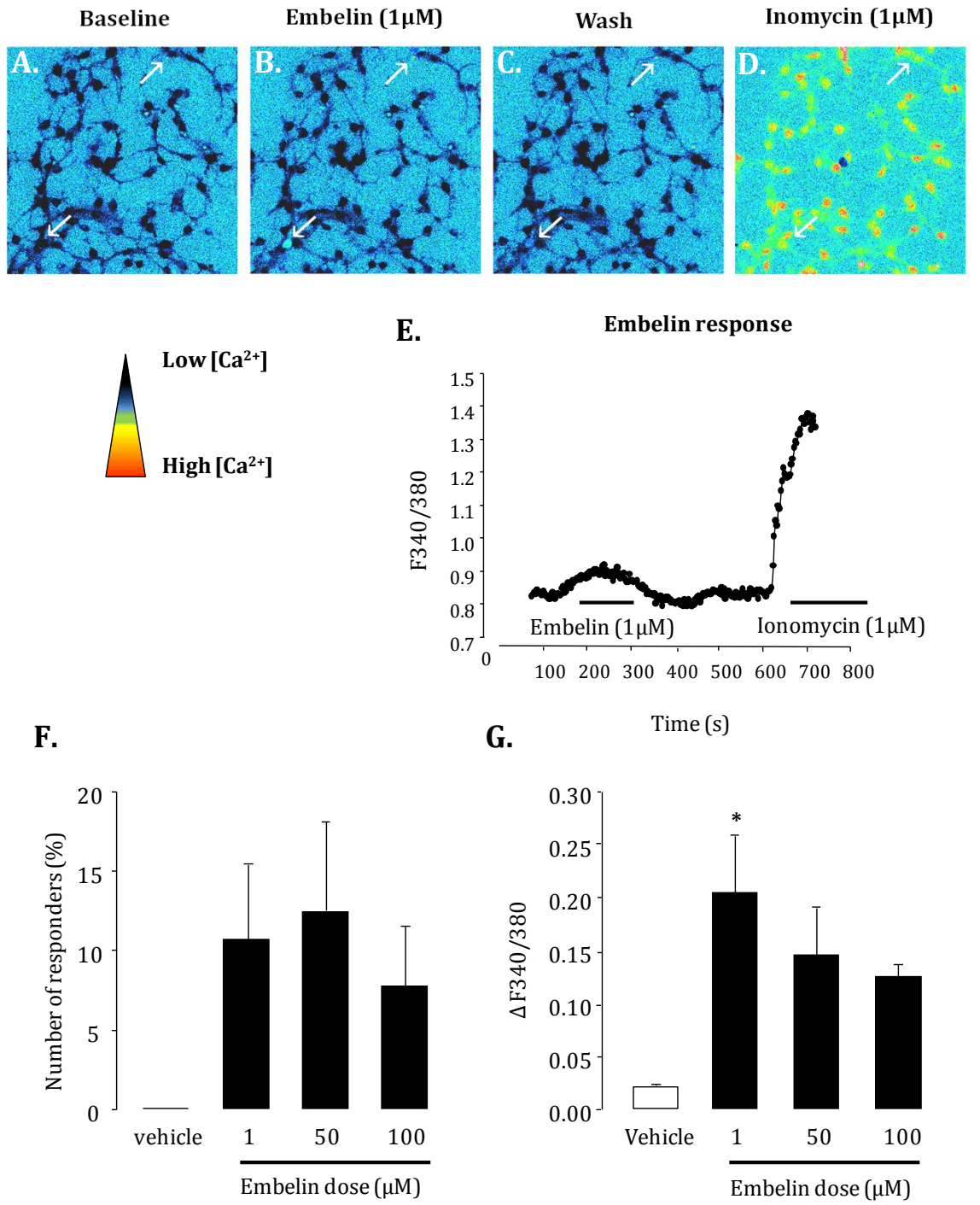

Figure 4.9: Embelin produces weak Ca^{2+} responses in microglial cells

(A-D) Embelin elicits a weak Ca^{2+} response in microglial cells. Representative trace of a single microglial cell showing the change in F340/380 in response to 1 µM embelin (E). Quantification of the number of cells responding to different doses of embelin was not significantly different from vehicle (F). Quantification of the Ca^{2+} response is represented as a ΔF340/380 emission ratio (G). There was a significant increase in $[Ca^{2+}]_i$ in microglial cells treated with 1 µM embelin compared to vehicle. Data are presented as the mean ± SEM. *p < 0.05 vs vehicle, one-way ANOVA (F); Kruskal-Wallis one-way ANOVA on ranks, post-hoc Dunn's method (G), n = 4 experiments; average of ≥ 30 cells.

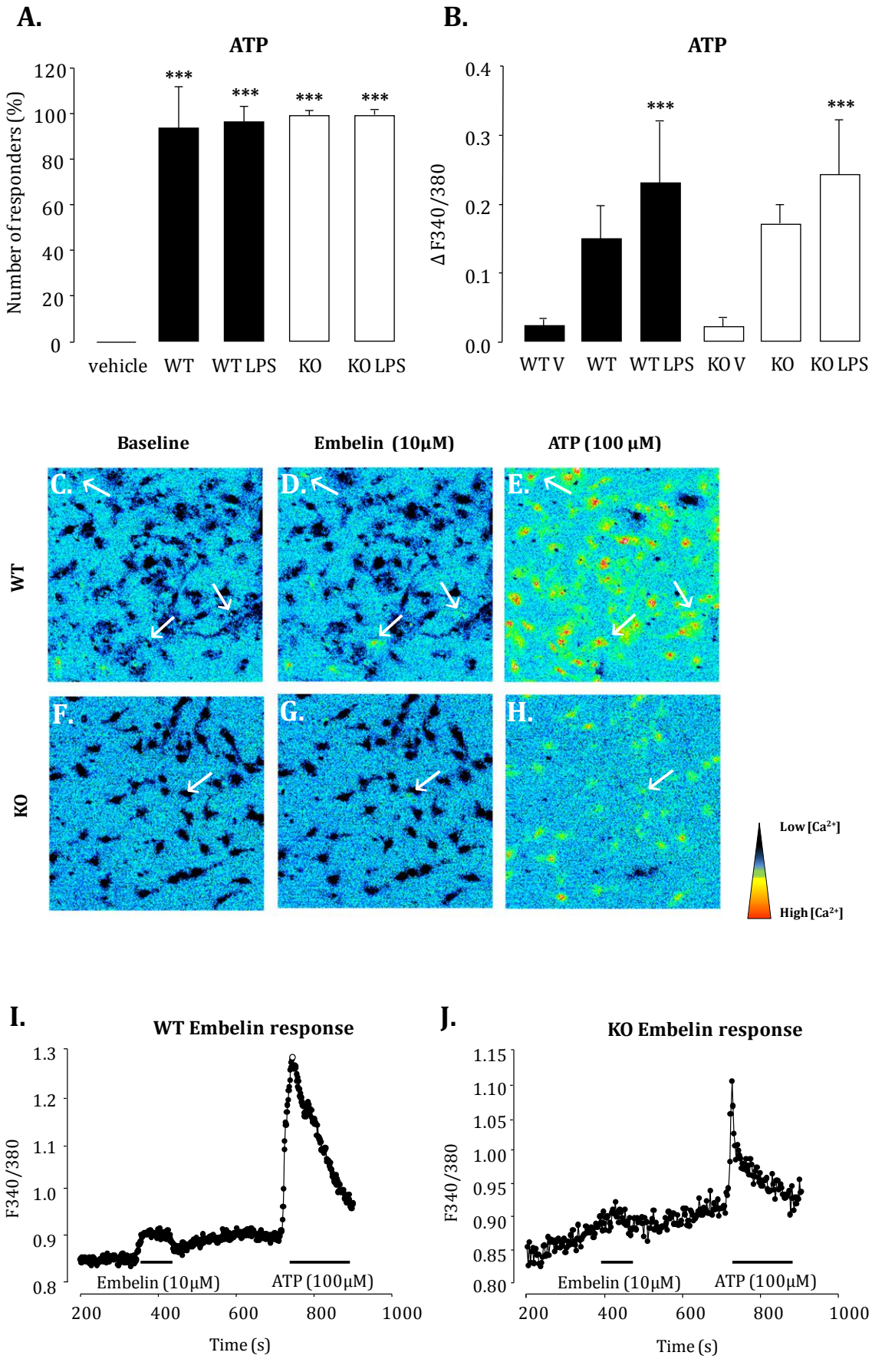
A.
ATP
Number of responders (%)
120
100
80
60
40
20
0
***
vehicle
WT
WT LPS
KO
KO LPS
B.
ATP
ΔF340/380
0.4
0.3
0.2
0.1
0.0
WT V
WT
WT LPS
KO V
KO
KO LPS
Baseline
Embelin (10μM)
ATP (100 μM)
C.
D.
E.
F.
G.
H.
WT
KO
Low [Ca2+]
High [Ca2+]
I.
WT Embelin response
F340/380
1.3
1.2
1.1
1.0
0.9
0.8
Embelin (10μM)
ATP (100μM)
200
400
600
800
1000
Time (s)
J.
KO Embelin response
F340/380
1.15
1.10
1.05
1.00
0.95
0.90
0.85
0.80
Embelin (10μM)
ATP (100μM)
200
400
600
800
1000
Time (s)

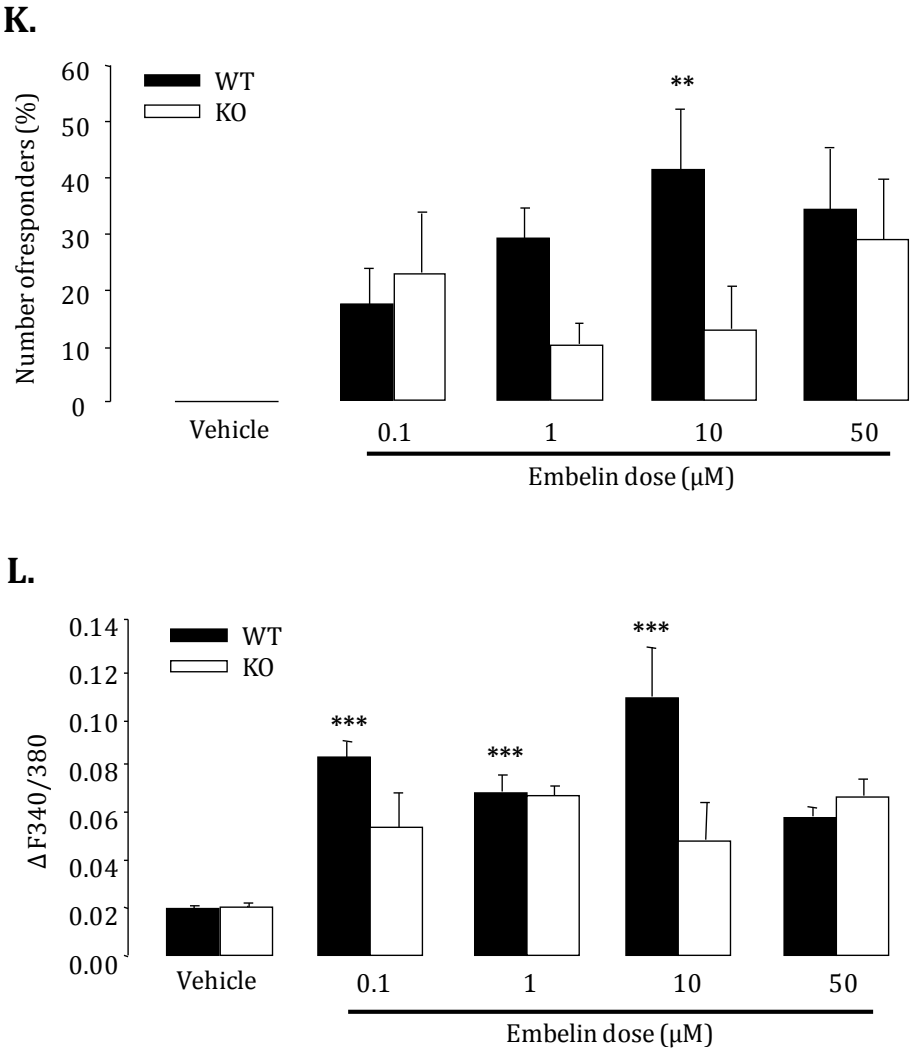

Figure 4.10: Embelin induced Ca^{2+} transients are attenuated in GPR84 KO macrophages

Quantification of percentage responders (A) and the Ca^{2+} response (B) to ATP (100 μM) in GPR84 WT and KO macrophages under non-stimulated and LPS stimulated conditions. There were a significant number of responders to ATP under non- and LPS stimulated conditions in both genotypes compared to vehicle. This correlated with an increase in $[Ca^{2+}]_i$, which was significant under LPS stimulated conditions compared to vehicle in both genotypes (WTV, KOV). (C-H) Embelin (10 μM) induced Ca^{2+} responses are greater in WT macrophages (D) than KO (G), as illustrated by the example traces from single WT (I) and KO (J) cells. Quantification of the number of responders (K) and the Ca^{2+} response (L) to 0.1, 1, 10 and 100 μM doses of embelin. The number of responders (at doses of 1, 10 and 50 μM) and changes in $[Ca^{2+}]_i$ (at doses of 0.1, 1 and 10 μM) was greater in WT than KO cells compared to vehicle. Increases in $[Ca^{2+}]_i$ are expressed as a Δ340/380 emission ratio. Data are presented as the mean ± SEM. **p < 0.01, ***p < 0.001 vs vehicle, Kruskal-Wallis one-way ANOVA on ranks, post-hoc Dunn's method, n = 3-6 experiments; average of ≥ 30 cells.

4.3.5 Capric acid elicits Ca^{2+} transients in microglial cells

To determine whether CA could produce Ca^{2+} responses in microglia and macrophage cells we utilised a similar approach to as previously presented. CA is a FFA with a carbon chain length of 10 and is postulated to be a natural ligand of GPR84 (Wang et al., 2006a). We found that CA was a successful inducer of Ca^{2+} transients in microglial cells as represented by the ΔF340/380 ratio, which was significant at doses of 1 and 10 μM (0.10 ± 0.02; 0.10 ± 0.03, respectively) compared to vehicle (0.02 ± $8x10^{-4}$; Fig. 4.11L). CA also recruited a greater number of responders compared to embelin, which was significant at doses of 1 and 100 μM (33.9 ± 14.0%; 31.6 ± 14.0%, respectively) vs vehicle (Fig. 4.11K). To extend these findings, we also investigated two additional parameters: desensitisation upon a second challenge and the effect of LPS stimulation. We previously showed that LPS up-regulates the expression of GPR84 (*Chapter 3*), which may enhance Ca^{2+} responses to CA. In addition, we also reported that 3 hrs of LPS stimulation does not attenuate Ca^{2+} responses (Fig. 4.10A, B) and so would not hinder the ability of cells to respond to succeeding challenges.

As illustrated in images (A-H) and the representative traces of single cells responding to 1 μM CA under non- (I) and LPS (J) stimulated conditions, LPS substantially enhanced CA induced Ca^{2+} transients and the responses of cells to a second challenge of CA were generally smaller (Fig. 4.11). Under LPS stimulated conditions, all doses tested (0.1 μM: 23.1 ± 4.9%; 1 μM: 26.8 ± 7.8%; 10 μM: 27.1 ± 11.9% and 100 μM: 47.6 ± 23.4%) produced a significant number of responders compared to vehicle (Fig. 4.11K). Correspondingly, LPS stimulation significantly enhanced Fura-2AM based Ca^{2+} signals compared to vehicle (0.02 ± $6x10^{-4}$) at every dose tested (0.1 μM: 0.09 ± 0.01; 1 μM: 0.22 ± 0.06; 10 μM: 0.17 ± 0.06 and 100 μM: 0.13 ± 0.01; Fig. 4.11L). Under non- or LPS stimulated conditions the percentage of responders or the ΔF340/380 ratio emissions to the second challenge were either reduced or remained unchanged compared to the first dose. Responses to a second challenge were significant compared to vehicle in LPS stimulated cells at 1 μM (0.12 ± 0.01), 10 μM (0.07 ± 0.01) and 100 μM (0.12 ± 0.02). These data suggest that CA induces Ca^{2+} responses in microglial cells, which can be enhanced via prior LPS exposure and that GPR84 may undergo receptor desensitisation upon further stimulation.

4.3.6 Capric acid shows weak selectivity for GPR84 in macrophages

In conjunction with our studies where we showed that different doses of CA elicit Ca^{2+} responses in microglia, we also investigated the selectivity of this ligand by comparing Ca^{2+} responses in WT and KO macrophages. As illustrated in the example images (Fig. 4.12A-L)

and traces (Fig. 4.12M-P), CA (1 μM) induces Ca^{2+} responses in both WT and KO macrophages that are enhanced by LPS stimulation (3hrs, 1 μg/ml). However it is apparent that at this particular dose (under both non- and LPS-stimulated conditions) a greater number of WT than KO cells are responsive (Fig. 4.12A-L) and under non-stimulated conditions WT cells also exhibited a greater change in $[Ca^{2+}]_i$ than KO cells (Fig. 4.12M-P).

Quantification of the percentage of responders revealed that there was a significant number of CA responding cells at 1 μM in WT (54.1 ± 10.7%) and 10 μM in both genotypes (WT: 46.3 ± 11.2%; KO: 48.8 ± 13.9%) following LPS exposure compared to vehicle (Fig. 4.12Q). Doses of 0.1 μM and 100 μM of CA failed to stimulate a significant number of cells compared to vehicle under non- and LPS-stimulated conditions. However, despite a greater percentage of WT than KO responders at 1 μM CA, there was an equivalent induction in $[Ca^{2+}]_i$ in both genotypes (WT: 0.10 ± 0.01; KO: 0.09 ± 0.01) compared to vehicle (WT: 0.02 ± 0.002; KO: 0.02 ± 0.001; Fig. 4.12R). There was also a significant increase in $[Ca^{2+}]_i$ in LPS stimulated WT and non-stimulated KO cells at 10 μM and 100 μM doses of CA compared to vehicle (WT: 10 μM, 0.08 ± 0.001; 100 μM; 0.08 ± 0.003; KO: vehicle, 0.02 ± 0.002; 10 μM 0.07 ± 0.003; 100 μM, 0.08 ± 0.004; Fig. 4.12R). In general, the data shows that the effects of CA on macrophage Ca^{2+} responses lack a concentration dependent effect (although the dose-response curve could be bell-shaped) and that the relationship between the percentage of responders and the ΔF340/380 ratio was variable. CA failed to show consistent selectivity for GPR84 except at a dose of 1 μM in terms of the percentage of responders (under both conditions) and the ΔF340/380 ratio under non-stimulated conditions. Together, these data suggest that CA and embelin only show selectivity for GPR84 at particular doses (1 μM and 10 μM, respectively). Therefore the data must be interpreted with caution and further experiments are required to validate these findings.

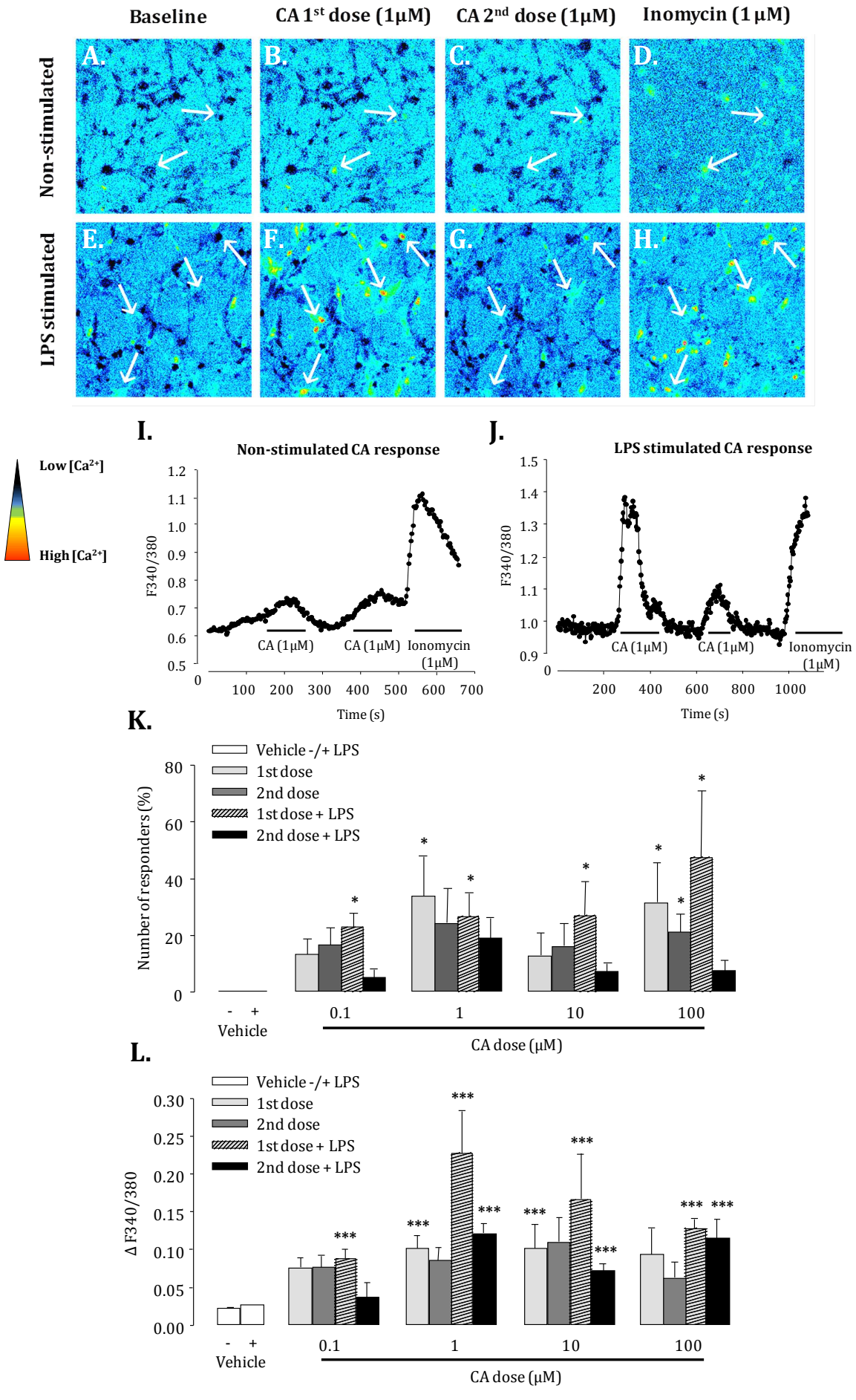
Baseline
CA 1st dose (1µM)
CA 2nd dose (1µM)
Inomycin (1 µM)
Non-stimulated
LPS stimulated
A.
B.
C.
D.
E.
F.
G.
H.
Low [Ca2+]
High [Ca2+]
I.
Non-stimulated CA response
F340/380
CA (1µM)
CA (1µM)
Ionomycin (1µM)
Time (s)
J.
LPS stimulated CA response
F340/380
CA (1µM)
CA (1µM)
Ionomycin (1µM)
Time (s)
K.
Vehicle -/+ LPS
1st dose
2nd dose
1st dose + LPS
2nd dose + LPS
Number of responders (%)
Vehicle
CA dose (µM)
L.
Vehicle -/+ LPS
1st dose
2nd dose
1st dose + LPS
2nd dose + LPS
Δ F340/380
Vehicle
CA dose (µM)

Figure 4.11: Capric acid produces a Ca^{2+} response in microglia, which is enhanced by LPS

Under non-stimulated conditions capric acid (CA, 1 μM) produces weak Ca^{2+} responses in microglial cells as illustrated in the top row (panels A-D) and the example trace (I). However, subsequent to 3 hrs LPS stimulation (1 μg/mL) Ca^{2+} signals generated by the 1st and 2nd challenges of CA are much greater (E-H, J). Under non-stimulated conditions, 1 μM and 100 μM doses recruited a significant number of responders to the 1st CA challenge, whereas under LPS stimulated conditions all doses recruited a significant number of responders compared to vehicle (K). The number of responders to 2nd challenges of CA were smaller or unchanged compared to the 1st challenge. Increases in $[Ca^{2+}]_i$ in response to the 1st and 2nd CA challenge at different doses are quantified in (L). Again, the 1st CA challenge produced a significant increase in $[Ca^{2+}]_i$ at all doses tested under LPS stimulated conditions, whereas only 1 μM and 10 μM CA produced a significant increase in $[Ca^{2+}]_i$ under non-stimulated conditions compared to vehicle. Responses to 2nd CA challenges were smaller or unchanged compared to the 1st challenge. Increases in $[Ca^{2+}]_i$ are expressed as a Δ340/380 emission ratio. Data are presented as the mean ± SEM. *p < 0.05, ***p < 0.001 vs vehicle, Kruskal-Wallis one-way ANOVA on ranks, post-hoc Dunn's method, n = 5-6 experiments; average of ≥ 30 cells.

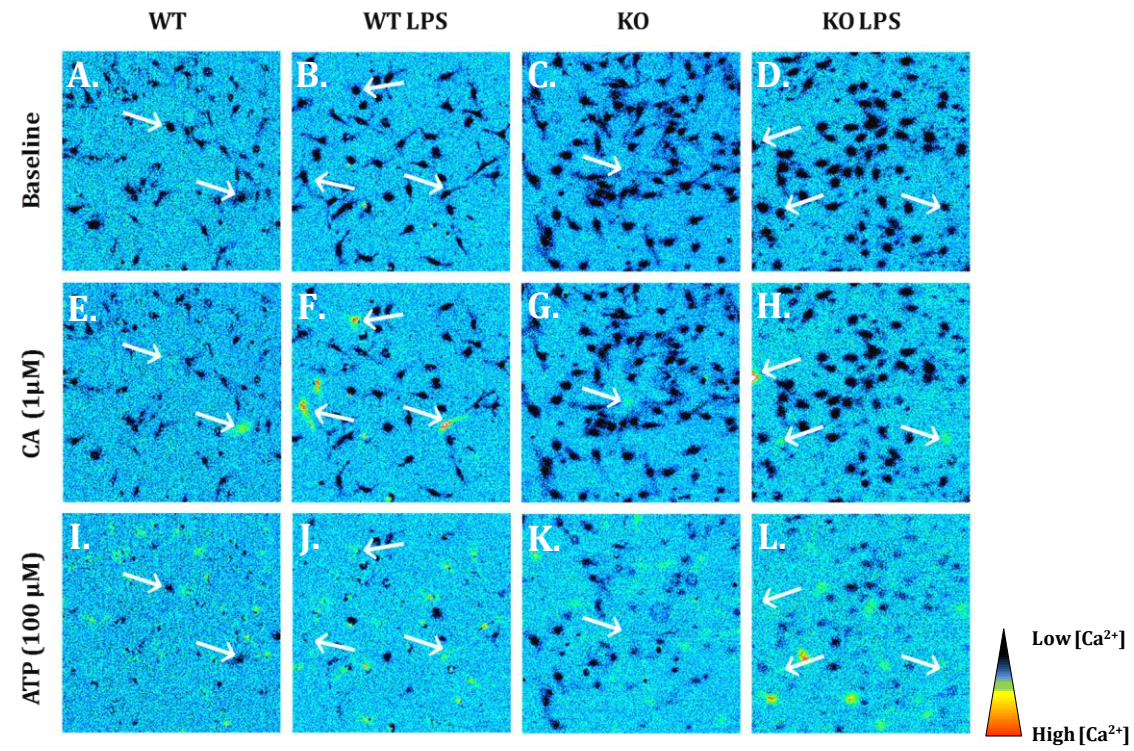
WT
WT LPS
KO
KO LPS
Baseline
CA (1µM)
ATP (100 µM)
A.
B.
C.
D.
E.
F.
G.
H.
I.
J.
K.
L.
Low [Ca2+]
High [Ca2+]

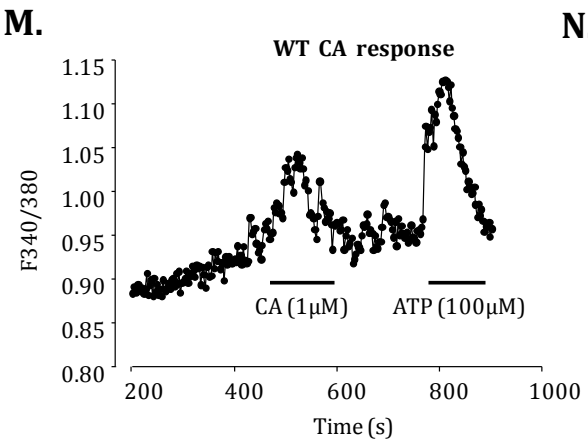
M.
WT CA response
F340/380
1.15
1.10
1.05
1.00
0.95
0.90
0.85
0.80
200
400
600
800
1000
Time (s)
CA (1µM)
ATP (100µM)

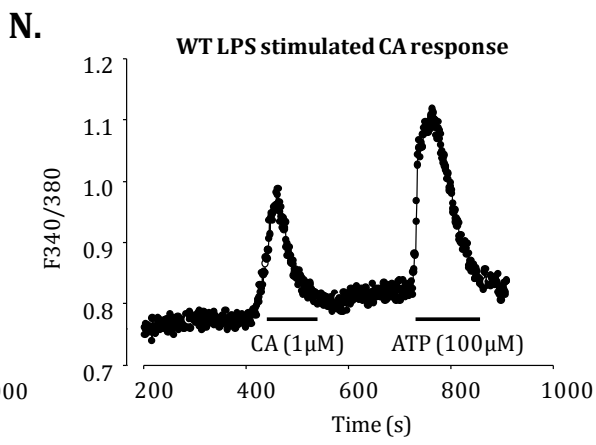
N.
WT LPS stimulated CA response
F340/380
1.2
1.1
1.0
0.9
0.8
0.7
200
400
600
800
1000
Time (s)
CA (1µM)
ATP (100µM)

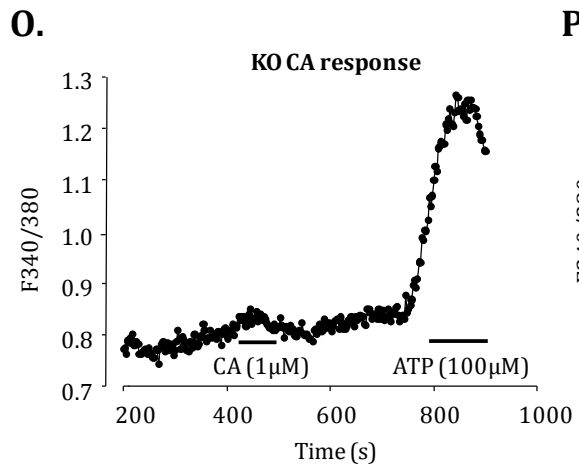
O.
KO CA response
F340/380
1.3
1.2
1.1
1.0
0.9
0.8
0.7
200
400
600
800
1000
Time (s)
CA (1µM)
ATP (100µM)

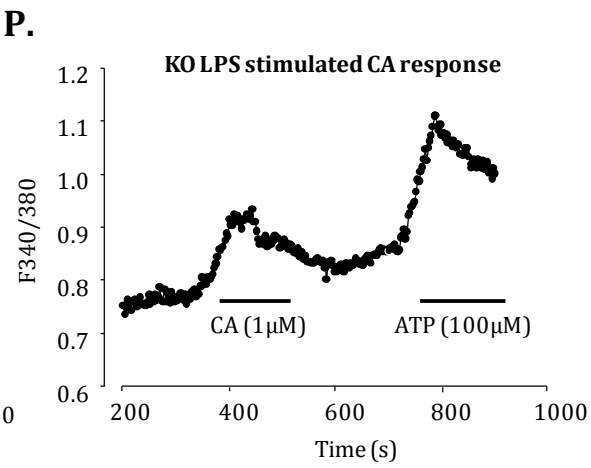
P.
KO LPS stimulated CA response
F340/380
1.2
1.1
1.0
0.9
0.8
0.7
0.6
200
400
600
800
1000
Time (s)
CA (1µM)
ATP (100µM)

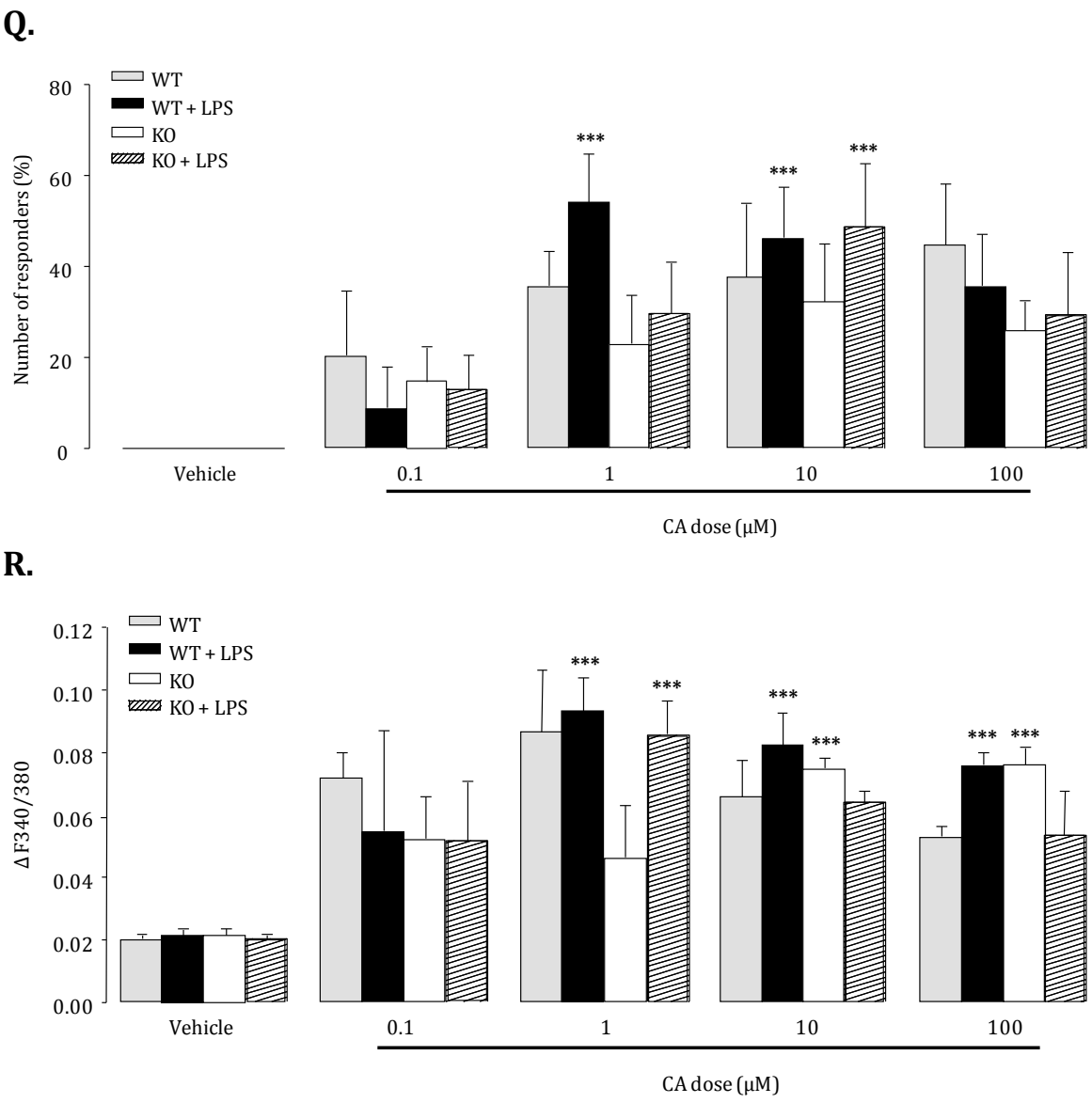

Figure 4.12: Capric acid shows weak selectivity for GPR84 in macrophages

Capric acid (CA, 1μM) generates Ca^{2+} transients in WT (E and F) and KO (G and H) macrophages under control (E and G) and LPS stimulated (F and H) conditions. Panels M-P illustrate images and example traces of WT (M and N) and KO (O and P) macrophage cells under non-stimulated (M and O) and LPS stimulated (N and P) conditions. The number of responders to different doses of CA are quantified in (Q). LPS stimulation enhanced the percentage of responding WT cells at 1 μM and in both genotypes at 10 μM compared to non-stimulated cells, which was significant in comparison to vehicle. LPS stimulation also significantly enhanced $[Ca^{2+}]_i$ responses in WT cells to doses of 1, 10 and 100 μM of CA and in the KO to a dose of 1 μM (R) compared to vehicle. Under non- and LPS stimulated conditions there were no significant differences between genotypes. Increases in $[Ca^{2+}]_i$ are expressed as a Δ340/380 emission ratio. Data are presented as the mean ± SEM. ***$p < 0.001$ vs vehicle, Kruskal-Wallis one-way ANOVA on ranks, post-hoc Dunn's method, n = 3-8 experiments; average of ≥ 30 cells.

4.3.7 cAMP assay

Although embelin and CA generated Ca^{2+} transients in microglia and macrophage cells this response was considerably variable, resembled an unlikely bell-shaped dose-response curve and the relationship between the number of responders and ΔF340/380 ratio was inconsistent. This suggests that examining Ca^{2+} responses to test ligand selectivity might not be the most appropriate assay for this receptor and that GPR84 mediated Ca^{2+} mobilisation may be complex and further down-stream in the signalling pathway rather than directly coupled to receptor activation. As we were unable to gain definitive answers from these studies we sought to investigate selectivity of embelin, CA and CNV by examining changes in cAMP levels, based on evidence that GPR84 is directly coupled to the $G_{i/o}$ G-protein family (Wang et al., 2006a). Here, CA was shown to reduce forskolin-stimulated cAMP production in a dose-dependent fashion in GPR84 transfected CHO cells (Wang et al., 2006a). We therefore hypothesised that a selective ligand would inhibit forskolin-induced cAMP in WT macrophages, but have no effect on KO macrophages. Forskolin is a valuable and widely used compound due to its ability to directly interact with the catalytic subunit of AC and increase the synthesis of cAMP (Insel and Ostrom, 2003) and thus provides an excellent positive control for the study of cAMP in our studies.

The cAMP-screen direct chemiluminescent ELISA system provides a rapid and sensitive quantification of cellular cAMP for functional assays examining receptor activation and can be used for receptor characterisation and ligand identification. In principle, the system is a competitive immunoassay where the addition of an AP-labelled cAMP conjugate competes with cAMP from sample extracts for a highly specific anti-cAMP antibody. AP is an enzyme that removes phosphate groups from a substrate via hydrolysis in a process termed dephosphorylation and is most effective in alkaline environments. Subsequent to the competitive antibody reaction the addition of the chemiluminescent substrate, CSPD, results in enzymatic dephosphorylation by AP, which leads to the formation of a metastable phenolate anion that decomposes to emit light at a maximum wavelength of 477 nm. CSPD requires an alkaline hydrophobic environment for rapid decomposition and emission of bright chemiluminescent signals, which is provided by an enhancer such as sapphire-II. In practise, the less cAMP present in the sample, the more cAMP-AP is bound to the antibody and the greater the amount of light emitted. Thus the light signal intensity, measured by a luminometer, is inversely proportional to the concentration of cAMP in the sample.

4.3.8 The effects of embelin, capric acid and CNV on forskolin-induced cAMP levels in WT and KO B-GEPMs

We examined inhibition of cAMP in non- and LPS stimulated conditions in WT B-GEPMs to determine if increased expression of GPR84 enhances ligand efficacy, which would be apparent by augmented inhibition of cAMP levels. GPR84 KO B-GEPMs were only examined under non-stimulated conditions. Three doses of each ligand, CA (A), embelin (B) or CNV (C) were comparatively examined in both WT and KO macrophages (Fig. 4.13). Despite testing two doses of forskolin which are documented to elicit marked increases in intracellular cAMP levels (Chang et al., 1984; Kreckler et al., 2009), we were unable to induce cAMP in WT macrophages. In general, under LPS stimulated conditions there was a greater induction of cAMP and each of the ligands exhibited a slight inhibitory trend, however due to the small difference between basal levels and forskolin-induced cAMP levels there was a limited window to observe a clear inhibitory effect (Fig. 4.13A, B, C). In contrast, KO cells showed a striking induction of cAMP (64.7 ± 6.5 fmol/mL (A); 216 ± 17.0 fmol/mL (B); 469.0 ± 53.9 fmol/mL (C)) which was significant compared to control (26.2 ± 0.3 fmol/mL (A); 54.2 ± 1.9 fmol/mL (A); 122.7 ± 3.2 fmol/mL (C)) and forskolin stimulated WT cells (23.4 ± 0.5 fmol/mL (A); 79.6 ± 0.6 fmol/mL (C)). In KO cells, CA elicited a significant inhibition of cAMP levels at the 1 μM dose (38.3 ± 2.3 fmol/mL) compared to the positive forskolin control (Fig. 4.13B). The inhibitory effect of CA in KO cells appeared to have a dose-dependent trend, suggesting that CA could indeed be exerting non-GPR84 selective effects. However, this assumption is difficult to ascertain without a comparative effect in the WT. Despite this we were able to show that subsequent to appropriate stimulation, KO cells are capable of inducing greater cAMP responses than WT cells (KO + FSK: 342.5 ± 37.9 fmol/mL vs WT + FSK: 121.2 ± 6.4 fmol/mL), compared to control (WT: 68.5 ± 2.8 fmol/mL vs KO: 88.4 ± 7.8 fmol/mL; Fig 4.13D). This elevated cAMP phenotype in the KO is particularly interesting with regards to the immunosuppressive role of this second messenger (Bourne et al., 1974; Serezani et al., 2008; Peters-Golden, 2009) and may be associated with the KO behavioural phenotype in experimental models of persistent pain (*Chapters 2 and 3*).

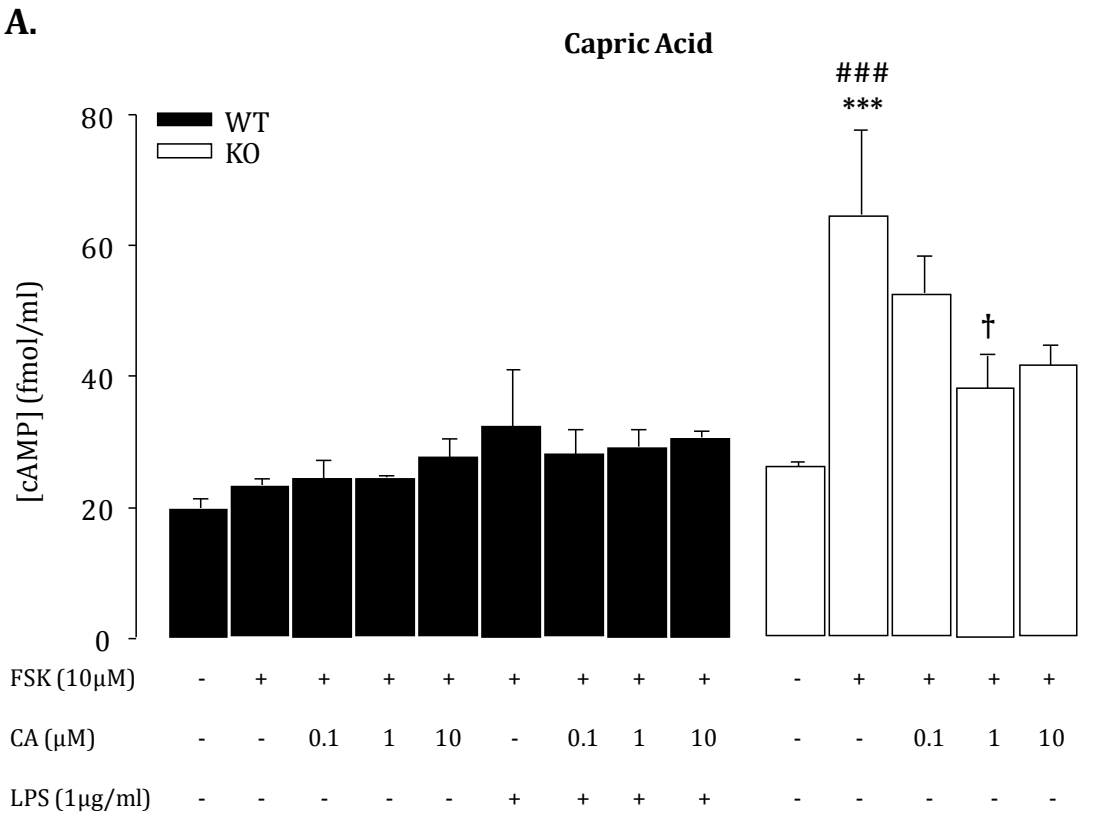
A.
Capric Acid
WT
KO
[cAMP] (fmol/ml)
80
60
40
20
0
###
***
†
FSK (10μM) - + + + + + + + + - + + + +
CA (μM) - - 0.1 1 10 - 0.1 1 10 - - 0.1 1 10
LPS (1μg/ml) - - - - - + + + + - - - - -

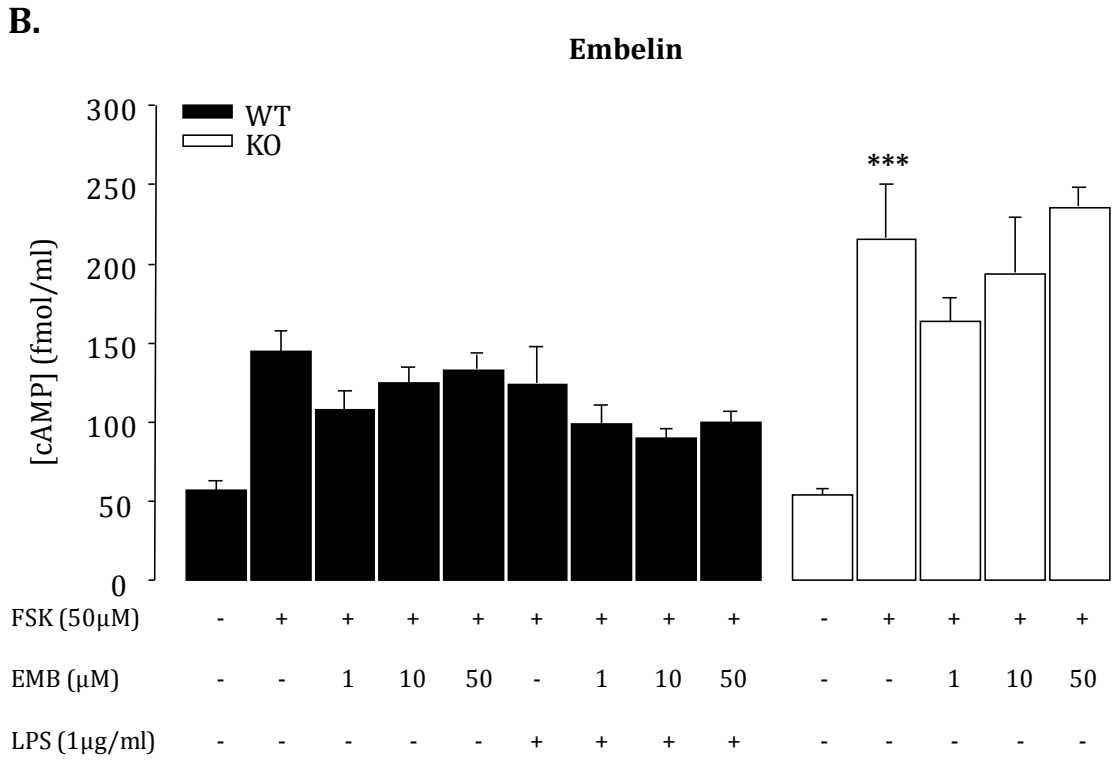
B.
Embelin
WT
KO
[cAMP] (fmol/ml)
300
250
200
150
100
50
0
***
FSK (50μM) - + + + + + + + + - + + + +
EMB (μM) - - 1 10 50 - 1 10 50 - - 1 10 50
LPS (1μg/ml) - - - - - + + + + - - - - -

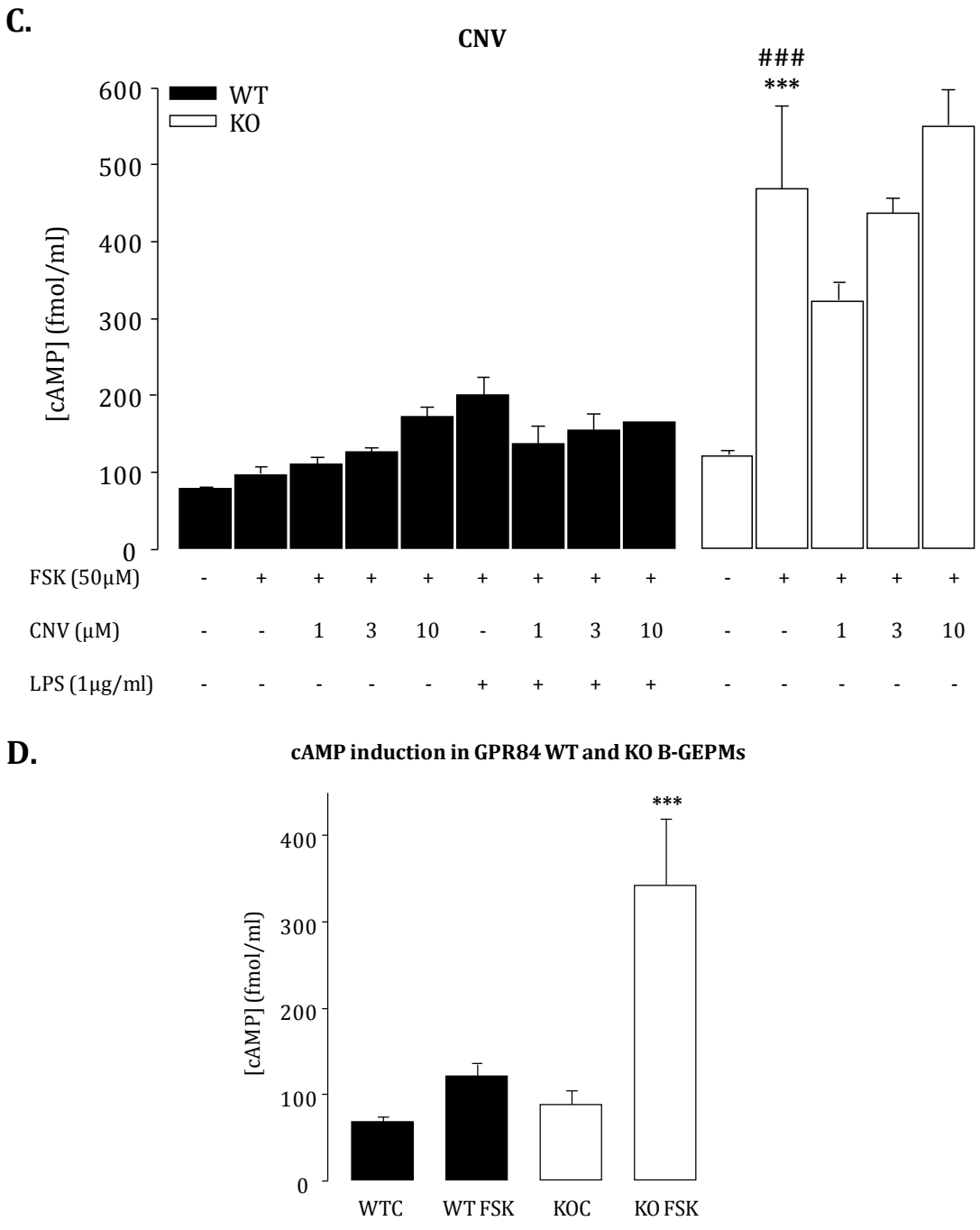

Figure 4.13: The effects of putative GPR84 ligands on forskolin-induced cAMP levels in WT and KO B-GEPMs

Examining the production of cAMP in GPR84 WT and KO B-GEPMs to test the selectivity of capric acid (CA; A), embelin (EMB; B) and CNV (C). None of the three ligands inhibited forskolin (FSK)-induced cAMP in WT cells under non- and LPS stimulated conditions (3hrs; 1µg/ml). Mean ± SEM; ***$p<0.001$, *$p<0.05$ vs appropriate control (-); ###$p<0.001$ KO+FSK vs WT+FSK; †$p<0.05$ CA+FSK vs FSK. One-way ANOVA with Tukey's post-hoc. n = 4-6 wells/condition. (D) GPR84 KO cells show greater FSK induced cAMP production (KO FSK) than WT cells (WT FSK) in comparison to control cells (KOC, WTC, respectively). Mean ± SEM; ***$p<0.001$ vs appropriate control. Kruskal-Wallis one-way ANOVA on ranks with Tukey's. n = 12 wells/condition.

4.4 Discussion

Pharmacological tools have been widely exploited in experimental studies investigating the physiological role and signalling pathways of receptors *in vitro* and *in vivo* systems. Throughout this thesis, we have utilised transgenic mice to investigate GPR84 in chronic pain mechanisms, and have shown that this receptor contributes to pain-associated behaviours in a model of nerve injury (PNL) and inflammation (CFA) (*Chapter 2 and 3*). However, a lack of commercially available agonists or antagonists selective for GPR84 has prevented further characterisation of this receptor. GPR84 is an orphan receptor and its signalling pathway is currently unknown, with only a single study postulating that CA is the natural ligand (Wang et al., 2006a). Based on this limited evidence we explored the efficacy and selectivity of three potential GPR84 ligands (embelin, CA and CNV) in microglia and WT and KO macrophages via Ca^{2+} and cAMP signalling assays to identify a selective agonist that could be utilised in further functional studies. We report that embelin and CA generate Ca^{2+} transients in microglia and WT macrophage cells and exhibited selectivity for GPR84 at doses of 10 μM and 1 μM, respectively. We were unable to conclusively show CA, embelin or CNV -induced inhibition of cAMP formation and so could not validate ligand efficacy and selectivity in this assay. However, interestingly we observed that KO macrophages showed a greater increase in forskolin induced cAMP than control WT cells.

4.4.1 GPR84 and Ca^{2+} signalling

Spinal microglia and peripheral macrophages express a number of chemokine receptors such as CCR2, CCR4, CCR5 and CX_3CR1, which are altered under chronic pain conditions; conversely pain-associated behaviours are attenuated in null mice or via the administration of chemokine receptor neutralising antibodies (Kieseier et al., 2002; Abbadie et al., 2003; Thacker et al., 2009; Kiguchi et al., 2010b; Staniland et al., 2010). Activation of chemokine receptors initiates rapid mobilisation of PLC, the subsequent generation of IP_3 and a resultant increase in cytosolic $[Ca^{2+}]_i$. This pathway is characteristic of chemokine signalling and can be utilised to investigate the responsiveness of these receptors to different ligands. PI3K is also a key player in chemokine signalling and initiates the subsequent activation of the MAPK cascade, particularly involving ERK (Bajetto et al., 2002). Elevated levels of $[Ca^{2+}]_i$ have been experimentally demonstrated in microglia, monocytes and macrophages following exposure to CCL2, CCL3, CCL5, CXCL5 and CX_3CL1, whereas pharmacological antagonism correspondingly blocks Ca^{2+} signalling (Harrison et al., 1998; Boddeke et al., 1999; Cardaba and Mueller, 2009; Serrano et al., 2010; Dawes et al., 2011; Clark and Malcangio, 2012). The GPR84 signalling pathway is currently unknown, but is postulated to

be coupled to the $G\alpha_{i/o}$ family (Wang et al., 2006a) where its activation may lead to the mobilisation of intracellular Ca^{2+} in a similar pathway to that of a chemokine receptor. However, there is some evidence that GPR84 signalling may be independent of a *Pertussis* toxin sensitive pathway (Versleijen et al., 2009). Chemokine receptors may also activate several other intracellular effectors including PLA_2, PI3K and MAPK (Murdoch and Finn, 2000), leading to the mobilisation of $[Ca^{2+}]_i$ and the activation of the p38 MAPK pathway (Kreideweiss et al., 1999; Elzi et al., 2001). Upon phosphorylation, p38 MAPK enters the nucleus where it phosphorylates transcription factors such as NF-κB, which mediate the biosynthesis of many pro-inflammatory factors documented to contribute to nociceptive transmission (Jana et al., 2003; Kumar et al., 2003; Ji and Suter, 2007).

Circumstantial evidence has suggested that GPR84 is activated by MCFFAs and cytokines (IL-1β, TNF-α) capable of stimulating the NF-κB pathway and that the activation of this receptor elicits the release of CXCL1, IL-8 and IL-12p40 (Hwang, 2000; Wang et al., 2006a; Bouchard et al., 2007; Suzuki et al., 2013). It has been reported that MCFFAs demonstrate efficacy in GPR84 transfected CHO cells and are able to activate leucocytes by increasing $[Ca^{2+}]_i$ (Wanten et al., 2004; Wanten and Naber, 2004; Wanten, 2006). Therefore, we postulated that as a pro-inflammatory receptor, GPR84 activation may be coupled to the mobilisation of Ca^{2+} and thus a functional assay examining Ca^{2+} responses in microglia and macrophages would be a relevant approach to examine the selectivity of embelin and CA.

In accordance with literature we verified the ability to obtain Ca^{2+} responses in rat spinal microglia and GPR84 WT and KO mouse peritoneal macrophages to challenges of ATP (Walz et al., 1993; McLarnon et al., 1999; Moller et al., 2000; Hoffmann et al., 2003; McLarnon, 2005; Farber and Kettenmann, 2006b). Purinergic signalling in these cells is mediated by the ionotropic $P2X_4$ and $P2X_7$ receptors and metabotropic P2Y receptors (McLarnon, 2005). Activation of $P2X_{4/7}$ receptors results in the influx of Na^+ and Ca^{2+} and efflux of K^+ and subsequent depolarisation, whereas activation of the P2Y receptor leads to an increase in $[Ca^{2+}]_i$ as a result of intracellular store depletion and subsequent SOC activation (McLarnon, 2005). Having successfully shown that ATP elicits Ca^{2+} responses we then investigated whether we could show the same with embelin and CA in microglia and WT macrophage cells, where ligand selectivity would be evidential by an attenuated/abolished Ca^{2+} response in KO cells. We found that both ligands produced Ca^{2+} transients in microglia and macrophage cells, but these responses tended to be inconsistent and the number of responders did not correlate with changes in $[Ca^{2+}]_i$. Usually dose-response relationships of a GPCR ligand are sigmoidal; at low concentrations the biological effect is small but when a certain threshold is met the effect increases until it reaches a plateau. However, some drugs

may exhibit a bell-shaped relationship, which is characterised by low dose responses but loss of the effect at higher doses. Both embelin and CA exhibited bell-shaped dose response curves, with a trend towards GPR84 selectively particularly at doses of 10 μM for embelin and 1 μM for CA.

Based on the fact that CA is a suggested natural ligand for GPR84 and the fact that CA recruited a greater number of microglial cells than embelin, we explored two additional parameters using CA to further complement our studies. We examined the concept of desensitisation by challenging the cells twice and also looked at the effect of LPS stimulation, which increases the expression of GPR84 in immune cells (Wang et al., 2006a; Bouchard et al., 2007). Desensitisation is a phenomenon that occurs subsequent to receptor activation via a number of mechanisms. These include phosphorylation of the receptor via second messenger kinases such as PKA and PKC, leading to the uncoupling of the receptor from its respective G-protein, or GRK-mediated phosphorylation and consequential sterical inhibition as a result of arrestin binding. Internalisation and sequestration of GPCRs via clathrin coated vesicles may also occur (Pierce et al., 2002). Accordingly, we showed that under normal and LPS stimulated conditions microglia exhibited reduced or unchanged CA responses to a second challenge at every dose tested. We also demonstrated that LPS substantially enhanced CA-induced Ca^{2+} transients in microglia and WT macrophages. However, as LPS stimulated KO cells also exhibited increased Ca^{2+} transients, whether this LPS-enhancing effect was due to increased expression of GPR84 is unknown. In conclusion, although embelin and CA clearly showed a degree of efficacy and selectivity at particular doses, the lack of consistency and residual responses in KO cells adds caution to the interpretation of a specific interaction with GPR84. Furthermore, selectivity at the 1 μM CA dose was lost in LPS stimulated cells as both WT and KO macrophages showed equivalent Ca^{2+} transients. This indicates a lack of selectivity or the possibility that other FFA-sensitive cell membrane receptors (as well as GPR84) may be up-regulated by LPS exposure, and may account for the greater Ca^{2+} responses observed in both genotypes compared to unstimulated conditions.

4.4.2 GPR84 and cAMP signalling

Our findings indicate that our initial approach using Ca^{2+} fluorometry to validate ligand selectivity for GPR84 may not have been the most appropriate assay for this receptor. GPR84 mediated Ca^{2+} mobilisation could be further down-stream of receptor activation rather than being directly coupled. We therefore supplemented our investigations on the selectivity of embelin, CA and CNV by assessing cAMP levels, based on evidence that GPR84

is coupled to the inhibitory $G\alpha_{i/o}$ family (Wang et al., 2006a). Here, Wang et al. (2006) employed a GPR84 heterologous expression system and showed that CA reduced forskolin-induced cAMP production in a dose-dependent fashion and that this effect could be abolished by *Pertussis* toxin pre-treatment (Wang et al., 2006a). We therefore hypothesised that a selective ligand would inhibit forskolin-induced cAMP in WT macrophages but have little or no effect on KO macrophages.

As we were unable to induce a sufficient level of cAMP in WT macrophages it is difficult to determine whether CA, embelin or CNV exerted inhibitory actions on cAMP formation and thus a comparison between WT and KO cells cannot be made. The induction of cAMP in macrophages is usually very small and within the picomolar range. However, forskolin induced formation of cAMP in macrophage cells is well documented, and many groups have shown the ability to increase cAMP levels using similar concentrations and incubation periods to the ones we employed (Chang et al., 1984; Osawa et al., 2006; Kreckler et al., 2009; Ballinger et al., 2010). Therefore, the poor cAMP responses we obtained should be improved by altering experimental conditions such as using higher doses of forskolin and extending the incubation period. In contrast, GPR84 KO macrophages exhibited striking increases in forskolin-induced intracellular cAMP levels compared to vehicle, which we postulate is due to the absence of inhibitory GPR84 signalling. Surprisingly, 1 μM of CA significantly inhibited forskolin-induced cAMP in KO cells, which was a dose that appeared to be particularly selective in the Ca^{2+} fluorometry assays. Therefore we did not attempt to repeat a second cAMP assay study to test CA with a higher dose of forskolin due to this non-selective action. However, we used a higher dose of forskolin (50 μM) in subsequent studies (embelin, CNV) in attempt to elicit greater cAMP responses in WT macrophages, which was disappointingly unsuccessful.

The role of cAMP in macrophage function has historically been the centre of debate owning to conflicting data; while some thought that this second messenger enhanced phagocytosis and collagen production (Muschel et al., 1977; McCarthy et al., 1980) others believed that cAMP in fact did the opposite. However, it is now well established that elevated cAMP levels exert a broad range of immunosuppressive actions, including down- or up- regulation of pro- or anti-inflammatory mediators, respectively, and a reduction in phagocytic activity (Bourne et al., 1974; Aronoff et al., 2005; Serezani et al., 2008; Peters-Golden, 2009; Wall et al., 2009) as previously discussed (section 4.1.2). These effects are primarily coordinated by two effector molecules, PKA and the exchange proteins, Epac 1 and 2, which are directly activated by cAMP and play distinct, redundant or opposing roles in immune cell function (Wall et al., 2009; Ballinger et al., 2010). In light of this evidence, the KO macrophage

phenotype is very intriguing as upon forskolin stimulation these cells exhibited a robust cAMP up-regulation in contrast to WT macrophages, moreover despite a lack of significance, KO macrophages also possess slightly greater basal levels of cAMP. This may suggest that macrophage cells have a greater polarity towards an anti-inflammatory M2 state in the absence of GPR84. Accordingly, we observed increased expression of the M2 macrophage marker, ARG1, in the injured sciatic nerves of KO mice (*Chapter 2*) and have shown that KO macrophages exhibit attenuated production of some pro-inflammatory mediators in response to LPS (*Chapter 3*). Therefore, it is feasible that nerve injury and/or inflammation leads to an increase in cAMP levels in GPR84 KO microglia/macrophages, which inhibits the release of some pro-inflammatory mediators and hence alleviates pain-associated behaviours. Furthermore, it has been reported that forskolin increases cellular proliferation and differentiation via cAMP-dependent activation of PKA and Epac (Misra and Pizzo, 2005). This is consistent with our previous findings of an ipsilateral increase in Iba1 positive cells in the spinal cords of KO PNL and CFA treated mice and in the sciatic nerves of KO PNL mice (see *Chapters 2* and *3*). However, we must note that elevated cAMP has also been reported to suppress macrophage proliferation (Vairo et al., 1990).

In contrast to its immunosuppressive role in immune cells, cAMP was one of the first second messengers to be implicated in nociceptive transmission (Hucho and Levine, 2007). At the site of inflammation nociceptor sensitisors such as PGE_2 and adenosine activate AC via their $G\alpha_s$ coupled GPCRs, which initiates cAMP synthesis. Increased levels of cAMP enhances neuronal excitability via the phosphorylation dependent actions of its binding partner, PKA, which has been demonstrated to modulate voltage-gated channels ($Na_v1.8$) and ligand-gated channels (TRPV1) as well as augment neurotransmitter release (Hingtgen et al., 1995; Fitzgerald et al., 1999; Bhave et al., 2002). Elevated levels of cAMP is also associated with increased neuronal excitability in experimental models of chronic pain and the administration of cAMP inducing agents such as forskolin produces dose-dependent hyperalgesia in rats that can be prolonged via PDE inhibitors or blocked by the cAMP analog, RP-cAMP (Taiwo and Levine, 1991). Conversely, pre-treatment with AC inhibitors decreases PGE_2 induced behavioural hyperalgesia and administration of PKA inhibitors pre or post PGE_2 treatment produced a similar inhibitory effect on pain behaviours. Thus indicating that PKA plays a key role in the maintenance of hypersensitivity (Aley and Levine, 1999). Knock-out mice have also been utilised in a number of studies exploring the roles of specific isoforms of AC in nociceptive transmission. Behavioural responses to PNL or subcutaneous administration of formalin or CFA was attenuated or abolished in AC type 1 and 8 double KO mice (Wei et al., 2002). Similarly, AC type 5 null mice demonstrated attenuated formalin or SNL evoked pain responses (Kim et al., 2007b). In light of this evidence and with regards to

our findings, the development of immune cell specific AC agonists or drugs exploiting cAMP function could be therapeutically beneficial in combating chronic inflammatory diseases associated with pain. Fascinatingly, several pathogenic microorganisms (*Bordetella pertussis*, *Vibrio cholerae* and *Escherichia coli*) have evolved cAMP enhancing mechanisms to disable host innate immune defences (Serezani et al., 2008). However, the selectivity of such drugs would be crucial, as non-selective effects at other cell types may result in pain.

4.4.3 Future work

In this chapter we tested the efficacy and selectivity of three putative GPR84 ligands (embelin, CA and CNV) using Ca^{2+} and cAMP assays. In the Ca^{2+} assays, we found that CA and embelin exhibited some selectivity for GPR84 at doses of 1 μM and 10 μM, respectively, and that LPS increased Ca^{2+} responses to CA but selectivity was lost. Notably, CA and embelin recruited a modest number of responding cells. Thus in light of previous findings, which suggested that GPR84 is only expressed by a subset of microglial cells (*Chapter 3*), it may be interesting to characterise which populations of microglia and macrophages express GPR84.

Data from the cAMP assays were inconclusive as we were unable to generate sufficient forskolin-induced cAMP responses in WT macrophages. It would therefore be necessary to repeat the cAMP studies using an optimised stimulation protocol to achieve a greater cAMP induction window where the inhibitory effects of GPR84 ligands can be fully assessed. It would also be interesting to further investigate the elevated cAMP/M2 phenotype of KO macrophages via immunocytological assessment of cAMP and other relevant markers (p38 MAPK, ARG1, iNOS) in ligand stimulated WT and KO macrophage cells. Here the development of selective agonists or antagonists would permit an extensive immunocytological evaluation of the cAMP phenotype. Previously we presented a selective antibody for GPR84 (*Chapter 3*), however as it possesses an intracellular epitope it is not appropriate for blocking GPR84 in live cells. Therefore, the development of a selective antibody possessing an extracellular epitope may enable further functional analysis of GPR84 *in vitro* and *in vivo*. Cyclic AMP signalling is also synonymous with the activity of its binding partner, PKA, thus it would be interesting to immunohistochemically examine immune cell-expressed phosphorylated PKA in the sciatic nerves and spinal cords of PNL and CFA treated WT and KO mice.

In the Ca^{2+} and cAMP signalling assays, we utilised resident and B-GEPMs, respectively, due to different protocol demands in cell yields. B-GEPMs consist of a mixture of resident and infiltrating cells, and so are representative of the *in vivo* situation in addition to providing

greater yields. This population of macrophages differ in their respiratory and phagocytic capacity and chemokine responsiveness compared to resident cells (Zhang et al., 2008). It is worth noting that different types of cell cultures or the use of different populations of macrophages in primary cell cultures accounts for many of the discrepancies throughout the literature. Although B-GEPMs are perhaps the most relevant source of macrophages to use in our studies in comparison to other sources such as BMMs, under normal conditions the expression of GPR84 is the lowest in this population (Lattin et al., 2008), which could possibly account for a lack of potency of the ligands tested. Attempts to increase GPR84 expression using LPS enhanced Ca^{2+} responses to ligands in some cases but not always specifically in WT cells and only markedly improved inhibition of forskolin-induced cAMP. Therefore the consideration of alternative populations of macrophages for future studies may be critical in aiding our understanding of the function of GPR84.

Chapter 5

General Discussion

5.1 Summary of experimental findings

Owning to the compelling body of evidence on the interaction between neurons, immune and glial cells in nociceptive transmission (Marchand et al., 2005; Scholz and Woolf, 2007; Thacker et al., 2007; Austin and Moalem-Taylor, 2010; Calvo et al., 2012), experimental research on immune cell expressed targets is well underway in the chronic pain field. The exclusive expression of GPR84 in immune cells and its pro-inflammatory profile warrants this receptor as an exciting new candidate in pain pathways. Therefore the aim of this thesis was to explore GPR84 signalling in animal models of persistent pain. The main findings are:

1. GPR84 mRNA is up-regulated in microglia and macrophage cells upon LPS stimulation as well as in the sciatic nerve and spinal cord tissue of neuropathic mice.
2. GPR84 KO mice do not develop neuropathic pain behaviours in a model of traumatic nerve injury.
3. Subsets of mediators, particularly ARG1, are dysregulated between the ipsilateral sciatic nerve and spinal cord tissues of nerve injured WT and KO mice.
4. GPR84 KO mice exhibit attenuated pain behaviours in a model of inflammatory pain.
5. LPS-induced up-regulation of some cytokines/chemokines including CCL2, CCL3 and CXCL5 are attenuated in KO macrophages.
6. KO macrophages exhibit elevated basal and forskolin-induced levels of cAMP compared to WT cells.

Using transgenic mice we have shown, for the first time to the best of our knowledge, that GPR84 KO mice have attenuated neuropathic and inflammatory pain. This indicates that GPR84 is necessary for the development of persistent pain and thus pharmacological manipulation of GPR84 signalling in immune cells may alleviate pain behaviours. Accordingly, the immunomodulatory role of GPR84 is evident by our gene profiling studies, where subsets of immune-derived pro-inflammatory mediators were dysregulated between nerve injured WT and KO mice. Although not significant, nerve injury-induced expression of IL-1β, IL-12p40, CCL3 and NOS2 was attenuated in the sciatic nerves and spinal cords of KO mice 21 days post PNL. These mediators are known to contribute directly or via second messengers to peripheral and/or central sensitisation (Sommer and Kress, 2004; Abbadie, 2005; Austin and Moalem-Taylor, 2010), as previously discussed (*Chapter 1*), and so collectively their diminished expression in the KO may account for the absence of pain behaviours subsequent to nerve injury. Using a similar approach, we also observed decreased LPS-induced expression of a selection of chemokines and cytokines in KO

macrophages, including pro-nociceptive CCL2, CCL3 and CXCL5 (Abbadie et al., 2003; Kiguchi et al., 2010b; Dawes et al., 2011).

In both neuropathic and inflammatory pain models, spinal microglia and peripheral macrophage responses were equivalent between genotypes, although our immunohistological assessment was restricted to Iba1 and p-p38 MAPK. Likewise, LPS stimulated KO macrophages appeared just as capable as WT macrophages in launching a pro-inflammatory response, except for the attenuated expression of some chemokines. Despite the unaltered microglia/macrophage response, an explanation for the behavioural phenotype in the KO could indeed lie with reduced chemokine signalling. It is apparent in the literature that the interruption of a single receptor or signalling molecule can completely abolish pain behaviours due to the integrated nature of the nociceptive transmission system. On the other hand, our data could in fact argue against a critical role of microglia and macrophages in the pathogenesis of chronic pain. In this thesis we have reported that GPR84 mediated signalling contributes to the initiation of nerve injury-induced neuropathic pain and the maintenance of CFA-induced inflammatory pain. However, we did not observe a corresponding immune cell response via immunohistochemical analysis. Dissociation between a microglial or macrophage cell contribution and behavioural hypersensitivity in animal models of neuropathic and inflammatory pain has also been previously documented (Colburn et al., 1997; Molander et al., 1997; Colburn et al., 1999; Hashizume et al., 2000; Honore et al., 2000; Rutkowski et al., 2000; Winkelstein and DeLeo, 2002; Raghavendra et al., 2003a; Zhang et al., 2003; Barclay et al., 2007; Clark et al., 2007a; Shi et al., 2011). Furthermore, in models that are more representative of disease-associated pain conditions such as chemotherapeutic, bone cancer, HIV or VZV -induced neuropathy microgliosis was absent (Honore et al., 2000; Zheng et al., 2011a; Blackbeard et al., 2012; Zhang et al., 2012a). It was also found that minocycline failed to alleviate mechanical allodynia in painful diabetic neuropathy (Liao et al., 2011). Likewise, the clinical evidence for a role of microglia and macrophages in chronic pain patients is limited and unclear. For example, propentofylline was ineffective for the treatment of post-herpetic neuralgia in a randomised controlled trial (Landry et al., 2012) and the CCR2 antagonist AZD2423, bore no efficacy in patients with post-traumatic neuralgia (Kalliomaki et al., 2013).

Despite the fact that some pre-clinical and clinical evidence suggests a limited role of microglia and macrophages in chronic pain, differences in disease aetiologies, failure of translational research and caveats in clinical trial design argue against this. Undoubtedly, there is a significant body of basic research supporting microglia and macrophages as active participants in chronic pain (discussed in *Chapter 1*), which is supported by growing clinical

evidence. For example, reactive microglia have been detected in the ipsilateral thalamus of amputees with chronic phantom limb pain by positron emission tomography (PET) using a radiolabelled ligand for the peripheral benzodiazepine receptor (Banati et al., 2001). This technique has also been employed to investigate the neural bases of pain, including the involvement of microglia in other types of neuronal injury. PET as well as functional magnetic resonance imaging (fMRI) have already exemplified success in animal research and therefore provide excellent alternatives to study microglia in humans in a non-invasive manner (Imamoto et al., 2013). Besides an obvious change in morphological phenotype and numbers, mediators released by microglia are well documented to contribute to behavioural hypersensitivity in animal models of chronic pain. Heightened levels of pro-inflammatory cytokines were detected in the CSF fluid of two CRPS patients and this increase correlated with pain intensity (Alexander et al., 2005; Backonja et al., 2008). However, since a number of cell types are capable of producing cytokines, these findings do not conclusively indicate microglial activation. A pro-inflammatory monocyte phenotype has also been documented in CRPS patients (Ritz et al., 2011) and an increase in inflammatory cell recruitment has been reported in nerve biopsies from neuropathic pain patients, where the extent of infiltration correlated with the pain experienced (Lindenlaub and Sommer, 2003). Despite previous failures, clinical trials examining alternative microglial modulators are well underway (NCT01314482) (Grace et al., 2011) and the p38 MAPK inhibitor SB-681323, which may also effect macrophages, was efficacious for neuropathic pain in a small double-blind crossover trial (Anand et al., 2011).

It is possibile that the up-regulation of GPR84 expression alone is driving the pain behaviours. Tsuda et al. (2003) demonstrated that the up-regulation of $P2X_4$ receptors in hyperactive microglia in the spinal cord is crucial for nerve injury-induced allodynia. Pharmacological blockade or intraspinal administration of $P2X_4$ receptor antisense oligodeoxynucleotides suppressed pain behaviours, whereas intraspinal transfer of $P2X_4$-expressing microglia generated behavioural hypersensitivity in naïve rats (Tsuda et al., 2003). Here we demonstrate that GPR84 mRNA is strikingly up-regulated in the sciatic nerve and more modestly in the spinal cord at 7 days post PNL, and this increase persisted up to day 21. We also demonstrated that GPR84 mRNA was considerably up-regulated in peritoneal macrophages and moderately in cortical microglia subsequent to LPS stimulation. Immunohistochemical assessment revealed GPR84 up-regulation in a majority of microglial cells in LPS-treated spinal cords, indicating that this receptor may represent a sub-population specific marker. Together, these data suggest a prominent role of GPR84 signalling in peripheral macrophages.

Interestingly, we found that under normal conditions GRP84 expression was undetectable, however upon appropriate immunostimulation there was an increase in transcript and protein levels. Therefore, GPR84 may be a silent receptor that is recruited only under pathological circumstances. Accordingly, GPR84 up-regulation has been reported in clinically relevant animal models of diabesity and EAE, which feature pain-associated pathologies (Bouchard et al., 2007; Nagasaki et al., 2012). This response-specific up-regulation is a particularly appealing property for the development of selective ligands as only erroneous immune activity would be targeted whilst normal nociceptive transmission would remain unaffected, limiting the possibility of detrimental side effects. Likewise, pharmacological blockade of $P2X_4$ had no effect on acute pain behaviours of naïve rats but suppressed tactile allodynia in neuropathic animals (Tsuda et al., 2003).

One of the most intriguing outcomes of the gene profiling studies was the considerable up-regulation of the anti-inflammatory M2 macrophage marker, ARG1, in the sciatic nerve of KO mice 7 days post PNL, in contrast to WT controls. ARG1 is associated with the alternative pathway, which entails the metabolism of L-arginine to produce L-ornithine and urea. In mammals there are two isoforms of ARG, cytosolic ARGI and mitochondrial ARGII, both of which carry out the same reaction (Bogdan, 2001). Ornithine amino transferase may then synthesise proline from ornithine, which is crucial in collagen production, whereas ornithine decarboxylase generates polyamines that are involved in cellular proliferation. Together these pathways contribute to cell growth and differentiation as well as the formation of the ECM (Kreider et al., 2007). On the other hand, pro-inflammatory M1 macrophages are associated with the expression of inducible nitric oxide synthase (iNOS), which catalyses the oxidation of the substrate L-arginine to form NO and L-citrulline. The transfer of electrons by iNOS subunits to the co-substrate O_2 results in the formation of superoxide (O^-_2). Superoxide may then react with NO or L-citrulline to produce the reactive nitrogen oxide species, peroxynitrite, or may react with water to form hydrogen peroxide. Both of these highly reactive agents are able to cross the membrane and damage biological targets (Bronte and Zanovello, 2005). NO exerts multiple immunoregulatory functions in host protection such as antimicrobial activity, cytokine modulation and Th cell development. Hence the expression of NO in macrophages is tightly regulated by the competing enzymes, iNOS and ARG, for their common substrate, L-arginine, where the induction of one enzyme suppresses the expression of the other and vice versa (Modolell et al., 1995; Sonoki et al., 1997; Chang et al., 1998). Notably, there are three isoforms of NOS, neuronal NOS (nNOS), endothelial NOS (eNOS, NOS3) and iNOS, with the former two collectively known as cNOS due to their constitutive expression. All three isoforms operate in the immune system and catalyse the same reaction. Importantly, iNOS expression in macrophages depends on

localised chemokine profiles. Thus, Th-1-derived IL-2, IL-12 and INF-γ increase iNOS expression and promote M1 polarity. Conversely, Th-2-derived IL-4, IL-10 and IL-13 induce ARG1 activity while IL-4, IL-13 also inhibit iNOS mRNA expression and so promote M2 polarity (Modolell et al., 1995; Munder et al., 1998; Bogdan, 2001).

In the context of neuropathic pain, $iNOS^{+}/ARG^{-}$ M1 macrophages have been reported to rapidly infiltrate the injured nerve as soon as day 1, while $iNOS^{-}/ARG^{+}$ M2 macrophages infiltrate the DRG by day 2, suggesting distinct roles of macrophage populations in different tissues (Komori et al., 2011). In a similar study, M1 macrophage infiltration in the nerve was observed 1-2 days post PNL, while in IL-1R1/TNFR1 null mice, M1 macrophage infiltration was attenuated by 90% on day 1 post injury (Nadeau et al., 2011). M1 macrophage infiltration has also been observed in the inflamed paws of CFA treated mice, which correlated with mechanical hyperalgesia. Administration of the peroxisome proliferator-activated receptor-γ agonist, rosiglitazone, alleviated pain behaviours by promoting M2 infiltration at inflamed sites (Hasegawa-Moriyama et al., 2013). In addition to chronic pain, the pro-inflammatory M1 macrophage phenotype has been implicated in numerous diseases such as cancer and diabetes (Mosser and Edwards, 2008) whereas the M2 phenotype is generally perceived as M1 suppressive and pro-healing/repair. This is supported by studies demonstrating the beneficial effects of pro-M2 polarity. For example, clinical severity scores in a model of EAN were attenuated in TNF-α null mice, correlating with a pro-M2 macrophage phenotype (Zhang et al., 2012b). In the same model, treatment with compound A (a plant-derived glucocorticoid receptor ligand) inhibited the progression of mechanical allodynia and increased numbers of M2 macrophages in the sciatic nerve by promoting M2 polarity (Zhang et al., 2009). These studies are consistent with our own findings of a pro-M2 state in GPR84 KO mice and diminished chronic pain behaviours and thus provides a credible explanation for the behavioural phenotype.

Although the M1/M2 classification is useful in pertaining discrete macrophage populations to particular physiological functions, discrepancies in the literature suggest that such a broad segregation may not always be appropriate since it undermines the complexity of these cells. For instance, whilst ARG1 expression is considered a hallmark of alternative activation in murine macrophages, other studies have reported an increase in the expression of this marker following LPS stimulation (Sonoki et al., 1997; Menzies et al., 2010). Therefore it is evident that ARG1 is induced by both innate (LPS) and alternative cues and so experimental classification of macrophages should ideally be carried out with more than one marker. For example, dectin-1 and MRC-1 can be used as early markers (6 hours) of alternative activation involved in pathogen recognition and combating fungal

infections, whereas fizz1, ym1 and ARG1 can be used as late markers (24 hours) of alternative activation and are associated with tissue repair, wound healing and the control of parasitic infections. Evidentially, M2 classification encompasses different subtypes of macrophage cells, which exhibit a spectrum of overlapping functions and characteristics, as discussed in *Chapter 1* (Menzies et al., 2010; David and Kroner, 2011). Hence caution should be applied when interpreting studies that have used broad markers such as ARG1, as this group of cells are not solely involved in passive healing and anti-inflammatory functions.

Nevertheless, in conjunction with our findings of a pro-M2 macrophage polarity in nerve injured KO animals, we also observed greater intracellular cAMP production in KO macrophages than in WT. Elevated cAMP is associated with a broad range of immunosuppressive actions, including the down- or up- regulation of pro- or anti-inflammatory mediators, respectively, as well as a reduction in phagocytic activity (Bourne et al., 1974; Aronoff et al., 2005; Serezani et al., 2008; Peters-Golden, 2009; Wall et al., 2009) as previously discussed (*Chapter 4*). In light of this evidence, we postulate that under pathological conditions the ability of GPR84 KO macrophages to launch an inflammatory response and release certain subsets of chemokines/cytokines is compromised. Therefore, we propose that GPR84 is a pro-inflammatory receptor that suppresses intracellular cAMP via $G\alpha_{i/o}$ coupled signalling mechanism and contributes to peripheral and central sensitisation via the release of pro-nociceptive CCL2, CCL3 and CXCL5. As GPR84 expression is regulated by LPS and other stimulators of the NF-κB pathway (IL-1β, TNF-α) (Bouchard et al., 2007), we suggest that GPR84 may signal in a similar way to chemokine receptors. Thus, GPR84 activation may initiate hydrolytic activity of PLA_2, leading to the mobilisation of intracellular Ca^{2+} and possibly the activation of several other intracellular effectors including, PI3K and p38 MAPK (see Fig. 5.1) (Murdoch and Finn, 2000). According to our findings and the literature, GPR84 is also likely to be involved in the induction of NF-κB mediated transcription of pro-inflammatory mediators such as CXCL1, IL-8/CXCL8 and IL-12p40 (Hwang, 2000; Wang et al., 2006a; Bouchard et al., 2007; Suzuki et al., 2013), as well as CCL2, CCL3 and CXCL5. We propose that under pathological conditions GPR84 is a FFA sensor trans-activated by TLR4 or activated via autocrine cytokine/chemokine signalling.

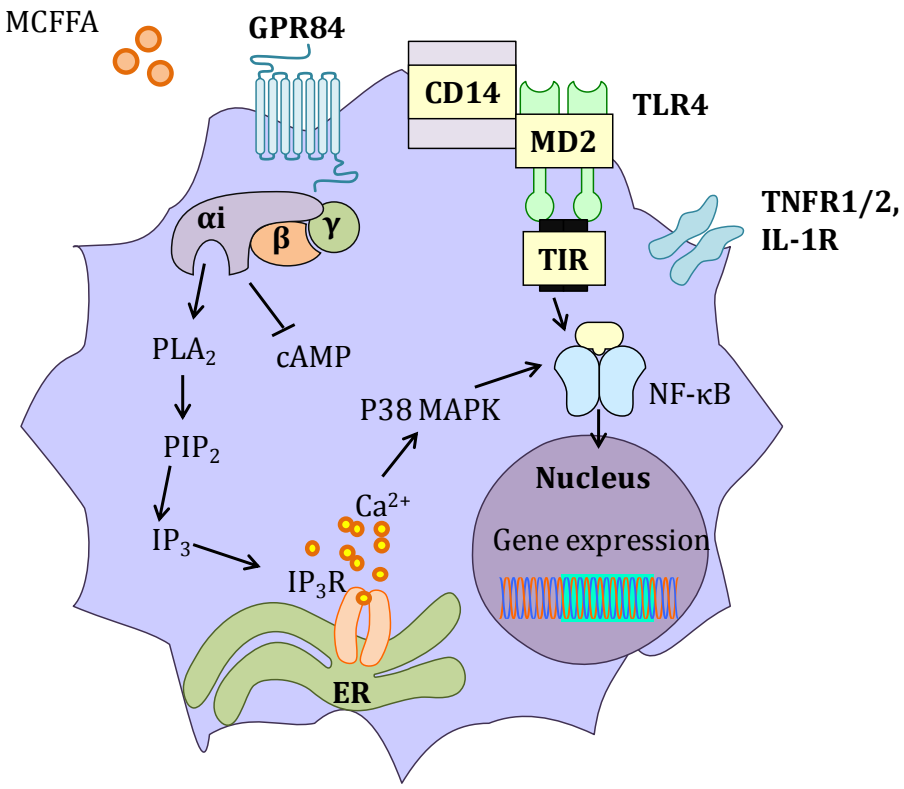

Figure 5.1: GPR84 signalling pathway in a microglia/macrophage cell

MCFFAs bind to GPR84, inhibiting the production of cAMP and initiating the hydrolytic activity of PLA_2 via a $G\alpha_{i/o}$ coupled pathway. This leads to mobilisation of Ca^{2+} from intracellular stores (ER), the phosphorylation of p38 MAPK and the activation of NF-κB, which mediates the transcription of target genes. GPR84 expression is regulated via the activation of TLR4, TNFR1/2 and IL-1R.

As GPR84 expression was more greatly induced by LPS in macrophages than microglia, as well as in nerve than spinal cord of neuropathic mice, GPR84 signalling may play a more prominent role in peripheral macrophages. Consistent with this, we ruled out microglial involvement as we did not observe an altered microglial response between genotypes in the PNL, CFA and LPS models of persistent/acute pain, despite an attenuation of pain behaviours in the KO. Although we did not see a difference in the injury-induced macrophage response in the sciatic nerve between genotypes, we only examined one marker (Iba1) at a single time point (7 days) and in a single model (PNL) and so there is scope for further investigation. It is also possible that the differences between WT and KO macrophages may not be detectable by staining for these traditional markers of activation. So far we have only found subtle differences in the capability of KO macrophages to produce

some chemokines and cytokines rather than gross differences in their ability to become activated, proliferate or infiltrate sites of injury. The question is precisely how these subtle differences account for the absence of mechanical allodynia and thermal hyperalgesia in nerve injured KO mice.

Macrophages are well-documented to contribute to mechanical and thermal hyperalgesia in models of neuropathic and inflammatory pain (Myers et al., 1996; Izikson et al., 2000; Liu et al., 2000; Abbadie et al., 2003; Barclay et al., 2007; Ulmann et al., 2010), but are reported to have a limited role in mechanical allodynia, since neither systemic or perineural administration of a macrophage inhibitor nor depletion or transfer of activated macrophages to the perineurium altered mechanical thresholds (Rutkowski et al., 2000; Barclay et al., 2007). This indicates that the absence of mechanical allodynia in nerve injured KO mice cannot be entirely attributed to a compromised macrophage response. However, in PNL injured mice engineered to express green fluorescent protein (GFP) in bone marrow, GFP^+ monocytes infiltrated the spinal cord, proliferated and differentiated into activated microglia (Zhang et al., 2007). The authors concluded that both resident microglia and bone marrow-derived macrophages contribute to centrally driven mechanical allodynia and are equally important targets in therapeutic treatment. It has also been shown that intraneural injection of anti-inflammatory TGF-β1 alleviated mechanical allodynia and thermal hyperalgesia by reducing the numbers of pro-inflammatory macrophages in the injured sciatic nerve (Echeverry et al., 2013). Furthermore, a recent study using TLR2 null mice supported a prominent role of peripheral macrophages in behavioural hypersensitivity and found no evidence of microglial involvement (Shi et al., 2011). Here, it was reported that thermal hyperalgesia was abolished in nerve injured TLR2 KO mice whilst mechanical allodynia was partially attenuated, correlating with a reduction in macrophage infiltration (Shi et al., 2011). Therefore, although the contribution of reactive microglial cells to mechanisms underlying mechanical allodynia is well established, there is some evidence for the involvement of macrophages, however, these cells are unlikely to be the only drivers in GPR84 nociceptive signalling.

5.2 Future directions and a critical analysis

Immunohistochemistry	
Advantages	**Disadvantages**
• Short procedure • Inexpensive • Maintains morphology of surrounding tissue • Cell numbers and IR can be quantified	• Antibodies vary in specificity and sensitivity • No standard threshold for positivity • Non-specific staining • Staining can be variable based on tissue preparation • Overlapping of fluorophore signals can lead to false positives • A limited number of antibodies can be used simultaneously • Semi-quantitative, subjective interpretation of results
Western blotting	
Advantages	**Disadvantages**
• Effectively detects and characterises proteins in small amounts • Sensitive	• Antibodies vary in specificity and sensitivity • Non-specific staining • No morphological correlation • Inadequate protein transfer time can produce false negatives • Technically demanding and time consuming • Semi-quantitative
Flow cytometry	
Advantages	**Disadvantages**
• Short procedure • Quantitative, accurate and reproducible • Distinct cell populations are defined by their size and granularity and can be sorted • Sensitive • 5-6 antibodies can be assessed simultaneously • Cell number and IR can be quantified	• Antibodies vary in specificity and sensitivity • No morphological correlation • Overlapping of fluorophore signals can lead to false positives if compensation is ineffective • A large number of cells are required • Expensive
qRT-PCR	
Advantages	**Disadvantages**
• Quantitative, accurate and reproducible • High through-put cards enables many genes to be examined simultaneously • Sensitive • Changes in the mRNA expression of cell markers and associated cytokines can be measured	• Genomic contamination or faulty reactions can lead to inaccurate quantification • Time consuming • RNA degradation means there's less/poor quality starting material • Protein verification is required • Non-specific amplification can lead to false-positives • Expensive

Table 5.1: Advantages and disadvantages of immune cell quantification techniques

The findings of this thesis support that pro-inflammatory GPR84 is a novel marker of chronic pain states primarily in macrophage cells. Hence an important extension of this work is to verify the differences in gene expression seen in the PNL model between genotypes, with a particular focus on the pro-M2 phenotype in the KO sciatic nerve. As previously mentioned quantification of the immune cell response in the PNL and CFA models was limited to the examination of two commonly used immunohistochemical markers. Therefore a range of alternative immune cell markers associated with M1/M2 polarity could be examined in WT and KO mice in models of chronic pain. However, since immunohistochemistry bears a number of technical limitations, alternative methods such as genetic profiling, western blotting and flow cytometry should be considered for quantifying the immune cell response. As presented in Table 5.1, each method possesses advantages and disadvantages and so the complementary use of more than one method is likely to be more informative and reliable. Finally, mediators that have shown reduced induction in LPS-stimulated KO macrophages should be verified *in vivo* to examine their effects on acute pain thresholds and to determine which ones contribute to GPR84-mediated nociceptive transmission.

The development of transgenic technology has enabled the robust study of single targets in a physiological context. This has led to great progression in pain research and an increase in published work featuring the mouse (Mogil, 2009). However, the KO mouse is not without its interpretational confounds. Genes tend to act in concert with one another and so gene targeting can result in compensatory up- (or even down-) regulation of other genes (Wilson and Mogil, 2001). Consequentially the observed behavioural phenotype we report could be the result of a number of developmental, physiological or behavioural processes that have altered to compensate for the null mutation. It is therefore possible that a number of phenotypical changes have occurred that are not necessarily related to the function of GPR84. Such compensatory effects may have masked any phenotypical differences between WT and KO microglia and macrophages, or may even be responsible for the absence of pain-associated behaviours rather than GPR84 itself.

Behavioural phenotypes can also be related to the genetic background of the mutant. Transgenic mice have been historically bred onto a C57BL/6 genetic background, which is not the most representative strain of pain sensitivity in a typical laboratory mouse (Mogil, 2009). Nevertheless, most gene targeting is carried out on embryonic stem cells derived from the 129 strain and are placed on a C57BL/6 background strain. Both of which differ considerably in terms of pain-related traits (Wilson and Mogil, 2001). Therefore the gene alleles surrounding the locus of interest will be derived from the 129 strain in the null

mutants and B6 strain in the WT littermates. Consequentially, any phenotypical differences observed between the WT and KO mice could be due to the null mutation or a false positive generated by differences in genetic backgrounds. However, in this case an obvious solution would be to use a B6 cell line for gene targeting to prevent background genotype effects, which has exemplified previous success (Gerlai, 2001).

To avoid the contingency of compensation compromising experimental results, more refined transgenic technology such as the inducible KO can be utilised. This allows genes to be switched on or off on demand, which facilitates the comparison of pre- and post-induction phenotypes (Gerlai, 2001). Therefore enabling the circumvention of compensatory mechanisms occuring during development that can lead to long-term changes in gene expression. However, due to the lack of pure bred backgrounds, experiments using these mice are also associated with interpretational complications (Gerlai, 2001). In our case a conventional pharmacological approach would provide a more feasible way to complement our studies and consolidate that the behavioural phenotype is a result of GPR84 deletion. Moreover, a selective agonist or antagonist would permit further *in vitro* and *in vivo* studies that directly examine the contribution of GPR84 to pain pathways.

It is worth noting that no other developmental or behavioural abnormalities were observed in GPR84 KO mice, which exhibited normal acute pain thresholds and locomotor ability. However, this does not exclude the possibility of other undetected abnormalities, especially since WT littermates alone are not necessarily adequate controls due to the potential genetic background effects. Therefore, our experimental findings could possess greater credibility with additional non-littermate WT control groups. Furthermore, throughout this thesis sham-operated or saline-treated mice have served as experimental control groups. Although these groups serve as adequate controls for experimental variability introduced by surgery, general anaesthetic and handling, the potential effects of sham surgery or intrathecal saline administration on experimental results are not accounted for. Hence additional WT and KO naïve control groups should be considered in future experiments. Although this means that more animals are required, this is ethically justified with regards to the importance of good experimental design and the capability to adequately test an experimental hypothesis.

Poorly designed studies and a failure to report methods and results appropriately is damaging to the efforts of researchers and the scientific community (Rice et al., 2013). The Animal Research: Reporting of *In Vivo* Experiments (ARRIVE) guidelines, developed by the

National Centre for the Replacement, Refinement and Reduction of Animals in Research (NC3Rs), advocate that published research should provide all necessary information to enable other researchers to critically evaluate and utilise the work. These guidelines have steadily been adopted by an increasing number of journals and institutions and it has been shown that adherence to these reporting standards reduces bias and enforces better experimental design. This will not only improve confidence in pre-clinical research but will also increase the likelihood of developing effective therapies upon translation to humans (Rice et al., 2013).

In light of these guidelines, a number of factors related to the work in this thesis should be considered. Firstly, as stated in the methods sections, age and sex-matched animals were allocated to experimental groups via the process of random selection. According to the ARRIVE guidelines this method does not provide adequate randomisation as manually selecting animals can introduce experimental bias; however, in our case this was necessary due to the limitations of an in-house transgenic colony. Even so, software-generated allocation would provide a preferable method of randomisation that we could adopt in future studies (Macleod et al., 2009). Another potentially impeding factor was the use of mixed sex animals, which introduces a number of variables such as hormonally driven differences in pain behaviours. Furthermore, the use of young and genetically identical mice is hardly a representation of the complex human chronic pain condition that is known to mainly affect women and the elderly. Likewise, the nerve injury and inflammatory models employed do not reflect the heterogeneity of clinical presentations of pain-related conditions or the associated comorbidities that many patients experience. In addition, although the outcome measures tested bear some similarity to symptoms of allodynia and hyperalgesia seen in the clinic, they do not account for spontaneous pain or the overall effect on quality of life in these patients (Andrews et al., 2012). Therefore, we could consider using elderly female mice and objective assays of innate behaviour such as spontaneous burrowing tests, alongside the conventional reflex based tests. We could also adopt alternative animal models that are more representative of the human condition in our studies.

Allocation concealment was strictly carried out in every experiment reported in this thesis by assigning each mouse an individual identification number. However, it must be noted that although the genotype and treatment group of each mouse was blinded, in some cases the treatment group was visibly evident during testing due to hind paw swelling, limping or licking behaviours. Importantly, there were no visually obvious phenotypic differences between GPR84 WT and KO mice and so the genotype of the animals always remained

unknown until blinding was broken at the end of the experiment. In the same way as the behavioural studies, immunohistochemical assessment was carried out blind to treatment and genotype. However, the analysis could be improved by implementing more objective criteria to determine cell positivity such as a particular IR threshold, in addition to our prior requirement that a cell must be co-stained with a nuclear marker.

Within the limited literature available, it is apparent that GPR84 is emerging as a functionally important receptor in fatty acid metabolism and immunoregulation, with some implications in metabolic diseases. Obesity and type 2 diabetes are associated with elevated levels of plasma FFAs, which can cause an accumulation of lipids and insulin resistance in pancreatic β-cells. Chronic exposure to FFAs may impair insulin secretion and contribute to hyper/hypoinsulinemia, which are characteristic of type 2 diabetes (Haber et al., 2003). Thus FFA-sensitive GPCRs are of particular interest in the development of therapeutic treatments against diabetes and other related disorders. In the past decade an increasing number of GPCRs have been deorphanised, leading to the identification of a number of FFA-sensitive receptors such as GPR40/FFAR1, GPR41/FFAR3, GPR42 (functional polymorph of GPR41), GPR43/FFAR2, GPR84, GPR119 and GPR120 (Ichimura et al., 2009), which respond to FFAs of particular chain lengths, as previously discussed (*Chapter 4*). Obesity and type 2 diabetes are usually accompanied by chronic low-grade metabolic inflammation that is related to immunological changes occurring in adipose tissue, liver, brain, islets and vasculature tissues in addition to changes in circulating leukocytes and their cytokine/chemokine profiles (Donath and Shoelson, 2011; Gregor and Hotamisligil, 2011).

The contribution of macrophages to low-grade metabolic inflammation is of particular interest as they are the most abundant leukocyte population in the periphery and the key effector cells in inflammation-mediated insulin resistance. Macrophages have also been implicated in a number of other human diseases including RA, cancer, IBS, MS and psoriasis (Wynn et al., 2013). Macrophages express multiple GPCRs that contribute to immunological and inflammatory processes, including the newly identified GPR84, which has received substantial interest with regards to its immunoregulatory role in obesity and diabetes. Recruitment of inflammatory macrophages to adipose tissues and the consequential release of immune mediators is believed to promote inflammation and reduce insulin sensitivity in localised cells. Thus highlighting a link between the immune system and the incidence of adiposity and diabetes. In mice subjected to a high fat diet, GPR84 mRNA was up-regulated in fat pad tissues as a result of TNF-α release from invading macrophages, indicating that GPR84 may be directly involved in exacerbating the inflammatory changes occurring to adipocytes (Nagasaki et al., 2012). GPR40 has also been associated with impaired glucose

homeostasis and is highly expressed in pancreatic β-cells, where it plays a role in FFA mediated augmentation of insulin secretion (Talukdar et al., 2011). Interestingly, supraspinal GPR40 signalling has been implicated in pain; in the formalin model, intracerebroventricular injection of a selective GPR40 agonist (GW9508) attenuated pain behaviours, indicating an endogenous anti-nociceptive role of this receptor (Nakamoto et al., 2012). So far, GPR40 is the latest FFA-sensing GPCR that has been linked to nociceptive signalling.

Painful diabetic neuropathy is one of the most prevalent complications in diabetes. Given the contribution of GPR84 signalling in chronic pain mechanisms and insulin resistance in inflamed adipocytes, it would be interesting to examine the involvement of GPR84 in diabetes. One of the most characterised models of painful diabetic neuropathy is the STZ-induced neuropathy model in *Psammomys obesus* (Fat Sand rats), which show persistent mechanical, but not thermal, hyperalgesia starting at 2 weeks post STZ injection (Wuarin-Bierman et al., 1987; Malcangio and Tomlinson, 1998). It would thus be informative to characterise pain responses and investigate the progression of obesity-induced adipocyte inflammation and insulin resistance in GPR84 transgenics. As previously discussed, the use of clinically relevant models such as the STZ-induced neuropathy model is an important step towards improving translational pain research. In addition, such approaches may reveal a critical role for GPR84 in low-grade metabolic diseases associated with chronic pain pathology. These metabolic diseases pose an increasing problem in the clinic, with the prevalence of obesity continuing to rise at alarming rates. However, encouragingly therapeutic interventions that inhibit inflammatory pathways in obesity by targeting the immune system are found to be effective and reduce the incidence of insulin sensitivity.

In conclusion, the development of effective analgesics for chronic pain states remains a major challenge. However, our comprehension of the underlying mechanisms that contribute to pain pathophysiology has improved substantially. We now appreciate that the immune system is an important player in chronic pain and many related diseases. Therefore, the identification of novel immune cell targets like GPR84 holds a promising future for the development of superior therapies and enhanced patient care.

The authors declare no conflict of interest. The identity of CNV is proprietary to GSK/Convergence Pharmaceuticals. Funding was obtained from GSK and BBSRC.

Bibliography

Abbadie C (2005) Chemokines, chemokine receptors and pain. Trends Immunol 26:529-534.

Abbadie C, Bhangoo S, De Koninck Y, Malcangio M, Melik-Parsadaniantz S, White FA (2009) Chemokines and pain mechanisms. Brain Res Rev 60:125-134.

Abbadie C, Lindia JA, Cumiskey AM, Peterson LB, Mudgett JS, Bayne EK, DeMartino JA, MacIntyre DE, Forrest MJ (2003) Impaired neuropathic pain responses in mice lacking the chemokine receptor CCR2. Proceedings of the National Academy of Sciences of the United States of America 100:7947-7952.

Ahn KS, Sethi G, Aggarwal BB (2007) Embelin, an inhibitor of X chromosome-linked inhibitor-of-apoptosis protein, blocks nuclear factor-kappaB (NF-kappaB) signaling pathway leading to suppression of NF-kappaB-regulated antiapoptotic and metastatic gene products. Molecular Pharmacology 71:209-219.

Alexander GM, van Rijn MA, van Hilten JJ, Perreault MJ, Schwartzman RJ (2005) Changes in cerebrospinal fluid levels of pro-inflammatory cytokines in CRPS. Pain 116:213-219.

Aley KO, Levine JD (1999) Role of protein kinase A in the maintenance of inflammatory pain. Journal of Neuroscience 19:2181-2186.

Aley KO, Reichling DB, Levine JD (1996) Vincristine hyperalgesia in the rat: a model of painful vincristine neuropathy in humans. Neuroscience 73:259-265.

Aley KO, McCarter G, Levine JD (1998) Nitric oxide signaling in pain and nociceptor sensitization in the rat. Journal of Neuroscience 18:7008-7014.

Aloisi F, Penna G, Cerase J, Menendez Iglesias B, Adorini L (1997) IL-12 production by central nervous system microglia is inhibited by astrocytes. Journal of Immunology 159:1604-1612.

Alvarez FJ, Villalba RM, Carr PA, Grandes P, Somohano PM (2000) Differential distribution of metabotropic glutamate receptors 1a, 1b, and 5 in the rat spinal cord. Journal of Comparative Neurology 422:464-487.

Amaya F, Shimosato G, Nagano M, Ueda M, Hashimoto S, Tanaka Y, Suzuki H, Tanaka M (2004) NGF and GDNF differentially regulate TRPV1 expression that contributes to development of inflammatory thermal hyperalgesia. European Journal of Neuroscience 20:2303-2310.

Amaya F, Wang H, Costigan M, Allchorne AJ, Hatcher JP, Egerton J, Stean T, Morisset V, Grose D, Gunthorpe MJ, Chessell IP, Tate S, Green PJ, Woolf CJ (2006) The voltage-gated sodium channel Na(v)1.9 is an effector of peripheral inflammatory pain hypersensitivity. Journal of Neuroscience 26:12852-12860.

Amir R, Kocsis JD, Devor M (2005) Multiple interacting sites of ectopic spike electrogenesis in primary sensory neurons. Journal of Neuroscience 25:2576-2585.

Anand P, Shenoy R, Palmer JE, Baines AJ, Lai RY, Robertson J, Bird N, Ostenfeld T, Chizh BA (2011) Clinical trial of the p38 MAP kinase inhibitor dilmapimod in neuropathic pain following nerve injury. Eur J Pain 15:1040-1048.

Andersson PB, Perry VH, Gordon S (1992a) Intracerebral injection of proinflammatory cytokines or leukocyte chemotaxins induces minimal myelomonocytic cell recruitment to the parenchyma of the central nervous system. Journal of Experimental Medicine 176:255-259.

Andersson PB, Perry VH, Gordon S (1992b) The acute inflammatory response to lipopolysaccharide in CNS parenchyma differs from that in other body tissues. Neuroscience 48:169-186.

Andrade EL, Meotti FC, Calixto JB (2012) TRPA1 antagonists as potential analgesic drugs. Pharmacology and Therapeutics 133:189-204.

Andres C, Meyer S, Dina OA, Levine JD, Hucho T (2010) Quantitative automated microscopy (QuAM) elucidates growth factor specific signalling in pain sensitization. Mol Pain 6:98.

Andrews N, Harper S, Issop Y, Rice AS (2011) Novel, nonreflex tests detect analgesic action in rodents at clinically relevant concentrations. Annals of the New York Academy of Sciences 1245:11-13.

Andrews N, Legg E, Lisak D, Issop Y, Richardson D, Harper S, Pheby T, Huang W, Burgess G, Machin I, Rice AS (2012) Spontaneous burrowing behaviour in the rat is reduced by peripheral nerve injury or inflammation associated pain. Eur J Pain 16:485-495.

Antal M, Fukazawa Y, Eordogh M, Muszil D, Molnar E, Itakura M, Takahashi M, Shigemoto R (2008) Numbers, densities, and colocalization of AMPA- and NMDA-type glutamate receptors at individual synapses in the superficial spinal dorsal horn of rats. Journal of Neuroscience 28:9692-9701.

Antunes-Martins A, Perkins JR, Lees J, Hildebrandt T, Orengo C, Bennett DL (2013) Systems biology approaches to finding novel pain mediators. Wiley Interdiscip Rev Syst Biol Med 5:11-35.

Arai KI, Lee F, Miyajima A, Miyatake S, Arai N, Yokota T (1990) Cytokines: coordinators of immune and inflammatory responses. Annual Review of Biochemistry 59:783-836.

Aravalli RN, Peterson PK, Lokensgard JR (2007) Toll-like receptors in defense and damage of the central nervous system. J Neuroimmune Pharmacol 2:297-312.

Aronoff DM, Canetti C, Serezani CH, Luo M, Peters-Golden M (2005) Cutting edge: macrophage inhibition by cyclic AMP (cAMP): differential roles of protein kinase A and exchange protein directly activated by cAMP-1. Journal of Immunology 174:595-599.

Aronoff DM, Carstens JK, Chen GH, Toews GB, Peters-Golden M (2006) Short communication: differences between macrophages and dendritic cells in the cyclic

AMP-dependent regulation of lipopolysaccharide-induced cytokine and chemokine synthesis. Journal of Interferon and Cytokine Research 26:827-833.

Ato M, Nakano H, Kakiuchi T, Kaye PM (2004) Localization of marginal zone macrophages is regulated by C-C chemokine ligands 21/19. Journal of Immunology 173:4815-4820.

Aumeerally N, Allen G, Sawynok J (2004) Glutamate-evoked release of adenosine and regulation of peripheral nociception. Neuroscience 127:1-11.

Austin PJ, Moalem-Taylor G (2010) The neuro-immune balance in neuropathic pain: involvement of inflammatory immune cells, immune-like glial cells and cytokines. Journal of Neuroimmunology 229:26-50.

Averill S, McMahon SB, Clary DO, Reichardt LF, Priestley JV (1995) Novel classes of responsive and unresponsive C nociceptors in human skin. Eur J Neurosci 7:1484-1494.

Backonja MM, Coe CL, Muller DA, Schell K (2008) Altered cytokine levels in the blood and cerebrospinal fluid of chronic pain patients. Journal of Neuroimmunology 195:157-163.

Baek YH, Choi DY, Yang HI, Park DS (2005) Analgesic effect of electroacupuncture on inflammatory pain in the rat model of collagen-induced arthritis: mediation by cholinergic and serotonergic receptors. Brain Research 1057:181-185.

Baeuerle PA, Henkel T (1994) Function and Activation of NF-kappaB in the Immune System. Annual Review of Immunology 12:141-179.

Bajetto A, Bonavia R, Barbero S, Schettini G (2002) Characterization of chemokines and their receptors in the central nervous system: physiopathological implications. Journal of Neurochemistry 82:1311-1329.

Ballinger MN, Welliver T, Straight S, Peters-Golden M, Swanson JA (2010) Transient increase in cyclic AMP localized to macrophage phagosomes. PLoS One 5:1362-1371.

Banati RB, Cagnin A, Brooks DJ, Gunn RN, Myers R, Jones T, Birch R, Anand P (2001) Long-term trans-synaptic glial responses in the human thalamus after peripheral nerve injury. Neuroreport 12:3439-3442.

Barclay J, Clark AK, Ganju P, Gentry C, Patel S, Wotherspoon G, Buxton F, Song C, Ullah J, Winter J, Fox A, Bevan S, Malcangio M (2007) Role of the cysteine protease cathepsin S in neuropathic hyperalgesia. Pain 130:225-234.

Baron R, Binder A, Wasner G (2010) Neuropathic pain: diagnosis, pathophysiological mechanisms, and treatment. Lancet Neurol 9:807-819.

Basbaum AI, Bautista DM, Scherrer G, Julius D (2009) Cellular and molecular mechanisms of pain. Cell 139:267-284.

Bastos KR, Alvarez JM, Marinho CR, Rizzo LV, Lima MR (2002) Macrophages from IL-12p40-deficient mice have a bias toward the M2 activation profile. Journal of Leukocyte Biology 71:271-278.

Bautista DM, Siemens J, Glazer JM, Tsuruda PR, Basbaum AI, Stucky CL, Jordt SE, Julius D (2007) The menthol receptor TRPM8 is the principal detector of environmental cold. Nature 448:204-208.

Bautista DM, Jordt SE, Nikai T, Tsuruda PR, Read AJ, Poblete J, Yamoah EN, Basbaum AI, Julius D (2006) TRPA1 mediates the inflammatory actions of environmental irritants and proalgesic agents. Cell 124:1269-1282.

Bazan JF, Timans JC, Kastelein RA (1996) A newly defined interleukin-1? Nature 379:591.

Beggs S, Currie G, Salter MW, Fitzgerald M, Walker SM (2012) Priming of adult pain responses by neonatal pain experience: maintenance by central neuroimmune activity. Brain 135:404-417.

Benamar K, Geller EB, Adler MW (2008) Elevated level of the proinflammatory chemokine, RANTES/CCL5, in the periaqueductal grey causes hyperalgesia in rats. European Journal of Pharmacology 592:93-95.

Benjamini Y, Drai D, Elmer G, Kafkafi N, Golani I (2001) Controlling the false discovery rate in behavior genetics research. Behavioural Brain Research 125:279-284.

Bennett DL, Boucher TJ, Armanini MP, Poulsen KT, Michael GJ, Priestley JV, Phillips HS, McMahon SB, Shelton DL (2000) The glial cell line-derived neurotrophic factor family receptor components are differentially regulated within sensory neurons after nerve injury. Journal of Neuroscience 20:427-437.

Bennett DL, Boucher TJ, Michael GJ, Popat RJ, Malcangio M, Averill SA, Poulsen KT, Priestley JV, Shelton DL, McMahon SB (2006) Artemin has potent neurotrophic actions on injured C-fibres. Journal of the Peripheral Nervous System 11:330-345.

Bennett GJ (1999) Does a neuroimmune interaction contribute to the genesis of painful peripheral neuropathies? Proceedings of the National Academy of Sciences of the United States of America 96:7737-7738.

Bennett GJ, Xie YK (1988) A peripheral mononeuropathy in rat that produces disorders of pain sensation like those seen in man. Pain 33:87-107.

Bessou P, Perl ER (1969) Response of cutaneous sensory units with unmyelinated fibers to noxious stimuli. Journal of Neurophysiology 32:1025-1043.

Bhattacharyya S, Gill R, Chen ML, Zhang F, Linhardt RJ, Dudeja PK, Tobacman JK (2008) Toll-like receptor 4 mediates induction of the Bcl10-NFkappaB-interleukin-8 inflammatory pathway by carrageenan in human intestinal epithelial cells. Journal of Biological Chemistry 283:10550-10558.

Bhave G, Zhu W, Wang H, Brasier DJ, Oxford GS, Gereau RWt (2002) cAMP-dependent protein kinase regulates desensitization of the capsaicin receptor (VR1) by direct phosphorylation. Neuron 35:721-731.

Bhave G, Hu HJ, Glauner KS, Zhu W, Wang H, Brasier DJ, Oxford GS, Gereau RWt (2003) Protein kinase C phosphorylation sensitizes but does not activate the capsaicin receptor transient receptor potential vanilloid 1 (TRPV1). Proceedings of the National Academy of Sciences of the United States of America 100:12480-12485.

Biber K, Tsuda M, Tozaki-Saitoh H, Tsukamoto K, Toyomitsu E, Masuda T, Boddeke H, Inoue K (2011) Neuronal CCL21 up-regulates microglia P2X4 expression and initiates neuropathic pain development. The EMBO Journal 30:1864-1873.

Binshtok AM, Wang H, Zimmermann K, Amaya F, Vardeh D, Shi L, Brenner GJ, Ji RR, Bean BP, Woolf CJ, Samad TA (2008) Nociceptors Are Interleukin-1 Sensors. Journal of Neuroscience 28:14062-14073.

Bishnoi M, Bosgraaf CA, Abooj M, Zhong L, Premkumar LS (2011) Streptozotocin-induced early thermal hyperalgesia is independent of glycemic state of rats: role of transient receptor potential vanilloid 1(TRPV1) and inflammatory mediators. Mol Pain 7:52.

Blackbeard J, Wallace VC, O'Dea KP, Hasnie F, Segerdahl A, Pheby T, Field MJ, Takata M, Rice AS (2012) The correlation between pain-related behaviour and spinal microgliosis in four distinct models of peripheral neuropathy. Eur J Pain 16:1357-1367.

Boddeke EW, Meigel I, Frentzel S, Gourmala NG, Harrison JK, Buttini M, Spleiss O, Gebicke-Harter P (1999) Cultured rat microglia express functional beta-chemokine receptors. Journal of Neuroimmunology 98:176-184.

Bogdan C (2001) Nitric oxide and the immune response. Nat Immunol 2:907-916.

Bogen O, Joseph EK, Chen X, Levine JD (2008) GDNF hyperalgesia is mediated by PLCgamma, MAPK/ERK, PI3K, CDK5 and Src family kinase signaling and dependent on the IB4-binding protein versican. European Journal of Neuroscience 28:12-19.

Boivin A, Pineau I, Barrette B, Filali M, Vallieres N, Rivest S, Lacroix S (2007) Toll-like receptor signaling is critical for Wallerian degeneration and functional recovery after peripheral nerve injury. Journal of Neuroscience 27:12565-12576.

Bos JL (2006) Epac proteins: multi-purpose cAMP targets. Trends in Biochemical Sciences 31:680-686.

Bouchard C, Page J, Bedard A, Tremblay P, Vallieres L (2007) G protein-coupled receptor 84, a microglia-associated protein expressed in neuroinflammatory conditions. Glia 55:790-800.

Boucher TJ (2000) Potent Analgesic Effects of GDNF in Neuropathic Pain States. Science 290:124-127.

Bouhassira D, Lanteri-Minet M, Attal N, Laurent B, Touboul C (2008) Prevalence of chronic pain with neuropathic characteristics in the general population. Pain 136:380-387.

Bourne HR, Lichtenstein LM, Melmon KL, Henney CS, Weinstein Y, Shearer GM (1974) Modulation of inflammation and immunity by cyclic AMP. Science 184:19-28.

Brack A, Rittner HL, Machelska H, Leder K, Mousa SA, Schafer M, Stein C (2004) Control of inflammatory pain by chemokine-mediated recruitment of opioid-containing polymorphonuclear cells. Pain 112:229-238.

Bradbury EJ, Burnstock G, McMahon SB (1998) P2X3 is expressed by DRG neurons that terminate in inner lamina II. Mol Cell Neurosci 12:256-268.

Braz JM, Nassar MA, Wood JN, Basbaum AI (2005) Parallel "pain" pathways arise from subpopulations of primary afferent nociceptor. Neuron 47:787-793.

Breivik H, Collett B, Ventafridda V, Cohen R, Gallacher D (2006) Survey of chronic pain in Europe: prevalence, impact on daily life, and treatment. Eur J Pain 10:287-333.

Bridges D, Thompson SW, Rice AS (2001) Mechanisms of neuropathic pain. British Journal of Anaesthesia 87:12-26.

Bridges D, Rice AS, Egertova M, Elphick MR, Winter J, Michael GJ (2003) Localisation of cannabinoid receptor 1 in rat dorsal root ganglion using in situ hybridisation and immunohistochemistry. Neuroscience 119:803-812.

Brisby H, Olmarker K, Larsson K, Nutu M, Rydevik B (2002) Proinflammatory cytokines in cerebrospinal fluid and serum in patients with disc herniation and sciatica. European Spine Journal 11:62-66.

Briscoe CP et al. (2003) The orphan G protein-coupled receptor GPR40 is activated by medium and long chain fatty acids. Journal of Biological Chemistry 278:11303-11311.

Bronte V, Zanovello P (2005) Regulation of immune responses by L-arginine metabolism. Nat Rev Immunol 5:641-654.

Brown AJ et al. (2003) The Orphan G protein-coupled receptors GPR41 and GPR43 are activated by propionate and other short chain carboxylic acids. Journal of Biological Chemistry 278:11312-11319.

Bryn T, Mahic M, Enserink JM, Schwede F, Aandahl EM, Tasken K (2006) The cyclic AMP-Epac1-Rap1 pathway is dissociated from regulation of effector functions in monocytes but acquires immunoregulatory function in mature macrophages. Journal of Immunology 176:7361-7370.

Burgos E, Gomez-Nicola D, Pascual D, Martin MI, Nieto-Sampedro M, Goicoechea C (2012) Cannabinoid agonist WIN 55,212-2 prevents the development of paclitaxel-induced peripheral neuropathy in rats. Possible involvement of spinal glial cells. European Journal of Pharmacology 682:62-72.

Butt AM (2011) ATP: a ubiquitous gliotransmitter integrating neuron-glial networks. Seminars in Cell and Developmental Biology 22:205-213.

Cabrera-Vera TM, Vanhauwe J, Thomas TO, Medkova M, Preininger A, Mazzoni MR, Hamm HE (2003) Insights into G protein structure, function, and regulation. Endocrine Reviews 24:765-781.

Caggiano AO, Kraig RP (1999) Prostaglandin E receptor subtypes in cultured rat microglia and their role in reducing lipopolysaccharide-induced interleukin-1beta production. Journal of Neurochemistry 72:565-575.

Cahill CM, Dray A, Coderre TJ (2003) Enhanced thermal antinociceptive potency and anti-allodynic effects of morphine following spinal administration of endotoxin. Brain Research 960:209-218.

Caielli S, Banchereau J, Pascual V (2012) Neutrophils come of age in chronic inflammation. Current Opinion in Immunology 24:671-677.

Calvo M, Bennett DL (2012) The mechanisms of microgliosis and pain following peripheral nerve injury. Experimental Neurology 234:271-282.

Calvo M, Dawes JM, Bennett DL (2012) The role of the immune system in the generation of neuropathic pain. The Lancet Neurology 11:629-642.

Calvo M, Zhu N, Grist J, Ma Z, Loeb JA, Bennett DL (2011) Following nerve injury neuregulin-1 drives microglial proliferation and neuropathic pain via the MEK/ERK pathway. Glia 59:554-568.

Calvo M, Zhu N, Tsantoulas C, Ma Z, Grist J, Loeb JA, Bennett DL (2010) Neuregulin-ErbB signaling promotes microglial proliferation and chemotaxis contributing to microgliosis and pain after peripheral nerve injury. Journal of Neuroscience 30:5437-5450.

Campana WM (2007) Schwann cells: activated peripheral glia and their role in neuropathic pain. Brain, Behavior, and Immunity 21:522-527.

Canetti C, Silva JS, Ferreira SH, Cunha FQ (2001) Tumour necrosis factor-alpha and leukotriene B(4) mediate the neutrophil migration in immune inflammation. British Journal of Pharmacology 134:1619-1628.

Cao L, DeLeo JA (2008) CNS-infiltrating CD4+ T lymphocytes contribute to murine spinal nerve transection-induced neuropathic pain. European Journal of Immunology 38:448-458.

Cao YQ (2006) Voltage-gated calcium channels and pain. Pain 126:5-9.

Cao Z, Henzel WJ, Gao X (1996a) IRAK: a kinase associated with the interleukin-1 receptor. Science 271:1128-1131.

Cao Z, Xiong J, Takeuchi M, Kurama T, Goeddel DV (1996b) TRAF6 is a signal transducer for interleukin-1. Nature 383:443-446.

Carafoli E (1994) Biogenesis: plasma membrane calcium ATPase: 15 years of work on the purified enzyme. FASEB Journal 8:993-1002.

Cardaba CM, Mueller A (2009) Distinct modes of molecular regulation of CCL3 induced calcium flux in monocytic cells. Biochemical Pharmacology 78:974-982.

Cardenas LM, Cardenas CG, Scroggs RS (2001) 5HT increases excitability of nociceptor-like rat dorsal root ganglion neurons via cAMP-coupled TTX-resistant Na(+) channels. Journal of Neurophysiology 86:241-248.

Caterina MJ (2000) Impaired Nociception and Pain Sensation in Mice Lacking the Capsaicin Receptor. Science 288:306-313.

Caterina MJ, Schumacher MA, Tominaga M, Rosen TA, Levine JD, Julius D (1997) The capsaicin receptor: a heat-activated ion channel in the pain pathway. Nature 389:816-824.

Chang CI, Liao JC, Kuo L (1998) Arginase modulates nitric oxide production in activated macrophages. American Journal of Physiology 274:342-348.

Chang J, Cherney ML, Moyer JA, Lewis AJ (1984) Effect of forskolin on prostaglandin synthesis by mouse resident peritoneal macrophages. European Journal of Pharmacology 103:303-312.

Chaplan SR, Bach FW, Pogrel JW, Chung JM, Yaksh TL (1994) Quantitative assessment of tactile allodynia in the rat paw. Journal of Neuroscience Methods 53:55-63.

Chapman GA, Moores K, Harrison D, Campbell CA, Stewart BR, Strijbos PJ (2000) Fractalkine cleavage from neuronal membranes represents an acute event in the inflammatory response to excitotoxic brain damage. Journal of Neuroscience 20:RC87.

Chapman RW, Phillips JE, Hipkin RW, Curran AK, Lundell D, Fine JS (2009) CXCR2 antagonists for the treatment of pulmonary disease. Pharmacology and Therapeutics 121:55-68.

Charo IF, Ransohoff RM (2006) The many roles of chemokines and chemokine receptors in inflammation. New England Journal of Medicine 354:610-621.

Chen CC, Chiu KT, Sun YT, Chen WC (1999) Role of the cyclic AMP-protein kinase A pathway in lipopolysaccharide-induced nitric oxide synthase expression in RAW 264.7 macrophages. Involvement of cyclooxygenase-2. Journal of Biological Chemistry 274:31559-31564.

Chen IF, Khan J, Noma N, Hadlaq E, Teich S, Benoliel R, Eliav E (2013) Anti-nociceptive effect of IL-12p40 in a rat model of neuropathic pain. Cytokine 62:401-406.

Chessell IP, Hatcher JP, Bountra C, Michel AD, Hughes JP, Green P, Egerton J, Murfin M, Richardson J, Peck WL, Grahames CB, Casula MA, Yiangou Y, Birch R, Anand P, Buell GN (2005) Disruption of the P2X7 purinoceptor gene abolishes chronic inflammatory and neuropathic pain. Pain 114:386-396.

Chien LY, Cheng JK, Chu D, Cheng CF, Tsaur ML (2007) Reduced expression of A-type potassium channels in primary sensory neurons induces mechanical hypersensitivity. Journal of Neuroscience 27:9855-9865.

Chiu IM, von Hehn CA, Woolf CJ (2012) Neurogenic inflammation and the peripheral nervous system in host defense and immunopathology. Nature Neuroscience 15:1063-1067.

Chuang HH, Prescott ED, Kong H, Shields S, Jordt SE, Basbaum AI, Chao MV, Julius D (2001) Bradykinin and nerve growth factor release the capsaicin receptor from PtdIns(4,5)P2-mediated inhibition. Nature 411:957-962.

Clapham DE (1995) Calcium signaling. Cell 80:259-268.

Clark-Lewis I, Schumacher C, Baggiolini M, Moser B (1991) Structure-activity relationships of interleukin-8 determined using chemically synthesized analogs. Critical role of NH2-terminal residues and evidence for uncoupling of neutrophil chemotaxis, exocytosis, and receptor binding activities. Journal of Biological Chemistry 266:23128-23134.

Clark AK, Malcangio M (2012) Microglial signalling mechanisms: Cathepsin S and Fractalkine. Experimental Neurology 234:283-292.

Clark AK, Yip PK, Malcangio M (2009) The liberation of fractalkine in the dorsal horn requires microglial cathepsin S. Journal of Neuroscience 29:6945-6954.

Clark AK, Staniland AA, Malcangio M (2011) Fractalkine/CX3CR1 signalling in chronic pain and inflammation. Curr Pharm Biotechnol 12:1707-1714.

Clark AK, Gentry C, Bradbury EJ, McMahon SB, Malcangio M (2007a) Role of spinal microglia in rat models of peripheral nerve injury and inflammation. Eur J Pain 11:223-230.

Clark AK, Wodarski R, Guida F, Sasso O, Malcangio M (2010a) Cathepsin S release from primary cultured microglia is regulated by the P2X7 receptor. Glia 58:1710-1726.

Clark AK, Grist J, Al-Kashi A, Perretti M, Malcangio M (2012) Spinal cathepsin S and fractalkine contribute to chronic pain in the collagen-induced arthritis model. Arthritis and Rheumatism 64:2038-2047.

Clark AK, D'Aquisto F, Gentry C, Marchand F, McMahon SB, Malcangio M (2006) Rapid co-release of interleukin 1beta and caspase 1 in spinal cord inflammation. Journal of Neurochemistry 99:868-880.

Clark AK, Staniland AA, Marchand F, Kaan TK, McMahon SB, Malcangio M (2010b) P2X7-dependent release of interleukin-1beta and nociception in the spinal cord following lipopolysaccharide. Journal of Neuroscience 30:573-582.

Clark AK, Yip PK, Grist J, Gentry C, Staniland AA, Marchand F, Dehvari M, Wotherspoon G, Winter J, Ullah J, Bevan S, Malcangio M (2007b) Inhibition of spinal microglial cathepsin S for the reversal of neuropathic pain. Proceedings of the National Academy of Sciences of the United States of America 104:10655-10660.

Clatworthy AL, Illich PA, Castro GA, Walters ET (1995) Role of peri-axonal inflammation in the development of thermal hyperalgesia and guarding behavior in a rat model of neuropathic pain. Neuroscience Letters 184:5-8.

Cloez-Tayarani I, Changeux JP (2007) Nicotine and serotonin in immune regulation and inflammatory processes: a perspective. Journal of Leukocyte Biology 81:599-606.

Cockayne DA, Dunn PM, Zhong Y, Rong W, Hamilton SG, Knight GE, Ruan HZ, Ma B, Yip P, Nunn P, McMahon SB, Burnstock G, Ford AP (2005) P2X2 knockout mice and P2X2/P2X3 double knockout mice reveal a role for the P2X2 receptor subunit in mediating multiple sensory effects of ATP. J Physiol 567:621-639.

Coggeshall RE, Zhou S, Carlton SM (1997) Opioid receptors on peripheral sensory axons. Brain Research 764:126-132.

Coggeshall RE, Tate S, Carlton SM (2004) Differential expression of tetrodotoxin-resistant sodium channels Nav1.8 and Nav1.9 in normal and inflamed rats. Neuroscience Letters 355:45-48.

Colburn RW, Rickman AJ, DeLeo JA (1999) The effect of site and type of nerve injury on spinal glial activation and neuropathic pain behavior. Experimental Neurology 157:289-304.

Colburn RW, DeLeo JA, Rickman AJ, Yeager MP, Kwon P, Hickey WF (1997) Dissociation of microglial activation and neuropathic pain behaviors following peripheral nerve injury in the rat. Journal of Neuroimmunology 79:163-175.

Colton CA, Jia M, Li MX, Gilbert DL (1994) K+ modulation of microglial superoxide production: involvement of voltage-gated Ca2+ channels. American Journal of Physiology 266:C1650-1655.

Comerford I, Harata-Lee Y, Bunting MD, Gregor C, Kara EE, McColl SR (2013) A myriad of functions and complex regulation of the CCR7/CCL19/CCL21 chemokine axis in the adaptive immune system. Cytokine & Growth Factor Reviews 24:269-283.

Conti G, Scarpini E, Baron P, Livraghi S, Tiriticco M, Bianchi R, Vedeler C, Scarlato G (2002) Macrophage infiltration and death in the nerve during the early phases of experimental diabetic neuropathy: a process concomitant with endoneurial induction of IL-1beta and p75NTR. Journal of the Neurological Sciences 195:35-40.

Coste B, Crest M, Delmas P (2007) Pharmacological dissection and distribution of NaN/Nav1.9, T-type Ca2+ currents, and mechanically activated cation currents in different populations of DRG neurons. J Gen Physiol 129:57-77.

Costigan M, Scholz J, Woolf CJ (2009a) Neuropathic pain: a maladaptive response of the nervous system to damage. Annual Review of Neuroscience 32:1-32.

Costigan M, Befort K, Karchewski L, Griffin RS, D'Urso D, Allchorne A, Sitarski J, Mannion JW, Pratt RE, Woolf CJ (2002) Replicate high-density rat genome oligonucleotide microarrays reveal hundreds of regulated genes in the dorsal root ganglion after peripheral nerve injury. BMC Neurosci 3:16.

Costigan M, Moss A, Latremoliere A, Johnston C, Verma-Gandhu M, Herbert TA, Barrett L, Brenner GJ, Vardeh D, Woolf CJ, Fitzgerald M (2009b) T-cell infiltration and signaling in the adult dorsal spinal cord is a major contributor to neuropathic pain-like hypersensitivity. Journal of Neuroscience 29:14415-14422.

Coull JA, Boudreau D, Bachand K, Prescott SA, Nault F, Sik A, De Koninck P, De Koninck Y (2003) Trans-synaptic shift in anion gradient in spinal lamina I neurons as a mechanism of neuropathic pain. Nature 424:938-942.

Coull JA, Beggs S, Boudreau D, Boivin D, Tsuda M, Inoue K, Gravel C, Salter MW, De Koninck Y (2005) BDNF from microglia causes the shift in neuronal anion gradient underlying neuropathic pain. Nature 438:1017-1021.

Coutinho AE, Chapman KE (2011) The anti-inflammatory and immunosuppressive effects of glucocorticoids, recent developments and mechanistic insights. Molecular and Cellular Endocrinology 335:2-13.

Cox JJ, Reimann F, Nicholas AK, Thornton G, Roberts E, Springell K, Karbani G, Jafri H, Mannan J, Raashid Y, Al-Gazali L, Hamamy H, Valente EM, Gorman S, Williams R, McHale DP, Wood JN, Gribble FM, Woods CG (2006) An SCN9A channelopathy causes congenital inability to experience pain. Nature 444:894-898.

Cui JG, Holmin S, Mathiesen T, Meyerson BA, Linderoth B (2000) Possible role of inflammatory mediators in tactile hypersensitivity in rat models of mononeuropathy. Pain 88:239-248.

Cunha FQ, Lorenzetti BB, Poole S, Ferreira SH (1991) Interleukin-8 as a mediator of sympathetic pain. British Journal of Pharmacology 104:765-767.

Cunha FQ, Poole S, Lorenzetti BB, Ferreira SH (1992) The pivotal role of tumour necrosis factor alpha in the development of inflammatory hyperalgesia. British Journal of Pharmacology 107:660-664.

Cunha JM, Cunha FQ, Poole S, Ferreira SH (2000) Cytokine-mediated inflammatory hyperalgesia limited by interleukin-1 receptor antagonist. British Journal of Pharmacology 130:1418-1424.

Cunha TM, Verri WA, Jr., Schivo IR, Napimoga MH, Parada CA, Poole S, Teixeira MM, Ferreira SH, Cunha FQ (2008a) Crucial role of neutrophils in the development of mechanical inflammatory hypernociception. Journal of Leukocyte Biology 83:824-832.

Cunha TM, Barsante MM, Guerrero AT, Verri WA, Jr., Ferreira SH, Coelho FM, Bertini R, Di Giacinto C, Allegretti M, Cunha FQ, Teixeira MM (2008b) Treatment with DF 2162, a non-competitive allosteric inhibitor of CXCR1/2, diminishes neutrophil influx and inflammatory hypernociception in mice. British Journal of Pharmacology 154:460-470.

D'Mello R, Dickenson AH (2008) Spinal cord mechanisms of pain. British Journal of Anaesthesia 101:8-16.

Dai Y, Fukuoka T, Wang H, Yamanaka H, Obata K, Tokunaga A, Noguchi K (2004) Contribution of sensitized P2X receptors in inflamed tissue to the mechanical hypersensitivity revealed by phosphorylated ERK in DRG neurons. Pain 108:258-266.

Daulhac L, Mallet C, Courteix C, Etienne M, Duroux E, Privat AM, Eschalier A, Fialip J (2006) Diabetes-induced mechanical hyperalgesia involves spinal mitogen-activated protein kinase activation in neurons and microglia via N-methyl-D-aspartate-dependent mechanisms. Molecular Pharmacology 70:1246-1254.

David S, Kroner A (2011) Repertoire of microglial and macrophage responses after spinal cord injury. Nat Rev Neurosci 12:388-399.

Davies AL, Hayes KC, Dekaban GA (2007) Clinical correlates of elevated serum concentrations of cytokines and autoantibodies in patients with spinal cord injury. Archives of Physical Medicine and Rehabilitation 88:1384-1393.

Dawes JM, Calvo M, Perkins JR, Paterson KJ, Kiesewetter H, Hobbs C, Kaan TK, Orengo C, Bennett DL, McMahon SB (2011) CXCL5 mediates UVB irradiation-induced pain. Sci Transl Med 3:90.

De Castro Costa M, De Sutter P, Gybels J, Van Hees J (1981) Adjuvant-induced arthritis in rats: a possible animal model of chronic pain. Pain 10:173-185.

Decosterd I, Woolf CJ (2000) Spared nerve injury: an animal model of persistent peripheral neuropathic pain. Pain 87:149-158.

Del Valle L, Schwartzman RJ, Alexander G (2009) Spinal cord histopathological alterations in a patient with longstanding complex regional pain syndrome. Brain, Behavior, and Immunity 23:85-91.

DeLeo JA, Yezierski RP (2001) The role of neuroinflammation and neuroimmune activation in persistent pain. Pain 90:1-6.

DeLeo JA, Colburn RW, Nichols M, Malhotra A (1996) Interleukin-6-mediated hyperalgesia/allodynia and increased spinal IL-6 expression in a rat mononeuropathy model. Journal of Interferon and Cytokine Research 16:695-700.

Di Virgilio F, Steinberg TH, Swanson JA, Silverstein SC (1988) Fura-2 secretion and sequestration in macrophages. A blocker of organic anion transport reveals that these processes occur via a membrane transport system for organic anions. Journal of Immunology 140:915-920.

Dib-Hajj SD, Fjell J, Cummins TR, Zheng Z, Fried K, LaMotte R, Black JA, Waxman SG (1999) Plasticity of sodium channel expression in DRG neurons in the chronic constriction injury model of neuropathic pain. Pain 83:591-600.

Dickenson AH, Sullivan AF (1987) Peripheral origins and central modulation of subcutaneous formalin-induced activity of rat dorsal horn neurones. Neuroscience Letters 83:207-211.

Dixon WJ (1980) Efficient analysis of experimental observations. Annual Review of Pharmacology and Toxicology 20:441-462.

Djouhri L, Lawson SN (2004) Abeta-fiber nociceptive primary afferent neurons: a review of incidence and properties in relation to other afferent A-fiber neurons in mammals. Brain Research Brain Research Reviews 46:131-145.

Donath MY, Shoelson SE (2011) Type 2 diabetes as an inflammatory disease. Nat Rev Immunol 11:98-107.

Dowdall T, Robinson I, Meert TF (2005) Comparison of five different rat models of peripheral nerve injury. Pharmacology, Biochemistry and Behavior 80:93-108.

Doyle CA, Hunt SP (1999) Substance P receptor (neurokinin-1)-expressing neurons in lamina I of the spinal cord encode for the intensity of noxious stimulation: a c-Fos study in rat. Neuroscience 89:17-28.

Doyle SL, O'Neill LA (2006) Toll-like receptors: from the discovery of NFkappaB to new insights into transcriptional regulations in innate immunity. Biochemical Pharmacology 72:1102-1113.

Drel VR, Lupachyk S, Shevalye H, Vareniuk I, Xu W, Zhang J, Delamere NA, Shahidullah M, Slusher B, Obrosova IG (2010) New therapeutic and biomarker discovery for peripheral diabetic neuropathy: PARP inhibitor, nitrotyrosine, and tumor necrosis factor-{alpha}. Endocrinology 151:2547-2555.

Dubuisson D, Dennis SG (1977) The formalin test: a quantitative study of the analgesic effects of morphine, meperidine, and brain stem stimulation in rats and cats. Pain 4:161-174.

Durrenberger PF, Facer P, Casula MA, Yiangou Y, Gray RA, Chessell IP, Day NC, Collins SD, Bingham S, Wilson AW, Elliot D, Birch R, Anand P (2006) Prostanoid receptor EP1 and Cox-2 in injured human nerves and a rat model of nerve injury: a time-course study. BMC Neurol 6:1.

Dworkin RH et al. (2010) Recommendations for the pharmacological management of neuropathic pain: an overview and literature update. Mayo Clinic Proceedings 85:S3-14.

Echeverry S, Wu Y, Zhang J (2013) Selectively reducing cytokine/chemokine expressing macrophages in injured nerves impairs the development of neuropathic pain. Experimental Neurology 240:205-218.

Eddy NB, Leimbach D (1953) Synthetic analgesics. II. Dithienylbutenyl- and dithienylbutylamines. Journal of Pharmacology and Experimental Therapeutics 107:385-393.

Eder C (2005) Regulation of microglial behavior by ion channel activity. Journal of Neuroscience Research 81:314-321.

Elzi DJ, Bjornsen AJ, MacKenzie T, Wyman TH, Silliman CC (2001) Ionomycin causes activation of p38 and p42/44 mitogen-activated protein kinases in human neutrophils. Am J Physiol Cell Physiol 281:350-360.

Empl M, Renaud S, Erne B, Fuhr P, Straube A, Schaeren-Wiemers N, Steck AJ (2001) TNF-alpha expression in painful and nonpainful neuropathies. Neurology 56:1371-1377.

Evans RM, Barish GD, Wang YX (2004) PPARs and the complex journey to obesity. Nature Medicine 10:355-361.

Fan H, Williams DL, Zingarelli B, Breuel KF, Teti G, Tempel GE, Spicher K, Boulay G, Birnbaumer L, Halushka PV, Cook JA (2007) Differential regulation of lipopolysaccharide and Gram-positive bacteria induced cytokine and chemokine production in macrophages by Galpha(i) proteins. Immunology 122:116-123.

Fang M, Wang Y, He QH, Sun YX, Deng LB, Wang XM, Han JS (2003) Glial cell line-derived neurotrophic factor contributes to delayed inflammatory hyperalgesia in adjuvant rat pain model. Neuroscience 117:503-512.

Farber K, Kettenmann H (2006a) Functional role of calcium signals for microglial function. Glia 54:656-665.

Farber K, Kettenmann H (2006b) Purinergic signaling and microglia. Pflugers Archiv European Journal of Physiology 452:615-621.

Fauve RM, Jusforgues H, Hevin B (1983) Maintenance of granuloma macrophages in serum-free medium. J Immunol Methods 64:345-351.

Felts PA, Woolston AM, Fernando HB, Asquith S, Gregson NA, Mizzi OJ, Smith KJ (2005) Inflammation and primary demyelination induced by the intraspinal injection of lipopolysaccharide. Brain 128:1649-1666.

Feng WG, Wang YB, Zhang JS, Wang XY, Li CL, Chang ZL (2002) cAMP elevators inhibit LPS-induced IL-12 p40 expression by interfering with phosphorylation of p38 MAPK in murine peritoneal macrophages. Cell Research 12:331-337.

Ferreira SH (1980) Peripheral analgesia: mechanism of the analgesic action of aspirin-like drugs and opiate-antagonists. British Journal of Clinical Pharmacology 10:237-245.

Ferreira SH, Lorenzetti BB, Bristow AF, Poole S (1988) Interleukin-1 beta as a potent hyperalgesic agent antagonized by a tripeptide analogue. Nature 334:698-700.

Feske S, Gwack Y, Prakriya M, Srikanth S, Puppel SH, Tanasa B, Hogan PG, Lewis RS, Daly M, Rao A (2006) A mutation in Orai1 causes immune deficiency by abrogating CRAC channel function. Nature 441:179-185.

Finnerup NB, Sindrup SH, Jensen TS (2010) The evidence for pharmacological treatment of neuropathic pain. Pain 150:573-581.

Fitzgerald EM, Okuse K, Wood JN, Dolphin AC, Moss SJ (1999) cAMP-dependent phosphorylation of the tetrodotoxin-resistant voltage-dependent sodium channel SNS. J Physiol 516:433-446.

Flatters SJL, Fox AJ, Dickenson AH (2003) Spinal interleukin-6 (IL-6) inhibits nociceptive transmission following neuropathy. Brain Research 984:54-62.

Flatters SJL, Fox AJ, Dickenson AH (2004) Nerve injury alters the effects of interleukin-6 on nociceptive transmission in peripheral afferents. European Journal of Pharmacology 484:183-191.

Fleetwood-Walker SM, Quinn JP, Wallace C, Blackburn-Munro G, Kelly BG, Fiskerstrand CE, Nash AA, Dalziel RG (1999) Behavioural changes in the rat following infection with varicella-zoster virus. Journal of General Virology 80:2433-2436.

Fleming JC, Bao F, Chen Y, Hamilton EF, Gonzalez-Lara LE, Foster PJ, Weaver LC (2009) Timing and duration of anti-alpha4beta1 integrin treatment after spinal cord injury: effect on therapeutic efficacy. J Neurosurg Spine 11:575-587.

Flynn G, Maru S, Loughlin J, Romero IA, Male D (2003) Regulation of chemokine receptor expression in human microglia and astrocytes. Journal of Neuroimmunology 136:84-93.

Follenfant RL, Nakamura-Craig M, Henderson B, Higgs GA (1989) Inhibition by neuropeptides of interleukin-1 beta-induced, prostaglandin-independent hyperalgesia. British Journal of Pharmacology 98:41-43.

Franchini L, Levi G, Visentin S (2004) Inwardly rectifying K+ channels influence Ca2+ entry due to nucleotide receptor activation in microglia. Cell Calcium 35:449-459.

Franciosi S, Choi HB, Kim SU, McLarnon JG (2002) Interferon-gamma acutely induces calcium influx in human microglia. Journal of Neuroscience Research 69:607-613.

Franke H, Schepper C, Illes P, Krugel U (2007) Involvement of P2X and P2Y receptors in microglial activation in vivo. Purinergic Signal 3:435-445.

Freund J (1947) Some Aspects of Active Immunization. Annual Review of Microbiology 1:291-308.

Fu KY, Light AR, Matsushima GK, Maixner W (1999) Microglial reactions after subcutaneous formalin injection into the rat hind paw. Brain Research 825:59-67.

Funk CD (2001) Prostaglandins and leukotrienes: advances in eicosanoid biology. Science 294:1871-1875.

Galli SJ, Kalesnikoff J, Grimbaldeston MA, Piliponsky AM, Williams CM, Tsai M (2005) Mast cells as "tunable" effector and immunoregulatory cells: recent advances. Annual Review of Immunology 23:749-786.

Gamper N, Shapiro MS (2003) Calmodulin mediates Ca2+-dependent modulation of M-type K+ channels. Journal of General Physiology 122:17-31.

Gao R, Gao X, Xia J, Tian Y, Barrett JE, Dai Y, Hu H (2013) Potent analgesic effects of a store-operated calcium channel inhibitor. Pain 154:2034-2044.

Gao YD, Hanley PJ, Rinne S, Zuzarte M, Daut J (2010) Calcium-activated K(+) channel (K(Ca)3.1) activity during Ca(2+) store depletion and store-operated Ca(2+) entry in human macrophages. Cell Calcium 48:19-27.

Gao YJ, Zhang L, Samad OA, Suter MR, Yasuhiko K, Xu ZZ, Park JY, Lind AL, Ma Q, Ji RR (2009) JNK-induced MCP-1 production in spinal cord astrocytes contributes to central sensitization and neuropathic pain. Journal of Neuroscience 29:4096-4108.

Garcia-Anoveros J, Samad TA, Zuvela-Jelaska L, Woolf CJ, Corey DP (2001) Transport and localization of the DEG/ENaC ion channel BNaC1alpha to peripheral mechanosensory terminals of dorsal root ganglia neurons. Journal of Neuroscience 21:2678-2686.

Gardell LR et al. (2003) Multiple actions of systemic artemin in experimental neuropathy. Nature Medicine 9:1383-1389.

Garrison CJ, Dougherty PM, Kajander KC, Carlton SM (1991) Staining of glial fibrillary acidic protein (GFAP) in lumbar spinal cord increases following a sciatic nerve constriction injury. Brain Research 565:1-7.

Gaudet AD, Popovich PG, Ramer MS (2011) Wallerian degeneration: gaining perspective on inflammatory events after peripheral nerve injury. J Neuroinflammation 8:110.

George A, Buehl A, Sommer C (2004) Wallerian degeneration after crush injury of rat sciatic nerve increases endo- and epineurial tumor necrosis factor-alpha protein. Neuroscience Letters 372:215-219.

George A, Buehl A, Sommer C (2005) Tumor necrosis factor receptor 1 and 2 proteins are differentially regulated during Wallerian degeneration of mouse sciatic nerve. Experimental Neurology 192:163-166.

Gerlai R (2001) Gene targeting: technical confounds and potential solutions in behavioral brain research. Behavioural Brain Research 125:13-21.

Gilabert JA, Parekh AB (2000) Respiring mitochondria determine the pattern of activation and inactivation of the store-operated Ca(2+) current I(CRAC). EMBO Journal 19:6401-6407.

Gilden DH (2005) Infectious causes of multiple sclerosis. Lancet Neurol 4:195-202.

Gillen C, Jander S, Stoll G (1998) Sequential expression of mRNA for proinflammatory cytokines and interleukin-10 in the rat peripheral nervous system: comparison between immune-mediated demyelination and Wallerian degeneration. Journal of Neuroscience Research 51:489-496.

Goghari V, Franciosi S, Kim SU, Lee YB, McLarnon JG (2000) Acute application of interleukin-1beta induces Ca(2+) responses in human microglia. Neuroscience Letters 281:83-86.

Gold MS, Reichling DB, Shuster MJ, Levine JD (1996) Hyperalgesic agents increase a tetrodotoxin-resistant Na+ current in nociceptors. Proceedings of the National Academy of Sciences of the United States of America 93:1108-1112.

Gollob JA, Mier JW, Veenstra K, McDermott DF, Clancy D, Clancy M, Atkins MB (2000) Phase I trial of twice-weekly intravenous interleukin 12 in patients with metastatic renal cell cancer or malignant melanoma: ability to maintain IFN-gamma induction is associated with clinical response. Clinical Cancer Research 6:1678-1692.

Goncharov NV, Jenkins RO, Radilov AS (2006) Toxicology of fluoroacetate: a review, with possible directions for therapy research. Journal of Applied Toxicology 26:148-161.

Gordon S (2007) The macrophage: past, present and future. European Journal of Immunology 37:9-17.

Gosselin RD, Varela C, Banisadr G, Mechighel P, Rostene W, Kitabgi P, Melik-Parsadaniantz S (2005) Constitutive expression of CCR2 chemokine receptor and inhibition by MCP-1/CCL2 of GABA-induced currents in spinal cord neurones. Journal of Neurochemistry 95:1023-1034.

Gould HJ, England JD, Soignier RD, Nolan P, Minor LD, Liu ZP, Levinson SR, Paul D (2004) Ibuprofen blocks changes in nav 1.7 and 1.8 sodium channels associated with complete freund's adjuvant–induced inflammation in rat. The Journal of Pain 5:270-280.

Grace PM, Rolan PE, Hutchinson MR (2011) Peripheral immune contributions to the maintenance of central glial activation underlying neuropathic pain. Brain, Behavior, and Immunity 25:1322-1332.

Graeber MB, Streit WJ, Kreutzberg GW (1988) Axotomy of the rat facial nerve leads to increased CR3 complement receptor expression by activated microglial cells. Journal of Neuroscience Research 21:18-24.

Gregor MF, Hotamisligil GS (2011) Inflammatory mechanisms in obesity. Annual Review of Immunology 29:415-445.

Guo W, Wang H, Watanabe M, Shimizu K, Zou S, LaGraize SC, Wei F, Dubner R, Ren K (2007) Glial-cytokine-neuronal interactions underlying the mechanisms of persistent pain. Journal of Neuroscience 27:6006-6018.

Haber EP, Ximenes HM, Procopio J, Carvalho CR, Curi R, Carpinelli AR (2003) Pleiotropic effects of fatty acids on pancreatic beta-cells. J Cell Physiol 194:1-12.

Hamilton SG, Wade A, McMahon SB (1999) The effects of inflammation and inflammatory mediators on nociceptive behaviour induced by ATP analogues in the rat. British Journal of Pharmacology 126:326-332.

Hamm HE (1998) The Many Faces of G Protein Signaling. Journal of Biological Chemistry 273:669-672.

Han P, Zhao J, Liu SB, Yang CJ, Wang YQ, Wu GC, Xu DM, Mi WL (2013) Interleukin-33 mediates formalin-induced inflammatory pain in mice. Neuroscience 241:59-66.

Hansen RR, Malcangio M (2013) Astrocytes-Multitaskers in chronic pain. European Journal of Pharmacology 716:120-128.

Haraoui B (2005) The anti-tumor necrosis factor agents are a major advance in the treatment of rheumatoid arthritis. Journal of Rheumatology Supplement 72:46-47.

Hargreaves K, Dubner R, Brown F, Flores C, Joris J (1988) A new and sensitive method for measuring thermal nociception in cutaneous hyperalgesia. Pain 32:77-88.

Harper AA, Lawson SN (1985a) Electrical properties of rat dorsal root ganglion neurones with different peripheral nerve conduction velocities. J Physiol 359:47-63.

Harper AA, Lawson SN (1985b) Spinal termination of functionally identified primary afferent neurons with slowly conducting myelinated fibers. J Physiol 359:31-46.

Harrison JK, Jiang Y, Chen S, Xia Y, Maciejewski D, McNamara RK, Streit WJ, Salafranca MN, Adhikari S, Thompson DA, Botti P, Bacon KB, Feng L (1998) Role for neuronally derived fractalkine in mediating interactions between neurons and CX3CR1-expressing microglia. Proceedings of the National Academy of Sciences of the United States of America 95:10896-10901.

Harvey RJ, Depner UB, Wassle H, Ahmadi S, Heindl C, Reinold H, Smart TG, Harvey K, Schutz B, Abo-Salem OM, Zimmer A, Poisbeau P, Welzl H, Wolfer DP, Betz H, Zeilhofer HU, Muller U (2004) GlyR alpha3: an essential target for spinal PGE2-mediated inflammatory pain sensitization. Science 304:884-887.

Hasegawa-Moriyama M, Kurimoto T, Nakama M, Godai K, Kojima M, Kuwaki T, Kanmura Y (2013) Peroxisome proliferator-activated receptor-gamma agonist rosiglitazone attenuates inflammatory pain through the induction of heme oxygenase-1 in macrophages. Pain 154:1402-1412.

Hashizume H, DeLeo JA, Colburn RW, Weinstein JN (2000) Spinal glial activation and cytokine expression after lumbar root injury in the rat. Spine 25:1206-1217.

Herbert MK, Just H, Schmidt RF (2001) Histamine excites groups III and IV afferents from the cat knee joint depending on their resting activity. Neuroscience Letters 305:95-98.

Herzberg U, Sagen J (2001) Peripheral nerve exposure to HIV viral envelope protein gp120 induces neuropathic pain and spinal gliosis. Journal of Neuroimmunology 116:29-39.

Hijioka T, Rosenberg RL, Lemasters JJ, Thurman RG (1992) Kupffer cells contain voltage-dependent calcium channels. Molecular Pharmacology 41:435-440.

Hill R (2000) NK1 (substance P) receptor antagonists--why are they not analgesic in humans? Trends in Pharmacological Sciences 21:244-246.

Hingtgen CM, Waite KJ, Vasko MR (1995) Prostaglandins facilitate peptide release from rat sensory neurons by activating the adenosine 3',5'-cyclic monophosphate transduction cascade. Journal of Neuroscience 15:5411-5419.

Hirasawa A, Tsumaya K, Awaji T, Katsuma S, Adachi T, Yamada M, Sugimoto Y, Miyazaki S, Tsujimoto G (2005) Free fatty acids regulate gut incretin glucagon-like peptide-1 secretion through GPR120. Nature Medicine 11:90-94.

Hoffmann A, Kann O, Ohlemeyer C, Hanisch UK, Kettenmann H (2003) Elevation of basal intracellular calcium as a central element in the activation of brain macrophages (microglia): suppression of receptor-evoked calcium signaling and control of release function. Journal of Neuroscience 23:4410-4419.

Holmes FE, Arnott N, Vanderplank P, Kerr NC, Longbrake EE, Popovich PG, Imai T, Combadiere C, Murphy PM, Wynick D (2008) Intra-neural administration of fractalkine attenuates neuropathic pain-related behaviour. Journal of Neurochemistry 106:640-649.

Homma Y, Brull SJ, Zhang JM (2002) A comparison of chronic pain behavior following local application of tumor necrosis factor alpha to the normal and mechanically compressed lumbar ganglia in the rat. Pain 95:239-246.

Honore P, Rogers SD, Schwei MJ, Salak-Johnson JL, Luger NM, Sabino MC, Clohisy DR, Mantyh PW (2000) Murine models of inflammatory, neuropathic and cancer pain each generates a unique set of neurochemical changes in the spinal cord and sensory neurons. Neuroscience 98:585-598.

Hoogerwerf WA, Gondesen K, Xiao SY, Winston JH, Willis WD, Pasricha PJ (2005) The role of mast cells in the pathogenesis of pain in chronic pancreatitis. BMC Gastroenterol 5:8.

Horvath RJ, Nutile-McMenemy N, Alkaitis MS, Deleo JA (2008) Differential migration, LPS-induced cytokine, chemokine, and NO expression in immortalized BV-2 and HAPI cell lines and primary microglial cultures. Journal of Neurochemistry 107:557-569.

Hoth M, Penner R (1992) Depletion of intracellular calcium stores activates a calcium current in mast cells. Nature 355:353-356.

Hu JH, Zheng XY, Yang JP, Wang LN, Ji FH (2012) Involvement of spinal monocyte chemoattractant protein-1 (MCP-1) in cancer-induced bone pain in rats. Neuroscience Letters 517:60-63.

Hu P, McLachlan EM (2002) Macrophage and lymphocyte invasion of dorsal root ganglia after peripheral nerve lesions in the rat. Neuroscience 112:23-38.

Hua XY, Svensson CI, Matsui T, Fitzsimmons B, Yaksh TL, Webb M (2005) Intrathecal minocycline attenuates peripheral inflammation-induced hyperalgesia by inhibiting p38 MAPK in spinal microglia. European Journal of Neuroscience 22:2431-2440.

Hucho T, Levine JD (2007) Signaling Pathways in Sensitization: Toward a Nociceptor Cell Biology. Neuron 55:365-376.

Hudson LJ, Bevan S, Wotherspoon G, Gentry C, Fox A, Winter J (2001) VR1 protein expression increases in undamaged DRG neurons after partial nerve injury. European Journal of Neuroscience 13:2105-2114.

Hunt SP, Mantyh PW (2001) The molecular dynamics of pain control. Nat Rev Neurosci 2:83-91.

Hwang D (2000) Fatty acids and immune responses--a new perspective in searching for clues to mechanism. Annual Review of Nutrition 20:431-456.

Hylden JL, Wilcox GL (1980) Intrathecal morphine in mice: a new technique. European Journal of Pharmacology 67:313-316.

Ichimura A, Hirasawa A, Hara T, Tsujimoto G (2009) Free fatty acid receptors act as nutrient sensors to regulate energy homeostasis. Prostaglandins and Other Lipid Mediators 89:82-88.

Imamoto K, Leblond CP (1978) Radioautographic investigation of gliogenesis in the corpus callosum of young rats. II. Origin of microglial cells. Journal of Comparative Neurology 180:139-163.

Imamoto N, Momosaki S, Fujita M, Omachi S, Yamato H, Kimura M, Kanegawa N, Shinohara S, Abe K (2013) [11C]PK11195 PET imaging of spinal glial activation after nerve injury in rats. NeuroImage 79:121-128.

Ingram SL, Williams JT (1994) Opioid inhibition of Ih via adenylyl cyclase. Neuron 13:179-186.

Insel PA, Ostrom RS (2003) Forskolin as a tool for examining adenylyl cyclase expression, regulation, and G protein signaling. Cellular and Molecular Neurobiology 23:305-314.

Iwamoto T, Okamoto H, Toyama Y, Momohara S (2008) Molecular aspects of rheumatoid arthritis: chemokines in the joints of patients. FEBS J 275:4448-4455.

Iwasaki K, Noguchi K, Endo H, Kondo H, Ishikawa I (2003) Prostaglandin E2 downregulates interleukin-12 production through EP4 receptors in human monocytes stimulated with lipopolysaccharide from Actinobacillus actinomycetemcomitans and interferon-gamma. Oral Microbiology and Immunology 18:150-155.

Izikson L, Klein RS, Charo IF, Weiner HL, Luster AD (2000) Resistance to experimental autoimmune encephalomyelitis in mice lacking the CC chemokine receptor (CCR)2. Journal of Experimental Medicine 192:1075-1080.

Jacobus WE, Taylor GJt, Hollis DP, Nunnally RL (1977) Phosphorus nuclear magnetic resonance of perfused working rat hearts. Nature 265:756-758.

Jana M, Dasgupta S, Saha RN, Liu X, Pahan K (2003) Induction of tumor necrosis factor-alpha (TNF-alpha) by interleukin-12 p40 monomer and homodimer in microglia and macrophages. Journal of Neurochemistry 86:519-528.

Ji RR, Woolf CJ (2001) Neuronal plasticity and signal transduction in nociceptive neurons: implications for the initiation and maintenance of pathological pain. Neurobiology of Disease 8:1-10.

Ji RR, Suter MR (2007) p38 MAPK, microglial signaling, and neuropathic pain. Mol Pain 3:33.

Ji RR, Baba H, Brenner GJ, Woolf CJ (1999) Nociceptive-specific activation of ERK in spinal neurons contributes to pain hypersensitivity. Nature Neuroscience 2:1114-1119.

Ji RR, Kohno T, Moore KA, Woolf CJ (2003) Central sensitization and LTP: do pain and memory share similar mechanisms? Trends in Neurosciences 26:696-705.

Ji RR, Gereau RWt, Malcangio M, Strichartz GR (2009) MAP kinase and pain. Brain Res Rev 60:135-148.

Ji RR, Samad TA, Jin SX, Schmoll R, Woolf CJ (2002) p38 MAPK activation by NGF in primary sensory neurons after inflammation increases TRPV1 levels and maintains heat hyperalgesia. Neuron 36:57-68.

Ji RR, Kawasaki Y, Zhuang ZY, Wen YR, Decosterd I (2006) Possible role of spinal astrocytes in maintaining chronic pain sensitization: review of current evidence with focus on bFGF/JNK pathway. Neuron Glia Biol 2:259-269.

Joosten LA, Lubberts E, Helsen MM, van den Berg WB (1997) Dual role of IL-12 in early and late stages of murine collagen type II arthritis. Journal of Immunology 159:4094-4102.

Julius D, Basbaum AI (2001) Molecular mechanisms of nociception. Nature 413:203-210.

Kalamidas SA, Kuehnel MP, Peyron P, Rybin V, Rauch S, Kotoulas OB, Houslay M, Hemmings BA, Gutierrez MG, Anes E, Griffiths G (2006) cAMP synthesis and degradation by phagosomes regulate actin assembly and fusion events: consequences for mycobacteria. Journal of Cell Science 119:3686-3694.

Kalish BT, Fallon EM, Puder M (2012) A tutorial on fatty acid biology. JPEN Journal of Parenteral and Enteral Nutrition 36:380-388.

Kalliomaki J, Attal N, Jonzon B, Bach FW, Huizar K, Ratcliffe S, Eriksson B, Janecki M, Danilov A, Bouhassira D (2013) A randomized, double-blind, placebo-controlled trial of a chemokine receptor 2 (CCR2) antagonist in posttraumatic neuralgia. Pain 154:761-767.

Kalyan Kumar G, Dhamotharan R, Kulkarni NM, Mahat MY, Gunasekaran J, Ashfaque M (2011) Embelin reduces cutaneous TNF-alpha level and ameliorates skin edema in acute and chronic model of skin inflammation in mice. European Journal of Pharmacology 662:63-69.

Kamerman PR, Moss PJ, Weber J, Wallace VC, Rice AS, Huang W (2012) Pathogenesis of HIV-associated sensory neuropathy: evidence from in vivo and in vitro experimental models. Journal of the Peripheral Nervous System 17:19-31.

Katsura H, Obata K, Mizushima T, Yamanaka H, Kobayashi K, Dai Y, Fukuoka T, Tokunaga A, Sakagami M, Noguchi K (2006) Antisense knock down of TRPA1, but not TRPM8, alleviates cold hyperalgesia after spinal nerve ligation in rats. Experimental Neurology 200:112-123.

Kawabata A, Kawao N, Kuroda R, Tanaka A, Itoh H, Nishikawa H (2001) Peripheral PAR-2 triggers thermal hyperalgesia and nociceptive responses in rats. Neuroreport 12:715-719.

Kawabata A, Ishiki T, Nagasawa K, Yoshida S, Maeda Y, Takahashi T, Sekiguchi F, Wada T, Ichida S, Nishikawa H (2007) Hydrogen sulfide as a novel nociceptive messenger. Pain 132:74-81.

Kawahara H, Sakamoto A, Takeda S, Onodera H, Imaki J, Ogawa R (2001) A prostaglandin E2 receptor subtype EP1 receptor antagonist (ONO-8711) reduces hyperalgesia, allodynia, and c-fos gene expression in rats with chronic nerve constriction. Anesthesia and Analgesia 93:1012-1017.

Kawamura N, Dyck PJ, Schmeichel AM, Engelstad JK, Low PA, Dyck PJ (2008) Inflammatory mediators in diabetic and non-diabetic lumbosacral radiculoplexus neuropathy. Acta Neuropathol 115:231-239.

Kawasaki Y, Zhang L, Cheng JK, Ji RR (2008) Cytokine mechanisms of central sensitization: distinct and overlapping role of interleukin-1beta, interleukin-6, and tumor necrosis factor-alpha in regulating synaptic and neuronal activity in the superficial spinal cord. Journal of Neuroscience 28:5189-5194.

Kawasaki Y, Kohno T, Zhuang ZY, Brenner GJ, Wang H, Van Der Meer C, Befort K, Woolf CJ, Ji RR (2004) Ionotropic and metabotropic receptors, protein kinase A, protein kinase C, and Src contribute to C-fiber-induced ERK activation and cAMP response element-binding protein phosphorylation in dorsal horn neurons, leading to central sensitization. Journal of Neuroscience 24:8310-8321.

Kerr BJ, Souslova V, McMahon SB, Wood JN (2001) A role for the TTX-resistant sodium channel Nav 1.8 in NGF-induced hyperalgesia, but not neuropathic pain. Neuroreport 12:3077-3080.

Kerstein PC, del Camino D, Moran MM, Stucky CL (2009) Pharmacological blockade of TRPA1 inhibits mechanical firing in nociceptors. Mol Pain 5:19.

Kettenmann H, Hanisch UK, Noda M, Verkhratsky A (2011) Physiology of microglia. Physiological Reviews 91:461-553.

Kieseier BC, Tani M, Mahad D, Oka N, Ho T, Woodroofe N, Griffin JW, Toyka KV, Ransohoff RM, Hartung HP (2002) Chemokines and chemokine receptors in inflammatory demyelinating neuropathies: a central role for IP-10. Brain 125:823-834.

Kiguchi N, Kobayashi Y, Kishioka S (2012) Chemokines and cytokines in neuroinflammation leading to neuropathic pain. Current Opinion in Pharmacology 12:55-61.

Kiguchi N, Maeda T, Kobayashi Y, Kishioka S (2008a) Up-regulation of tumor necrosis factor-alpha in spinal cord contributes to vincristine-induced mechanical allodynia in mice. Neuroscience Letters 445:140-143.

Kiguchi N, Maeda T, Kobayashi Y, Fukazawa Y, Kishioka S (2010a) Macrophage inflammatory protein-1alpha mediates the development of neuropathic pain following peripheral nerve injury through interleukin-1beta up-regulation. Pain 149:305-315.

Kiguchi N, Kobayashi Y, Maeda T, Saika F, Kishioka S (2010b) CC-chemokine MIP-1alpha in the spinal cord contributes to nerve injury-induced neuropathic pain. Neuroscience Letters 484:17-21.

Kiguchi N, Maeda T, Kobayashi Y, Kondo T, Ozaki M, Kishioka S (2008b) The critical role of invading peripheral macrophage-derived interleukin-6 in vincristine-induced mechanical allodynia in mice. European Journal of Pharmacology 592:87-92.

Kim D, Kim MA, Cho IH, Kim MS, Lee S, Jo EK, Choi SY, Park K, Kim JS, Akira S, Na HS, Oh SB, Lee SJ (2007a) A critical role of toll-like receptor 2 in nerve injury-induced spinal cord glial cell activation and pain hypersensitivity. Journal of Biological Chemistry 282:14975-14983.

Kim DS, Figueroa KW, Li KW, Boroujerdi A, Yolo T, Luo ZD (2009) Profiling of dynamically changed gene expression in dorsal root ganglia post peripheral nerve injury and a critical role of injury-induced glial fibrillary acidic protein in maintenance of pain behaviors. Pain 143:114-122.

Kim KJ, Yoon YW, Chung JM (1997) Comparison of three rodent neuropathic pain models. Experimental Brain Research 113:200-206.

Kim KS, Kim J, Back SK, Im JY, Na HS, Han PL (2007b) Markedly attenuated acute and chronic pain responses in mice lacking adenylyl cyclase-5. Genes, Brain and Behavior 6:120-127.

Kim SH, Chung JM (1992) An experimental model for peripheral neuropathy produced by segmental spinal nerve ligation in the rat. Pain 50:355-363.

Kim SY, Bae JC, Kim JY, Lee HL, Lee KM, Kim DS, Cho HJ (2002) Activation of p38 MAP kinase in the rat dorsal root ganglia and spinal cord following peripheral inflammation and nerve injury. Neuroreport 13:2483-2486.

Kitamura T, Miyake T, Fujita S (1984) Genesis of resting microglia in the gray matter of mouse hippocampus. Journal of Comparative Neurology 226:421-433.

Kohler RE, Comerford I, Townley S, Haylock-Jacobs S, Clark-Lewis I, McColl SR (2008) Antagonism of the chemokine receptors CXCR3 and CXCR4 reduces the pathology of experimental autoimmune encephalomyelitis. Brain Pathology 18:504-516.

Komori T, Morikawa Y, Inada T, Hisaoka T, Senba E (2011) Site-specific subtypes of macrophages recruited after peripheral nerve injury. Neuroreport 22:911-917.

Kong SK, Choy YM, Fung KP, Lee CY (1992) Membrane depolarization induced DNA synthesis in PU5-1.8 cells. Role of voltage-operated Ca2+ channel and protein kinase C. Biological Signals 1:12-22.

Korotzer AR, Whittemore ER, Cotman CW (1995) Differential regulation by beta-amyloid peptides of intracellular free Ca2+ concentration in cultured rat microglia. European Journal of Pharmacology 288:125-130.

Kreckler LM, Gizewski E, Wan TC, Auchampach JA (2009) Adenosine suppresses lipopolysaccharide-induced tumor necrosis factor-alpha production by murine macrophages through a protein kinase A- and exchange protein activated by cAMP-independent signaling pathway. Journal of Pharmacology and Experimental Therapeutics 331:1051-1061.

Kreider T, Anthony RM, Urban JF, Jr., Gause WC (2007) Alternatively activated macrophages in helminth infections. Current Opinion in Immunology 19:448-453.

Kreideweiss S, Ahlers C, Nordheim A, Ruhlmann A (1999) Ca2+-induced p38/SAPK signalling inhibited by the immunosuppressant cyclosporin A in human peripheral blood mononuclear cells. European Journal of Biochemistry 265:1075-1084.

Kreutzberg GW (1996) Microglia: a sensor for pathological events in the CNS. Trends in Neurosciences 19:312-318.

Kumar GK, Dhamotharan R, Kulkarni NM, Honnegowda S, Murugesan S (2011) Embelin ameliorates dextran sodium sulfate-induced colitis in mice. Int Immunopharmacol 11:724-731.

Kumar S, Boehm J, Lee JC (2003) p38 MAP kinases: key signalling molecules as therapeutic targets for inflammatory diseases. Nat Rev Drug Discov 2:717-726.

Lai AY, Todd KG (2006) Hypoxia-activated microglial mediators of neuronal survival are differentially regulated by tetracyclines. Glia 53:809-816.

Lambright DG, Sondek J, Bohm A, Skiba NP, Hamm HE, Sigler PB (1996) The 2.0 A crystal structure of a heterotrimeric G protein. Nature 379:311-319.

Landry RP, Jacobs VL, Romero-Sandoval EA, DeLeo JA (2012) Propentofylline, a CNS glial modulator does not decrease pain in post-herpetic neuralgia patients: in vitro evidence for differential responses in human and rodent microglia and macrophages. Experimental Neurology 234:340-350.

Latremoliere A, Woolf CJ (2009) Central sensitization: a generator of pain hypersensitivity by central neural plasticity. J Pain 10:895-926.

Latremoliere A, Mauborgne A, Masson J, Bourgoin S, Kayser V, Hamon M, Pohl M (2008) Differential implication of proinflammatory cytokine interleukin-6 in the development of cephalic versus extracephalic neuropathic pain in rats. Journal of Neuroscience 28:8489-8501.

Lattin JE, Schroder K, Su AI, Walker JR, Zhang J, Wiltshire T, Saijo K, Glass CK, Hume DA, Kellie S, Sweet MJ (2008) Expression analysis of G Protein-Coupled Receptors in mouse macrophages. Immunome Res 4:4-5.

Lawson SN (2002) 5HT increases excitability of nociceptor-like rat dorsal root ganglion neurons via cAMP-coupled TTX-resistant Na(+) channels. Exp Physiol 87:239-244.

Ledeboer A, Sloane EM, Milligan ED, Frank MG, Mahony JH, Maier SF, Watkins LR (2005) Minocycline attenuates mechanical allodynia and proinflammatory cytokine expression in rat models of pain facilitation. Pain 115:71-83.

Ledeboer A, Jekich BM, Sloane EM, Mahoney JH, Langer SJ, Milligan ED, Martin D, Maier SF, Johnson KW, Leinwand LA, Chavez RA, Watkins LR (2007) Intrathecal interleukin-10 gene therapy attenuates paclitaxel-induced mechanical allodynia and proinflammatory cytokine expression in dorsal root ganglia in rats. Brain, Behavior, and Immunity 21:686-698.

Lee H-N, Surh Y-J (2012) Therapeutic potential of resolvins in the prevention and treatment of inflammatory disorders. Biochemical Pharmacology 84:1340-1350.

Lee JY, Sohn KH, Rhee SH, Hwang D (2001) Saturated fatty acids, but not unsaturated fatty acids, induce the expression of cyclooxygenase-2 mediated through Toll-like receptor 4. Journal of Biological Chemistry 276:16683-16689.

Lee KM, Jeon SM, Cho HJ (2010) Interleukin-6 induces microglial CX3CR1 expression in the spinal cord after peripheral nerve injury through the activation of p38 MAPK. Eur J Pain 14:682.

Lee WY, Wang CJ, Lin TY, Hsiao CL, Luo CW (2013) CXCL17, an orphan chemokine, acts as a novel angiogenic and anti-inflammatory factor. Am J Physiol Endocrinol Metab 304:32-40.

Lehnardt S, Lachance C, Patrizi S, Lefebvre S, Follett PL, Jensen FE, Rosenberg PA, Volpe JJ, Vartanian T (2002) The toll-like receptor TLR4 is necessary for lipopolysaccharide-induced oligodendrocyte injury in the CNS. Journal of Neuroscience 22:2478-2486.

Levine JD, Fields HL, Basbaum AI (1993) Peptides and the primary afferent nociceptor. Journal of Neuroscience 13:2273-2286.

Levine JD, Lau W, Kwiat G, Goetzl EJ (1984) Leukotriene B4 produces hyperalgesia that is dependent on polymorphonuclear leukocytes. Science 225:743-745.

Levine JD, Gooding J, Donatoni P, Borden L, Goetzl EJ (1985) The role of the polymorphonuclear leukocyte in hyperalgesia. Journal of Neuroscience 5:3025-3029.

Lewis C, Neidhart S, Holy C, North RA, Buell G, Surprenant A (1995) Coexpression of P2X2 and P2X3 receptor subunits can account for ATP-gated currents in sensory neurons. Nature 377:432-435.

Li Y, Gamper N, Hilgemann DW, Shapiro MS (2005) Regulation of Kv7 (KCNQ) K+ channel open probability by phosphatidylinositol 4,5-bisphosphate. J Neurosci 25:9825-9835.

Liao YH, Zhang GH, Jia D, Wang P, Qian NS, He F, Zeng XT, He Y, Yang YL, Cao DY, Zhang Y, Wang DS, Tao KS, Gao CJ, Dou KF (2011) Spinal astrocytic activation contributes to mechanical allodynia in a mouse model of type 2 diabetes. Brain Research 1368:324-335.

Light AR, Perl ER (1979a) Reexamination of the dorsal root projection to the spinal dorsal horn including observations on the differential termination of coarse and fine fibers. J Comp Neurol 186:133-150.

Light AR, Perl ER (1979b) Spinal termination of functionally identified primary afferent neurons with slowly conducting myelinated fibers. Journal of Comparative Neurology 186:133-150.

Lindenlaub T, Sommer C (2003) Cytokines in sural nerve biopsies from inflammatory and non-inflammatory neuropathies. Acta Neuropathol 105:593-602.

Ling EA, Penney D, Leblond CP (1980) Use of carbon labeling to demonstrate the role of blood monocytes as precursors of the 'ameboid cells' present in the corpus callosum of postnatal rats. Journal of Comparative Neurology 193:631-657.

Linley JE, Rose K, Ooi L, Gamper N (2010) Understanding inflammatory pain: ion channels contributing to acute and chronic nociception. Pflügers Archiv - European Journal of Physiology 459:657-669.

Liu CC, Lu N, Cui Y, Yang T, Zhao ZQ, Xin WJ, Liu XG (2010) Prevention of paclitaxel-induced allodynia by minocycline: Effect on loss of peripheral nerve fibers and infiltration of macrophages in rats. Mol Pain 6:76.

Liu M, Wood JN (2011) The roles of sodium channels in nociception: implications for mechanisms of neuropathic pain. Pain Med 12 Suppl 3:S93-99.

Liu T, van Rooijen N, Tracey DJ (2000) Depletion of macrophages reduces axonal degeneration and hyperalgesia following nerve injury. Pain 86:25-32.

Lopshire JC, Nicol GD (1998) The cAMP transduction cascade mediates the prostaglandin E2 enhancement of the capsaicin-elicited current in rat sensory neurons: whole-cell and single-channel studies. Journal of Neuroscience 18:6081-6092.

Lu X, Richardson PM (1991) Inflammation near the nerve cell body enhances axonal regeneration. Journal of Neuroscience 11:972-978.

Lu YC, Yeh WC, Ohashi PS (2008) LPS/TLR4 signal transduction pathway. Cytokine 42:145-151.

Lytton J (2007) Na+/Ca2+ exchangers: three mammalian gene families control Ca2+ transport. Biochemical Journal 406:365-382.

Ma Q-P, Hill RG (1999) Neurokinin antagonists as potential agents for use in pain management. Curr Opin Invest Drugs 1:65-71.

Ma W, Quirion R (2002) Partial sciatic nerve ligation induces increase in the phosphorylation of extracellular signal-regulated kinase (ERK) and c-Jun N-terminal kinase (JNK) in astrocytes in the lumbar spinal dorsal horn and the gracile nucleus. Pain 99:175-184.

Ma W, Eisenach JC (2002) Morphological and pharmacological evidence for the role of peripheral prostaglandins in the pathogenesis of neuropathic pain. European Journal of Neuroscience 15:1037-1047.

Ma W, Eisenach JC (2003a) Intraplantar injection of a cyclooxygenase inhibitor ketorolac reduces immunoreactivities of substance P, calcitonin gene-related peptide, and dynorphin in the dorsal horn of rats with nerve injury or inflammation. Neuroscience 121:681-690.

Ma W, Eisenach JC (2003b) Cyclooxygenase 2 in infiltrating inflammatory cells in injured nerve is universally up-regulated following various types of peripheral nerve injury. Neuroscience 121:691-704.

Ma W, Quirion R (2007) Inflammatory mediators modulating the transient receptor potential vanilloid 1 receptor: therapeutic targets to treat inflammatory and neuropathic pain. Expert Opin Ther Targets 11:307-320.

Ma W, St-Jacques B, Duarte PC (2012) Targeting pain mediators induced by injured nerve-derived COX2 and PGE2 to treat neuropathic pain. Expert Opin Ther Targets 16:527-540.

Mack TG, Reiner M, Beirowski B, Mi W, Emanuelli M, Wagner D, Thomson D, Gillingwater T, Court F, Conforti L, Fernando FS, Tarlton A, Andressen C, Addicks K, Magni G, Ribchester RR, Perry VH, Coleman MP (2001) Wallerian degeneration of injured axons and synapses is delayed by a Ube4b/Nmnat chimeric gene. Nature Neuroscience 4:1199-1206.

Macleod MR, Fisher M, O'Collins V, Sena ES, Dirnagl U, Bath PM, Buchan A, van der Worp HB, Traystman R, Minematsu K, Donnan GA, Howells DW (2009) Good laboratory practice: preventing introduction of bias at the bench. Stroke 40:50-52.

Mahendran S, Thippeswamy BS, Veerapur VP, Badami S (2011a) Anticonvulsant activity of embelin isolated from Embelia ribes. Phytomedicine 18:186-188.

Mahendran S, Badami S, Ravi S, Thippeswamy BS, Veerapur VP (2011b) Synthesis and evaluation of analgesic and anti-inflammatory activities of most active free radical scavenging derivatives of embelin-A structure-activity relationship. Chemical and Pharmaceutical Bulletin 59:913-919.

Maingret F, Coste B, Padilla F, Clerc N, Crest M, Korogod SM, Delmas P (2008) Inflammatory mediators increase Nav1.9 current and excitability in nociceptors through a coincident detection mechanism. J Gen Physiol 131:211-225.

Makranz C, Cohen G, Reichert F, Kodama T, Rotshenker S (2006) cAMP cascade (PKA, Epac, adenylyl cyclase, Gi, and phosphodiesterases) regulates myelin phagocytosis mediated by complement receptor-3 and scavenger receptor-AI/II in microglia and macrophages. Glia 53:441-448.

Malcangio M, Tomlinson DR (1998) A pharmacologic analysis of mechanical hyperalgesia in streptozotocin/diabetic rats. Pain 76:151-157.

Malmberg AB, Basbaum AI (1998) Partial sciatic nerve injury in the mouse as a model of neuropathic pain: behavioral and neuroanatomical correlates. Pain 76:215-222.

Mamet J, Baron A, Lazdunski M, Voilley N (2002) Proinflammatory mediators, stimulators of sensory neuron excitability via the expression of acid-sensing ion channels. Journal of Neuroscience 22:10662-10670.

Mandadi S, Tominaga T, Numazaki M, Murayama N, Saito N, Armati PJ, Roufogalis BD, Tominaga M (2006) Increased sensitivity of desensitized TRPV1 by PMA occurs through PKCepsilon-mediated phosphorylation at S800. Pain 123:106-116.

Mannion RJ, Costigan M, Decosterd I, Amaya F, Ma QP, Holstege JC, Ji RR, Acheson A, Lindsay RM, Wilkinson GA, Woolf CJ (1999) Neurotrophins: peripherally and centrally acting modulators of tactile stimulus-induced inflammatory pain hypersensitivity. Proceedings of the National Academy of Sciences of the United States of America 96:9385-9390.

Mantyh PW (1997) Inhibition of Hyperalgesia by Ablation of Lamina I Spinal Neurons Expressing the Substance P Receptor. Science 278:275-279.

Mao-Ying QL, Wang XW, Yang CJ, Li X, Mi WL, Wu GC, Wang YQ (2012) Robust spinal neuroinflammation mediates mechanical allodynia in Walker 256 induced bone cancer rats. Mol Brain 5:16.

Marchand F, Perretti M, McMahon SB (2005) Role of the immune system in chronic pain. Nat Rev Neurosci 6:521-532.

Marchand F, Tsantoulas C, Singh D, Grist J, Clark AK, Bradbury EJ, McMahon SB (2009) Effects of Etanercept and Minocycline in a rat model of spinal cord injury. Eur J Pain 13:673-681.

Markel P, Shu P, Ebeling C, Carlson GA, Nagle DL, Smutko JS, Moore KJ (1997) Theoretical and empirical issues for marker-assisted breeding of congenic mouse strains. Nature Genetics 17:280-284.

Marmigere F, Ernfors P (2007) Specification and connectivity of neuronal subtypes in the sensory lineage. Nat Rev Neurosci 8:114-127.

Marta M, Meier UC, Lobell A (2009) Regulation of autoimmune encephalomyelitis by toll-like receptors. Autoimmun Rev 8:506-509.

Martin CA, Dorf ME (1991) Differential regulation of interleukin-6, macrophage inflammatory protein-1, and JE/MCP-1 cytokine expression in macrophage cell lines. Cellular Immunology 135:245-258.

Mayer ML, Westbrook GL, Guthrie PB (1984) Voltage-dependent block by Mg2+ of NMDA responses in spinal cord neurones. Nature 309:261-263.

Mayr B, Montminy M (2001) Transcriptional regulation by the phosphorylation-dependent factor CREB. Nat Rev Mol Cell Biol 2:599-609.

McCarthy JB, Wahl SM, Rees JC, Olsen CE, Sandberg L, Wahl LM (1980) Mediation of macrophage collagenase production by 3'-5' cyclic adenosine monophosphate. Journal of Immunology 124:2405-2409.

McCarthy PW, Lawson SN (1989) Cell type and conduction velocity of rat primary sensory neurons with substance P-like immunoreactivity. Neuroscience 28:745-753.

McLarnon JG (2005) Purinergic mediated changes in Ca2+ mobilization and functional responses in microglia: effects of low levels of ATP. Journal of Neuroscience Research 81:349-356.

McLarnon JG, Choi HB, Lue LF, Walker DG, Kim SU (2005) Perturbations in calcium-mediated signal transduction in microglia from Alzheimer's disease patients. Journal of Neuroscience Research 81:426-435.

McLarnon JG, Franciosi S, Wang X, Bae JH, Choi HB, Kim SU (2001) Acute actions of tumor necrosis factor-alpha on intracellular Ca(2+) and K(+) currents in human microglia. Neuroscience 104:1175-1184.

McLarnon JG, Zhang L, Goghari V, Lee YB, Walz W, Krieger C, Kim SU (1999) Effects of ATP and elevated K+ on K+ currents and intracellular Ca2+ in human microglia. Neuroscience 91:343-352.

McMahon SB, Malcangio M (2009) Current challenges in glia-pain biology. Neuron 64:46-54.

McMahon SB, Cafferty WBJ, Marchand F (2005) Immune and glial cell factors as pain mediators and modulators. Experimental Neurology 192:444-462.

McMahon SB, Armanini MP, Ling LH, Phillips HS (1994) Expression and coexpression of Trk receptors in subpopulations of adult primary sensory neurons projecting to identified peripheral targets. Neuron 12:1161-1171.

Medhurst SJ, Walker K, Bowes M, Kidd BL, Glatt M, Muller M, Hattenberger M, Vaxelaire J, O'Reilly T, Wotherspoon G, Winter J, Green J, Urban L (2002) A rat model of bone cancer pain. Pain 96:129-140.

Meller ST, Dykstra C, Grzybycki D, Murphy S, Gebhart GF (1994) The possible role of glia in nociceptive processing and hyperalgesia in the spinal cord of the rat. Neuropharmacology 33:1471-1478.

Melzack R, Wall PD (1965) Pain mechanisms: a new theory. Science 150:971-979.

Menzies FM, Henriquez FL, Alexander J, Roberts CW (2010) Sequential expression of macrophage anti-microbial/inflammatory and wound healing markers following innate, alternative and classical activation. Clin Exp Immunol 160:369-379.

Mert T, Gunay I, Ocal I, Guzel AI, Inal TC, Sencar L, Polat S (2009) Macrophage depletion delays progression of neuropathic pain in diabetic animals. Naunyn-Schmiedebergs Archives of Pharmacology 379:445-452.

Metcalfe DD, Baram D, Mekori YA (1997) Mast cells. Physiological Reviews 77:1033-1079.

Michael GJ, Priestley JV (1999) Differential expression of the mRNA for the vanilloid receptor subtype 1 in cells of the adult rat dorsal root and nodose ganglia and its downregulation by axotomy. Journal of Neuroscience 19:1844-1854.

Mika J, Zychowska M, Popiolek-Barczyk K, Rojewska E, Przewlocka B (2013) Importance of glial activation in neuropathic pain. European Journal of Pharmacology 716:106-119.

Milligan E, Zapata V, Schoeniger D, Chacur M, Green P, Poole S, Martin D, Maier SF, Watkins LR (2005) An initial investigation of spinal mechanisms underlying pain enhancement induced by fractalkine, a neuronally released chemokine. European Journal of Neuroscience 22:2775-2782.

Milligan ED, Mehmert KK, Hinde JL, Harvey LO, Martin D, Tracey KJ, Maier SF, Watkins LR (2000) Thermal hyperalgesia and mechanical allodynia produced by intrathecal administration of the human immunodeficiency virus-1 (HIV-1) envelope glycoprotein, gp120. Brain Research 861:105-116.

Minghetti L, Walsh DT, Levi G, Perry VH (1999) In vivo expression of cyclooxygenase-2 in rat brain following intraparenchymal injection of bacterial endotoxin and inflammatory cytokines. Journal of Neuropathology and Experimental Neurology 58:1184-1191.

Misharin AV, Saber R, Perlman H (2012) Eosinophil contamination of thioglycollate-elicited peritoneal macrophage cultures skews the functional readouts of in vitro assays. J Leukoc Biol 92:325-331.

Misra UK, Pizzo SV (2005) Coordinate regulation of forskolin-induced cellular proliferation in macrophages by protein kinase A/cAMP-response element-binding protein (CREB) and Epac1-Rap1 signaling: effects of silencing CREB gene expression on Akt activation. Journal of Biological Chemistry 280:38276-38289.

Miyoshi K, Obata K, Kondo T, Okamura H, Noguchi K (2008) Interleukin-18-mediated microglia/astrocyte interaction in the spinal cord enhances neuropathic pain processing after nerve injury. Journal of Neuroscience 28:12775-12787.

Mizoguchi Y, Monji A, Kato T, Seki Y, Gotoh L, Horikawa H, Suzuki SO, Iwaki T, Yonaha M, Hashioka S, Kanba S (2009) Brain-derived neurotrophic factor induces sustained elevation of intracellular Ca2+ in rodent microglia. Journal of Immunology 183:7778-7786.

Moalem-Taylor G, Allbutt HN, Iordanova MD, Tracey DJ (2007) Pain hypersensitivity in rats with experimental autoimmune neuritis, an animal model of human inflammatory demyelinating neuropathy. Brain, Behavior, and Immunity 21:699-710.

Moalem G, Tracey DJ (2006) Immune and inflammatory mechanisms in neuropathic pain. Brain Res Rev 51:240-264.

Moalem G, Xu K, Yu L (2004) T lymphocytes play a role in neuropathic pain following peripheral nerve injury in rats. Neuroscience 129:767-777.

Modolell M, Corraliza IM, Link F, Soler G, Eichmann K (1995) Reciprocal regulation of the nitric oxide synthase/arginase balance in mouse bone marrow-derived macrophages by TH1 and TH2 cytokines. Eur J Immunol 25:1101-1104.

Mogil JS (2009) Animal models of pain: progress and challenges. Nat Rev Neurosci 10:283-294.

Mogil JS, Wilson SG, Bon K, Lee SE, Chung K, Raber P, Pieper JO, Hain HS, Belknap JK, Hubert L, Elmer GI, Chung JM, Devor M (1999) Heritability of nociception I: responses of 11 inbred mouse strains on 12 measures of nociception. Pain 80:67-82.

Molander C, Hongpaisan J, Svensson M, Aldskogius H (1997) Glial cell reactions in the spinal cord after sensory nerve stimulation are associated with axonal injury. Brain Research 747:122-129.

Moller T (2002) Calcium signaling in microglial cells. Glia 40:184-194.

Moller T, Kann O, Verkhratsky A, Kettenmann H (2000) Activation of mouse microglial cells affects P2 receptor signaling. Brain Research 853:49-59.

Molliver DC, Wright DE, Leitner ML, Parsadanian AS, Doster K, Wen D, Yan Q, Snider WD (1997) Coexpression of P2X2 and P2X3 receptor subunits can account for ATP-gated currents in sensory neurons. Neuron 19:849-861.

Moore KA, Kohno T, Karchewski LA, Scholz J, Baba H, Woolf CJ (2002) Partial peripheral nerve injury promotes a selective loss of GABAergic inhibition in the superficial dorsal horn of the spinal cord. Journal of Neuroscience 22:6724-6731.

Morein B, Blomqvist G, Hu K (2007) Immune responsiveness in the neonatal period. Journal of Comparative Pathology 137:27-31.

Morenilla-Palao C, Planells-Cases R, Garcia-Sanz N, Ferrer-Montiel A (2004) Regulated exocytosis contributes to protein kinase C potentiation of vanilloid receptor activity. Journal of Biological Chemistry 279:25665-25672.

Morgan AJ, Jacob R (1994) Ionomycin enhances Ca2+ influx by stimulating store-regulated cation entry and not by a direct action at the plasma membrane. Biochemical Journal 300:665-672.

Morin N, Owolabi SA, Harty MW, Papa EF, Tracy TF, Jr., Shaw SK, Kim M, Saab CY (2007) Neutrophils invade lumbar dorsal root ganglia after chronic constriction injury of the sciatic nerve. Journal of Neuroimmunology 184:164-171.

Moriyama T, Higashi T, Togashi K, Iida T, Segi E, Sugimoto Y, Tominaga T, Narumiya S, Tominaga M (2005) Sensitization of TRPV1 by EP1 and IP reveals peripheral nociceptive mechanism of prostaglandins. Mol Pain 1:3.

Mosser DM, Edwards JP (2008) Exploring the full spectrum of macrophage activation. Nat Rev Immunol 8:958-969.

Muja N, DeVries GH (2004) Prostaglandin E(2) and 6-keto-prostaglandin F(1alpha) production is elevated following traumatic injury to sciatic nerve. Glia 46:116-129.

Munder M, Eichmann K, Modolell M (1998) Alternative metabolic states in murine macrophages reflected by the nitric oxide synthase/arginase balance: competitive regulation by CD4+ T cells correlates with Th1/Th2 phenotype. J Immunol 160:5347-5354.

Murdoch C, Finn A (2000) Chemokine receptors and their role in inflammation and infectious diseases. Blood 95:3032-3043.

Murinson BB, Griffin JW (2004) C-fiber structure varies with location in peripheral nerve. Journal of Neuropathology and Experimental Neurology 63:246-254.

Murphy PG, Grondin J, Altares M, Richardson PM (1995) Induction of interleukin-6 in axotomized sensory neurons. Journal of Neuroscience 15:5130-5138.

Murphy PG, Borthwick LA, Altares M, Gauldie J, Kaplan D, Richardson PM (2000) Reciprocal actions of interleukin-6 and brain-derived neurotrophic factor on rat and mouse primary sensory neurons. European Journal of Neuroscience 12:1891-1899.

Muschel RJ, Rosen N, Rosen OM, Bloom BR (1977) Modulation of Fc-mediated phagocytosis by cyclic AMP and insulin in a macrophage-like cell line. Journal of Immunology 119:1813-1820.

Mustafa SB (1998) Expression of Nitric-oxide Synthase in Rat Kupffer Cells Is Regulated by cAMP. Journal of Biological Chemistry 273:5073-5080.

Myers RR, Heckman HM, Rodriguez M (1996) Reduced hyperalgesia in nerve-injured WLD mice: relationship to nerve fiber phagocytosis, axonal degeneration, and regeneration in normal mice. Experimental Neurology 141:94-101.

Nadeau S, Filali M, Zhang J, Kerr BJ, Rivest S, Soulet D, Iwakura Y, de Rivero Vaccari JP, Keane RW, Lacroix S (2011) Functional recovery after peripheral nerve injury is dependent on the pro-inflammatory cytokines IL-1beta and TNF: implications for neuropathic pain. Journal of Neuroscience 31:12533-12542.

Nagano T, Kawasaki Y, Baba A, Takemura M, Matsuda T (2004) Up-regulation of Na(+)-Ca2+ exchange activity by interferon-gamma in cultured rat microglia. Journal of Neurochemistry 90:784-791.

Nagasaki H, Kondo T, Fuchigami M, Hashimoto H, Sugimura Y, Ozaki N, Arima H, Ota A, Oiso Y, Hamada Y (2012) Inflammatory changes in adipose tissue enhance expression of GPR84, a medium-chain fatty acid receptor: TNFalpha enhances GPR84 expression in adipocytes. FEBS Letters 586:368-372.

Nakamoto K, Nishinaka T, Matsumoto K, Kasuya F, Mankura M, Koyama Y, Tokuyama S (2012) Involvement of the long-chain fatty acid receptor GPR40 as a novel pain regulatory system. Brain Research 1432:74-83.

Nakanishi K, Yoshimoto T, Tsutsui H, Okamura H (2001) Interleukin-18 is a unique cytokine that stimulates both Th1 and Th2 responses depending on its cytokine milieu. Cytokine and Growth Factor Reviews 12:53-72.

Nassar MA, Levato A, Stirling LC, Wood JN (2005) Neuropathic pain develops normally in mice lacking both Na(v)1.7 and Na(v)1.8. Mol Pain 1:24.

Nassar MA, Stirling LC, Forlani G, Baker MD, Matthews EA, Dickenson AH, Wood JN (2004) Nociceptor-specific gene deletion reveals a major role for Nav1.7 (PN1) in acute and inflammatory pain. Proceedings of the National Academy of Sciences of the United States of America 101:12706-12711.

Nathan C (2006) Neutrophils and immunity: challenges and opportunities. Nat Rev Immunol 6:173-182.

Nathan CF (1987) Secretory products of macrophages. Journal of Clinical Investigation 79:319-326.

Nguyen KD, Fohner A, Booker JD, Dong C, Krensky AM, Nadeau KC (2008) XCL1 enhances regulatory activities of CD4+ CD25(high) CD127(low/-) T cells in human allergic asthma. Journal of Immunology 181:5386-5395.

Nguyen MD, Julien JP, Rivest S (2002) Innate immunity: the missing link in neuroprotection and neurodegeneration? Nat Rev Neurosci 3:216-227.

Ni M, Aschner M (2010) Neonatal rat primary microglia: isolation, culturing and selected applications. Curr Protoc Toxicol 12:12-17.

Nicol GD, Vasko MR, Evans AR (1997) Prostaglandins suppress an outward potassium current in embryonic rat sensory neurons. Journal of Neurophysiology 77:167-176.

Nikolovska-Coleska Z, Xu L, Hu Z, Tomita Y, Li P, Roller PP, Wang R, Fang X, Guo R, Zhang M, Lippman ME, Yang D, Wang S (2004) Discovery of embelin as a cell-permeable, small-molecular weight inhibitor of XIAP through structure-based computational screening of a traditional herbal medicine three-dimensional structure database. Journal of Medicinal Chemistry 47:2430-2440.

Nilius B, Appendino G, Owsianik G (2012) The transient receptor potential channel TRPA1: from gene to pathophysiology. Pflugers Archiv European Journal of Physiology 464:425-458.

Nordahl S, Alstergren P, Kopp S (2000) Tumor necrosis factor-alpha in synovial fluid and plasma from patients with chronic connective tissue disease and its relation to temporomandibular joint pain. Journal of Oral and Maxillofacial Surgery 58:525-530.

O'Connor AB, Dworkin RH (2009) Treatment of neuropathic pain: an overview of recent guidelines. American Journal of Medicine 122:S22-32.

O'Garra A, Arai N (2000) The molecular basis of T helper 1 and T helper 2 cell differentiation. Trends in Cell Biology 10:542-550.

Obata K, Katsura H, Miyoshi K, Kondo T, Yamanaka H, Kobayashi K, Dai Y, Fukuoka T, Akira S, Noguchi K (2008) Toll-like receptor 3 contributes to spinal glial activation and tactile allodynia after nerve injury. Journal of Neurochemistry 105:2249-2259.

Oberpenning F, van Ophoven A, Hertle L (2002) Interstitial cystitis: an update. Curr Opin Urol 12:321-332.

Ochi K, Kohriyama T, Higaki M, Ikeda J, Harada A, Nakamura S (2003) Changes in serum macrophage-related factors in patients with chronic inflammatory demyelinating polyneuropathy caused by intravenous immunoglobulin therapy. Journal of the Neurological Sciences 208:43-50.

Ohara PT, Vit JP, Bhargava A, Romero M, Sundberg C, Charles AC, Jasmin L (2009) Gliopathic pain: when satellite glial cells go bad. The Neuroscientist 15:450-463.

Ohtori S, Takahashi K, Moriya H, Myers RR (2004) TNF-alpha and TNF-alpha receptor type 1 upregulation in glia and neurons after peripheral nerve injury: studies in murine DRG and spinal cord. Spine 29:1082-1088.

Okamoto K, Martin DP, Schmelzer JD, Mitsui Y, Low PA (2001) Pro- and anti-inflammatory cytokine gene expression in rat sciatic nerve chronic constriction injury model of neuropathic pain. Experimental Neurology 169:386-391.

Olausson H, Cole J, Rylander K, McGlone F, Lamarre Y, Wallin BG, Kramer H, Wessberg J, Elam M, Bushnell MC, Vallbo A (2008) Functional role of unmyelinated tactile afferents in human hairy skin: sympathetic response and perceptual localization. Exp Brain Res 184:135-140.

Olechowski CJ, Truong JJ, Kerr BJ (2009) Neuropathic pain behaviours in a chronic-relapsing model of experimental autoimmune encephalomyelitis (EAE). Pain 141:156-164.

Opree A, Kress M (2000) Involvement of the proinflammatory cytokines tumor necrosis factor-alpha, IL-1 beta, and IL-6 but not IL-8 in the development of heat hyperalgesia: effects on heat-evoked calcitonin gene-related peptide release from rat skin. Journal of Neuroscience 20:6289-6293.

Osawa Y, Lee HT, Hirshman CA, Xu D, Emala CW (2006) Lipopolysaccharide-induced sensitization of adenylyl cyclase activity in murine macrophages. Am J Physiol Cell Physiol 290:143-151.

Pabreja K, Dua K, Sharma S, Padi SS, Kulkarni SK (2011) Minocycline attenuates the development of diabetic neuropathic pain: possible anti-inflammatory and anti-oxidant mechanisms. European Journal of Pharmacology 661:15-21.

Pahl HL (1999) Activators and target genes of Rel/NF-kappaB transcription factors. Oncogene 18:6853-6866.

Parada CA, Tambeli CH, Cunha FQ, Ferreira SH (2001) The major role of peripheral release of histamine and 5-hydroxytryptamine in formalin-induced nociception. Neuroscience 102:937-944.

Paredes RM, Etzler JC, Watts LT, Zheng W, Lechleiter JD (2008) Chemical calcium indicators. Methods 46:143-151.

Parekh AB (2010) Store-operated CRAC channels: function in health and disease. Nat Rev Drug Discov 9:399-410.

Paterson JA, Privat A, Ling EA, Leblond CP (1973) Investigation of glial cells in semithin sections. 3. Transformation of subependymal cells into glial cells, as shown by radioautography after 3 H-thymidine injection into the lateral ventricle of the brain of young rats. Journal of Comparative Neurology 149:83-102.

Perkins JR, Dawes JM, McMahon SB, Bennett DL, Orengo C, Kohl M (2012) ReadqPCR and NormqPCR: R packages for the reading, quality checking and normalisation of RT-qPCR quantification cycle (Cq) data. BMC Genomics 13:296.

Perkins NM, Tracey DJ (2000) Hyperalgesia due to nerve injury: role of neutrophils. Neuroscience 101:745-757.

Perrin FE, Lacroix S, Aviles-Trigueros M, David S (2005) Involvement of monocyte chemoattractant protein-1, macrophage inflammatory protein-1alpha and interleukin-1beta in Wallerian degeneration. Brain 128:854-866.

Perry VH, Hume DA, Gordon S (1985) Immunohistochemical localization of macrophages and microglia in the adult and developing mouse brain. Neuroscience 15:313-326.

Perry VH, Brown MC, Gordon S (1987) The macrophage response to central and peripheral nerve injury. A possible role for macrophages in regeneration. Journal of Experimental Medicine 165:1218-1223.

Peters-Golden M (2009) Putting on the brakes: cyclic AMP as a multipronged controller of macrophage function. Sci Signal 2:37.

Peters CM, Jimenez-Andrade JM, Kuskowski MA, Ghilardi JR, Mantyh PW (2007a) An evolving cellular pathology occurs in dorsal root ganglia, peripheral nerve and spinal cord following intravenous administration of paclitaxel in the rat. Brain Research 1168:46-59.

Peters CM, Jimenez-Andrade JM, Jonas BM, Sevcik MA, Koewler NJ, Ghilardi JR, Wong GY, Mantyh PW (2007b) Intravenous paclitaxel administration in the rat induces a peripheral sensory neuropathy characterized by macrophage infiltration and injury to sensory neurons and their supporting cells. Experimental Neurology 203:42-54.

Pezet S, McMahon SB (2006) Neurotrophins: mediators and modulators of pain. Annual Review of Neuroscience 29:507-538.

Pezet S, Marchand F, D'Mello R, Grist J, Clark AK, Malcangio M, Dickenson AH, Williams RJ, McMahon SB (2008) Phosphatidylinositol 3-kinase is a key mediator of central sensitization in painful inflammatory conditions. J Neurosci 28:4261-4270.

Phillips CJ (2006) Economic burden of chronic pain. Expert Rev Pharmacoecon Outcomes Res 6:591-601.

Pierce KL, Premont RT, Lefkowitz RJ (2002) Seven-transmembrane receptors. Nat Rev Mol Cell Biol 3:639-650.

Pillemer L, Eaker EE (1941) Anticomplementary factor in fresh yeast. Immunological:139-142.

Polomano RC, Mannes AJ, Clark US, Bennett GJ (2001) A painful peripheral neuropathy in the rat produced by the chemotherapeutic drug, paclitaxel. Pain 94:293-304.

Poltorak A (1998) Defective LPS Signaling in C3H/HeJ and C57BL/10ScCr Mice: Mutations in Tlr4 Gene. Science 282:2085-2088.

Prescott ED, Julius D (2003) A modular PIP2 binding site as a determinant of capsaicin receptor sensitivity. Science 300:1284-1288.

Priest BT, Murphy BA, Lindia JA, Diaz C, Abbadie C, Ritter AM, Liberator P, Iyer LM, Kash SF, Kohler MG, Kaczorowski GJ, MacIntyre DE, Martin WJ (2005) Contribution of the tetrodotoxin-resistant voltage-gated sodium channel NaV1.9 to sensory transmission and nociceptive behavior. Proceedings of the National Academy of Sciences of the United States of America 102:9382-9387.

Prinz M, Hausler KG, Kettenmann H, Hanisch U (2001) beta-adrenergic receptor stimulation selectively inhibits IL-12p40 release in microglia. Brain Research 899:264-270.

Putney JW, Jr. (1986) A model for receptor-regulated calcium entry. Cell Calcium 7:1-12.

Putney JW, Jr. (1990) Capacitative calcium entry revisited. Cell Calcium 11:611-624.

Racioppi L, Means AR (2008) Calcium/calmodulin-dependent kinase IV in immune and inflammatory responses: novel routes for an ancient traveller. Trends Immunol 29:600-607.

Racioppi L, Means AR (2012) Calcium/calmodulin-dependent protein kinase kinase 2: roles in signaling and pathophysiology. Journal of Biological Chemistry 287:31658-31665.

Racioppi L, Noeldner PK, Lin F, Arvai S, Means AR (2012) Calcium/calmodulin-dependent protein kinase kinase 2 regulates macrophage-mediated inflammatory responses. Journal of Biological Chemistry 287:11579-11591.

Raghavendra V, Tanga F, DeLeo JA (2003a) Inhibition of microglial activation attenuates the development but not existing hypersensitivity in a rat model of neuropathy. Journal of Pharmacology and Experimental Therapeutics 306:624-630.

Raghavendra V, Tanga FY, DeLeo JA (2004) Complete Freunds adjuvant-induced peripheral inflammation evokes glial activation and proinflammatory cytokine expression in the CNS. European Journal of Neuroscience 20:467-473.

Raghavendra V, Tanga F, Rutkowski MD, DeLeo JA (2003b) Anti-hyperalgesic and morphine-sparing actions of propentofylline following peripheral nerve injury in rats: mechanistic implications of spinal glia and proinflammatory cytokines. Pain 104:655-664.

Ralston HJ, 3rd, Light AR, Ralston DD, Perl ER (1984) Morphology and synaptic relationships of physiologically identified low-threshold dorsal root axons stained with intra-axonal horseradish peroxidase in the cat and monkey. Journal of Neurophysiology 51:777-792.

Ramer MS, Bradbury EJ, McMahon SB (2001) Nerve growth factor induces P2X(3) expression in sensory neurons. Journal of Neurochemistry 77:864-875.

Ramer MS, Bradbury EJ, Michael GJ, Lever IJ, McMahon SB (2003) Glial cell line-derived neurotrophic factor increases calcitonin gene-related peptide immunoreactivity in sensory and motoneurons in vivo. European Journal of Neuroscience 18:2713-2721.

Randall LO, Selitto JJ (1957) A method for measurement of analgesic activity on inflamed tissue. Archives Internationales de Pharmacodynamie et de Therapie 111:409-419.

Rankin EC, Choy EH, Kassimos D, Kingsley GH, Sopwith AM, Isenberg DA, Panayi GS (1995) The therapeutic effects of an engineered human anti-tumour necrosis factor alpha antibody (CDP571) in rheumatoid arthritis. British Journal of Rheumatology 34:334-342.

Ransohoff RM (2007) Microgliosis: the questions shape the answers. Nature Neuroscience 10:1507-1509.

Ransohoff RM, Perry VH (2009) Microglial physiology: unique stimuli, specialized responses. Annual Review of Immunology 27:119-145.

Rasband MN, Park EW, Vanderah TW, Lai J, Porreca F, Trimmer JS (2001) Distinct potassium channels on pain-sensing neurons. Proceedings of the National Academy of Sciences of the United States of America 98:13373-13378.

Rasley A, Bost KL, Olson JK, Miller SD, Marriott I (2002) Expression of functional NK-1 receptors in murine microglia. Glia 37:258-267.

Reeve AJ, Patel S, Fox A, Walker K, Urban L (2000) Intrathecally administered endotoxin or cytokines produce allodynia, hyperalgesia and changes in spinal cord neuronal responses to nociceptive stimuli in the rat. Eur J Pain 4:247-257.

Reimer MK, Brange C, Rosendahl A (2011) CCR8 signaling influences Toll-like receptor 4 responses in human macrophages in inflammatory diseases. Clin Vaccine Immunol 18:2050-2059.

Rexed B (1952) The cytoarchitectonic organization of the spinal cord in the cat. J Comp Neurol 96:414-495.

Ribeiro RA, Vale ML, Thomazzi SM, Paschoalato AB, Poole S, Ferreira SH, Cunha FQ (2000) Involvement of resident macrophages and mast cells in the writhing nociceptive response induced by zymosan and acetic acid in mice. European Journal of Pharmacology 387:111-118.

Rice AS, Cimino-Brown D, Eisenach JC, Kontinen VK, Lacroix-Fralish ML, Machin I, Mogil JS, Stohr T (2008) Animal models and the prediction of efficacy in clinical trials of analgesic drugs: a critical appraisal and call for uniform reporting standards. Pain 139:243-247.

Rice ASC, Morland R, Huang W, Currie GL, S. Sena ES, Macleod MR (2013) Transparency in the reporting of in vivo pre-clinical pain research: The relevance and implications of the ARRIVE (Animal Research: Reporting In Vivo Experiments) guidelines. Scandinavian Journal of Pain 4:58-62.

Ritz BW, Alexander GM, Nogusa S, Perreault MJ, Peterlin BL, Grothusen JR, Schwartzman RJ (2011) Elevated blood levels of inflammatory monocytes (CD14+ CD16+) in patients with complex regional pain syndrome. Clinical and Experimental Immunology 164:108-117.

Rodin BE, Kruger L (1984) Deafferentation in animals as a model for the study of pain: an alternative hypothesis. Brain Research 319:213-228.

Rouzaire-Dubois B, Milandri JB, Bostel S, Dubois JM (2000) Control of cell proliferation by cell volume alterations in rat C6 glioma cells. Pflügers Archiv European Journal of Physiology 440:881-888.

Rueff A, Dray A (1993) Pharmacological characterization of the effects of 5-hydroxytryptamine and different prostaglandins on peripheral sensory neurons in vitro. Agents and Actions 38:13-15.

Rueff A, Mendell LM (1996) Nerve growth factor NT-5 induce increased thermal sensitivity of cutaneous nociceptors in vitro. Journal of Neurophysiology 76:3593-3596.

Rutkowski MD, Pahl JL, Sweitzer S, van Rooijen N, DeLeo JA (2000) Limited role of macrophages in generation of nerve injury-induced mechanical allodynia. Physiology and Behavior 71:225-235.

Safieh-Garabedian B, Poole S, Allchorne A, Winter J, Woolf CJ (1995) Contribution of interleukin-1 beta to the inflammation-induced increase in nerve growth factor levels and inflammatory hyperalgesia. British Journal of Pharmacology 115:1265-1275.

Saijo K, Glass CK (2011) Microglial cell origin and phenotypes in health and disease. Nat Rev Immunol 11:775-787.

Samad TA, Sapirstein A, Woolf CJ (2002) Prostanoids and pain: unraveling mechanisms and revealing therapeutic targets. Trends Mol Med 8:390-396.

Sandkuhler J (2009) Models and mechanisms of hyperalgesia and allodynia. Physiol Rev 89:707-758.

Sassone-Corsi P (2012) The cyclic AMP pathway. Cold Spring Harb Perspect Biol 4.

Scapini P, Lapinet-Vera JA, Gasperini S, Calzetti F, Bazzoni F, Cassatella MA (2000) The neutrophil as a cellular source of chemokines. Immunological Reviews 177:195-203.

Schafers M, Geis C, Svensson CI, Luo ZD, Sommer C (2003a) Selective increase of tumour necrosis factor-alpha in injured and spared myelinated primary afferents after chronic constrictive injury of rat sciatic nerve. European Journal of Neuroscience 17:791-804.

Schafers M, Lee DH, Brors D, Yaksh TL, Sorkin LS (2003b) Increased sensitivity of injured and adjacent uninjured rat primary sensory neurons to exogenous tumor necrosis factor-alpha after spinal nerve ligation. Journal of Neuroscience 23:3028-3038.

Schmid CD, Melchior B, Masek K, Puntambekar SS, Danielson PE, Lo DD, Sutcliffe JG, Carson MJ (2009) Differential gene expression in LPS/IFNgamma activated microglia and macrophages: in vitro versus in vivo. Journal of Neurochemistry 109:117-125.

Schmidt R, Schmelz M, Forster C, Ringkamp M, Torebjork E, Handwerker H (1995) Novel classes of responsive and unresponsive C nociceptors in human skin. Journal of Neuroscience 15:333-341.

Schmittgen TD, Livak KJ (2008) Analyzing real-time PCR data by the comparative C(T) method. Nat Protoc 3:1101-1108.

Schmitz K, Pickert G, Wijnvoord N, Haussler A, Tegeder I (2013) Dichotomy of CCL21 and CXCR3 in nerve injury-evoked and autoimmunity-evoked hyperalgesia. Brain, Behavior, and Immunity 32:186–200.

Schneider MR, Wolf E (2009) The epidermal growth factor receptor ligands at a glance. Journal of Cellular Physiology 218:460-466.

Scholz J, Woolf CJ (2002) Can we conquer pain? Nature Neuroscience 5:1062-1067.

Scholz J, Woolf CJ (2007) The neuropathic pain triad: neurons, immune cells and glia. Nature Neuroscience 10:1361-1368.

Schwarz BA, Bhandoola A (2006) Trafficking from the bone marrow to the thymus: a prerequisite for thymopoiesis. Immunological Reviews 209:47-57.

Seltzer Z, Dubner R, Shir Y (1990) A novel behavioral model of neuropathic pain disorders produced in rats by partial sciatic nerve injury. Pain 43:205-218.

Semenova SB, Kiselev KI, Mozhaeva GN (1999) Low-conductivity calcium channels in the macrophage plasma membrane: activation by inositol-1,4,5-triphosphate. Neuroscience and Behavioral Physiology 29:339-345.

Serezani CH, Ballinger MN, Aronoff DM, Peters-Golden M (2008) Cyclic AMP: master regulator of innate immune cell function. American Journal of Respiratory Cell and Molecular Biology 39:127-132.

Serrano A, Pare M, McIntosh F, Elmes SJ, Martino G, Jomphe C, Lessard E, Lembo PM, Vaillancourt F, Perkins MN, Cao CQ (2010) Blocking spinal CCR2 with AZ889 reversed hyperalgesia in a model of neuropathic pain. Mol Pain 6:90.

Shamash S, Reichert F, Rotshenker S (2002) The cytokine network of Wallerian degeneration: tumor necrosis factor-alpha, interleukin-1alpha, and interleukin-1beta. Journal of Neuroscience 22:3052-3060.

Sherrington CS (1906) Observations on the scratch-reflex in the spinal dog. J Physiol 34:1-50.

Shi XQ, Zekki H, Zhang J (2011) The role of TLR2 in nerve injury-induced neuropathic pain is essentially mediated through macrophages in peripheral inflammatory response. Glia 59:231-241.

Shubayev VI, Myers RR (2000) Upregulation and interaction of TNFalpha and gelatinases A and B in painful peripheral nerve injury. Brain Research 855:83-89.

Siderovski DP, Willard FS (2005) The GAPs, GEFs, and GDIs of heterotrimeric G-protein alpha subunits. Int J Biol Sci 1:51-66.

Siebert H, Sachse A, Kuziel WA, Maeda N, Bruck W (2000) The chemokine receptor CCR2 is involved in macrophage recruitment to the injured peripheral nervous system. Journal of Neuroimmunology 110:177-185.

Sivilotti L, Woolf CJ (1994) The contribution of GABAA and glycine receptors to central sensitization: disinhibition and touch-evoked allodynia in the spinal cord. Journal of Neurophysiology 72:169-179.

Smyth EM, Grosser T, Wang M, Yu Y, FitzGerald GA (2009) Prostanoids in health and disease. Journal of Lipid Research 50:423-428.

Snider WD, McMahon SB (1998) Tackling pain at the source: new ideas about nociceptors. Neuron 20:629-632.

Soderling TR (1999) The Ca-calmodulin-dependent protein kinase cascade. Trends in Biochemical Sciences 24:232-236.

Sola C, Barron S, Tusell JM, Serratosa J (1999) The Ca2+/calmodulin signaling system in the neural response to excitability. Involvement of neuronal and glial cells. Progress in Neurobiology 58:207-232.

Sommer C, Kress M (2004) Recent findings on how proinflammatory cytokines cause pain: peripheral mechanisms in inflammatory and neuropathic hyperalgesia. Neuroscience Letters 361:184-187.

Sommer C, Schafers M, Marziniak M, Toyka KV (2001) Etanercept reduces hyperalgesia in experimental painful neuropathy. Journal of the Peripheral Nervous System 6:67-72.

Sonoki T, Nagasaki A, Gotoh T, Takiguchi M, Takeya M, Matsuzaki H, Mori M (1997) Coinduction of nitric-oxide synthase and arginase I in cultured rat peritoneal macrophages and rat tissues in vivo by lipopolysaccharide. Journal of Biological Chemistry 272:3689-3693.

Sorkin LS, Xiao WH, Wagner R, Myers RR (1997) Tumour necrosis factor-alpha induces ectopic activity in nociceptive primary afferent fibres. Neuroscience 81:255-262.

Souza GE, Cunha FQ, Mello R, Ferreira SH (1988) Neutrophil migration induced by inflammatory stimuli is reduced by macrophage depletion. Agents and Actions 24:377-380.

St-Jacques B, Ma W (2011) Role of prostaglandin E2 in the synthesis of the pro-inflammatory cytokine interleukin-6 in primary sensory neurons: an in vivo and in vitro study. Journal of Neurochemistry 118:841-854.

Staiano RI, Granata F, Secondo A, Petraroli A, Loffredo S, Annunziato L, Triggiani M, Marone G (2013) Human macrophages and monocytes express functional Na(+)/Ca (2+) exchangers 1 and 3. Advances in Experimental Medicine and Biology 961:317-326.

Staniland AA, Clark AK, Wodarski R, Sasso O, Maione F, D'Acquisto F, Malcangio M (2010) Reduced inflammatory and neuropathic pain and decreased spinal microglial response in fractalkine receptor (CX3CR1) knockout mice. Journal of Neurochemistry 114:1143-1157.

Staton PC, Wilson AW, Bountra C, Chessell IP, Day NC (2007) Changes in dorsal root ganglion CGRP expression in a chronic inflammatory model of the rat knee joint: differential modulation by rofecoxib and paracetamol. Eur J Pain 11:283-289.

Stein AT, Ufret-Vincenty CA, Hua L, Santana LF, Gordon SE (2006) Phosphoinositide 3-kinase binds to TRPV1 and mediates NGF-stimulated TRPV1 trafficking to the plasma membrane. J Gen Physiol 128:509-522.

Strong JA, Xie W, Coyle DE, Zhang JM (2012) Microarray analysis of rat sensory ganglia after local inflammation implicates novel cytokines in pain. PLoS One 7.

Suh HW, Lee HK, Seo YJ, Kwon MS, Shim EJ, Lee JY, Choi SS, Lee JH (2005) Kainic acid (KA)-induced Ca2+/calmodulin-dependent protein kinase II (CaMK II) expression in the neurons, astrocytes and microglia of the mouse hippocampal CA3 region, and the phosphorylated CaMK II only in the hippocampal neurons. Neuroscience Letters 381:223-227.

Sun S, Cao H, Han M, Li TT, Pan HL, Zhao ZQ, Zhang YQ (2007) New evidence for the involvement of spinal fractalkine receptor in pain facilitation and spinal glial activation in rat model of monoarthritis. Pain 129:64-75.

Sung CS, Wen ZH, Chang WK, Ho ST, Tsai SK, Chang YC, Wong CS (2004) Intrathecal interleukin-1beta administration induces thermal hyperalgesia by activating inducible nitric oxide synthase expression in the rat spinal cord. Brain Research 1015:145-153.

Sung CS, Wen ZH, Chang WK, Chan KH, Ho ST, Tsai SK, Chang YC, Wong CS (2005) Inhibition of p38 mitogen-activated protein kinase attenuates interleukin-1beta-induced thermal hyperalgesia and inducible nitric oxide synthase expression in the spinal cord. Journal of Neurochemistry 94:742-752.

Sutherland EW, Rall TW (1958) Fractionation and characterization of a cyclic adenine ribonucleotide formed by tissue particles. Journal of Biological Chemistry 232:1077-1091.

Suyama H, Kawamoto M, Gaus S, Yuge O (2004) Effect of etodolac, a COX-2 inhibitor, on neuropathic pain in a rat model. Brain Research 1010:144-150.

Suzuki M, Takaishi S, Nagasaki M, Onozawa Y, Iino I, Maeda H, Komai T, Oda T (2013) Medium-chain Fatty Acid-sensing Receptor, GPR84, Is a Proinflammatory Receptor. Journal of Biological Chemistry 288:10684-10691.

Suzuki N, Hasegawa-Moriyama M, Takahashi Y, Kamikubo Y, Sakurai T, Inada E (2011) Lidocaine attenuates the development of diabetic-induced tactile allodynia by inhibiting microglial activation. Anesthesia and Analgesia 113:941-946.

Suzuki R, Dickenson A (2005) Spinal and supraspinal contributions to central sensitization in peripheral neuropathy. Neurosignals 14:175-181.

Suzuki T, Hide I, Ido K, Kohsaka S, Inoue K, Nakata Y (2004) Production and release of neuroprotective tumor necrosis factor by P2X7 receptor-activated microglia. Journal of Neuroscience 24:1-7.

Svensson CI, Hua XY, Protter AA, Powell HC, Yaksh TL (2003a) Spinal p38 MAP kinase is necessary for NMDA-induced spinal PGE(2) release and thermal hyperalgesia. Neuroreport 14:1153-1157.

Svensson CI, Schafers M, Jones TL, Powell H, Sorkin LS (2005) Spinal blockade of TNF blocks spinal nerve ligation-induced increases in spinal P-p38. Neuroscience Letters 379:209-213.

Svensson CI, Marsala M, Westerlund A, Calcutt NA, Campana WM, Freshwater JD, Catalano R, Feng Y, Protter AA, Scott B, Yaksh TL (2003b) Activation of p38 mitogen-activated protein kinase in spinal microglia is a critical link in inflammation-induced spinal pain processing. Journal of Neurochemistry 86:1534-1544.

Sweitzer SM, Schubert P, DeLeo JA (2001) Propentofylline, a glial modulating agent, exhibits antiallodynic properties in a rat model of neuropathic pain. Journal of Pharmacology and Experimental Therapeutics 297:1210-1217.

Sweitzer SM, Colburn RW, Rutkowski M, DeLeo JA (1999) Acute peripheral inflammation induces moderate glial activation and spinal IL-1beta expression that correlates with pain behavior in the rat. Brain Research 829:209-221.

Sweitzer SM, Medicherla S, Almirez R, Dugar S, Chakravarty S, Shumilla JA, Yeomans DC, Protter AA (2004) Antinociceptive action of a p38alpha MAPK inhibitor, SD-282, in a diabetic neuropathy model. Pain 109:409-419.

Taiwo YO, Levine JD (1991) Further confirmation of the role of adenyl cyclase and of cAMP-dependent protein kinase in primary afferent hyperalgesia. Neuroscience 44:131-135.

Takeda M, Kitagawa J, Takahashi M, Matsumoto S (2008) Activation of interleukin-1beta receptor suppresses the voltage-gated potassium currents in the small-diameter trigeminal ganglion neurons following peripheral inflammation. Pain 139:594-602.

Takeda M, Tanimoto T, Ikeda M, Nasu M, Kadoi J, Yoshida S, Matsumoto S (2006) Enhanced excitability of rat trigeminal root ganglion neurons via decrease in A-type potassium currents following temporomandibular joint inflammation. Neuroscience 138:621-630.

Takeda M, Tanimoto T, Kadoi J, Nasu M, Takahashi M, Kitagawa J, Matsumoto S (2007) Enhanced excitability of nociceptive trigeminal ganglion neurons by satellite glial cytokine following peripheral inflammation. Pain 129:155-166.

Talukdar S, Olefsky JM, Osborn O (2011) Targeting GPR120 and other fatty acid-sensing GPCRs ameliorates insulin resistance and inflammatory diseases. Trends Pharmacol Sci 32:543-550.

Tanga FY, Raghavendra V, DeLeo JA (2004) Quantitative real-time RT-PCR assessment of spinal microglial and astrocytic activation markers in a rat model of neuropathic pain. Neurochemistry International 45:397-407.

Tanga FY, Nutile-McMenemy N, DeLeo JA (2005) The CNS role of Toll-like receptor 4 in innate neuroimmunity and painful neuropathy. Proceedings of the National Academy of Sciences of the United States of America 102:5856-5861.

Tannenbaum CS, Hamilton TA (1989) Lipopolysaccharide-induced gene expression in murine peritoneal macrophages is selectively suppressed by agents that elevate intracellular cAMP. Journal of Immunology 142:1274-1280.

Taub DD, Lloyd AR, Conlon K, Wang JM, Ortaldo JR, Harada A, Matsushima K, Kelvin DJ, Oppenheim JJ (1993) Recombinant human interferon-inducible protein 10 is a chemoattractant for human monocytes and T lymphocytes and promotes T cell adhesion to endothelial cells. Journal of Experimental Medicine 177:1809-1814.

Tawfik VL, Regan MR, Haenggeli C, Lacroix-Fralish ML, Nutile-McMenemy N, Perez N, Rothstein JD, DeLeo JA (2008) Propentofylline-induced astrocyte modulation leads to alterations in glial glutamate promoter activation following spinal nerve transection. Neuroscience 152:1086-1092.

Taylor SS, Knighton DR, Zheng J, Ten Eyck LF, Sowadski JM (1992) Structural framework for the protein kinase family. Annual Review of Cell Biology 8:429-462.

Thacker MA, Clark AK, Marchand F, McMahon SB (2007) Pathophysiology of peripheral neuropathic pain: immune cells and molecules. Anesthesia and Analgesia 105:838-847.

Thacker MA, Clark AK, Bishop T, Grist J, Yip PK, Moon LD, Thompson SW, Marchand F, McMahon SB (2009) CCL2 is a key mediator of microglia activation in neuropathic pain states. Eur J Pain 13:263-272.

Thippeswamy BS, Nagakannan P, Shivasharan BD, Mahendran S, Veerapur VP, Badami S (2011a) Protective effect of embelin from Embelia ribes Burm. against transient global ischemia-induced brain damage in rats. Neurotox Res 20:379-386.

Thippeswamy BS, Mahendran S, Biradar MI, Raj P, Srivastava K, Badami S, Veerapur VP (2011b) Protective effect of embelin against acetic acid induced ulcerative colitis in rats. European Journal of Pharmacology 654:100-105.

Thomazzi SM, Ribeiro RA, Campos DI, Cunha FQ, Ferreira SH (1997) Tumor necrosis factor, interleukin-1 and interleukin-8 mediate the nociceptive activity of the supernatant of LPS-stimulated macrophages. Mediators of Inflammation 6:195-200.

Ting E, Guerrero AT, Cunha TM, Verri WA, Jr., Taylor SM, Woodruff TM, Cunha FQ, Ferreira SH (2008) Role of complement C5a in mechanical inflammatory hypernociception: potential use of C5a receptor antagonists to control inflammatory pain. British Journal of Pharmacology 153:1043-1053.

Todd AJ (2010) Neuronal circuitry for pain processing in the dorsal horn. Nat Rev Neurosci 11:823-836.

Todd AJ, Spike RC, Polgar E (1998) A quantitative study of neurons which express neurokinin-1 or somatostatin sst2a receptor in rat spinal dorsal horn. Neuroscience 85:459-473.

Toescu EC, Moller T, Kettenmann H, Verkhratsky A (1998) Long-term activation of capacitative Ca2+ entry in mouse microglial cells. Neuroscience 86:925-935.

Tofaris GK, Patterson PH, Jessen KR, Mirsky R (2002) Denervated Schwann cells attract macrophages by secretion of leukemia inhibitory factor (LIF) and monocyte chemoattractant protein-1 in a process regulated by interleukin-6 and LIF. Journal of Neuroscience 22:6696-6703.

Ton BH, Chen Q, Gaina G, Tucureanu C, Georgescu A, Strungaru C, Flonta ML, Sah D, Ristoiu V (2013) Activation profile of dorsal root ganglia Iba-1 (+) macrophages varies with the type of lesion in rats. Acta Histochemica 115: 840–850.

Treede RD, Jensen TS, Campbell JN, Cruccu G, Dostrovsky JO, Griffin JW, Hansson P, Hughes R, Nurmikko T, Serra J (2008) Neuropathic pain: redefinition and a grading system for clinical and research purposes. Neurology 70:1630-1635.

Tsantoulas C, McMahon SB (2014) Opening paths to novel analgesics: the role of potassium channels in chronic pain. Trends in Neurosciences.

Tsantoulas C, Zhu L, Yip P, Grist J, Michael GJ, McMahon SB (2014) Kv2 dysfunction after peripheral axotomy enhances sensory neuron responsiveness to sustained input. Experimental Neurology 251:115-126.

Tsantoulas C, Zhu L, Shaifta Y, Grist J, Ward JP, Raouf R, Michael GJ, McMahon SB (2012) Sensory neuron downregulation of the Kv9.1 potassium channel subunit mediates neuropathic pain following nerve injury. Journal of Neuroscience 32:17502-17513.

Tsuda M, Mizokoshi A, Shigemoto-Mogami Y, Koizumi S, Inoue K (2004) Activation of p38 mitogen-activated protein kinase in spinal hyperactive microglia contributes to pain hypersensitivity following peripheral nerve injury. Glia 45:89-95.

Tsuda M, Ueno H, Kataoka A, Tozaki-Saitoh H, Inoue K (2008) Activation of dorsal horn microglia contributes to diabetes-induced tactile allodynia via extracellular signal-regulated protein kinase signaling. Glia 56:378-386.

Tsuda M, Shigemoto-Mogami Y, Koizumi S, Mizokoshi A, Kohsaka S, Salter MW, Inoue K (2003) P2X4 receptors induced in spinal microglia gate tactile allodynia after nerve injury. Nature 424:778-783.

Ubogu EE, Cossoy MB, Ransohoff RM (2006) The expression and function of chemokines involved in CNS inflammation. Trends in Pharmacological Sciences 27:48-55.

Uceyler N, Rogausch JP, Toyka KV, Sommer C (2007a) Differential expression of cytokines in painful and painless neuropathies. Neurology 69:42-49.

Uceyler N, Eberle T, Rolke R, Birklein F, Sommer C (2007b) Differential expression patterns of cytokines in complex regional pain syndrome. Pain 132:195-205.

Uchiya Ki, Groisman EA, Nikai T (2004) Involvement of Salmonella Pathogenicity Island 2 in the Up-Regulation of Interleukin-10 Expression in Macrophages: Role of Protein Kinase A Signal Pathway. Infection and Immunity 72:1964-1973.

Ulmann L, Hirbec H, Rassendren F (2010) P2X4 receptors mediate PGE2 release by tissue-resident macrophages and initiate inflammatory pain. EMBO Journal 29:2290-2300.

Ulven T (2012) Short-chain free fatty acid receptors FFA2/GPR43 and FFA3/GPR41 as new potential therapeutic targets. Front Endocrinol 3:111.

Upchurch KS, Kay J (2012) Evolution of treatment for rheumatoid arthritis. Rheumatology 51:28-36.

Urb M, Sheppard DC (2012) The role of mast cells in the defence against pathogens. PLoS Pathog 8.

Vairo G, Argyriou S, Bordun AM, Whitty G, Hamilton JA (1990) Inhibition of the signaling pathways for macrophage proliferation by cyclic AMP. Lack of effect on early responses to colony stimulating factor-1. Journal of Biological Chemistry 265:2692-2701.

Vanegas H, Schaible HG (2001) Prostaglandins and cyclooxygenases [correction of cycloxygenases] in the spinal cord. Progress in Neurobiology 64:327-363.

Vasko MR (1995) Prostaglandin-induced neuropeptide release from spinal cord. Progress in Brain Research 104:367-380.

Venkataraman C, Kuo F (2005) The G-protein coupled receptor, GPR84 regulates IL-4 production by T lymphocytes in response to CD3 crosslinking. Immunology Letters 101:144-153.

Verkhratsky A, Parpura V (2013) Store-operated calcium entry in neuroglia. Neurosci Bull.

Verkhratsky A, Orkand RK, Kettenmann H (1998) Glial calcium: homeostasis and signaling function. Physiological Reviews 78:99-141.

Verpoorten N, Claeys KG, Deprez L, Jacobs A, Van Gerwen V, Lagae L, Arts WF, De Meirleir L, Keymolen K, Ceuterick-de Groote C, De Jonghe P, Timmerman V, Nelis E (2006) Novel frameshift and splice site mutations in the neurotrophic tyrosine kinase receptor type 1 gene (NTRK1) associated with hereditary sensory neuropathy type IV. Neuromuscular Disorders 16:19-25.

Verri WA (2005) Nociceptive Effect of Subcutaneously Injected Interleukin-12 Is Mediated by Endothelin (ET) Acting on ETB Receptors in Rats. Journal of Pharmacology and Experimental Therapeutics 315:609-615.

Verri WA, Cunha TM, Parada CA, Poole S, Cunha FQ, Ferreira SH (2006) Hypernociceptive role of cytokines and chemokines: Targets for analgesic drug development? Pharmacology & Therapeutics 112:116-138.

Versleijen MW, van Esterik JC, Roelofs HM, van Emst-de Vries SE, Willems PH, Wanten GJ (2009) Parenteral medium-chain triglyceride-induced neutrophil activation is not mediated by a Pertussis Toxin sensitive receptor. Clin Nutr 28:59-64.

Vig M, Kinet JP (2009) Calcium signaling in immune cells. Nat Immunol 10:21-27.

Voilley N, de Weille J, Mamet J, Lazdunski M (2001) Nonsteroid anti-inflammatory drugs inhibit both the activity and the inflammation-induced expression of acid-sensing ion channels in nociceptors. Journal of Neuroscience 21:8026-8033.

Vulchanova L, Riedl MS, Shuster SJ, Stone LS, Hargreaves KM, Buell G, Surprenant A, North RA, Elde R (1998) P2X3 is expressed by DRG neurons that terminate in inner lamina II. European Journal of Neuroscience 10:3470-3478.

Wagner R, Myers RR (1996) Endoneurial injection of TNF-alpha produces neuropathic pain behaviors. Neuroreport 7:2897-2901.

Wakeland E, Morel L, Achey K, Yui M, Longmate J (1997) Speed congenics: a classic technique in the fast lane (relatively speaking). Immunology Today 18:472-477.

Wall EA, Zavzavadjian JR, Chang MS, Randhawa B, Zhu X, Hsueh RC, Liu J, Driver A, Bao XR, Sternweis PC, Simon MI, Fraser ID (2009) Suppression of LPS-induced TNF-alpha production in macrophages by cAMP is mediated by PKA-AKAP95-p105. Sci Signal 2:2.

Wall PD, Devor M, Inbal R, Scadding JW, Schonfeld D, Seltzer Z, Tomkiewicz MM (1979) Autotomy following peripheral nerve lesions: experimental anaesthesia dolorosa. Pain 7:103-111.

Wallace VC, Blackbeard J, Segerdahl AR, Hasnie F, Pheby T, McMahon SB, Rice AS (2007a) Characterization of rodent models of HIV-gp120 and anti-retroviral-associated neuropathic pain. Brain 130:2688-2702.

Wallace VC, Blackbeard J, Pheby T, Segerdahl AR, Davies M, Hasnie F, Hall S, McMahon SB, Rice AS (2007b) Pharmacological, behavioural and mechanistic analysis of HIV-1 gp120 induced painful neuropathy. Pain 133:47-63.

Walz W, Ilschner S, Ohlemeyer C, Banati R, Kettenmann H (1993) Extracellular ATP activates a cation conductance and a K+ conductance in cultured microglial cells from mouse brain. Journal of Neuroscience 13:4403-4411.

Wang H, Dai Y, Fukuoka T, Yamanaka H, Obata K, Tokunaga A, Noguchi K (2004) Enhancement of stimulation-induced ERK activation in the spinal dorsal horn and gracile nucleus neurons in rats with peripheral nerve injury. European Journal of Neuroscience 19:884-890.

Wang J, Wu X, Simonavicius N, Tian H, Ling L (2006a) Medium-chain fatty acids as ligands for orphan G protein-coupled receptor GPR84. Journal of Biological Chemistry 281:34457-34464.

Wang LN, Yang JP, Zhan Y, Ji FH, Wang XY, Zuo JL, Xu QN (2012a) Minocycline-induced reduction of brain-derived neurotrophic factor expression in relation to cancer-induced bone pain in rats. Journal of Neuroscience Research 90:672-681.

Wang LN, Yao M, Yang JP, Peng J, Peng Y, Li CF, Zhang YB, Ji FH, Cheng H, Xu QN, Wang XY, Zuo JL (2011) Cancer-induced bone pain sequentially activates the ERK/MAPK pathway in different cell types in the rat spinal cord. Mol Pain 7:48.

Wang R, Guo W, Ossipov MH, Vanderah TW, Porreca F, Lai J (2003) Glial cell line-derived neurotrophic factor normalizes neurochemical changes in injured dorsal root ganglion neurons and prevents the expression of experimental neuropathic pain. Neuroscience 121:815-824.

Wang S, Dai Y, Fukuoka T, Yamanaka H, Kobayashi K, Obata K, Cui X, Tominaga M, Noguchi K (2008) Phospholipase C and protein kinase A mediate bradykinin sensitization of TRPA1: a molecular mechanism of inflammatory pain. Brain 131:1241-1251.

Wang X, Li WG, Yu Y, Xiao X, Cheng J, Zeng WZ, Peng Z, Xi Zhu M, Xu TL (2013) Serotonin facilitates peripheral pain sensitivity in a manner that depends on the nonproton ligand sensing domain of ASIC3 channel. Journal of Neuroscience 33:4265-4279.

Wang XW, Li TT, Zhao J, Mao-Ying QL, Zhang H, Hu S, Li Q, Mi WL, Wu GC, Zhang YQ, Wang YQ (2012b) Extracellular signal-regulated kinase activation in spinal astrocytes and microglia contributes to cancer-induced bone pain in rats. Neuroscience 217:172-181.

Wang Z, Dillon TJ, Pokala V, Mishra S, Labudda K, Hunter B, Stork PJ (2006b) Rap1-mediated activation of extracellular signal-regulated kinases by cyclic AMP is dependent on the mode of Rap1 activation. Molecular and Cellular Biology 26:2130-2145.

Wanten G (2006) An update on parenteral lipids and immune function: only smoke, or is there any fire? Curr Opin Clin Nutr Metab Care 9:79-83.

Wanten G, Kusters A, van Emst-de Vries SE, Tool A, Roos D, Naber T, Willems P (2004) Lipid effects on neutrophil calcium signaling induced by opsonized particles: platelet activating factor is only part of the story. Clinical Nutrition 23:623-630.

Wanten GJ, Naber AH (2004) Cellular and physiological effects of medium-chain triglycerides. Mini Rev Med Chem 4:847-857.

Watkins LR, Maier SF (2003) Glia: a novel drug discovery target for clinical pain. Nat Rev Drug Discov 2:973-985.

Watkins LR, Milligan ED, Maier SF (2001) Glial activation: a driving force for pathological pain. Trends in Neurosciences 24:450-455.

Watkins LR, Martin D, Ulrich P, Tracey KJ, Maier SF (1997) Evidence for the involvement of spinal cord glia in subcutaneous formalin induced hyperalgesia in the rat. Pain 71:225-235.

Wei F, Vadakkan KI, Toyoda H, Wu LJ, Zhao MG, Xu H, Shum FW, Jia YH, Zhuo M (2006) Calcium calmodulin-stimulated adenylyl cyclases contribute to activation of extracellular signal-regulated kinase in spinal dorsal horn neurons in adult rats and mice. Journal of Neuroscience 26:851-861.

Wei F, Qiu CS, Kim SJ, Muglia L, Maas JW, Pineda VV, Xu HM, Chen ZF, Storm DR, Muglia LJ, Zhuo M (2002) Genetic elimination of behavioral sensitization in mice lacking calmodulin-stimulated adenylyl cyclases. Neuron 36:713-726.

Wei XQ, Leung BP, Arthur HM, McInnes IB, Liew FY (2001) Reduced incidence and severity of collagen-induced arthritis in mice lacking IL-18. Journal of Immunology 166:517-521.

Wells TN, Power CA, Shaw JP, Proudfoot AE (2006) Chemokine blockers--therapeutics in the making? Trends in Pharmacological Sciences 27:41-47.

Wemmie JA, Price MP, Welsh MJ (2006) Acid-sensing ion channels: advances, questions and therapeutic opportunities. Trends in Neurosciences 29:578-586.

White GE, Iqbal AJ, Greaves DR (2013) CC chemokine receptors and chronic inflammation--therapeutic opportunities and pharmacological challenges. Pharmacological Reviews 65:47-89.

Wieseler-Frank J, Maier SF, Watkins LR (2005) Immune-to-brain communication dynamically modulates pain: physiological and pathological consequences. Brain, Behavior, and Immunity 19:104-111.

Wild KD, Bian D, Zhu D, Davis J, Bannon AW, Zhang TJ, Louis JC (2007) Antibodies to nerve growth factor reverse established tactile allodynia in rodent models of neuropathic pain without tolerance. Journal of Pharmacology and Experimental Therapeutics 322:282-287.

Willis D, Li KW, Zheng JQ, Chang JH, Smit AB, Kelly T, Merianda TT, Sylvester J, van Minnen J, Twiss JL (2005) Differential transport and local translation of cytoskeletal, injury-response, and neurodegeneration protein mRNAs in axons. Journal of Neuroscience 25:778-791.

Wilson SG, Mogil JS (2001) Measuring pain in the (knockout) mouse: big challenges in a small mammal. Behavioural Brain Research 125:65-73.

Winkelstein BA, DeLeo JA (2002) Nerve root injury severity differentially modulates spinal glial activation in a rat lumbar radiculopathy model: considerations for persistent pain. Brain Research 956:294-301.

Witko-Sarsat V, Rieu P, Descamps-Latscha B, Lesavre P, Halbwachs-Mecarelli L (2000) Neutrophils: molecules, functions and pathophysiological aspects. Laboratory Investigation 80:617-653.

Wittenberger T, Schaller HC, Hellebrand S (2001) An expressed sequence tag (EST) data mining strategy succeeding in the discovery of new G-protein coupled receptors. Journal of Molecular Biology 307:799-813.

Wodarski R, Clark AK, Grist J, Marchand F, Malcangio M (2009) Gabapentin reverses microglial activation in the spinal cord of streptozotocin-induced diabetic rats. Eur J Pain 13:807-811.

Woolf CJ (1983) Evidence for a central component of post-injury pain hypersensitivity. Nature 306:686-688.

Woolf CJ (1996) Phenotypic modification of primary sensory neurons: the role of nerve growth factor in the production of persistent pain. Philosophical Transactions of the Royal Society of London Series B: Biological Sciences 351:441-448.

Woolf CJ, Salter MW (2000) Neuronal plasticity: increasing the gain in pain. Science 288:1765-1769.

Woolf CJ, Ma Q (2007) Nociceptors—Noxious Stimulus Detectors. Neuron 55:353-364.

Woolf CJ, Ma QP, Allchorne A, Poole S (1996) Peripheral cell types contributing to the hyperalgesic action of nerve growth factor in inflammation. Journal of Neuroscience 16:2716-2723.

Woolf CJ, Allchorne A, Safieh-Garabedian B, Poole S (1997) Cytokines, nerve growth factor and inflammatory hyperalgesia: the contribution of tumour necrosis factor alpha. British Journal of Pharmacology 121:417-424.

Worley PF, Zeng W, Huang GN, Yuan JP, Kim JY, Lee MG, Muallem S (2007) TRPC channels as STIM1-regulated store-operated channels. Cell Calcium 42:205-211.

Wu Y, Willcockson HH, Maixner W, Light AR (2004) Suramin inhibits spinal cord microglia activation and long-term hyperalgesia induced by formalin injection. J Pain 5:48-55.

Wuarin-Bierman L, Zahnd GR, Kaufmann F, Burcklen L, Adler J (1987) Hyperalgesia in spontaneous and experimental animal models of diabetic neuropathy. Diabet 30:653-658.

Wynn TA, Chawla A, Pollard JW (2013) Macrophage biology in development, homeostasis and disease. Nature 496:445-455.

Xiao HS, Huang QH, Zhang FX, Bao L, Lu YJ, Guo C, Yang L, Huang WJ, Fu G, Xu SH, Cheng XP, Yan Q, Zhu ZD, Zhang X, Chen Z, Han ZG, Zhang X (2002) Identification of gene expression profile of dorsal root ganglion in the rat peripheral axotomy model of neuropathic pain. Proceedings of the National Academy of Sciences of the United States of America 99:8360-8365.

Xu GY, Huang LY (2002) Peripheral inflammation sensitizes P2X receptor-mediated responses in rat dorsal root ganglion neurons. Journal of Neuroscience 22:93-102.

Yaqoob P (2004) Fatty acids and the immune system: from basic science to clinical applications. Proceedings of the Nutrition Society 63:89-104.

Yeo JF, Liu HP, Leong SK (2001) Sustained Microglial Immunoreactivity in the Caudal Spinal Trigeminal Nucleus after Formalin Injection. Journal of Dental Research 80:1524-1529.

Yoon SY, Patel D, Dougherty PM (2012) Minocycline blocks lipopolysaccharide induced hyperalgesia by suppression of microglia but not astrocytes. Neuroscience 221:214-224.

Yousefi S, Cooper PR, Potter SL, Mueck B, Jarai G (2001) An expressed sequence tag (EST) data mining strategy succeeding in the discovery of new G-protein coupled receptors. J Leukoc Biol 69:1045-1052.

Zarpelon AC, Cunha TM, Alves-Filho JC, Pinto LG, Ferreira SH, McInnes IB, Xu D, Liew FY, Cunha FQ, Verri WA (2013) IL-33/ST2 signalling contributes to carrageenin-induced innate inflammation and inflammatory pain: role of cytokines, endothelin-1 and prostaglandin E2. British Journal of Pharmacology 169:90-101.

Zelenka M, Schafers M, Sommer C (2005) Intraneural injection of interleukin-1beta and tumor necrosis factor-alpha into rat sciatic nerve at physiological doses induces signs of neuropathic pain. Pain 116:257-263.

Zhang H, Yoon SY, Zhang H, Dougherty PM (2012a) Evidence that spinal astrocytes but not microglia contribute to the pathogenesis of Paclitaxel-induced painful neuropathy. J Pain 13:293-303.

Zhang HL, Hassan MY, Zheng XY, Azimullah S, Quezada HC, Amir N, Elwasila M, Mix E, Adem A, Zhu J (2012b) Attenuated EAN in TNF-alpha deficient mice is associated with an altered balance of M1/M2 macrophages. PLoS One 7:38157.

Zhang J, Hoffert C, Vu HK, Groblewski T, Ahmad S, O'Donnell D (2003) Induction of CB2 receptor expression in the rat spinal cord of neuropathic but not inflammatory chronic pain models. European Journal of Neuroscience 17:2750-2754.

Zhang J, Shi XQ, Echeverry S, Mogil JS, De Koninck Y, Rivest S (2007) Expression of CCR2 in both resident and bone marrow-derived microglia plays a critical role in neuropathic pain. Journal of Neuroscience 27:12396-12406.

Zhang N, Inan S, Cowan A, Sun R, Wang JM, Rogers TJ, Caterina M, Oppenheim JJ (2005a) A proinflammatory chemokine, CCL3, sensitizes the heat- and capsaicin-gated ion channel TRPV1. Proceedings of the National Academy of Sciences of the United States of America 102:4536-4541.

Zhang R-X, Ren K (2010) Animal Models of Inflammatory Pain. In: Animal Models of Pain, pp 23-40.

Zhang RX, Liu B, Wang L, Ren K, Qiao JT, Berman BM, Lao L (2005b) Spinal glial activation in a new rat model of bone cancer pain produced by prostate cancer cell inoculation of the tibia. Pain 118:125-136.

Zhang SL, Yu Y, Roos J, Kozak JA, Deerinck TJ, Ellisman MH, Stauderman KA, Cahalan MD (2005c) STIM1 is a Ca2+ sensor that activates CRAC channels and migrates from the Ca2+ store to the plasma membrane. Nature 437:902-905.

Zhang X, Mosser DM (2008) Macrophage activation by endogenous danger signals. Journal of Pathology 214:161-178.

Zhang X, Huang J, McNaughton PA (2005d) NGF rapidly increases membrane expression of TRPV1 heat-gated ion channels. EMBO Journal 24:4211-4223.

Zhang X, Goncalves R, Mosser DM (2008) The isolation and characterization of murine macrophages. Curr Protoc Immunol 14.

Zhang Z, Zhang ZY, Schluesener HJ (2009) Compound A, a plant origin ligand of glucocorticoid receptors, increases regulatory T cells and M2 macrophages to attenuate experimental autoimmune neuritis with reduced side effects. Journal of Immunology 183:3081-3091.

Zheng FY, Xiao WH, Bennett GJ (2011a) The response of spinal microglia to chemotherapy-evoked painful peripheral neuropathies is distinct from that evoked by traumatic nerve injuries. Neuroscience 176:447-454.

Zheng W, Ouyang H, Zheng X, Liu S, Mata M, Fink DJ, Hao S (2011b) Glial TNFalpha in the spinal cord regulates neuropathic pain induced by HIV gp120 application in rats. Mol Pain 7:40.

Zhu W, Oxford GS (2007) Phosphoinositide-3-kinase and mitogen activated protein kinase signaling pathways mediate acute NGF sensitization of TRPV1. Molecular and Cellular Neurosciences 34:689-700.

Zhuang ZY, Kawasaki Y, Tan PH, Wen YR, Huang J, Ji RR (2007) Role of the CX3CR1/p38 MAPK pathway in spinal microglia for the development of neuropathic pain following nerve injury-induced cleavage of fractalkine. Brain, Behavior, and Immunity 21:642-651.

Zimmermann M (2001) Pathobiology of neuropathic pain. European Journal of Pharmacology 429:23-37.

Zlotnik A, Yoshie O (2000) Chemokines: a new classification system and their role in immunity. Immunity 12:121-127.

Zuo Y, Perkins NM, Tracey DJ, Geczy CL (2003) Inflammation and hyperalgesia induced by nerve injury in the rat: a key role of mast cells. Pain 105:467-479.

Appendix

Appendix Table 1: Raw CT values of genes screened in the sciatic nerve of GPR84 WT sham and PNL operated mice 7 days post surgery

Table 1	WT Sciatic nerve 7 days post SHAM				WT Sciatic nerve 7 days post PNL			
Gene	**1**	**2**	**3**	**4**	**1**	**2**	**3**	**4**
Allograft inflammatory factors -1 (Iba1; AIF)	29.5	29.8	29.7	28.5	27.7	28.7	27.6	27.4
Amphiregulin (AREG)	ND	ND	37.6	ND	ND	34.6	32.9	33.8
Arginase 1 (ARG1)	26.9	27.2	28.9	30.1	25.9	26.7	26.1	26.5
Artemin (ARTN)	30.0	31.8	31.3	31.0	29.1	30.8	28.5	29.1
Brain-derived neurotrophic factor (BDNF)	33.8	31.8	33.1	31.2	30.5	31.2	29.0	29.5
Betacellulin (BTC)	28.6	28.9	29.8	28.6	27.0	28.4	26.5	28.1
Chemokine (C-C motif) ligand 1 (CCL1)	ND	34.2	35.8	34.1	ND	35.7	ND	34.0
Chemokine (C-C motif) ligand 11 (CCL11)	22.2	22.2	22.2	22.0	23.7	25.1	23.7	24.5
Chemokine (C-C motif) ligand 17 (CCL17)	31.8	33.0	34.6	31.0	ND	33.8	34.0	33.2
Chemokine (C-C motif) ligand 19 (CCL19)	28.0	27.5	28.2	27.3	29.5	30.1	28.7	29.1
Chemokine (C-C motif) ligand 2 (CCL2)	27.5	27.3	27.7	26.6	26.8	27.8	25.8	27.2
Chemokine (C-C motif) ligand 20 (CCL20)	ND	ND	ND	ND	ND	ND	ND	ND
Chemokine (C-C motif) ligand 21a,b (CCL21a,b)	21.8	21.8	23.3	21.5	25.0	25.0	23.9	23.1
Chemokine (C-C motif) ligand 22 (CCL22)	30.8	31.0	30.5	29.2	28.7	29.7	28.9	28.6
Chemokine (C-C motif) ligand 24 (CCL24)	27.9	28.5	28.8	27.2	30.1	30.6	30.9	30.6
Chemokine (C-C motif) ligand 25 (CCL25)	28.5	27.7	27.9	27.8	28.5	29.8	29.7	29.4
Chemokine (C-C motif) ligand 27a,b (CCL27a,b)	25.3	24.8	25.1	25.0	26.9	27.4	27.3	27.2
Chemokine (C-C motif) ligand 3 (CCL3)	33.0	34.0	33.9	32.9	30.5	31.2	30.7	30.2
Chemokine (C-C motif) ligand 4 (CCL4)	31.8	31.6	31.5	31.4	28.6	29.9	29.0	28.6
Chemokine (C-C motif) ligand 5 (CCL5)	30.7	29.5	30.0	28.7	27.3	28.4	27.8	27.4
Chemokine (C-C motif) ligand 6 (CCL6)	21.9	22.7	22.6	20.3	20.8	21.3	21.5	21.0
Chemokine (C-C motif) ligand 7 (CCL7)	27.5	27.0	27.3	26.3	26.6	28.6	25.2	27.0
Chemokine (C-C motif) ligand 8 (CCL8)	28.5	26.3	27.8	22.6	23.9	24.0	24.0	23.9
Chemokine (C-C motif) ligand 9 (CCL9)	23.9	25.5	25.0	22.9	23.7	24.1	24.3	24.0
T-cell surface glycoprotein CD3 delta chain (CD3D)	36.8	36.0	33.9	33.9	33.1	ND	34.7	31.8
Colony stimulating factor 1 (macrophage) (CSF1)	24.6	24.6	25.0	24.2	25.6	26.5	25.6	25.9
Colony stimulating factor 2 (granulocyte-macrophage) (CSF2)	ND	33.5	35.2	32.4	ND	ND	34.0	33.3
Colony stimulating factor 3 (granulocyte) (CSF3)	ND	31.3	35.0	31.8	32.7	33.3	30.2	33.6
Colony stimulating factor 3 (granulocyte) receptor (CSF3R)	29.3	29.4	29.8	27.7	26.6	27.4	26.8	26.5
Chemokine (CX3-C motif) ligand 1 (CX3CL1)	27.1	26.7	26.9	26.2	26.3	27.6	26.6	26.7
Chemokine (C-X-C motif) ligand 1 (CXCL1)	29.9	28.0	30.5	27.7	30.0	32.6	29.4	29.5
Chemokine (C-X-C motif) ligand 10 (CXCL10)	28.7	28.5	29.2	27.5	27.3	29.0	28.9	27.5
Chemokine (C-X-C motif) ligand 11 (CXCL11)	28.1	28.0	27.9	27.8	30.9	30.5	32.7	31.4
Chemokine (C-X-C motif) ligand 12 (CXCL12)	28.6	28.7	29.6	28.8	27.5	29.2	28.4	27.5
Chemokine (C-X-C motif) ligand 13 (CXCL13)	24.6	25.1	25.6	23.5	28.3	28.2	29.2	29.3
Chemokine (C-X-C motif) ligand 14 (CXCL14)	23.7	24.7	24.3	23.9	23.9	24.2	24.3	24.8
Chemokine (C-X-C motif) ligand 16 (CXCL16)	26.9	26.5	27.0	25.7	24.6	25.3	24.5	23.9
Chemokine (C-X-C motif) ligand 17 (CXCL17)	32.5	32.6	32.6	31.7	ND	33.5	ND	32.5
Chemokine (C-X-C motif) ligand 2 (CXCL2)	32.6	32.2	33.6	30.9	28.0	29.3	28.0	28.9
Chemokine (C-X-C motif) ligand 3 (CXCL3)	ND	ND	ND	ND	29.8	32.3	29.8	31.0
Chemokine (C-X-C motif) ligand 5 (CXCL5)	34.5	32.4	ND	33.3	26.2	28.3	24.9	25.8
Chemokine (C-X-C motif) ligand 9 (CXCL9)	29.5	29.2	30.3	28.9	28.0	28.2	29.0	27.7
Chemokine (C-X-C motif) receptor 3 (CXCR3)	29.0	30.1	30.5	28.8	29.3	29.7	30.1	28.1
Epstein-Barr virus induced gene 3 (EBI3)	29.6	29.8	29.5	28.3	28.8	29.3	29.6	29.1
Epiregulin (EREG)	ND	33.5	ND	ND	33.1	31.9	29.5	32.0
Fibroblast growth factor 7 (keratinocyte growth factor; FGF7)	24.7	24.7	24.6	24.9	26.3	27.8	27.0	27.0
G-protein receptor 84 (GPR84)	ND	ND	ND	34.6	31.2	31.7	31.4	33.7
Heparin-binding EGF-like growth factor (HBEGF)	25.0	24.2	24.4	24.5	26.5	27.0	26.5	27.1
Interleukin 10 (IL10)	34.1	35.9	34.3	31.3	32.9	33.5	32.8	32.3
Interleukin 11 (IL11)	32.0	31.1	31.5	31.3	32.1	32.5	31.1	32.0

Table 1	WT Sciatic nerve 7 days post SHAM				WT Sciatic nerve 7 days post PNL			
Gene	**1**	**2**	**3**	**4**	**1**	**2**	**3**	**4**
Interleukin 12 alpha (IL12a)	31.7	30.8	30.5	31.4	33.9	32.2	33.5	33.3
Interleukin 12 beta (IL12b)	ND	34.9	ND	35.5	33.5	ND	33.2	32.5
Interleukin 13 (IL13)	33.4	34.0	ND	36.6	ND	ND	ND	34.3
Interleukin 15 (IL15)	27.2	27.1	27.5	26.8	27.9	28.9	28.4	27.9
Interleukin 16 (IL16)	22.4	21.8	22.1	22.3	24.1	24.9	25.3	24.7
Interleukin 17 alpha (IL17a)	ND	35.7	ND	ND	ND	ND	ND	ND
Interleukin 18 (IL18)	28.1	27.9	28.6	27.0	28.1	29.5	29.3	28.3
Interleukin 19 (IL19)	34.1	ND	34.5	ND	34.5	ND	ND	ND
Interleukin 1 alpha (IL1a)	ND	ND	ND	35.3	31.3	31.1	31.1	31.1
Interleukin 1 beta (IL1b)	31.8	30.2	32.9	29.2	26.5	28.3	26.1	26.9
Interleukin 2 (IL2)	37.6	ND	ND	ND	ND	ND	ND	ND
Interleukin 20 (IL20)	ND	ND	ND	ND	ND	ND	ND	ND
Interleukin 21 (IL21)	35.8	34.6	34.7	ND	33.9	ND	ND	ND
Interleukin 22 (IL22)	ND	ND	ND	ND	ND	ND	ND	ND
Interleukin 23 alpha (IL23a)	30.1	29.7	30.4	30.9	32.0	32.9	32.1	32.6
Interleukin 24 (IL24)	ND	ND	ND	ND	ND	ND	ND	ND
Interleukin 25 (IL25)	32.1	32.7	31.2	34.8	37.9	ND	33.6	33.6
Interleukin 27 (IL27)	32.7	ND	34.5	32.6	32.9	34.2	32.3	33.8
Interleukin 28 beta (IL28b)	ND	ND	ND	ND	ND	ND	ND	ND
Interleukin 3 (IL3)	ND	ND	ND	ND	34.6	ND	ND	ND
Interleukin 31 (IL31)	ND	ND	ND	ND	ND	ND	ND	ND
Interleukin 33 (IL33)	23.1	23.0	23.0	23.0	24.6	25.1	24.7	24.5
Interleukin 34 (IL34)	29.0	28.3	28.7	28.8	30.5	30.9	32.3	31.8
Interleukin 4 (IL4)	ND	ND	ND	ND	ND	ND	ND	ND
Interleukin 5 (IL5)	32.3	34.3	34.5	33.0	ND	33.2	34.5	32.9
Interleukin 6 (IL6)	32.6	30.0	32.5	30.5	31.1	34.2	28.2	30.8
Interleukin 7 (IL7)	30.5	30.1	31.3	29.6	31.2	33.0	30.7	31.0
Interleukin 9 (IL9)	ND	ND	ND	ND	ND	ND	ND	ND
Integrin alpha M (ITGAM); (CD11B)	25.3	25.8	26.0	24.0	23.3	24.1	23.6	23.4
Mannose receptor, C type 1 (MRC1)	23.9	24.0	24.1	22.4	23.4	23.9	23.4	23.5
Nerve growth factor (NGF)	26.9	26.4	27.5	26.2	26.8	28.4	26.5	27.1
Nitric oxide synthase, inducible (NOS2)	30.6	30.7	29.7	29.9	28.2	29.3	28.7	29.2
Neuregulin 1 (NRG1)	29.5	29.1	29.4	29.0	29.3	31.2	28.8	29.1
Platelet factor 4 (PF4; CXCL4)	24.4	24.7	24.6	23.1	22.6	24.3	23.1	23.2
Pro-platelet basic protein (chemokine (C-X-C motif) ligand 7	27.0	29.1	27.2	25.3	28.0	29.3	28.2	29.1
Prostaglandin E synthase (PTGES)	26.0	25.4	25.9	25.3	26.3	27.8	26.8	26.7
Prostaglandin-endoperoxide synthase 2 (COX-2; PTGS2)	32.4	29.8	33.0	29.9	31.2	32.1	29.6	30.9
Signal Transducer and Activator of Transcription protein 4 (STAT4)	29.6	29.7	29.7	30.1	30.1	30.5	29.6	29.9
Toll-like receptor 4 (TLR4)	25.5	25.7	25.7	24.9	25.7	26.7	25.8	25.8
Tumor necrosis factor (TNF)	30.8	30.6	31.6	30.2	28.2	29.2	28.7	28.1
Alpha-taxilin (TXLNA)	24.8	24.4	24.6	24.5	25.0	25.8	24.7	25.0
Chemokine (C motif) ligand 1 (XCL1)	35.8	ND	36.2	35.9	32.8	35.3	ND	32.9
Housekeeping genes								
Beta-actin (ACTB)	18.7	18.4	18.7	18.3	18.6	19.4	18.7	18.8
Glyceraldehyde 3-phosphate dehydrogenase (GAPDH)	20.0	19.5	18.8	19.1	20.9	19.9	21.0	20.7
Hypoxanthine-guanine phosphoribosyltransferase (HPRT)	25.3	25.5	25.4	25.1	25.6	26.9	25.9	25.5
18s (X18S)	13.4	13.3	13.3	13.2	13.1	13.3	13.1	13.2

Appendix Table 2: Raw CT values of genes screened in the sciatic nerve of GPR84 KO sham and PNL operated mice 7 days post surgery

Table 2	KO Sciatic nerve 7 days post SHAM				KO Sciatic nerve 7 days post PNL			
Gene	**1**	**2**	**3**	**4**	**1**	**2**	**3**	**4**
Allograft inflammatory factors -1 (Iba1; AIF)	29.2	29.4	30.1	30.0	28.0	25.5	27.2	27.2
Amphiregulin (AREG)	ND	ND	ND	ND	ND	ND	ND	ND
Arginase 1 (ARG1)	29.5	29.9	32.0	29.9	26.7	25.4	25.9	27.9
Artemin (ARTN)	30.5	32.4	30.6	31.7	29.9	29.5	31.6	31.0
Brain-derived neurotrophic factor (BDNF)	33.1	33.0	32.6	33.1	30.3	30.4	30.5	31.4
Betacellulin (BTC)	29.0	29.6	29.2	28.8	26.4	28.0	30.5	29.6
Chemokine (C-C motif) ligand 1 (CCL1)	ND	ND	ND	ND	ND	35.3	33.7	34.9
Chemokine (C-C motif) ligand 11 (CCL11)	21.7	21.6	22.3	21.8	23.6	24.4	24.2	25.4
Chemokine (C-C motif) ligand 17 (CCL17)	34.5	32.9	32.7	33.9	35.4	33.5	32.4	31.4
Chemokine (C-C motif) ligand 19 (CCL19)	27.5	28.1	27.8	27.3	29.1	30.0	28.2	29.3
Chemokine (C-C motif) ligand 2 (CCL2)	28.1	28.0	28.3	28.5	27.1	24.9	26.6	27.1
Chemokine (C-C motif) ligand 20 (CCL20)	ND	ND	ND	ND	ND	ND	ND	35.5
Chemokine (C-C motif) ligand 21a,b (CCL21a,b)	21.3	22.7	22.5	23.0	23.6	24.9	22.8	23.7
Chemokine (C-C motif) ligand 22 (CCL22)	29.8	30.1	30.4	30.8	31.1	27.6	28.4	28.3
Chemokine (C-C motif) ligand 24 (CCL24)	28.4	28.1	29.0	28.4	31.1	29.4	30.3	29.7
Chemokine (C-C motif) ligand 25 (CCL25)	27.4	28.0	28.1	27.6	28.7	28.7	29.7	29.1
Chemokine (C-C motif) ligand 27a,b (CCL27a,b)	24.8	24.9	25.1	24.9	27.2	27.1	27.4	26.8
Chemokine (C-C motif) ligand 3 (CCL3)	33.3	33.5	34.6	33.8	30.6	28.3	29.8	29.8
Chemokine (C-C motif) ligand 4 (CCL4)	31.7	32.5	33.0	32.2	29.1	26.4	27.6	28.2
Chemokine (C-C motif) ligand 5 (CCL5)	29.4	29.5	29.9	29.9	29.0	26.1	27.3	27.4
Chemokine (C-C motif) ligand 6 (CCL6)	21.9	22.2	22.2	22.5	21.9	19.6	20.6	21.1
Chemokine (C-C motif) ligand 7 (CCL7)	28.4	28.2	28.9	28.8	27.6	24.2	26.2	26.6
Chemokine (C-C motif) ligand 8 (CCL8)	27.3	27.6	28.1	27.3	25.2	21.5	23.7	24.2
Chemokine (C-C motif) ligand 9 (CCL9)	24.4	25.0	25.2	25.2	24.6	22.1	23.6	23.4
T-cell surface glycoprotein CD3 delta chain (CD3D)	34.4	33.8	34.6	33.7	33.6	30.5	32.4	31.9
Colony stimulating factor 1 (macrophage) (CSF1)	24.3	24.7	24.8	24.6	26.4	25.3	26.1	26.3
Colony stimulating factor 2 (granulocyte-macrophage) (CSF2)	34.9	33.9	ND	ND	34.9	33.0	ND	33.6
Colony stimulating factor 3 (granulocyte) (CSF3)	34.6	ND	35.2	ND	ND	34.2	32.7	32.9
Colony stimulating factor 3 (granulocyte) receptor (CSF3R)	29.1	29.8	29.2	29.4	26.9	25.2	26.0	26.4
Chemokine (CX3-C motif) ligand 1 (CX3CL1)	26.5	26.9	27.1	27.1	28.0	27.1	26.9	28.2
Chemokine (C-X-C motif) ligand 1 (CXCL1)	30.3	29.3	30.4	30.0	29.9	27.9	29.6	30.7
Chemokine (C-X-C motif) ligand 10 (CXCL10)	28.1	29.1	29.4	29.0	28.3	24.9	26.9	27.5
Chemokine (C-X-C motif) ligand 11 (CXCL11)	27.3	27.3	27.7	27.4	29.9	31.0	30.7	33.1
Chemokine (C-X-C motif) ligand 12 (CXCL12)	28.3	28.6	29.0	28.9	29.7	27.8	28.8	28.2
Chemokine (C-X-C motif) ligand 13 (CXCL13)	24.3	25.2	24.6	24.3	27.5	30.1	29.3	30.7
Chemokine (C-X-C motif) ligand 14 (CXCL14)	24.0	25.4	24.6	25.5	24.2	24.5	23.9	25.4
Chemokine (C-X-C motif) ligand 16 (CXCL16)	26.1	26.7	26.7	26.8	25.1	23.4	24.1	24.3
Chemokine (C-X-C motif) ligand 17 (CXCL17)	31.2	33.4	33.3	31.9	32.9	33.9	33.8	35.2
Chemokine (C-X-C motif) ligand 2 (CXCL2)	34.3	32.1	32.8	32.9	28.6	26.8	27.8	27.8
Chemokine (C-X-C motif) ligand 3 (CXCL3)	ND	ND	ND	34.4	31.9	29.3	29.4	29.8
Chemokine (C-X-C motif) ligand 5 (CXCL5)	ND	34.0	34.5	33.8	28.2	24.1	24.9	25.9
Chemokine (C-X-C motif) ligand 9 (CXCL9)	29.7	30.8	30.2	30.5	29.5	25.9	27.1	27.5
Chemokine (C-X-C motif) receptor 3 (CXCR3)	29.7	30.1	30.0	29.8	30.1	27.5	28.5	28.9
Epstein-Barr virus induced gene 3 (EBI3)	29.2	29.2	29.2	29.1	31.1	28.3	29.3	29.5
Epiregulin (EREG)	33.9	ND	ND	33.8	32.4	30.0	30.5	33.1
Fibroblast growth factor 7 (keratinocyte growth factor; FGF7)	24.3	24.2	24.7	24.5	26.2	26.4	27.0	28.0
G-protein receptor 84 (GPR84)	ND	ND	ND	ND	ND	ND	ND	ND
Heparin-binding EGF-like growth factor (HBEGF)	24.3	24.3	24.5	24.4	26.8	26.5	27.7	28.6
Interleukin 10 (IL10)	34.1	32.9	33.1	34.1	34.0	29.4	31.7	31.6
Interleukin 11 (IL11)	31.2	31.1	31.8	32.0	32.7	32.1	33.1	33.1

Table 2	KO Sciatic nerve 7 days post SHAM				KO Sciatic nerve 7 days post PNL			
Gene	**1**	**2**	**3**	**4**	**1**	**2**	**3**	**4**
Interleukin 12 alpha (IL12a)	31.5	30.5	31.6	30.6	35.7	32.4	33.8	30.8
Interleukin 12 beta (IL12b)	ND	ND	34.8	35.0	33.0	31.6	33.2	31.1
Interleukin 13 (IL13)	ND	ND	ND	ND	ND	ND	34.9	ND
Interleukin 15 (IL15)	26.2	26.9	27.7	27.3	28.3	27.2	28.3	28.3
Interleukin 16 (IL16)	21.6	21.3	22.1	21.7	24.4	24.3	24.8	25.9
Interleukin 17 alpha (IL17a)	36.9	ND	ND	ND	ND	ND	ND	ND
Interleukin 18 (IL18)	27.8	28.2	28.7	28.3	28.5	26.8	28.5	28.8
Interleukin 19 (IL19)	36.6	ND	ND	34.7	12.4	34.8	ND	ND
Interleukin 1 alpha (IL1a)	ND	ND	ND	35.1	30.7	30.2	32.0	32.0
Interleukin 1 beta (IL1b)	31.6	30.8	32.2	31.9	27.2	24.5	25.8	26.1
Interleukin 2 (IL2)	34.8	35.5	34.8	ND	35.0	33.9	ND	ND
Interleukin 20 (IL20)	32.8	35.4	ND	ND	ND	ND	ND	35.6
Interleukin 21 (IL21)	37.0	34.6	ND	ND	ND	ND	ND	35.4
Interleukin 22 (IL22)	ND	ND	ND	ND	ND	ND	ND	ND
Interleukin 23 alpha (IL23a)	30.4	29.5	30.5	30.3	32.7	31.4	32.0	ND
Interleukin 24 (IL24)	ND	ND	ND	35.0	ND	ND	ND	ND
Interleukin 25 (IL25)	30.6	32.2	33.7	32.3	32.7	33.2	ND	34.4
Interleukin 27 (IL27)	32.8	34.5	ND	32.3	33.3	30.7	31.9	32.6
Interleukin 28 beta (IL28b)	ND	ND	ND	ND	ND	ND	ND	ND
Interleukin 3 (IL3)	38.0	ND	ND	ND	ND	ND	ND	ND
Interleukin 31 (IL31)	ND	ND	ND	ND	ND	ND	ND	ND
Interleukin 33 (IL33)	22.7	23.1	23.1	23.0	24.7	25.5	24.0	25.7
Interleukin 34 (IL34)	28.6	28.1	29.0	28.0	30.0	31.4	32.9	34.0
Interleukin 4 (IL4)	ND	ND	ND	ND	ND	ND	ND	ND
Interleukin 5 (IL5)	33.2	33.3	34.0	33.4	ND	ND	ND	ND
Interleukin 6 (IL6)	33.4	34.6	34.4	34.3	32.4	28.4	30.4	32.0
Interleukin 7 (IL7)	29.5	30.3	30.9	30.3	31.8	30.5	32.2	31.4
Interleukin 9 (IL9)	ND	ND	ND	ND	ND	ND	ND	ND
Integrin alpha M (ITGAM); (CD11B)	25.4	25.5	25.5	25.8	24.4	22.3	23.3	23.5
Mannose receptor, C type 1 (MRC1)	23.8	24.0	24.2	24.0	24.5	21.9	23.5	23.8
Nerve growth factor (NGF)	27.3	27.3	27.7	27.9	28.2	27.5	28.0	28.2
Nitric oxide synthase, inducible (NOS2)	30.4	30.2	31.2	30.6	30.3	27.4	28.4	28.8
Neuregulin 1 (NRG1)	29.5	28.7	29.4	29.6	29.6	28.3	30.2	29.6
Platelet factor 4 (PF4; CXCL4)	24.0	24.4	24.7	24.3	24.4	21.4	22.7	23.3
Pro-platelet basic protein (chemokine (C-X-C motif) ligand 7	27.9	29.1	28.9	25.2	27.8	26.7	27.9	28.8
Prostaglandin E synthase (PTGES)	25.4	25.8	26.0	25.6	27.2	26.6	27.6	27.8
Prostaglandin-endoperoxide synthase 2 (COX-2; PTGS2)	30.6	30.2	32.1	32.3	31.5	29.4	30.9	30.8
Signal Transducer and Activator of Transcription protein 4 (STAT4)	29.5	29.3	30.1	29.7	30.4	27.8	29.2	29.5
Toll-like receptor 4 (TLR4)	25.4	25.8	25.6	25.4	25.7	24.3	25.8	26.1
Tumor necrosis factor (TNF)	30.2	31.3	31.5	32.2	28.7	26.7	27.8	27.2
Alpha-taxilin (TXLNA)	24.1	24.1	24.6	24.3	25.6	24.6	25.9	25.8
Chemokine (C motif) ligand 1 (XCL1)	35.8	34.7	35.4	ND	33.7	30.3	32.3	32.3
Housekeeping genes								
Beta-actin (ACTB)	18.5	18.3	18.7	18.7	20.1	18.5	19.1	19.5
Glyceraldehyde 3-phosphate dehydrogenase (GAPDH)	19.4	19.5	19.9	19.8	21.3	20.0	20.9	18.9
Hypoxanthine-guanine phosphoribosyltransferase (HPRT)	25.0	25.2	25.4	25.1	25.5	24.8	26.0	26.1
18s (X18S)	13.2	13.1	13.3	13.1	13.3	13.3	13.5	13.3

Appendix Table 3: Raw CT values of genes screened in the spinal cord of GPR84 WT sham and PNL operated mice 7 days post surgery

Table 3	WT Spinal cord 7 days post SHAM				WT Spinal cord 7 days post PNL			
Gene	**1**	**2**	**3**	**4**	**1**	**2**	**3**	**4**
Allograft inflammatory factors -1 (Iba1; AIF)	28.5	26.9	27.2	26.9	26.8	27.6	27.6	28.0
Amphiregulin (AREG)	ND	ND	33.9	ND	34.0	34.9	ND	ND
Arginase 1 (ARG1)	32.9	31.3	32.1	30.7	31.8	31.9	32.3	33.0
Artemin (ARTN)	30.9	29.9	30.9	29.6	30.1	30.4	30.8	30.5
Brain-derived neurotrophic factor (BDNF)	27.6	27.4	27.7	27.0	27.3	27.1	28.0	27.6
Betacellulin (BTC)	29.3	28.4	28.0	27.3	27.7	29.0	28.9	29.1
Chemokine (C-C motif) ligand 1 (CCL1)	ND	ND	ND	ND	ND	ND	ND	ND
Chemokine (C-C motif) ligand 11 (CCL11)	27.3	26.4	25.8	26.1	25.6	25.4	27.7	27.7
Chemokine (C-C motif) ligand 17 (CCL17)	ND	32.6	35.3	ND	34.0	ND	ND	36.7
Chemokine (C-C motif) ligand 19 (CCL19)	28.1	25.5	26.0	26.3	26.2	27.6	27.7	27.9
Chemokine (C-C motif) ligand 2 (CCL2)	31.3	30.6	31.6	30.0	27.5	29.0	29.5	30.3
Chemokine (C-C motif) ligand 20 (CCL20)	ND	ND	ND	ND	ND	ND	ND	ND
Chemokine (C-C motif) ligand 21a,b (CCL21a,b)	26.0	24.7	24.1	25.4	24.6	24.5	25.7	26.0
Chemokine (C-C motif) ligand 22 (CCL22)	30.6	30.2	29.3	29.2	29.4	30.7	30.6	30.5
Chemokine (C-C motif) ligand 24 (CCL24)	31.3	31.0	31.6	31.0	31.7	31.5	31.9	32.4
Chemokine (C-C motif) ligand 25 (CCL25)	26.0	25.7	25.5	25.1	25.3	25.8	26.0	26.0
Chemokine (C-C motif) ligand 27a,b (CCL27a,b)	23.2	22.8	22.9	22.3	22.7	23.1	23.5	23.3
Chemokine (C-C motif) ligand 3 (CCL3)	34.6	32.6	32.3	32.8	32.7	33.7	33.6	34.1
Chemokine (C-C motif) ligand 4 (CCL4)	32.8	31.0	30.5	29.9	30.8	31.4	31.4	32.8
Chemokine (C-C motif) ligand 5 (CCL5)	30.6	28.6	29.4	28.8	28.3	29.2	29.9	30.7
Chemokine (C-C motif) ligand 6 (CCL6)	25.8	24.0	24.7	24.7	24.5	23.9	25.9	26.0
Chemokine (C-C motif) ligand 7 (CCL7)	32.2	30.9	30.9	29.8	26.4	27.1	27.8	27.6
Chemokine (C-C motif) ligand 8 (CCL8)	32.6	29.8	32.8	30.7	30.2	31.2	31.3	33.0
Chemokine (C-C motif) ligand 9 (CCL9)	27.2	25.9	26.3	26.3	25.9	25.7	26.4	27.1
T-cell surface glycoprotein CD3 delta chain (CD3D)	33.7	31.7	33.3	33.2	32.4	33.3	ND	33.9
Colony stimulating factor 1 (macrophage) (CSF1)	24.4	23.6	23.1	23.0	23.1	23.7	23.9	24.0
Colony stimulating factor 2 (granulocyte-macrophage) (CSF2)	ND	ND	35.1	35.1	ND	ND	ND	ND
Colony stimulating factor 3 (granulocyte) (CSF3)	ND	35.1	ND	ND	34.4	34.8	ND	ND
Colony stimulating factor 3 (granulocyte) receptor (CSF3R)	27.6	25.8	26.5	26.4	26.0	26.3	27.3	27.1
Chemokine (CX3-C motif) ligand 1 (CX3CL1)	21.2	20.8	20.9	20.0	20.5	21.1	21.6	21.2
Chemokine (C-X-C motif) ligand 1 (CXCL1)	33.2	30.4	31.8	31.4	31.2	32.1	33.7	34.6
Chemokine (C-X-C motif) ligand 10 (CXCL10)	31.3	30.4	28.3	29.0	28.8	29.2	29.0	29.7
Chemokine (C-X-C motif) ligand 11 (CXCL11)	31.7	30.2	29.4	29.1	29.4	29.9	31.0	32.0
Chemokine (C-X-C motif) ligand 12 (CXCL12)	31.3	30.5	30.7	30.5	30.8	30.8	31.4	31.4
Chemokine (C-X-C motif) ligand 13 (CXCL13)	33.7	29.2	31.9	33.7	30.5	29.3	32.6	31.3
Chemokine (C-X-C motif) ligand 14 (CXCL14)	22.1	21.2	21.4	21.1	21.3	21.9	22.4	22.0
Chemokine (C-X-C motif) ligand 16 (CXCL16)	27.4	25.2	26.0	25.5	25.9	26.5	26.5	27.5
Chemokine (C-X-C motif) ligand 17 (CXCL17)	35.0	32.4	32.9	32.2	32.9	33.8	33.5	35.0
Chemokine (C-X-C motif) ligand 2 (CXCL2)	ND	35.2	35.4	35.9	33.5	ND	ND	ND
Chemokine (C-X-C motif) ligand 3 (CXCL3)	ND	34.7	ND	34.5	34.6	34.7	ND	34.8
Chemokine (C-X-C motif) ligand 5 (CXCL5)	30.2	30.2	29.7	29.4	29.1	30.5	31.3	31.4
Chemokine (C-X-C motif) ligand 9 (CXCL9)	35.7	34.7	34.3	34.8	31.5	33.0	31.4	34.3
Chemokine (C-X-C motif) receptor 3 (CXCR3)	32.6	29.9	31.4	30.7	31.6	31.2	31.9	33.1
Epstein-Barr virus induced gene 3 (EBI3)	30.6	29.7	29.7	29.3	29.6	30.2	30.8	30.5
Epiregulin (EREG)	ND	ND	ND	36.1	34.9	ND	ND	ND
Fibroblast growth factor 7 (keratinocyte growth factor; FGF7)	28.5	28.1	27.7	27.5	27.1	27.5	28.8	28.6
G-protein receptor 84 (GPR84)	31.7	29.4	29.4	29.8	27.8	28.5	29.3	30.2
Heparin-binding EGF-like growth factor (HBEGF)	26.0	25.5	25.3	24.2	24.9	25.5	26.0	26.1
Interleukin 10 (IL10)	ND	36.4	ND	ND	ND	35.3	35.8	ND
Interleukin 11 (IL11)	31.8	32.0	31.5	31.0	31.7	32.5	33.0	33.3

Table 3	WT Spinal cord 7 days post SHAM				WT Spinal cord 7 days post PNL			
Gene	**1**	**2**	**3**	**4**	**1**	**2**	**3**	**4**
Interleukin 12 alpha (IL12a)	30.9	29.7	29.6	30.1	30.4	30.4	31.0	30.8
Interleukin 12 beta (IL12b)	ND	34.1	32.7	33.8	34.9	34.3	34.1	ND
Interleukin 13 (IL13)	ND	35.3	ND	34.1	ND	ND	ND	ND
Interleukin 15 (IL15)	28.9	28.4	28.5	27.6	28.1	29.0	28.9	29.9
Interleukin 16 (IL16)	25.9	24.5	24.1	24.6	24.0	24.4	26.0	26.0
Interleukin 17 alpha (IL17a)	ND	ND	ND	ND	34.3	ND	ND	ND
Interleukin 18 (IL18)	25.1	24.0	23.9	23.4	23.7	24.6	25.3	24.7
Interleukin 19 (IL19)	34.0	31.5	30.7	31.6	32.6	32.4	33.0	32.6
Interleukin 1 alpha (IL1a)	31.7	30.4	31.2	30.1	29.2	30.0	30.5	30.8
Interleukin 1 beta (IL1b)	30.4	31.7	31.3	30.4	28.2	28.9	31.2	32.6
Interleukin 2 (IL2)	ND	ND	ND	ND	ND	ND	ND	ND
Interleukin 20 (IL20)	ND	ND	34.7	36.0	ND	ND	ND	ND
Interleukin 21 (IL21)	31.9	32.7	31.5	32.5	33.2	32.7	33.6	33.3
Interleukin 22 (IL22)	ND	ND	ND	ND	ND	ND	ND	ND
Interleukin 23 alpha (IL23a)	30.3	29.6	29.0	28.6	29.7	29.8	30.0	29.8
Interleukin 24 (IL24)	ND	ND	ND	ND	34.5	34.2	33.6	ND
Interleukin 25 (IL25)	31.8	30.9	31.4	30.8	30.0	30.2	31.7	31.7
Interleukin 27 (IL27)	ND	ND	33.7	33.1	32.9	34.7	34.4	ND
Interleukin 28 beta (IL28b)	ND	ND	ND	ND	ND	ND	ND	ND
Interleukin 3 (IL3)	ND	ND	ND	ND	ND	ND	ND	ND
Interleukin 31 (IL31)	35.5	ND	ND	ND	ND	ND	ND	ND
Interleukin 33 (IL33)	22.8	22.3	22.2	21.2	21.8	22.6	22.8	22.7
Interleukin 34 (IL34)	30.6	28.4	29.4	28.6	29.3	29.8	30.8	30.8
Interleukin 4 (IL4)	ND	ND	ND	ND	ND	ND	ND	ND
Interleukin 5 (IL5)	32.0	31.4	31.1	32.1	31.2	31.6	33.3	32.2
Interleukin 6 (IL6)	34.4	32.4	31.6	33.0	30.8	31.8	34.4	33.1
Interleukin 7 (IL7)	30.0	29.6	30.0	29.1	29.0	29.7	30.4	30.0
Interleukin 9 (IL9)	ND	ND	ND	ND	ND	ND	ND	ND
Integrin alpha M (ITGAM; CD11B)	25.2	23.6	24.3	23.9	23.4	23.2	24.2	24.3
Mannose receptor, C type 1 (MRC1)	27.4	25.1	25.9	25.3	25.9	25.8	26.6	27.3
Nerve growth factor (NGF)	29.1	27.4	27.6	26.9	27.4	27.8	28.4	28.5
Nitric oxide synthase, inducible (NOS2)	30.1	30.0	29.1	28.3	29.2	30.0	30.2	30.1
Neuregulin 1 (NRG1)	23.0	22.2	21.9	21.7	21.8	22.6	23.2	23.0
Platelet factor 4 (PF4; CXCL4)	25.5	25.6	26.0	25.4	24.0	25.1	26.4	27.6
Pro-platelet basic protein (chemokine (C-X-C motif) ligand 7	25.0	25.8	25.8	25.8	23.5	24.7	25.9	27.2
Prostaglandin E synthase (PTGES)	28.1	27.0	26.9	26.6	26.6	27.7	28.2	28.3
Prostaglandin-endoperoxide synthase 2 (COX-2; PTGS2)	31.2	29.3	31.0	30.3	28.9	30.9	31.8	31.8
Signal Transducer and Activator of Transcription protein 4 (STAT4)	31.7	30.5	31.9	30.2	31.2	31.2	32.1	31.5
Toll-like receptor 4 (TLR4)	28.9	26.9	27.4	27.2	27.2	27.3	28.2	28.6
Tumor necrosis factor (TNF)	31.3	30.8	31.8	32.5	29.8	30.1	31.5	31.4
Alpha-taxilin (TXLNA)	24.2	23.5	23.5	23.0	22.9	23.7	24.3	24.0
Chemokine (C motif) ligand 1 (XCL1)	ND	34.0	35.4	33.6	34.6	35.3	34.3	36.0
Housekeeping genes								
Beta-actin (ACTB)	18.4	17.7	17.6	17.2	17.3	17.9	18.4	18.3
Glyceraldehyde 3-phosphate dehydrogenase (GAPDH)	17.4	17.0	16.9	16.6	16.7	17.2	17.7	17.5
Hypoxanthine-guanine phosphoribosyltransferase (HPRT)	23.2	22.5	22.4	21.8	22.1	22.9	23.4	23.2
18s (X18S)	13.3	13.2	13.2	13.2	13.1	13.2	13.3	13.2

Appendix Table 4: Raw CT values of genes screened in the spinal cord tissue of GPR84 KO sham and PNL operated mice 7 days post surgery

Table 4	KO Spinal cord 7 days post SHAM				KO Spinal cord 7 days post PNL			
Gene	**1**	**2**	**3**	**4**	**1**	**2**	**3**	**4**
Allograft inflammatory factors -1 (Iba1; AIF)	27.8	27.9	27.8	28.0	27.7	27.8	27.5	27.2
Amphiregulin (AREG)	ND	34.9	34.4	ND	ND	ND	34.8	ND
Arginase 1 (ARG1)	33.3	31.9	32.6	32.2	33.2	32.6	32.5	32.0
Artemin (ARTN)	31.1	31.1	30.6	30.0	31.4	31.1	30.8	31.0
Brain-derived neurotrophic factor (BDNF)	27.3	28.0	27.8	27.2	28.2	28.2	27.7	28.0
Betacellulin (BTC)	29.1	28.5	28.6	29.2	29.1	28.6	28.2	28.7
Chemokine (C-C motif) ligand 1 (CCL1)	ND	ND	ND	ND	ND	ND	35.8	ND
Chemokine (C-C motif) ligand 11 (CCL11)	26.9	25.8	26.1	26.9	27.4	27.5	27.7	27.4
Chemokine (C-C motif) ligand 17 (CCL17)	35.2	35.6	35.6	ND	36.0	35.7	35.9	35.9
Chemokine (C-C motif) ligand 19 (CCL19)	26.7	27.7	26.3	27.0	28.0	27.7	27.9	27.5
Chemokine (C-C motif) ligand 2 (CCL2)	31.4	32.8	31.2	31.6	29.1	29.9	30.1	29.2
Chemokine (C-C motif) ligand 20 (CCL20)	ND	35.2	ND	ND	ND	ND	ND	ND
Chemokine (C-C motif) ligand 21a,b (CCL21a,b)	25.6	26.3	25.0	24.9	25.0	24.6	24.6	24.7
Chemokine (C-C motif) ligand 22 (CCL22)	29.8	30.7	30.2	29.8	30.9	31.7	30.4	30.4
Chemokine (C-C motif) ligand 24 (CCL24)	32.5	32.9	32.9	31.5	32.6	33.7	33.1	32.0
Chemokine (C-C motif) ligand 25 (CCL25)	25.4	25.8	25.7	25.6	26.5	26.2	25.8	25.9
Chemokine (C-C motif) ligand 27a,b (CCL27a,b)	22.8	23.2	22.9	22.8	23.5	23.4	23.0	23.0
Chemokine (C-C motif) ligand 3 (CCL3)	33.0	33.1	32.3	33.3	33.7	33.8	32.8	33.6
Chemokine (C-C motif) ligand 4 (CCL4)	32.0	31.3	31.0	31.7	31.9	31.7	30.7	31.8
Chemokine (C-C motif) ligand 5 (CCL5)	30.8	29.5	29.3	30.3	30.3	29.1	27.1	29.5
Chemokine (C-C motif) ligand 6 (CCL6)	25.3	25.1	25.2	25.6	25.9	25.3	24.6	25.5
Chemokine (C-C motif) ligand 7 (CCL7)	31.9	32.3	30.7	32.2	27.3	27.7	28.6	26.8
Chemokine (C-C motif) ligand 8 (CCL8)	34.7	32.7	31.9	32.2	32.2	31.4	30.5	30.7
Chemokine (C-C motif) ligand 9 (CCL9)	26.6	27.0	26.3	26.8	27.6	27.1	26.4	27.0
T-cell surface glycoprotein CD3 delta chain (CD3D)	ND	33.7	34.5	34.8	34.4	33.5	32.3	34.0
Colony stimulating factor 1 (macrophage) (CSF1)	23.7	24.0	23.7	24.0	24.2	24.0	23.7	23.8
Colony stimulating factor 2 (granulocyte-macrophage) (CSF2)	ND	ND	ND	ND	ND	ND	ND	ND
Colony stimulating factor 3 (granulocyte) (CSF3)	33.9	34.1	ND	ND	ND	35.7	32.4	ND
Colony stimulating factor 3 (granulocyte) receptor (CSF3R)	26.8	27.3	26.6	27.2	26.9	26.7	26.1	26.6
Chemokine (CX3-C motif) ligand 1 (CX3CL1)	20.7	21.2	21.0	20.6	21.5	21.3	21.0	21.1
Chemokine (C-X-C motif) ligand 1 (CXCL1)	33.9	32.4	31.6	32.4	ND	32.7	31.0	33.1
Chemokine (C-X-C motif) ligand 10 (CXCL10)	30.7	29.9	29.6	30.2	30.6	29.5	28.3	29.0
Chemokine (C-X-C motif) ligand 11 (CXCL11)	30.5	28.9	30.2	30.1	30.6	31.2	30.9	30.9
Chemokine (C-X-C motif) ligand 12 (CXCL12)	31.5	30.3	30.7	31.4	32.5	30.9	30.7	31.4
Chemokine (C-X-C motif) ligand 13 (CXCL13)	32.5	34.5	30.9	34.0	32.5	31.4	30.4	32.0
Chemokine (C-X-C motif) ligand 14 (CXCL14)	21.3	21.7	21.6	21.4	22.2	21.9	21.9	22.0
Chemokine (C-X-C motif) ligand 16 (CXCL16)	26.8	26.4	25.9	26.7	27.5	26.3	26.6	26.5
Chemokine (C-X-C motif) ligand 17 (CXCL17)	33.0	32.8	33.0	ND	34.2	34.4	32.1	34.1
Chemokine (C-X-C motif) ligand 2 (CXCL2)	ND	ND	32.6	35.6	ND	ND	35.1	ND
Chemokine (C-X-C motif) ligand 3 (CXCL3)	ND	35.2	ND	ND	ND	ND	ND	ND
Chemokine (C-X-C motif) ligand 5 (CXCL5)	29.8	29.7	30.8	30.3	31.0	30.8	30.7	31.2
Chemokine (C-X-C motif) ligand 9 (CXCL9)	34.9	31.6	33.9	33.3	33.0	32.8	29.2	31.0
Chemokine (C-X-C motif) receptor 3 (CXCR3)	38.0	31.9	32.8	32.0	32.3	31.5	29.7	31.1
Epstein-Barr virus induced gene 3 (EBI3)	29.9	31.3	29.9	30.5	31.0	30.2	29.0	30.7
Epiregulin (EREG)	ND	ND	ND	ND	ND	ND	34.9	ND
Fibroblast growth factor 7 (keratinocyte growth factor; FGF7)	28.2	27.1	27.7	27.9	28.7	28.6	28.5	28.3
G-protein receptor 84 (GPR84)	ND	ND	ND	ND	ND	ND	ND	ND
Heparin-binding EGF-like growth factor (HBEGF)	25.6	25.5	25.7	25.6	26.2	25.8	25.5	25.6
Interleukin 10 (IL10)	35.9	ND	ND	35.0	ND	34.8	34.9	35.5
Interleukin 11 (IL11)	32.2	32.7	32.2	32.0	33.2	33.2	32.4	32.1

Table 4	KO Spinal cord 7 days post SHAM				KO Spinal cord 7 days post PNL			
Gene	**1**	**2**	**3**	**4**	**1**	**2**	**3**	**4**
Interleukin 12 alpha (IL12a)	29.7	30.1	30.2	30.4	30.9	30.7	31.2	30.8
Interleukin 12 beta (IL12b)	35.8	34.9	ND	34.9	ND	34.3	34.3	ND
Interleukin 13 (IL13)	34.8	ND	ND	ND	ND	ND	ND	34.6
Interleukin 15 (IL15)	29.2	29.1	28.9	29.1	29.5	29.4	28.9	28.9
Interleukin 16 (IL16)	25.3	24.5	24.4	24.9	25.4	26.1	25.7	25.1
Interleukin 17 alpha (IL17a)	ND	ND	ND	ND	ND	ND	ND	ND
Interleukin 18 (IL18)	24.3	24.6	24.6	24.5	25.0	25.0	25.0	24.8
Interleukin 19 (IL19)	31.7	31.9	31.7	33.2	37.4	32.8	33.3	32.6
Interleukin 1 alpha (IL1a)	30.9	31.5	30.9	30.9	30.6	30.2	30.9	29.4
Interleukin 1 beta (IL1b)	31.9	31.3	31.5	32.4	32.9	31.7	28.3	31.9
Interleukin 2 (IL2)	ND	ND	ND	ND	ND	ND	ND	ND
Interleukin 20 (IL20)	34.9	ND	ND	ND	ND	ND	ND	ND
Interleukin 21 (IL21)	31.8	31.9	31.9	32.2	33.0	31.9	32.6	32.5
Interleukin 22 (IL22)	ND	ND	38.0	ND	ND	ND	ND	ND
Interleukin 23 alpha (IL23a)	29.4	29.2	29.4	29.4	30.7	30.4	29.7	29.9
Interleukin 24 (IL24)	ND	ND	ND	ND	35.2	ND	34.8	34.9
Interleukin 25 (IL25)	30.6	31.2	31.3	30.1	31.0	30.8	30.7	31.2
Interleukin 27 (IL27)	35.2	ND	34.3	31.9	ND	ND	32.6	35.2
Interleukin 28 beta (IL28b)	ND	ND	ND	ND	ND	ND	ND	ND
Interleukin 3 (IL3)	ND	ND	ND	ND	ND	ND	ND	ND
Interleukin 31 (IL31)	ND	ND	ND	ND	ND	ND	ND	35.6
Interleukin 33 (IL33)	22.4	22.1	22.6	22.3	23.0	22.7	22.2	22.4
Interleukin 34 (IL34)	29.8	30.1	29.6	30.0	30.3	30.1	29.9	31.0
Interleukin 4 (IL4)	ND	37.4	ND	ND	ND	ND	ND	ND
Interleukin 5 (IL5)	31.3	32.1	32.5	31.4	32.4	31.8	30.6	33.3
Interleukin 6 (IL6)	32.6	33.6	33.5	33.6	33.4	32.2	32.0	31.8
Interleukin 7 (IL7)	29.6	30.0	29.5	29.9	29.9	30.2	30.0	29.6
Interleukin 9 (IL9)	ND	ND	ND	ND	ND	ND	ND	ND
Integrin alpha M (ITGAM; CD11B)	24.7	24.6	24.4	24.8	24.4	24.0	24.0	23.7
Mannose receptor, C type 1 (MRC1)	26.8	26.3	25.8	26.7	27.6	26.9	26.7	26.4
Nerve growth factor (NGF)	27.9	28.6	28.0	28.0	28.2	28.2	27.7	27.9
Nitric oxide synthase, inducible (NOS2)	29.8	29.6	30.4	29.7	30.6	30.3	28.9	29.3
Neuregulin 1 (NRG1)	22.2	22.5	22.5	22.4	22.8	22.7	22.6	22.7
Platelet factor 4 (PF4; CXCL4)	26.3	24.9	26.5	26.3	26.2	27.7	24.6	26.6
Pro-platelet basic protein (chemokine (C-X-C motif) ligand 7	25.9	24.0	26.9	25.6	25.3	28.3	23.3	26.3
Prostaglandin E synthase (PTGES)	27.5	27.4	27.4	27.4	28.2	28.0	27.6	27.7
Prostaglandin-endoperoxide synthase 2 (COX-2; PTGS2)	30.8	30.8	30.4	30.6	30.8	31.1	28.5	31.3
Signal Transducer and Activator of Transcription protein 4 (STAT4)	32.8	31.7	30.9	33.6	32.9	31.1	30.4	32.9
Toll-like receptor 4 (TLR4)	28.2	27.9	27.7	28.1	28.4	28.4	27.3	28.0
Tumor necrosis factor (TNF)	34.2	32.1	32.1	31.3	31.1	30.2	30.6	30.7
Alpha-taxilin (TXLNA)	23.5	23.6	23.7	23.5	24.3	23.9	23.9	23.7
Chemokine (C motif) ligand 1 (XCL1)	36.7	33.4	35.8	36.6	ND	34.7	35.3	34.9
Housekeeping genes								
Beta-actin (ACTB)	17.9	17.9	18.0	17.9	18.3	18.2	17.8	17.9
Glyceraldehyde 3-phosphate dehydrogenase (GAPDH)	16.9	17.1	17.0	17.0	17.5	17.4	17.2	17.2
Hypoxanthine-guanine phosphoribosyltransferase (HPRT)	22.3	22.9	22.8	22.5	23.1	23.2	23.2	22.9
18s (X18S)	13.2	13.2	13.0	13.1	13.3	13.2	13.2	13.2

Appendix Table 5: Raw CT values of genes screened in the sciatic nerve of GPR84 WT sham and PNL operated mice 21 days post surgery

Table 5	WT Sciatic nerve 21 days post SHAM				WT Sciatic nerve 21 days post PNL			
Gene	**1**	**2**	**3**	**4**	**1**	**2**	**3**	**4**
Allograft inflammatory factors -1 (Iba1; AIF)	29.8	30.3	32.3	32.9	31.3	31.0	32.5	30.4
Amphiregulin (AREG)	37.6	36.5	ND	ND	ND	ND	ND	ND
Artemin (ARTN)	32.4	32.1	33.6	31.6	32.9	35.0	32.9	31.6
Brain-derived neurotrophic factor (BDNF)	ND	33.5	ND	ND	32.7	32.7	32.8	ND
Betacellulin (BTC)	30.5	30.1	32.1	31.0	28.9	30.9	29.3	29.3
Chemokine (C-C motif) ligand 1 (CCL1)	ND	ND	ND	ND	ND	ND	ND	ND
Chemokine (C-C motif) ligand 11 (CCL11)	23.7	22.8	24.4	23.9	24.7	25.6	25.6	24.9
Chemokine (C-C motif) ligand 17 (CCL17)	34.8	34.8	34.3	ND	ND	32.4	35.6	34.2
Chemokine (C-C motif) ligand 19 (CCL19)	30.5	29.3	31.5	30.9	31.0	33.6	31.7	31.6
Chemokine (C-C motif) ligand 2 (CCL2)	30.2	29.7	30.8	31.9	30.2	30.4	30.3	29.8
Chemokine (C-C motif) ligand 20 (CCL20)	ND	ND	ND	ND	ND	ND	ND	ND
Chemokine (C-C motif) ligand 21a,b (CCL21a,b)	23.6	22.8	23.6	24.6	25.6	26.0	26.9	25.6
Chemokine (C-C motif) ligand 22 (CCL22)	31.7	32.3	32.7	34.4	34.6	30.2	30.4	30.3
Chemokine (C-C motif) ligand 24 (CCL24)	29.5	29.6	30.4	30.2	32.0	33.1	32.9	31.0
Chemokine (C-C motif) ligand 25 (CCL25)	25.4	29.2	31.5	30.8	31.8	30.7	30.8	31.7
Chemokine (C-C motif) ligand 26 (CCL26)	ND	ND	ND	ND	ND	ND	ND	ND
Chemokine (C-C motif) ligand 27a,b (CCL27a,b)	27.0	26.0	27.4	26.9	28.8	28.4	28.7	27.9
Chemokine (C-C motif) ligand 28 (CCL28)	29.4	30.9	32.6	32.4	33.2	32.6	34.7	32.5
Chemokine (C-C motif) ligand 3 (CCL3)	36.9	36.9	ND	ND	35.0	33.9	34.0	31.2
Chemokine (C-C motif) ligand 4 (CCL4)	35.7	34.9	35.2	35.2	33.5	32.5	32.9	31.0
Chemokine (C-C motif) ligand 5 (CCL5)	31.3	32.3	31.5	31.7	30.5	30.0	30.9	30.5
Chemokine (C-C motif) ligand 6 (CCL6)	24.1	23.8	24.2	24.3	24.8	24.0	25.3	23.0
Chemokine (C-C motif) ligand 7 (CCL7)	28.5	30.2	30.3	30.6	30.8	31.2	32.8	30.3
Chemokine (C-C motif) ligand 8 (CCL8)	29.1	30.1	30.5	30.3	28.8	28.2	28.3	28.7
Chemokine (C-C motif) ligand 9 (CCL9)	25.7	25.9	26.3	26.6	27.9	27.0	28.2	25.4
T-cell surface glycoprotein CD3 delta chain (CD3D)	33.9	ND	ND	ND	ND	ND	32.7	34.5
Colony stimulating factor 1 (macrophage) (CSF1)	27.2	25.7	27.3	27.0	27.8	27.6	28.2	27.0
Colony stimulating factor 1 (macrophage) receptor (CSF1R)	25.6	24.6	26.0	25.6	26.7	25.8	26.4	24.8
Colony stimulating factor 2 (granulocyte-macrophage) (CSF2)	27.9	36.0	ND	ND	ND	ND	34.6	33.5
Colony stimulating factor 3 (granulocyte) (CSF3)	ND	ND	ND	ND	33.6	ND	ND	35.0
Chemokine (CX3-C motif) ligand 1 (CX3CL1)	29.6	28.2	30.7	29.6	30.5	30.8	30.7	29.7
Chemokine (C-X-C motif) ligand 1 (CXCL1)	33.7	35.9	33.5	34.9	31.9	33.8	34.3	34.3
Chemokine (C-X-C motif) ligand 10 (CXCL10)	28.3	28.2	32.0	31.5	30.0	30.2	29.8	29.2
Chemokine (C-X-C motif) ligand 11 (CXCL11)	29.7	29.0	31.0	30.2	33.4	31.4	32.6	30.9
Chemokine (C-X-C motif) ligand 12 (CXCL12)	32.0	30.9	31.9	31.7	33.4	33.0	33.1	30.8
Chemokine (C-X-C motif) ligand 13 (CXCL13)	26.7	26.2	26.3	26.6	27.7	29.9	32.6	29.7
Chemokine (C-X-C motif) ligand 14 (CXCL14)	25.4	25.7	27.5	26.8	25.4	27.0	27.0	25.8
Chemokine (C-X-C motif) ligand 16 (CXCL16)	28.8	27.7	29.7	29.1	28.1	27.8	28.3	26.5
Chemokine (C-X-C motif) ligand 17 (CXCL17)	35.5	32.1	34.0	34.9	35.0	33.6	35.1	ND
Chemokine (C-X-C motif) ligand 2 (CXCL2)	34.5	ND	ND	34.2	ND	32.2	ND	30.2
Chemokine (C-X-C motif) ligand 3 (CXCL3)	37.6	ND	ND	ND	ND	32.9	32.5	32.4
Chemokine (C-X-C motif) ligand 5 (CXCL5)	ND	34.1	ND	ND	ND	31.8	32.6	29.0
Chemokine (C-X-C motif) ligand 9 (CXCL9)	31.1	29.3	30.7	30.6	30.1	30.4	30.0	30.9
Chemokine (C-X-C motif) receptor 3 (CXCR3)	31.3	31.4	32.5	31.7	30.9	31.4	30.5	30.3
Epstein-Barr virus induced gene 3 (EBI3)	31.5	30.6	33.0	31.7	32.7	31.4	32.4	30.0
Epiregulin (EREG)	35.2	ND	ND	ND	ND	34.1	ND	33.8
Fibroblast growth factor 7 (keratinocyte growth factor; FGF7)	25.6	25.8	27.1	26.9	29.4	29.1	28.8	27.6
G-protein receptor 84 (GPR84)	ND	36.4	ND	ND	ND	35.1	37.3	33.6
Histocompatibility 2, class II antigen E beta (H2.EB1)	25.3	24.4	26.1	25.7	26.5	26.4	26.3	25.8

Table 5	WT Sciatic nerve 21 days post SHAM				WT Sciatic nerve 21 days post PNL			
Gene	**1**	**2**	**3**	**4**	**1**	**2**	**3**	**4**
Heparin-binding EGF-like growth factor (HBEGF)	27.1	26.2	27.9	27.1	29.2	29.1	29.4	28.2
Interleukin 10 (IL10)	29.6	35.8	ND	ND	35.3	ND	ND	ND
Interleukin 11 (IL11)	32.2	33.7	ND	34.2	ND	34.9	ND	36.1
Interleukin 12 alpha (IL12a)	33.7	31.3	32.8	34.0	35.5	34.0	35.5	35.3
Interleukin 12 beta (IL12b)	ND	ND	ND	ND	ND	34.4	ND	35.0
Interleukin 13 (IL13)	32.3	ND	ND	ND	ND	ND	ND	ND
Interleukin 15 (IL15)	29.8	28.6	29.8	29.8	30.2	30.0	30.4	29.6
Interleukin 16 (IL16)	24.3	23.1	24.8	23.9	26.0	26.4	25.7	24.8
Interleukin 17 alpha (IL17a)	33.5	ND	ND	ND	37.3	ND	ND	ND
Interleukin 18 (IL18)	29.0	29.8	31.4	30.8	33.4	32.0	32.7	30.6
Interleukin 19 (IL19)	ND	ND	ND	ND	34.9	ND	ND	ND
Interleukin 1 alpha (IL1a)	ND	ND	ND	ND	35.6	ND	33.8	31.5
Interleukin 1 beta (IL1b)	ND	34.8	35.4	ND	33.3	30.9	31.5	29.6
Interleukin 2 (IL2)	36.9	ND	ND	ND	ND	ND	ND	ND
Interleukin 20 (IL20)	ND	ND	ND	ND	ND	ND	ND	ND
Interleukin 21 (IL21)	ND	ND	ND	ND	ND	ND	ND	ND
Interleukin 22 (IL22)	ND	ND	ND	ND	ND	ND	ND	ND
Interleukin 23 alpha (IL23a)	31.6	32.1	32.7	33.3	33.4	34.4	ND	35.1
Interleukin 24 (IL24)	ND	32.9	ND	ND	ND	ND	ND	ND
Interleukin 25 (IL25)	33.6	34.2	33.3	ND	ND	33.7	ND	33.4
Interleukin 27 (IL27)	35.5	ND	ND	ND	32.9	33.8	34.7	32.9
Interleukin 28 beta (IL28b)	ND	ND	ND	ND	ND	ND	ND	ND
Interleukin 3 (IL3)	ND	ND	ND	ND	ND	ND	ND	ND
Interleukin 31 (IL31)	26.9	ND	ND	ND	37.9	ND	ND	ND
Interleukin 33 (IL33)	25.2	24.6	25.3	24.9	27.3	27.7	28.1	26.7
Interleukin 34 (IL34)	30.6	30.1	32.8	31.7	33.4	34.0	34.0	32.2
Interleukin 4 (IL4)	ND	ND	ND	ND	ND	ND	ND	ND
Interleukin 5 (IL5)	32.9	34.3	ND	33.3	ND	ND	37.9	ND
Interleukin 6 (IL6)	30.6	36.1	ND	ND	34.2	35.4	ND	ND
Interleukin 7 (IL7)	31.0	31.9	32.4	33.7	33.6	33.3	34.5	32.9
Interleukin 9 (IL9)	ND	ND	ND	ND	ND	ND	ND	ND
Integrin alpha M (ITGAM; CD11B)	28.0	27.3	28.9	28.4	28.8	27.5	27.8	25.4
Nerve growth factor (NGF)	27.9	28.3	29.3	29.6	28.5	29.7	31.0	29.9
Nitric oxide synthase, inducible (NOS2)	31.9	31.0	33.5	ND	32.1	31.8	32.0	31.0
Platelet factor 4 (PF4; CXCL4)	26.6	26.6	28.1	27.2	28.8	27.6	28.3	26.9
Pro-platelet basic protein (chemokine (C-X-C motif) ligand 7	29.9	28.9	29.3	31.4	30.3	30.9	33.3	31.3
Prostaglandin E synthase (PTGES)	27.9	26.8	29.0	28.4	29.2	30.7	29.9	28.7
Prostaglandin-endoperoxide synthase 2 (COX-2; PTGS2)	33.6	33.0	33.4	34.1	32.6	34.3	36.7	33.8
Signal Transducer and Activator of Transcription protein 4 (STAT4)	30.3	30.5	32.0	31.2	34.2	33.8	37.5	32.4
Toll-like receptor 4 (TLR4)	27.0	26.5	27.6	27.5	28.5	28.4	29.3	27.4
Tumor necrosis factor (TNF)	33.2	32.1	32.1	32.7	34.2	31.2	31.1	29.1
Alpha-taxilin (TXLNA)	27.4	26.4	28.4	27.9	28.0	27.9	28.0	27.9
Chemokine (C motif) ligand 1 (XCL1)	36.6	ND	ND	ND	25.3	ND	34.6	37.0
Housekeeping genes								
Beta-actin (ACTB)	20.6	19.5	20.7	20.4	21.3	21.3	21.7	20.1
Glyceraldehyde 3-phosphate dehydrogenase (GAPDH)	21.5	20.6	22.5	21.9	23.7	19.7	22.6	21.9
Hypoxanthine-guanine phosphoribosyltransferase (HPRT)	27.6	26.7	28.9	28.3	26.8	28.9	29.1	28.1
18s (X18S)	15.5	14.1	18.0	16.2	15.9	15.6	14.7	15.0

Appendix Table 6: Raw CT values of genes screened in the sciatic nerve of GPR84 KO sham and PNL operated mice 21 days post surgery

Table 6	KO Sciatic nerve 21 days post SHAM				KO Sciatic nerve 21 days post PNL			
Gene	**1**	**2**	**3**	**4**	**1**	**2**	**3**	**4**
Allograft inflammatory factors -1 (Iba1; AIF)	30.3	30.7	31.8	31.2	31.9	30.4	31.9	31.3
Amphiregulin (AREG)	ND	ND	ND	ND	ND	ND	ND	ND
Artemin (ARTN)	30.7	31.3	34.5	32.3	33.2	33.9	33.8	31.9
Brain-derived neurotrophic factor (BDNF)	ND	34.4	ND	ND	33.8	34.8	33.4	34.4
Betacellulin (BTC)	30.5	31.9	30.9	32.0	31.1	29.9	30.1	31.0
Chemokine (C-C motif) ligand 1 (CCL1)	ND	ND	ND	ND	ND	ND	ND	ND
Chemokine (C-C motif) ligand 11 (CCL11)	22.2	22.7	23.1	23.6	26.3	25.0	25.9	25.8
Chemokine (C-C motif) ligand 17 (CCL17)	32.0	33.8	33.9	ND	34.6	36.6	ND	35.1
Chemokine (C-C motif) ligand 19 (CCL19)	28.3	29.4	30.5	31.6	30.9	33.7	32.2	31.1
Chemokine (C-C motif) ligand 2 (CCL2)	28.8	30.0	30.2	30.6	30.5	31.1	31.3	29.6
Chemokine (C-C motif) ligand 20 (CCL20)	ND	ND	ND	ND	ND	ND	ND	ND
Chemokine (C-C motif) ligand 21a,b (CCL21a,b)	23.2	24.4	24.3	27.1	26.2	29.3	26.8	26.4
Chemokine (C-C motif) ligand 22 (CCL22)	29.9	30.9	31.3	31.8	30.7	33.4	32.9	29.6
Chemokine (C-C motif) ligand 24 (CCL24)	28.7	30.0	30.3	31.1	32.2	32.3	32.9	32.0
Chemokine (C-C motif) ligand 25 (CCL25)	29.5	29.6	30.0	30.8	32.6	32.0	32.0	32.1
Chemokine (C-C motif) ligand 26 (CCL26)	36.0	ND	ND	ND	ND	ND	ND	ND
Chemokine (C-C motif) ligand 27a,b (CCL27a,b)	25.9	25.9	26.4	26.4	29.8	28.6	28.0	28.6
Chemokine (C-C motif) ligand 28 (CCL28)	30.3	30.8	31.1	31.5	ND	34.0	33.3	35.1
Chemokine (C-C motif) ligand 3 (CCL3)	33.0	35.0	36.6	ND	36.3	35.6	35.6	33.3
Chemokine (C-C motif) ligand 4 (CCL4)	32.2	33.6	33.3	35.1	33.7	33.5	35.3	31.0
Chemokine (C-C motif) ligand 5 (CCL5)	29.5	31.2	31.2	32.8	30.9	31.0	31.8	30.4
Chemokine (C-C motif) ligand 6 (CCL6)	22.2	24.2	25.1	25.8	24.5	25.3	25.2	23.9
Chemokine (C-C motif) ligand 7 (CCL7)	28.1	29.0	29.9	29.7	31.7	32.6	33.2	30.1
Chemokine (C-C motif) ligand 8 (CCL8)	28.6	30.5	30.3	32.5	28.5	28.1	28.7	27.7
Chemokine (C-C motif) ligand 9 (CCL9)	25.0	26.9	27.5	28.0	27.9	27.8	28.7	27.1
T-cell surface glycoprotein CD3 delta chain (CD3D)	33.1	35.2	34.4	ND	ND	ND	ND	ND
Colony stimulating factor 1 (macrophage) (CSF1)	25.5	25.8	26.4	26.9	28.6	27.7	28.7	27.5
Colony stimulating factor 1 (macrophage) receptor (CSF1R)	24.0	24.6	26.2	26.0	26.3	25.9	26.5	25.6
Colony stimulating factor 2 (granulocyte-macrophage) (CSF2)	34.6	ND	34.9	ND	ND	ND	ND	ND
Colony stimulating factor 3 (granulocyte) (CSF3)	ND	ND	ND	ND	ND	ND	ND	ND
Chemokine (CX3-C motif) ligand 1 (CX3CL1)	28.8	28.7	28.6	28.6	30.3	29.5	29.4	29.8
Chemokine (C-X-C motif) ligand 1 (CXCL1)	33.9	33.3	34.9	32.2	34.5	35.4	ND	32.2
Chemokine (C-X-C motif) ligand 10 (CXCL10)	28.7	29.2	29.0	29.8	30.5	29.7	30.7	30.3
Chemokine (C-X-C motif) ligand 11 (CXCL11)	28.4	28.8	29.1	29.4	ND	32.3	32.5	32.8
Chemokine (C-X-C motif) ligand 12 (CXCL12)	29.0	31.3	31.3	32.3	32.9	32.9	32.9	31.4
Chemokine (C-X-C motif) ligand 13 (CXCL13)	24.6	26.4	27.9	28.8	32.3	31.0	30.0	30.3
Chemokine (C-X-C motif) ligand 14 (CXCL14)	24.1	26.4	28.1	27.8	25.9	25.9	26.9	27.1
Chemokine (C-X-C motif) ligand 16 (CXCL16)	26.7	27.9	28.5	29.0	28.3	28.0	28.7	27.6
Chemokine (C-X-C motif) ligand 17 (CXCL17)	32.7	ND	ND	ND	33.3	35.0	35.0	35.1
Chemokine (C-X-C motif) ligand 2 (CXCL2)	32.8	34.9	34.7	ND	34.1	ND	35.1	31.0
Chemokine (C-X-C motif) ligand 3 (CXCL3)	ND	ND	ND	ND	35.0	ND	ND	32.5
Chemokine (C-X-C motif) ligand 5 (CXCL5)	ND	ND	ND	ND	35.2	ND	35.0	30.1
Chemokine (C-X-C motif) ligand 9 (CXCL9)	30.3	30.9	29.8	31.4	30.9	30.9	30.4	30.1
Chemokine (C-X-C motif) receptor 3 (CXCR3)	29.9	31.0	29.8	33.0	30.9	31.3	31.4	30.5
Epstein-Barr virus induced gene 3 (EBI3)	30.2	30.3	31.0	31.0	33.9	31.6	32.6	31.3
Epiregulin (EREG)	ND	ND	ND	ND	ND	ND	ND	ND
Fibroblast growth factor 7 (keratinocyte growth factor; FGF7)	25.4	25.4	25.4	25.9	26.4	28.6	29.2	28.9
G-protein receptor 84 (GPR84)	ND	ND	ND	ND	ND	ND	ND	ND
Histocompatibility 2, class II antigen E beta (H2.EB1)	24.0	24.9	25.2	25.6	26.6	26.2	26.4	26.1

Table 6	KO Sciatic nerve 21 days post SHAM				KO Sciatic nerve 21 days post PNL			
Gene	**1**	**2**	**3**	**4**	**1**	**2**	**3**	**4**
Heparin-binding EGF-like growth factor (HBEGF)	26.2	25.9	26.3	26.2	29.9	29.4	28.8	29.2
Interleukin 10 (IL10)	ND	36.0	ND	ND	ND	ND	ND	ND
Interleukin 11 (IL11)	33.2	33.0	33.9	32.7	34.7	ND	36.0	ND
Interleukin 12 alpha (IL12a)	31.6	31.6	31.4	31.9	ND	35.3	31.8	35.5
Interleukin 12 beta (IL12b)	ND	ND	ND	34.8	ND	35.5	ND	34.4
Interleukin 13 (IL13)	ND	ND	ND	ND	ND	ND	ND	ND
Interleukin 15 (IL15)	28.7	28.8	29.1	29.7	32.2	31.3	29.4	29.8
Interleukin 16 (IL16)	22.9	23.0	23.4	23.4	27.3	26.0	26.7	26.5
Interleukin 17 alpha (IL17a)	ND	ND	ND	ND	33.9	ND	ND	ND
Interleukin 18 (IL18)	28.2	29.9	30.4	30.4	32.6	32.0	32.8	31.9
Interleukin 19 (IL19)	ND	ND	ND	ND	ND	ND	ND	ND
Interleukin 1 alpha (IL1a)	ND	ND	33.9	ND	34.5	32.8	34.5	35.8
Interleukin 1 beta (IL1b)	30.1	33.1	32.8	34.8	32.4	33.5	34.6	29.6
Interleukin 2 (IL2)	ND	ND	ND	ND	ND	ND	ND	ND
Interleukin 20 (IL20)	ND	ND	ND	ND	ND	ND	ND	ND
Interleukin 21 (IL21)	ND	ND	ND	ND	ND	ND	ND	ND
Interleukin 22 (IL22)	ND	ND	ND	ND	ND	ND	ND	ND
Interleukin 23 alpha (IL23a)	30.6	32.2	31.5	31.4	ND	ND	ND	33.1
Interleukin 24 (IL24)	ND	ND	ND	ND	ND	ND	ND	ND
Interleukin 25 (IL25)	34.9	33.7	34.2	ND	ND	ND	ND	ND
Interleukin 27 (IL27)	33.2	34.6	ND	ND	ND	ND	34.6	34.7
Interleukin 28 beta (IL28b)	ND	ND	ND	ND	ND	ND	ND	ND
Interleukin 3 (IL3)	37.0	ND	ND	ND	ND	ND	ND	ND
Interleukin 31 (IL31)	36.4	ND	35.6	ND	ND	ND	ND	ND
Interleukin 33 (IL33)	24.2	24.8	25.0	25.4	28.8	27.7	28.8	27.8
Interleukin 34 (IL34)	30.2	30.4	31.2	30.4	28.2	32.3	35.2	33.3
Interleukin 4 (IL4)	35.8	ND	ND	ND	ND	ND	ND	ND
Interleukin 5 (IL5)	ND	34.3	33.9	ND	ND	ND	ND	34.7
Interleukin 6 (IL6)	32.6	33.8	34.1	35.2	ND	36.3	ND	ND
Interleukin 7 (IL7)	29.2	32.9	34.0	36.1	33.9	34.2	33.8	35.2
Interleukin 9 (IL9)	ND	ND	ND	ND	ND	ND	ND	ND
Integrin alpha M (ITGAM; CD11B)	25.9	27.2	29.1	29.5	27.6	28.3	28.6	26.6
Nerve growth factor (NGF)	27.5	28.5	28.6	28.9	31.0	30.2	30.4	29.8
Nitric oxide synthase, inducible (NOS2)	31.0	32.5	31.9	30.8	33.5	31.5	31.0	31.6
Platelet factor 4 (PF4; CXCL4)	25.2	26.5	27.0	27.4	28.4	28.4	28.0	27.1
Pro-platelet basic protein (chemokine (C-X-C motif) ligand 7	27.3	29.8	26.3	29.1	32.1	32.3	33.4	32.2
Prostaglandin E synthase (PTGES)	26.3	26.9	27.3	27.7	31.2	29.3	30.0	29.0
Prostaglandin-endoperoxide synthase 2 (COX-2; PTGS2)	31.5	33.5	33.5	34.0	36.8	ND	37.2	34.0
Signal Transducer and Activator of Transcription protein 4 (STAT4)	30.1	30.9	29.6	33.2	35.4	34.2	34.5	32.8
Toll-like receptor 4 (TLR4)	26.1	26.9	31.0	27.9	29.6	28.7	29.5	28.0
Tumor necrosis factor (TNF)	30.4	31.1	32.1	34.3	31.8	32.1	33.3	30.4
Alpha-taxilin (TXLNA)	25.9	26.2	26.9	26.9	28.8	28.0	28.1	27.9
Chemokine (C motif) ligand 1 (XCL1)	33.6	37.5	37.5	ND	ND	35.1	37.0	37.3
Housekeeping genes								
Beta-actin (ACTB)	19.5	19.7	19.8	20.1	22.0	21.5	22.0	21.2
Glyceraldehyde 3-phosphate dehydrogenase (GAPDH)	20.5	19.8	20.2	20.9	24.2	21.2	18.5	22.6
Hypoxanthine-guanine phosphoribosyltransferase (HPRT)	26.3	27.3	27.7	27.8	30.3	29.4	29.4	28.7
18s (X18S)	13.9	14.1	14.4	14.2	15.2	15.2	14.5	14.5

Appendix Table 7: Raw CT values of genes screened in the spinal cord of GPR84 WT sham and PNL operated mice 21 days post surgery

Table 7	WT Spinal cord 21 days post SHAM				WT Spinal cord 21 days post PNL			
Gene	**1**	**2**	**3**	**4**	**1**	**2**	**3**	**4**
Allograft inflammatory factors -1 (Iba1; AIF)	28.9	28.8	28.5	27.9	27.5	28.7	28.1	28.7
Amphiregulin (AREG)	ND	36.7	34.9	ND	33.9	ND	ND	ND
Artemin (ARTN)	31.8	31.1	31.5	33.3	31.3	32.2	32.6	32.4
Brain-derived neurotrophic factor (BDNF)	28.7	28.4	28.7	29.1	28.8	28.6	28.4	29.3
Betacellulin (BTC)	30.0	29.9	29.7	29.1	28.9	29.8	28.9	29.7
Chemokine (C-C motif) ligand 1 (CCL1)	ND	ND	ND	35.4	ND	ND	ND	ND
Chemokine (C-C motif) ligand 11 (CCL11)	29.6	29.3	27.8	26.4	27.2	30.1	27.2	28.8
Chemokine (C-C motif) ligand 17 (CCL17)	37.4	33.9	34.7	ND	ND	34.7	33.9	ND
Chemokine (C-C motif) ligand 19 (CCL19)	29.2	28.2	27.5	27.5	27.9	29.8	28.0	29.0
Chemokine (C-C motif) ligand 2 (CCL2)	30.9	ND	32.3	31.9	29.6	31.3	31.2	31.3
Chemokine (C-C motif) ligand 20 (CCL20)	ND	ND	ND	ND	ND	ND	ND	ND
Chemokine (C-C motif) ligand 21a,b (CCL21a,b)	26.9	25.9	25.8	25.3	26.3	27.4	26.2	26.2
Chemokine (C-C motif) ligand 22 (CCL22)	33.2	31.5	32.3	30.8	30.8	32.4	30.4	32.5
Chemokine (C-C motif) ligand 24 (CCL24)	34.2	35.0	32.6	34.8	30.7	33.6	32.9	34.0
Chemokine (C-C motif) ligand 25 (CCL25)	26.2	26.3	26.6	26.3	26.4	27.1	26.0	27.1
Chemokine (C-C motif) ligand 26 (CCL26)	37.0	ND	ND	ND	ND	ND	ND	ND
Chemokine (C-C motif) ligand 27a,b (CCL27a,b)	23.9	23.5	23.6	23.6	23.6	24.2	23.3	24.4
Chemokine (C-C motif) ligand 28 (CCL28)	28.9	29.0	29.1	29.0	28.9	28.9	29.1	29.9
Chemokine (C-C motif) ligand 3 (CCL3)	36.1	35.7	34.2	34.4	35.2	34.9	33.9	34.2
Chemokine (C-C motif) ligand 4 (CCL4)	32.7	34.5	32.2	31.1	31.7	32.7	30.8	32.7
Chemokine (C-C motif) ligand 5 (CCL5)	31.0	31.1	30.3	29.0	30.0	32.1	29.8	30.5
Chemokine (C-C motif) ligand 6 (CCL6)	27.6	26.8	26.3	25.9	26.1	27.4	26.2	26.8
Chemokine (C-C motif) ligand 7 (CCL7)	30.4	33.6	31.4	31.6	29.3	31.0	32.8	31.1
Chemokine (C-C motif) ligand 8 (CCL8)	ND	32.3	32.5	33.5	31.7	32.7	31.6	35.0
Chemokine (C-C motif) ligand 9 (CCL9)	29.3	28.0	27.7	27.3	27.9	28.8	27.7	28.6
T-cell surface glycoprotein CD3 delta chain (CD3D)	34.6	ND	34.6	32.2	34.5	34.7	34.9	ND
Colony stimulating factor 1 (macrophage) (CSF1)	25.9	25.4	24.9	24.7	24.2	25.8	25.1	25.2
Colony stimulating factor 1 (macrophage) receptor (CSF1R)	24.3	23.7	23.6	23.2	23.0	24.0	23.5	24.1
Colony stimulating factor 2 (granulocyte-macrophage) (CSF2)	ND	ND	35.0	34.9	ND	ND	ND	ND
Colony stimulating factor 3 (granulocyte) (CSF3)	34.4	ND	ND	ND	29.4	ND	ND	ND
Chemokine (CX3-C motif) ligand 1 (CX3CL1)	22.5	21.9	22.2	22.0	22.0	22.7	21.7	22.7
Chemokine (C-X-C motif) ligand 1 (CXCL1)	32.8	34.9	ND	33.1	28.8	ND	34.8	34.7
Chemokine (C-X-C motif) ligand 10 (CXCL10)	31.9	32.2	31.0	31.3	29.4	31.6	28.5	31.0
Chemokine (C-X-C motif) ligand 11 (CXCL11)	32.2	30.3	30.4	29.6	30.5	32.2	30.7	31.1
Chemokine (C-X-C motif) ligand 12 (CXCL12)	33.8	34.0	32.0	32.6	32.7	33.3	31.8	32.4
Chemokine (C-X-C motif) ligand 13 (CXCL13)	ND	35.1	ND	34.3	32.2	34.3	34.7	ND
Chemokine (C-X-C motif) ligand 14 (CXCL14)	23.7	22.7	22.8	22.2	22.5	23.3	22.5	23.1
Chemokine (C-X-C motif) ligand 16 (CXCL16)	28.1	28.0	27.5	26.9	26.3	28.3	27.3	28.6
Chemokine (C-X-C motif) ligand 17 (CXCL17)	ND	ND	34.9	34.4	33.9	34.8	33.4	34.9
Chemokine (C-X-C motif) ligand 2 (CXCL2)	ND	ND	36.1	35.1	31.2	ND	ND	ND
Chemokine (C-X-C motif) ligand 3 (CXCL3)	ND	ND	ND	ND	ND	ND	ND	ND
Chemokine (C-X-C motif) ligand 5 (CXCL5)	32.8	31.1	33.5	30.0	31.2	31.8	31.1	31.6
Chemokine (C-X-C motif) ligand 9 (CXCL9)	35.0	35.4	34.2	32.5	35.4	34.9	30.5	33.8
Chemokine (C-X-C motif) receptor 3 (CXCR3)	32.6	ND	33.5	32.5	31.8	33.1	31.5	32.8
Epstein-Barr virus induced gene 3 (EBI3)	32.2	31.3	31.0	32.0	30.7	31.6	31.8	32.1
Epiregulin (EREG)	ND	ND	ND	ND	ND	ND	ND	ND
Fibroblast growth factor 7 (keratinocyte growth factor; FGF7)	28.3	28.6	27.9	27.4	27.7	29.5	27.8	28.6
G-protein receptor 84 (GPR84)	32.0	31.3	31.3	31.2	31.1	31.6	31.0	31.3
Histocompatibility 2, class II antigen E beta (H2.EB1)	27.8	27.7	26.8	26.0	26.5	28.0	26.7	28.0

Table 7	WT Spinal cord 21 days post SHAM				WT Spinal cord 21 days post PNL			
Gene	**1**	**2**	**3**	**4**	**1**	**2**	**3**	**4**
Heparin-binding EGF-like growth factor (HBEGF)	26.3	25.9	26.2	25.7	25.2	26.8	25.6	26.3
Interleukin 10 (IL10)	35.8	ND	ND	ND	35.6	ND	ND	36.0
Interleukin 11 (IL11)	32.1	32.7	34.8	33.3	33.3	33.5	32.9	34.5
Interleukin 12 alpha (IL12a)	31.1	31.5	31.4	30.7	30.0	32.5	31.1	32.0
Interleukin 12 beta (IL12b)	35.5	ND	ND	34.3	33.9	35.9	ND	33.9
Interleukin 13 (IL13)	ND	ND	ND	34.0	ND	ND	ND	ND
Interleukin 15 (IL15)	29.8	29.8	29.6	29.7	28.6	30.0	29.3	29.5
Interleukin 16 (IL16)	27.5	26.7	26.1	25.6	25.9	27.8	26.0	26.6
Interleukin 17 alpha (IL17a)	ND	ND	ND	ND	ND	ND	ND	ND
Interleukin 18 (IL18)	26.3	25.6	25.5	24.8	25.0	26.1	25.1	25.7
Interleukin 19 (IL19)	33.5	33.6	33.3	32.1	31.3	33.1	33.2	32.6
Interleukin 1 alpha (IL1a)	34.5	32.1	31.9	31.5	30.9	31.8	31.2	31.7
Interleukin 1 beta (IL1b)	32.5	31.9	32.8	31.2	31.3	34.8	32.4	33.4
Interleukin 2 (IL2)	ND	ND	35.0	ND	ND	ND	ND	ND
Interleukin 20 (IL20)	ND	ND	36.4	ND	ND	ND	ND	ND
Interleukin 21 (IL21)	33.8	33.5	33.3	32.0	33.5	33.5	32.6	33.6
Interleukin 22 (IL22)	37.9	37.7	ND	37.9	ND	ND	ND	ND
Interleukin 23 alpha (IL23a)	32.0	31.2	31.3	30.7	30.7	31.0	30.9	31.0
Interleukin 24 (IL24)	ND	ND	ND	ND	ND	ND	ND	ND
Interleukin 25 (IL25)	32.9	32.2	32.7	34.0	32.1	32.9	31.9	32.3
Interleukin 27 (IL27)	ND	34.6	34.5	ND	34.5	ND	34.6	ND
Interleukin 28 beta (IL28b)	ND	ND	ND	ND	ND	ND	ND	ND
Interleukin 3 (IL3)	ND	ND	ND	ND	ND	ND	ND	ND
Interleukin 31 (IL31)	ND	ND	ND	ND	ND	ND	ND	ND
Interleukin 33 (IL33)	23.6	23.1	23.2	22.5	22.5	23.7	22.7	23.3
Interleukin 34 (IL34)	30.8	31.3	30.9	31.0	30.9	32.2	31.1	31.8
Interleukin 4 (IL4)	ND	ND	ND	ND	ND	ND	ND	ND
Interleukin 5 (IL5)	32.7	33.9	32.7	31.9	32.1	33.2	32.1	ND
Interleukin 6 (IL6)	31.9	33.9	33.3	32.1	31.5	34.7	32.9	32.8
Interleukin 7 (IL7)	31.0	30.7	30.9	30.4	28.8	31.4	30.6	30.7
Interleukin 9 (IL9)	ND	ND	ND	ND	ND	ND	ND	ND
Integrin alpha M (ITGAM; CD11B)	26.6	26.1	26.1	25.6	25.5	26.8	25.7	26.3
Nerve growth factor (NGF)	29.6	29.7	29.7	28.6	28.7	30.6	29.3	29.6
Nitric oxide synthase, inducible (NOS2)	31.2	30.6	30.6	30.2	29.2	30.9	30.3	31.1
Platelet factor 4 (PF4; CXCL4)	29.5	28.7	28.1	25.8	26.5	28.8	27.5	27.3
Pro-platelet basic protein (chemokine (C-X-C motif) ligand 7	31.1	28.3	28.5	25.6	26.0	27.8	27.1	27.0
Prostaglandin E synthase (PTGES)	29.7	28.7	28.4	27.9	27.9	29.6	28.0	28.9
Prostaglandin-endoperoxide synthase 2 (COX-2; PTGS2)	31.8	31.5	32.6	32.5	28.4	33.2	31.9	32.8
Signal Transducer and Activator of Transcription protein 4 (STAT4)	33.7	32.7	32.4	31.8	33.4	34.2	32.5	34.9
Toll-like receptor 4 (TLR4)	30.4	29.0	28.9	28.7	28.2	29.7	28.9	29.6
Tumor necrosis factor (TNF)	35.1	34.8	33.3	32.1	31.5	ND	33.0	33.5
Alpha-taxilin (TXLNA)	25.7	25.1	25.1	24.5	24.5	25.5	24.5	25.2
Chemokine (C motif) ligand 1 (XCL1)	37.5	36.6	ND	35.1	ND	37.2	35.6	37.5
Housekeeping genes								
Beta-actin (ACTB)	19.7	19.2	19.1	18.8	18.5	19.8	18.6	19.3
Glyceraldehyde 3-phosphate dehydrogenase (GAPDH)	18.9	18.3	18.5	17.9	18.0	18.8	17.9	18.7
Hypoxanthine-guanine phosphoribosyltransferase (HPRT)	23.5	23.3	23.3	22.8	23.1	23.8	22.9	23.7
18s (X18S)	14.9	14.6	14.8	14.9	14.8	14.8	14.7	14.8

Appendix Table 8: Raw CT values of genes screened in the spinal cord of GPR84 KO sham and PNL operated mice 21 days post surgery

Table 8	KO Spinal cord 21 days post SHAM				KO Spinal cord 21 days post PNL			
Gene	**1**	**2**	**3**	**4**	**1**	**2**	**3**	**4**
Allograft inflammatory factors -1 (Iba1; AIF)	27.8	28.2	27.9	28.9	28.0	29.1	27.8	27.6
Amphiregulin (AREG)	33.6	ND	ND	34.9	33.8	ND	34.5	33.1
Artemin (ARTN)	31.5	31.0	31.1	31.3	31.6	32.3	30.9	31.8
Brain-derived neurotrophic factor (BDNF)	28.6	28.5	27.8	29.0	28.9	28.9	27.7	28.6
Betacellulin (BTC)	30.0	29.9	29.1	29.9	30.1	30.0	29.6	29.2
Chemokine (C-C motif) ligand 1 (CCL1)	ND	ND	35.8	ND	ND	ND	ND	ND
Chemokine (C-C motif) ligand 11 (CCL11)	28.0	29.7	28.2	28.9	29.3	31.5	27.9	27.8
Chemokine (C-C motif) ligand 17 (CCL17)	34.3	34.7	ND	ND	ND	ND	35.0	35.0
Chemokine (C-C motif) ligand 19 (CCL19)	27.7	28.3	27.8	28.6	28.0	28.9	27.3	28.0
Chemokine (C-C motif) ligand 2 (CCL2)	34.7	32.5	31.0	32.0	29.6	32.2	30.9	29.8
Chemokine (C-C motif) ligand 20 (CCL20)	ND	ND	ND	ND	ND	ND	ND	ND
Chemokine (C-C motif) ligand 21a,b (CCL21a,b)	25.9	25.6	26.4	26.8	26.3	25.4	25.5	26.1
Chemokine (C-C motif) ligand 22 (CCL22)	30.7	30.7	30.6	31.6	32.1	32.5	30.7	30.9
Chemokine (C-C motif) ligand 24 (CCL24)	32.8	32.7	31.6	33.5	32.4	33.9	32.7	32.0
Chemokine (C-C motif) ligand 25 (CCL25)	25.9	26.0	26.1	26.9	26.4	26.7	26.2	26.3
Chemokine (C-C motif) ligand 26 (CCL26)	30.7	ND	ND	ND	ND	ND	ND	ND
Chemokine (C-C motif) ligand 27a,b (CCL27a,b)	23.4	23.6	23.4	24.0	23.9	23.8	23.1	23.5
Chemokine (C-C motif) ligand 28 (CCL28)	28.3	28.1	30.2	29.6	29.4	28.5	29.0	29.0
Chemokine (C-C motif) ligand 3 (CCL3)	35.0	34.4	34.4	36.0	35.0	35.1	34.0	34.7
Chemokine (C-C motif) ligand 4 (CCL4)	33.0	32.7	31.5	32.4	31.8	32.8	31.9	31.0
Chemokine (C-C motif) ligand 5 (CCL5)	31.3	29.8	29.5	30.9	30.5	30.7	28.7	28.8
Chemokine (C-C motif) ligand 6 (CCL6)	26.8	27.6	26.2	27.0	26.3	28.0	26.2	26.3
Chemokine (C-C motif) ligand 7 (CCL7)	33.2	32.0	30.8	32.9	29.6	31.0	29.0	28.0
Chemokine (C-C motif) ligand 8 (CCL8)	34.0	31.7	31.8	35.5	31.1	32.8	30.9	30.9
Chemokine (C-C motif) ligand 9 (CCL9)	28.1	28.7	28.3	28.6	28.0	28.9	27.8	28.2
T-cell surface glycoprotein CD3 delta chain (CD3D)	ND	34.5	34.4	ND	35.0	35.9	33.4	ND
Colony stimulating factor 1 (macrophage) (CSF1)	24.9	25.1	24.5	25.3	25.1	25.5	24.7	24.4
Colony stimulating factor 1 (macrophage) receptor (CSF1R)	23.8	23.9	23.3	24.1	23.5	23.9	23.0	23.0
Colony stimulating factor 2 (granulocyte-macrophage) (CSF2)	ND	ND	ND	ND	ND	ND	34.4	ND
Colony stimulating factor 3 (granulocyte) (CSF3)	ND	ND	ND	ND	34.6	ND	34.5	ND
Chemokine (CX3-C motif) ligand 1 (CX3CL1)	22.2	22.1	21.8	22.5	22.2	22.5	21.6	21.8
Chemokine (C-X-C motif) ligand 1 (CXCL1)	33.0	ND	34.3	34.2	33.0	35.2	ND	33.4
Chemokine (C-X-C motif) ligand 10 (CXCL10)	31.3	31.4	30.7	30.9	30.5	29.4	29.3	30.6
Chemokine (C-X-C motif) ligand 11 (CXCL11)	31.6	32.2	30.7	30.6	31.9	32.1	30.0	30.6
Chemokine (C-X-C motif) ligand 12 (CXCL12)	32.5	32.7	31.6	31.8	32.8	33.7	31.4	32.1
Chemokine (C-X-C motif) ligand 13 (CXCL13)	ND	34.1	33.5	ND	33.5	ND	31.0	32.4
Chemokine (C-X-C motif) ligand 14 (CXCL14)	22.7	22.7	22.6	23.5	22.9	23.1	22.4	22.6
Chemokine (C-X-C motif) ligand 16 (CXCL16)	27.9	27.9	26.9	27.9	27.6	28.9	27.2	27.1
Chemokine (C-X-C motif) ligand 17 (CXCL17)	34.0	34.0	ND	34.0	33.0	33.9	34.0	34.7
Chemokine (C-X-C motif) ligand 2 (CXCL2)	ND	34.9	34.0	ND	ND	36.8	ND	33.4
Chemokine (C-X-C motif) ligand 3 (CXCL3)	33.2	34.2	ND	ND	ND	33.1	ND	33.4
Chemokine (C-X-C motif) ligand 5 (CXCL5)	30.8	31.6	30.2	32.8	31.2	31.3	30.9	31.3
Chemokine (C-X-C motif) ligand 9 (CXCL9)	34.4	31.7	33.2	ND	34.7	34.0	31.0	32.6
Chemokine (C-X-C motif) receptor 3 (CXCR3)	34.1	32.9	32.5	32.7	33.4	34.4	31.3	32.2
Epstein-Barr virus induced gene 3 (EBI3)	31.9	32.8	31.1	31.8	31.9	31.6	30.5	30.8
Epiregulin (EREG)	ND	ND	ND	34.9	ND	ND	ND	34.6
Fibroblast growth factor 7 (keratinocyte growth factor; FGF7)	27.8	28.6	27.5	28.6	29.3	29.8	28.0	27.9
G-protein receptor 84 (GPR84)	ND	ND	ND	ND	ND	ND	ND	ND
Histocompatibility 2, class II antigen E beta (H2.EB1)	27.5	27.3	26.6	27.5	27.6	29.6	26.6	26.6

Table 8	KO Spinal cord 21 days post SHAM				KO Spinal cord 21 days post PNL			
Gene	**1**	**2**	**3**	**4**	**1**	**2**	**3**	**4**
Heparin-binding EGF-like growth factor (HBEGF)	26.1	26.0	25.5	26.3	26.1	26.6	25.7	25.6
Interleukin 10 (IL10)	ND	ND	ND	ND	ND	ND	ND	ND
Interleukin 11 (IL11)	32.9	32.2	31.7	33.5	32.9	34.8	34.5	32.7
Interleukin 12 alpha (IL12a)	30.8	30.3	30.8	31.0	31.4	30.7	30.9	31.2
Interleukin 12 beta (IL12b)	35.0	34.2	35.0	33.6	ND	ND	34.5	34.0
Interleukin 13 (IL13)	ND	ND	ND	ND	34.7	ND	ND	ND
Interleukin 15 (IL15)	28.8	28.8	29.0	29.9	29.2	30.1	28.7	28.8
Interleukin 16 (IL16)	26.6	27.2	26.1	26.9	27.2	28.3	25.7	25.8
Interleukin 17 alpha (IL17a)	ND	ND	ND	ND	ND	ND	ND	ND
Interleukin 18 (IL18)	25.7	25.5	25.0	26.0	25.7	25.9	25.0	25.1
Interleukin 19 (IL19)	ND	32.5	33.0	ND	32.9	ND	33.2	33.1
Interleukin 1 alpha (IL1a)	31.2	32.7	31.6	32.0	30.8	32.6	31.0	31.1
Interleukin 1 beta (IL1b)	32.5	31.8	32.1	32.7	31.6	32.3	32.2	31.0
Interleukin 2 (IL2)	ND	ND	ND	ND	33.4	ND	ND	ND
Interleukin 20 (IL20)	ND	ND	ND	ND	ND	ND	ND	ND
Interleukin 21 (IL21)	33.5	32.7	32.6	32.3	33.6	33.0	33.7	32.3
Interleukin 22 (IL22)	ND	37.3	ND	ND	ND	ND	ND	ND
Interleukin 23 alpha (IL23a)	31.5	32.0	30.0	31.4	31.2	ND	30.4	30.5
Interleukin 24 (IL24)	ND	ND	ND	ND	ND	ND	ND	ND
Interleukin 25 (IL25)	31.7	31.4	32.0	33.5	33.2	32.6	31.0	31.9
Interleukin 27 (IL27)	34.6	ND	ND	34.9	34.8	34.3	ND	ND
Interleukin 28 beta (IL28b)	ND	ND	ND	ND	ND	ND	ND	ND
Interleukin 3 (IL3)	30.6	ND	ND	ND	ND	ND	ND	ND
Interleukin 31 (IL31)	ND	ND	ND	ND	ND	ND	ND	ND
Interleukin 33 (IL33)	23.0	22.9	22.8	23.6	23.1	23.5	22.4	22.6
Interleukin 34 (IL34)	30.7	30.6	30.9	32.0	31.9	31.7	30.8	30.9
Interleukin 4 (IL4)	ND	ND	ND	ND	ND	ND	ND	ND
Interleukin 5 (IL5)	31.8	32.1	32.8	ND	32.9	32.1	32.4	33.2
Interleukin 6 (IL6)	33.3	33.7	33.1	33.8	33.9	33.7	33.2	32.5
Interleukin 7 (IL7)	30.5	31.3	30.1	31.0	30.8	31.2	30.3	29.9
Interleukin 9 (IL9)	ND	37.1	ND	ND	ND	ND	ND	ND
Integrin alpha M (ITGAM; CD11B)	26.5	26.1	25.7	26.7	25.7	26.4	25.4	25.2
Nerve growth factor (NGF)	29.5	29.8	29.6	29.3	29.3	29.9	28.9	28.8
Nitric oxide synthase, inducible (NOS2)	30.4	30.7	29.5	31.0	30.2	31.6	30.2	30.4
Platelet factor 4 (PF4; CXCL4)	28.5	27.9	27.1	28.1	27.4	27.8	26.4	27.7
Pro-platelet basic protein (chemokine (C-X-C motif) ligand 7	29.0	27.4	27.7	27.7	26.7	26.5	25.4	28.1
Prostaglandin E synthase (PTGES)	28.4	28.2	28.0	28.8	28.9	29.7	28.5	28.4
Prostaglandin-endoperoxide synthase 2 (COX-2; PTGS2)	31.4	31.8	31.3	33.4	30.2	32.6	31.8	32.6
Signal Transducer and Activator of Transcription protein 4 (STAT4)	33.9	33.5	31.4	ND	34.4	33.1	32.9	33.0
Toll-like receptor 4 (TLR4)	29.1	29.3	28.3	29.2	29.3	29.8	28.4	28.7
Tumor necrosis factor (TNF)	32.1	33.2	32.1	32.1	32.7	32.2	31.5	31.5
Alpha-taxilin (TXLNA)	24.8	24.8	24.2	25.4	25.0	25.6	24.4	24.5
Chemokine (C motif) ligand 1 (XCL1)	35.9	34.6	36.5	ND	36.4	ND	35.9	35.8
Housekeeping genes								
Beta-actin (ACTB)	19.1	18.9	18.6	19.5	19.0	19.0	18.4	18.6
Glyceraldehyde 3-phosphate dehydrogenase (GAPDH)	18.2	18.3	18.0	18.6	18.3	18.5	17.9	18.2
Hypoxanthine-guanine phosphoribosyltransferase (HPRT)	22.9	23.0	22.6	23.6	23.1	23.9	22.9	23.0
18s (X18S)	14.5	14.5	14.6	14.9	14.7	15.6	14.9	14.9

Appendix Table 9: Raw CT values of genes screened in GPR84 WT B-GEPMs in control conditions or after 3 hours of LPS stimulation

Table 9	WT control				WT LPS			
Gene	**1.0**	**2.0**	**3.0**	**4.0**	**1.0**	**2.0**	**3.0**	**4.0**
Allograft inflammatory factors -1 (Iba1; AIF)	24.4	26.9	24.6	24.9	25.8	25.4	25.4	25.5
Amphiregulin (AREG)	33.6	31.9	33.2	38.0	28.9	27.7	29.2	28.4
Artemin (ARTN)	33.9	32.7	33.0	31.0	28.1	27.6	27.8	27.4
Brain-derived neurotrophic factor (BDNF)	33.3	34.4	33.1	32.8	34.0	33.1	38.0	35.2
Betacellulin (BTC)	31.1	32.1	31.3	31.0	33.0	31.5	31.0	31.0
Chemokine (C-C motif) ligand 1 (CCL1)	38.0	38.0	38.0	33.8	38.0	34.1	34.8	38.0
Chemokine (C-C motif) ligand 11 (CCL11)	38.0	38.0	38.0	38.0	38.0	38.0	33.7	35.3
Chemokine (C-C motif) ligand 17 (CCL17)	34.1	38.0	38.0	34.1	30.0	29.7	26.4	28.3
Chemokine (C-C motif) ligand 19 (CCL19)	38.0	38.0	38.0	38.0	32.4	31.4	32.4	32.7
Chemokine (C-C motif) ligand 2 (CCL2)	24.9	26.4	26.2	25.9	22.3	21.0	20.5	22.1
Chemokine (C-C motif) ligand 20 (CCL20)	38.0	32.2	35.0	34.0	30.4	29.7	31.1	30.0
Chemokine (C-C motif) ligand 21a,b (CCL21a,b)	38.0	36.8	37.4	34.0	38.0	34.6	35.3	38.0
Chemokine (C-C motif) ligand 22 (CCL22)	32.7	33.0	31.5	33.0	22.8	22.7	20.3	21.1
Chemokine (C-C motif) ligand 24 (CCL24)	23.6	25.7	24.0	24.7	23.3	23.0	22.6	24.2
Chemokine (C-C motif) ligand 25 (CCL25)	26.7	27.6	27.3	27.5	29.9	28.9	28.9	29.2
Chemokine (C-C motif) ligand 26 (CCL26)	38.0	38.0	38.0	38.0	38.0	38.0	38.0	38.0
Chemokine (C-C motif) ligand 27a,b (CCL27a,b)	27.1	27.7	26.8	27.0	28.8	28.3	28.8	28.7
Chemokine (C-C motif) ligand 28 (CCL28)	30.8	31.1	31.5	34.1	33.0	34.7	32.8	33.1
Chemokine (C-C motif) ligand 3 (CCL3)	27.3	26.8	27.7	26.6	20.4	19.4	19.0	19.2
Chemokine (C-C motif) ligand 4 (CCL4)	24.9	25.9	26.0	25.0	18.1	17.0	17.3	17.1
Chemokine (C-C motif) ligand 5 (CCL5)	22.9	23.6	22.9	22.4	16.8	16.3	16.5	16.3
Chemokine (C-C motif) ligand 6 (CCL6)	16.9	17.5	17.1	17.7	18.8	18.3	17.5	18.4
Chemokine (C-C motif) ligand 7 (CCL7)	26.5	27.4	28.1	27.3	23.1	22.1	21.1	23.1
Chemokine (C-C motif) ligand 8 (CCL8)	22.1	25.6	23.4	23.6	24.9	24.2	23.8	25.8
Chemokine (C-C motif) ligand 9 (CCL9)	19.7	20.3	19.6	20.4	17.5	16.9	16.5	16.8
T-cell surface glycoprotein CD3 delta chain (CD3D)	33.7	38.0	38.0	38.0	38.0	38.0	33.8	34.6
Colony stimulating factor 1 (macrophage) (CSF1)	23.6	22.9	24.3	23.6	22.3	21.4	21.4	21.3
Colony stimulating factor 1 (macrophage) receptor (CSF1R)	17.7	17.9	17.8	17.7	19.3	18.9	19.1	18.9
Colony stimulating factor 2 (granulocyte-macrophage) (CSF2)	32.1	34.7	33.3	34.5	22.6	21.9	20.1	20.6
Colony stimulating factor 3 (granulocyte) (CSF3)	32.4	31.8	33.3	31.9	24.2	23.2	22.8	22.9
Chemokine (CX3-C motif) ligand 1 (CX3CL1)	30.1	31.1	29.9	30.0	28.1	28.4	27.2	27.0
Chemokine (C-X-C motif) ligand 1 (CXCL1)	26.4	27.3	26.6	26.1	18.4	17.5	18.0	17.7
Chemokine (C-X-C motif) ligand 10 (CXCL10)	26.1	27.0	26.5	25.6	19.8	19.3	19.6	19.4
Chemokine (C-X-C motif) ligand 11 (CXCL11)	33.8	35.3	33.5	34.7	30.0	29.8	29.4	29.1
Chemokine (C-X-C motif) ligand 12 (CXCL12)	31.6	32.6	31.3	31.5	32.3	33.3	33.3	31.7
Chemokine (C-X-C motif) ligand 13 (CXCL13)	25.7	29.7	25.9	26.2	25.9	25.9	24.6	24.3
Chemokine (C-X-C motif) ligand 14 (CXCL14)	23.0	25.0	22.9	23.0	24.8	23.8	24.5	23.9
Chemokine (C-X-C motif) ligand 16 (CXCL16)	20.4	21.4	20.4	20.0	20.1	19.1	19.1	19.0
Chemokine (C-X-C motif) ligand 17 (CXCL17)	38.0	38.0	34.7	38.0	38.0	38.0	38.0	38.0
Chemokine (C-X-C motif) ligand 2 (CXCL2)	23.6	24.4	24.6	23.5	16.9	16.0	16.2	15.7
Chemokine (C-X-C motif) ligand 3 (CXCL3)	26.7	27.7	27.0	26.1	17.8	17.3	17.3	16.9
Chemokine (C-X-C motif) ligand 5 (CXCL5)	27.0	27.8	28.4	28.6	23.7	23.6	23.1	22.6
Chemokine (C-X-C motif) ligand 9 (CXCL9)	32.7	34.1	34.9	32.0	29.7	29.0	29.0	28.9
Chemokine (C-X-C motif) receptor 3 (CXCR3)	27.4	29.1	27.7	28.1	28.9	28.7	28.4	28.5
Epstein-Barr virus induced gene 3 (EBI3)	22.9	22.7	22.9	22.9	23.0	22.3	22.0	22.1
Epiregulin (EREG)	30.2	28.7	29.6	29.4	25.9	25.2	25.9	25.0
Fibroblast growth factor 7 (keratinocyte growth factor; FGF7)	32.7	32.4	31.9	32.5	33.4	33.3	34.3	34.5
G-protein receptor 84 (GPR84)	25.5	25.8	25.8	24.5	21.7	20.7	20.8	20.1
Histocompatibility 2, class II antigen E beta (H2.EB1)	21.6	22.1	20.7	21.0	21.5	21.2	20.9	21.5

Table 9	WT control				WT LPS			
Gene	**1.0**	**2.0**	**3.0**	**4.0**	**1.0**	**2.0**	**3.0**	**4.0**
Heparin-binding EGF-like growth factor (HBEGF)	27.7	27.1	27.6	27.7	27.0	26.4	25.2	26.2
Interleukin 10 (IL10)	31.9	35.7	31.8	33.7	27.4	26.5	25.4	26.2
Interleukin 11 (IL11)	34.1	34.3	33.8	33.1	34.5	32.8	34.4	34.1
Interleukin 12 alpha (IL12a)	30.7	30.6	31.3	30.2	21.7	20.9	20.7	20.4
Interleukin 12 beta (IL12b)	28.7	29.1	29.5	28.2	19.2	18.6	18.5	18.9
Interleukin 13 (IL13)	38.0	38.0	38.0	38.0	36.2	33.0	38.0	34.5
Interleukin 15 (IL15)	24.7	25.8	25.1	25.3	22.5	21.8	22.0	22.1
Interleukin 16 (IL16)	23.4	24.0	23.5	23.9	27.1	26.6	26.2	26.0
Interleukin 17 alpha (IL17a)	38.0	38.0	38.0	38.0	38.0	38.0	38.0	38.0
Interleukin 18 (IL18)	25.3	25.9	25.6	25.4	24.7	23.9	23.4	23.7
Interleukin 19 (IL19)	33.6	34.8	38.0	38.0	28.9	28.5	28.4	29.0
Interleukin 1 alpha (IL1a)	24.8	24.6	25.8	24.8	18.0	17.4	16.5	16.9
Interleukin 1 beta (IL1b)	25.7	25.8	25.1	24.6	17.0	16.3	15.6	15.6
Interleukin 2 (IL2)	38.0	38.0	38.0	38.0	38.0	38.0	33.9	35.7
Interleukin 20 (IL20)	38.0	38.0	38.0	38.0	35.0	33.0	35.9	34.7
Interleukin 21 (IL21)	32.4	38.0	38.0	38.0	38.0	38.0	38.0	38.0
Interleukin 22 (IL22)	38.0	38.0	38.0	38.0	38.0	38.0	35.4	38.0
Interleukin 23 alpha (IL23a)	33.4	31.4	32.3	31.3	23.4	22.2	21.5	21.6
Interleukin 24 (IL24)	33.3	38.0	38.0	38.0	38.0	38.0	38.0	34.1
Interleukin 25 (IL25)	38.0	38.0	38.0	38.0	38.0	38.0	38.0	38.0
Interleukin 27 (IL27)	28.3	29.0	28.9	28.3	20.7	19.8	20.1	19.7
Interleukin 28 beta (IL28b)	38.0	38.0	38.0	38.0	38.0	38.0	38.0	38.0
Interleukin 3 (IL3)	38.0	38.0	38.0	38.0	38.0	38.0	38.0	38.0
Interleukin 31 (IL31)	38.0	38.0	38.0	38.0	38.0	38.0	38.0	38.0
Interleukin 33 (IL33)	30.6	31.1	31.6	32.2	29.4	29.5	28.5	27.9
Interleukin 34 (IL34)	38.0	35.7	35.1	34.7	38.0	35.5	38.0	34.6
Interleukin 4 (IL4)	38.0	38.0	38.0	38.0	38.0	38.0	38.0	38.0
Interleukin 5 (IL5)	33.0	38.0	34.2	34.4	38.0	38.0	34.9	38.0
Interleukin 6 (IL6)	29.5	30.0	30.4	29.1	19.9	19.4	19.0	19.0
Interleukin 7 (IL7)	29.6	29.8	29.4	29.5	28.9	28.5	28.7	28.3
Interleukin 9 (IL9)	38.0	38.0	38.0	38.0	38.0	38.0	38.0	38.0
Integrin alpha M (ITGAM; CD11B)	18.1	18.8	18.2	18.4	19.9	18.8	19.3	19.1
Nerve growth factor (NGF)	28.3	26.8	29.2	28.3	29.2	27.5	27.3	27.0
Nitric oxide synthase, inducible (NOS2)	31.0	31.7	33.0	31.2	25.7	25.1	24.2	25.3
Platelet factor 4 (PF4; CXCL4)	19.1	22.5	19.4	19.5	20.2	19.6	19.8	20.3
Pro-platelet basic protein (chemokine (C-X-C motif) ligand 7	28.5	30.3	27.8	28.6	28.8	28.7	28.3	29.0
Prostaglandin E synthase (PTGES)	23.8	24.1	24.9	24.5	20.9	19.9	19.6	18.7
Prostaglandin-endoperoxide synthase 2 (COX-2; PTGS2)	29.8	27.0	29.1	28.8	19.4	19.0	18.6	18.6
Signal Transducer and Activator of Transcription protein 4 (STAT4)	28.7	29.7	28.4	28.4	28.8	28.3	28.1	27.9
Toll-like receptor 4 (TLR4)	22.0	23.0	22.3	22.2	23.6	22.9	22.3	22.5
Tumor necrosis factor (TNF)	22.6	22.0	23.1	21.5	16.1	15.5	15.4	15.4
Alpha-taxilin (TXLNA)	23.0	23.8	23.3	23.2	24.9	23.9	24.1	23.9
Chemokine (C motif) ligand 1 (XCL1)	33.1	37.1	35.3	34.3	35.7	34.5	33.9	34.5
Housekeeping genes								
Beta-actin (ACTB)	15.9	16.2	16.0	16.1	15.8	15.7	15.7	15.9
Glyceraldehyde 3-phosphate dehydrogenase (GAPDH)	17.6	17.8	18.1	18.0	18.7	18.2	18.6	18.4
Hypoxanthine-guanine phosphoribosyltransferase (HPRT)	21.5	22.8	22.0	21.7	22.7	22.3	22.7	22.8
18s (X18S)	13.2	13.5	13.1	13.3	15.8	13.0	13.1	13.1

Appendix Table 10: Raw CT values of genes screened in GPR84 KO B-GEPMs in control conditions or after 3 hours of LPS stimulation

Table 10	KO control				KO LPS			
Gene	**1.0**	**2.0**	**3.0**	**4.0**	**1.0**	**2.0**	**3.0**	**4.0**
Allograft inflammatory factors -1 (Iba1; AIF)	24.5	23.3	25.0	24.9	25.1	27.1	26.8	26.1
Amphiregulin (AREG)	33.4	31.4	34.6	38.0	27.0	30.9	30.5	29.4
Artemin (ARTN)	32.9	32.3	35.0	32.9	28.1	29.5	29.0	27.7
Brain-derived neurotrophic factor (BDNF)	33.7	35.0	34.4	33.7	32.8	38.0	32.6	35.1
Betacellulin (BTC)	33.0	31.0	31.0	30.6	33.6	31.5	29.4	31.3
Chemokine (C-C motif) ligand 1 (CCL1)	38.0	38.0	38.0	34.1	38.0	38.0	38.0	35.3
Chemokine (C-C motif) ligand 11 (CCL11)	38.0	38.0	38.0	38.0	38.0	33.4	34.8	34.7
Chemokine (C-C motif) ligand 17 (CCL17)	38.0	38.0	38.0	35.1	31.9	30.2	30.1	28.1
Chemokine (C-C motif) ligand 19 (CCL19)	38.0	38.0	38.0	38.0	38.0	38.0	35.0	38.0
Chemokine (C-C motif) ligand 2 (CCL2)	24.9	25.6	26.4	25.7	22.1	22.9	22.3	22.5
Chemokine (C-C motif) ligand 20 (CCL20)	32.1	34.9	38.0	38.0	28.8	32.9	30.4	29.5
Chemokine (C-C motif) ligand 21a,b (CCL21a,b)	38.0	34.1	38.0	33.2	38.0	38.0	38.0	35.2
Chemokine (C-C motif) ligand 22 (CCL22)	30.0	31.7	32.4	31.8	25.4	22.5	22.1	20.2
Chemokine (C-C motif) ligand 24 (CCL24)	24.5	22.7	24.6	24.7	23.4	24.0	23.7	24.2
Chemokine (C-C motif) ligand 25 (CCL25)	27.3	26.2	27.6	27.7	28.3	29.8	29.9	29.0
Chemokine (C-C motif) ligand 26 (CCL26)	38.0	38.0	38.0	38.0	38.0	38.0	38.0	38.0
Chemokine (C-C motif) ligand 27a,b (CCL27a,b)	27.4	26.8	27.1	27.3	28.7	29.6	29.3	28.6
Chemokine (C-C motif) ligand 28 (CCL28)	38.0	31.6	31.8	31.8	32.9	34.0	33.1	35.3
Chemokine (C-C motif) ligand 3 (CCL3)	26.5	26.0	27.4	26.9	19.6	20.8	20.0	19.7
Chemokine (C-C motif) ligand 4 (CCL4)	25.5	24.5	26.4	26.4	16.8	19.1	18.6	18.0
Chemokine (C-C motif) ligand 5 (CCL5)	22.0	22.1	24.0	23.6	16.8	18.0	17.7	16.8
Chemokine (C-C motif) ligand 6 (CCL6)	16.6	16.5	17.5	17.3	17.8	18.8	18.8	18.4
Chemokine (C-C motif) ligand 7 (CCL7)	25.4	28.1	27.8	27.0	24.0	23.2	22.8	23.6
Chemokine (C-C motif) ligand 8 (CCL8)	23.9	21.8	23.4	23.0	23.0	25.3	24.5	24.1
Chemokine (C-C motif) ligand 9 (CCL9)	19.3	19.5	20.0	20.1	17.1	17.7	17.2	17.0
T-cell surface glycoprotein CD3 delta chain (CD3D)	34.3	38.0	38.0	38.0	38.0	38.0	38.0	38.0
Colony stimulating factor 1 (macrophage) (CSF1)	24.5	23.8	24.4	24.0	22.5	22.7	22.2	21.1
Colony stimulating factor 1 (macrophage) receptor (CSF1R)	18.1	17.3	18.1	18.2	18.5	20.0	20.0	19.0
Colony stimulating factor 2 (granulocyte-macrophage) (CSF2)	31.2	33.7	38.0	38.0	24.6	22.7	21.9	21.0
Colony stimulating factor 3 (granulocyte) (CSF3)	30.8	32.7	33.7	33.4	24.7	24.6	24.1	23.8
Chemokine (CX3-C motif) ligand 1 (CX3CL1)	32.8	29.9	29.9	30.0	28.9	28.9	28.0	27.0
Chemokine (C-X-C motif) ligand 1 (CXCL1)	26.6	26.5	28.1	27.8	18.3	20.7	20.0	18.0
Chemokine (C-X-C motif) ligand 10 (CXCL10)	25.3	25.2	26.8	26.2	18.8	19.8	19.6	19.0
Chemokine (C-X-C motif) ligand 11 (CXCL11)	38.0	34.5	38.0	38.0	31.0	29.6	29.6	29.0
Chemokine (C-X-C motif) ligand 12 (CXCL12)	33.8	31.5	31.1	31.0	31.6	34.0	32.8	33.3
Chemokine (C-X-C motif) ligand 13 (CXCL13)	27.0	26.3	26.6	25.6	27.3	26.8	25.8	27.1
Chemokine (C-X-C motif) ligand 14 (CXCL14)	23.9	22.5	22.9	23.4	22.8	24.8	24.9	24.3
Chemokine (C-X-C motif) ligand 16 (CXCL16)	21.4	20.0	21.3	21.0	19.2	20.8	20.2	19.3
Chemokine (C-X-C motif) ligand 17 (CXCL17)	38.0	38.0	38.0	38.0	38.0	38.0	38.0	38.0
Chemokine (C-X-C motif) ligand 2 (CXCL2)	24.5	23.2	25.0	25.4	16.1	18.3	17.8	16.6
Chemokine (C-X-C motif) ligand 3 (CXCL3)	25.5	25.8	28.0	28.3	17.4	19.5	19.2	17.6
Chemokine (C-X-C motif) ligand 5 (CXCL5)	25.5	28.5	28.5	27.0	23.7	24.8	24.4	22.7
Chemokine (C-X-C motif) ligand 9 (CXCL9)	31.8	32.0	33.6	30.8	29.5	29.9	29.1	28.4
Chemokine (C-X-C motif) receptor 3 (CXCR3)	27.6	27.3	27.8	27.7	27.8	29.7	29.7	29.1
Epstein-Barr virus induced gene 3 (EBI3)	22.7	22.4	23.8	23.7	23.1	23.9	23.6	21.8
Epiregulin (EREG)	29.9	30.0	30.6	29.8	24.3	26.7	26.5	25.1
Fibroblast growth factor 7 (keratinocyte growth factor; FGF7)	32.6	31.4	34.0	33.8	37.6	38.0	38.0	35.6
G-protein receptor 84 (GPR84)	38.0	38.0	38.0	38.0	38.0	38.0	38.0	38.0
Histocompatibility 2, class II antigen E beta (H2.EB1)	20.3	20.8	21.5	21.2	21.3	22.4	22.6	21.6

Table 10	KO control				KO LPS			
Gene	**1.0**	**2.0**	**3.0**	**4.0**	**1.0**	**2.0**	**3.0**	**4.0**
Heparin-binding EGF-like growth factor (HBEGF)	28.4	28.1	28.4	28.2	27.4	28.0	27.1	27.1
Interleukin 10 (IL10)	30.1	32.5	32.2	32.3	26.6	27.2	27.8	26.9
Interleukin 11 (IL11)	36.5	33.6	33.5	34.0	33.7	38.0	38.0	34.0
Interleukin 12 alpha (IL12a)	29.1	30.1	32.1	31.8	21.7	22.2	21.9	20.6
Interleukin 12 beta (IL12b)	28.8	27.5	30.2	30.1	19.0	19.9	19.7	19.0
Interleukin 13 (IL13)	38.0	38.0	38.0	38.0	34.8	38.0	38.0	38.0
Interleukin 15 (IL15)	24.7	24.5	25.9	25.6	22.5	23.0	22.9	22.2
Interleukin 16 (IL16)	23.8	22.7	23.9	23.8	27.0	27.8	27.7	26.6
Interleukin 17 alpha (IL17a)	38.0	38.0	38.0	38.0	38.0	38.0	38.0	38.0
Interleukin 18 (IL18)	25.1	24.6	25.8	25.9	24.8	25.5	24.9	23.6
Interleukin 19 (IL19)	35.0	33.6	38.0	34.8	28.4	29.4	30.4	29.5
Interleukin 1 alpha (IL1a)	24.8	24.8	25.6	25.9	18.0	18.1	17.8	17.2
Interleukin 1 beta (IL1b)	25.8	24.9	26.9	26.8	16.9	17.9	17.4	16.2
Interleukin 2 (IL2)	38.0	38.0	38.0	38.0	38.0	38.0	38.0	38.0
Interleukin 20 (IL20)	38.0	38.0	38.0	38.0	34.6	34.8	38.0	35.8
Interleukin 21 (IL21)	38.0	38.0	38.0	38.0	38.0	38.0	38.0	38.0
Interleukin 22 (IL22)	38.0	38.0	38.0	38.0	38.0	36.9	38.0	35.3
Interleukin 23 alpha (IL23a)	38.0	32.1	32.0	33.3	23.2	24.4	23.9	22.0
Interleukin 24 (IL24)	38.0	38.0	38.0	38.0	38.0	38.0	38.0	38.0
Interleukin 25 (IL25)	38.0	38.0	38.0	38.0	38.0	38.0	38.0	38.0
Interleukin 27 (IL27)	28.8	28.0	29.6	29.2	20.3	21.5	21.2	20.0
Interleukin 28 beta (IL28b)	38.0	38.0	38.0	38.0	38.0	38.0	38.0	38.0
Interleukin 3 (IL3)	38.0	38.0	38.0	38.0	37.9	38.0	38.0	38.0
Interleukin 31 (IL31)	38.0	38.0	38.0	38.0	38.0	38.0	38.0	36.5
Interleukin 33 (IL33)	30.6	32.3	32.2	30.8	28.5	29.5	28.9	27.8
Interleukin 34 (IL34)	38.0	33.5	36.0	38.0	38.0	38.0	36.1	35.9
Interleukin 4 (IL4)	38.0	38.0	38.0	38.0	38.0	38.0	38.0	38.0
Interleukin 5 (IL5)	34.7	33.8	38.0	33.3	38.0	38.0	38.0	38.0
Interleukin 6 (IL6)	28.7	29.2	31.4	30.9	19.9	21.3	20.9	19.1
Interleukin 7 (IL7)	29.5	29.2	29.7	29.7	29.3	29.7	30.2	28.5
Interleukin 9 (IL9)	38.0	38.0	38.0	38.0	38.0	38.0	38.0	38.0
Integrin alpha M (ITGAM; CD11B)	18.5	17.8	18.5	19.1	18.2	20.1	20.3	19.3
Nerve growth factor (NGF)	27.8	29.2	28.9	28.7	28.6	28.8	27.9	27.0
Nitric oxide synthase, inducible (NOS2)	31.0	31.5	32.5	32.0	26.0	24.3	24.4	24.5
Platelet factor 4 (PF4; CXCL4)	19.3	18.5	19.6	19.7	19.3	21.4	21.3	20.6
Pro-platelet basic protein (chemokine (C-X-C motif) ligand 7	27.4	28.3	28.8	28.7	28.3	28.9	29.8	28.9
Prostaglandin E synthase (PTGES)	25.5	24.0	25.9	25.8	20.1	21.7	21.4	19.5
Prostaglandin-endoperoxide synthase 2 (COX-2; PTGS2)	28.0	28.9	29.6	29.9	19.5	20.1	19.5	18.9
Signal Transducer and Activator of Transcription protein 4 (STAT4)	28.5	28.1	29.5	29.0	28.2	28.3	28.7	28.0
Toll-like receptor 4 (TLR4)	22.2	21.8	22.7	22.6	23.3	24.2	23.7	22.9
Tumor necrosis factor (TNF)	23.4	21.9	23.3	23.5	15.3	16.2	15.9	15.5
Alpha-taxilin (TXLNA)	23.3	22.3	23.5	23.7	24.0	25.5	25.1	24.3
Chemokine (C motif) ligand 1 (XCL1)	37.1	33.7	37.2	34.0	35.3	36.9	35.1	34.3
Housekeeping genes								
Beta-actin (ACTB)	16.1	15.5	16.2	16.3	15.8	16.5	16.4	16.0
Glyceraldehyde 3-phosphate dehydrogenase (GAPDH)	17.5	17.2	18.2	18.3	18.1	19.1	19.2	18.8
Hypoxanthine-guanine phosphoribosyltransferase (HPRT)	22.3	20.8	22.5	22.3	22.0	24.5	24.2	23.5
18s (X18S)	13.1	13.4	13.1	13.0	13.2	13.7	13.4	13.1

Appendix Table 11: FC values of genes profiled in the sciatic nerve and spinal cord at 7 and 21 days post PNL and in B-GEPMs 3 hours post LPS stimulation in GPR84 WT mice

Table 11	WT				
	Sciatic nerve		Spinal cord		Macrophages
Gene	7 days post PNL	21 days post PNL	7 days post PNL	21 days post PNL	3 hours post LPS
Allograft inflammatory factors -1 (Iba1; AIF)	4.3**	1.2	1.1	1.2	1.0
Amphiregulin (AREG)	12.2	ND	ND	-1.1	64.0*
Arginase-1 (ARG-1)	5.7	X	-1.2	X	X
Artemin (ARTN)	4.5*	-1.3	1.1	-1.2	38.5**
Brain-derived neurotrophic factor (BDNF)	7.9*	8.3	1.1	-1.1	-2.5
Betacellulin (BTC)	4.1*	2.8	-1.1	1.3	1.1
Chemokine (C-C motif) ligand 1 (CCL1)	-1.3	ND	ND	ND	ND
Chemokine (C-C motif) ligand 11 (CCL11)	-3.0*	-2.4	1.0	1.0	4.3
Chemokine (C-C motif) ligand 17 (CCL17)	-3.0	1.5	-1.4	-1.1	224.2**
Chemokine (C-C motif) ligand 19 (CCL19)	-2.1*	-2.3	-1.6	-1.5	71.0***
Chemokine (C-C motif) ligand 2 (CCL2)	1.9	1.6	4.2	5.4	27.2***
Chemokine (C-C motif) ligand 20 (CCL20)	ND	ND	ND	ND	28.7
Chemokine (C-C motif) ligand 21a,b (CCL21a,b)	-2.9*	-4.5	1.0	-1.5	1.4
Chemokine (C-C motif) ligand 22 (CCL22)	3.8*	3.1	-1.2	1.4	2360.1***
Chemokine (C-C motif) ligand 24 (CCL24)	-3.6*	-4.2	-1.3	2.5	3.0*
Chemokine (C-C motif) ligand 25 (CCL25)	-1.8*	-3.5	1.0	-1.3	-3.0***
Chemokine (C-C motif) ligand 26 (CCL26)	X	ND	X	ND	ND
Chemokine (C-C motif) ligand 27a,b (CCL27a,b)	-3.0**	-2.6	-1.1	-1.2	-2.1**
Chemokine (C-C motif) ligand 28 (CCL28)	X	-3.2	X	-1.1	-2.2
Chemokine (C-C motif) ligand 3 (CCL3)	10.2**	17.8	-1.2	1.5	249.5***
Chemokine (C-C motif) ligand 4 (CCL4)	8.3**	8.0	-1.2	1.6	341.3***
Chemokine (C-C motif) ligand 5 (CCL5)	5.8*	2.8	1.0	-1.2	114.4***
Chemokine (C-C motif) ligand 6 (CCL6)	2.4	1.0	1.0	-1.0	-1.5
Chemokine (C-C motif) ligand 7 (CCL7)	1.6	-2.2	15.8*	1.6	41.4***
Chemokine (C-C motif) ligand 8 (CCL8)	7.6	3.3	1.2	2.4	-1.5
Chemokine (C-C motif) ligand 9 (CCL9)	1.8	-1.7	1.3	-1.1	10.7***
T-cell surface glycoprotein CD3 delta chain (CD3D)	2.5	2.6	-2.3	-1.6	ND
Colony stimulating factor 1 (macrophage) (CSF1)	-1.7*	-1.5	1.0	1.1	5.1**
Colony stimulating factor 1 (macrophage) receptor (CSF1R)	X	-1.2	X	1.0	-1.9**
Colony stimulating factor 2 (granulocyte-macrophage) (CSF2)	-1.4	-1.8	ND	ND	6884.0***
Colony stimulating factor 3 (granulocyte) (CSF3)	4.4	ND	ND	ND	689.8***
Colony stimulating factor 3 (granulocyte) receptor (CSF3R)	6.9*	X	1.1	X	X
Chemokine (CX3-C motif) ligand 1 (CX3CL1)	1.4	-1.6	-1.1	-1.1	7.8**
Chemokine (C-X-C motif) ligand 1 (CXCL1)	-1.7	2.2	-1.9	1.5	517.8***
Chemokine (C-X-C motif) ligand 10 (CXCL10)	1.8	1.3	1.7	2.7	140.6***
Chemokine (C-X-C motif) ligand 11 (CXCL11)	-7.4*	-3.7	-1.2	-1.4	35.1***
Chemokine (C-X-C motif) ligand 12 (CXCL12)	2.5	-1.6	-1.1	1.4	-1.5
Chemokine (C-X-C motif) ligand 13 (CXCL13)	-11.7**	-9.9	2.7	2.9	4.2
Chemokine (C-X-C motif) ligand 14 (CXCL14)	1.3	1.2	-1.2	1.0	-1.4
Chemokine (C-X-C motif) ligand 16 (CXCL16)	5.5**	2.6	-1.3	1.0	3.0
Chemokine (C-X-C motif) ligand 17 (CXCL17)	-6.2	-2.1	-1.4	4.2	ND
Chemokine (C-X-C motif) ligand 2 (CXCL2)	20.0**	3.5	-1.4	1.4	289.9***

Table 11	WT				
	Sciatic nerve		Spinal cord		Macrophages
Gene	7 days post PNL	21 days post PNL	7 days post PNL	21 days post PNL	3 hours post LPS
Chemokine (C-X-C motif) ligand 3 (CXCL3)	226.2**	18.1	2.0	ND	959.8***
Chemokine (C-X-C motif) ligand 5 (CXCL5)	445.9**	21.2	-1.4	1.3	33.7***
Chemokine (C-X-C motif) ligand 9 (CXCL9)	3.5*	1.3	6.0	1.5	25.4**
Chemokine (C-X-C motif) receptor 3 (CXCR3)	1.7	2.3	-1.5	3.5	-1.1
Epstein-Barr virus induced gene 3 (EBI3)	1.5	1.2	-1.1	1.0	1.8
Epiregulin (EREG)	55.3*	2.9	ND	ND	19.7**
Fibroblast growth factor 7 (keratinocyte growth factor; FGF7)	-3.5**	-4.5	1.1	-1.3	-2.2
G-protein receptor 84 (GPR84)	51.3**	3.6	2.6	1.1	30.8***
Histocompatibility 2, class II antigen E beta (H2.EB1)	X	-1.6	X	-1.2	1.4
Heparin-binding EGF-like growth factor (HBEGF)	-3.3**	-3.2*	-1.1	1.0	3.2*
Interleukin 10 (IL10)	3.0	-3.4	2.1	1.5	153.2**
Interleukin 11 (IL11)	1.1	-4.0	-1.7	-1.2	1.2
Interleukin 12 alpha (IL12a)	-3.0*	-3.7	-1.2	-1.2	1121.8***
Interleukin 12 beta (IL12b)	7.1	ND	-1.4	2.0	1399.8***
Interleukin 13 (IL13)	-2.1	ND	-2.7	ND	7.7
Interleukin 15 (IL15)	-1.6*	-1.3	-1.3	1.3	11.1***
Interleukin 16 (IL16)	-4.1**	-2.8	-1.1	-1.1	-5.4***
Interleukin 17 alpha (IL17a)	ND	ND	ND	ND	ND
Interleukin 18 (IL18)	-1.3	-3.2	-1.2	1.1	4.0**
Interleukin 19 (IL19)	ND	ND	-1.4	1.4	219.6*
Interleukin 1 alpha (IL1a)	103.3**	11.5	2.0	2.1	288.4***
Interleukin 1 beta (IL1b)	24.9*	42.8	1.9	-1.8	749.5***
Interleukin 2 (IL2)	ND	ND	ND	ND	ND
Interleukin 20 (IL20)	ND	ND	-2.1	ND	13.1*
Interleukin 21 (IL21)	-1.6	ND	-1.8	-1.1	ND
Interleukin 22 (IL22)	ND	ND	ND	-1.1	ND
Interleukin 23 alpha (IL23a)	-3.0*	-6.0	-1.1	1.3	1227.4***
Interleukin 24 (IL24)	ND	ND	9.0	ND	ND
Interleukin 25 (IL25)	-5.7	-1.7	1.5	1.6	ND
Interleukin 27 (IL27)	3.2	16.4	1.9	1.0	475.3***
Interleukin 28 beta (IL28b)	ND	ND	ND	ND	ND
Interleukin 3 (IL3)	ND	ND	ND	ND	ND
Interleukin 31 (IL31)	ND	ND	ND	ND	ND
Interleukin 33 (IL33)	2.3**	-4.7	-1.1	1.0	7.5**
Interleukin 34 (IL34)	4.5*	-3.6	-1.6	-1.5	-1.2
Interleukin 4 (IL4)	ND	ND	ND	ND	ND
Interleukin 5 (IL5)	-1.5	-8.7	-1.1	-2.1	-3.9
Interleukin 6 (IL6)	1.8	-1.4	1.5	-1.1	1785.4***
Interleukin 7 (IL7)	-1.5	-2.1	1.1	1.3	2.6**
Interleukin 9 (IL9)	ND	ND	ND	ND	ND
Integrin alpha M (ITGAM; CD11B)	4.6*	2.0	1.6	1.0	-1.4
Mannose receptor, C type 1 (MRC1)	1.5	X	-1.2	X	X
Nerve growth factor (NGF)	1.0	-1.8	1.0	-1.1	1.7
Nitric oxide synthase, inducible (NOS2)	3.8**	4.3	-1.2	1.2	130.0***
Neuregulin 1 (NRG1)	1.1	X	-1.2	X	X
Platelet factor 4 (PF4; CXCL4)	2.7*	-1.5	1.1	1.4	1.4
Pro-platelet basic protein (chemokine (C-X-C motif) ligand 7	-1.9	-2.6	1.4	2.6	1.4
Prostaglandin E synthase (PTGES)	1.6	-2.6	-1.2	1.0	30.1***
Prostaglandin-endoperoxide synthase 2 (COX-2; PTGS2)	1.8	-1.5	-1.1	1.4	1120.5**
Signal Transducer and Activator of Transcription protein 4 (STAT4)	1.2	-9.4	-1.1	-2.2	1.8
Toll-like receptor 4 (TLR4)	-1.0	-2.0	-1.0	1.1	-1.1

Table 11	WT				
	Sciatic nerve		Spinal cord		Macrophages
Gene	7 days post PNL	21 days post PNL	7 days post PNL	21 days post PNL	3 hours post LPS
Tumor necrosis factor (TNF)	6.8**	2.6	2.2	-1.1	134.6***
Alpha-taxilin (TXLNA)	1.0	-1.1	1.0	1.1	-1.4**
Chemokine (C motif) ligand 1 (XCL1)	4.7	17.2	1.3	-1.2	1.5

Appendix Table 12: FC values of genes profiled in the sciatic nerve and spinal cord at 7 and 21 days post PNL and in B-GEPMs 3 hours post LPS stimulation in GPR84 KO mice

Table 12	KO				
	Sciatic nerve		Spinal cord		Macrophages
Gene	7 days post PNL	21 days post PNL	7 days post PNL	21 days post PNL	3 hours post LPS
Allograft inflammatory factors -1 (Iba1; AIF)	9.2**	2.3	1.5*	1.1	-2.2*
Amphiregulin (AREG)	ND	ND	-1.6	2.6	49.0*
Arginase-1 (ARG-1)	20.7**	X	1.1	X	X
Artemin (ARTN)	2.4	1.4	-1.1	-1.3	43.2***
Brain-derived neurotrophic factor (BDNF)	7.0**	23.0	-1.2	1.0	1.2
Betacellulin (BTC)	2.0	5.0*	1.3	1.0	1.6
Chemokine (C-C motif) ligand 1 (CCL1)	8.0	ND	ND	ND	ND
Chemokine (C-C motif) ligand 11 (CCL11)	-4.1	-2.5	-1.8	-1.3	11.3
Chemokine (C-C motif) ligand 17 (CCL17)	1.8	-1.1	1.4	-1.1	243.7**
Chemokine (C-C motif) ligand 19 (CCL19)	-2.0	-1.5	-1.5	1.1	ND
Chemokine (C-C motif) ligand 2 (CCL2)	4.9*	1.7	5.4*	4.0	15.6***
Chemokine (C-C motif) ligand 20 (CCL20)	ND	ND	ND	ND	66.6*
Chemokine (C-C motif) ligand 21a,b (CCL21a,b)	-1.9	-1.9	1.9	1.3	ND
Chemokine (C-C motif) ligand 22 (CCL22)	3.9	1.8	-1.4	-1.4	798.4**
Chemokine (C-C motif) ligand 24 (CCL24)	-2.2*	-1.7	-1.1	1.0	2.1
Chemokine (C-C motif) ligand 25 (CCL25)	-1.8	-1.6	-1.2	1.0	-2.5**
Chemokine (C-C motif) ligand 26 (CCL26)	X	ND	X	ND	ND
Chemokine (C-C motif) ligand 27a,b (CCL27a,b)	-3.3*	-2.1**	-1.0	1.1	-2.3**
Chemokine (C-C motif) ligand 28 (CCL28)	X	-6.4	X	1.1	1.2
Chemokine (C-C motif) ligand 3 (CCL3)	25.7***	4.0	-1.2	1.2	165.1***
Chemokine (C-C motif) ligand 4 (CCL4)	32.0**	3.3	1.2	1.5	307.5***
Chemokine (C-C motif) ligand 5 (CCL5)	6.5*	3.2	2.3	1.7	82.2**
Chemokine (C-C motif) ligand 6 (CCL6)	3.8*	2.2	1.2	1.2	-1.6*
Chemokine (C-C motif) ligand 7 (CCL7)	7.6*	-2.4	21.5*	7.5	21.3**
Chemokine (C-C motif) ligand 8 (CCL8)	21.0*	13.4	3.8	3.7	-1.4
Chemokine (C-C motif) ligand 9 (CCL9)	4.2*	1.4	-1.1	1.2	9.3***
T-cell surface glycoprotein CD3 delta chain (CD3D)	5.9*	-2.5	3.9	1.7	ND
Colony stimulating factor 1 (macrophage) (CSF1)	-1.9*	-1.4	1.1	1.1	6.9**
Colony stimulating factor 1 (macrophage) receptor (CSF1R)	X	1.6	X	1.4	-1.6**
Colony stimulating factor 2 (granulocyte-macrophage) (CSF2)	3.5	-1.1	ND	ND	11030**
Colony stimulating factor 3 (granulocyte) (CSF3)	5.7	ND	1.2	ND	531.1***
Colony stimulating factor 3 (granulocyte) receptor (CSF3R)	13.6***	X	1.6	X	X
Chemokine (CX3-C motif) ligand 1 (CX3CL1)	-1.1	1.3	1.0	1.1	9.0*
Chemokine (C-X-C motif) ligand 1 (CXCL1)	1.9	1.0	-1.8	1.1	428.9***
Chemokine (C-X-C motif) ligand 10 (CXCL10)	5.5*	1.3	2.0	2.2	158.4***
Chemokine (C-X-C motif) ligand 11 (CXCL11)	-9.6*	-11.1	-1.7	1.2	268.9***
Chemokine (C-X-C motif) ligand 12 (CXCL12)	1.5	1.0	-1.1	-1.2	-1.3
Chemokine (C-X-C motif) ligand 13 (CXCL13)	-20.1*	-5.5	3.1	4.7	1.3
Chemokine (C-X-C motif) ligand 14 (CXCL14)	1.9	3.2	-1.2	1.1	-1.2
Chemokine (C-X-C motif) ligand 16 (CXCL16)	7.3**	2.6	1.0	1.0	3.5**
Chemokine (C-X-C motif) ligand 17 (CXCL17)	-1.9	12.1	1.7	2.2	ND
Chemokine (C-X-C motif) ligand 2 (CXCL2)	55.9**	4.3	-2.0	-1.2	261.1***

Table 12	KO				
	Sciatic nerve		Spinal cord		Macrophages
Gene	7 days post PNL	21 days post PNL	7 days post PNL	21 days post PNL	3 hours post LPS
Chemokine (C-X-C motif) ligand 3 (CXCL3)	184.4**	12.4	ND	1.2	597.2***
Chemokine (C-X-C motif) ligand 5 (CXCL5)	882.3**	31.2	-1.5	1.2	18.5*
Chemokine (C-X-C motif) ligand 9 (CXCL9)	9.8*	2.9	4.5	2.5	11.8**
Chemokine (C-X-C motif) receptor 3 (CXCR3)	3.1*	2.7	7.0	1.2	-1.7
Epstein-Barr virus induced gene 3 (EBI3)	1.1	-1.2	1.4	1.7	1.7
Epiregulin (EREG)	30.5*	ND	ND	ND	35.6***
Fibroblast growth factor 7 (keratinocyte growth factor; FGF7)	-3.8*	-2.4	-1.5	-1.5	-12.1**
G-protein receptor 84 (GPR84)	ND	ND	ND	ND	ND
Histocompatibility 2, class II antigen E beta (H2.EB1)	X	1.1	X	-1.3	-1.2
Heparin-binding EGF-like growth factor (HBEGF)	-5.7*	-3.1**	1.1	1.0	3.1*
Interleukin 10 (IL10)	5.2	ND	2.2	ND	42.2**
Interleukin 11 (IL11)	-1.7*	-3.9	-1.1	-2.1	-1.7
Interleukin 12 alpha (IL12a)	-3.0	-3.9	-1.5	-1.2	959.5***
Interleukin 12 beta (IL12b)	26.2*	4.7	1.0	-3.1	1385.0***
Interleukin 13 (IL13)	ND	ND	ND	ND	ND
Interleukin 15 (IL15)	-1.4	1.0	1.1	1.0	9.5***
Interleukin 16 (IL16)	-6.3*	-3.7	-1.5	1.0	-8.0***
Interleukin 17 alpha (IL17a)	ND	ND	ND	ND	ND
Interleukin 18 (IL18)	1.5	-2.1	-1.1	1.1	2.6
Interleukin 19 (IL19)	ND	ND	-3.1	2.2	100.0**
Interleukin 1 alpha (IL1a)	91.0**	17.3	2.1	1.5	302.5***
Interleukin 1 beta (IL1b)	79.9***	3.2	1.8	1.4	823.4***
Interleukin 2 (IL2)	1.0	ND	ND	ND	ND
Interleukin 20 (IL20)	ND	ND	ND	ND	7.6*
Interleukin 21 (IL21)	ND	ND	-1.2	-1.2	ND
Interleukin 22 (IL22)	ND	ND	ND	ND	ND
Interleukin 23 alpha (IL23a)	-7.3	-14.3	-1.5	-2.3	2374.0**
Interleukin 24 (IL24)	ND	ND	5.7	ND	ND
Interleukin 25 (IL25)	-3.7	-2.4	1.1	1.1	ND
Interleukin 27 (IL27)	6.8	2.2	-1.8	1.1	470.0***
Interleukin 28 beta (IL28b)	ND	ND	ND	ND	ND
Interleukin 3 (IL3)	ND	ND	ND	ND	ND
Interleukin 31 (IL31)	ND	1.4	ND	ND	ND
Interleukin 33 (IL33)	-2.8	-3.7	1.0	1.2	11.5**
Interleukin 34 (IL34)	-8.7	-1.1	-1.1	-1.2	ND
Interleukin 4 (IL4)	ND	ND	ND	ND	ND
Interleukin 5 (IL5)	-16.2***	1.3	1.0	2.1	-5.0
Interleukin 6 (IL6)	14.3*	-4.4	2.4	1.2	1438.0***
Interleukin 7 (IL7)	-1.6	1.2	1.1	1.2	1.8
Interleukin 9 (IL9)	ND	ND	ND	ND	ND
Integrin alpha M (ITGAM; CD11B)	6.4**	3.2	1.8*	1.6	-1.2
Mannose receptor, C type 1 (MRC1)	2.2	X	-1.2	X	X
Nerve growth factor (NGF)	1.1	-1.4	1.3	1.3	2.5
Nitric oxide synthase, inducible (NOS2)	5.3*	2.2	1.3	-1.1	204.2**
Neuregulin 1 (NRG1)	1.3	X	1.0	X	X
Platelet factor 4 (PF4; CXCL4)	3.7	1.1	1.0	1.6	-1.5
Pro-platelet basic protein (chemokine (C-X-C motif) ligand 7	1.4	-7.1	1.0	2.5	1.0
Prostaglandin E synthase (PTGES)	-2.2	-2.5	-1.1	-1.4	41.1***
Prostaglandin-endoperoxide synthase 2 (COX-2; PTGS2)	2.2	-3.7	1.4	1.2	1292.0***
Signal Transducer and Activator of Transcription protein 4 (STAT4)	1.9	-3.4	1.6	1.9	2.3*
Toll-like receptor 4 (TLR4)	1.5	1.4	1.2	1.0	-1.4

Table 12	KO				
	Sciatic nerve		Spinal cord		Macrophages
Gene	7 days post PNL	21 days post PNL	7 days post PNL	21 days post PNL	3 hours post LPS
Tumor necrosis factor (TNF)	18.3**	3.0	4.1	1.4	266.6***
Alpha-taxilin (TXLNA)	-1.6*	-1.2	-1.1	1.0	-1.7*
Chemokine (C motif) ligand 1 (XCL1)	19.8*	2.5	1.1	-1.1	1.8